DOE/NV/10461--T64

TRAC *Technology and Resource Assessment Corporation*

3800 Arapahoe Avenue, Suite 225
Boulder, Colorado 80303
(303) 443-3700 FAX No. (303) 443-8626

DIALOGS BY JERRY SZYMANSKI REGARDING THE YUCCA MOUNTAIN CONTROVERSY FROM DECEMBER, 1990 TO MARCH, 1991

VOLUME II

SPECIAL REPORT No. 9
CONTRACT No. 92/94.0004

SPECIAL REPORT Submitted to the
Nuclear Waste Project Office
State of Nevada

July, 1993

Not a conf. material incomplete
jcp 3-1-96

Assembled by:

Jerry Szymanski
D. E. Livngston

Dialogs by Jerry Szymanski Regarding the Yucca Mountain Controversy from December, 1990 to March, 1991

Volume II

REPORT ORGANIZATION

PART 1
Materials Prepared for and Presented to the
Penrose Conference of Bodega Bay, California

J. S. Szymanski

PART 2
Materials Prepared for and Presented to
NRC/NAS Panel Field Trip,
April 23-25, 1991

J. S. Szymanski

PART 1

Materials Prepared for and Presented to the Penrose Conference of Bodega Bay, California

WBS 1.2.9
QA: N/A

MAR 11 1991

Ina B. Alterman, Ph.D.
Senior Program Officer
Board on Radioactive Waste Management
National Academy of Sciences National
Research Council
2101 Constitution Avenue, N.W.
Washington, DC 20418

TRANSMITTAL OF PENROSE CONFERENCE PRESENTATION

Enclosed please find a copy of the presentation I have prepared for the Penrose Conference on "Flow and Associated Transport in Basins: Driving Forces, Coupling, and Geologic Controls." You may recall that this copy has been requested by Dr. C. Berry Raleigh.

Should you have any questions concerning the enclosed material, please do not hesitate to contact me. I am looking forward to our field trip in early April 1991.

"ORIGINAL SIGNED BY"
JERRY SZYMANSKI
Jerry S. Szymanski
Technical Analysis Branch
Regulatory & Site Evaluation Division

RSED:JSS-2572

Enclosure:
Presentation Package

cc w/encl:
Leon Reiter, NWTRB, Arlington, VA
P. T. Prestholt, NRC, Las Vegas, NV
C. B. Archambeau, University of
Colorado, Boulder, CO
N. J. Price, Balloon House,
Lincolnshire PE9 2BW, UK
John Rudnicki, Northwestern University,
Evanston, IL
Leslie Smith, University of British
Columbia, Vancouver, BC, Canada
Dennis Powers, Anthony, TX
Jack Evernden, USGS, Menlo Park, CA
J. R. Dyer, YMP, NV
D. E. Livingston, YMP, NV
A. M. Simmons, YMP, NV

CONCUR
RTG.
YMP
INITL
Szym
3/11
RTG.
INITIA
DATE
RTG. S
INITIAL
DATE
RTG. S
INITIAL
DATE
RTG. S
INITIAL
DATE
RTG. S
INITIAL
DATE
RTG. SY
INITIAL
DATE
JR-26
RTG. SY
INITIAL
DATE

The Nevada Test Site hydrosphere as a non equilibrium dynamic system; Isotopic evidence for self organization, fluctuations, and sink - - source transformations.

Part A - Behavioral patterns of a dynamic system - general remarks.

Part B - The Nevada Test Site hydrosphere as a non-equilibrium dynamic system - isotopic and chemical evidence for:

i) self-organization;

ii) periodic and quasi-periodic fluctuations; and

iii) "source" - - "sink" transformations.

ENCLOSURE

Content.

Figure 1.

General statement of the problem:

Part A - A fundamental question that underlies any consideration of a dynamic system (in this case, a fluid heat flow in a deforming fractured medium) is concerned with a behavior of this system.

- Stated specifically, this question is: **which one of the three fundamental modes of behavior of a dynamic system is pertinent?**

Part A - Behavioral patterns of a dynamic system - general remark.

Figure 2.

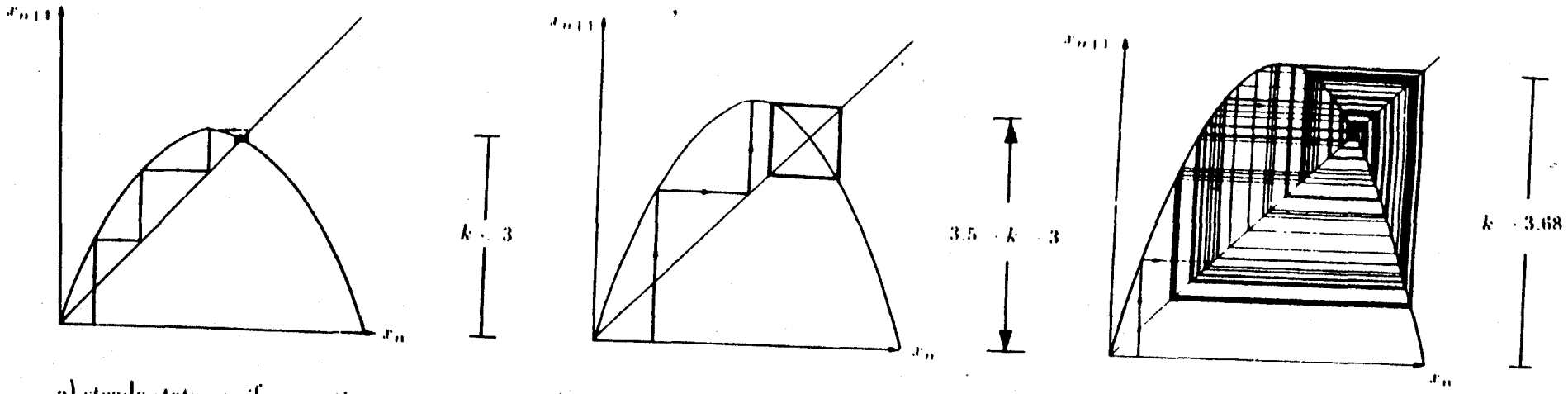

a) steady state - uniform motion.

b) periodic motion - marginally stable.

c) chaotic motion - unstable and diverging.

Note:

a) $x_{t+1} = kx_t(1 - x_t)$ - describes dynamic system, where $t = 0, 1, 2, 3, \ldots$ whole steps and k is constant;

b) k describes equilibrium status of a dynamic system; and

c) depending upon value of k a dynamic system exhibits three fundamentally different generic modes of behavior.

Cobweb diagram illustration of three generic modes of behavior of a dynamic system. From Stewart, 1989.

Figure 3.

Q: How understanding and definition of behavior of a dynamic system may be achieved?

A: Two general approaches are available:

i) **in enlarging time-space**, examine the relationship between forces that drive and resist motion; and

ii) **in enlarging time-space**, examine recorded history of system's behavior.

Note:

a) understanding of behavior of a dynamic system comes first;

b) numerical modeling comes second; and

c) serious errors in judgement may result from reversing the above sequence, e.g., the Yucca Mountain Project.

Specific statement of the problem.

Figure 4

Szymanski (1989) has shown that:

i) in a fixed time space, the Nevada Test Site flow system exhibits two fold soft loss of stability, namely: $Ra \rightarrow Rc$ (thermal) and $\tau_f \rightarrow \tau_{max}$, $U_s \rightarrow U_{sp}$ (mechanical);

ii) in enlarging time-space, $K_{(x,y,z,t)} \neq$ const; and consequently

iii) in enlarging time-space, $Ra_{(t)} \rightarrow Rc_{(t)} \neq$ const.

Expectation:

For enlarging time-space, the Nevada Test Site flow system does not possess a fixed level of disequilibrium, i.e., does not occupy a fixed position in the Feingenbaum sequence.

Explanation:

Ra - actual Rayleigh number;

Rc - critical Rayleigh number;

τ_f - shear stress along a fracture;

$\tau_{max} = C + tan\phi \cdot \sigma_{nfeff}$;

U_s - shear displacement along a fracture;

U_{sp} - peak shear displacement along a fracture; and

K - hydraulic conductivity.

Relationship between forces that drive and resist motion.

Figure 5.

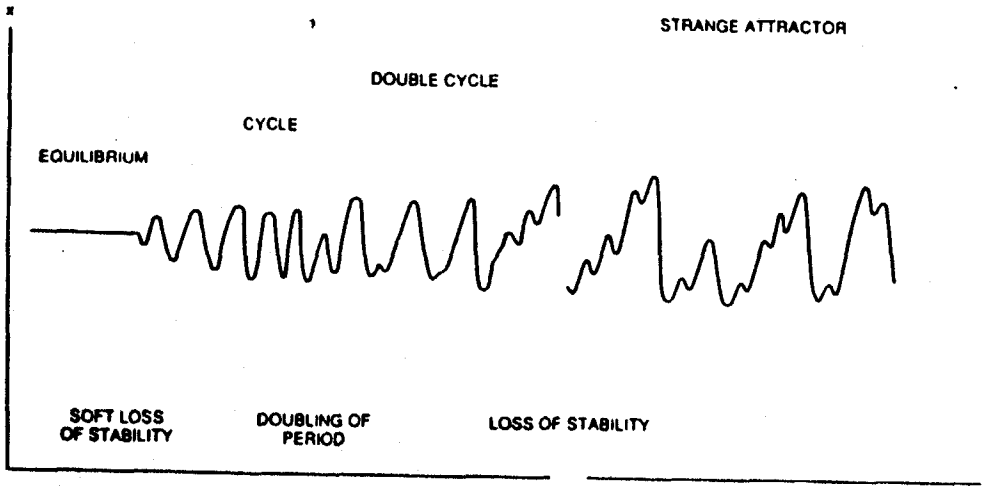

Note:

a) x denotes character of time series for any parameter that expresses system behavior, e.g., intensity of convection stream, temperature gradients, gradients describing chemical and isotopic compositions of fluids, etc.

b) y denotes distance from equilibrium, e.g. *Ra* — *Rc*, density of *in-situ* stress singularities, etc.

Feigenbaum sequence. From Ivlis Book, 1990

Figure 6

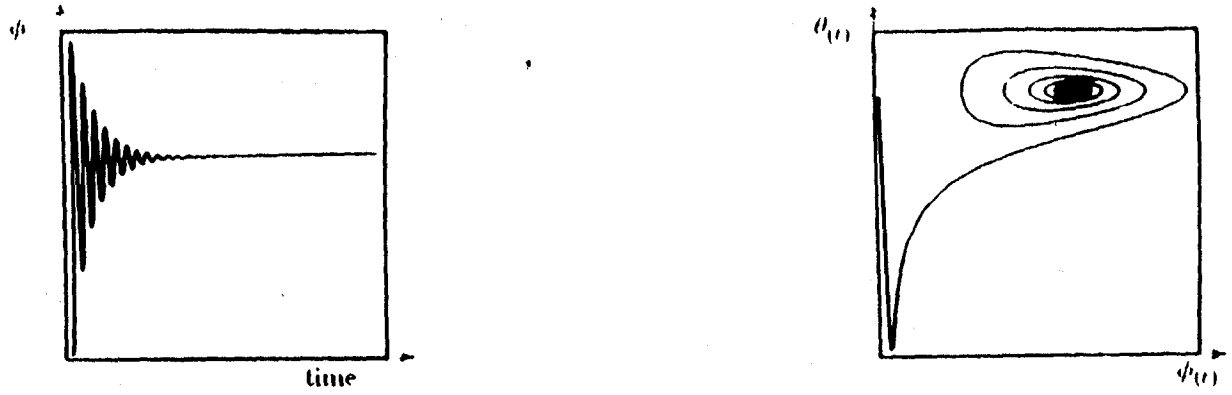

a) time-series

b) phase space

Note:

a) ϕ denotes vertical gradient of the hydraulic potential (dh/dz), θ denotes lateral gradient of the *in situ* temperature (dT/dx);

b) system has a stable-point attractor;

c) if perturbed, the system returns to initial mode of behavior; and

d) θ has a multitude of other expressions.

Typical behavior of a dynamic system, prior to the soft loss of stability. Modified from Gleick, 1988

Figure 7.

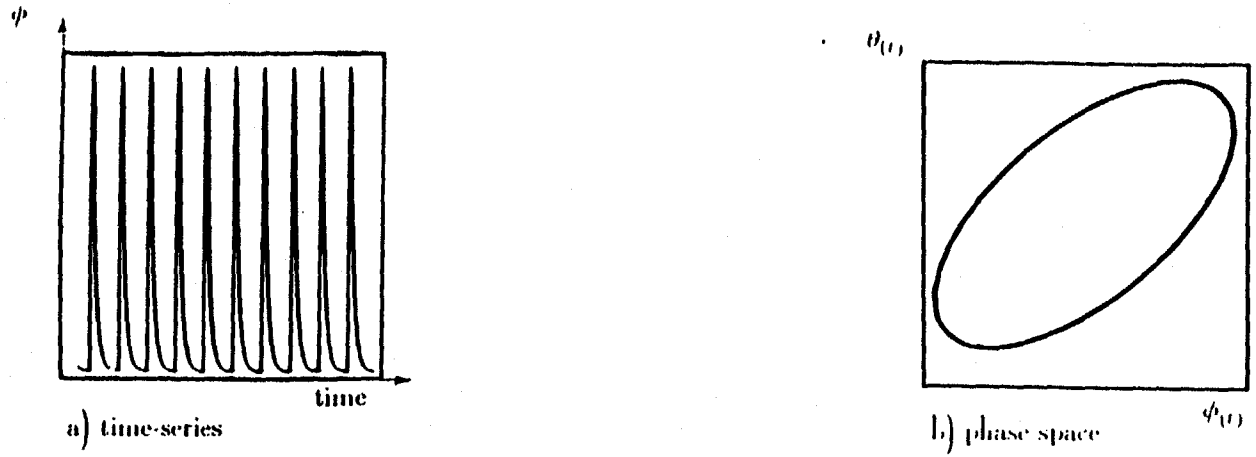

Note:

a) ϕ denotes vertical gradient of the hydraulic potential (dh/dz), θ denotes lateral gradient of the *in-situ* temperature (dT/dx);

b) system has a limit cycle as attractor, or so-called stable periodic attractor;

c) if perturbed, the system may change mode of behavior; and

d) ϕ has a multitude of other expressions.

Typical behavior of a dynamic system, immediately after the soft loss of stability. Modified from Gleick, 1988

Figure 8.

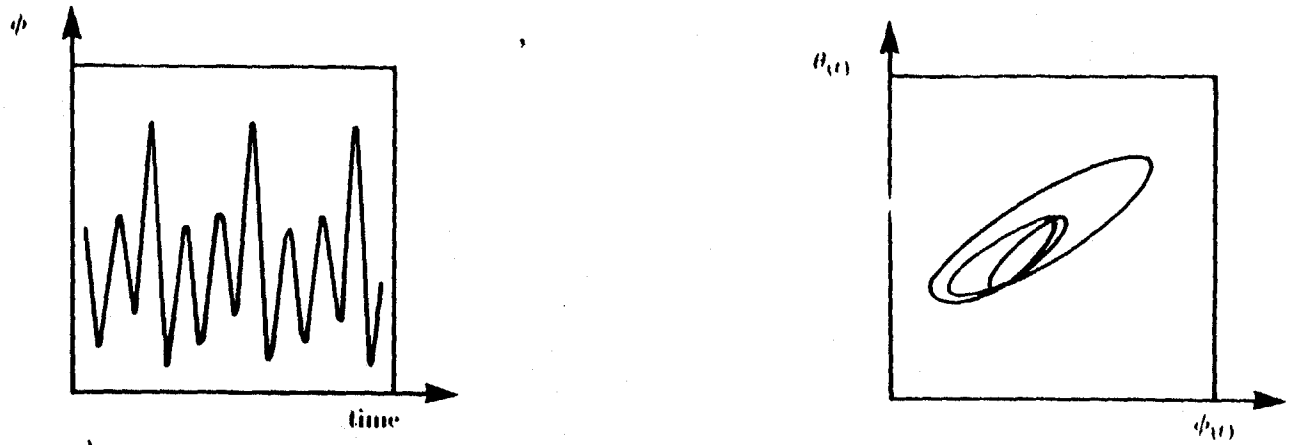

a) time-series

b) phase-space

Note:

a) ϕ denotes vertical gradient of the hydraulic potential (dh/dz), θ denotes gradient of the *in-situ* temperature (dT/dx);

b) system has a torus attractor;

c) if perturbed, the system will change mode of behavior; and

d) ϕ has a multitude of other expressions.

Typical behavior of a dynamic system, which is subject to the period doubling,bifurcations and frequency locking. Modified from Gleick, 1988.

Figure 9

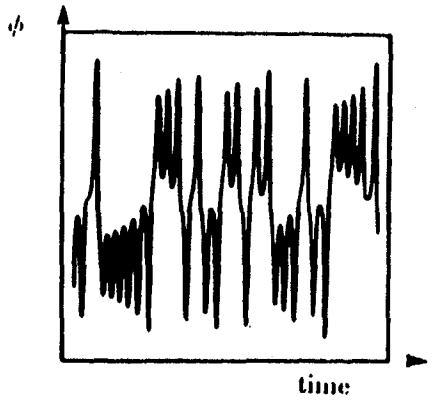

a) time-series

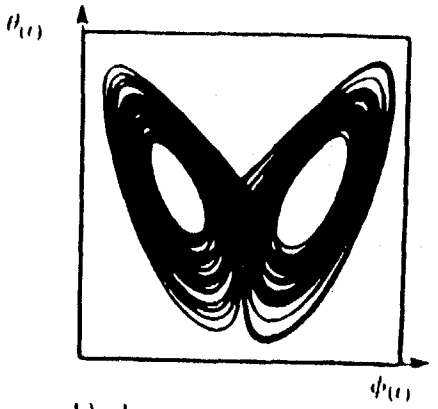

b) phase-space

Note:

a) ϕ denotes vertical gradient of the hydraulic potential (dh/dz), θ denotes gradient of the *in-situ* temperature (dT/dx);

b) system has "strange attractors";

c) system possesses an infinite sensitivity to perturbations; and

d) ϕ has a multitude of other expressions.

Typical behavior of a dynamic system - pass the "non-equilibrium turbulent chaos threshold". Modified from Gleick, 1988.

Figure 10

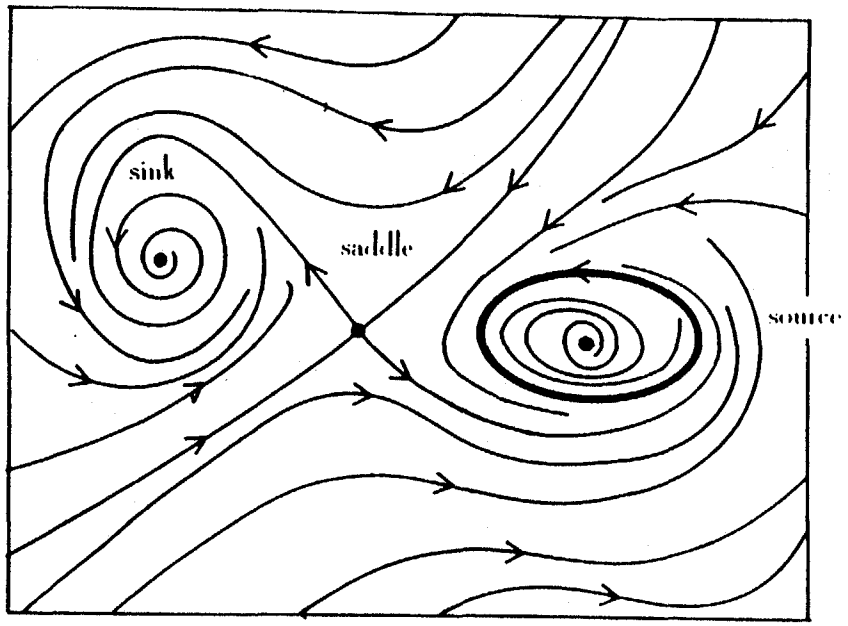

Note:

a) system is "structurally stable" if it's space phase representation includes sources, sinks, and saddles and whose attractors are: i) single points; and ii) stable limit cycles - Poincare - Bendixon theorem;

b) system may be "structurally unstable" if, in addition to the above features, exhibits quasi periodic fluctuations - possesses a torus attractor. Smale's conjecture.

Phase-space portrait of a self-organized dynamic system. From Stewart, 1989.

Figure 11

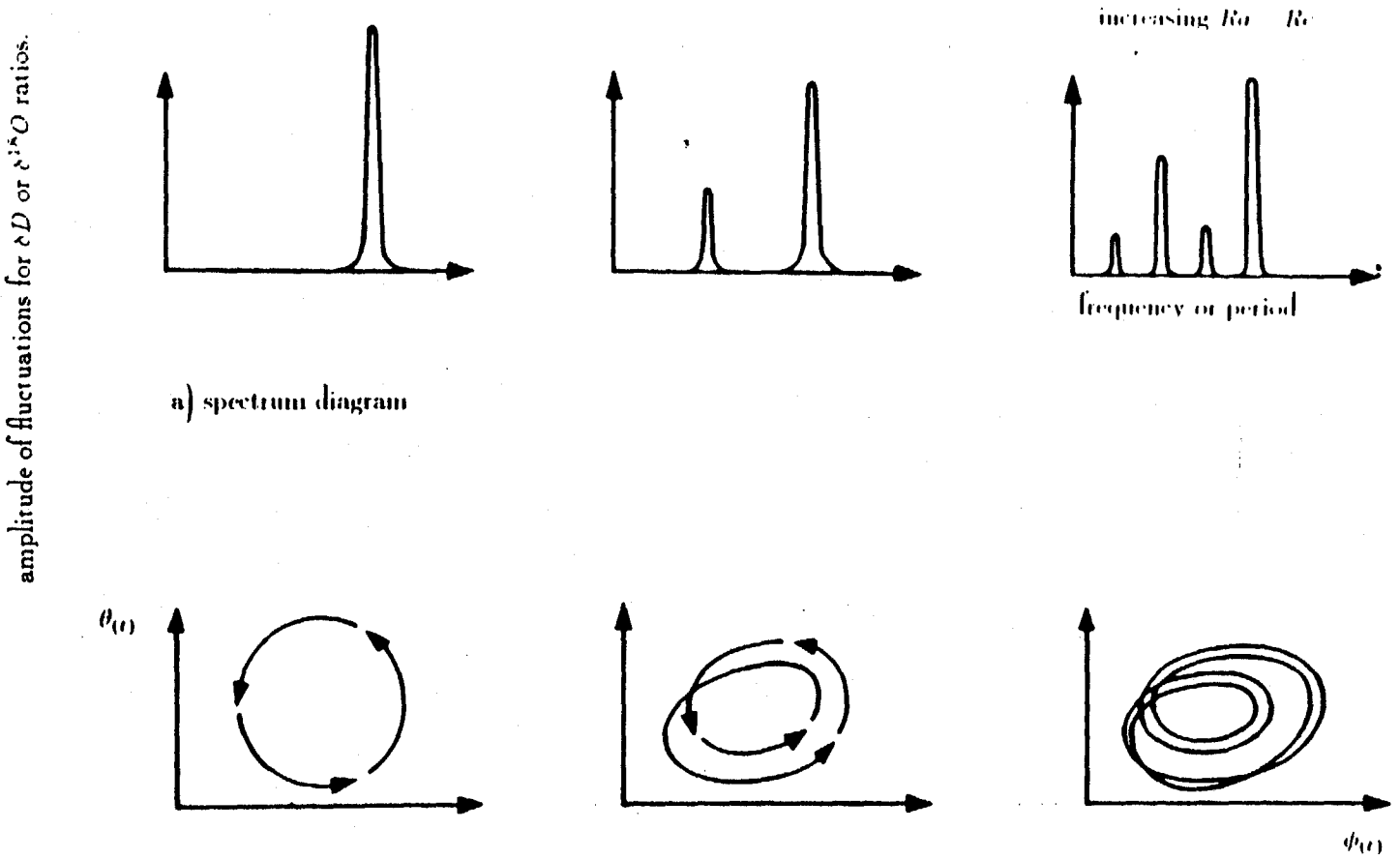

Note:

a) θ denotes vertical gradient of the hydraulic potential (dh/dz), ϕ denotes lateral gradient of the *in-situ* temperature (dT/dx);

b) δD or $\delta^{18}O$ f(θ); and

c) a non-Hamiltonian system exhibiting more than one frequency is subject to "frequency - locking" - two or more independent periodic motions interact, become entrained, and ultimately yield a combined periodic motion, see Ruelle and Takens, 1970.

Spectrum and phase-space diagrams illustrating periodic and quasi-periodic fluctuations of the hydrogen-oxygen isotopic signals. Fluids residing in the Benard - Rayleigh instability, for which level of disequilibrium ($Ra - Rc$) increases with time. Modified from Gleick, 1988.

Figure 12

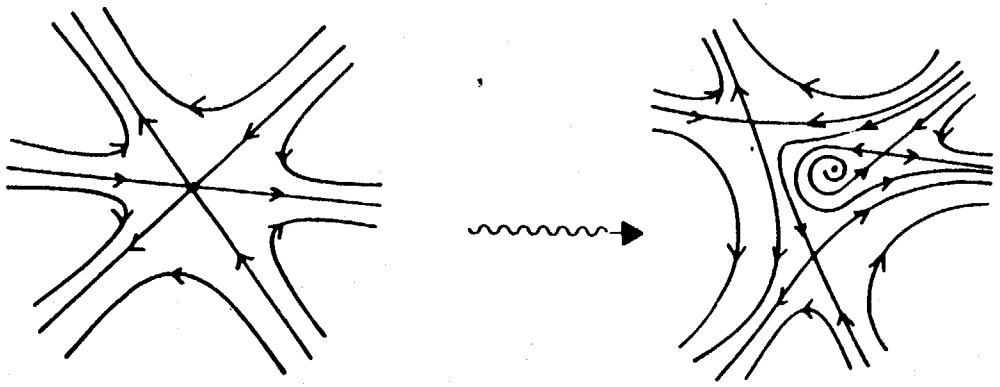

a) the Andronov - Pontryagin tranformation - under small perturbations, a saddle with three separatrices breaks down forming three separate saddles and a sink.

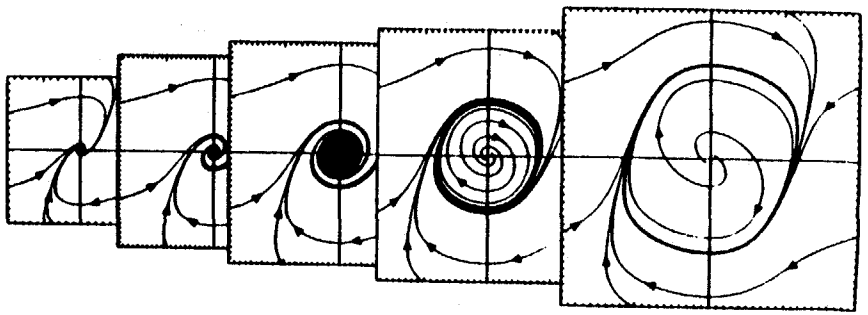

b) the Hopf - Landau transformation - under small perturbations, a sink loses stability and becomes a source (strictly speaking, the Hopf transformation pertains to Hamiltonian systems only).

Examples of "structural instability" - phase-space representations. From Stewart, 1989.

Figure 13

A dynamic system, for which level of disequilibrium undergoes spatio-temporal changes, may be expected to exhibit three general behavioral characteristics:

i) **self-organization**, i.e., development of macroscopic dissipative structures - for the Nevada Test Site flow system, such structures are: a) the Bernard - Rayleigh convection cells; and b) the *in-situ* stress field inclusions.

ii) **fluctuations**, i.e., periodic or quasi periodic changes of parameters that express system's behavior, e.g. fluid and heat fluxes and gradients thereof; fluid isotopic and chemical composition and gradients thereof.

iii) **in response to small perturbations, "structural instability"**, i.e., "sink ↔ source" and "saddle ↔ (sink) source" **transformations.**

Note:

a) **a dynamic system, exhibiting the above characteristics, though deterministic is unpredictable because prediction requires paradoxical precision in specifying the intial conditions; and**

b) **an approach to understanding such a system, amounting to breaking it down into small elements, is futile.**

The diagnostic characteristics of a non-equilibrium dynamic system.

Figure 11.

Isotopic and chemical evidence for:

i) self-organization;

ii) periodic and quasi-periodic fluctuations; and

iii) "source" - "sink" transformations.

Part B - The Nevada Test Site hydrosphere as a non-equilibrium dynamic system.

Figure 15.

Isotopic and chemical evidence for self-organization.

Step I - Delineation of the self organization produced macroscopic order, i.e., "sink" - "source" subdivision of the Nevada Test Site hydrosphere based on spatial distribution of: i) $dh/d\ell$: vertical hydraulic gradient; ii) $dT/d\ell$: geothermal gradient; and iii) fluid chemistry.

Step II - Isotopic expression of the delineated macroscopic order: i) uranium content and values of the $^{234}U/^{238}U$ ratio; ii) values of the $^{87}Sr/^{86}Sr$ ratio; iii) values of the $\delta^{13}C_{(PDB)}$ and $\delta^{13}C$ ratios; and iv) values of the δD and $\delta^{18}O$ ratios.

Self-organization. The Nevada Test Site hydrosphere.

Figure 16.

- Based on geothermal, hydraulic, and chemical characteristics the Nevada Test Site hydrosphere may be subdivided into two contrasting configurations:

  i) the hydraulic "source" regions - dh/dl: positive, dT/dl: high, $CL^- + SO_4^{--}$ content high; and

  ii) the hydraulic "sink" regions - dh/dl: negative or zero, dT/dl: low, $CL^- + SO_4^{--}$ content low.

Inference: The Nevada Test Site hydrosphere is a self-organized dynamic system, and consists of a number of the Benard Rayleigh dissipative structures.

Self-organization. The Nevada Test Site hydrosphere - chemical, geothermal, and hydraulic data.

Figure 17.

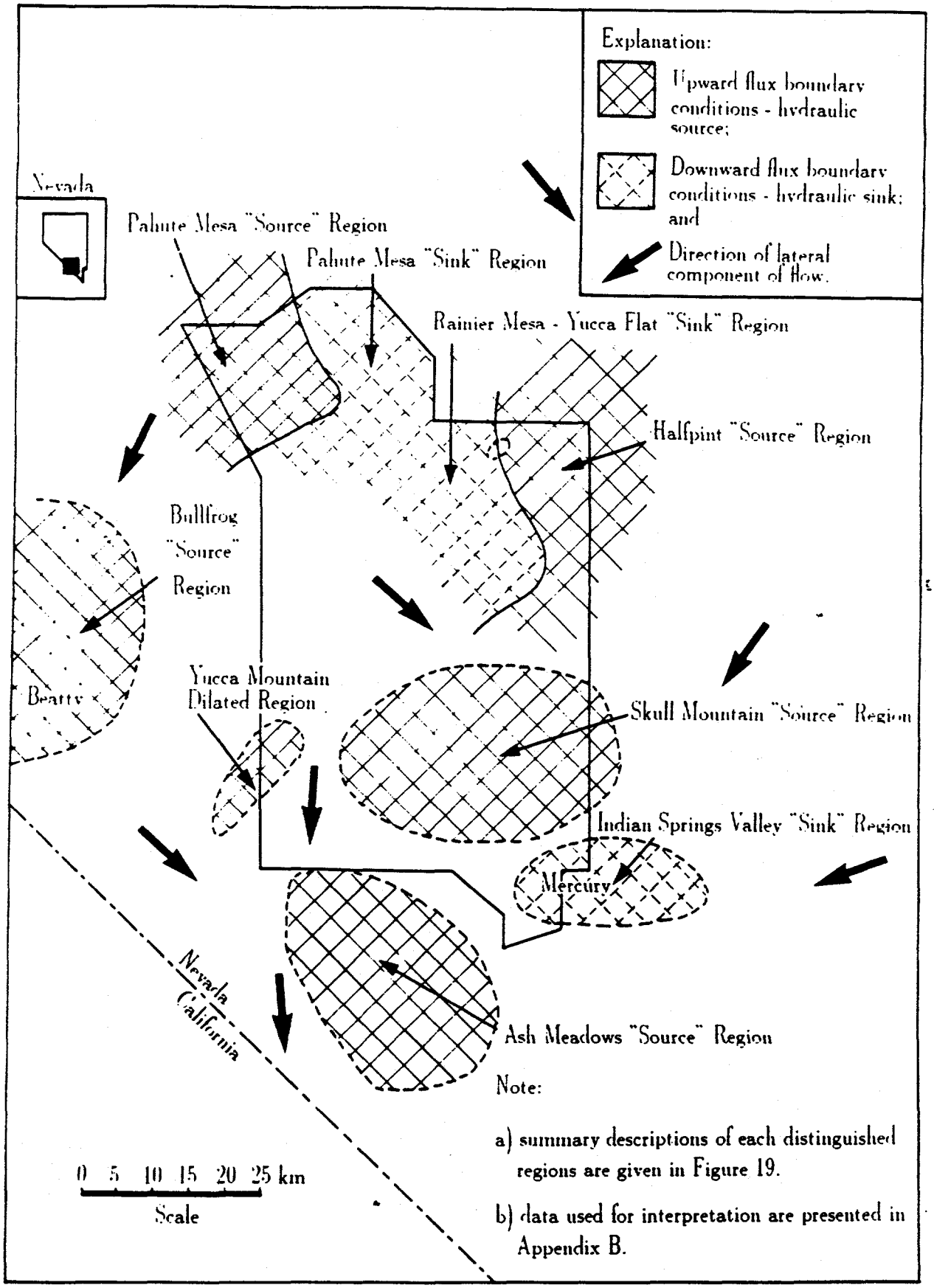

Inferred boundary conditions. The Nevada Test Site hydrosphere.

Figure 18

Paiute Mesa Hydraulic "Source" Region

Vertical hydraulic gradient dh/dz: upward (maximum known value is Δh 174 ft.).

Vertical geothermal gradient dT/dz: ranging from 30 to about 60°C/km.

Lateral geothermal gradient dT/dx 5°C/1 mile.

Possible upper thermal boundary layers.

Water chemistry: $Ca^{++} + Mg^{++}$ from 1 to 40 ppm

$Na^{+} + K^{+}$ from 40 to 250 ppm

$CL^{-} + SO_4^{--}$ from 35 to 250 ppm

HCO_3 from 90 to 270 ppm.

Paiute Mesa Hydraulic "Sink" Region

Vertical hydraulic gradient dh/dz - downward (maximum known value is Δh 41 ft.).

Vertical geothermal gradient dT/dz - 30°C/km.

Water chemistry: $Ca^{++} + Mg^{++}$ from 4 to 60 ppm

$Na^{+} + K^{+}$ from 35 to 95 ppm

$CL^{-} + SO_4^{--}$ from 15 to 70 ppm

HCO_3 from 60 to 450 ppm.

Boundary conditions. Interpretation bases. The Nevada Test Site hydrosphere.

Figure 19a.

Rainier Mesa - Yucca Flat Hydraulic "Sink" Region.

Vertical hydraulic gradient dh/dz: downward (maximum known value is Δh 1560 ft.)

Vertical geothermal gradient dT/dz: 20-25°C.

Water chemistry: $Ca^{++} + Mg^{++}$ from 2 to 40 ppm
$Na^{+} + K^{+}$ from 22 to 65 ppm
$CL^{-} + SO_4^{=}$ from 11 to 40 ppm
HCO_3^{-} from 50 to 230 ppm.

Note: $\sigma_C \doteq \frac{1}{3}\sigma_{oct}$ indicating that dilation is either very shallow or non existant.

Halfpint Hydraulic "Source" Region.

Vertical hydraulic gradient dh/dz - unknown.

Vertical geothermal gradient $dT/dz \sim 45°C/km$.

Water chemistry: $Ca^{++} + Mg^{++}$ from 55 to 400 ppm
$Na^{+} + K^{+}$ from 50 to 270 ppm
$CL^{-} + SO_4^{=}$ from 85 to 1100 ppm
HCO_3^{-} from 65 to 400 ppm.

Note: a) local water table is bent upward, maximum altitude is 4535 ft. amsl. (148 ft. above water table in upstream regions); and
b) lateral hydraulic gradient 1300 ft/mile and 820 ft/mile.

Boundary conditions. Interpretation bases. The Nevada Test Site hydrosphere.

Figure 19b.

Skull Mountain Hydraulic "Source" Region.

Vertical hydraulic gradient dh/dz - uncertain (upward gradient is suggested by hydraulic head observations made during drilling of Well 73 68).

Vertical geothermal gradient dT/dz: 45 50°C/km.

Water chemistry: $Ca^{++} + Mg^{++}$ from 4 to 470 ppm
$Na^{+} + K^{+}$ from 47 to 450 ppm
$CL^{-} + SO_4^{=}$ from 35 to 500 ppm
HCO_3^{-} from 100 to 1009 ppm.

Note: a) water table is bent upward, maximum altitude is 2982 ft. amsl. (about 600 ft. above water table in upstream regions);
b) samples of perched water display chemical affinity with water from below the water table, and
c) possible upper thermal boundary layer present in two boreholes.

Indian Springs Valley Hydraulic "Sink" Region.

Vertical hydraulic gradient dh/dz - unknown.

Vertical geothermal gradient dT/dz - 20°C/km.

Water chemistry: $Ca^{++} + Mg^{++}$ from 16 to 75 ppm
$Na^{+} + K^{+}$ from 6 to 40 ppm
$CL^{-} + SO_4^{=}$ from 8 to 70 ppm
HCO_3^{-} from 180 to 300 ppm.

Note: a) local water table is bent downward, minimum altitude is 2281 ft. amsl. (80 feet lower than water table downstream).

Boundary conditions. Interpretation bases. The Nevada Test Site hydrosphere.

Figure 19c

Ash Meadows Hydraulic "Source" Region.

Vertical hydraulic gradient dh/dz: upward (maximum value of Δh unknown).

Vertical geothermal gradient dT/dz: 40°C/km.

Water chemistry: $Ca^{++} + Mg^{++}$ from 12 to 270 ppm
$Na^{+} + K^{+}$ from 20 to 300 ppm
$Cl^{-} + SO_4^{--}$ from 45 to 1300 ppm
HCO_3^{-} from 120 to 380 ppm.

Note: a) water table appears to be bent upward; downstream water t^{++} altitude 2200 ft. amsl., maximum altitude 2365 ft., upstream at altitude 2281 ft; and
b) fault-line spring discharge, temperature ranging from 23 to 34.5°C.

Bullfrog Hydraulic "Source" Region.

Vertical hydraulic gradient dh/dz - upward (maximum value of Δh - unknown).

Vertical geothermal gradient dT/dz - unknown.

Water chemistry: $Ca^{++} + Mg^{++}$ from 8 to 50 ppm
$Na^{+} + K^{+}$ from 100 to 350 ppm
$Cl^{-} + SO_4^{--}$ from 90 to 350 ppm
HCO_3^{-} from 150 to 480 ppm.

Note: a) perched waters - discharge temperature 21-26.5°C and chemical affinity with deeper fluids suggest that these waters represent mixtures of deep fluids with infiltrating meteoric fluids; and
b) water table may be bent upward; downstream ± 2500 ft., maximum ± 4000 ft., upstream - 3800 ft.

Boundary conditions. Interpretation bases. The Nevada Test Site hydrosphere.

Figure 194

Yucca Mountain "Dilated" Region.

Vertical hydraulic gradient dh/dz: upward in deeper undilated regions; neutral immediately below the water table.

Vertical geothermal gradient dT/dz: 40 60 C/km in deeper undilated regions; dT/dz: 20 30 C/km immediately below the water table.

Water chemistry: dilated zone $Ca^{++} + Mg^{++}$ from 2 to 20 ppm
$Na^{+} + K^{+}$ from 40 to 120 ppm
$CL^{-} + SO_4^{--}$ from 21 to 55 ppm
HCO_3^{-} from 100 to 300 ppm.

undilated zone $Ca^{++} + Mg^{++}$ 140 ppm
$Na^{+} + K^{+}$ 162 ppm
$CL^{-} + SO_4^{--}$ 188 ppm
HCO_3^{-} from 569 ppm.

Note: a) local values of σ_c O, (indicating severe dilation) extend to a maximum depth of about 1300 m; and

b) the Yucca Mountain area is a source - sink hybrid.

The geothermal, hydraulic, and geochemical data used is subdividing ... Nevada Test Site hydrosphere, are from Walker (1962); Blankennagel and Weir (1973); Claassen (1973); Winograd and Thordenson (1975); White (1972); White et al. (1980); Garside and Schilling (1979); Sass and Lachenbruch (1982); Isherwood et al. (1982); Claassen (1985); and Benson and McKinley (1985).

Boundary conditions. Interpretation bases. The Nevada Test Site hydrosphere.

Figure 19c.

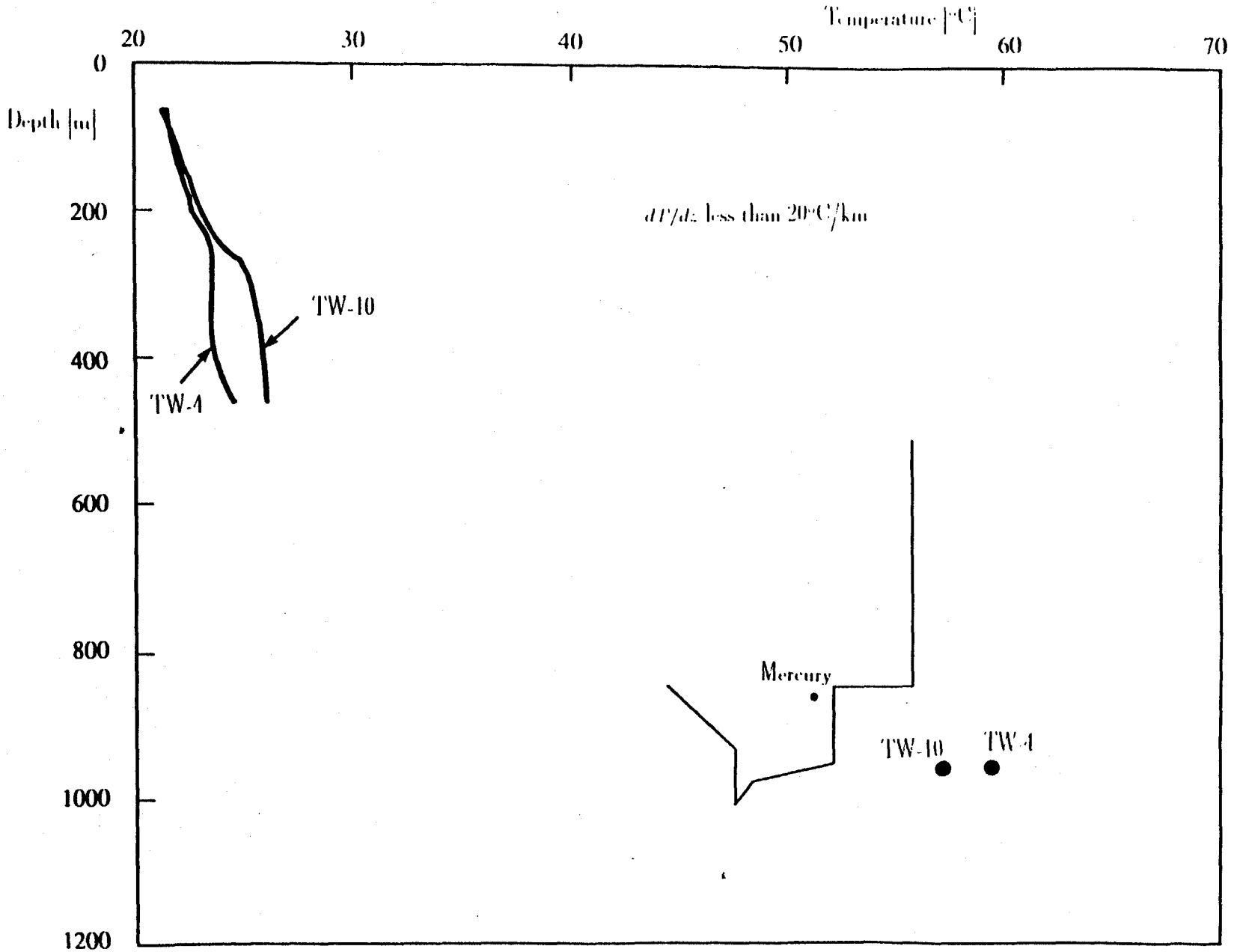

Downhole temperature profiles, Southern Indian Springs Valley From Sass and Lachenbruch, 1982.

Figure 20a.

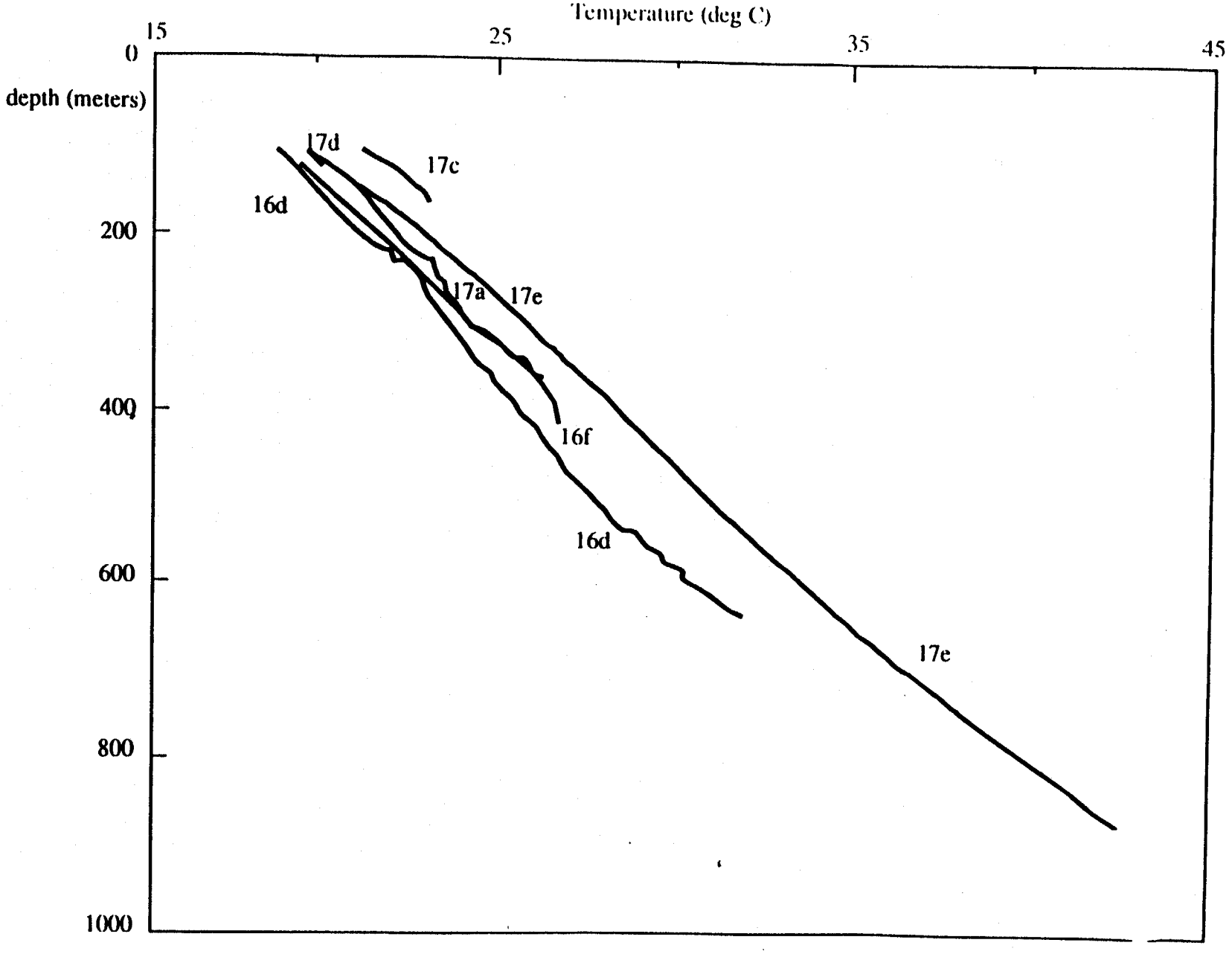

Downhole temperature profiles. Rainier Mesa - Yucca Flat hydraulic "sink" region. From Sass and Lachenbruch, 1982.

Figure 20b

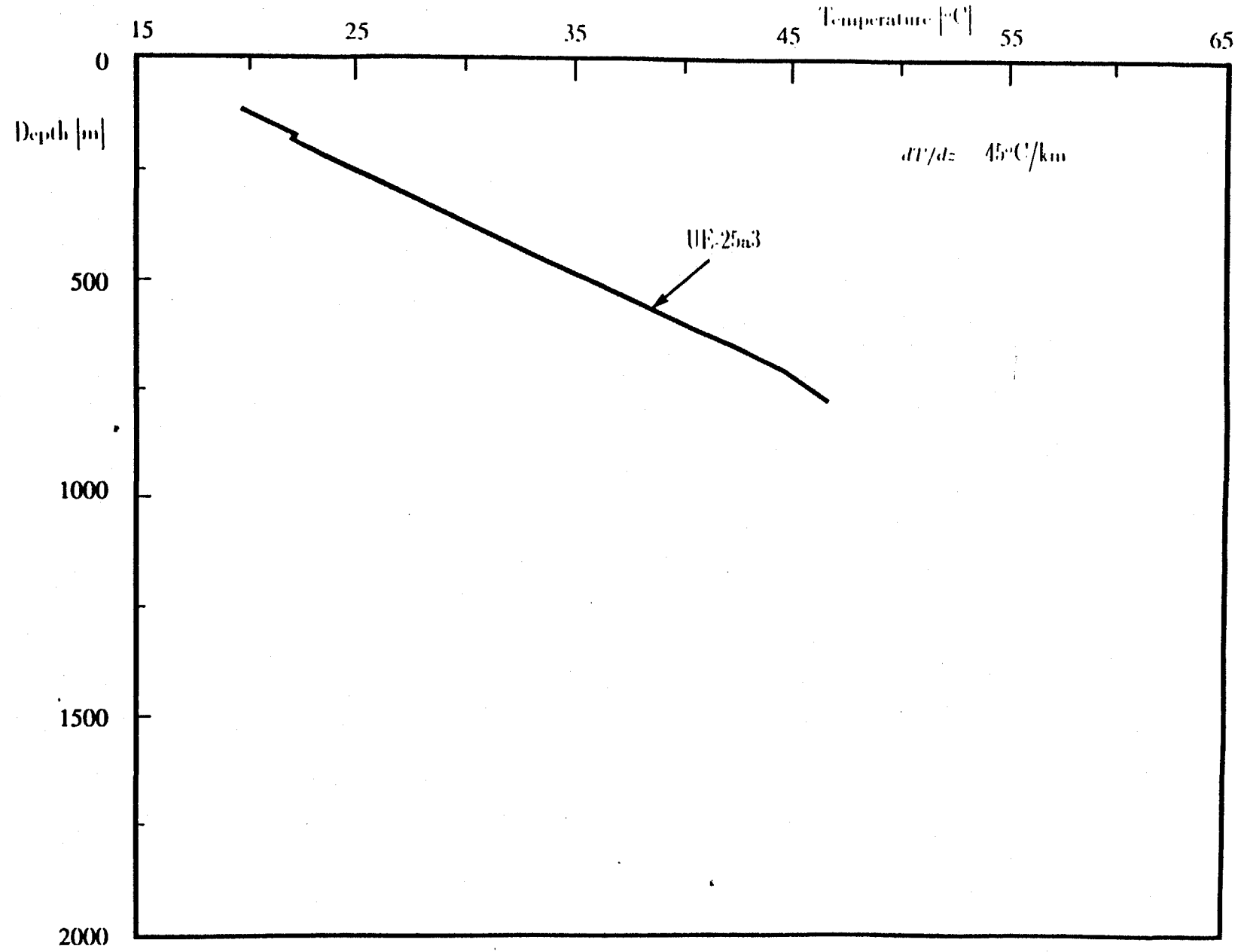

Downhole temperature profiles. Borehole UE-25a3. North-western margin of the Skull Mountain hydraulic "source". From Sass and Lachenbruch, 1982

Figure 20c.

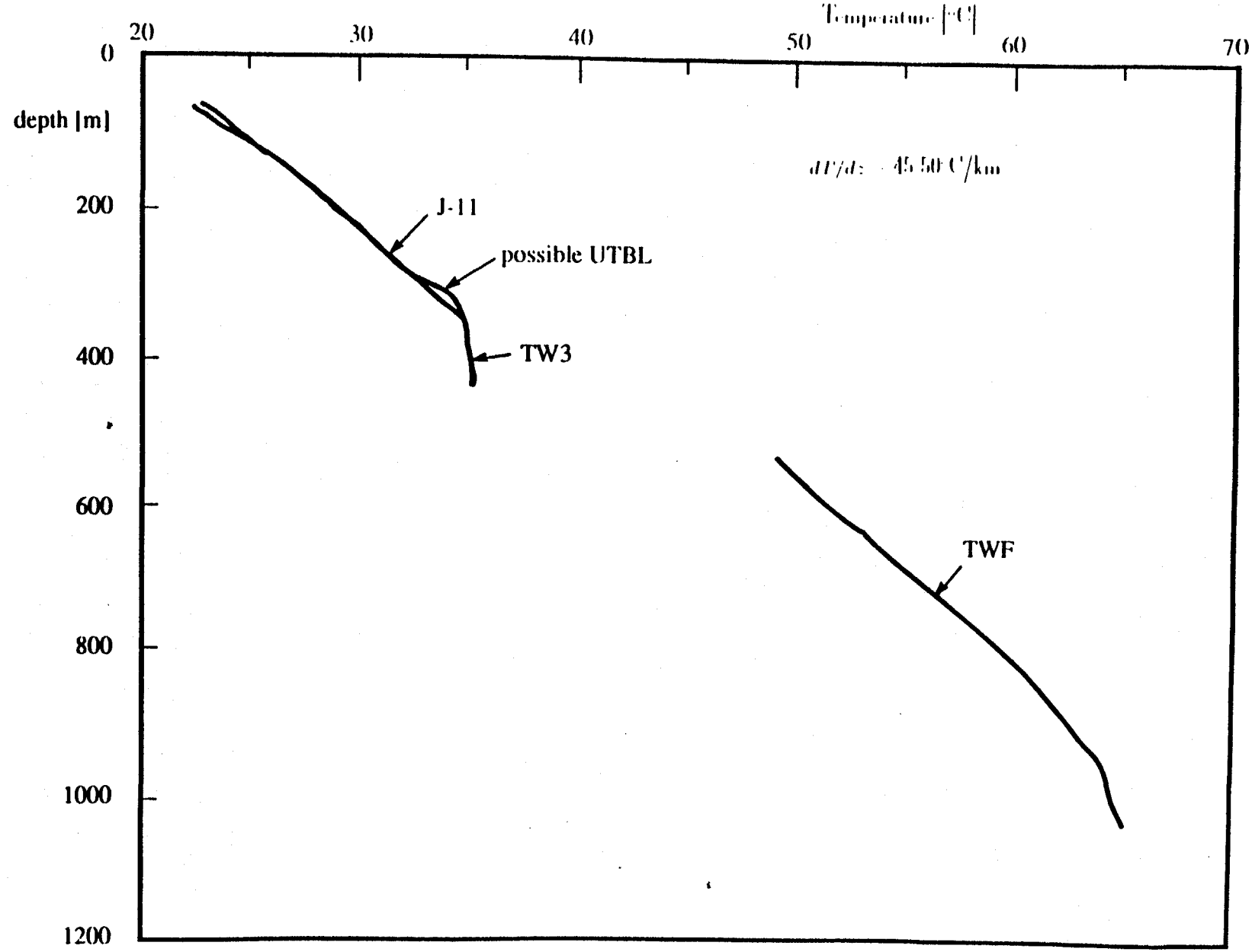

Downhole temperature profiles, Boreholes J-11, TWF, and TW3. Skull Mountain hydraulic "source" region. From Sass and Lachenbruch, 1982.

Figure 20d.

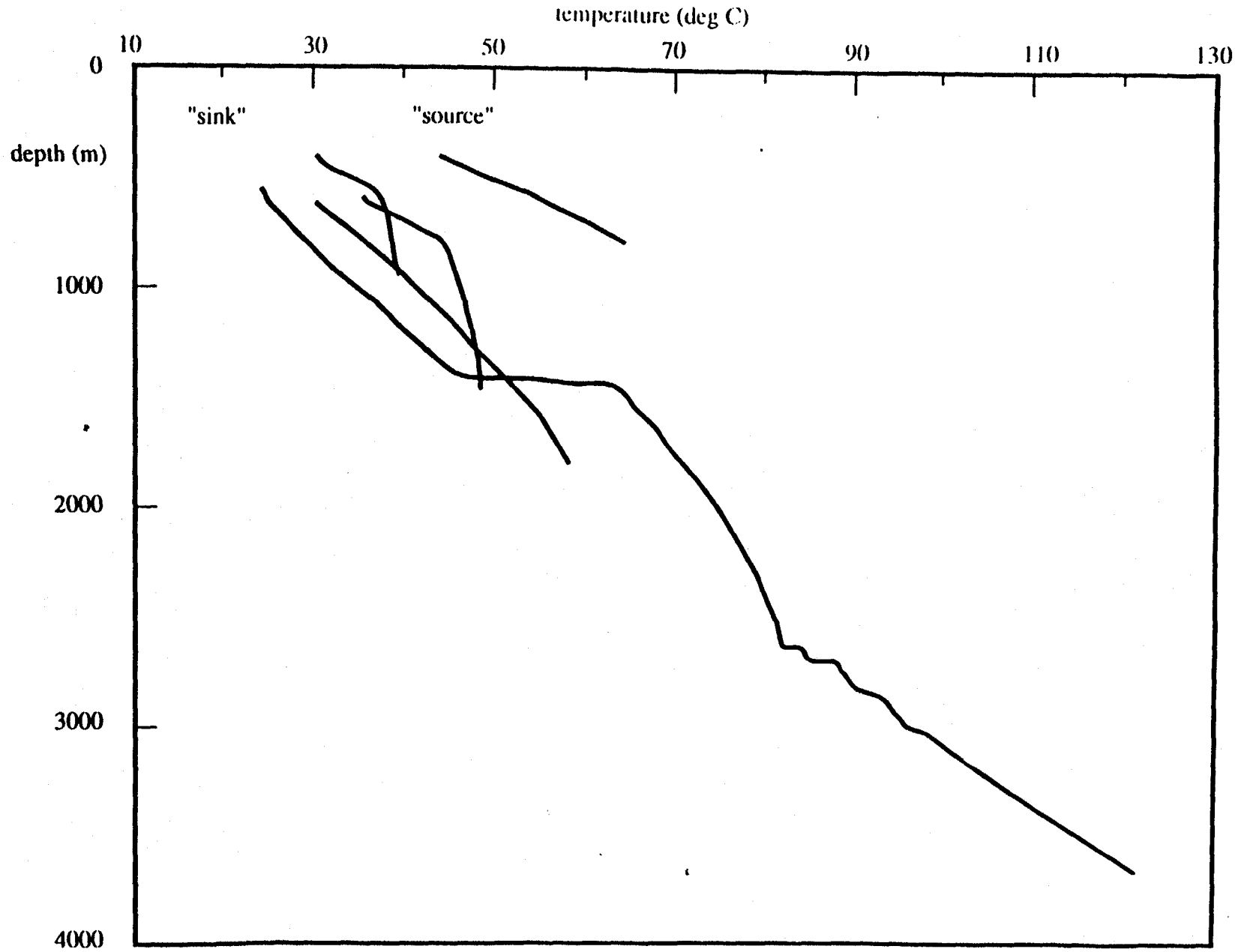

Composite temperature profile, Pahute Mesa hydraulic "sink and "source" regions. Modified From Sass and Lachenbruch, 1982.

Figure 20c

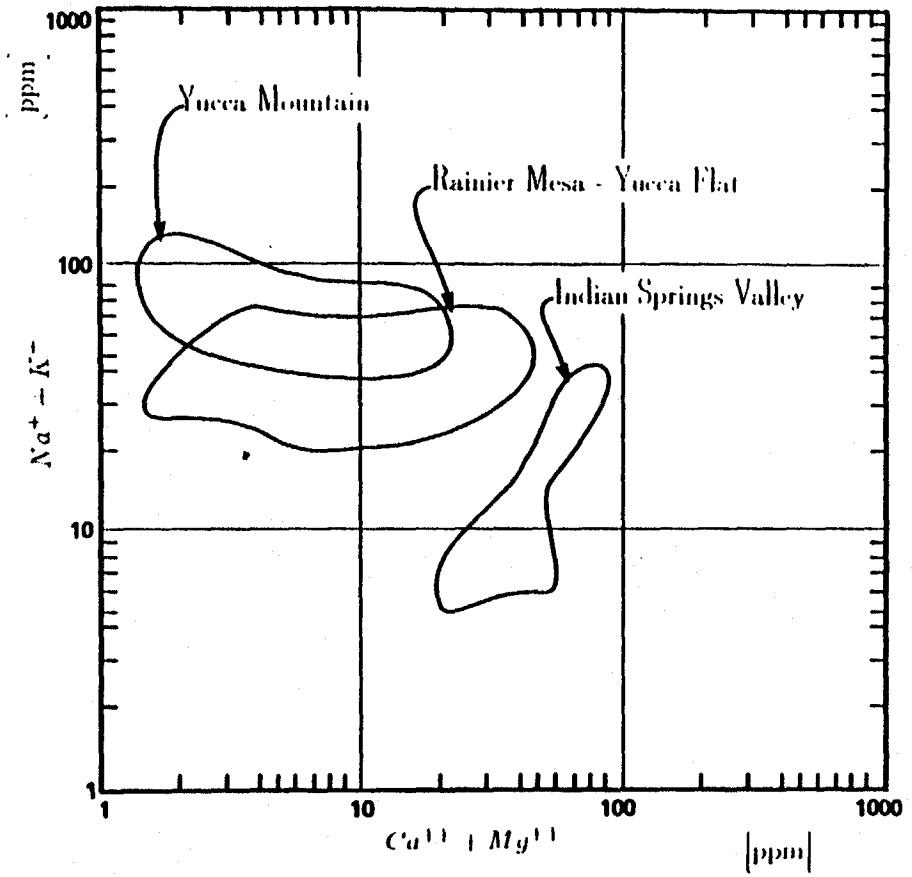

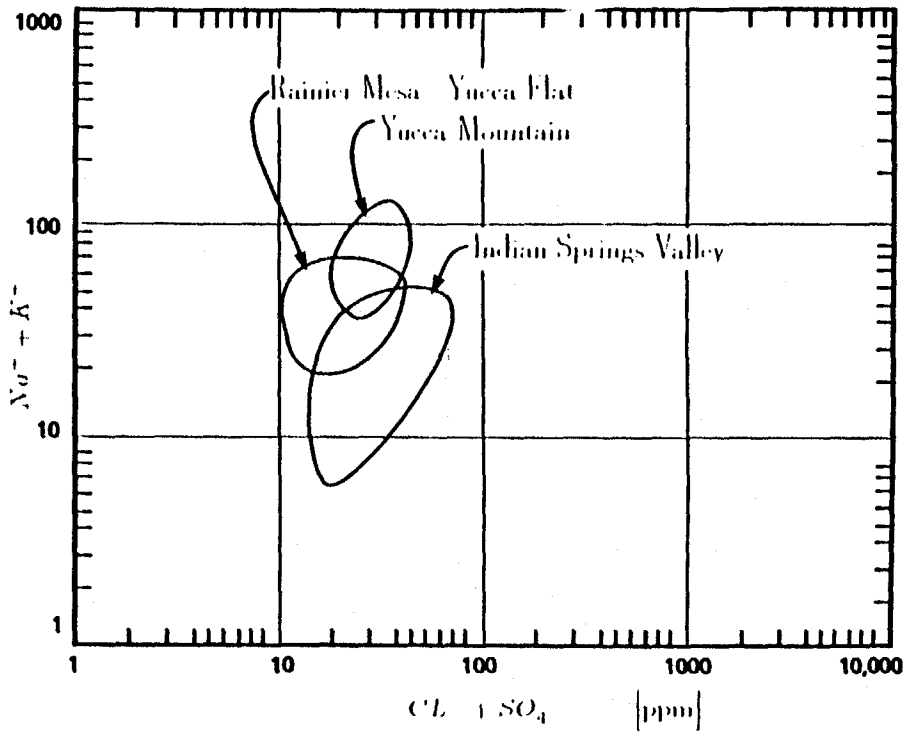

Groundwater chemistry. Hydraulic "sink" and dilated regions, The Nevada Test Site hydrosphere.

Figure 21a.

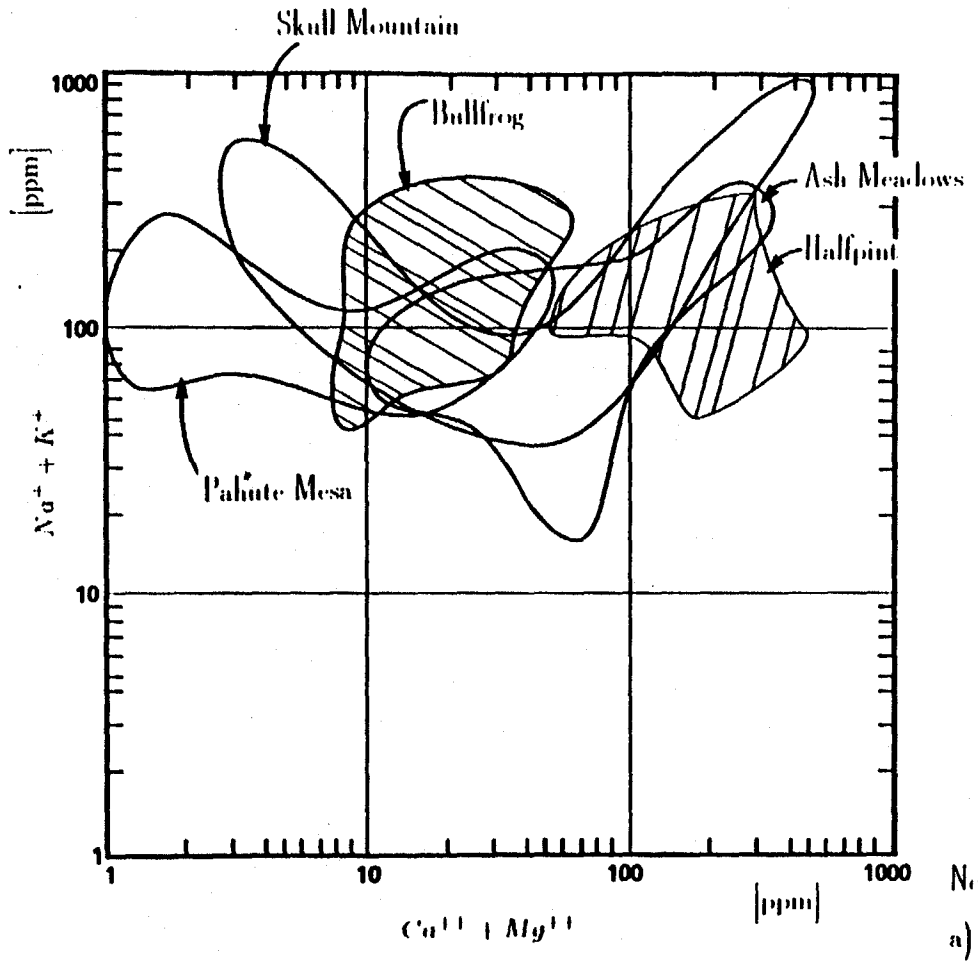

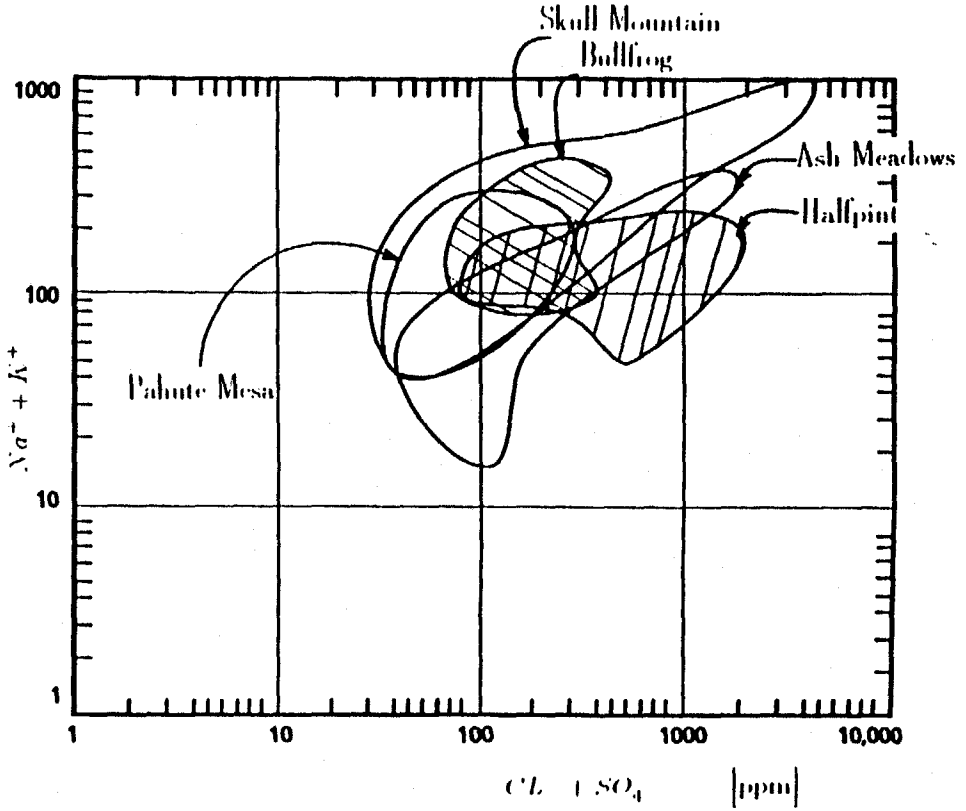

Note:

a) fluids result from intermixing of at least two end members;

b) one end member is represented by poorly evolved meteoric recharge; and

c) the other member is represented by deep and chemically evolved fluids.

Groundwater chemistry. Hydraulic "source" regions. The Nevada Test Site hydrosphere.

Figure 21b.

If the Nevada Test Site hydrosphere is a self organized system indeed then, it may be expected that the hydraulic "source" regions contain fluids which in terms of various isotopic signatures, are distinct from the hydraulic "sink" fluids.

Specifically, relative to the hydraulic "sink" fluids, fluids residing in the contemporary hydraulic "source" regions should exhibit:

a) higher concentrations of the dissolved uranium and lower values of the $^{234}U/^{238}U$ activity ratio;

b) higher values of the $^{87}Sr/^{86}Sr$ ratio;

c) higher values of the $\delta^{13}C$ ratio and lower carbon - 14 concentrations;

d) higher magnitudes of the "oxygen isotopic shift"; and

e) negative values of the "hydrogen isotopic shift".

Note:

a) each of the above expectations has a rational base;

b) the derivation of these expectations is a lengthy process and will not be presented here; and

c) other isotopic expressions are conceivable.

Expected relative isotopic expressions of the contemporary hydraulic "source" regions. The Nevada Test Site hydrosphere.

Figure 22

- At the Nevada Test Site, the U content vs. $^{234}U/^{238}U$ field from samples of the hydraulic "source" fluids is distinct from the corresponding field from samples of the hydraulic "sink" fluids.

Conclusion: The Nevada Test Site hydrosphere is a self-organized dynamic system and consists of a number of the Benard-Rayleigh dissipative structures.

Self-organization. The Nevada Test Site hydrosphere - dissolved uranium data.

Figure 23.

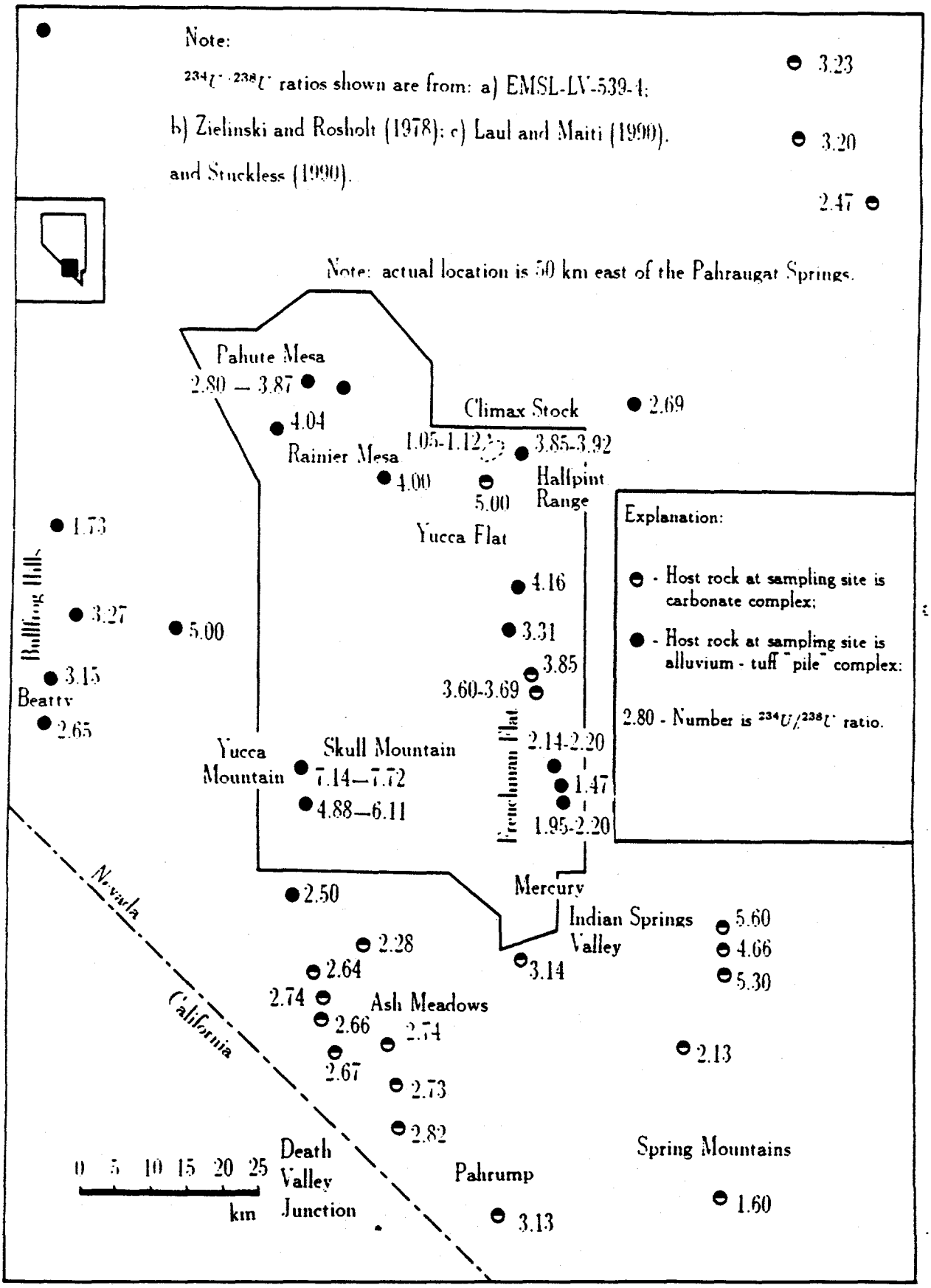

$^{234}U/^{238}U$ ratio. The Nevada Test Site hydrosphere.

Figure 24.

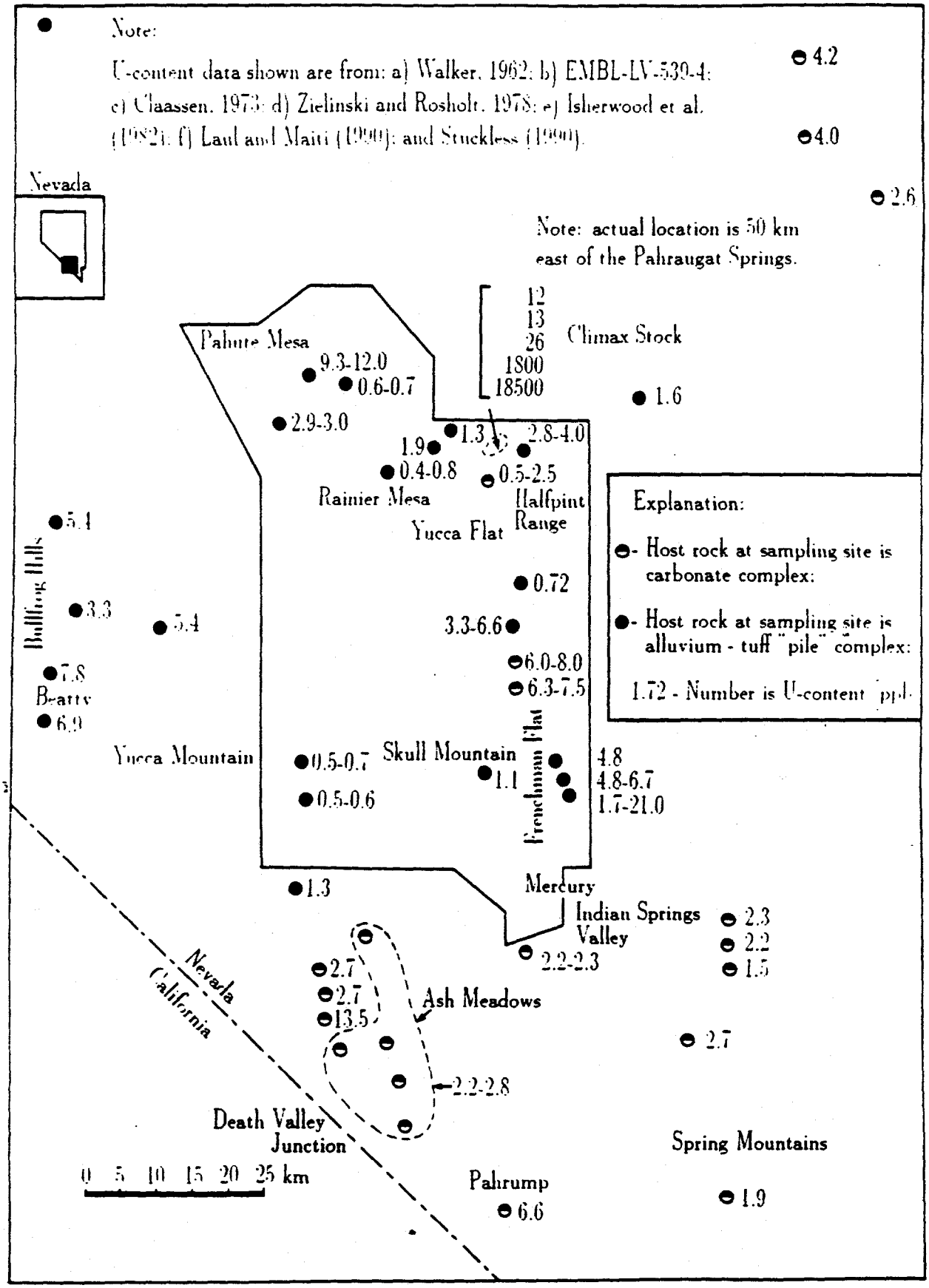

U-content. The Nevada Test Site hydrosphere.

Figure 25.

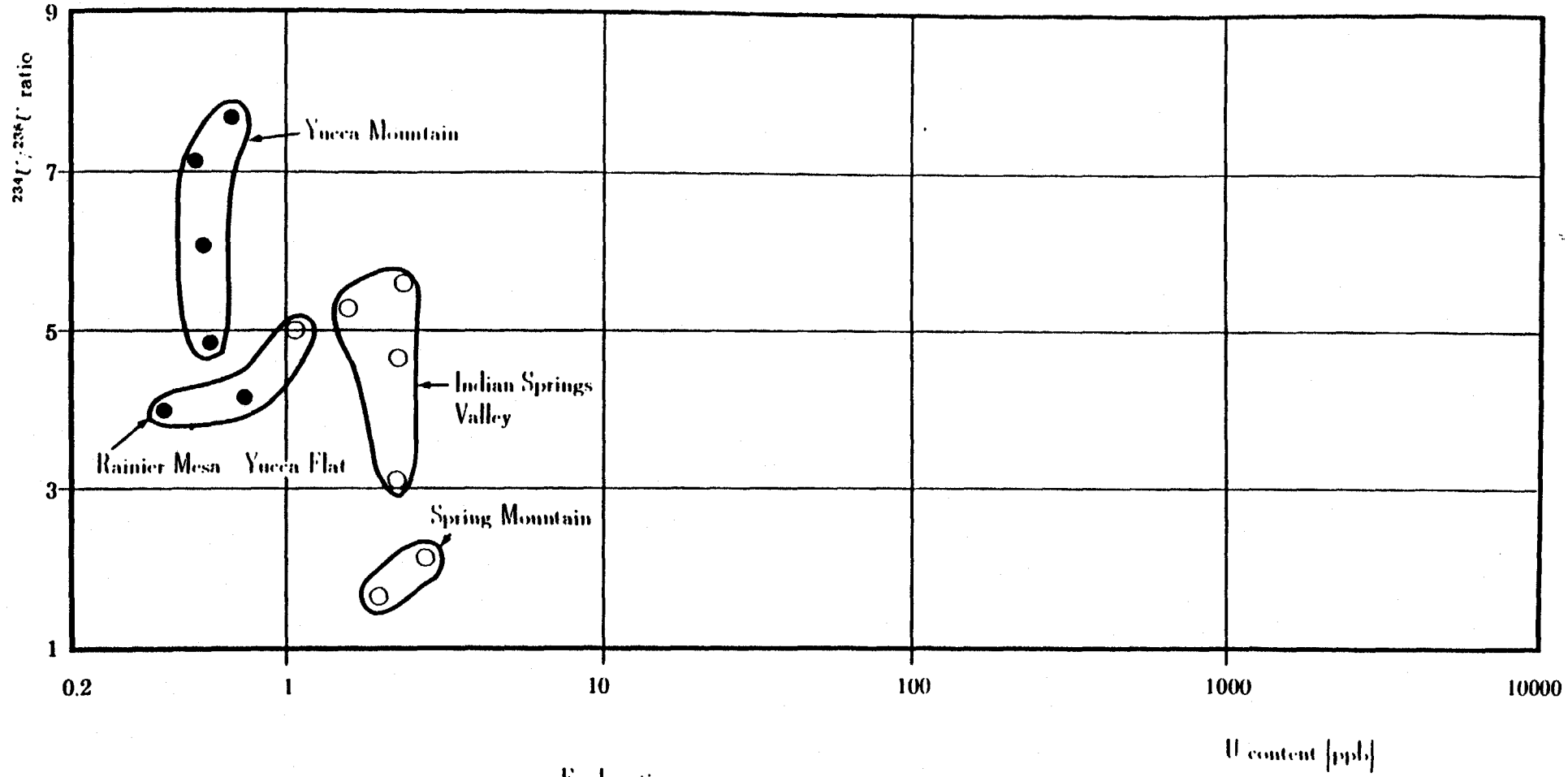

Explanation:

● - sample represents fluids from the tuff pile;

○ - sample represents fluids from the Paleozoic carbonates.

$^{234}U/^{238}U$ vs. U-content. Hydraulic sink and dilated regions. The Nevada Test Site hydrosphere.

Figure 26

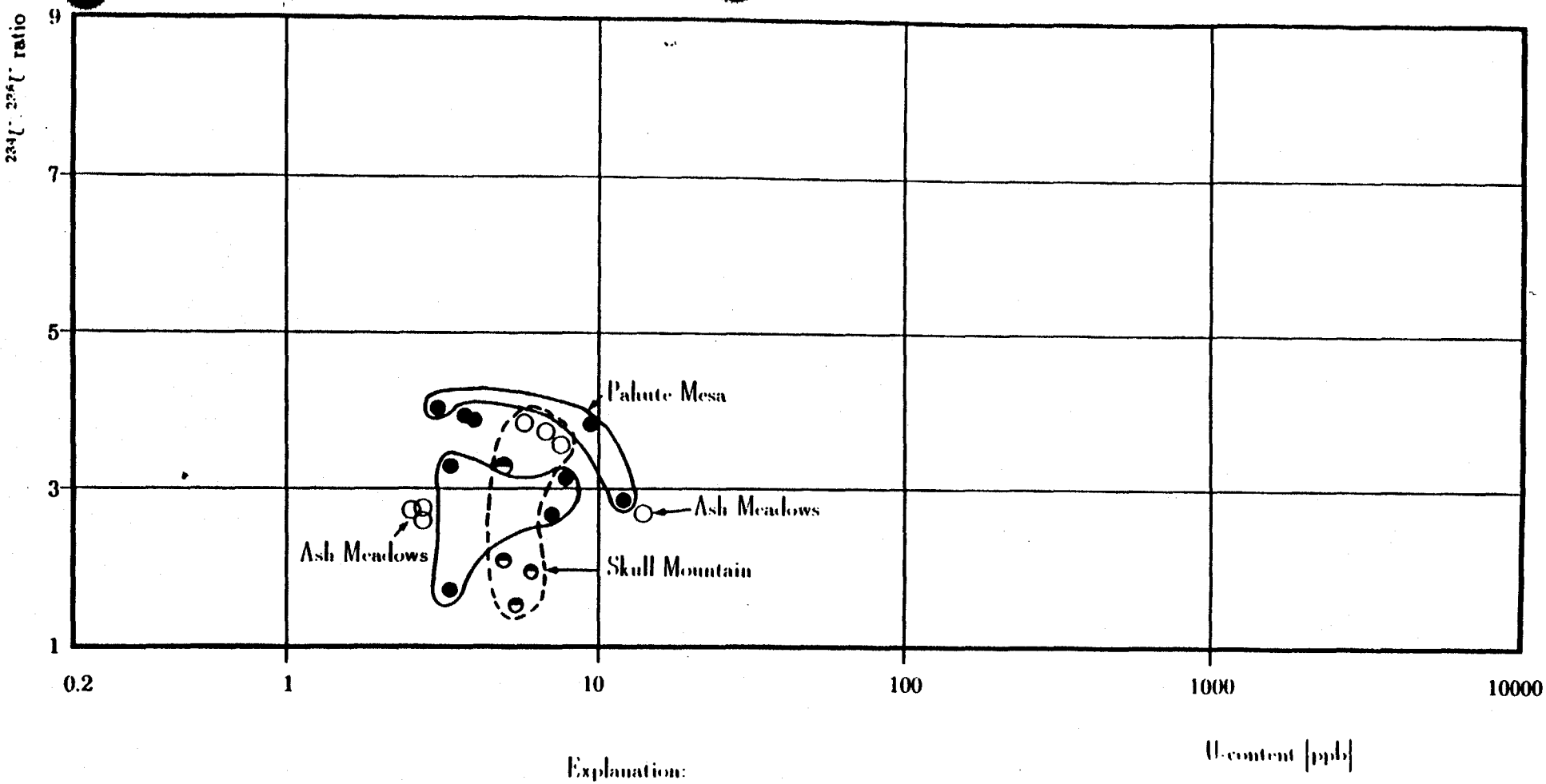

Explanation:

● - sample represents fluids from the tuff "pile";

○ - sample represents fluids from the Paleozoic carbonates; and

⊙ - sample represents fluids from alluvium.

Note:

a) the Climax Stock perched fluids were excluded from this plot.

$^{234}U/^{238}U$ vs. U-content. Hydraulic "source" regions. The Nevada Test Site hydrosphere.

Figure 27.

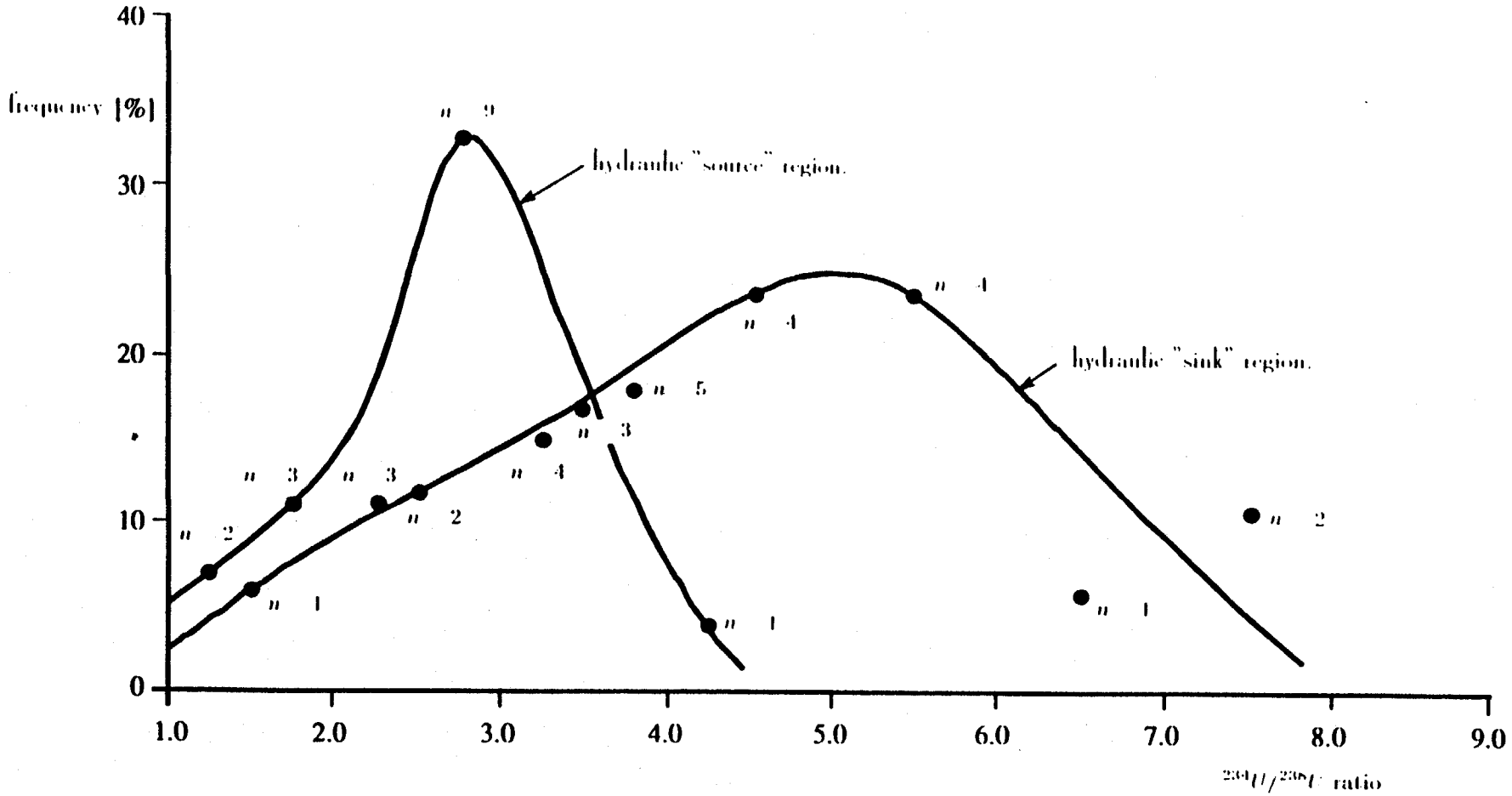

Note:

a) $n = 27$ for hydraulic "source" regions; $n = 17$ for hydraulic "sink" regions.

Isotopic character of dissolved uranium. Water samples from hydraulic "source" and "sink" regions.

Figure 28.

- At the Nevada Test Site, the $^{87}Sr/^{86}Sr$ ratios from samples of the hydraulic "source" fluids are distinct from the corresponding ratios from samples of the hydraulic "sink" fluids.

Conclusion: **The Nevada Test Site hydrosphere is a self-organized dynamic system and consists of a number of the Benard-Rayleigh dissipative structures.**

Self-organization. The Nevada Test Site hydrosphere - dissolved strontium data.

Figure 29.

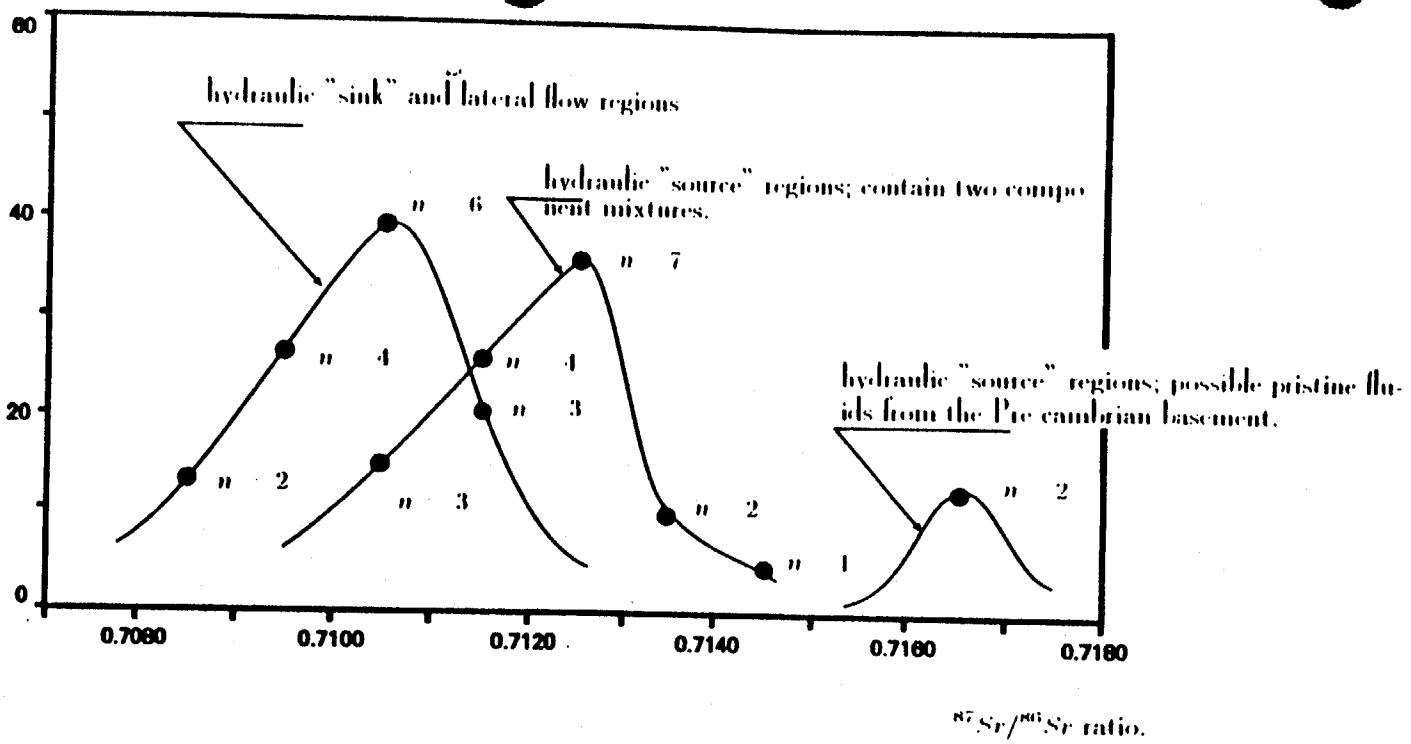

Note:

a) total number of samples: $n = 15$; and

b) isotopic data are from Stuckless (1990).

Comparison of the $^{87}Sr/^{86}Sr$ ratios. The Nevada Test Site "source" and "sink" regions.

Figure 30.

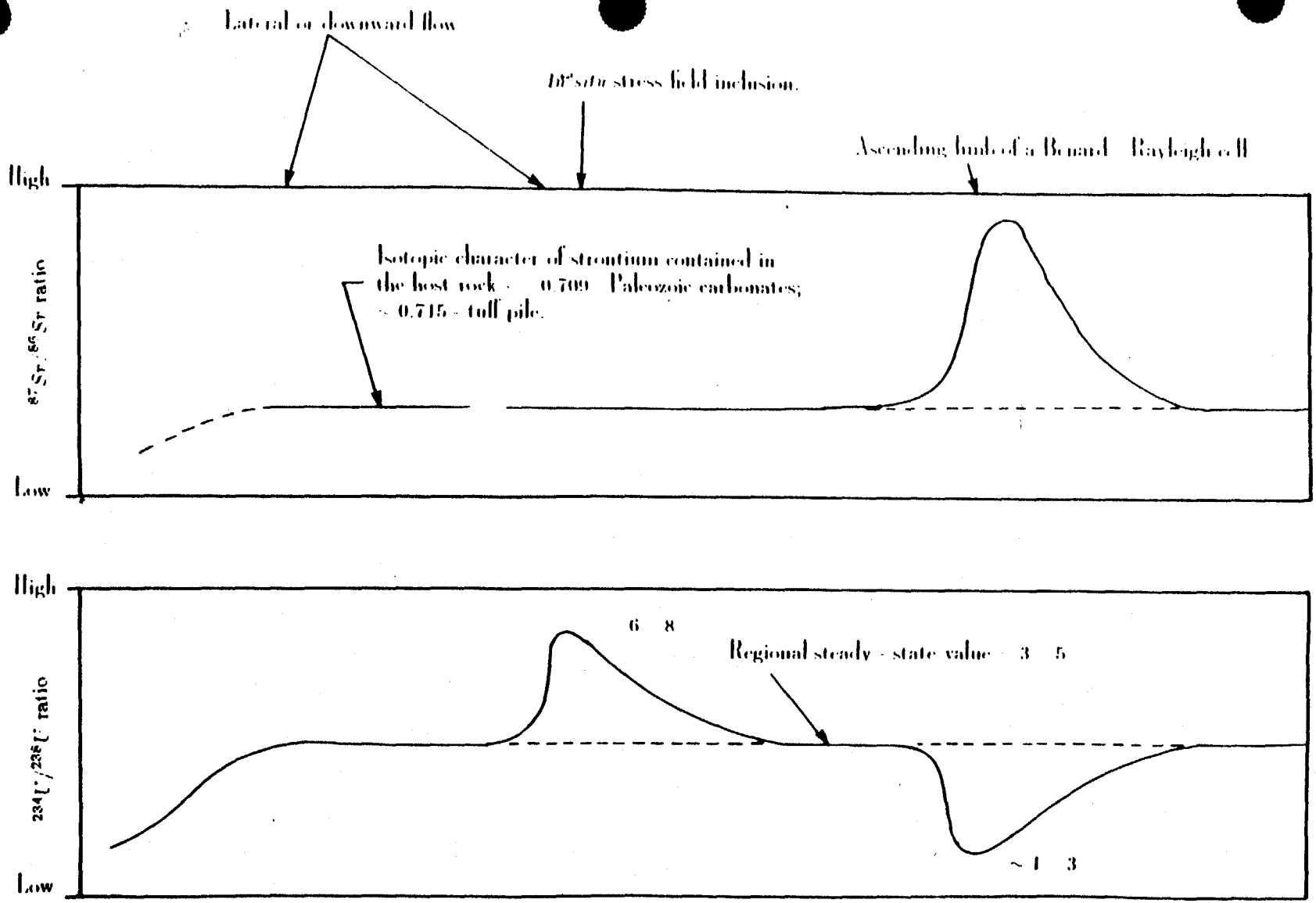

Note:

Fluids residing in the hydraulic "source" regions exhibit paired isotopic signature; relative to fluids from the hydraulic "sink" regions, the hydraulic "source" fluids simultaneously exhibit: i) lower values of the $^{234}U/^{238}U$ activity ratio; and ii) higher values of the $^{87}Sr/^{86}Sr$ ratio.

Conceptual understanding of spatial distribution of the strontium and uranium isotopic ratios. The contemporary Nevada Test Site hydrosphere.

Figure 31

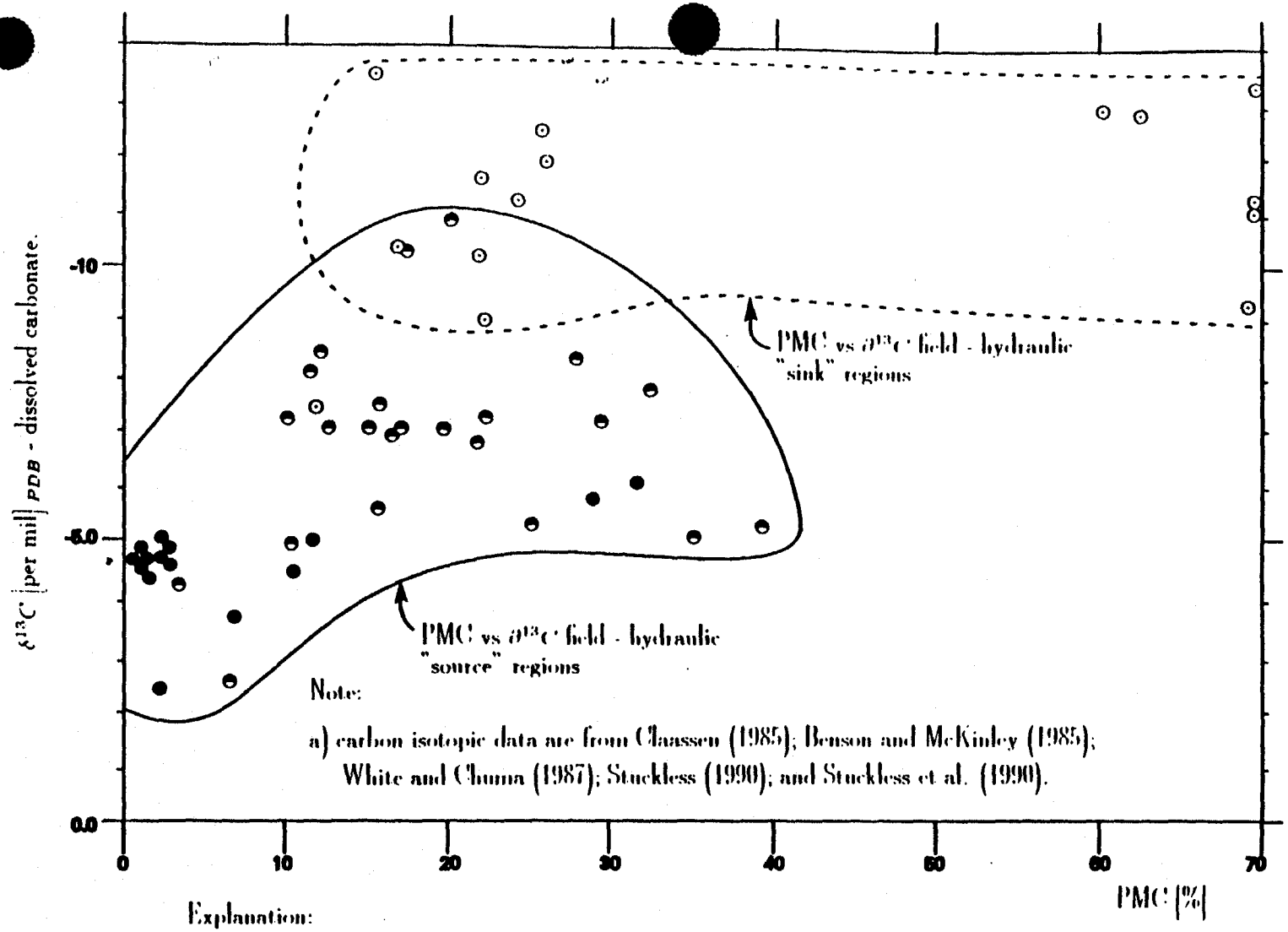

Explanation:

- ○ sample represents the tuff "pile" based hydraulic sink region;
- ◒ sample represents the tuff "pile" based hydraulic source region; and
- ● sample represents the Paleozoic carbonates based hydraulic source region.

$\delta^{13}C$ vs. PMC plot. Water samples from the Nevada Test Site hydrosphere.

Figure 38.

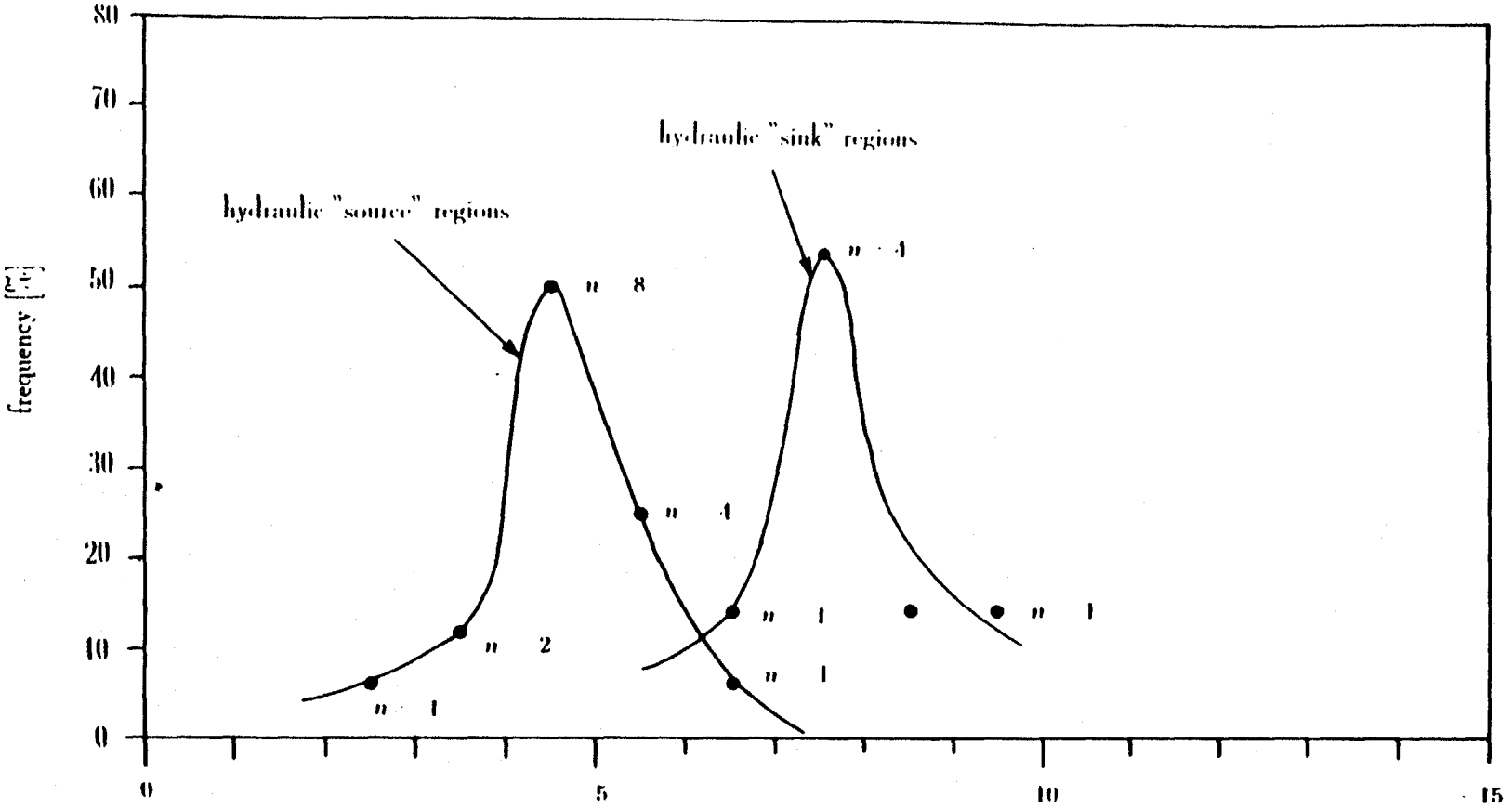

Note:

a) N = 16 for hydraulic "source" regions; N = 7 for hydraulic "sink" regions.

Isotopic character of carbon. Water samples from the Paleozoic carbonate based hydraulic "sink" and "source" regions.

Figure 39.

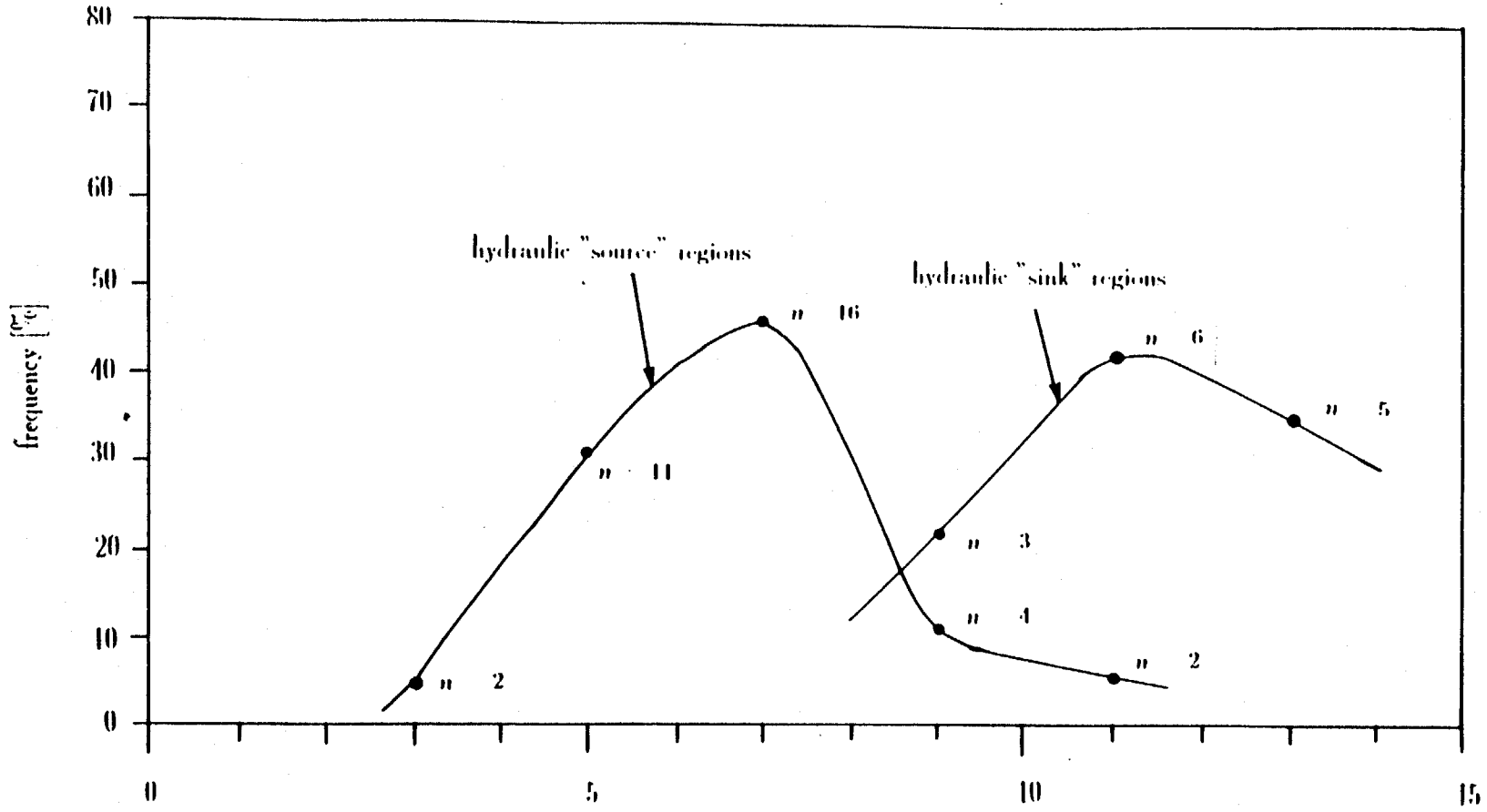

Note:

a) N 35 for hydraulic "source" regions; N 14 for hydraulic "sink" region.

Isotopic character of carbon. Water samples from the alluvium - tuff pile hydraulic "source" and "sink" regions.

Figure 40.

- At the Nevada Test Site, the "oxygen isotopic shift" from samples of the hydraulic "source" fluids is greater than that from samples of the hydraulic "sink" fluids.

- Both the deuterium content and the oxygen - 18 content, from samples of the Nevada Test Site subsurface fluids, reflect altitudes of the local land surface.

- Relative to the hydraulic "sink" fluids, the hydraulic "source" fluids exhibit both the negative "hydrogen isotopic shift" and the positive "oxygen isotopic shift".

Conclusion: a) **The Nevada Test Site hydrosphere is a self-organized dynamic system and consists of a number of the Benard-Rayleigh dissipative structures.**

b) **Partially, the Nevada Test Site subsurface fluids are derived from the local atmospheric precipitation. (i.e., recharge is widespread and not restricted to the high altitude regions.)**

c) **the Nevada Test Site subsurface fluids are, at least, two-component mixtures (oxygen shifted and deuterium depleated geothermal fluids intermixed with the recharging local atmospheric precipitation.)**

Self-organization. The Nevada Test Site hydrosphere - deuterium and oxygen data.

Figure 41.

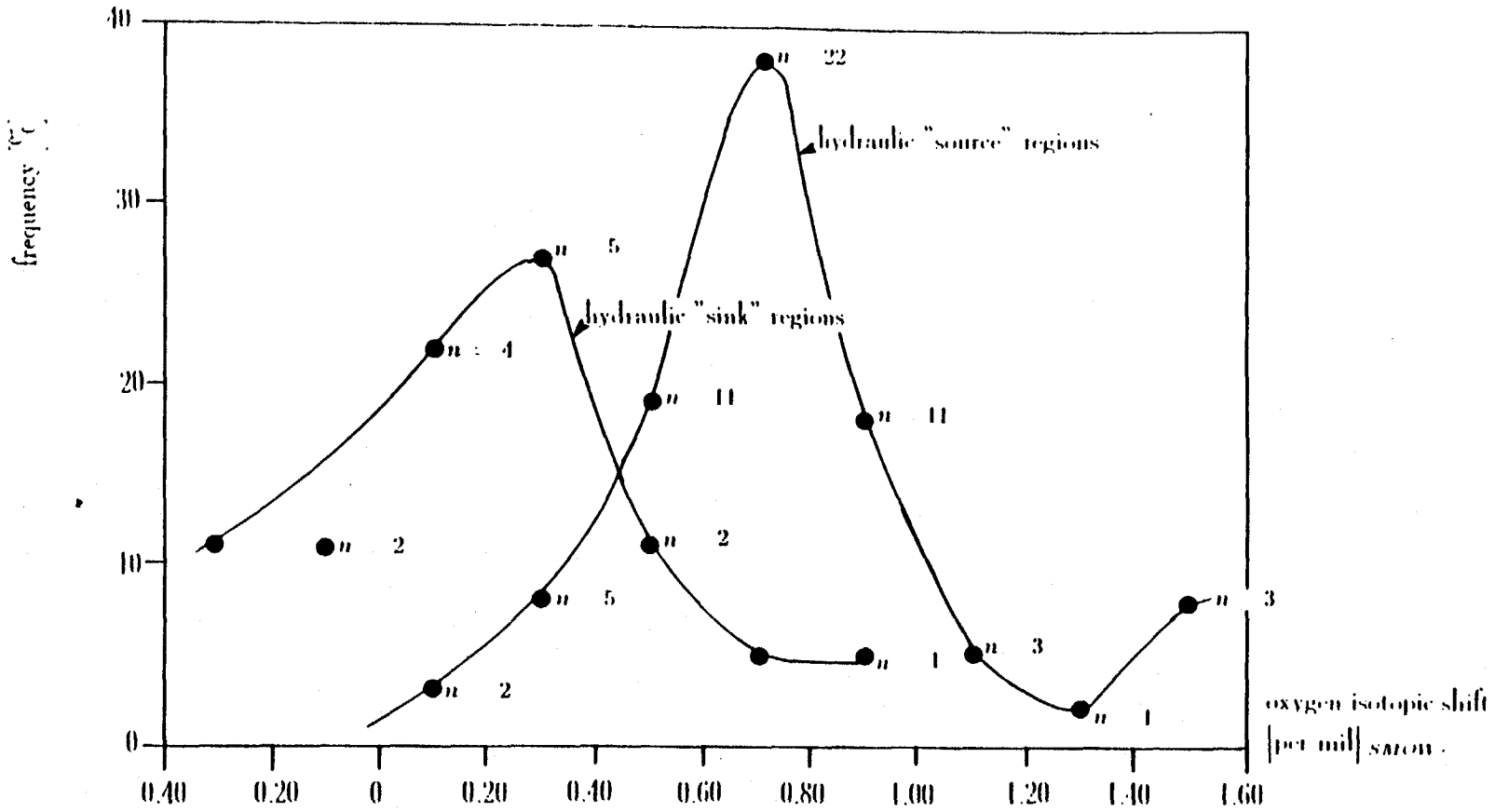

Note:

a) samples are bulk samples pumped out of large segments of exploratory wells - sampling "smoothing" may be involved, and the observed oxygen isotopic shift may be smaller than the actually present one;

b) oxygen isotopic shift $\Delta\delta^{18}O \quad (\delta D_{sl} \quad 10)/8 \quad \delta^{18}O_{sl}$; and

c) oxygen isotopic data are from Isherwood et al. (1982); Benson and McKinley (1985); Claassen (1985); White and Chuma (1987); Stuckless (1990); and Stuckless et al. (1990)

Comparison of magnitudes of the oxygen isotopic shift. The Nevada Test Site "sink" and "source" regions.

Figure 42.

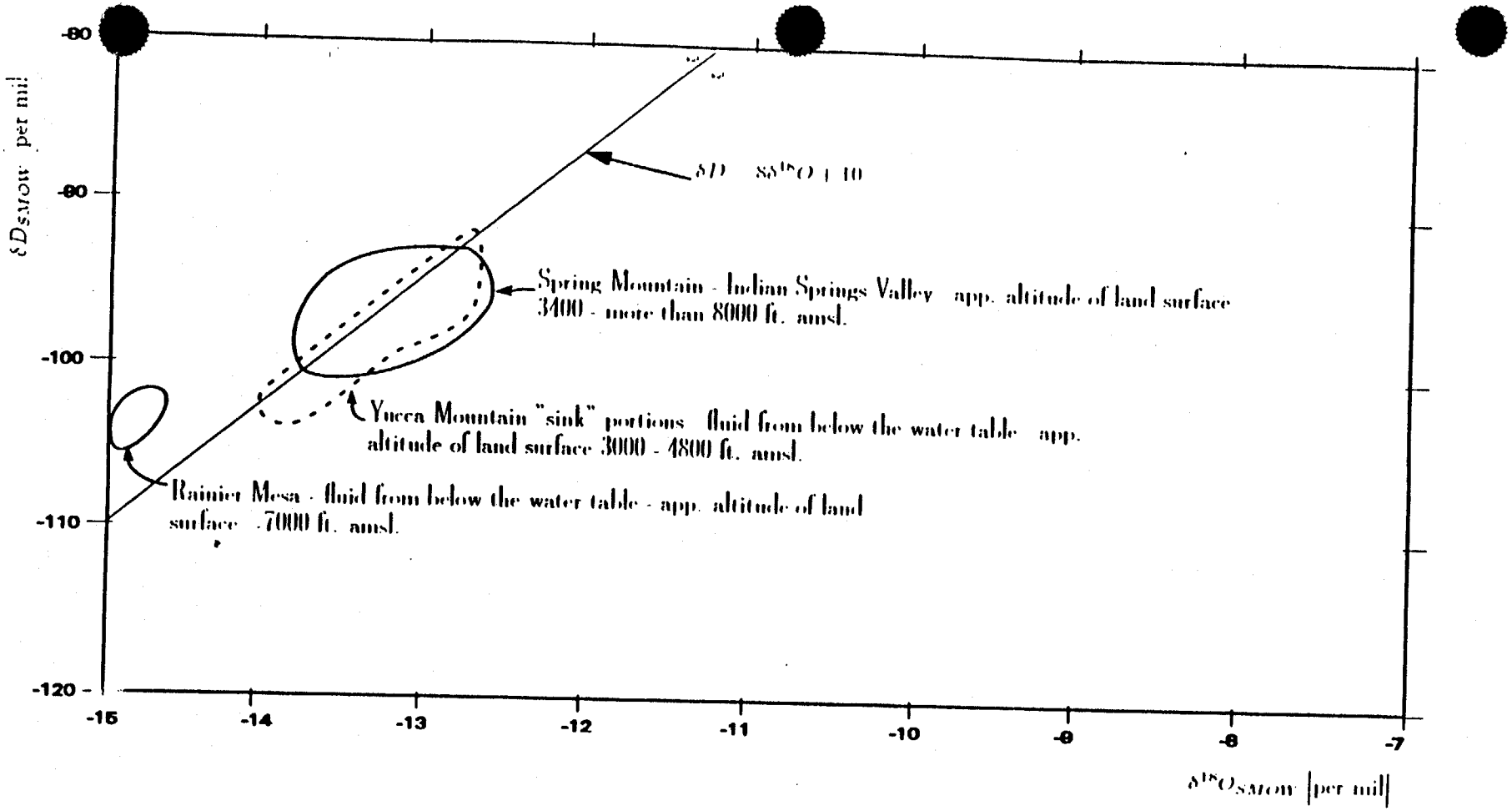

Note:

a) Rainier Mesa and Spring Mountain fluids are contemporary fluids; and

b) Yucca Mountain and Rainier Mesa fluids from below the water table are older fluids - ^{14}C ages are comparable to those of fluids from the "source" regions.

Relationship between compositions and altitude of the local land surface. Fluids from the hydraulic sink regions.

Figure 43.

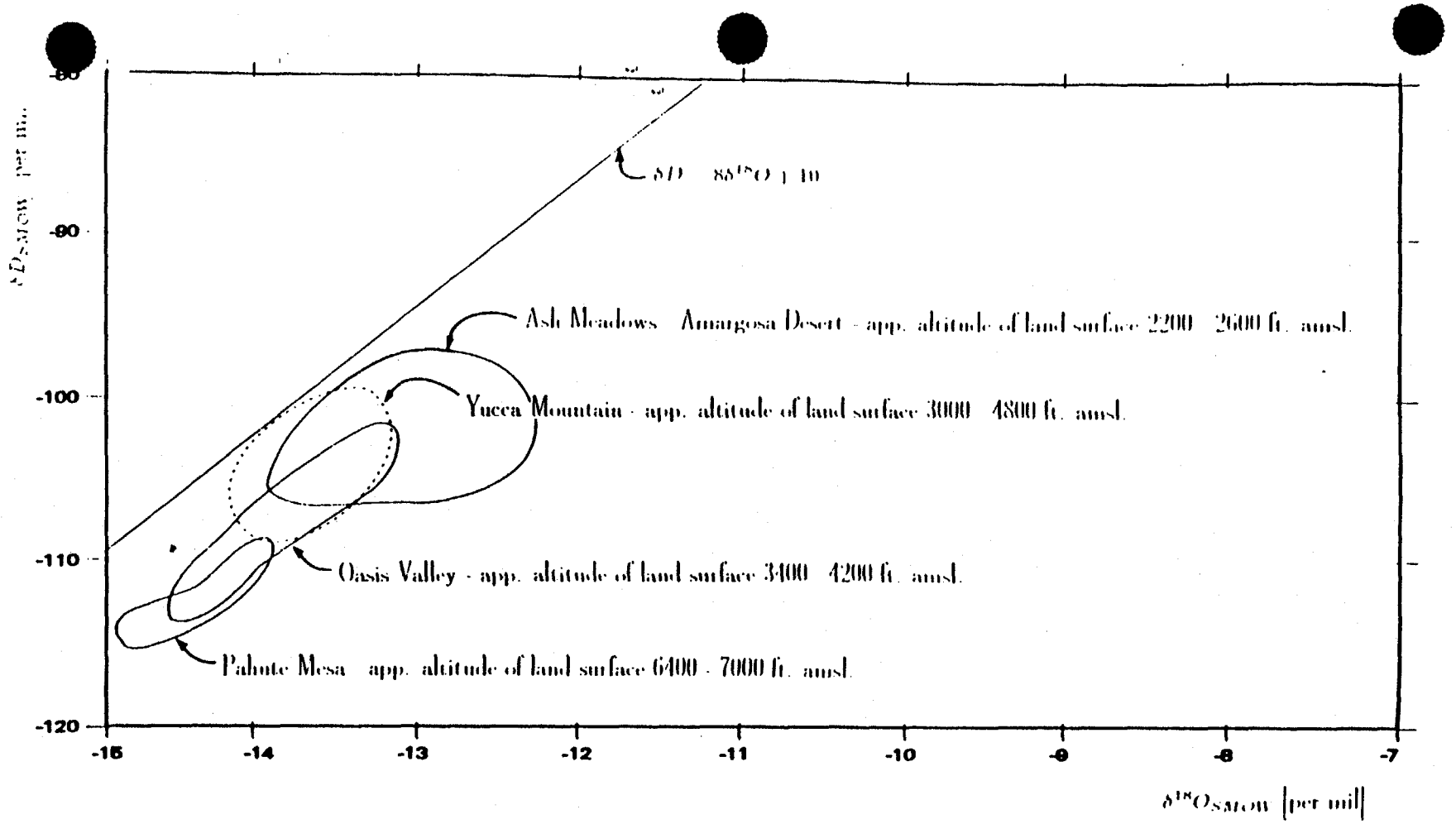

Relationship between isotopic compositions and altitudes of the local land surface. Fluids from the hydraulic source regions.

Figure 41

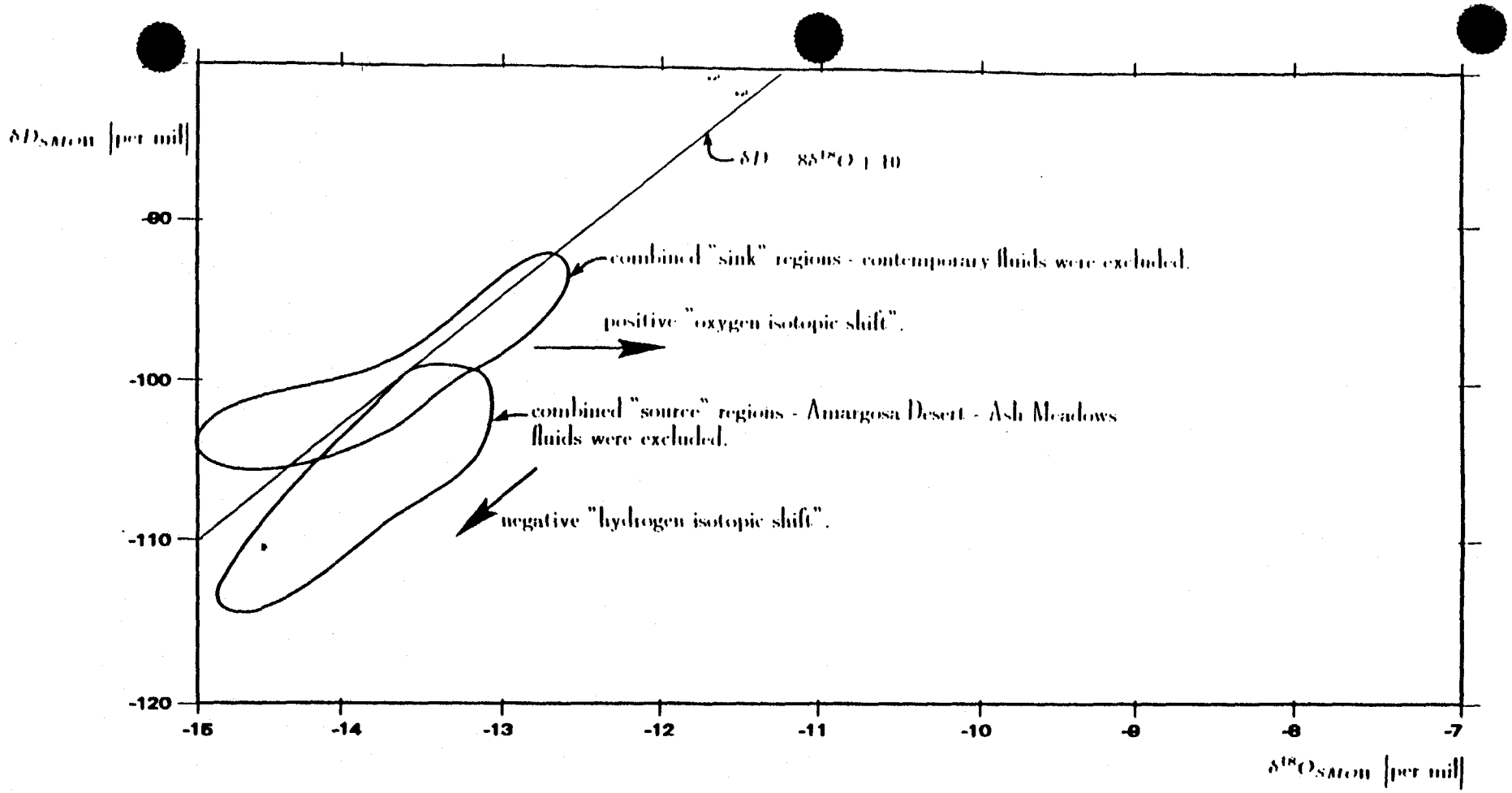

Note:

a) comparison is based on data from regions with comparable altitudes of the land surface; and

b) comparison is based on data from fluid samples with comparable PMC.

Comparison of isotopic compositions. Sink and "source" regions - The Nevada Test Site hydrosphere.

Figure 45.

Isotopic and chemical evidence for periodic and quasi-periodic fluctuations

- Contemporary data - short period fluctuations

  i) time series for values of the δD, $\delta^{13}C$, $\delta^{18}O$ ratios;

  ii) time series for U content, gross α values, and gross β values; and

  iii) partial time series for bulk fluid chemistry and temperature.

- Geological record - long-period fluctuations.

  i) time-series for values of the $^{87}Sr/^{86}Sr$ ratio;

  ii) time series for values of the δD ratio; and

  iii) time series for values of the $\delta^{18}O$ ratio.

Fluctuations. The Nevada Test Site hydrosphere.

Figure 46.

- The contemporary Nevada Test Site subsurface fluids exhibit the short period fluctuations. These fluctuations are known to involve: a) the $\delta^{13}C$ ratio, b) the $\delta^{18}O$ ratio [most likely the magnitude of "oxygen isotopic shift"], c) the δD ratio, $\Delta\delta D \quad \frac{1}{8}\Delta\delta^{18}O$, d) U concentrations; e) gross α values, $\Delta\alpha \neq \Delta\beta$; f) bulk fluid chemical composition; and g) fluid temperature (?).

- One possible explanation for the observed short period fluctuations is a transient mixing between the two end members, i.e., Q_{atm} and Q_{geoth}.

- Such transient mixing may be expressing the transient behavior of the local Benard Rayleigh instabilities.

Inference: **The Nevada Test Site Benard-Rayleigh instabilities are subject either to the period doubling bifurcations or to the persistant quasi-periodic motions.**

Short period fluctuations - isotopic, chemical, and geothermal data.

Figure 47.

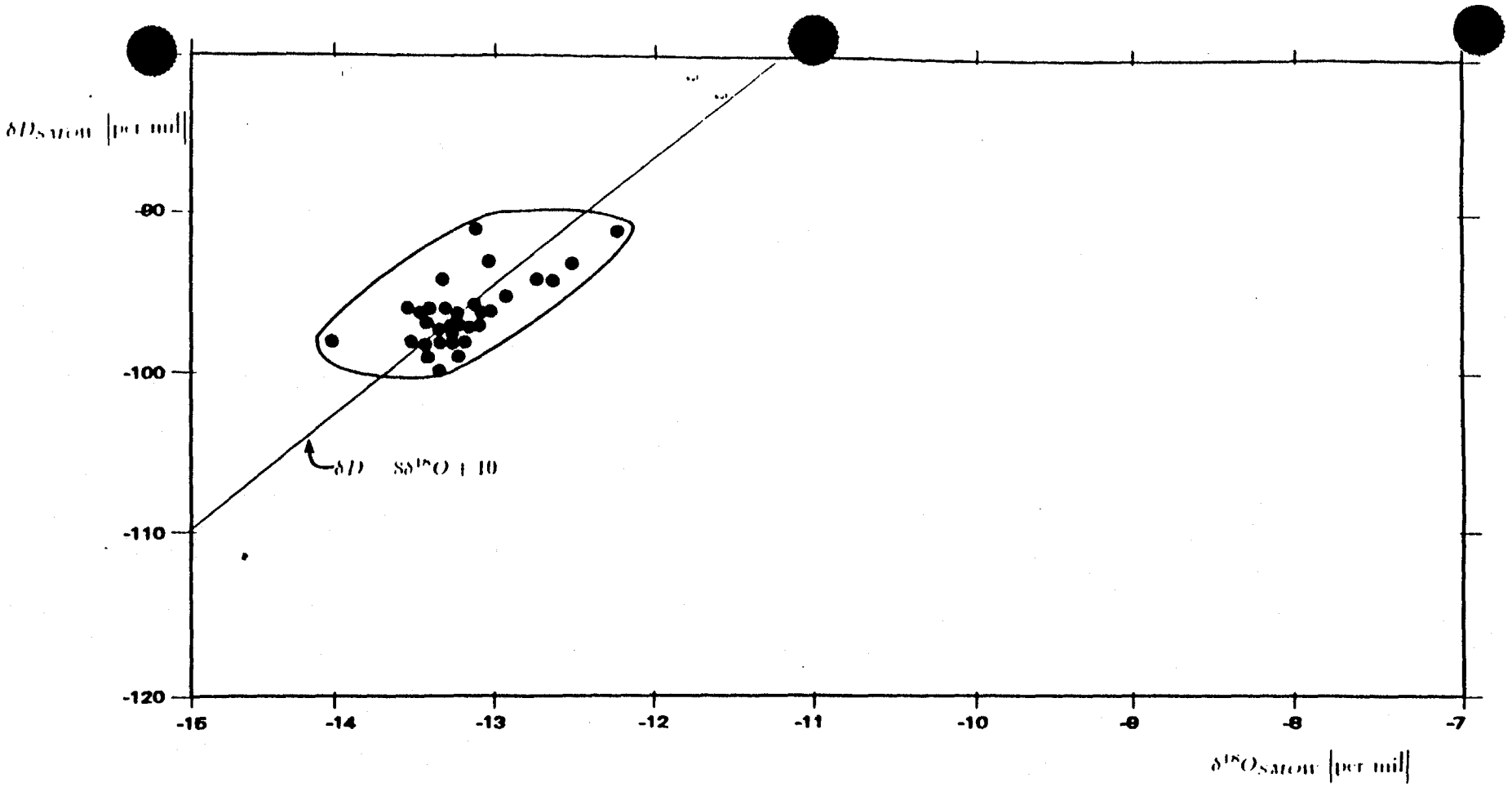

Note:

a) the U12n.03 seep is into tunnel, samples were obtained ~400m below the ground surface;

b) fluid is known to be directly from atmospheric precipitation;

c) fluid does not exhibit any oxygen shift, indicating that evaporative enrichment is nil;and

d) isotopic data are from Russell (1987).

Reference - evaporative enrichment in the Rainier Mesa recharge.

Figure 48.

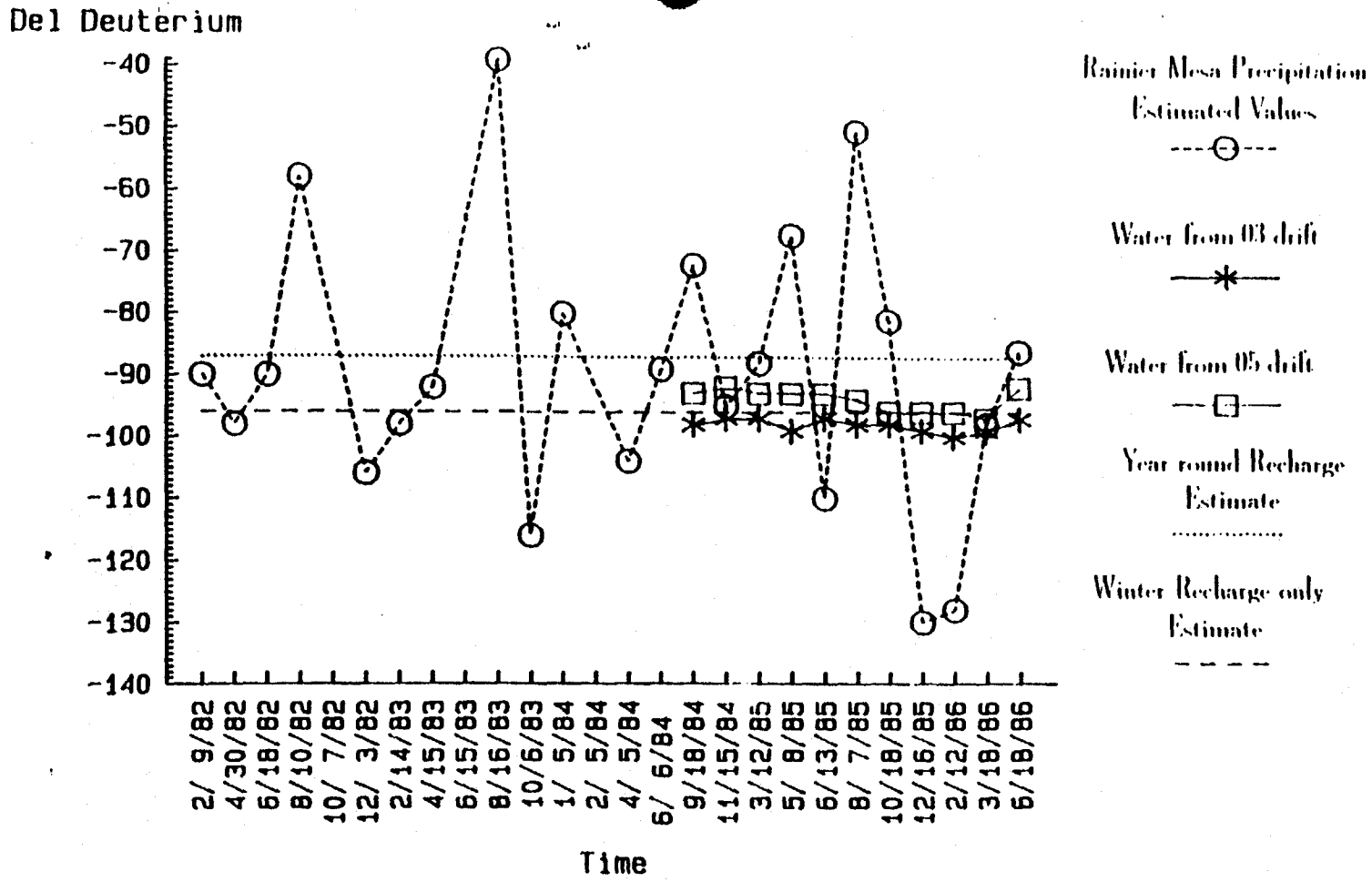

Note:

a) for the infiltrating recharge, δD fluctuations are very small;

b) mean value for the year round recharge is δD = -87 per mil $_{SMOW}$; and;

c) mean value for the winter recharge is δD = -96 per mil $_{SMOW}$.

Reference - temporal variability in value of the δD ratio, from samples of the infiltrating recharge. Rainier Mesa. From Russell, 1987.

Figure 49.

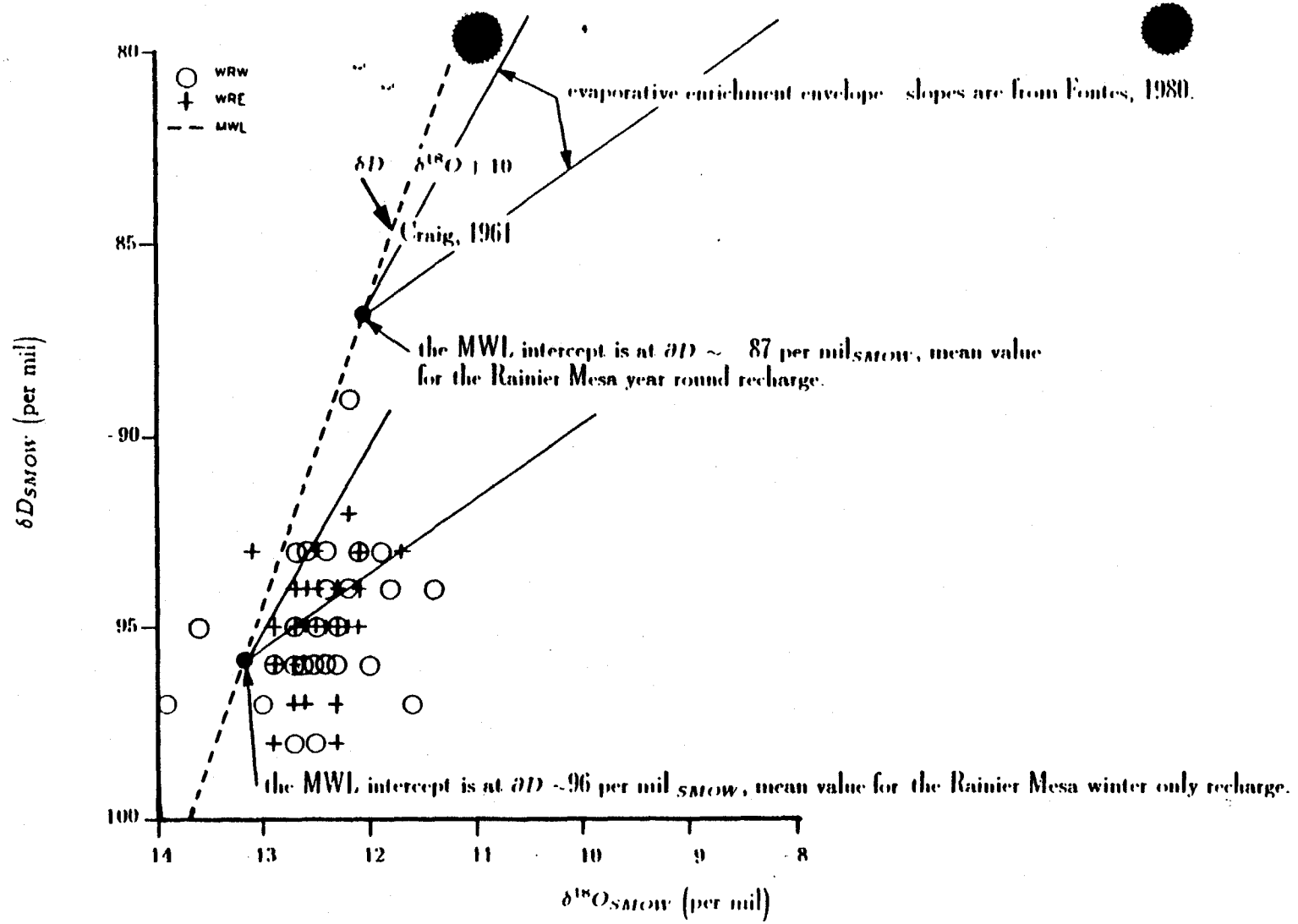

Note:

a) the White Rock Spring discharge is situated ~ 1000 ft. above the so called regional water table;

b) it occurs near the western edge of the Halfpint Hydraulic Source Region - the underlying perched body of water may be in part deep seated, some of the fluid contained may represent overflow from nearby hydraulic mound - Szymanski, 1989; and

c) the observed "oxygen isotopic shift" may be taken as supportive of the above conjecture.

Isotopic composition - fluids from the White Rock Spring discharge. Modified from Eyles et al. (1990)

Figure 50.

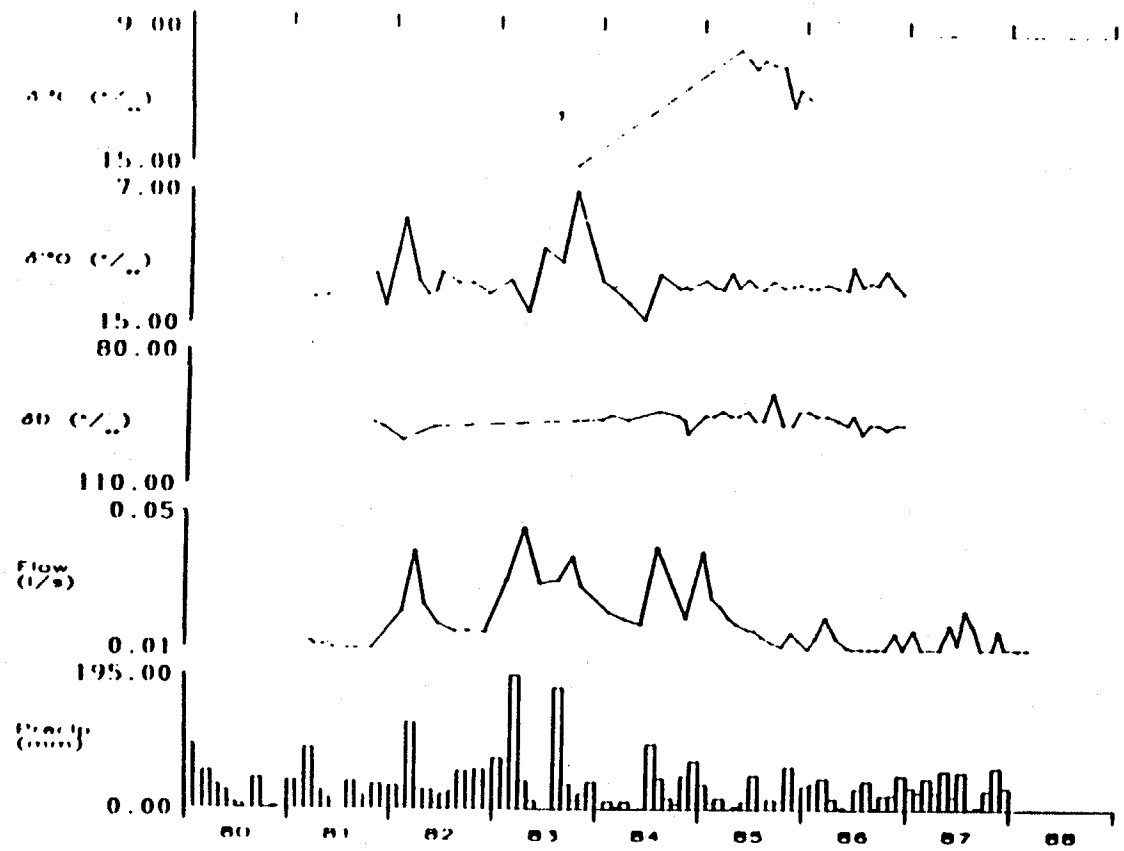

Time-series - fluids emerging from the White Rock West Spring discharge. From Lyles et al., 1990.

Figure 51.

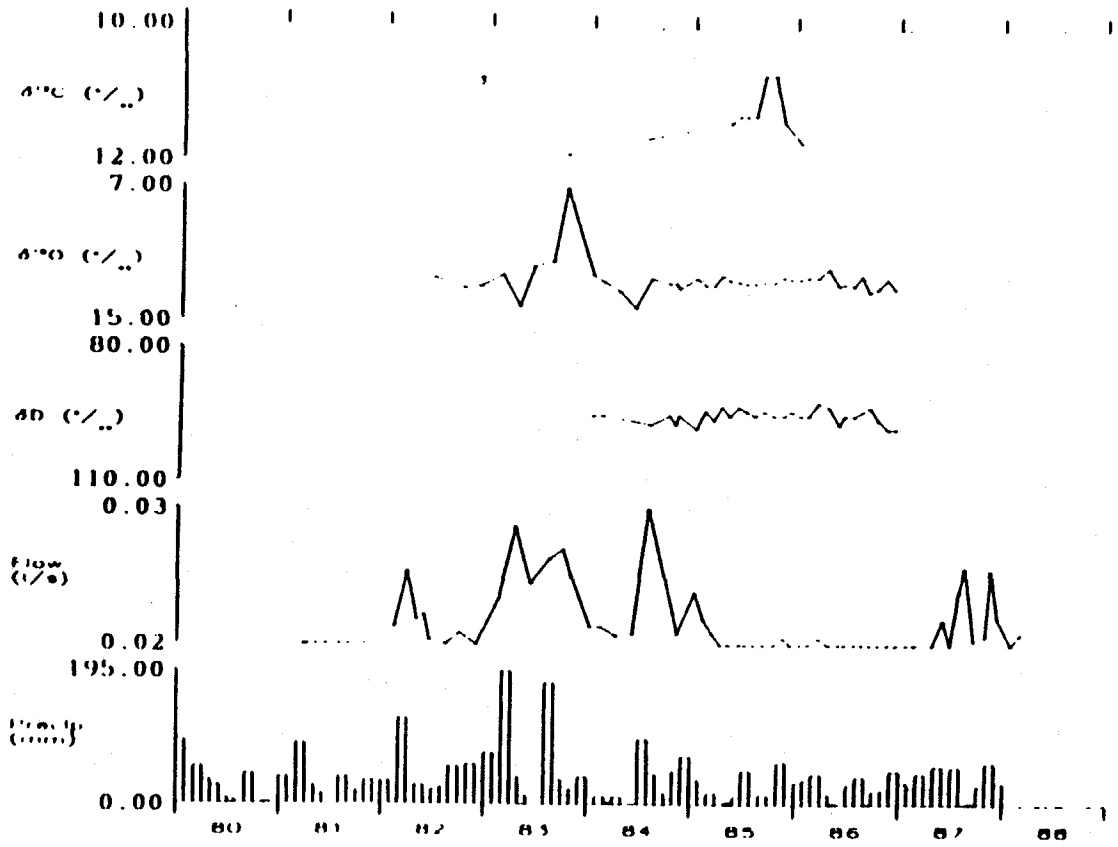

Time-series - fluids emerging from the White Rock East Spring discharge. From Lyles et al., 1990.

Figure 52.

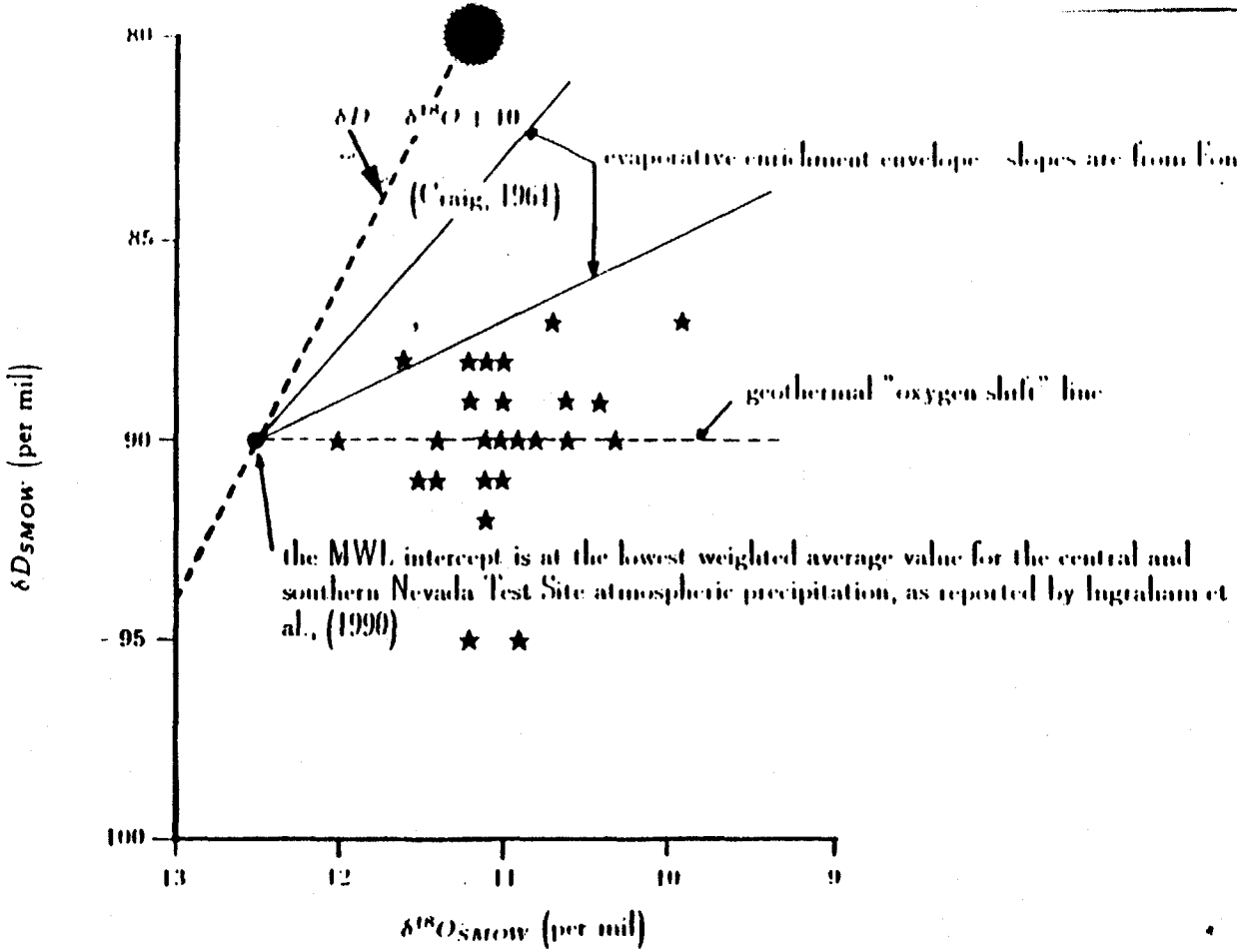

Note:

a) Cane Spring is situated some 1400 ft above the so- called regional water table, around the spring orifice there is an ongoing contemporary deposition of $CaCO_3$;

b) Based on a variety of data, Szymanski (1989) has postulated that both the Cane Spring discharge and the underlying perched bodies of ground water are deep seated and together express a contemporary hydraulic mound, presence of which is the result of past hydro tectonic activity;

c) The contemporary Cane Spring $CaCO_3$ deposits may be regarded as a modern analog for the Yucca Mountain calcite silica deposits; and

d) The observed "oxygen isotopic shift" fully supports the previous interpretations regarding the hydrologic setting of the Cane Spring area.

The contemporary Cane Spring deposits - a modern analog for the Yucca Mountain surficial calcite-silica deposits. Modified from Lyles et al. (1990)

Figure 53.

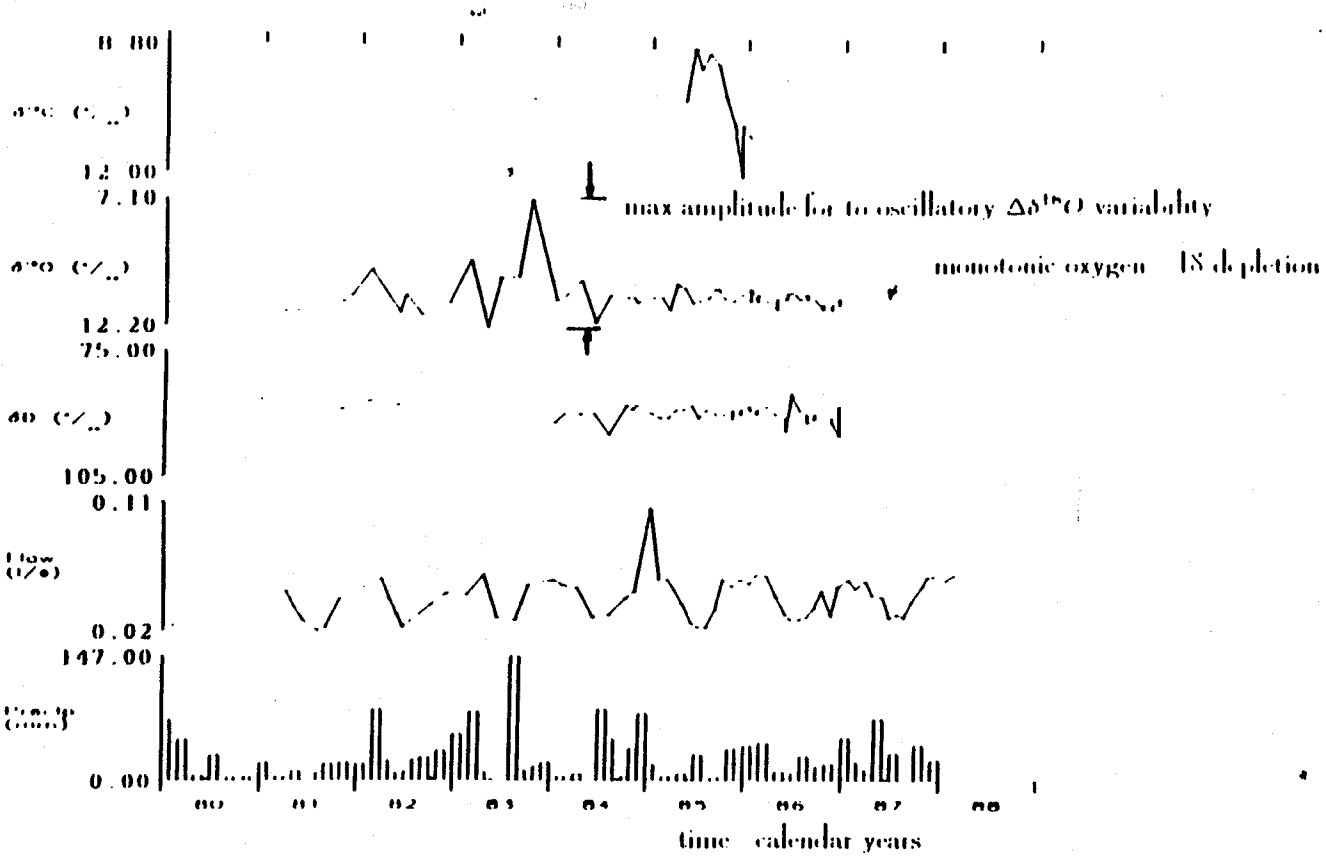

Note:

a) the time series suggests that, even during time-spans of a few years, the oxygen 18 content in the local subsurface fluids does not remain time invariant;

b) the observed monotonic oxygen 18 depletion is $\Delta\delta^{18}O \sim 1.2$ per mil $_{SMOW}$ in 6 years; and

c) the observed $\delta^{18}O$ oscillatory variability has a maximum amplitude of $\Delta\delta^{18}O \sim 5$ per mil $_{SMOW}$.

Time-series for the oxygen 18 content in fluids emerging from the local Cane Spring. From Lyles et al., 1990.

Figure 51.

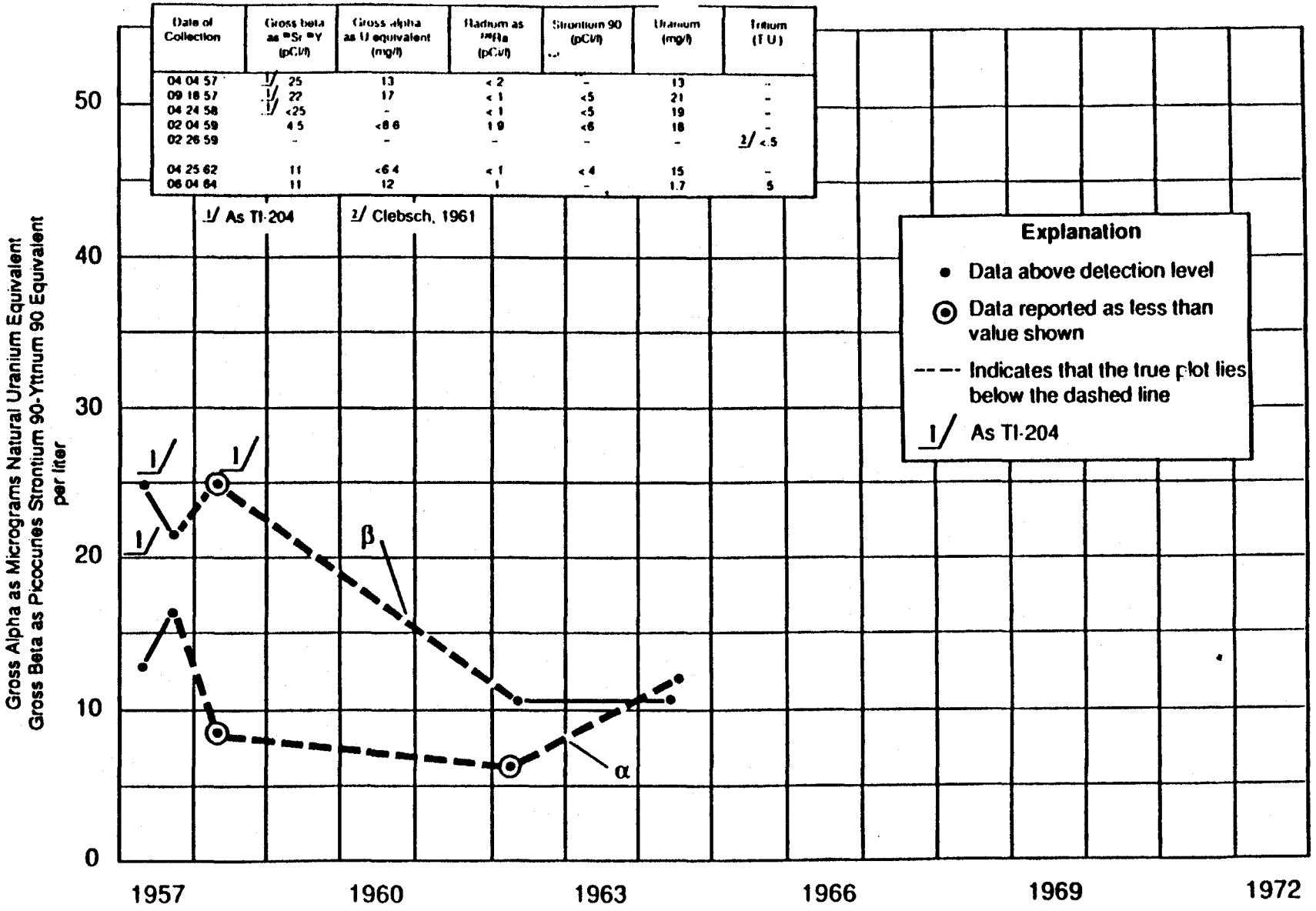

Date of Collection	Gross beta as ^{90}Sr-^{90}Y (pCi/l)	Gross alpha as U equivalent (mg/l)	Radium as ^{226}Ra (pCi/l)	Strontium 90 (pCi/l)	Uranium (mg/l)	Tritium (T U)
04 04 57	1/ 25	13	< 2	–	13	–
09 18 57	1/ 22	17	< 1	<5	21	–
04 24 58	1/ <25	–	< 1	<5	19	–
02 04 59	4 5	<8 6	1 9	<6	18	–
02 26 59	–	–	–	–	–	2/ <5
04 25 62	11	<6 4	< 1	< 4	15	–
06 04 64	11	12	1	–	1.7	5

Note.
$^{234}U/^{238}U$ - unknown.

Variations in gross alpha and gross beta values of water from Well 5A. From Claassen, 1973.

Figure 55.

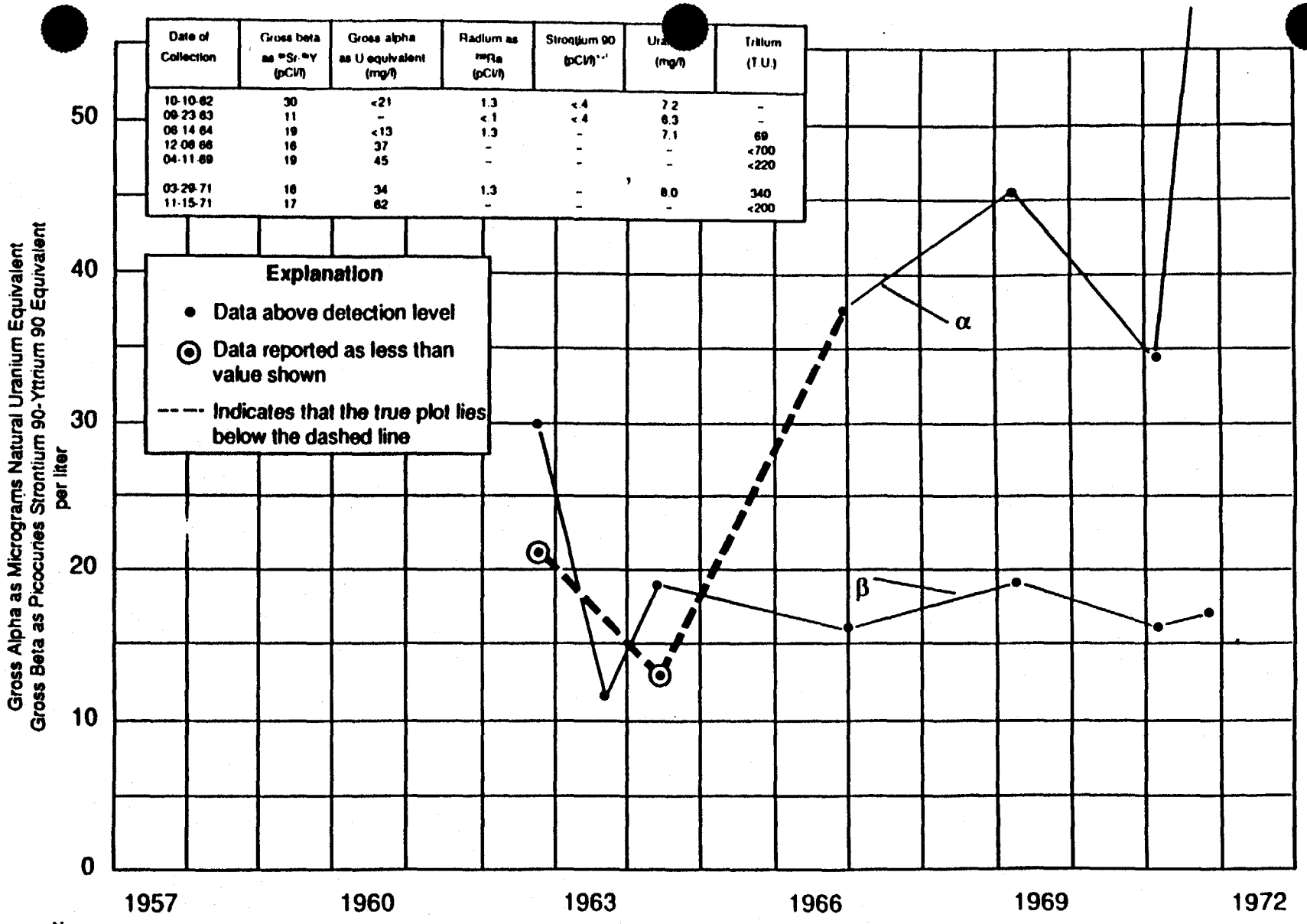

Date of Collection	Gross beta as ^{90}Sr-^{90}Y (pCi/l)	Gross alpha as U equivalent (mg/l)	Radium as ^{226}Ra (pCi/l)	Strontium 90 (pCi/l)	Uranium (mg/l)	Tritium (T.U.)
10-10-62	30	<21	1.3	<4	7.2	–
09-23-63	11	–	<1	<4	6.3	–
06-14-64	19	<13	1.3	–	7.1	69
12-06-66	16	37	–	–	–	<700
04-11-69	19	45	–	–	–	<220
03-29-71	16	34	1.3	–	8.0	340
11-15-71	17	62	–	–	–	<200

Note:
$^{234}U/^{238}U$ - 3.85 - 1975

Variations in gross alpha and gross beta values of water from Well C-1. From Claassen, 1973.

Figure 56.

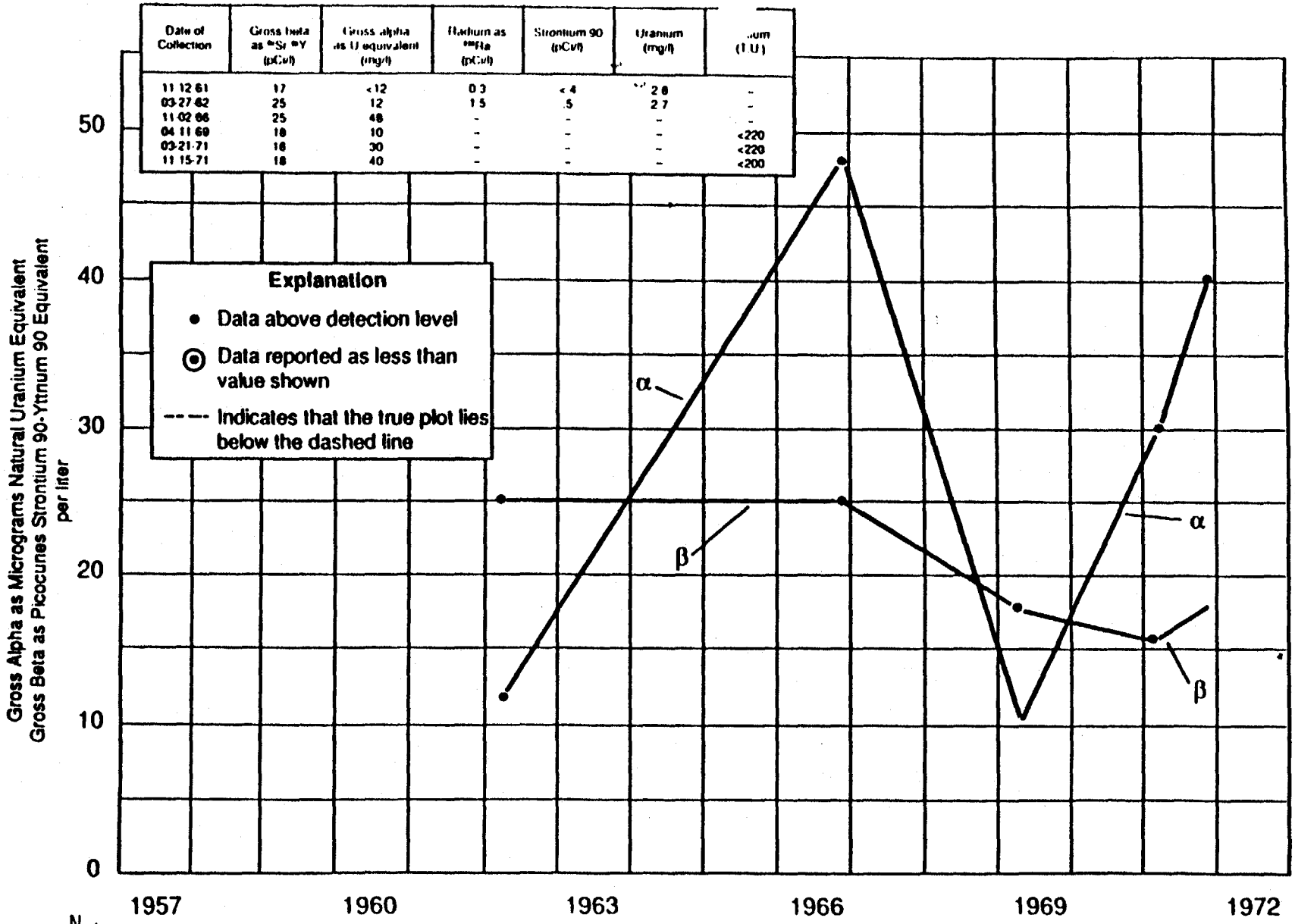

Date of Collection	Gross beta as ^{90}Sr-^{90}Y (pCi/l)	Gross alpha as U equivalent (mg/l)	Radium as ^{226}Ra (pCi/l)	Strontium 90 (pCi/l)	Uranium (mg/l)	...um (T.U.)
11-12-61	17	<12	0.3	< 4	2.8	-
03-27-62	25	12	1.5	5	2.7	-
11-02-66	25	48	-	-	-	-
04-11-69	18	10	-	-	-	<220
03-21-71	18	30	-	-	-	<220
11-15-71	18	40	-	-	-	<200

Note:

$^{234}U/^{238}U$ - 3.85 - November 15, 1971

3.92 - 1975

Variations in gross alpha and gross beta values of water from Well UE15d. From Claassen, 1973.

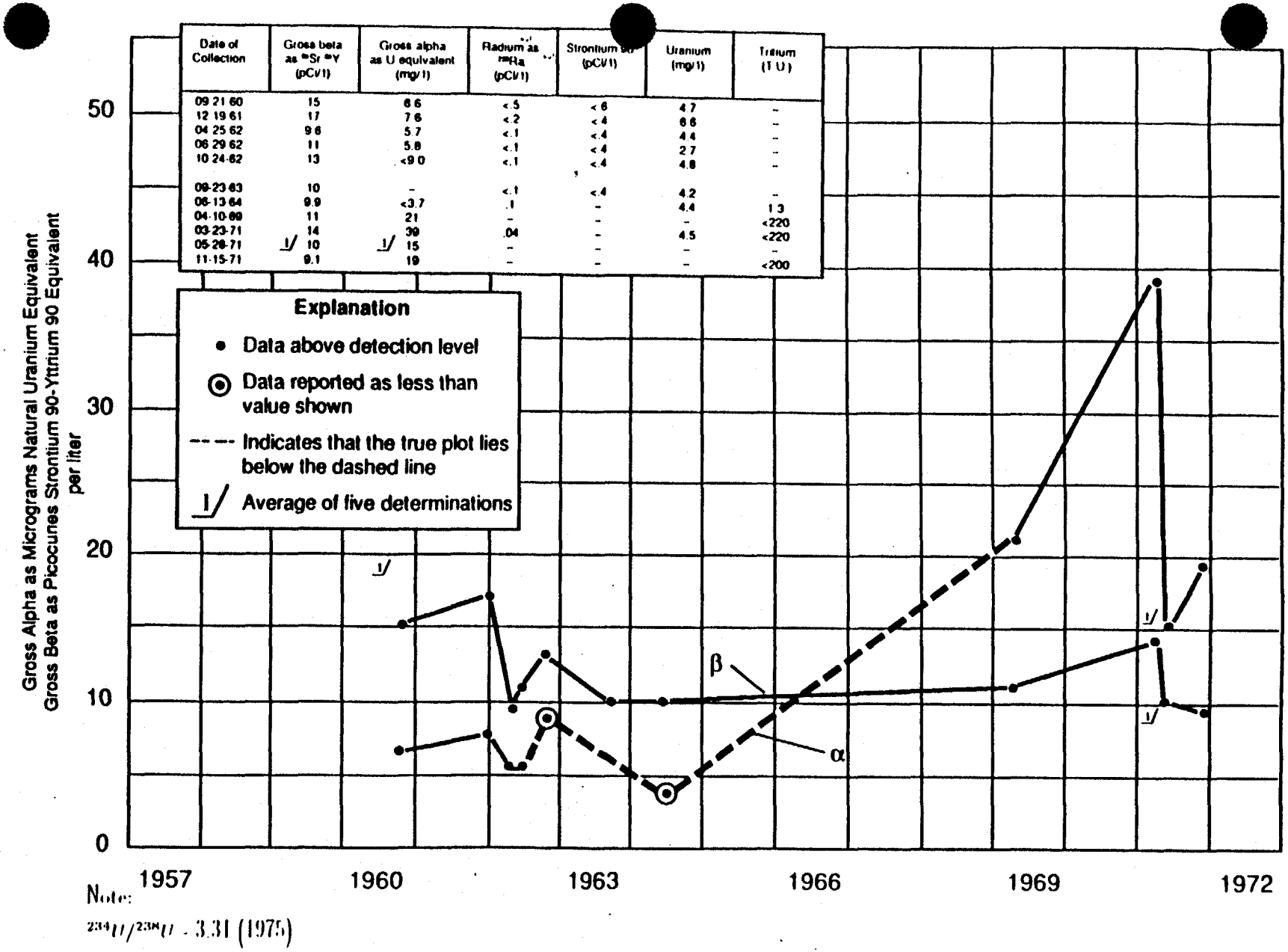

Date of Collection	Gross beta as ^{90}Sr-^{90}Y (pCi/l)	Gross alpha as U equivalent (mg/l)	Radium as ^{226}Ra (pCi/l)	Strontium 90 (pCi/l)	Uranium (mg/l)	Tritium (T.U.)
09 21 60	15	6.6	<.5	< 6	4.7	–
12 19 61	17	7.6	<.2	< 4	6.6	–
04 25 62	9.6	5.7	<.1	< 4	4.4	–
06 29 62	11	5.8	<.1	< 4	2.7	–
10 24 62	13	<9.0	<.1	< 4	4.8	–
09 23 63	10	–	<.1	< 4	4.2	–
06 13 64	9.9	<3.7	.1	–	4.4	1.3
04 10 69	11	21	–	–	–	<220
03 23 71	14	39	.04	–	4.5	<220
05 26 71	1/ 10	1/ 15	–	–	–	–
11 15 71	9.1	19	–	–	–	<200

Note: $^{234}U/^{238}U$ - 3.31 (1975)

Variations in gross alpha and gross beta values of water from Well A. From Claassen, 1973.

Figure 58.

Location: Devil's Hole.
Parameter: fluid temperature.
Source: Garside and Schilling, 1979.
Time-series: January 1953 - 91°F; January 1953 - 90°F; October 1964 - 81°F; and December 1966 - 92°F.

Location: Jack Rabbit Spring.
Parameter: total dissolved solids.
Source: Garside and Schilling, 1979.
Time-series: November 1966 - 412 ppm; November 1966 - 541 ppm; October 1970 - 2189 ppm; and October 1970 - 2140 ppm.

Location: Jack Rabbit Spring.
Parameter: $Cl + SO_4$.
Source: Garside and Schilling, 1979.
Time-series: November 1966 - 98 ppm; October 1970 - 1290 ppm.

Location: Soda Spring.
Parameter: SiO_2.
Source: Garside and Schilling, 1979.
Time-series: November 1966 - 35 ppm; October 1970 - 23 ppm.

Fluctuations. Groundwater from Ash Meadows, Nevada.

Figure 59.

- The Nevada Test Site deep seated fluids exhibit the long period fluctuations. These fluctuations are known to involve; a) the $^{87}Sr/^{86}Sr$ ratio; b) the δD ratio; and c) the $\delta^{18}O$ ratio.

- Both the normalized spectral comparison and the cross spectral comparison, between the SPECMAP and the DH 2 $\delta^{18}O$ time series, reveal that: a) for frequencies higher than ~ 0.05 cycles/10^3 years, the coherence between the two records breaks down; and b) for the entire range of the observed frequencies, the two records exhibit strong phase discords.

- The DH 2 $\delta^{18}O$ time series is, at best, a highly distorted record of the global climatic fluctuations.

- The local forcing function may readily be associated with the frequency locking modified isotopic signals resulting from the period doubling bifurcations.

Conclusion: **The Benard-Rayleigh instability, that underlies the Devil's Hole discharge point, is subject to the period doubling bifurcations.**

Note: seismic reflection data reported by Brocker et al. (1989) indicate that Devil's Hole is underlain by a deep-seated crustal magma body.

Long period fluctuations - strontium, deuterium, and oxygen 18 data.

Figure 60.

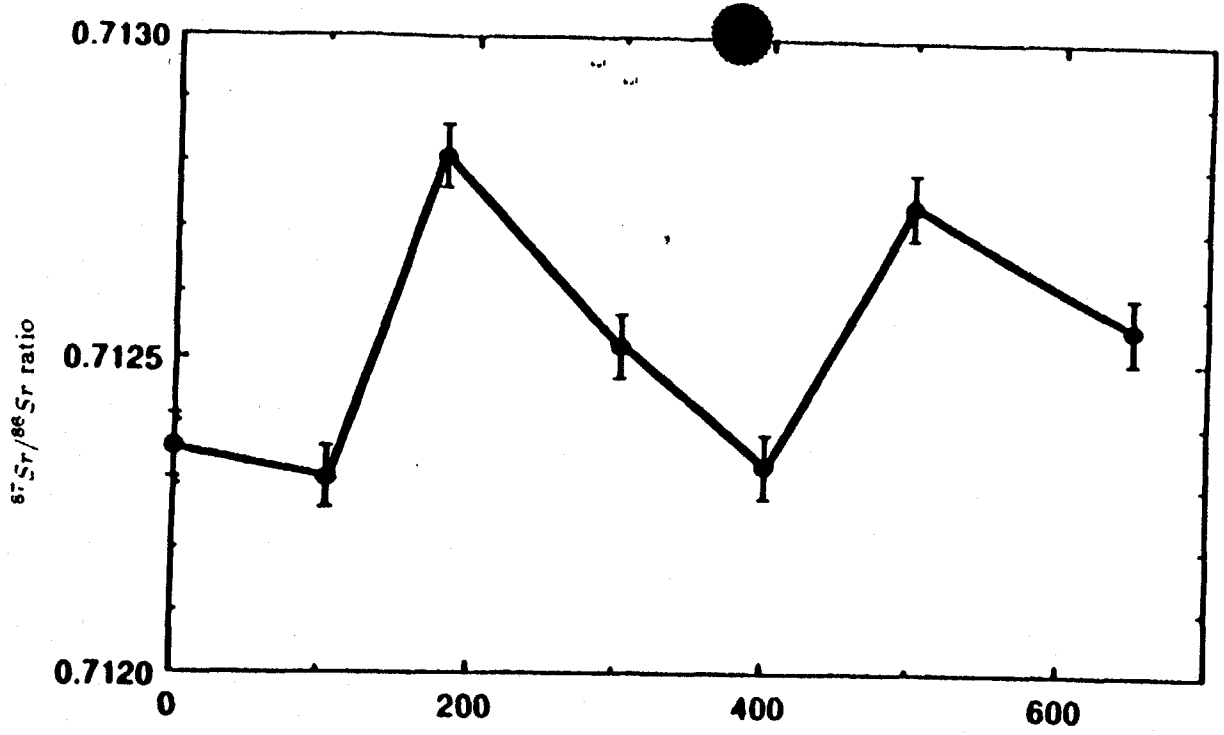

Fluctuations of value of the $^{87}Sr/^{86}Sr$ ratio. Calcitic veins from Devil's Hole, Ash Meadows, Nevada. From Stuckless, 1990.

Figure 61

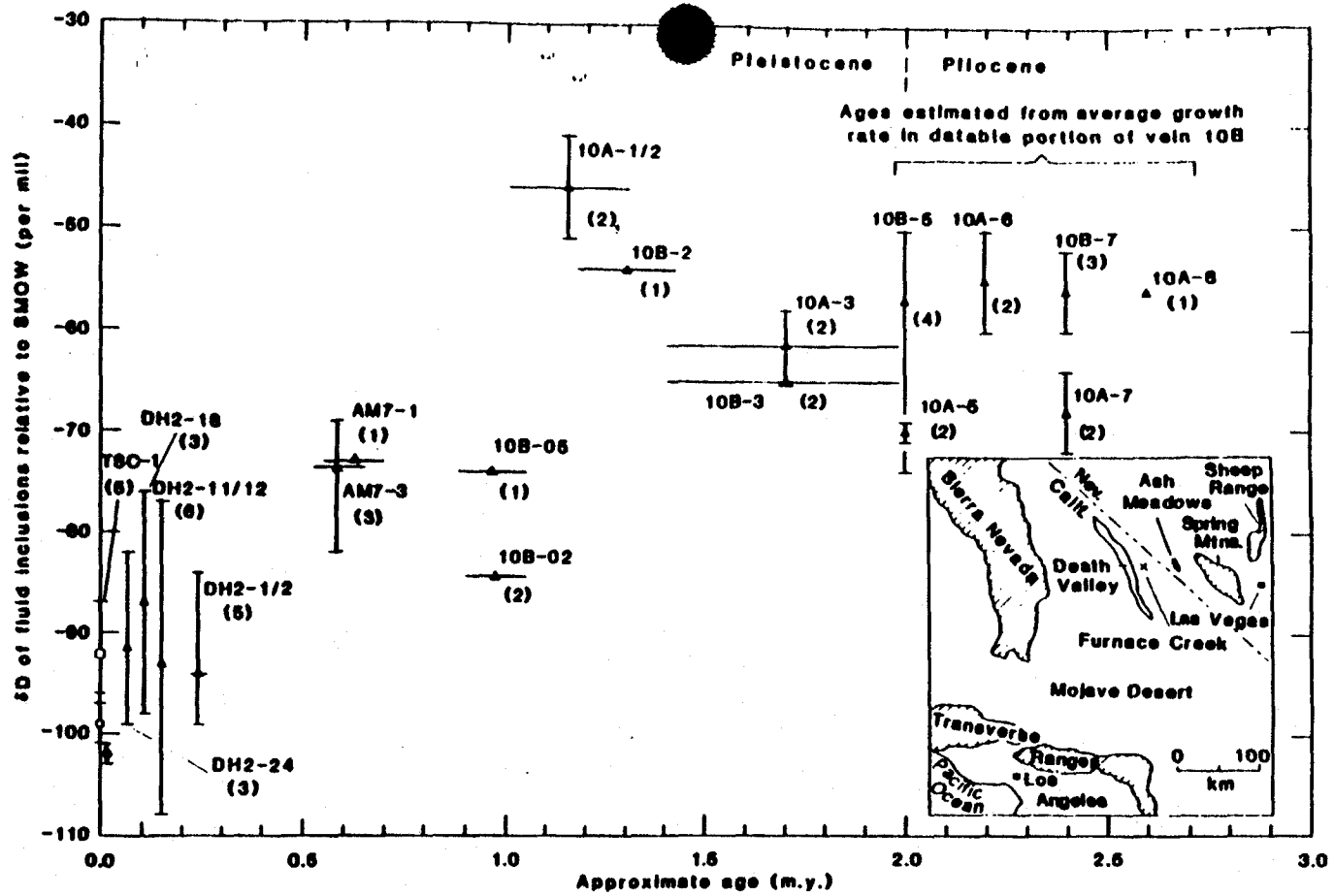

Explanation:

▲ - mean value of the δD ratio from a calcitic vein; vertical bar is the range; number in parentheses is the number of analyses;

□ - value of the δD ratio - sample of flowstone from Trout Springs Cave in Spring Mountains;

o - value of the δD ratio - water samples from springs in Spring Mountains;

● - value of the δD ratio - water samples from the Ash Meadows springs;

the horizontal bar denotes the error in the indicated age; and

TSC - sample from Trout Springs Cave, DH - sample from Devil's Hole, AM - sample from Ash Meadows, and 10A and 10B are samples from Furnace Creek Wash in Death Valley.

Time-series for deuterium content of fluid inclusions. Plio-Quaternary calcitic veins from southern Great Basin of California and Nevada. From Winograd et al., (1985).

Figure 62.

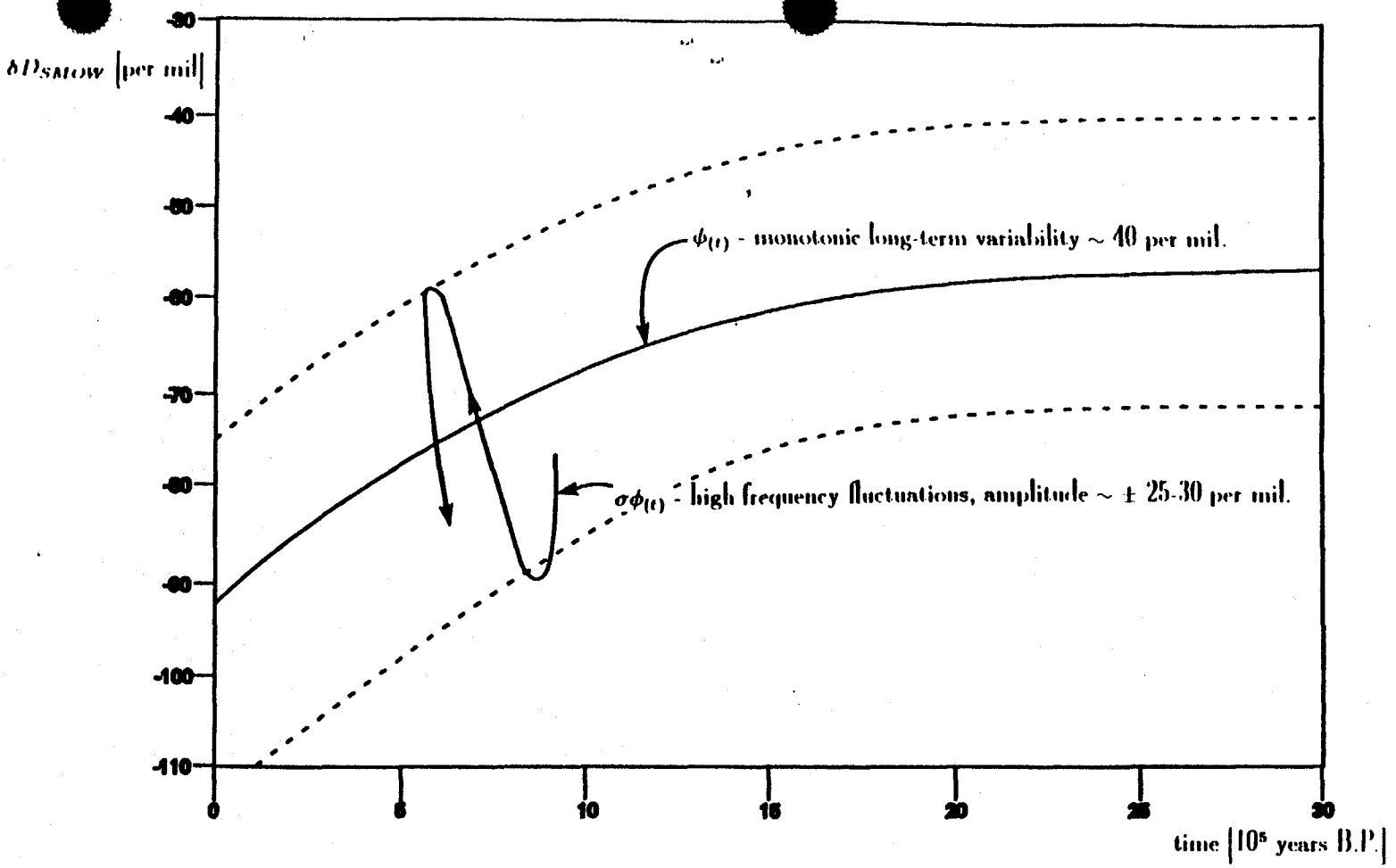

Note:

a) total temporal variability $\phi_{(t)} = \phi_{(t)} \pm \sigma\phi_{(t)}$; and

b) ϕ denotes deuterium content of parent fluids for the calcitic veins.

Schematic representation of time-series for deuterium content of fluid inclusions. Plio-Quaternary calcitic veins from southern Great Basin of California and Nevada.

Figure 63.

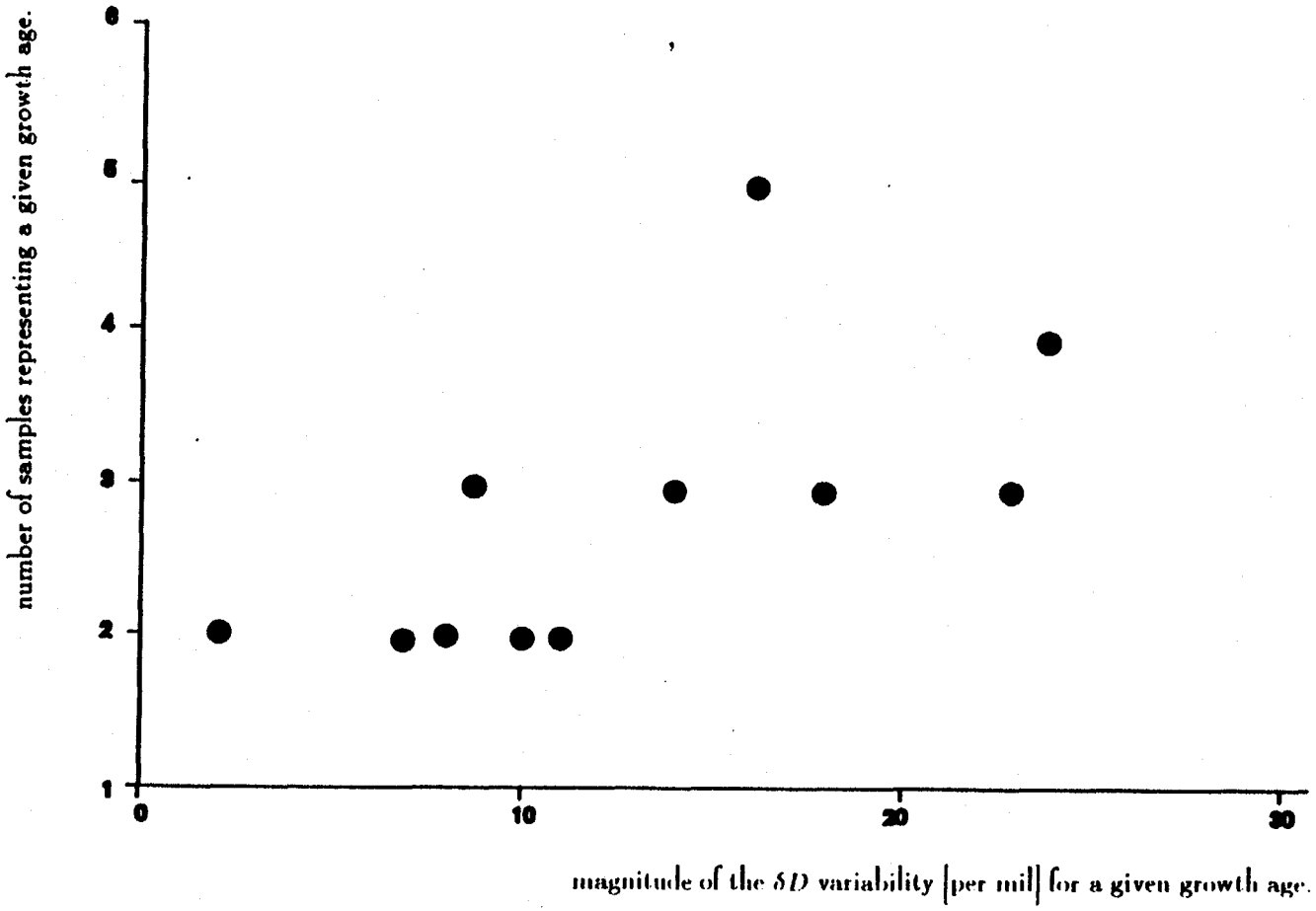

Note:

a) data are from Winograd et al. (1985).

Amplitude of the δD variability as a function of number of samples representing a given growth age. The DH-2 calcitic vein.

Figure 64

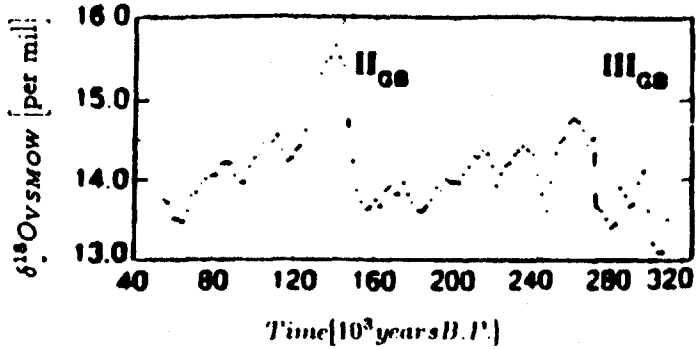

Note:

a) each dot represents a $\delta^{18}O$ analyzed sample;

b) the average sampling interval is 1.27mm - the corresponding $\delta^{18}O$ ratio represents a mean value fro a time span of 2300 ± 100 years; and

c) during the time span from 4 x 10^4 to about 3.5 x 10^5 years B.P.; which is equivalent to the time span represented by the Yucca Mountain sub-surface veins, the mean value for the $\delta^{18}O$ ration fluctuated with a maximum amplitude of about 2.7 per mil.

Time-series for the oxygen 18 content in the parent fluids for the Devils's Hole (DH-2) vein. From Winograd et al., (1988).

Figure 65.

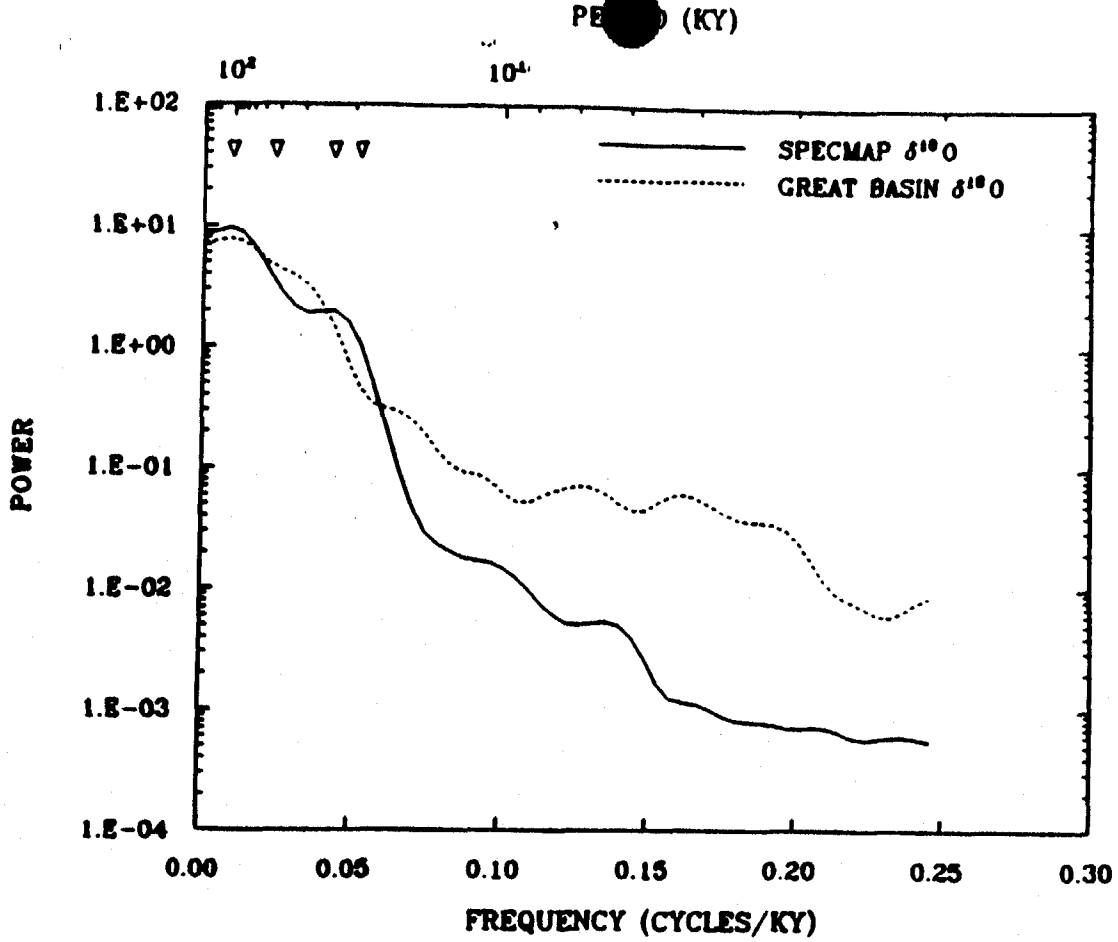

Note:

a) tick marks refer to dominant orbital periods of 100, 41, 23, and 19 KY.

A comparison of the smoothed spectral functions. The SPECMAP and Devil's Hole $\delta^{18}O$ records. From Crowley and Howard, 1990.

Figure 66.

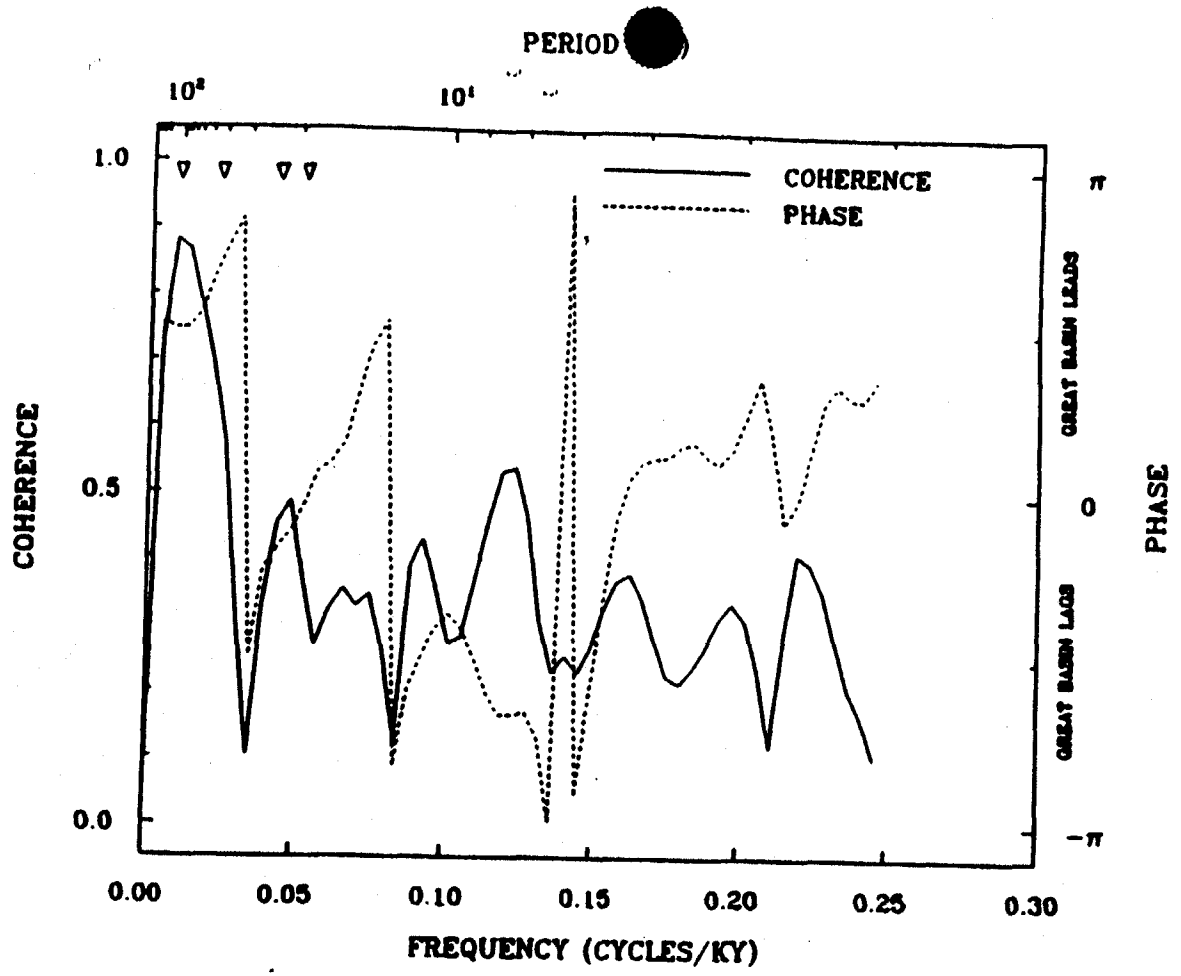

Note:

a) tick marks refer to dominant orbital periods of 100, 41, 23, and 19 KY.

Smoothed cross-spectral analyses. The SPECMAP and Devil's Hole $\delta^{18}O$ records. From Crowley and Howard, 1990).

Figure 67.

Isotopic and chemical evidence for "sink" ↔ "source" transformations.

o Chemical and isotopic affinity between the vadose zone interstitial fluids and the local geothermal fluids.

i) Rainier Mesa; and

ii) Yucca Mountain.

o Isotopic affinity between the parent fluids for the calcite-silica deposits and the local geothermal fluids.

i) the U content vs. $^{234}U/^{238}U$ ratio field;

ii) the $^{87}Sr/^{86}Sr$ ratio; and

iii) the $\delta^{18}O$ vs. $\delta^{13}C$ field.

o Geothermal circumstances of formation of the Yucca Mountain calcite-silica deposits.

i) the precipitation temperatures; and

ii) the paleo-geothermal gradients.

The "sink" ↔ "source" transformations. The Nevada Test Site hydrosphere.

Figure 68.

o At Rainier Mesa, the interstitial fluids are chemically distinct from the fracture based fluids, both from the vadose zone and from below the water table.

o The relative (i.e., fracture fluids vs. interstitial fluids) proportions of the $Na^{+} + K^{+}$, $Ca^{++} + Mg^{++}$, and $Cl^{-} + SO_4^{=}$ ions are the same as the corresponding relative (i.e., "sink" fluids vs. "source" fluids) proportions in the Pahute Mesa area.

Inference: **The Rainier Mesa interstitial fluids are relict geothermal fluids - they were introduced into the rock matrix during previous "sink" - "source" transformations.**

Chemical and isotopic affinity between the vadose zone interstitial fluids and the local geothermal fluids. Rainier Mesa.

Figure 69

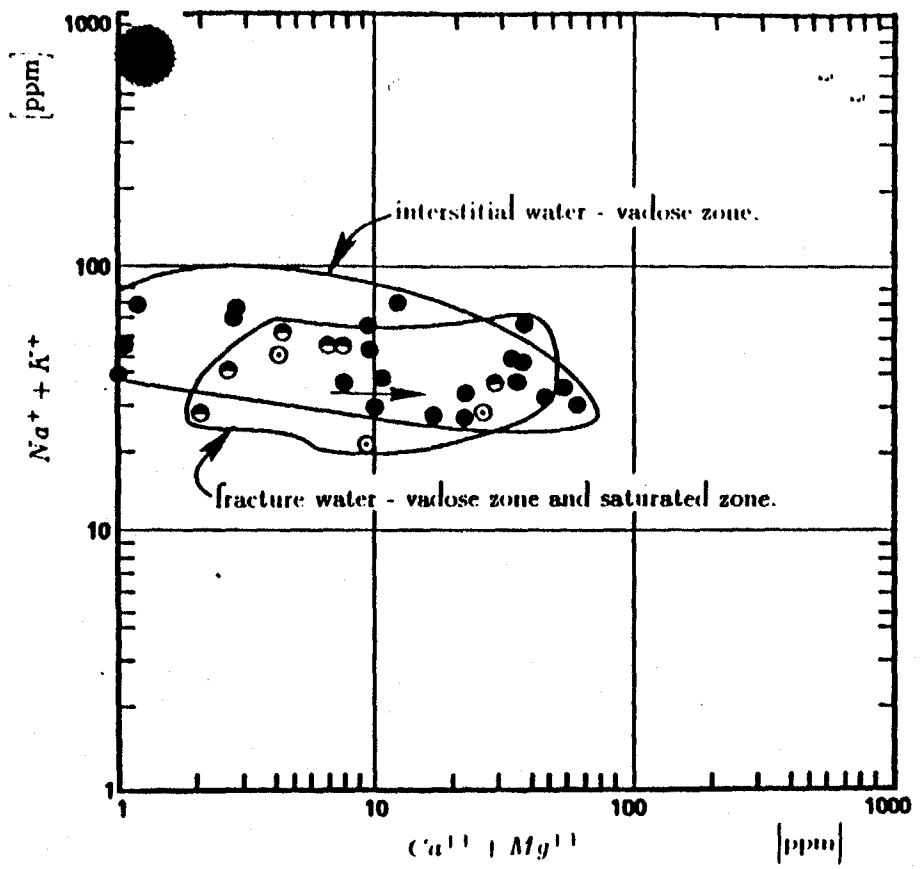

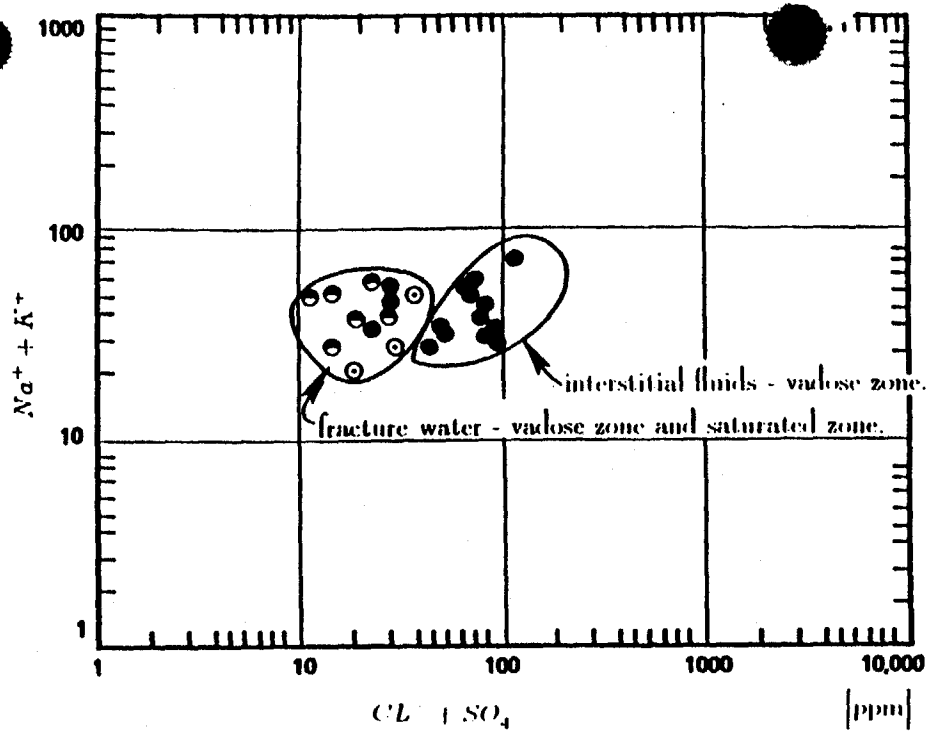

Explanation:

- ● - sample obtained from below the water table;
- ○ - sample obtained from spring;
- ◒ - sample represents fracture seep into a tunnel;
- ● - sample represents interstitial fluids from the vadose zone.

Note:

a) fluid chemistry data are from Claassen (1973); Blankennagel and Weir (1973); and White et al. (1980).

Figure 70.

Comparison of chemical compositions - fracture water against interstitial water. Rainier Mesa.

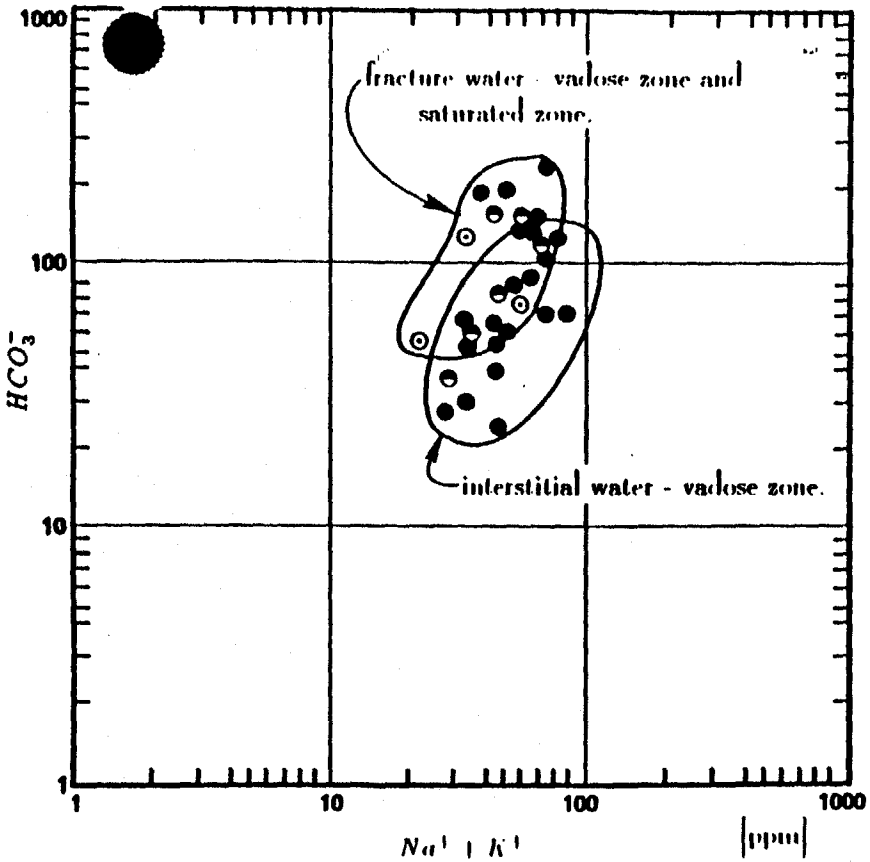

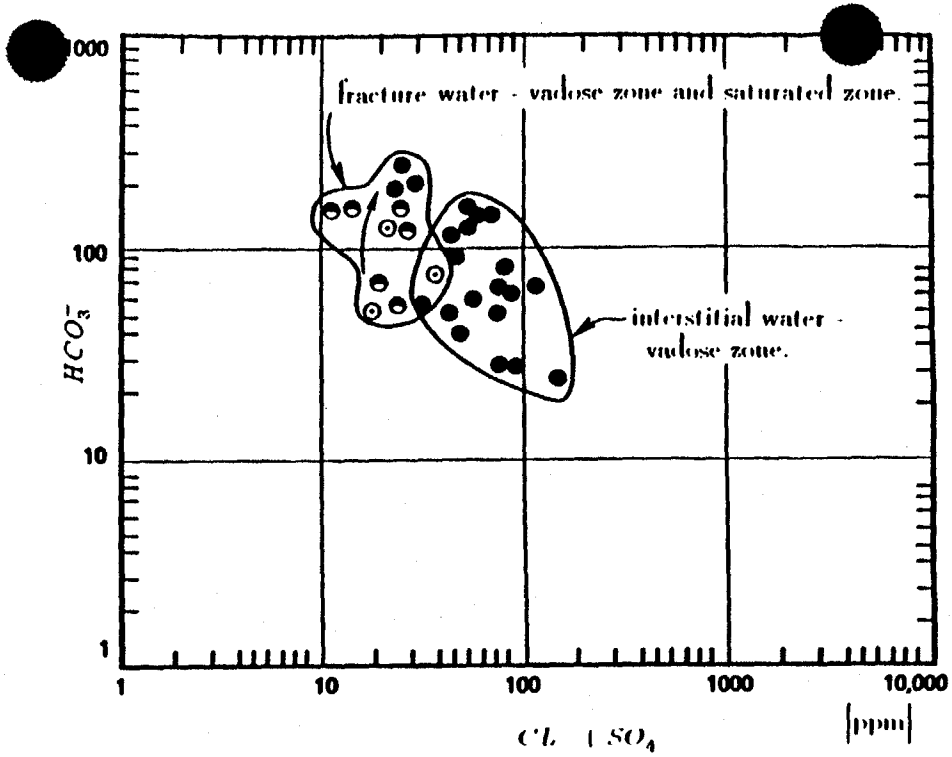

Explanation:

- ● - sample obtained from below the water table;
- ○ - sample obtained from spring;
- ◓ - sample represents fracture seep into a tunnel;
- ● - sample represents interstitial fluids from the vadose zone.

Comparison of chemical compositions - fracture water against interstitial water. Rainier Mesa.

Figure 71.

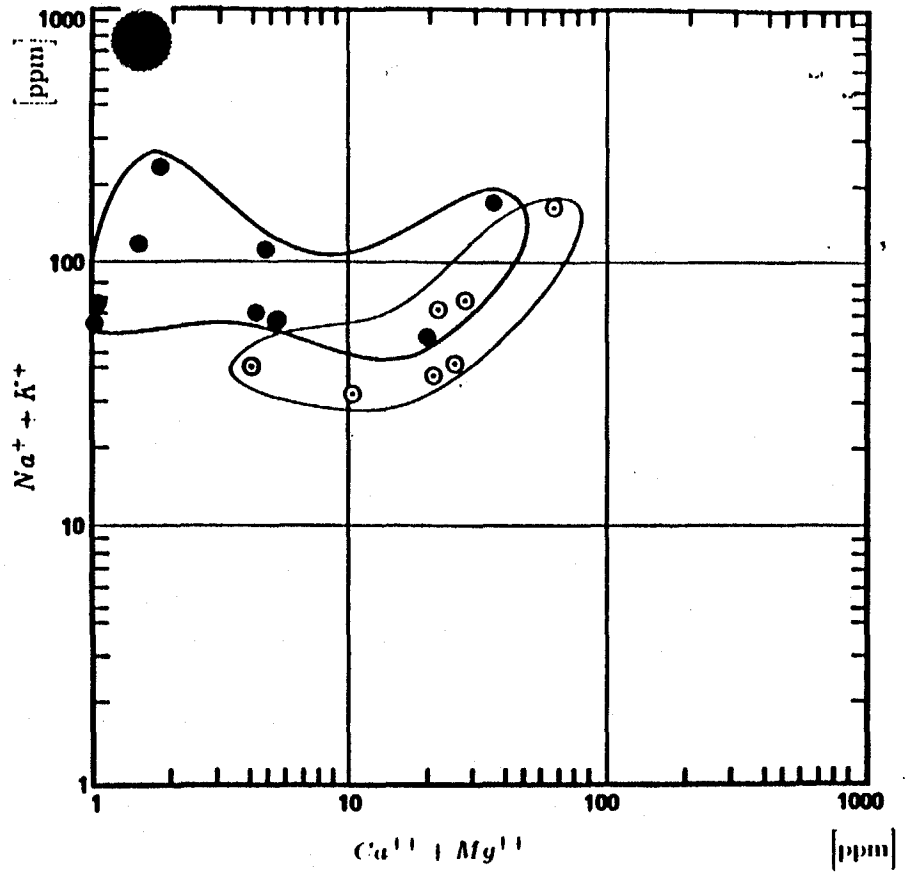

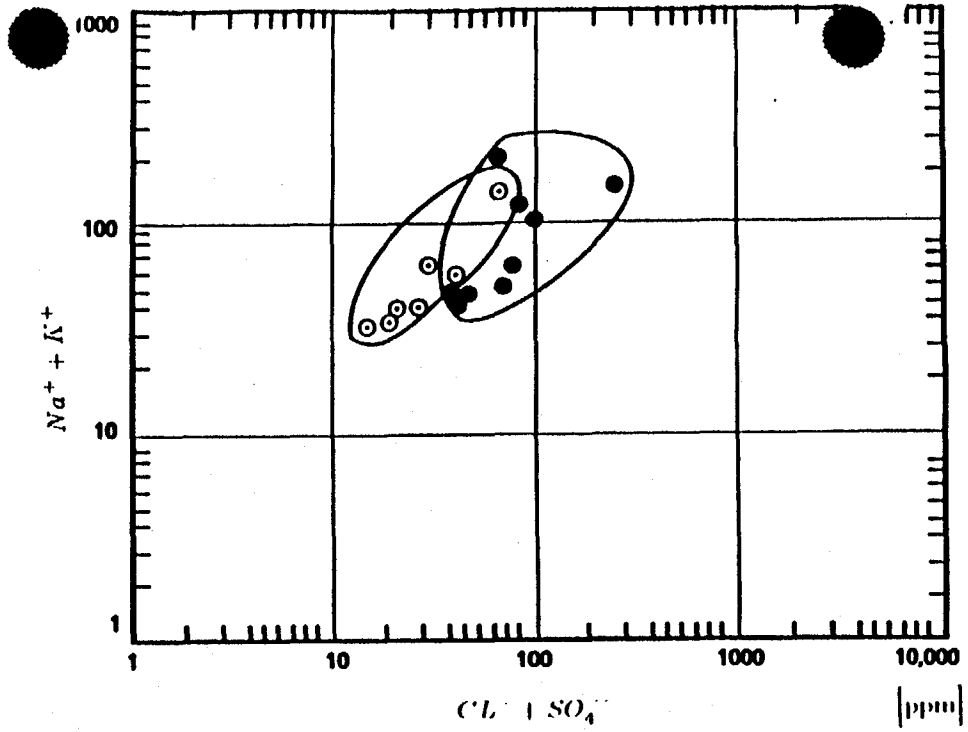

Explanation:

- ● - sample collected from hydraulic source area;
- ○ - sample collected from hydraulic sink area.

Comparison of chemical compositions - hydraulic "sink" region vs. hydraulic "source" region. Paiute Mesa.

Figure 72.

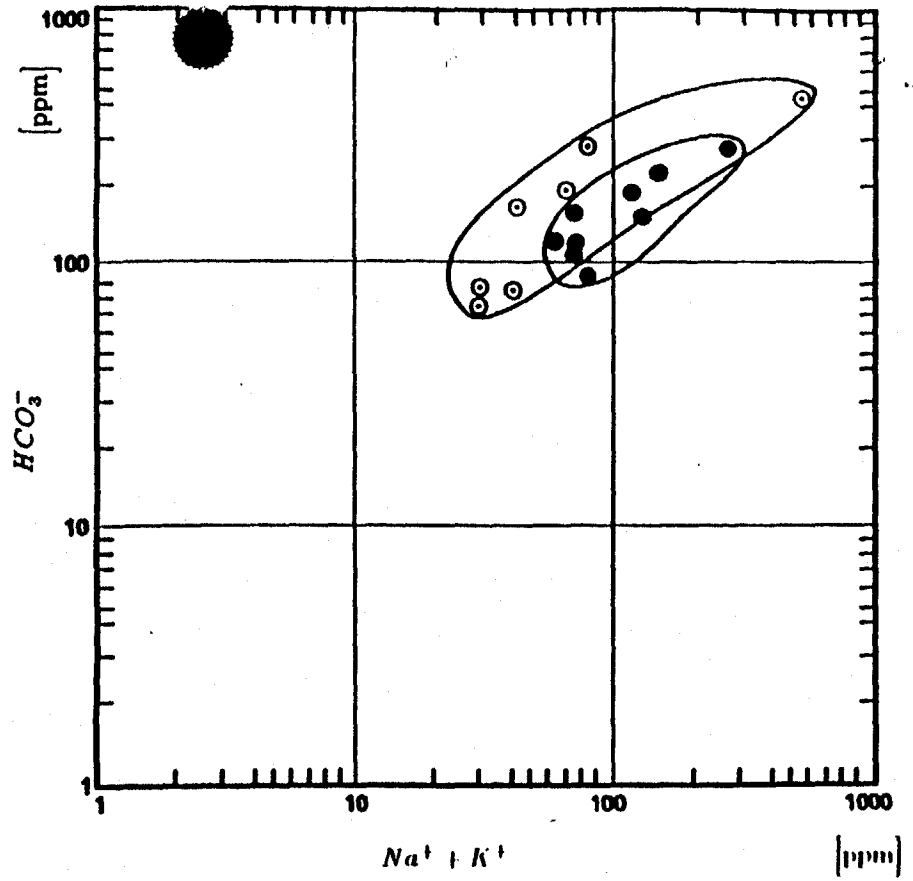

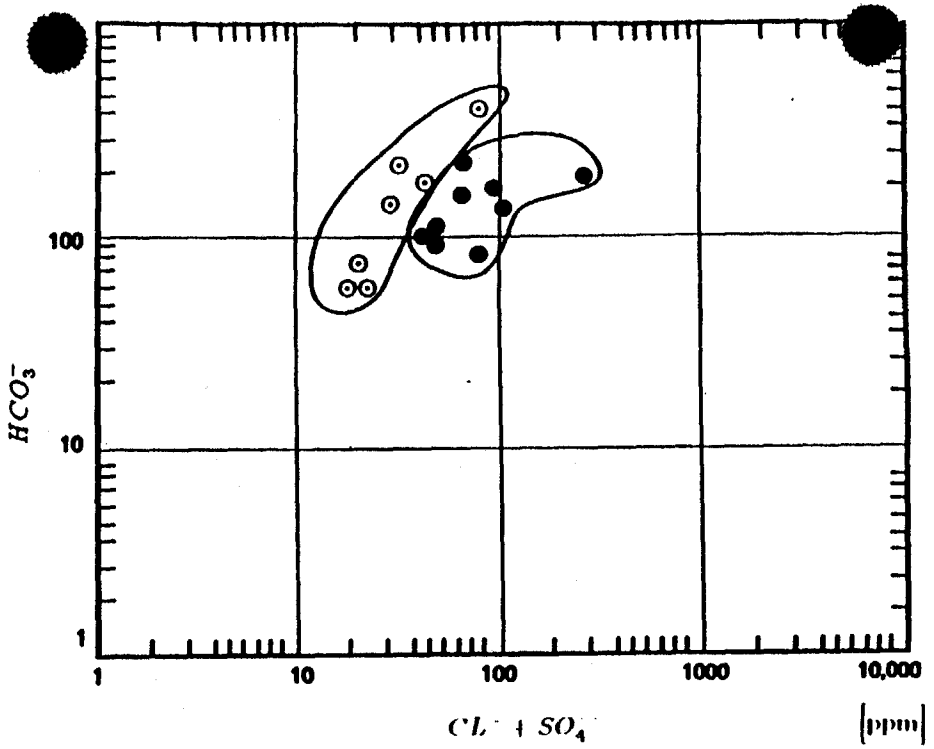

Explanation:

● - sample collected from hydraulic source area;

○ - sample collected from hydraulic sink area.

Comparison of chemical compositions - hydraulic "sink" region vs. hydraulic "source" region. Paiute Mesa.

Figure 73.

- At Yucca Mountain, the vadose zone interstitial fluids exhibit strong REE and bulk chemical affinity with the local deep seated geothermal fluids. The latter fluids are upwelling along the Tertiary/Paleozoic fault contact and were encountered in borehole UE 25p#1, depth ~ 1200m.

- The δD and $\delta^{18}O$ isotopic composition of the interstitial fluids may readily be explained by assuming that these fluids are the result of intermixing of fresh meteoric fluids with the older geothermal fluids. The observed "hydrogen-oxygen isotopic shift" is directly attributable to the *in-situ* evaporative deuterium and oxygen - 18 enrichment.

Conclusion: **The Yucca Mountain interstitial fluids are, in part, the relict geothermal fluids.**

Chemical and isotopic affinity between the vadose zone interstitial fluids and the local geothermal fluids. Yucca Mountain.

Figure 74.

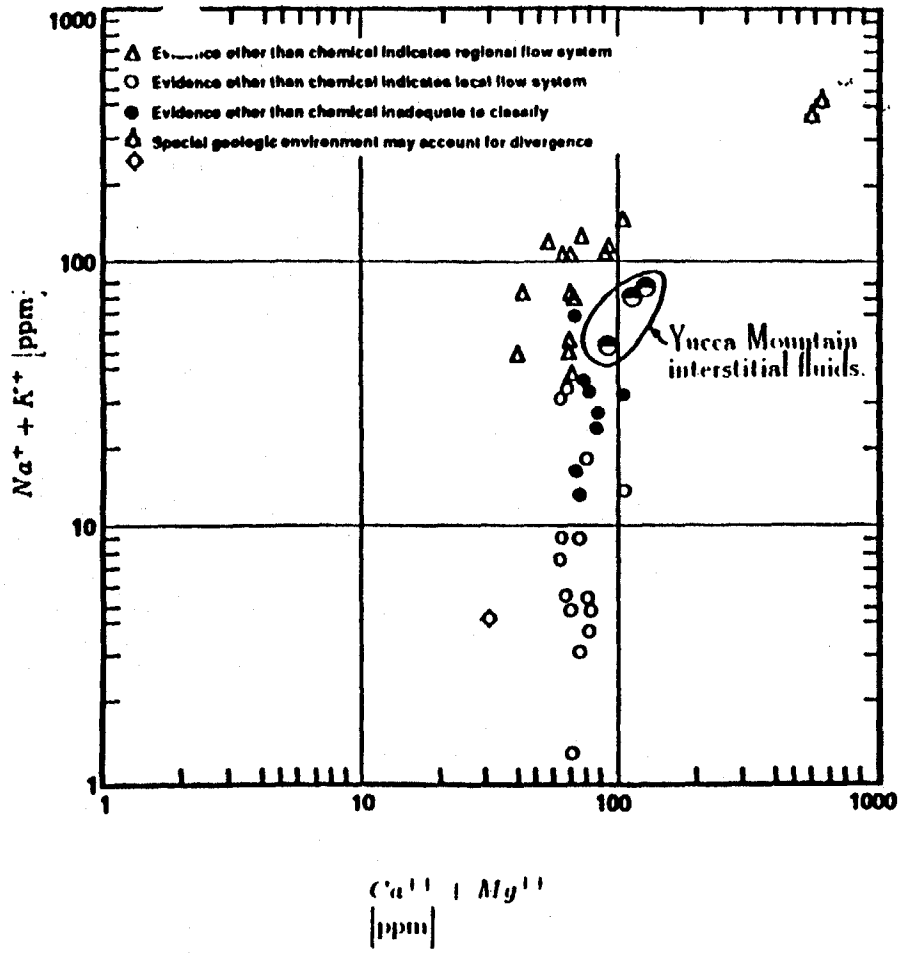

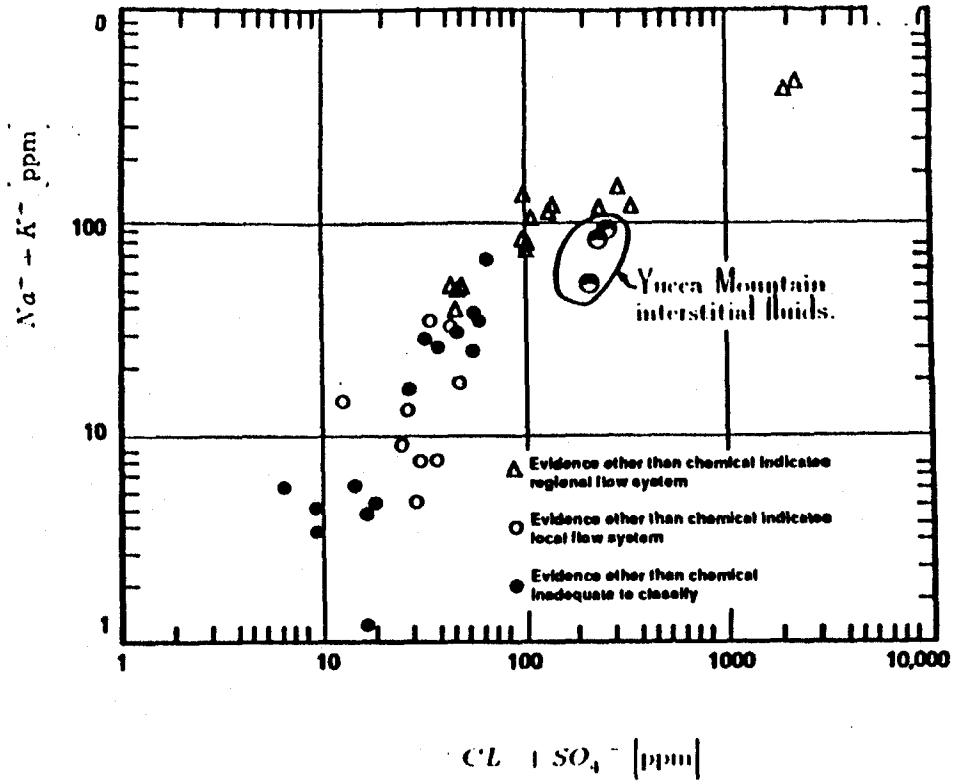

Note:

a) fluid chemistry data for the Yucca Mountain interstitial fluids are from Yang et al. (1989).

A comparison of geochemical compositions of fluids - the Yucca Mountain interstitial fluids and fluids from the carbonate - based flow system of Nevada. Modified from Domenico, 1972.

Figure 75

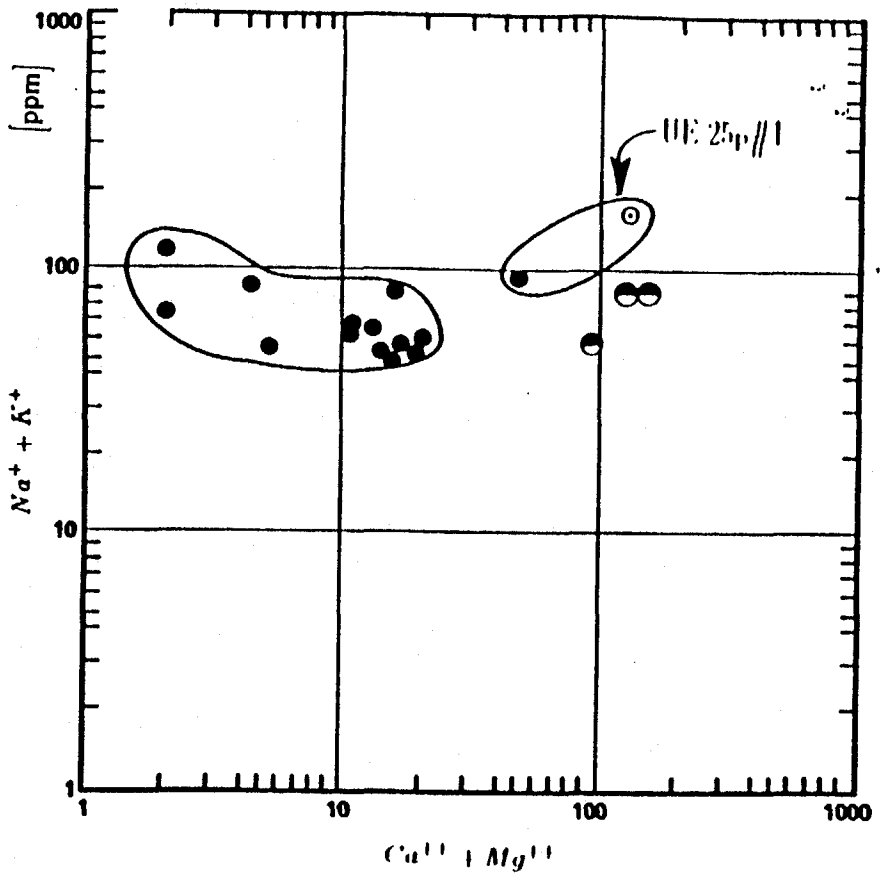

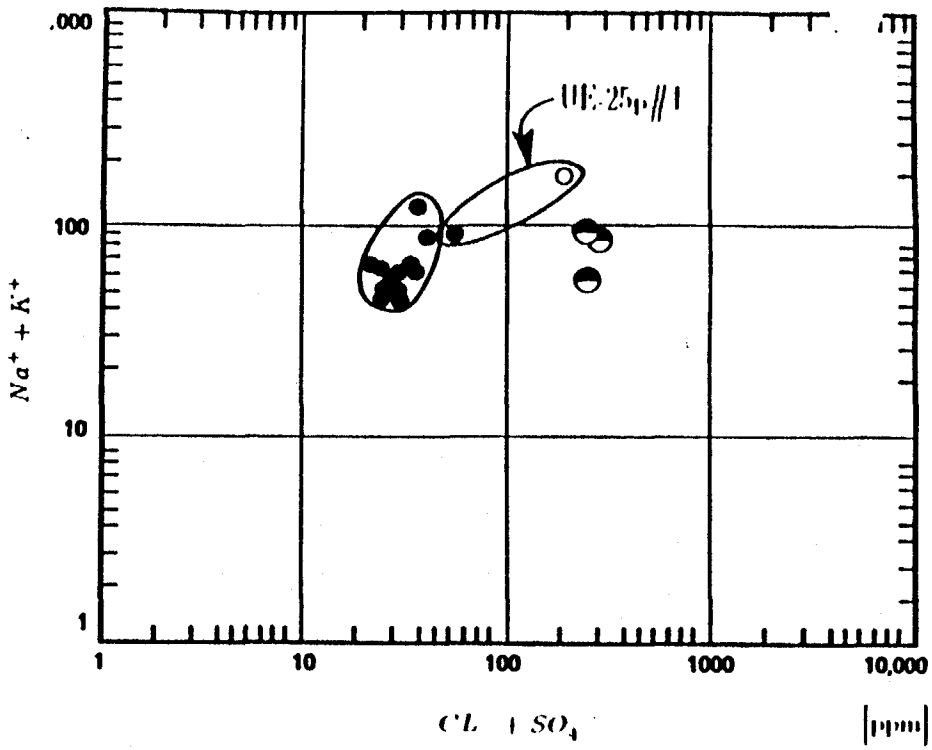

Note:

a) fluid chemistry data are from Benson and McKinley (1985) and Yang et al. (1989).

Explanation:

- ● - sample represents fluids from within the Yucca Mountain *in-situ* stress field inclusion;
- ○ - sample represents deeper fluids from the underlying hydraulic "source";
- ◓ - sample represents interstitial fluids from the local vadose zone.

Comparison of chemical compositions of subsurface fluids. Fracture water from below the water table against interstitial water from the vadose zone, Yucca Mountain.

Figure 76.

TABLE 3 Trace element data for J-12 and J-13 Well waters

Sample #	J-12	error	J-13	error	SLRS-1*	cert. val
pH (field)	7.3		--			
pH (lab)	7.89					
F(ppm)	2.00					
Cl(ppm)	7.5					
NO3(ppm)	8.2					
SO4(ppm)	22.2					
HCO3(ppm)	119					
Li	50	15	40	10	15	
B	130	10				
Na(ppm)	41.8	1.3				10.4
Mg(ppm)	2.45	0.15	2.4	0.2		5.95
Al	1.2	0.6	0.5			23.6
Si(ppm)	28.6	1.1	30	5		
Cl(ppm)	7.5	0.5				
K	5.6	0.7				1.3
Ca(ppm)	15	0.2	14	5	25	25.1
Sc	<1		<3		0.34	
Ti	0.08		0.1		0.7	
V	4	1	6	1	0.73	0.66
Cr	0.37	0.13	0.35	0.03	0.26	0.34
Mn	0.15	0.06	<0.3		1.19	1.77
Fe	3	1	3		27.3	31.6
Co	<0.01		<0.01		0.023	0.043
Ni	0.03	0.01	0.05	0.01	0.7	1.07
Cu	0.2	0.06	0.8	0.2	2.8	3.58
Zn	2.7	0.3	2.4	0.5	0.85	1.3
As	0	3	0	3	0.53	0.55
Rb	9.2	1.1	6.3	1	3.83	
Sr	35	1	33	2	133	136
Y	0.0025	0.0008	0.0025	0.0008	0.28	
Mo	5	0.5	5.3	0.1	0.62	0.76
Pd	<0.01		<0.01			
Cd	<0.05		<0.05		0.011	0.015
Sb	0.15	0.01	0.21	0.01	0.37	0.63
I	2		2		2.22	
Te	<0.01		<0.03		<0.01	
Cs	0.56	0.02	0.96	0.16	0.0032	
Ba	1.75	0.35	176.8		21.5	22.2
La	0.0004		0.0003		0.04	
Ce	<0.008		0.0006		0.069	
Pr	<0.001		<0.001		0.01	
Nd	<0.001		<0.001		0.057	
Sm	<0.001		<0.001		0.02	
Eu	<0.001		<0.001		0.0014	
Gd	<0.001		<0.001		0.005	
Tb	<0.001		<0.001		0.0007	
Dy	<0.001		<0.001		0.0035	
Ho	<0.001		<0.001		0.0006	
Er	<0.001		<0.001		0.003	
Tm	<0.001		<0.001		0.0003	
Yb	<0.001		<0.001		0.0028	
Lu	<0.001		<0.001		0.0004	
Hf	0.001		<0.002			
Ta	<0.001		<0.001			
W	1.0	0.2	2.0	0.4	0.13	
Re	0.044	0.01	0.0020.43		0.003	
Pt						
Au					0.0005	
Tl	0.01	0.004	0.004			
Pb	0.2	0.06	0.3	0.1	0.082	0.156
Bi	<0.001		<0.003		0.001	
Th	0.0001	0.00003	0.0004	0.0002	0.003	
U	0.55	0.13	0.4	0.14	0.25	0.28

* Riverine Water Reference Material for Trace Metals (Nawona) Research Council Canada)

Note:

a) concentrations are in ppb unless noted:

b) water samples are from below the water table;

c) host rock is rhyolitic tuff;

d) $logP_{CO_2}$ ranges from −2.10 to −2.11 atm. and PMC = 29.2 - 32.2 percent; and

e) SLRS-1. Riverine Reference Standard.

The results of trace element analyses. Water samples from J-12 and J-13 Wells. From Smith (1991).

TABLE 4. Trace element data for Pore Water Samples from UZ#4

Sample #	Pore wat 8110926	error	USGS (reported)	Pore wat 8110923	error	USGS (reported)
pH			8.5			8.5
SO4(ppm)						190
Li	80			85	10	
B						
Na(ppm)			46			53
Mg(ppm)	27	5	21	25		23
Al				<5		
Si(ppm)			74			78
Cl(ppm)			160			210
K			5			14
Ca(ppm)	120	10	120	110	10	130
Sc	<3	1		0.4		
Ti				<3		
Cr	<8	<3		0.6	0.1	
Mn	133	25	150	14	3	90
Fe	35	5	150	<20		<3
Co				<1		
Ni	40	10		<50	16	
Cu	40	10		10	1	
Zn	180	15		71	5	
Rb	23	2		12	2	
Sr	1020	110		1180	110	
Y	0.3	0.1		0.21	0.06	
Mo	1880	180		1400	30	
Cd				1.4	0.3	
Sb	1			0.7	0.2	
I	50			40		
Cs	0.5	0.1		0.44	0.06	
Ba	27	3		18	1	
La	<0.1			0.007	0.007	
Ce	<0.1			0.048	0.02	
Pr	<0.04			<0.008		
Nd	<2			<0.05		
Sm	<0.3			<0.006		
Eu	<0.06			<0.006		
Gd	<0.2			<0.003		
Tb	<0.03			0.013	0.005	
Dy	0.09	0.03		0.032	0.008	
Ho	<0.1			0.022	0.008	
Er	0.14	0.04		0.12	0.02	
Tm	0.05	0.02		0.04	0.01	
Yb	0.5	0.2		0.5	0.10	
Lu	0.14	0.06		0.16	0.05	
Hf	0.01			0.3	0.1	
Ta	0.5			<0.2		
W	900	200		330	50	
Re	0.2	0.09		0.2	0.1	
Pt	0.2	0.1		0.2	0.05	
Au	0.12	0.05		0.2	0.1	
Tl	0.2			0.2		
Pb	0.25	0.1		1.7	0.3	
Bi	<0.03			<0.1		
Th	0.0024	0.0006		<0.01		
U	0.45	0.09		0.13	0.03	

Note:

a) concentrations are in ppb unless noted;

b) samples represent the interstitial fluids from the Yucca Mountain vadose zone;

c) host rock is unwelded rhyolitic tuff; and

d) samples of fluid were extracted by centrifugation.

The results of trace element analyses. Interstitial fluids from the Yucca Mountain vadose zone (borehole UZ-4). From Smith (1991).

Figure 78.

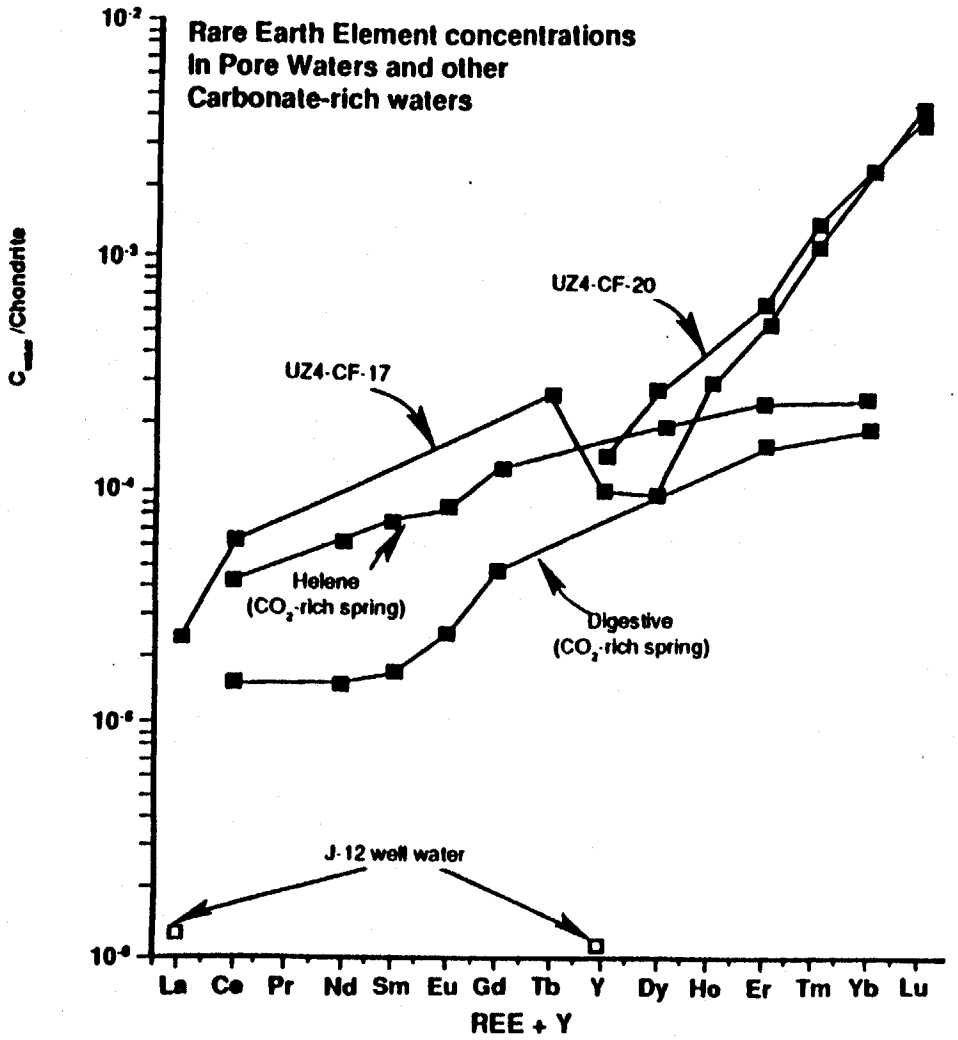

Note:

a) the expected REE abundance pattern for interstitial fluids from the rhyolitic tuffs is one of the high abundances of the light rare earth elements (i.e., La → Sm);

b) the observed REE abundance pattern is one of the high relative abundances of the heavy rare earth elements (Tb → Lu);

c) the interstitial fluids carry high concentrations of the alkaline earth elements (i.e., Mg, Ca, Sr, and Ba) - this suggests dissolution of the Paleozoic carbonates, which occur 1km below; and

d) the complexation of HREE by carbonate rich waters explains the abnormally high HREE concentrations.

Comparison of trace element abundances. The local subsurface fluids (Well J-12), the interstitial fluids from the Yucca Mountain vadose zone (U24-CF-17 and U24-CF-20), and the CO_2 - rich fluids from Vals-les-Baines (Helene and Digestive). From Smith, 1991.

Figure 79.

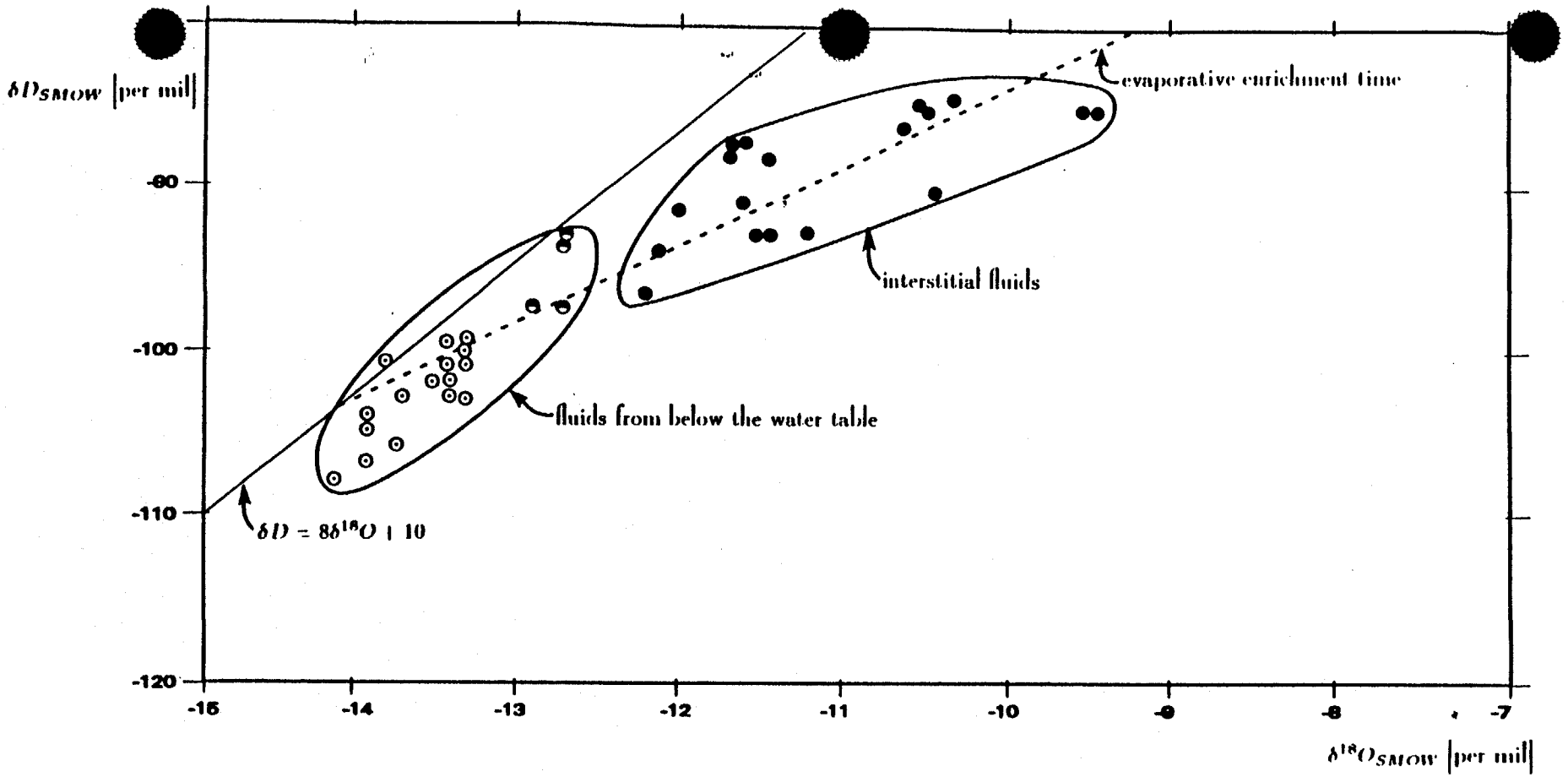

Explanation:

● - sample represents interstitial fluids from the vadose zone (^{14}C age ~ 10^3 - 4.9 x 10^3 years B.P.);

⊖ - sample represents fluids from below the water table (^{14}C age ~ 3.8 x 10^3 - 9.9 x 10^3 years B.P.);

○ - sample represents fluids from below the water table (^{14}C age ~ 12 x 10^3 - 18.5 years B.P.).

Note:

a) isotopic data are from Benson and McKinley (1985) and Yang et al. (1989).

A comparison of isotopic chemical compositions, interstitial fluids and fluids from below the water table. Yucca Mountain.

Figure 80.

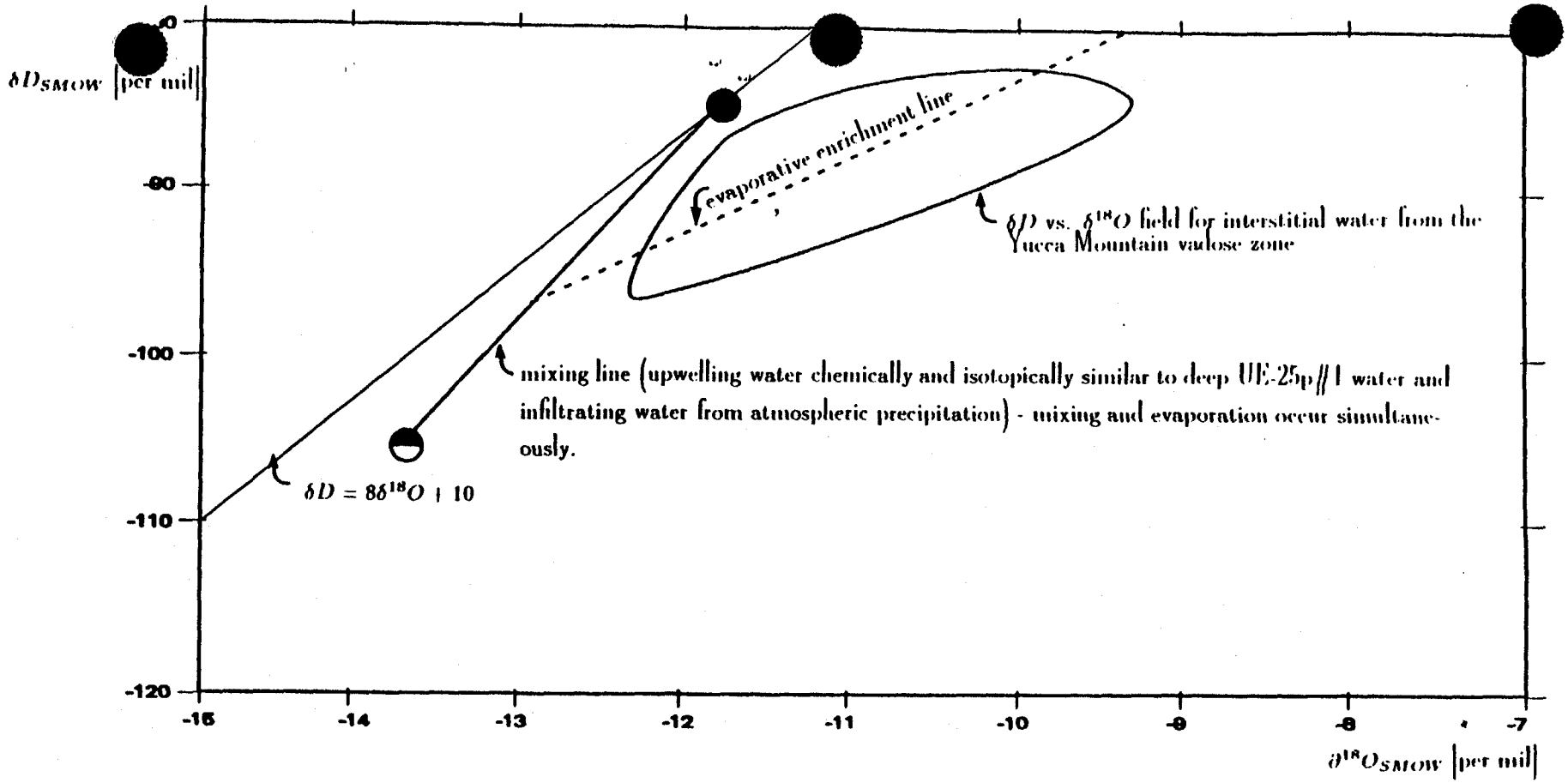

Explanation:

- isotopic composition of deep water from Well UE 25p#1 (Benson and McKinley, 1985);

- mean isotopic composition of the Yucca Mountain recharge (isotopic smoothing - based on studies at Rainier Mesa, altitude correction $d\delta D/dz \sim 1.3$ per mil per 10^2m, Dansgaard, 1964.)

Interpretation of meaning of chemical and isotopic compositions of interstitial water from the Yucca Mountain vadose zone.

Figure 81.

o The interpreted U-series characteristics of the parent fluids for the Nevada Test Site calcite-silica deposits are: a) value of the $^{234}U/^{238}U$ activity ratio ranging from 1.0 to ~ 3.5; and b) value of the U concentration varying over a range of 1-2 orders of magnitude;

o The interpreted U-content vs. $^{234}U/^{238}U$ field, for the parent fluids of the Nevada Test Site calcite-silica deposits, overlaps with the corresponding field from samples of the local geothermal fluids.

Conclusion: a) **The Nevada Test Site calcite-silica deposits, including: a) calcretes; b) surficial fault-infillings; and c) subsurface veins, were formed via the *per ascensum* process;**

b) **In the past, the Nevada Test Site hydrosphere have experienced the "source" ↔ "sink" transformations.**

Isotopic affinity between the parent fluids for the calcite-silica deposits and the local geothermal fluids - the U content vs. $^{234}U/^{238}U$ field.

Figure 82.

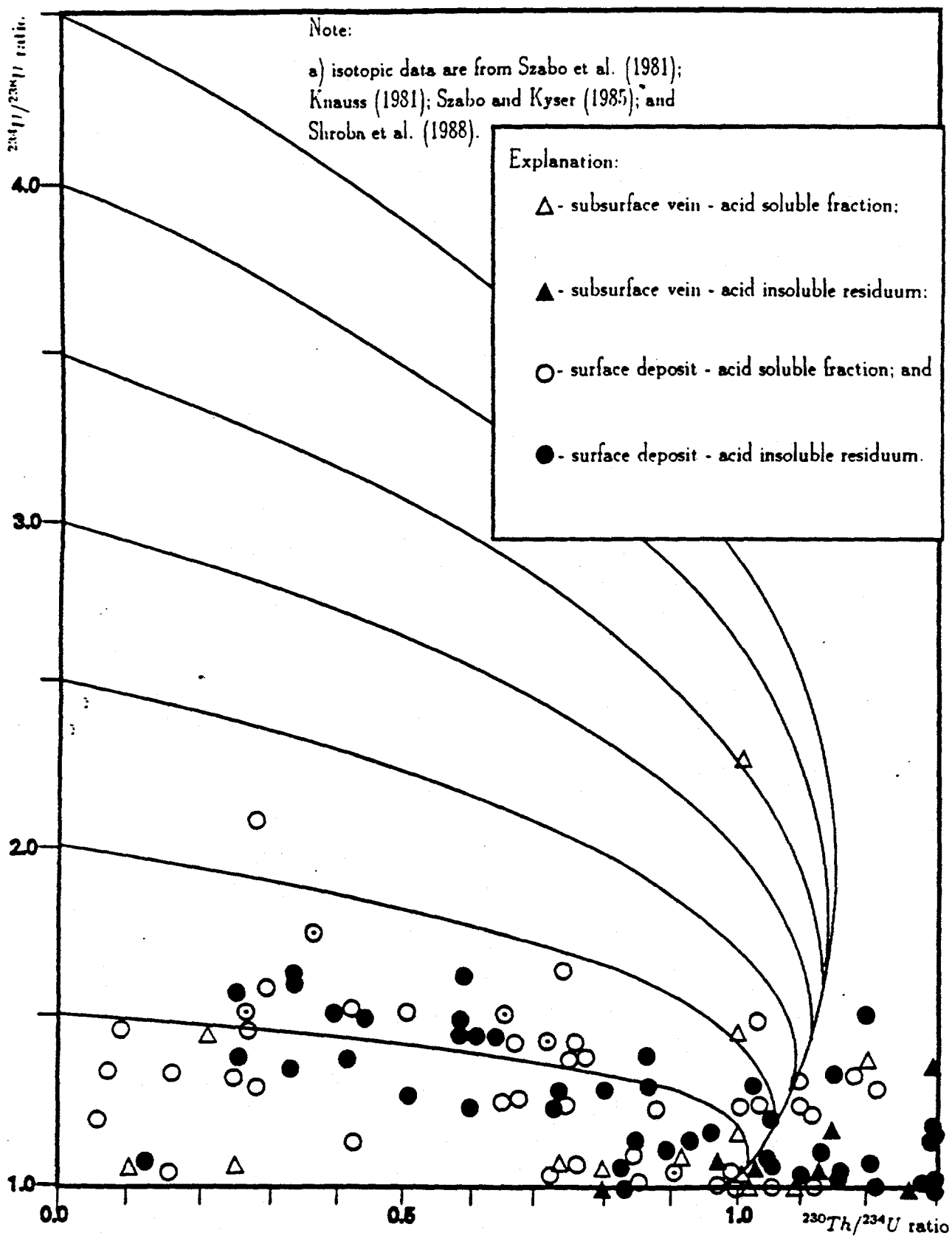

Variation of $^{234}U/^{238}U$ and $^{230}Th/^{234}U$ activity ratios. The Nevada Test Site hydrogenic deposits.

Figure 83.

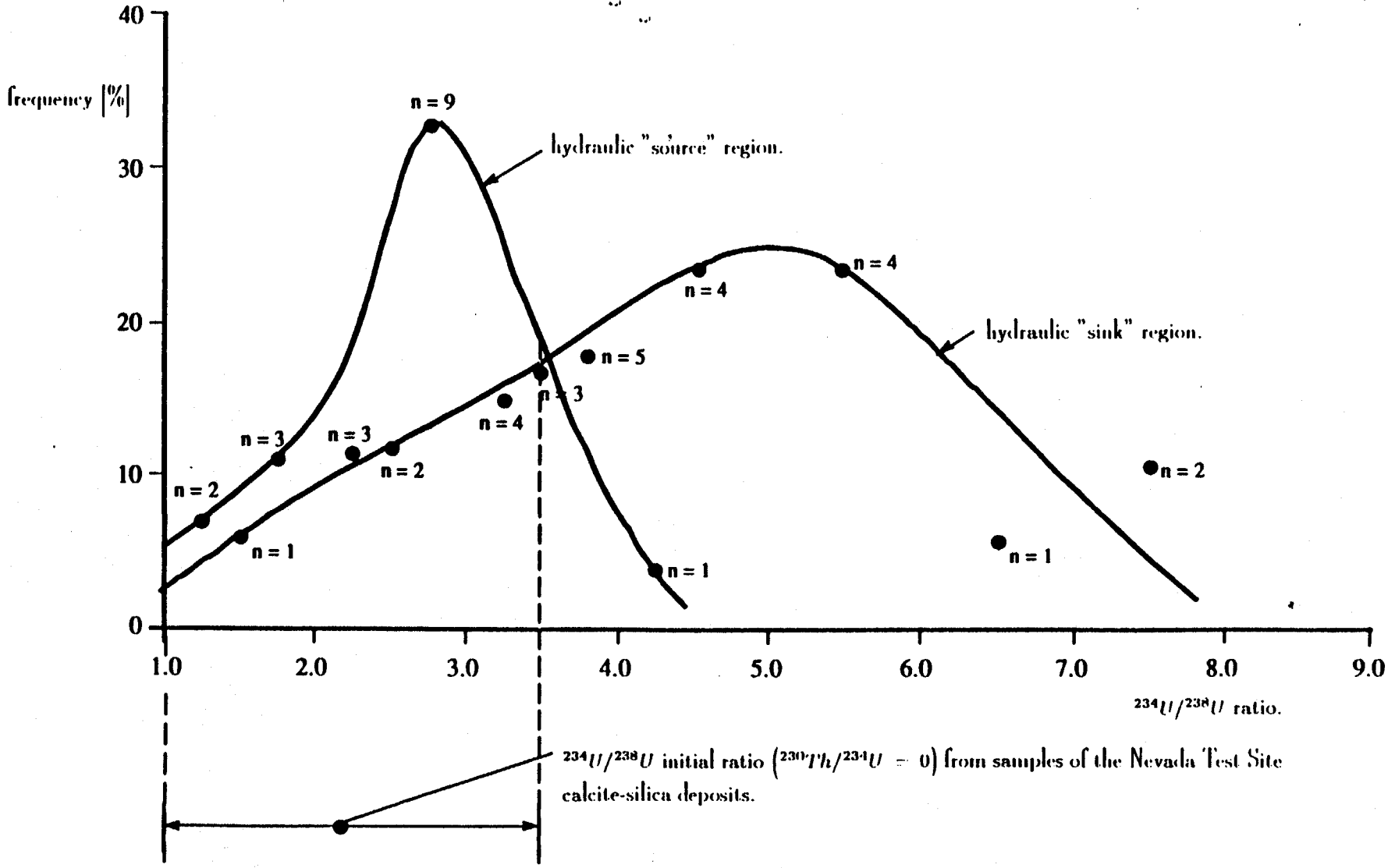

Comparison of the $^{234}U/^{238}U$ ratios. The Nevada Test Site calcite-silica deposits and the local hydraulic "source" regions.

Figure 81

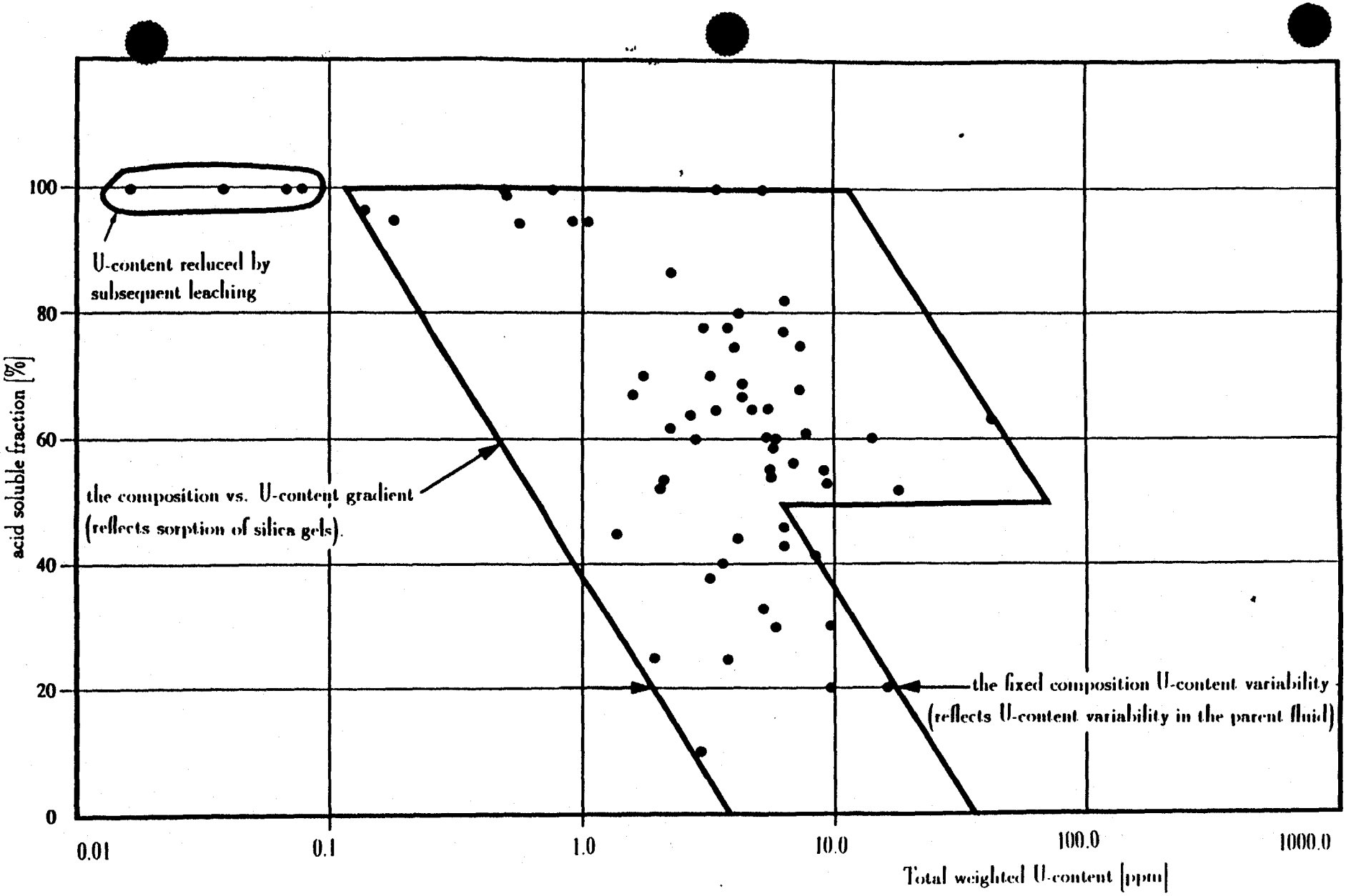

Total U-content vs. percentage of acid-soluble fraction. Hydrogenic deposits from the Nevada Test Site.

Figure 85.

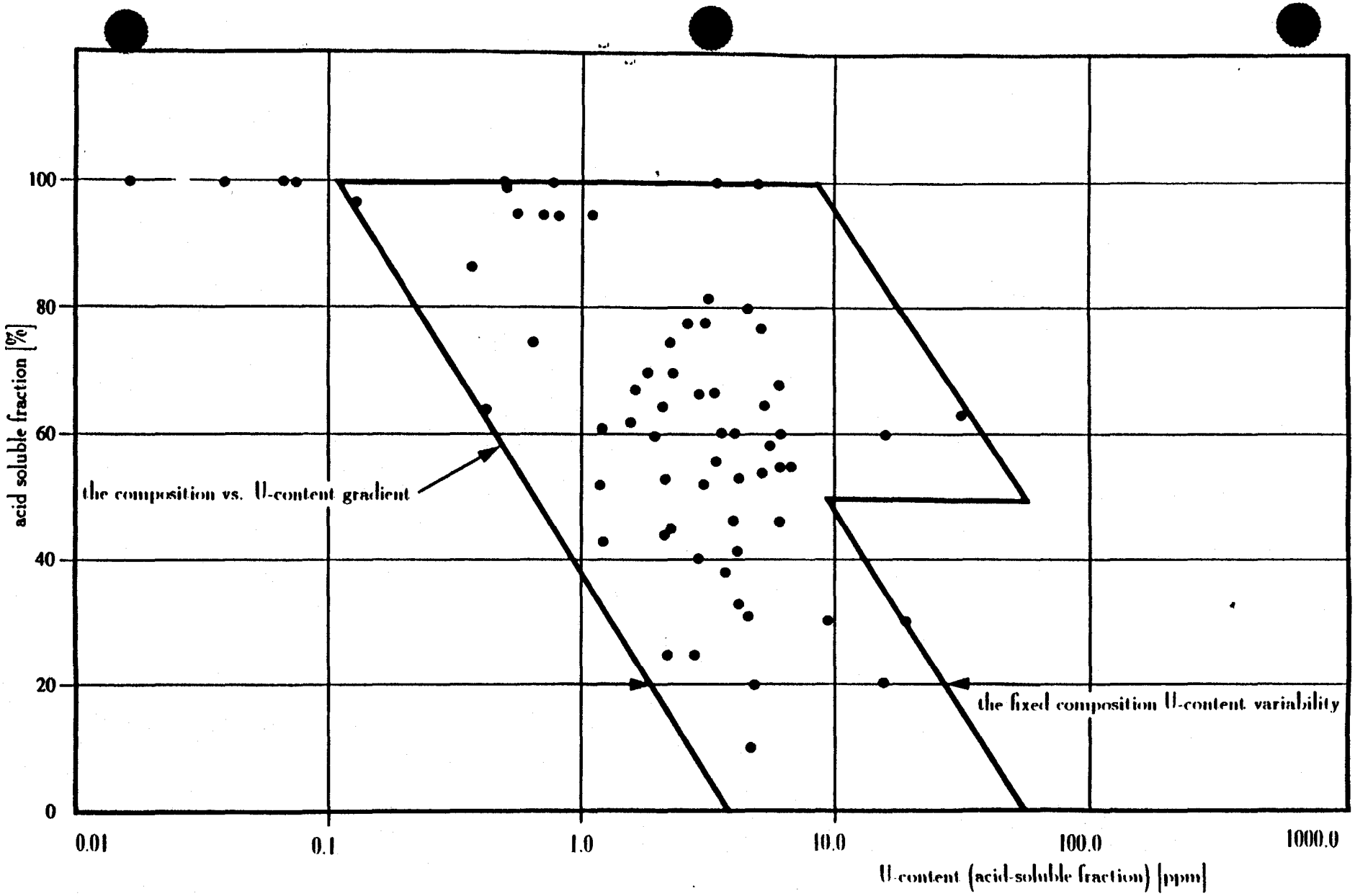

U-content vs. percentage of acid-soluble fraction. Hydrogenic deposits from the Nevada Test Site.

Figure 86.

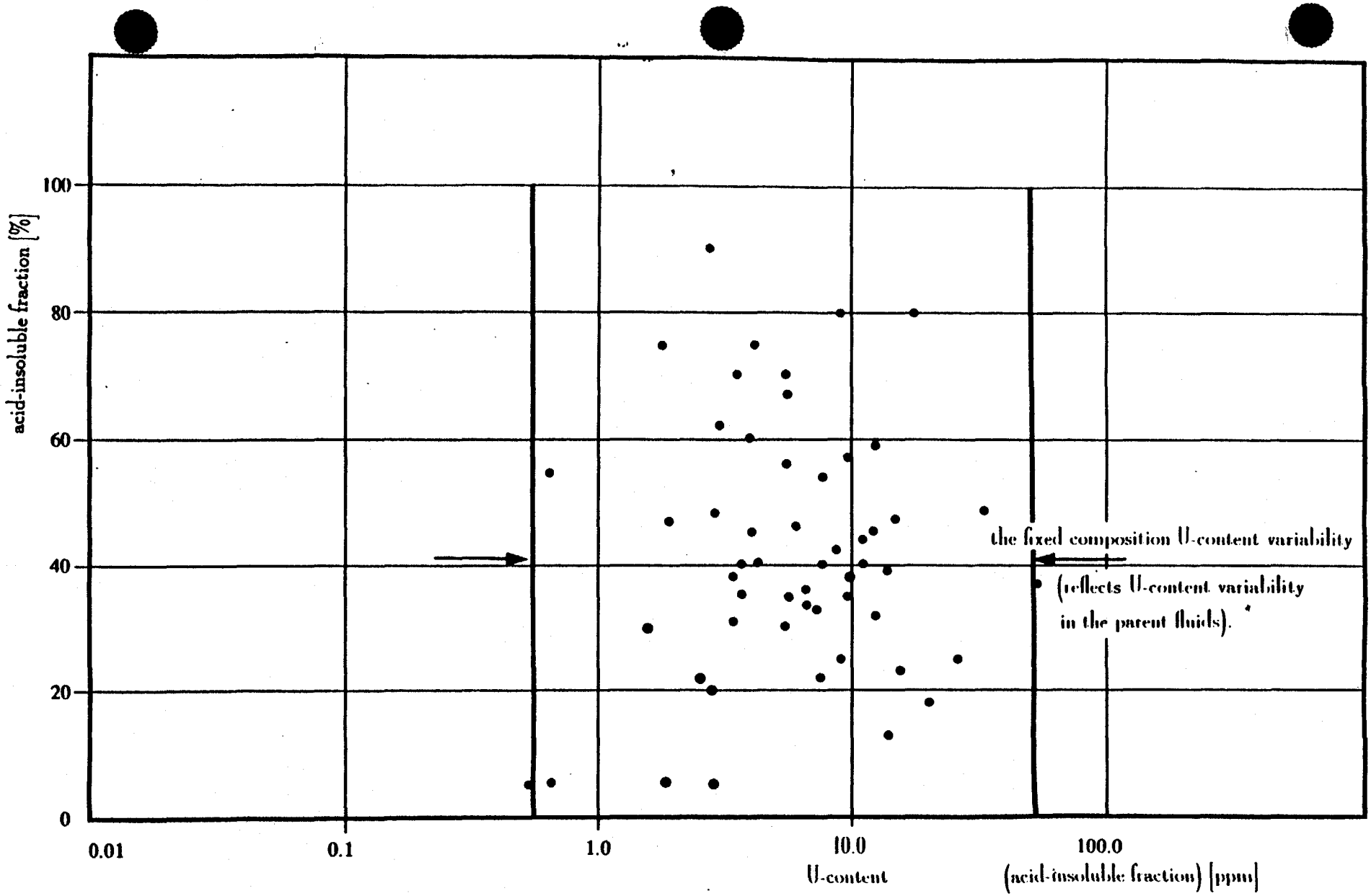

U-content vs. percentage of acid-insoluble fraction. Hydrogenic deposits from the Nevada Test Site.

Figure 87.

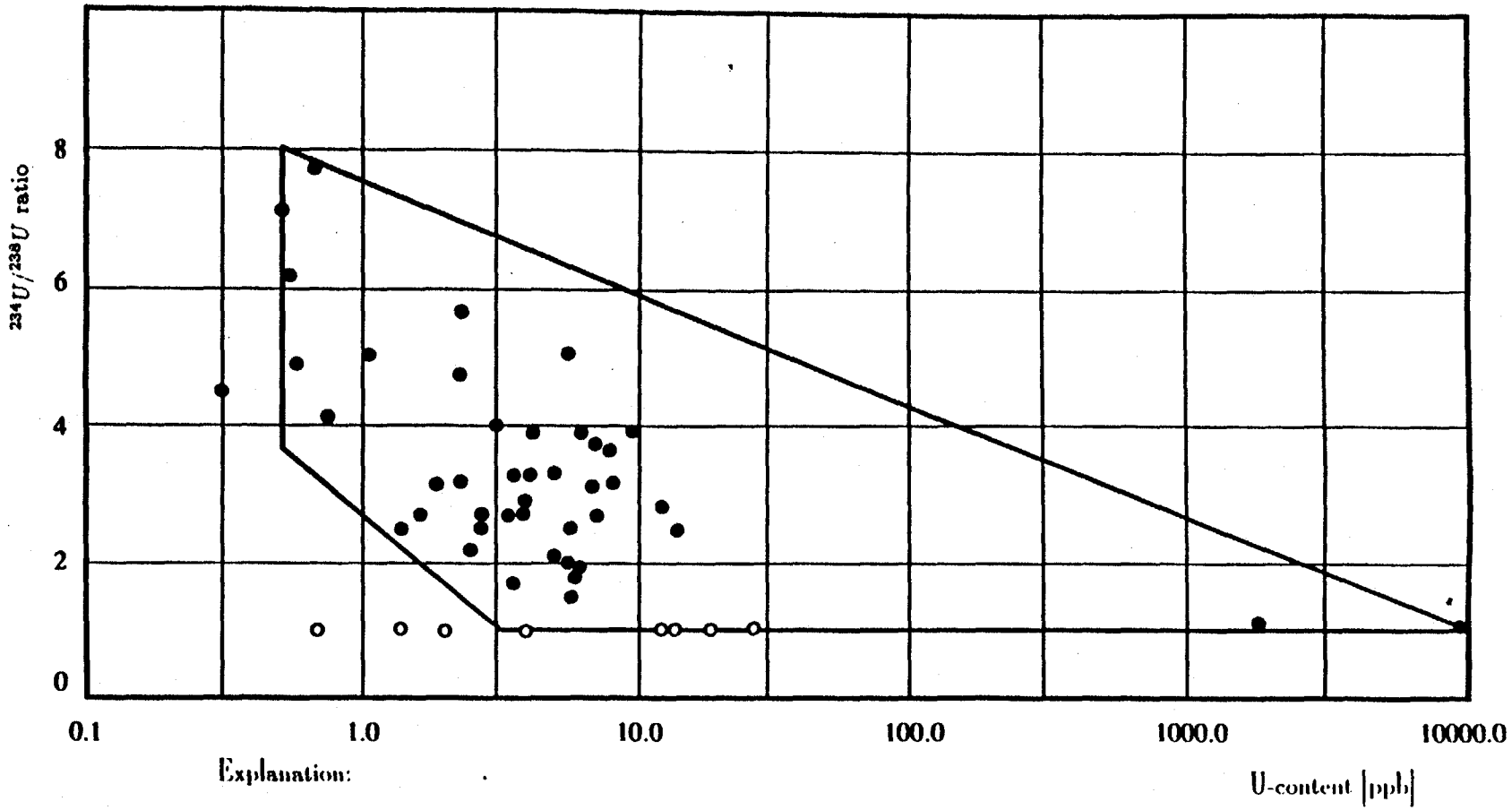

$^{234}U/^{238}U$ ratio vs. U-content field. Nevada Test Site subsurface fluids.

Figure 88.

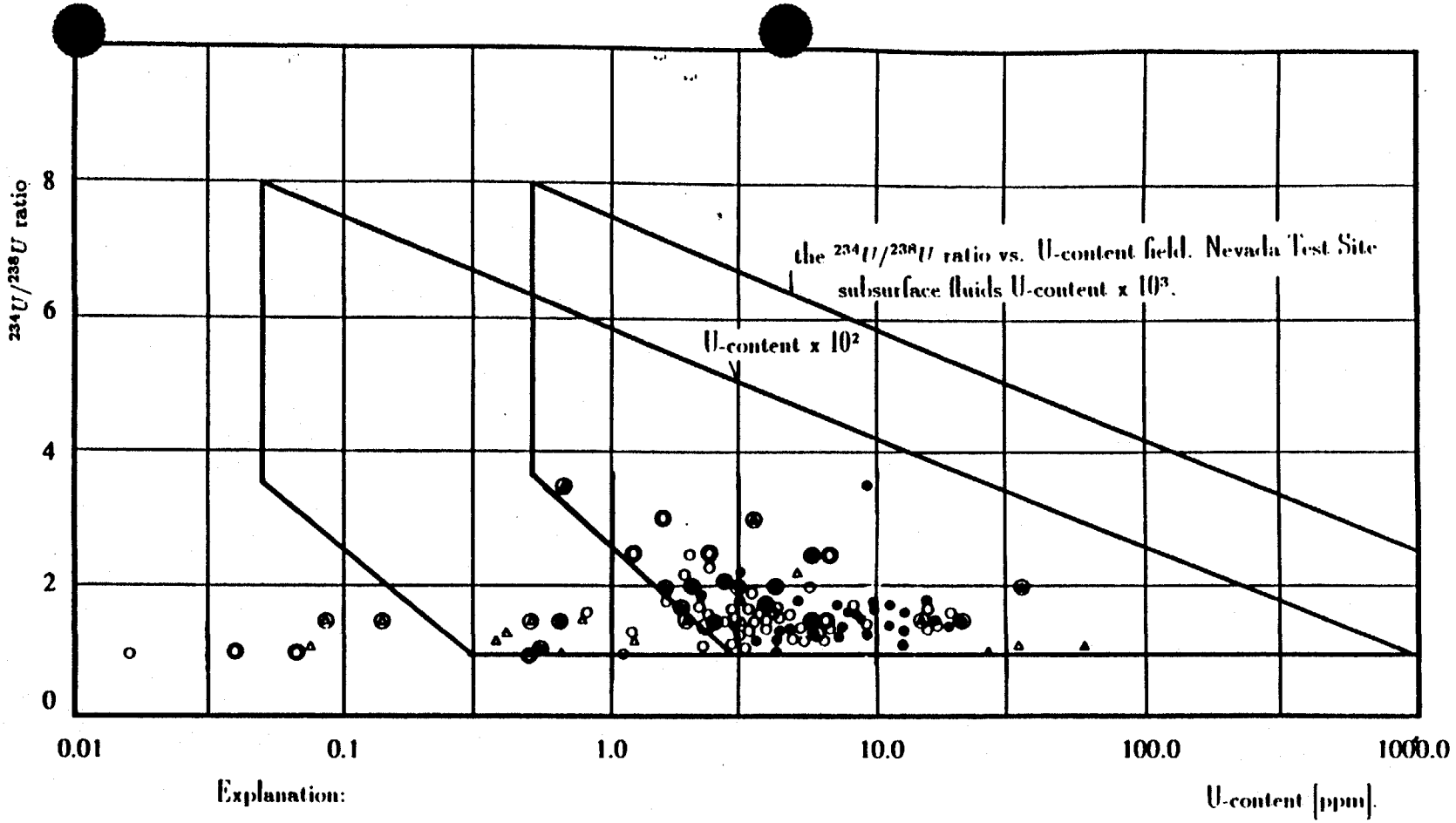

Explanation:

- ▲ - subsurface vein - acid soluble fraction;
- ▲ - subsurface vein - acid insoluble residuum;
- o - surficial deposit - acid soluble fraction;
- ● - surficial deposit - acid insoluble residuum;
- O - $^{234}U/^{238}U$ ratio plotted is a minimum value.

Comparison of $^{234}U/^{238}U$ ratio vs. U-content fields. Hydrogenic deposits and subsurface fluids. Nevada Test Site.

Figure 89.

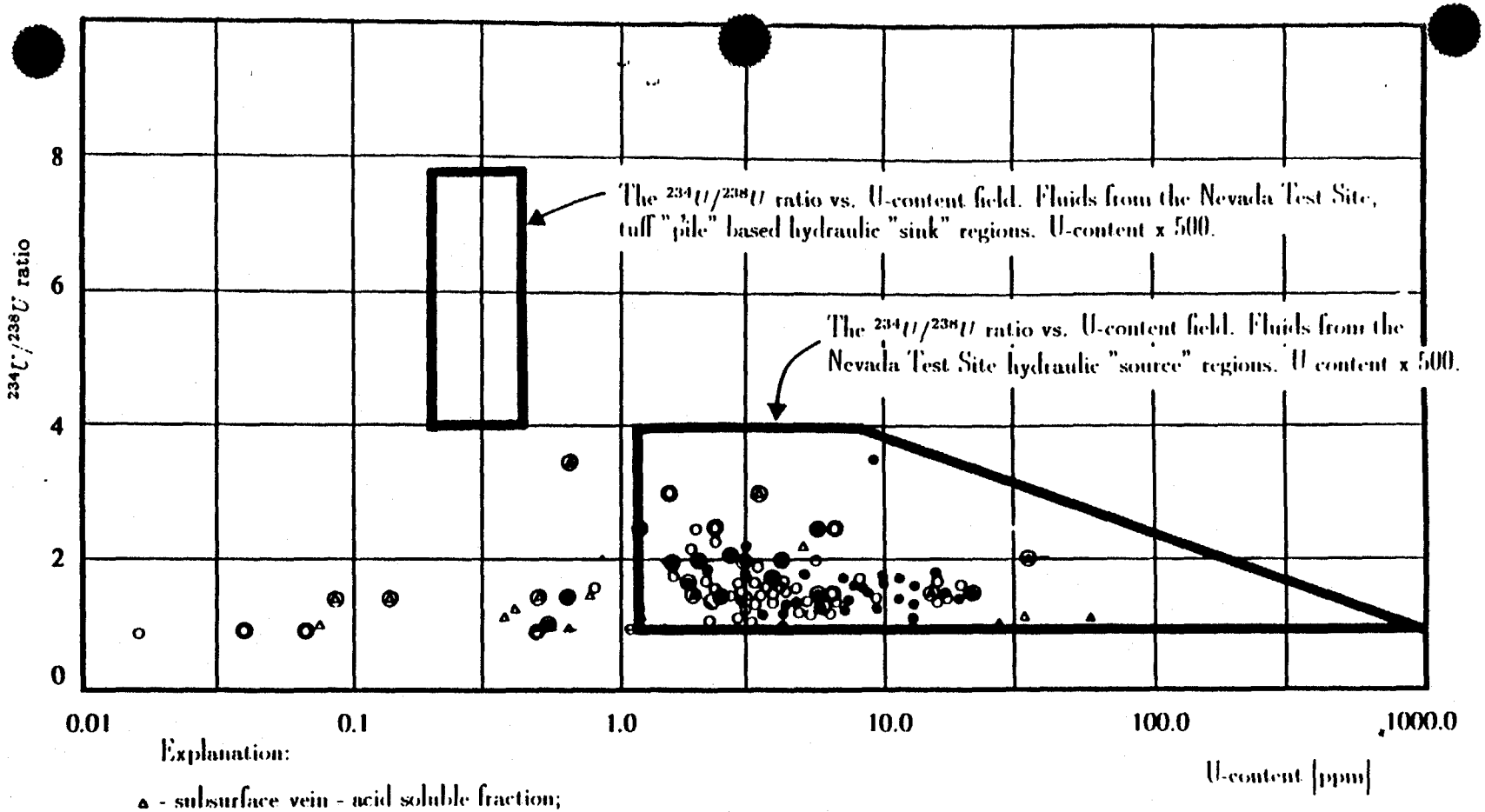

Comparison of $^{234}U/^{238}U$ ratio vs. U-content fields. Hydrogenic deposits and contemporary subsurface fluids. The Nevada Test Site hydrosphere.

Figure 90.

o The $^{87}Sr/^{86}Sr$ ratios, from samples of the Yucca Mountain surficial calcite-silica deposits, are similar to those from samples of the Northern and Southern Latium travertines.

o The $^{87}Sr/^{86}Sr$ ratios, from samples of the Yucca Mountain surficial calcite-silica deposits, are similar to those from samples of the local geothermal fluids.

Conclusion: a) **The Yucca Mountain surficial calcite-silica deposits were formed via the *per ascensum* process;**

b) **In the past, the Yucca Mountain hydrosphere have experienced the "source" ↔ "sink" transformations.**

Isotopic affinity between the parent fluids for the calcite-silica deposits and the local geothermal fluids - $^{87}Sr/^{86}Sr$ ratio.

Figure 91.

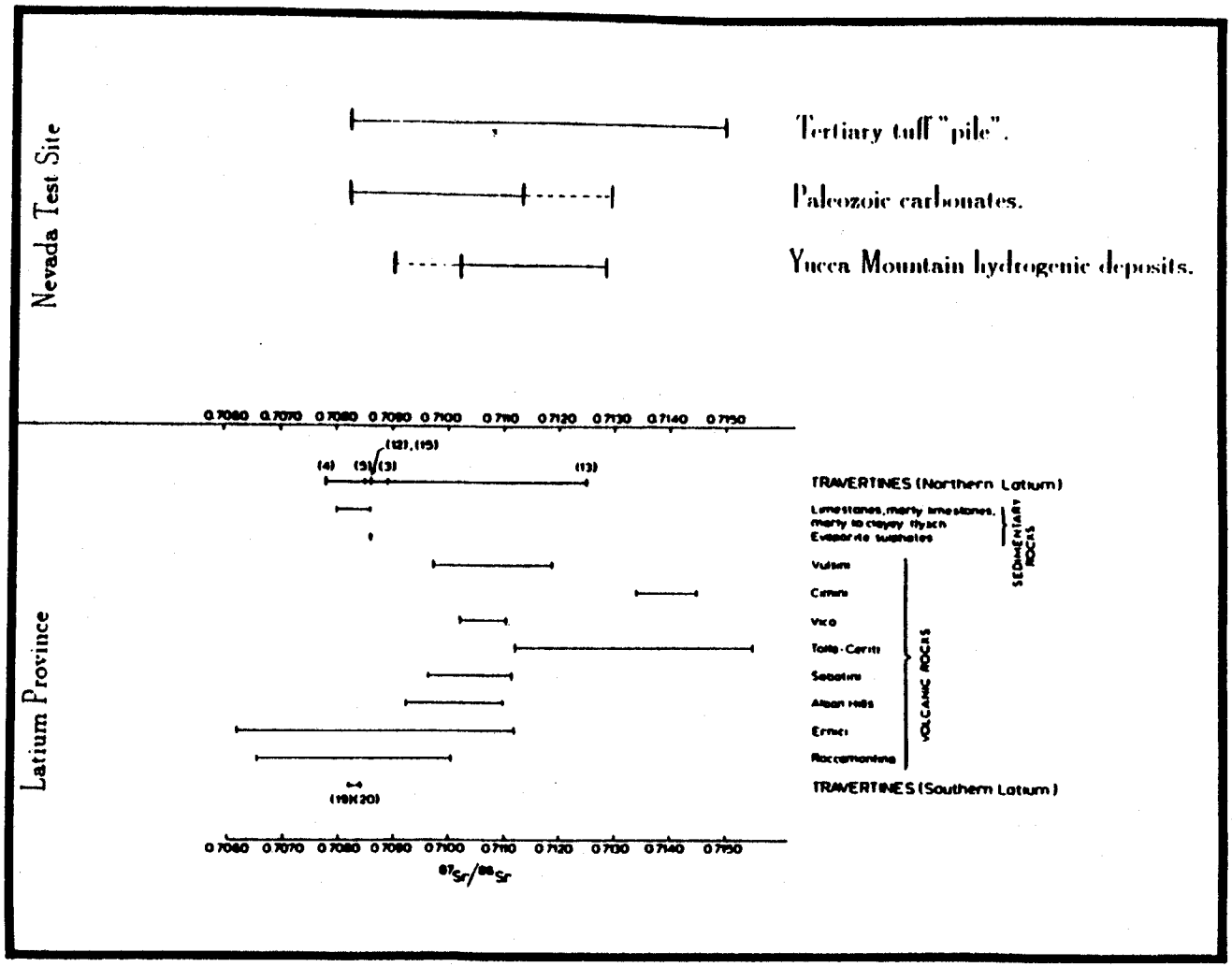

Comparison of the $^{87}Sr/^{86}Sr$ ratios from the Nevada Test Site with those from the Italian Latium Province. Modified from Turi, 1986.

Figure 92.

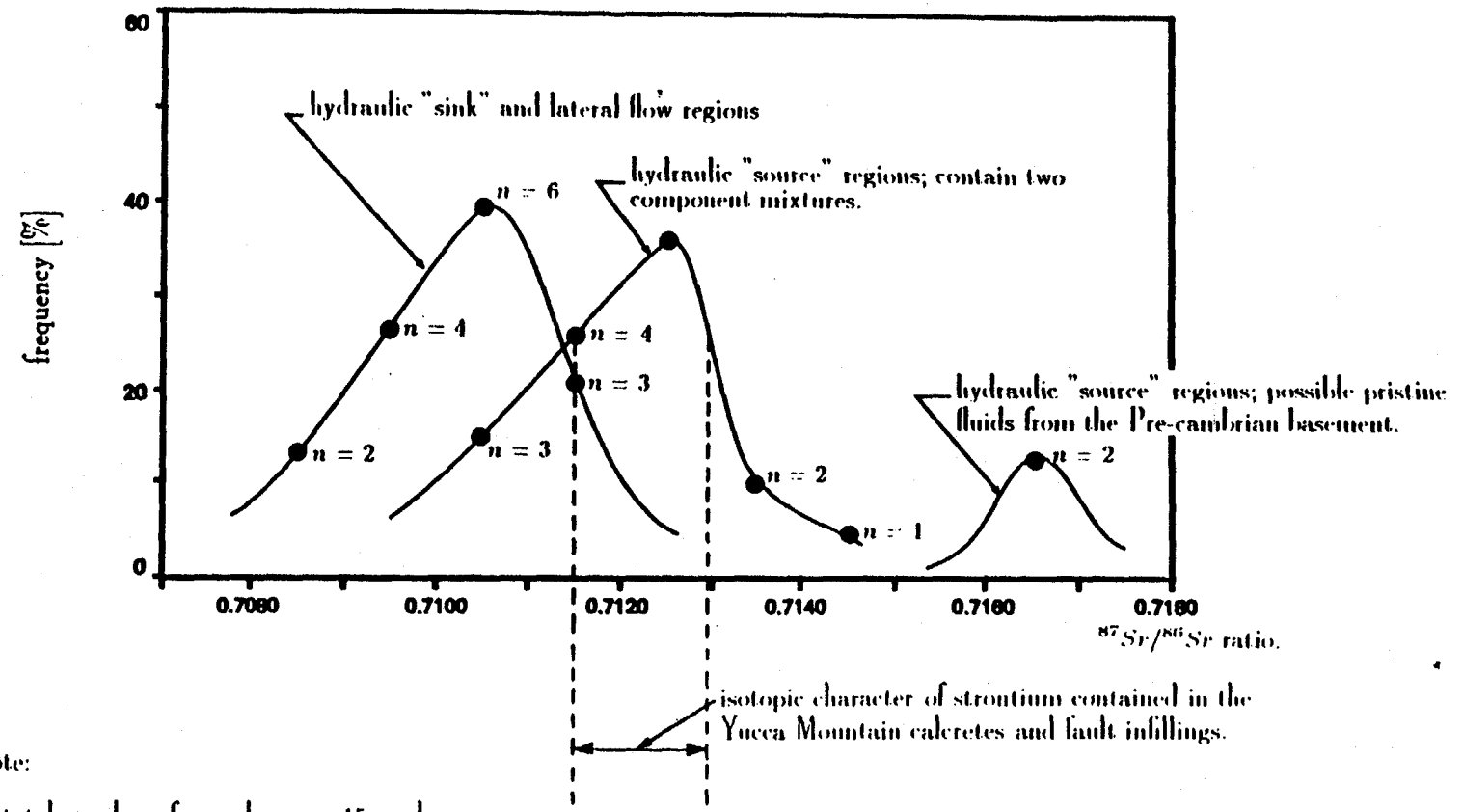

Note:

a) total number of samples: $n = 15$; and

b) isotopic data are from Marshall et al. (1990); Stuckless (1990); Peterman (1990); and Stuckless et al. (1990).

Comparison of the $^{87}Sr/^{86}Sr$ ratios. The Nevada Test Site hydraulic "source" regions and the Yucca Mountain calcite-silica deposits.

Figure 93

δ values of the $\delta^{13}C$ ratio from samples of the Yucca Mountain surficial calcite silica deposits are compatible with those: a) from the worldwide groundwater calcretes; b) from some of the worldwide travertines; c) from carbonate gangue veins from gold bearing hydrothermal ore deposits; d) from the Yucca Mountain subsurface veins (occurring down to a depth of at least ~ 600m); and e) from the local geothermal fluids.

Conclusion: a) **The Yucca Mountain calcite-silica deposits, including: a) calcretes; b) surficial fault in-fillings; and c) subsurface veins, were formed via the** *per ascensum* **process.**

b) **In the past, the Yucca Mountain have experienced the "sink" ↔ "source" transformations.**

Isotopic affinity between the parent fluids for the calcite-silica deposits and the geothermal fluids - carbon.

Figure 94.

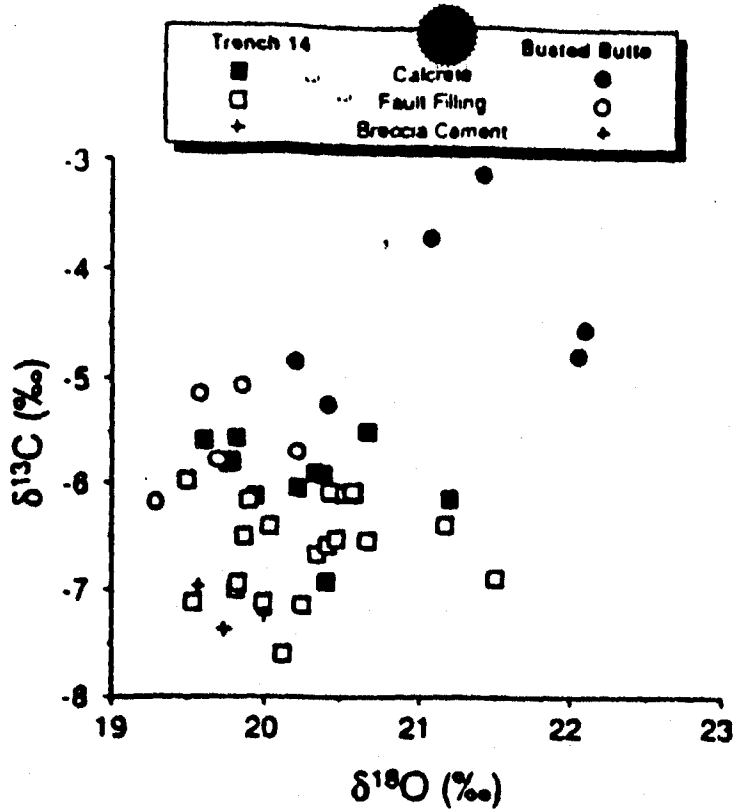

Note:

a) The carbon-oxygen part of the isotopic fingerprint, for the Yucca Mountain surficial calcite silica deposits, is a range of values for the $\delta^{18}O$ and $\delta^{13}C$ ratios;

b) The observed range for the $\delta^{13}C$ ratio is from 3.0 to 7.5 per mil *PDB*; and

c) The observed range for the $\delta^{18}O$ ratio is from 19.2 to 22.0 per mil *SMOW*.

Carbon-oxygen isotopic fingerprint. The Yucca Mountain surficial calcite- silica deposits. From Whelan and Stuckless, 1990.

Figure 95.

- For the Yucca Mountain area, a mean value for proportion of plants having the C3 metabolic pathway is ~ 85 percent, Quade and Cerling, 1989.
- A mean value for the $\delta^{13}C$ ratio for CO_2 produced by plants having the C3 metabolic pathway is ~ -27 per mil $_{PDB}$.
- A mean value for the $\delta^{13}C$ ratio for CO_2 produced by plants having the C4 metabolic pathway is ~ -12 per mil $_{PDB}$.
- A mean value for the $\delta^{13}C$ ratio for carbon dioxide produced by the local plants is ~ -24 per mil $_{PDB}$ - (-27 per mil · 85 percent + -12 per mil · 15 percent)/100.
- Dissolution of the locally produced biogenic CO_2 will yield fluids with values of the $\delta^{13}C$ ratio of about -16 per mil $_{PDB}$ ($10^3 \ln\alpha_{HCO_3^- - CO_2} \sim 8$ per mil $_{PDB}$).
- At temperatures less than 50°C, fluids carrying $\delta^{13}C \sim$ -16 per mil $_{PDB}$ may yield $CaCO_3$ deposits with values of the $\delta^{13}C$ ratio of about -14 per mil $_{PDB}$ ($10^3 \ln\alpha_{CaCO_3 - HCO_3^-} \sim 2$ per mil $_{PDB}$).

Note:

a) Carbon isotopic fractionation data are from Hoefs, 1987; and

b) Plant CO_2 data are from Deines, 1980.

Results of isotopic comparison: the observed Yucca Mountain range, from -3.0 to -7.5 per mil $_{PDB}$, is too "heavy" to be the result of the local biogenic activity alone.

Carbon isotopic file - isotopic character of carbon contained in $CaCO_3$ deposits precipitated in surficial fluids that own their CO_2 content to biogenic activity.

Figure 96.

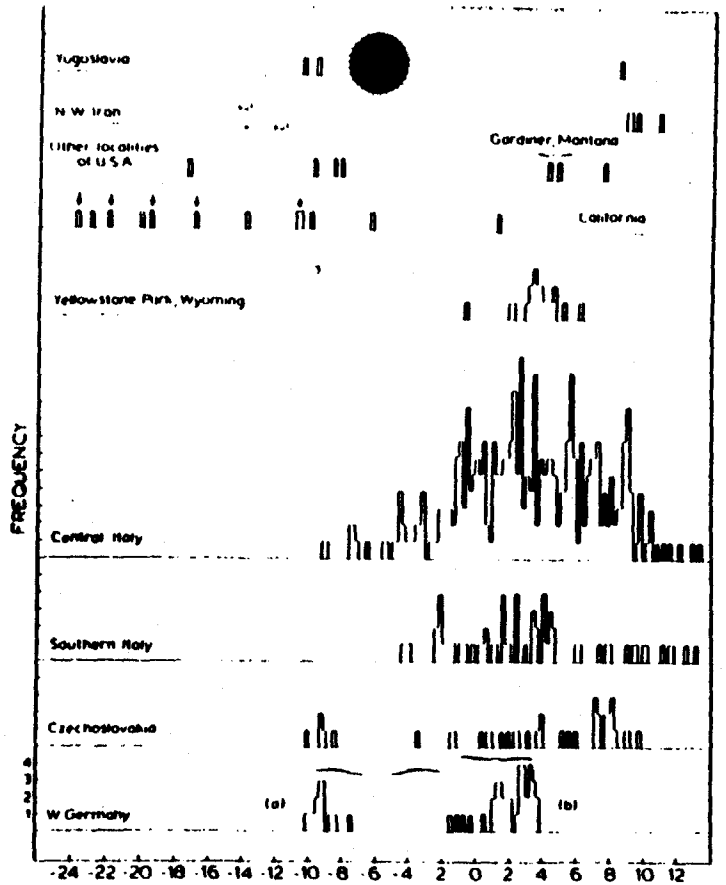

Note:

a) In some regions, carbon contained in travertine deposits is largely derived from dissolution of marine limestones and, therefore, mean values for the $\delta^{13}C$ ratio tend to be positive, say +3.0 per mil $_{PDB}$; and

b) In other regions, however, carbon contained in travertine deposits is isotopically "lighter" than that derived exclusively from marine limestones. A number of factors may be involved, including: i) participation of biogenically produced CO_2 ($\delta^{13}C$ values ranging from -35 to -10 per mil $_{PDB}$); and ii) participation of CO_2 from deep, igneous sources ($\delta^{13}C \sim -7$ per mil $_{PDB}$).

Results of isotopic comparison: the observed Yucca Mountain range, from -3.0 to -7.5 per mil $_{PDB}$, is "lighter" than that from travertines produced as the result of marine limestone dissolution alone.

Carbon isotopic file - isotopic character of carbon contained in travertines, worldwide data. From Turi, 1986.

Figure 97.

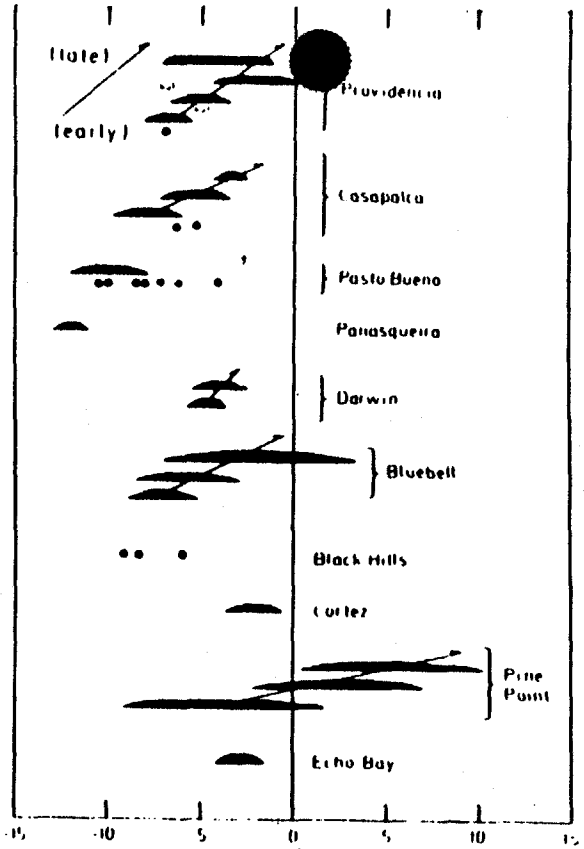

$\delta^{13}C$ (per mil)$_{PDB}$ - carbonate gangue from hydrothermal ore deposits

Note:

a) The isotopic character of carbon contained in CO_2 derived from deep-seated, igneous sources is described by a mean value of the $\delta^{13}C$ ration of about −7 per mil $_{PDB}$; and

b) Depending upon reaction temperature ($10^3 \ln \alpha_{HCO_3^-,\ CO_{2(g)}} = 9.483 \cdot 10^3 \cdot T^{-1} - 23.89$), dissolution of the igneous CO_2 may yield geothermal fluids with values of the $\delta^{13}C$ ratio ranging from +1 (temp. ~ 20°Celsius) to −14 per mil $_{PDB}$ (temp ~ 300°C).

Results of isotopic comparison: the observed Yucca Mountain range, from −3.0 to −7.5 per mil $_{PDB}$, is similar to that contained in carbonate gangue minerals from hydrothermal ore deposits.

Carbon isotopic file - isotopic character of carbon contained in carbonate gangue minerals from a number of hydrothermal ore deposits. From Hoefs, 1987.

Figure 98.

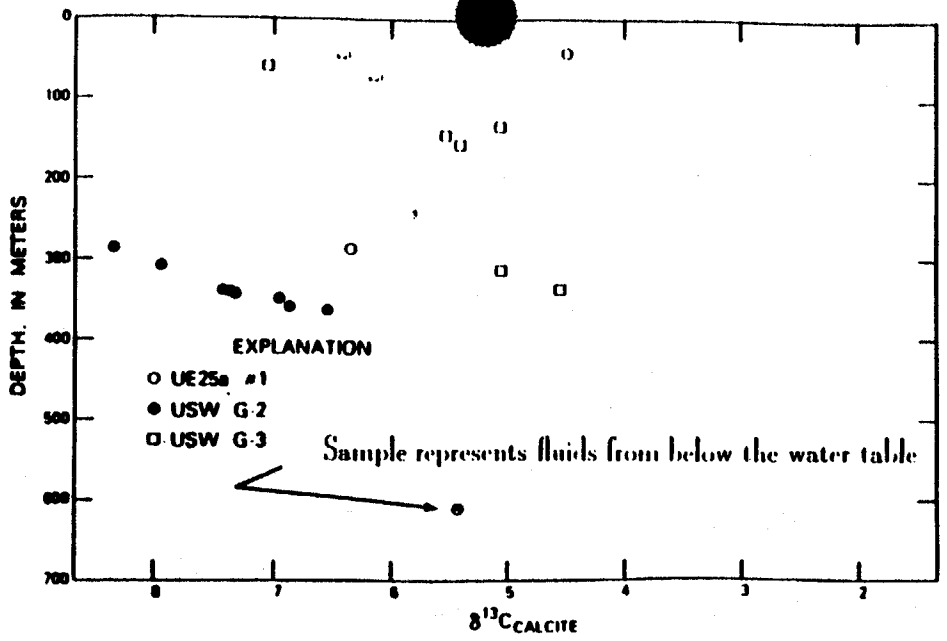

Note:

a) Values of the CO_2 partial pressure for the Yucca Mountain subsurface fluids, as calculated and reported by Kerrisk (1987), range from $\log P_{CO_2}$ = -0.79 to $\log P_{CO_2}$ = -2.86 atm. The mean local value of $\log P_{CO_2}$ is well above the CO_2 partial pressure in the atmosphere ($\log P_{CO_2} \sim -3.5$ atm);

b) The results of monitoring of the Yucca Mountain borehole UZ63 revealed that, during a 30-month long monitoring period, this borehole has exhaled ~1150 kg of carbon, Thorstenson et al., 1989; and

c) Both of the above observations suggest that, at Yucca Mountain, the net CO_2 flux is from hydrosphere → vadose zone → atmosphere, but not vice versa. A common sole source of carbon, contained in both the surficial deposits and the subsurface veins, may not be the atmosphere - biosphere system.

Results of isotopic comparison: the observed Yucca Mountain range (surficial deposits), from -3.0 to -7.5 per mil $_{PDB}$, is similar as that from samples of calcite silica veins from both the vadose zone and below the water table.

Carbon isotopic file - isotopic character of carbon contained in the Yucca Mountain subsurface veins. From Szabo and Kyser, 1990

Figure 99.

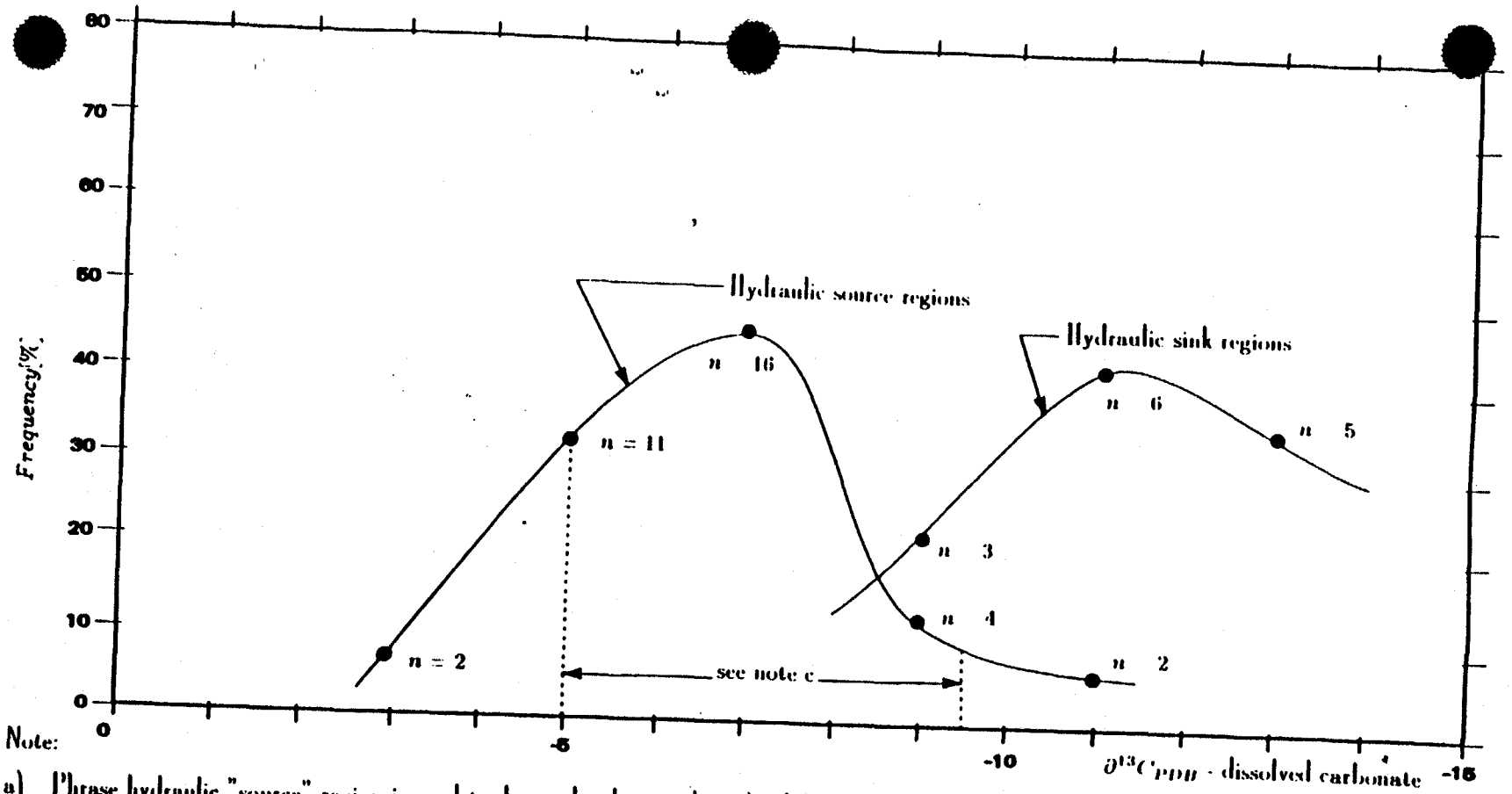

Note:

a) Phrase hydraulic "source" region is used to denote local areas that; i) exhibit positive values of the $d\phi/dz$ gradient - ϕ is hydraulic potential; ii) exhibit high values of the dt/dz gradient - $dt/dz \sim 35$ 55°Celsius per 1km of depth; and iii) contain fluids having relatively high concentrations of $CL^- + SO_4$ anions;

b) At precipitation temperatures ~50° Celsius, value of the isotopic fractionation factor $10^3 ln\alpha_{CaCO_3,\ HCO_3}$ is ~ 2 per mil *PDB*; and

c) The -3.0 to -7.5 per mil *PDB* range, from samples of the Yucca Mountain surficial deposits, indicates that the parent fluids for these deposits have carried values of the $\delta^{13}C$ ratio ranging from -5.0 to -9.5 per mil *PDB*.

Results of isotopic comparison: the observed Yucca Mountain range, from -3.0 to -7.5 per mil *PDB*, is similar to that expected for deposits produced by the local geothermal fluids

Carbon isotopic file - isotopic character of carbon contained in the local geothermal fluids; host rock is tuff pile. Data from - Claassen, 1985; Benson and McKinley, 1985; and White and Chuma, 1987

Figure 100

o Values of the $\delta^{18}O$ ratio from samples of the Yucca Mountain surficial calcite silica deposits are compatible with those: a) from some of the worldwide travertines; b) from the local deep-seated spring deposits; c) from the Yucca Mountain subsurface veins (occurring down to a depth of at least ~ 600m); d) from the Yucca Mountain subsurface fluids; and g) from the Yucca Mountain geothermal fluids.

Conclusion: a) **The Yucca Mountain calcite-silica deposits, including: a) calcretes; b) surficial fault in-fillings; and c) subsurface veins, were formed via the** *per ascensum* **process.**

b) **In the past, the Yucca Mountain hydrosphere have experienced the "sink" ↔ "source" transformations.**

Isotopic affinity between the parent fluids for the calcite-silica deposits and the geothermal fluids - oxygen.

Figure 101.

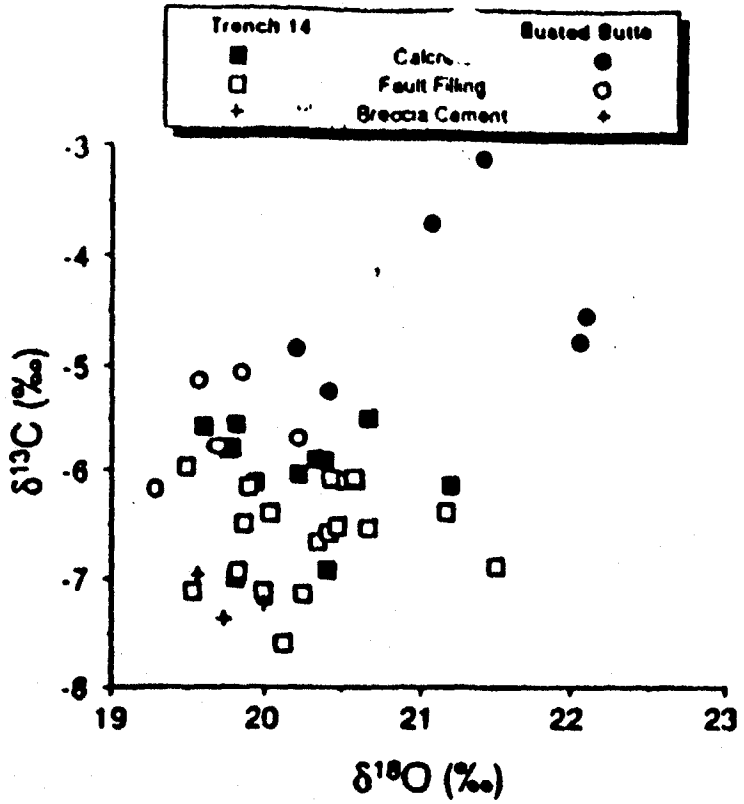

Note:

a) The carbon-oxygen part of the isotopic fingerprint, for the Yucca Mountain surficial calcite-silica deposits, is a range of values for the $\delta^{18}O$ and $\delta^{13}C$ ratios;

b) The observed range for the $\delta^{13}C$ ratio is from -3.0 to - 7.5 per mil $_{PDB}$; and

c) The observed range for the $\delta^{18}O$ ratio is from 19.2 to 22.0 per mil $_{SMOW}$.

Carbon-oxygen isotopic fingerprint. The Yucca Mountain surficial calicite- silica deposits. From Whelan and Stuckless, 1990.

Figure 102.

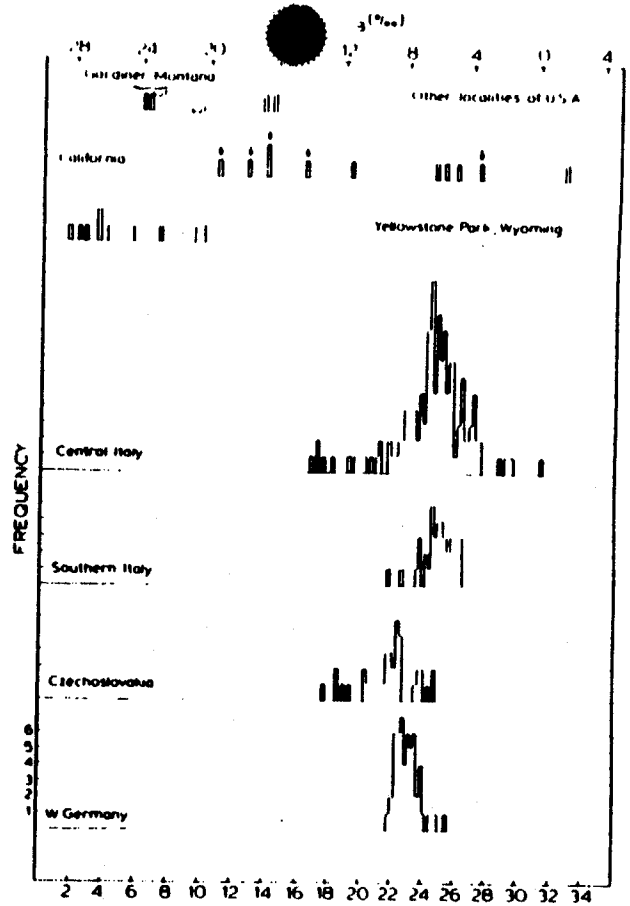

Note:

a) A value of the $\delta^{18}O$ ratio, from a sample of a particular travertine deposit, reflects three main factors, namely: i) oxygen 18 content for the parent fluid; ii) precipitation temperature; and iii) conditions of precipitation and the resulting value of the isotopic fractionation factor; and

b) Various combinations of the controlling factors are possible and, consequently, the worldwide travertine deposits exhibit a very wide range of the $\delta^{18}O$ ratio, from +2 to about +32 per mil $_{SMOW}$.

Results of isotopic comparison: the observed Yucca Mountain range, from 19.2 to 22.0 per mil $_{SMOW}$, is within the corresponding range from the worldwide travertine deposits.

Oxygen isotopic life - isotopic character of oxygen contained in travertines, worldwide data. From Turi, 1986.

Figure 103.

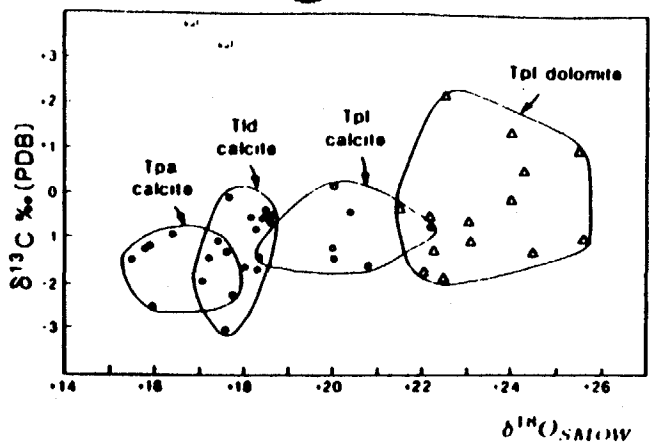

Note:

a) Both the $\delta^{13}C$ vs. lithology gradient and the $\delta^{18}O$ vs. lithology gradient may reasonably be attributed to an increasing residence time, at the topographic surface, of the deposits parent fluids;

b) The increasing residence time for the parent fluid, at the topographic surface, is accompanied by: i) decreasing precipitation temperature; ii) increasing kinetic fractionation effects; and iii) increasing oxygen 18 and carbon 13 evaporative enrichment - each of these factors may account for the observed gradients;

c) Tpa denotes soft - chalky limestone; Tld denotes dense nodular and fenestral limestone; Tpl denotes carbonate rocks and minerals disseminated in claystones;

d) At the Ash Meadows topographic surface, the ambient temperatures are likely to be 5 to 10° Celsius higher than the corresponding temperatures at Yucca Mountain - the resulting differences in the equilibrium fractionation factor range from 1 to 2 per mil $_{SMOW}$, the Yucca Mountain values being larger; and

e) Differences in values of the $\delta^{13}C$ ratio, between the Ash Meadows deposits and the Yucca Mountain surficial deposits, are directly attributable to the corresponding differences in the parent fluids host rocks.

Results of isotopic comparison: the observed Yucca Mountain range, from 19.2 to 22 per mil $_{SMOW}$, if adjusted for the differing equilibrium fractionation factors is compatible with the oxygen 18 content of the Ash Meadows spring carbonates.

Oxygen isotopic file - isotopic character of oxygen contained in the deep-seated spring deposits from the Ash Meadows Basin, Nevada. From Hay et al., (1986)

Figure 104.

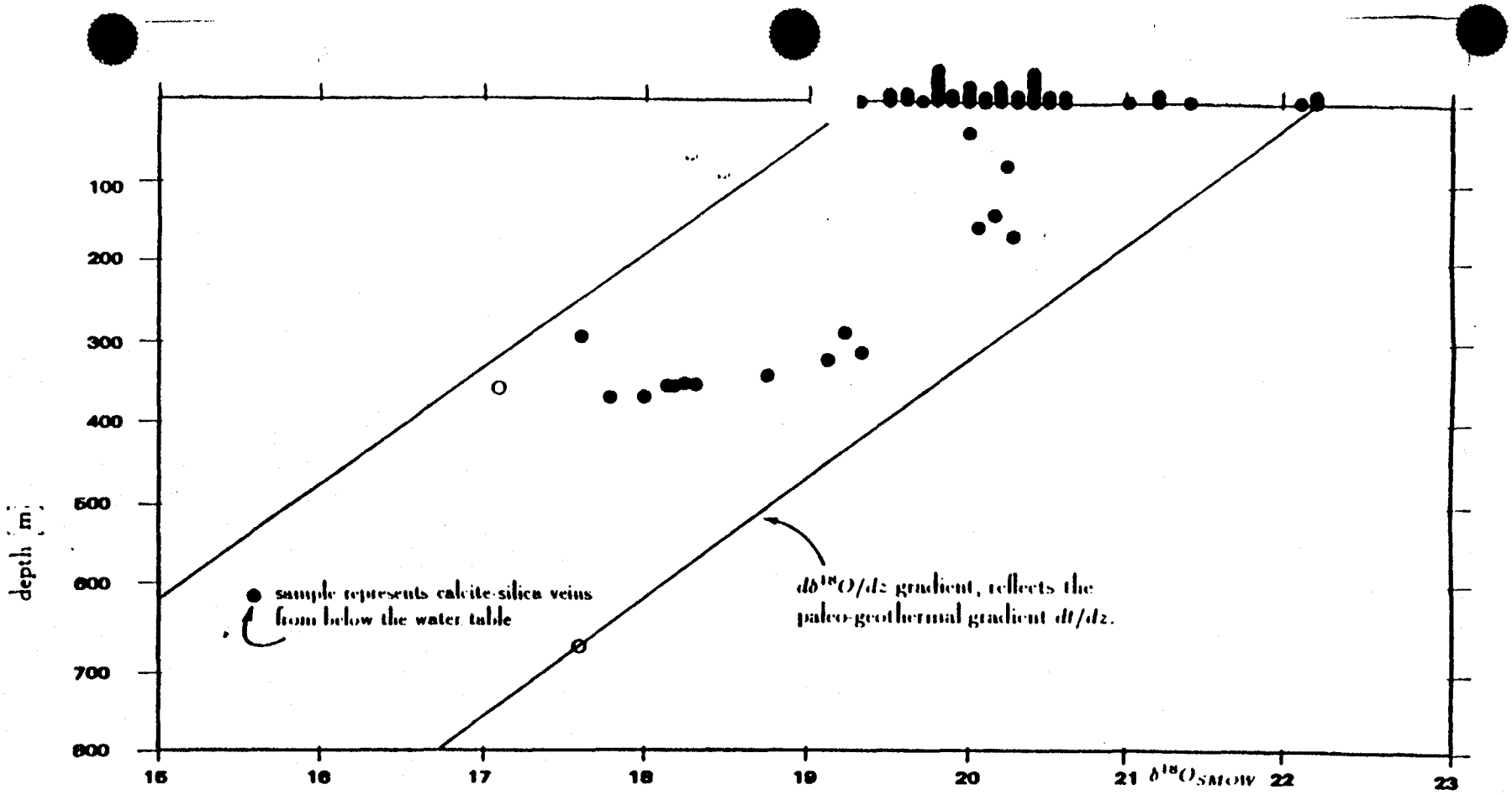

Note:

a) The entire observed Yucca Mountain range of the $\delta^{18}O$ ratios for carbonate deposits, from 15.4 to 22.0 per mil $_{SMOW}$, is very similar to that observed for the Ash Meadows Basin deposits, Figure 8; and

b) The above similarities suggest that, the differences in oxygen - 18 contents from samples of the respective surficial deposits are caused by the respective differences in either the precipitation temperatures or the isotopic fractionation factors, but not by major differences in the oxygen - 18 contents of the respective parent fluids.

Results of isotopic comparison: the observed Yucca Mountain range, from 19.2 to 22 $_{SMOW}$, if adjusted for the differing percipitation temperatures, is compatible with the observed oxygen - 18 content of the Yucca Mountain subsurface veins.

Oxygen isotopic life - isotopic character of oxygen contained in the Yucca Mountain calcite-silica subsurface veins. Data from Szabo and Kyser (1990) and Whelan and Stuckless (1990)

Figure 105.

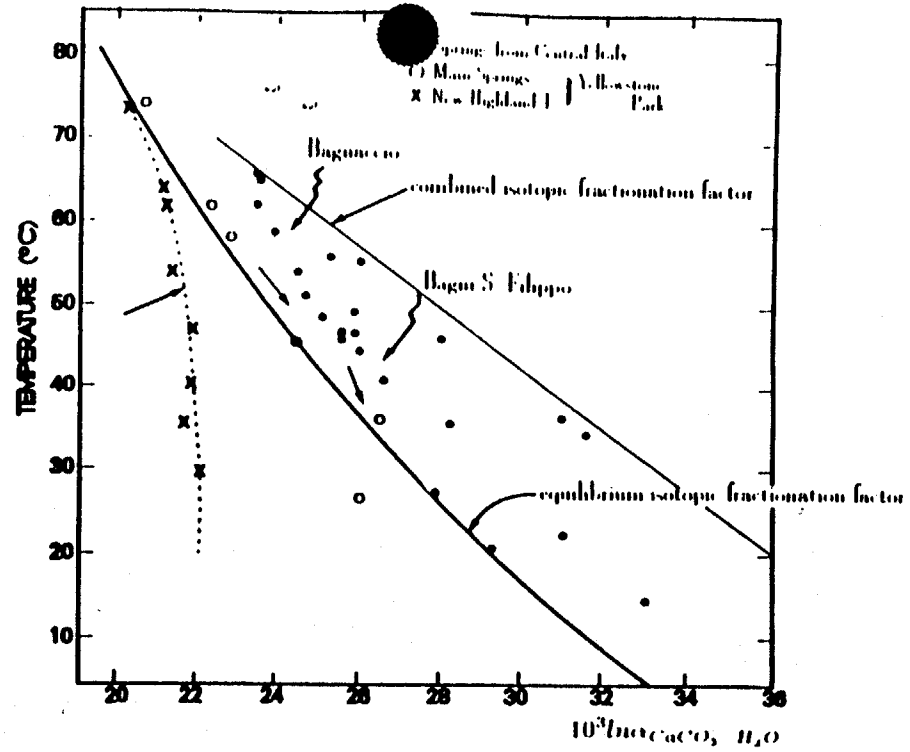

Note:

a) During natural depositions of travertines, the conditions of equilibrium isotopic fractionation are seldom attained, mainly as a consequence of the kinetic or non-equilibrium processes;

b) Depending upon conditions of precipitation, the combined or actual isotopic fractionation factor ($10^3 ln\alpha_{CaCO_3,\ H_2O}$) may be both larger and smaller than the equilibrium fractionation factor; and

c) At a precipitation temperature of t ~20° Celsius, the combined isotopic fractionation factor may be assumed to range from 22 to 36 per mil *SMOW*.

Oxygen isotopic fractionation data from travertine depositing springs of Central Italy and Yellowstone Park. From Turi, 1986.

Figure 106.

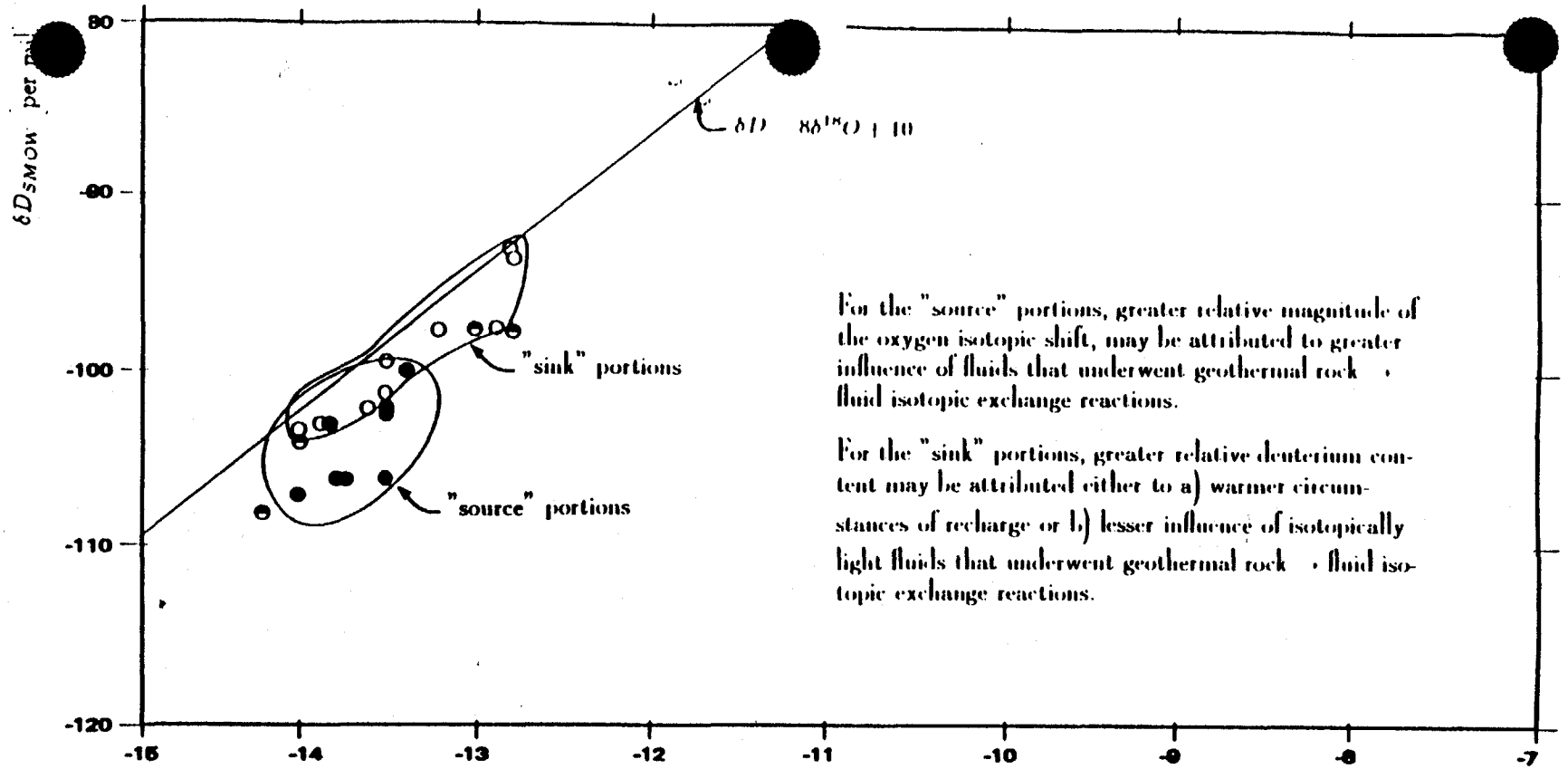

Note:

a) The observed range of values for the $\delta^{18}O$ ratio, from samples of the contemporary Yucca Mountain subsurface fluids, is from 14.2 to 12.7 per mil $_{SMOW}$; samples are bulk water samples pumped out of large segments of exploratory wells - sampling "smoothing" may be involved, and the observed range may be smaller than the actually present one; and

b) If the parent fluids, for the Yucca Mountain surficial deposits, have carried the same oxygen 18 contents then, the combined isotopic fractionation factor was in a range from 31.9 to 35.2 per mil $_{SMOW}$, which is permissible by the empirical fractionation data from Figure 106.

Results of isotopic comparison: the observed Yucca Mountain range, from 19.2 to 22 per mil $_{SMOW}$, is compatible with that expected for deposits produced by the contemporary Yucca Mountain subsurface fluids.

Oxygen isotopic file - isotopic character of oxygen contained in the contemporary Yucca Mountain subsurface fluids. Data from Benson and McKinley, 1985.

Figure 107.

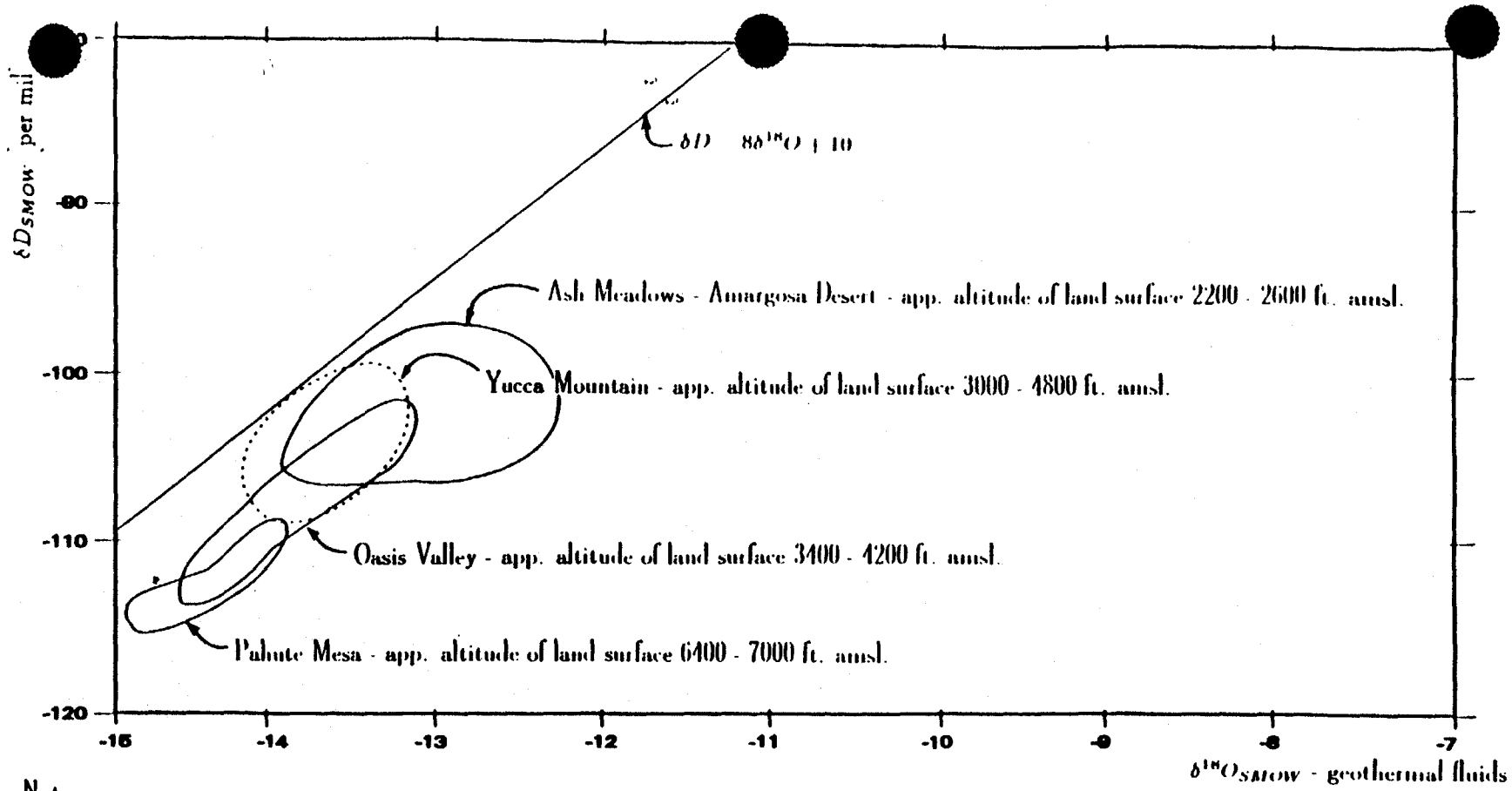

Note:

a) The observed range of values for the $\delta^{18}O$ ratio, from samples of the contemporary Nevada Test Site geothermal fluids, is from -14.8 to -12.3 *SMOW*; samples are bulk samples pumped out of large segments of exploratory wells - sampling "smoothing" may be involved, and the observed "oxygen isotopic shift" may be smaller than the actually present one; and

b) If the parent fluids, for the Yucca Mountain surficial deposits, have carried the same oxygen-18 contents then, the combined isotopic fractionation factor was in a range from 31.5 to 36.8 per mil *SMOW*, which again is permissible by the empirical fractionation data from Figure 106.

Results of isotopic comparison: the observed Yucca Mountain range, from 19.2 to 22.0 per mil *SMOW*, is compatible with that expected for deposits produced by the contemporary Nevada Test Site geothermal fluids.

Oxygen isotopic file - isotopic character of oxygen contained in the contemporary Nevada Test Site geothermal fluids. Data from Claassen, 1985; Benson and McKinley, 1985; and White and Claassen, 1987

Figure 108.

o Considerations of: a) the oxygen 18 content of the precipitates; b) the assumed oxygen 18 contents of the parent fluids; and c) the reasonable isotopic fractionation effects lead to a conclusion that, the precipitation temperatures for the Yucca Mountain surficial calcite-silica deposits may have been in a range from 15 to as much as 53° Celsius.

o The available data do not allow for further narrowing of the interpreted precipitation temperature range. Thus, the considerations of precipitation temperatures alone neither support nor contradict each of the two postulated modes of formation of the Yucca Mountain surficial calcite-silica deposits.

Conclusion: **Based on considerations of the precipitation temperatures alone, both the *per ascensum* origin and the *per descensum* origin, for the Yucca Mountain surficial calcite-silica deposits, are permissible.**

Precipitation (crystallization) temperatures, based on the oxygen 18 content of the Yucca Mountain surficial calcite-silica deposits.

Figure 109.

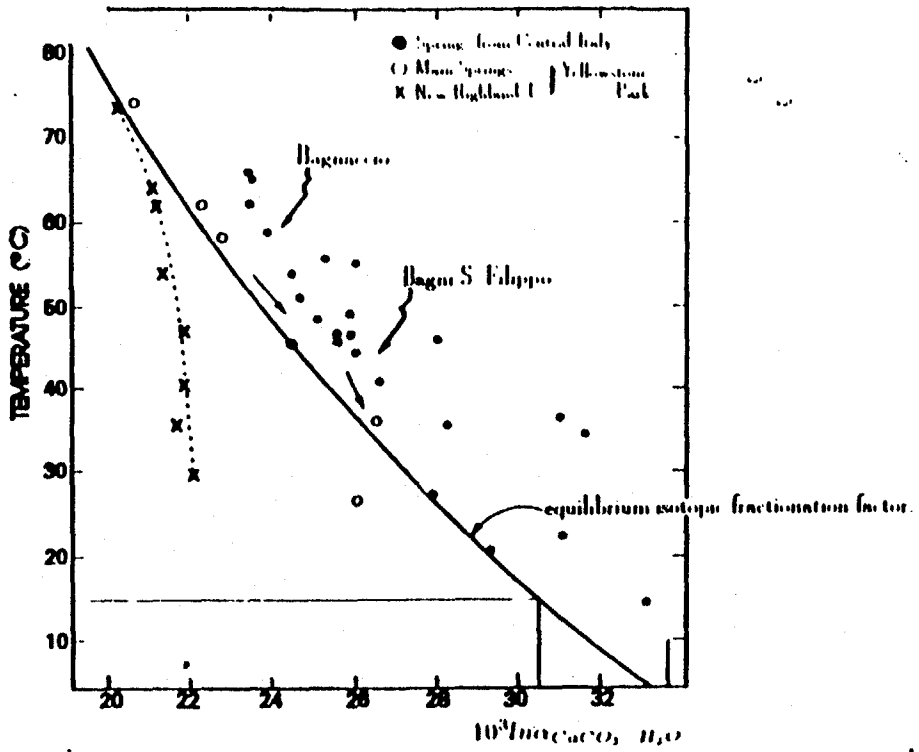

a) isotopic fractionation data, from Turi (1986).

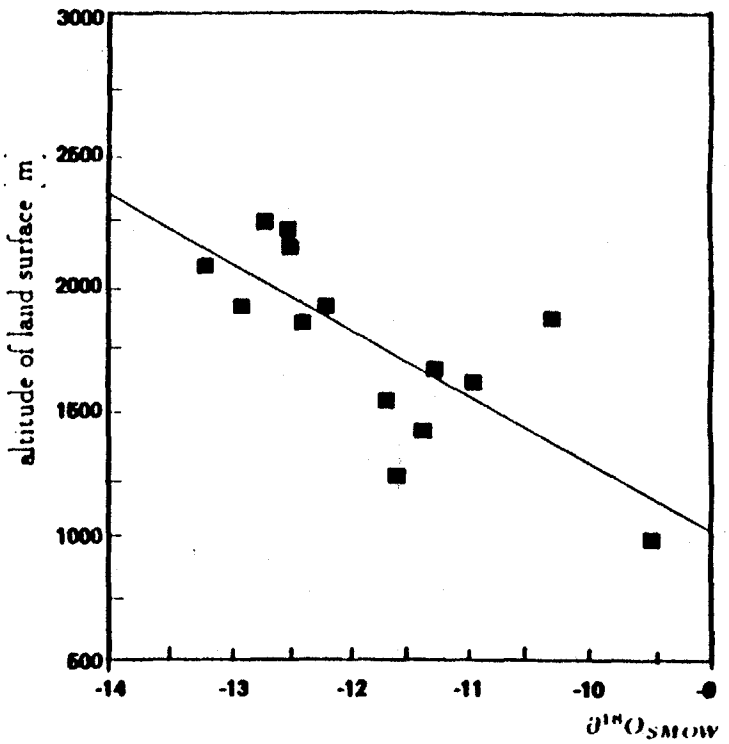

b) weighted average values of the $\delta^{18}O$ ratio - atmospheric precipitation at the Nevada Test Site, from Ingraham et al., (1990).

Note:

a) In performing this reconstruction, it has been assumed that: i) the parent fluids, for the Yucca Mountain surficial fluids, were isotopically identical to the contemporary atmospheric precipitation (at altitudes ranging from 1250 to 1400m, $\delta^{18}O$ values range from -11.7 to -11.3 per mil $_{SNOW}$), and ii) the non-equilibrium isotopic fractionation effects were absent, such that the combined isotopic fractionation factor $10^3 ln\alpha_{CaCO_3,\ H_2O} = 2.78 \cdot 10^6/T^2 - 2.82$;

b) The minimum and maximum values for the combined fractionation factor ($10^3 ln\alpha_{CaCO_3,\ H_2O} = 2.78 \cdot 10^6/T^2 - 2.82$) are 30.5 and 33.7, respectively;

c) The corresponding range for the precipitation temperatures is from 0 to -14° Celsius; and

d) The measured contemporary *in situ* temperatures, at and near the topographic surface, range from 15 to 21° Celsius, Sass et al., (1987) the paleo and contemporary temperatures discrepancy indicates that one or both of the assumptions, employed to determine the paleo temperature, are false.

Reconstruction A - the precipitation temperatures for the Yucca Mountain surficial deposits, based on oxygen-18 contents from samples of these deposits.

Figure 110.

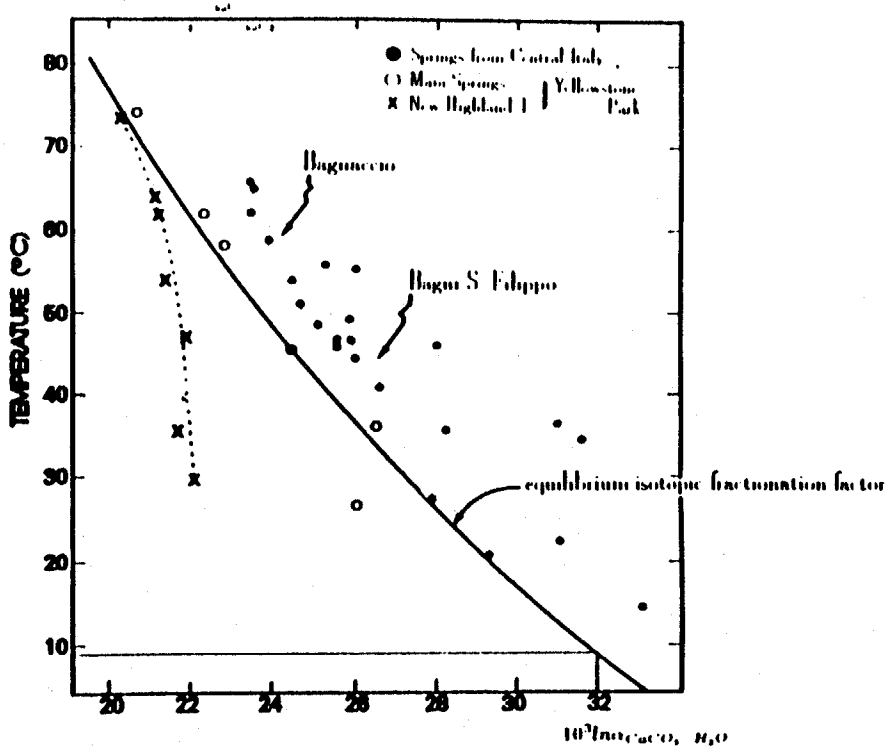

Note:

a) In performing this reconstruction, it has been assumed that: i) during a time span represented by the surficial deposits, the isotopic compositions of the parent fluids were the same as those observed below the water table at the present time ($\delta^{18}O$ values ranging from - 14.2 to - 12.7 per mil *SMOW*, Figure 11); and ii) the non equilibrium isotopic fractionation effects were absent, such that the combined isotopic fractionation factor $10^3 ln\alpha_{CaCO_3,\ H_2O} = 2.78 \cdot 10^6 / T^2 - 2.82$;

b) The minimum and maximum values for the combined fractionation factor ($10^3 ln\alpha_{CaCO_3,\ H_2O} - 2.78 \cdot 10^6 / T^2 - 2.82$) are 31.9 and 36.2 per mil *SMOW*, respectively; and

c) The corresponding range for the precipitation temperatures is from 8 to below 0° Celsius - this abnormally low range indicates that one or both of the employed assumptions are false.

Reconstruction B - the precipitation temperatures for the Yucca Mountain surficial deposits, based on the oxygen 18 contents from samples of these deposits.

Figure 111.

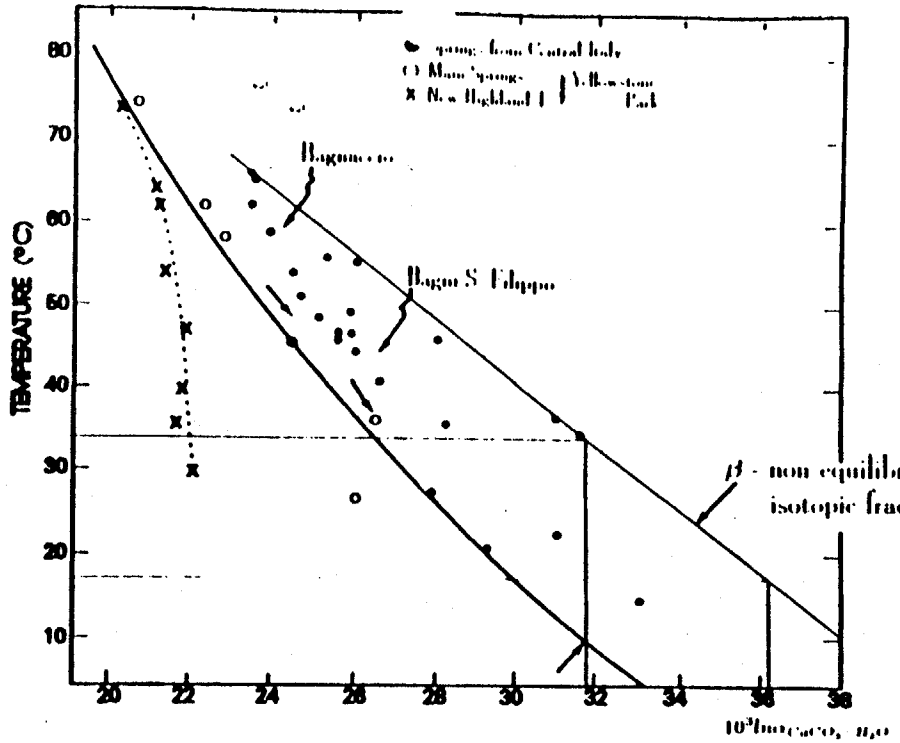

Note:

a) In performing this reconstruction, it has been assumed that: i) during a time span represented by the surficial deposits, the isotopic compositions of the parent fluids were the same as those observed below the water table at the present time ($\delta^{18}O$ values ranging from −14.2 to −12.7 per mil $_{SMOW}$, Figure 11), ii) the combined isotopic fractionation factor was larger that the equilibrium fractionation factor, such that $10^3 ln\alpha_{CaCO_3,\ H_2O}$ $2.78 \cdot 10^6/T^2$ 2.82 (β); and iii) the non equilibrium isotopic fractionation is caused by a rapid escape of CO_2 from the parent solution; isotopically lighter CO_2 is eliminated preferentially, and $CaCO_3$ acquires it's oxygen from both H_2O and CO_2;

b) The minimum and maximum values for the combined isotopic fractionation factor $(10^3 ln\alpha_{CaCO_3,\ H_2O}$ $2.78 \cdot 10^6/T^2$ 2.82 (β) are 31.9 and 36.2, respectively; and

c) The corresponding range for the precipitation temperatures is from 18 to 34° Celsius.

Reconstruction C - the precipitation temperatures for the Yucca Mountain surficial deposits, based on the oxygen 18 contents from samples of these deposits.

Figure 112.

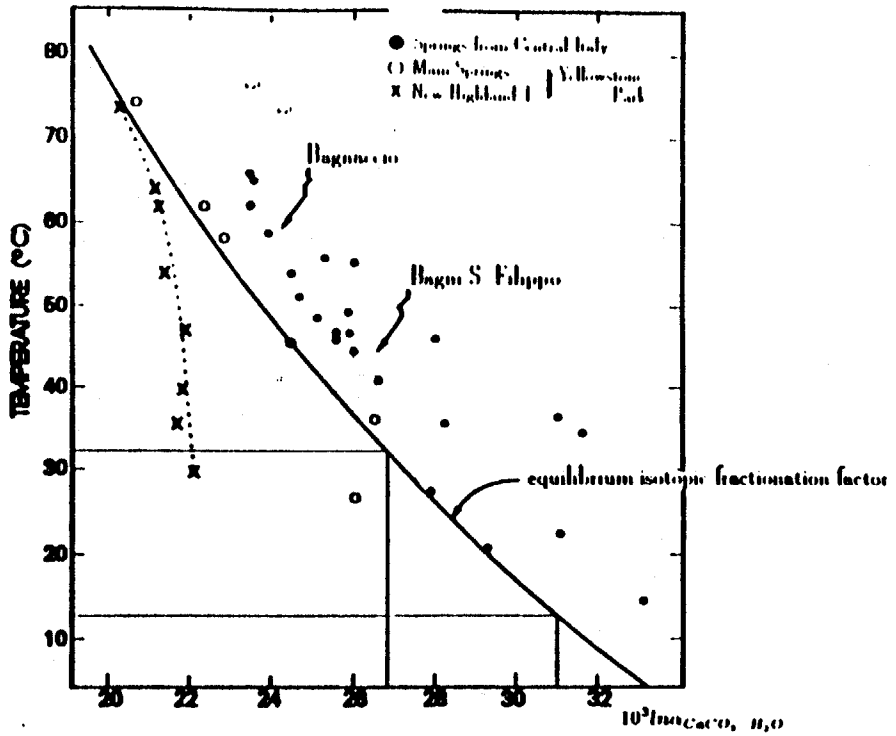

Note:

a) In performing this reconstruction, it has been assumed that: i) the parent fluids, for the Yucca Mountain surficial deposits, were isotopically heavier than the contemporary Yucca Mountain subsurface fluids, $\Delta\delta^{18}O \sim 5$ per mil $_{SMOW}$ (9.2 to 7.7 per mil $_{SMOW}$, Figure 18); and ii) the non-equilibrium isotopic fractionation effects were absent, such that the combined isotopic fractionation factor $10^3 ln\alpha_{CaCO_3-H_2O} = 2.78 \cdot 10^6/T^2 - 2.82$;

b) The minimum and maximum values for the combined fractionation factor ($10^3 ln\alpha_{CaCO_3-H_2O} = 2.78 \cdot 10^6/T^2 - 2.82$) are 26.9 and 31.2 per mil, respectively; and

c) The corresponding range for the precipitation temperatures is from 13 to ~ 32° Celsius.

Reconstruction D - the precipitation temperatures for the Yucca Mountain surficial deposits, based on the oxygen 18 contents from samples of these deposits.

Figure 113.

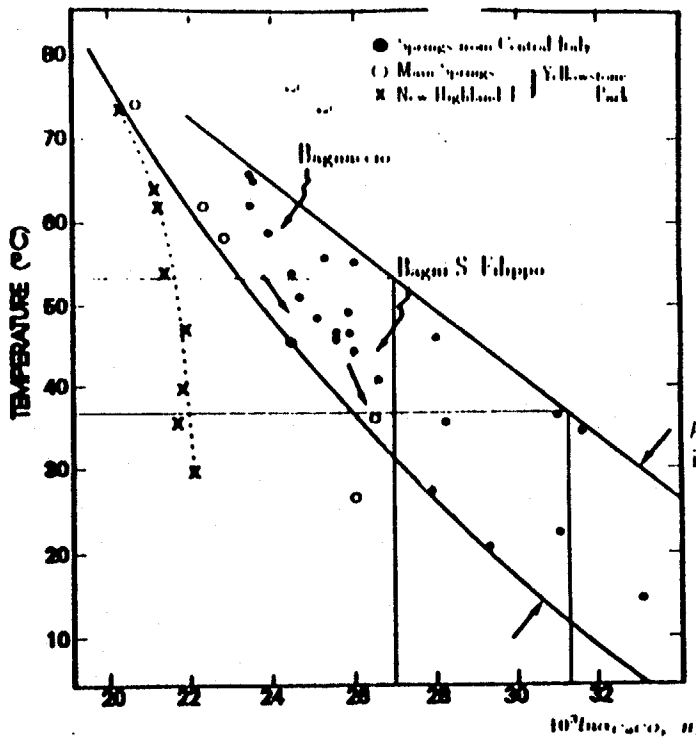

Note:

a) In performing this reconstruction, it has been assumed that: i) the parent fluids, for the Yucca Mountain surficial deposits, were isotopically heavier than the contemporary Yucca Mountain subsurface fluids, $\Delta\delta^{18}O \sim 5$ per mil $_{SMOW}$ (9.2 to 7.7 per mil $_{SMOW}$, Figure 18); the combined isotopic fractionation factor was larger than the equilibrium fractionation factor, such that $10^3 ln\alpha_{CaCO_3,\ H_2O}$ 2.78 $\cdot 10^6/T^2$ 2.82 (β); and iii) the non-equilibrium isotopic fractionation is caused by a rapid escape of CO_2 from the parent solution; isotopically lighter CO_2 is eliminated preferentially, and $CaCO_3$ acquires it's oxygen from both H_2O and CO_2;

b) The minimum and maximum values for the combined isotopic fractionation factor ($10^3 ln\alpha_{CaCO_3,\ H_2O}$ 2.78 $\cdot 10^6/T^2$ 2.82 (β)) are 26.9 and 31.2 per mil, respectively; and

c) The corresponding range for the precipitation temperatures is from 38 to 53° Celsius.

Reconstruction E - the precipitation temperatures for the Yucca Mountain surficial deposits, based on the oxygen 18 contents from samples of these deposits.

Figure 114.

- Without having reliable information regarding both the isotopic compositions for the parent fluids and the isotopic fractionation conditions, it is not possible to specify a reliable, but at the same time narrow, range for the precipitation temperatures for the Yucca Mountain surficial deposits. Based on information presently at hand all that may be said, with some degree of certainty, is that these temperatures could have been anywhere within a range from 15 to as much as 53° Celsius, consistently with the *per ascensum* origin for the deposits.

- The currently available data do not allow for ruling out the possibility that the precipitation temperatures, for all of the considered samples, were within the 15 - 20° Celsius ambient temperature range. As a consequence, based on the results of considerations of the precipitation temperature alone, the *per descensum* origin for the Yucca Mountain surficial deposits can not be rejected.

- A more reliable and definitive picture of the geothermal circumstances of precipitation, for the Yucca Mountain calcite silica deposits, may be derived from considerations of the paleo-geothermal gradients. This is so because such considerations may be performed on relativistic basis and therefore, do not require knowledge of the absolute isotopic composition for the deposits parent fluids.

Summary - the precipitation temperature reconstructions. The Yucca Mountain calcite-silica deposits.

Figure 115.

o Considerations of: a) the $d\delta^{18}O/dz$ from samples of the calcite-silica deposits; b) the reasonable spatio-temporal variability of the oxygen - 18 content for the parent fluids; and c) the reasonable isotopic fractionation effects lead to a conclusion that, during formation of the Yucca Mountain calcite-silica deposits, the geothermal gradient (dT/dz) was a factor 1.5-2.5 higher than the contemporary geothermal gradient.

Conclusion: **a) The paleo- and contemporary geothermal gradient discrepancy indicates that precipitation of the calcite-silica deposits was accompanied by a significant warming up of the vadose zone, and occurred as the *per ascensum* process.**

b) In the past, the Yucca Mountain hydrosphere have experienced the "sink" ↔ "source" transformations.

Paleo-geothermal gradient, based on the $d\delta^{18}O/dz$ gradient.

Figure 116.

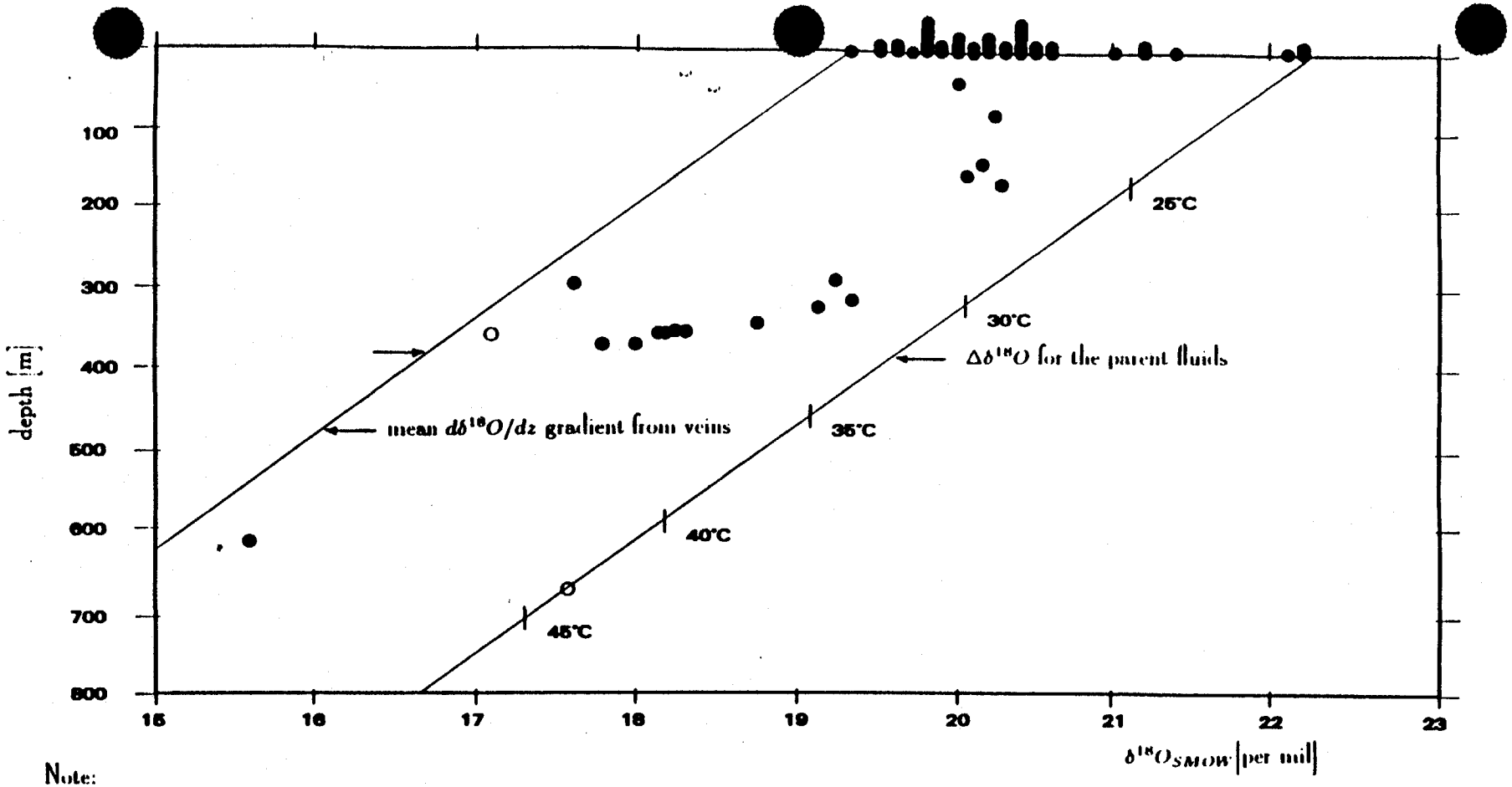

Note:

a) In performing this reconstruction, it has been assumed that: i) at the topographic surface, the precipitation temperature for calcretes and veins was $t \sim 20°$ Celsius; ii) the constant depth variability of the oxygen 18 content, from samples of the calcite-silica deposits, reflects the spatio-temporal variability of the oxygen 18 content in the parent fluids, $\Delta\delta^{18}O \sim 3$ per mil; and iii) the non equilibrium isotopic fractionation effects are absent and, therefore, $10^3 ln\alpha_{CaCO_3 - H_2O} = 2.78 \cdot 10^6/T^2 - 2.82$ - where T is precipitation temperature in ° Kelvin; and

b) Value of the paleo geothermal gradient is $dt/dz \sim 35°$ Celsius per 1km increase in depth - the corresponding contemporary geothermal gradient ranges from 20 to 24° Celsius per 1km increase in depth.

Reconstruction A - the Yucca Mountain paleo-geothermal, based on the oxygen 18 content of samples of the local calcite-silica deposits.

Figure 117.

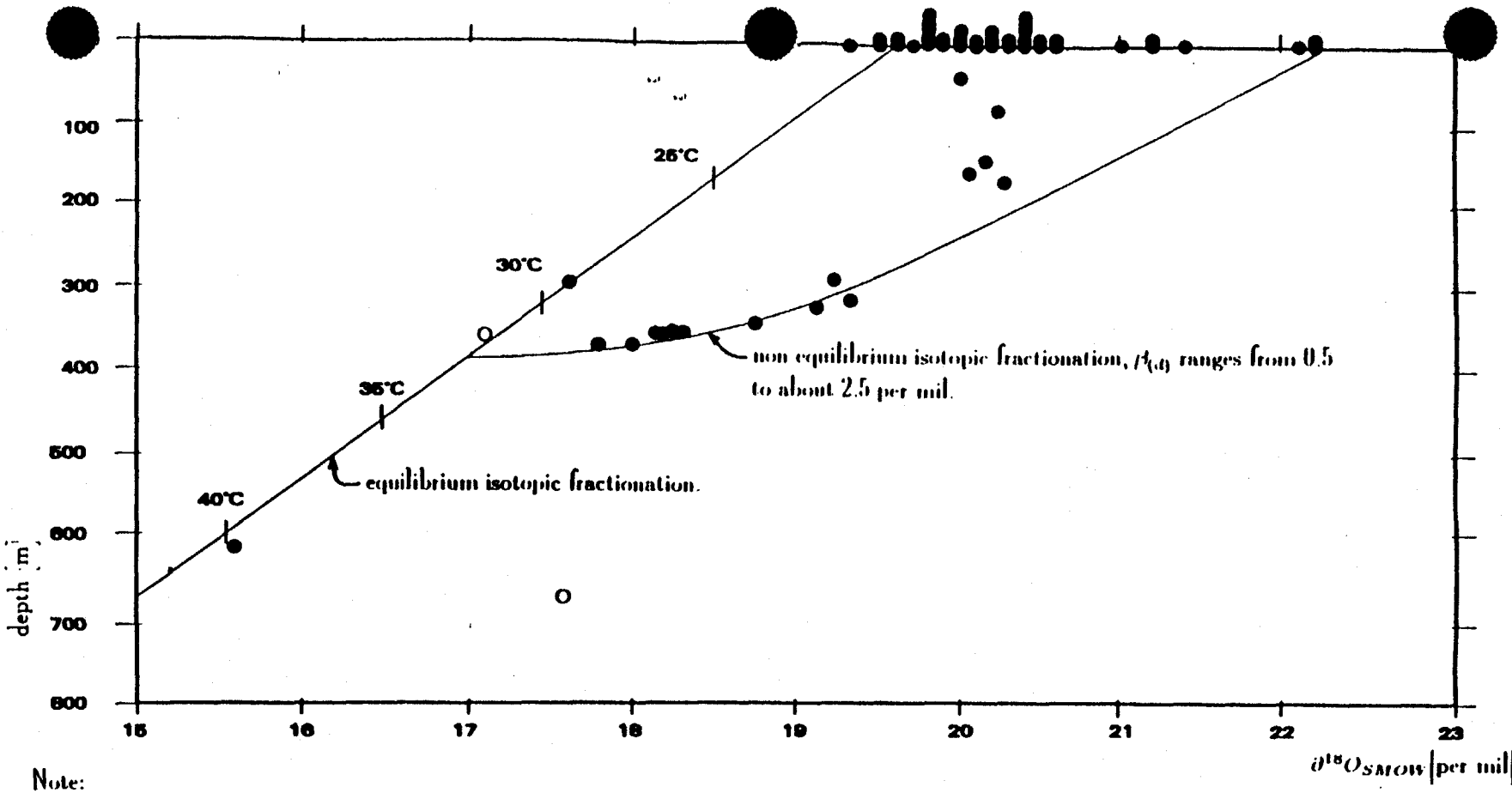

Note:

a) In performing this reconstruction, it has been assumed that: i) at the topographic surface, the precipitation temperature for calcretes and veins was $t \sim 20°$ Celsius; ii) the oxygen 18 content of the parent fluids, for spatio-temporally different samples, was the same; iii) the constant depth variability of the oxygen 18 content, from samples of the calcite-silica deposits, is attributable to the non-equilibrium isotopic fractionation effects, such that combined $10^3 \ln \alpha_{CaCO_3,\ H_2O} = 2.78 \cdot 10^6/T^2 - 2.82\ f_{(a)}$; and iv) the non-equilibrium fractionation is caused by a rapid, and depth variant escape of CO_2 from the parent solution - the CO_2 degassing rate decreases depthward, and $CaCO_3$ acquires its oxygen from both H_2O and CO_2; and

b) Value of the paleo-geothermal gradient is $dt/dz \sim 33°$ Celsius per 1km increase in depth - the corresponding contemporary geothermal gradient ranges from 20 to 24° Celsius per 1km increase in depth.

Reconstruction B - the Yucca Mountain paleo-geothermal gradient, based on the oxygen 18 content of samples of the local calcite-silica deposits.

Figure 119.

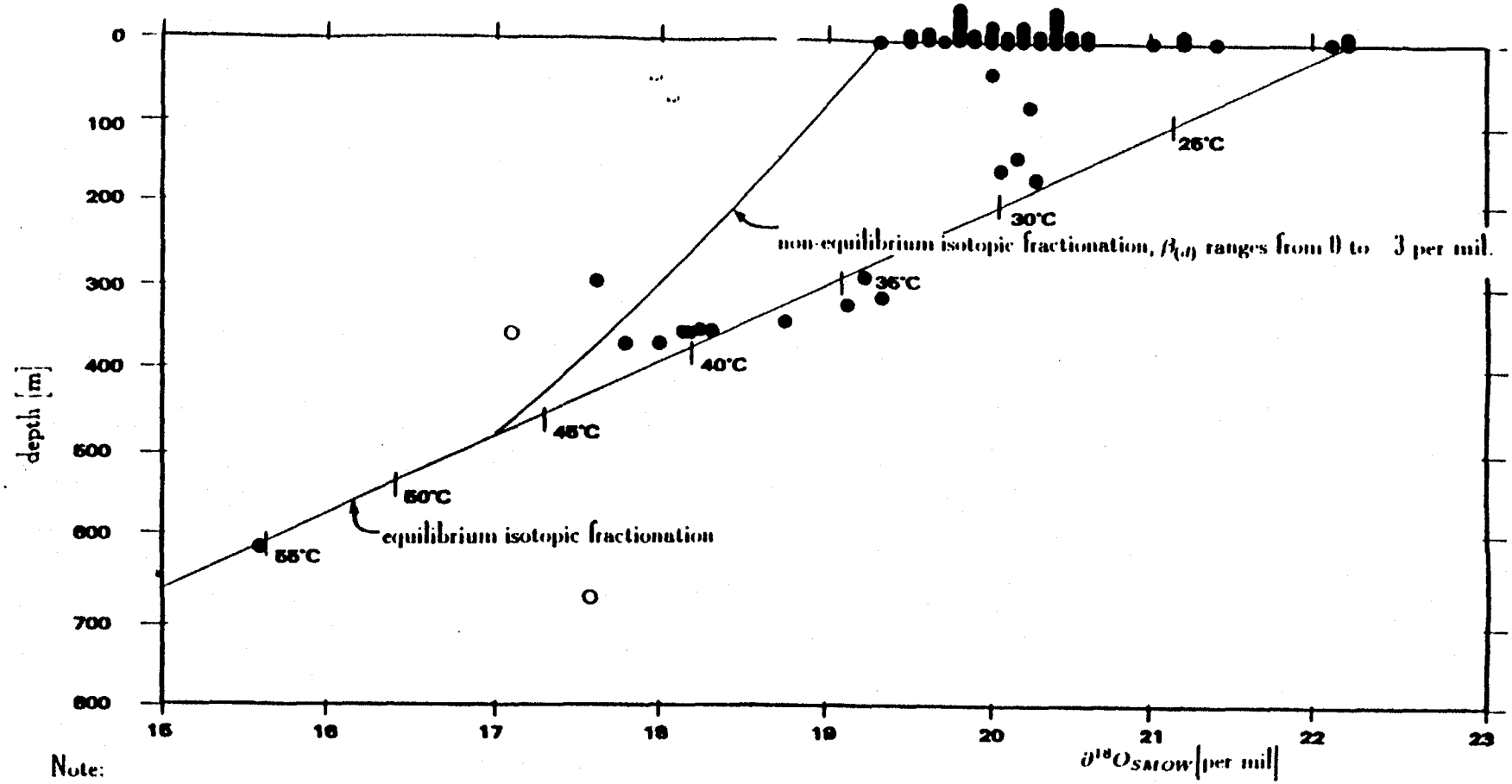

Note:

a) In performing this reconstruction, it has been assumed that: i) at the topographic surface, the precipitation temperature for calcretes and veins was $t \sim 20^{o}$ Celsius; ii) the oxygen 18 content of the parent fluids, for spatio-temporally different samples, was the same; iii) the constant depth variability of the oxygen 18 content, from samples of the calcite-silica deposits, is attributable to the non-equilibrium isotopic fractionation effects, such that combined $10^{3}\ln\alpha_{CaCO_3\,H_2O} = 2.78 \cdot 10^{6}/T^{2} - 2.82 - \beta_{(d)}$; and iv) the non-equilibrium fractionation is caused by a rapid upward movement of the parent fluids - the $CaCO_3$ nucleation occures prior to its deposition and, consequently, the deposited $CaCO_3$ records, temperatures that are higher than those prevailing at the actual deposition sites; and

b) Value of the paleo-geothermal gradient is $dt/dz \sim 58^{o}$ Celsius per 1km increase in depth - the corresponding contemporary geothermal gradient ranges from 20 to 24° Celsius per 1km increase in depth.

Reconstruction C - the Yucca Mountain paleo-geothermal gradient, based on the oxygen 18 content of samples of the local calcite-silica deposits.

Figure 120

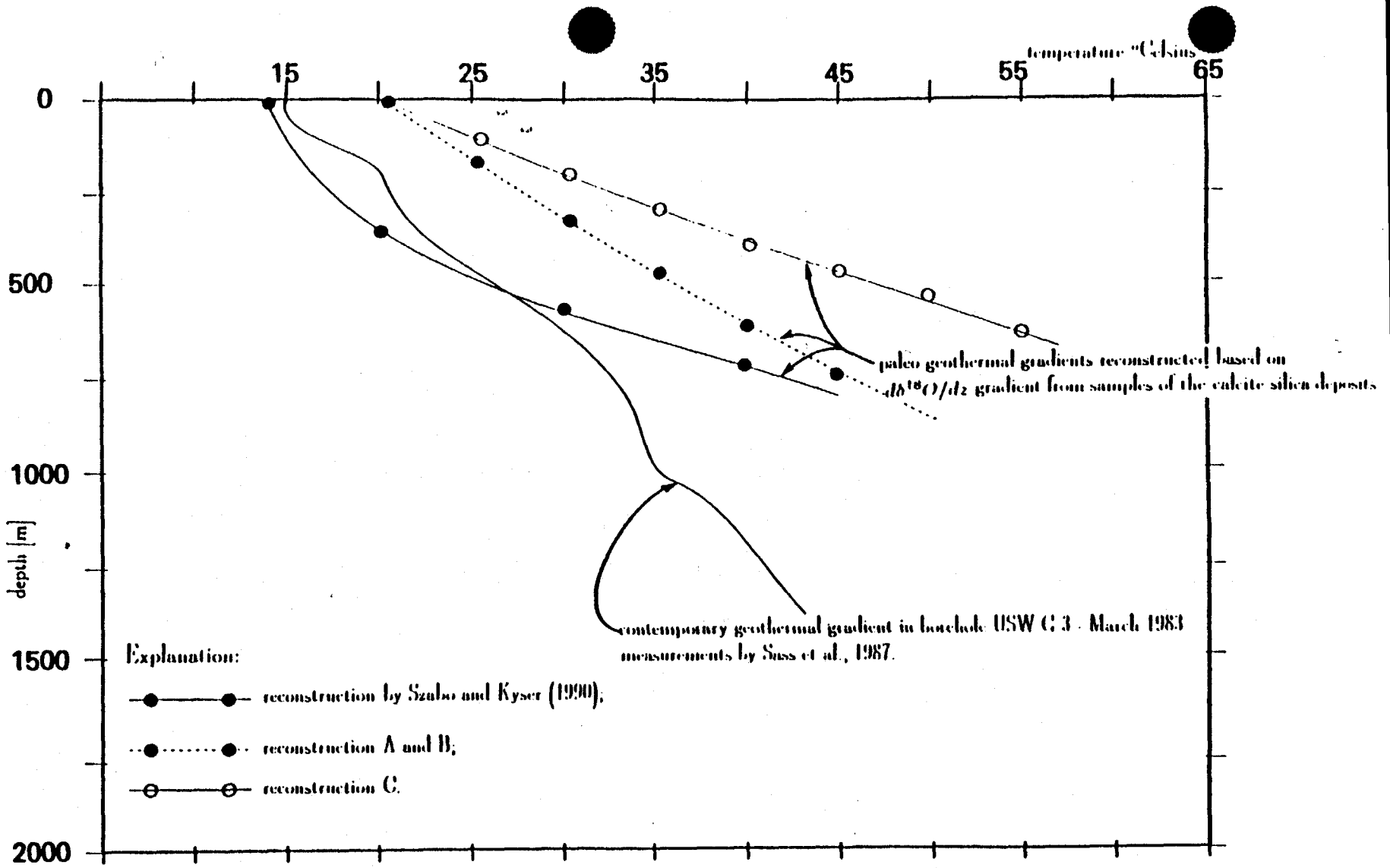

Note:

a) Each of the considered cases yields the paleo- geothermal gradient that is substantially higher than the contemporary geothermal gradient; and

b) The geothermal gradients discrepancy indicates that precipitation of the calcite-silica deposits was accompanied by a significant warming up of the vadose zone and, therefore, occurred as the *per ascensum* process.

Comparison between the contemporary geothermal gradient and the paleo-geothermal gradients, as reconstructed based on the $d\delta^{18}O/dz$ gradient from samples of the calcite-silica deposits and using various assumptions.

Figure 121

- Figure 4-3.44 presents a summary of reconstructions of the Yucca Mountain paleo-geothermal gradient. The contemporary geothermal gradient, as measured in Well USW G-3 by Sass et al., (1987), is used as a reference.

- In all cases considered, the reconstructed paleo-geothermal gradient is significantly greater than the geothermal gradient, as measured in the corresponding wells. Values of the contemporary geothermal gradient are: i) Well UE-25a, dT/dz ~ 22°Celsius per 1km of depth; ii) Well USW G-2, dT/dz ~ 24°Celsius per 1km of depth; iii) Well USW G-3, dT/dz ~ 22°Celsius per 1km of depth; and iv) Well USW G-4, dT/dz ~ 20°Celsius per 1km of depth.

- The reconstructed values of the paleo-geothermal gradient are: i) reconstruction by Szabo and Kyser (1990) - dT/dz ranging from 17, near the topographic surface, to 50°Celsius per 1km of depth, in deeper parts of the vadose zone; ii) reconstruction A - dT/dz ~ 35°Celsius per 1km of depth; iii) reconstruction B - dT/dz ~ 33°Celsius per 1km of depth; and iv) reconstruction C - dT/dz ~ 58°Celsius per 1km of depth.

- The interpreted temporal fluctuations of values of the geothermal gradient indicate that, the Yucca Mountain vadose zone was being episodically invaded by warm fluids from below the water table. Evidently, the resulting warming up of the vadose zone was accompanied, and recorded, by the episodic precipitation of the calcite-silica veins.

- As far as the origin of the calcite-silica deposits is concerned, the available oxygen -18 and carbon -13 data are convincing and clear. Both the surficial deposits and the subsurface veins were produced via the *per ascensum* process.

Summary - the paelo-geothermal gradient reconstruction.

PART 2

Materials Prepared for and Presented to NRC/NAS Field Trip, April 23-25, 1991

Department of Energy
Yucca Mountain Site Characterization
Project Office
P. O. Box 98608
Las Vegas, NV 89193-8608

WBS 1.2.9
QA: N/A

APR 19 1991

Ina B. Alterman, Ph.D.
Senior Program Officer
Board on Radioactive Waste Management
National Academy of Sciences National
Research Council
2101 Constitution Avenue, N.W.
Washington, DC 20418

TRANSMITTAL OF THE FIELD BRIEFING MATERIAL

Enclosed please find a copy of the presentations I have prepared for the forthcoming National Sciences Academy field trip. Should you have any questions regarding the enclosed material, please do not hesitate to contact me at (702) 794-7941 or FTS 544-7941.

Jerry S. Szymanski
Technical Analysis Branch
Regulatory & Site Evaluation Division

RSED:JSS-3375

Enclosure:
Presentation Package

cc w/encl:
Leon Reiter, NWTRB, Arlington, VA
P. T. Prestholt, NRC, Las Vegas, NV
C. B. Archambeau, University of
Colorado, Boulder, CO
N. J. Price, Balloon House,
Lincolnshire, United Kingdom
J. W. Rudnicki, Northwestern University,
Evanston, IL
J. L. Smith, University of British
Columbia, Vancouver, BC, Canada
Dennis Powers, Anthony, TX
Jack Evernden, USGS, Menlo Park, CA

THE NEVADA TEST SITE AREA

SUBJECT: **DIRECT FIELD OBSERVATIONS AND GEOCHEMICAL-ISOTOPIC EVIDENCE FOR THE CONCEPTUAL UNDERSTANDING OF THE NEVADA TEST SITE HYDROSPHERE, AS PROPOSED BY SZYMANSKI (1989).**

J. SZYMANSKI
SENIOR SCIENTIST
TECHNICAL ANALYSIS BRANCH
YUCCA MOUNTAIN SITE CHARACTERIZATION PROJECT OFFICE

APRIL 23-25, 1991

Table of Contents

Presentation #1 - Thermodynamic character of the Nevada Test Site Hydrosphere.

Table of Contents

Table of Contents

Table of Contents

Table of Contents

Table of Contents

Part III - Isotopic and geochemical evidence for the per ascensum origin of the Yucca Mountain calcretes and surficial veins. (continued)

Table of Contents

Part III - Isotopic and geochemical evidence for the per ascensum origin of the Yucca Mountain calcretes and surficial veins. (continued)

Table of Contents

Issue - Thermodynamic character of the Nevada Test Site hydrosphere.

Interpretation options

I - apart from changing climatic conditions, non-evolving flow system consisting of spatially fixed and uniform recharge and discharge regions.

II - a non-monotonically evolving self-organized flow system consisting of alternating "sink" and "source" regions.

Statement of the issue - presentation #1.

Figure 1-1

Isotopic and chemical evidence for self-organization

Step I - Delineation of the self-organization produced macroscopic order, i.e., "sink" - "source" subdivision of the Nevada Test Site hydrosphere based on spatial distribution of: i) dh/dz - vertical hydraulic gradient, ii) dT/dz - geothermal gradient, and iii) fluid chemistry.

Step II - Isotopic expression of the delineated macroscopic order: i) uranium content and values of the $^{234}U/^{238}U$ ratio, ii) values of the $^{87}Sr/^{86}Sr$ ratio, iii) values of the $\delta^{14}C$ (PMC) and $\delta^{13}C$ ratios, and iv) values of the δD and $\delta^{18}O$ ratios.

Note: Both the "source" and "sink" phrases have been borrowed from topological studies of various non-linear equations of motion, see Stewart (1989), for example. They are used in the context of the so-called phase space portraits of such equations.

Self-organization. The Nevada Test Site hydrosphere.

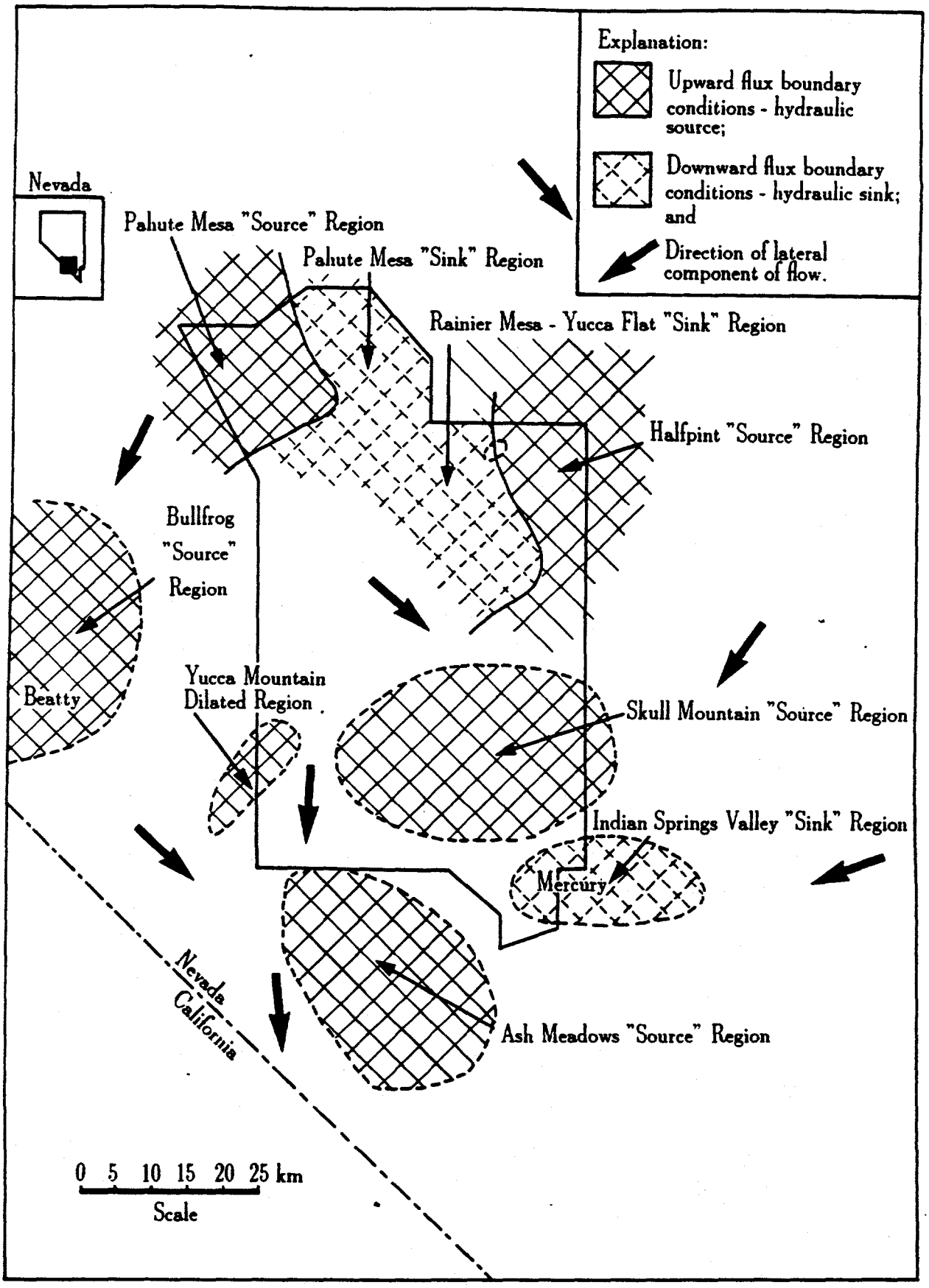

Inferred boundary conditions. The Nevada Test Site hydrosphere.

Pahute Mesa Hydraulic "Source" Region

Vertical hydraulic gradient dh/dz - upward (maximum known value is $\Delta h = 174$ ft.).

Vertical geothermal gradient dT/dz ranging from 30 to about 60°C/km.

Lateral geothermal gradient dT/dx 5°C/1 mile.

Possible upper thermal boundary layers.

Water chemistry:
$Ca^{++} + Mg^{++}$ from 1 to 40 ppm
$Na^{+} + K^{+}$ from 40 to 250 ppm
$CL^{-} + SO^{-}_{4}$ from 35 to 250 ppm
HCO_3^{-} from 90 to 270 ppm.

Pahute Mesa Hydraulic "Sink" Region

Vertical hydraulic gradient dh/dz - downward (maximum known value is $\Delta h = 41$ ft.).

Vertical geothermal gradient dT/dz ~ 30°C/km.

Water chemistry:
$Ca^{++} + Mg^{++}$ from 4 to 60 ppm
$Na^{+} + K^{+}$ from 35 to 95 ppm
$CL^{-} + SO_4^{--}$ from 15 to 70 ppm
HCO_3^{-} from 60 to 450 ppm.

Boundary conditions. Interpretation bases. The Nevada Test Site hydrosphere.

Rainier Mesa - Yucca Flat Hydraulic "Sink" Region.

Vertical hydraulic gradient dh/dz - downward (maximum known value is $\Delta h = 1560$ ft.).

Vertical geothermal gradient $dT/dz \simeq 20\text{-}25°C$.

Water chemistry: $Ca^{++} + Mg^{++}$ from 2 to 40 ppm
$Na^{+} + K^{+}$ from 22 to 65 ppm
$CL^{-} + SO_4^{--}$ from 11 to 40 ppm
HCO_3^{-} from 50 to 230 ppm.

Note: $\sigma_c \geq \frac{1}{3} \sigma_{ov}$ indicating that dilation is either very shallow or non-existant.

Halfpint Hydraulic "Source" Region.

Vertical hydraulic gradient dh/dz - unknown.

Vertical geothermal gradient $dT/dz \simeq 45°C/km$.

Water chemistry: $Ca^{++} + Mg^{++}$ from 55 to 400 ppm
$Na^{+} + K^{+}$ from 50 to 270 ppm
$CL^{-} + SO^{4--}$ from 85 to 1100 ppm
HCO_3^{-} from 65 to 400 ppm.

Note: a) local water table is bent upward, maximum altitude is 4535 ft. amsl. (148 ft. above water table in upstream regions); and

b) lateral hydraulic gradient 1300 ft/mile and 820 ft/mile.

Boundary conditions. Interpretation bases. The Nevada Test Site hydrosphere.

Skull Mountain Hydraulic "Source" Region.

Vertical hydraulic gradient dh/dz - uncertain (upward gradient is suggested by hydraulic head observations made during drilling of Well #73-68).

Vertical geothermal gradient dT/dz = 45-50°C/km.)

Water chemistry: $Ca^{++} + Mg^{++}$ from 4 to 470 ppm
$Na^{+} + K^{+}$ from 47 to 450 ppm
$CL^{-} + SO_4^{--}$ from 35 to 500 ppm
HCO_3^{-} from 100 to 1000 ppm.

Note: a) water table is bent upward, maximum altitude is 2982 ft. amsl. (about 600 ft. above water table in upstream regions);

b) samples of perched water display chemical affinity with water from below the water table; and

c) possible upper thermal boundary layer present in two boreholes.

Indian Springs Valley Hydraulic "Sink" Region.

Vertical hydraulic gradient dh/dz - unknown.

Vertical geothermal gradient dT/dz < 20°C/km.

Water chemistry: $Ca^{++} + Mg^{++}$ from 16 to 75 ppm
$Na^{+} + K^{+}$ from 6 to 40 ppm
$CL^{-} + SO_4^{--}$ from 8 to 70 ppm
HCO_3^{-} from 180 to 300 ppm.

Note: a) local water table is bent downward, minimum altitude is 2281 ft. amsl. (80 feet lower than water table downstream).

Boundary conditions. Interpretation bases. The Nevada Test Site hydrosphere.

Ash Meadows Hydraulic "Source" Region.

Vertical hydraulic gradient dh/dz - upward (maximum value of Δ h - unknown).

Vertical geothermal gradient dT/dz ~ 40°C/km.

Water chemistry: $Ca^{++} + Mg^{++}$ from 12 to 270 ppm
$Na^{+} + K^{+}$ from 20 to 300 ppm
$CL^{-} + SO_4^{--}$ from 45 to 1300 ppm
HCO_3^{-} from 120 to 380 ppm.

Note: a) water table appears to be bent upward; downstream water table altitude 2200 ft. amsl., maximum altitude 2365 ft., upstream at altitude 2281 ft; and

b) fault-line spring discharge, temperature ranging from 23 to 34.5°C.

Bullfrog Hydraulic "Source" Region.

Vertical hydraulic gradient dh/dz - upward (maximum value of Δ h - unknown).

Vertical geothermal gradient dT/dz - unknown.

Water chemistry: $Ca^{++} + Mg^{++}$ from 8 to 50 ppm
$Na^{+} + K^{+}$ from 100 to 350 ppm
$CL^{-} + SO_4^{--}$ from 90 to 350 ppm
HCO_3^{-} from 150 to 480 ppm.

Note: a) perched waters - discharge temperature 21-26.5°C and chemical affinity with deeper fluids suggest that these waters represent mixtures of deep fluids with infiltrating meteoric fluids; and

b) water table may be bent upward; downstream - 2500 ft., maximum ~ 4000 ft., upstream - 3800 ft.

Boundary conditions. Interpretation bases. The Nevada Test Site hydrosphere.

Yucca Mountain "Dilated" Region.

Vertical hydraulic gradient dh/dz - upward in deeper undilated regions; neutral immediately below the water table.

Vertical geothermal gradient dT/dz = 40-60°C/km in deeper undilated regions; dT/dz = 20-30°C/km immediately below the water table.

Water chemistry: dilated zone $Ca^{++} + Mg^{++}$ from 2 to 20 ppm
$Na^{+} + K^{+}$ from 40 to 120 ppm
$CL^{-} + SO_4^{-}$ from 21 to 55 ppm
HCO_3^{-} from 100 to 300 ppm.

undilated zone $Ca^{++} + Mg^{++}$ 140 ppm
$Na^{+} + K^{+}$ 162 ppm
$CL^{-} + SO_4^{-}$ 188 ppm
HCO_3^{-} 569 ppm.

Note: a) local values of $\dot{\sigma}_c \longrightarrow 0$, (indicating severe dilation) extend to a maximum depth of about ~ 1300 m; and

b) the Yucca Mountain area is a source - sink hybrid.

The geothermal, hydraulic, and geochemical data used is subdividing the Nevada Test Site hydrosphere, are from Walker (1962); Blankennagel and Weir (1973); Claassen (1973); Winograd and Thordenson (1975); White (1972); White et al. (1980); Garside and Schilling (1979); Sass and Lachenbruch (1982); Isherwood et al. (1982); Claassen (1985); and Benson and McKinley (1985).}

Boundary conditions. Interpretation bases. The Nevada Test Site hydrosphere.

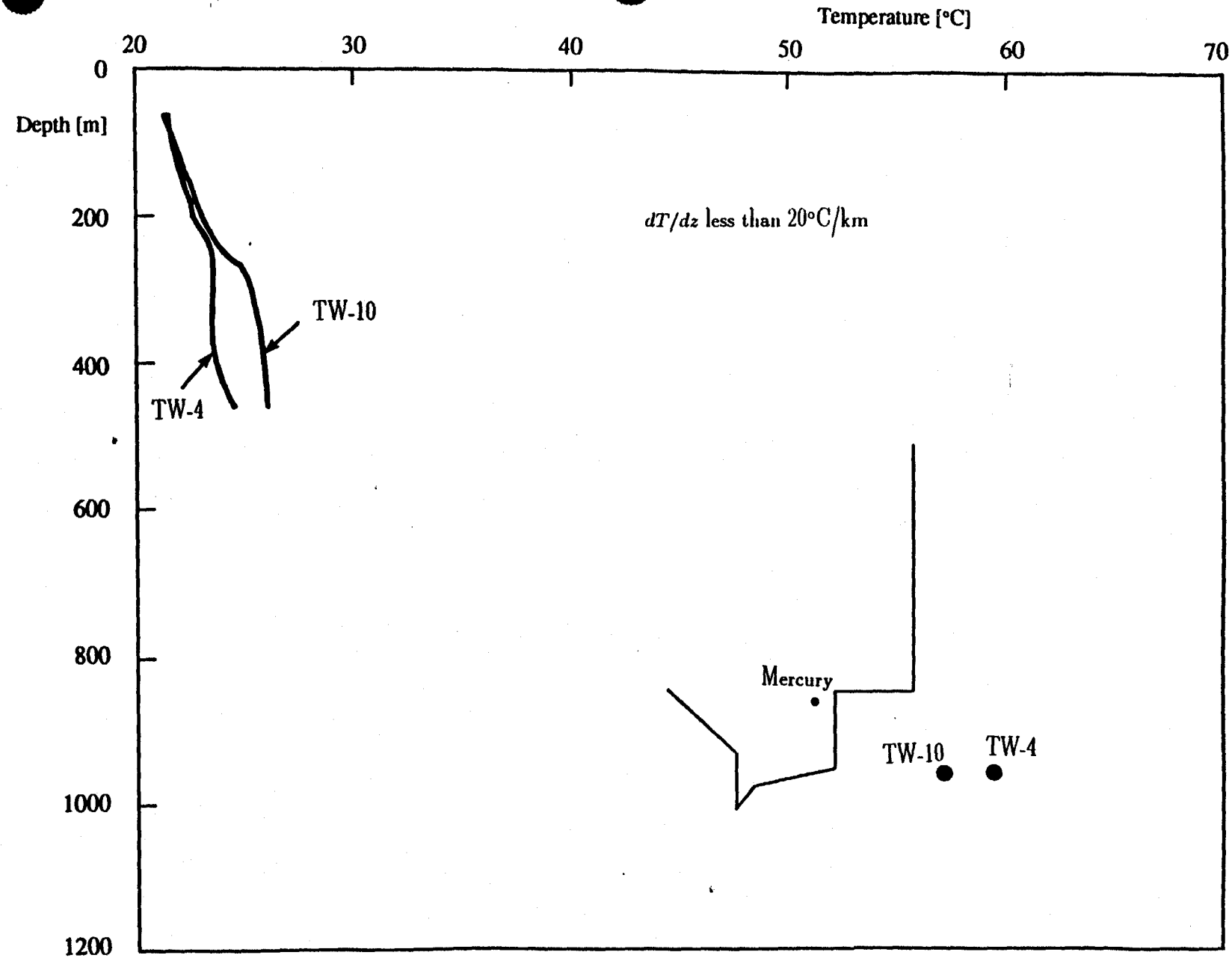

Downhole temperature profiles. Southern Indian Springs Valley "sink" region. From Sass and Lachenbruch, 1982.

Figure 1-5a

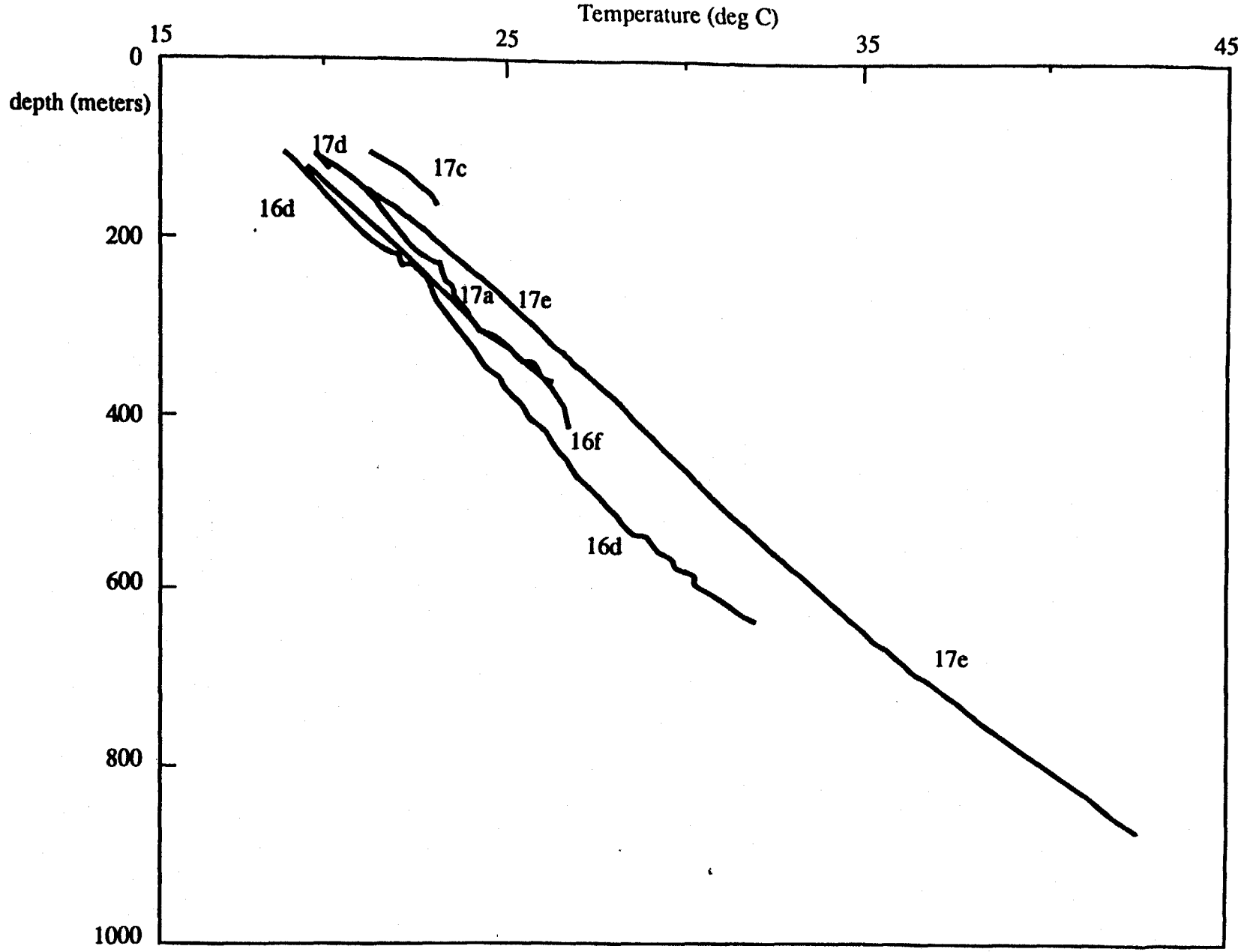

Downhole temperature profiles. Rainier Mesa - Yucca Flat hydraulic "sink" regions. From Sass and Lachenbruch, 1982.

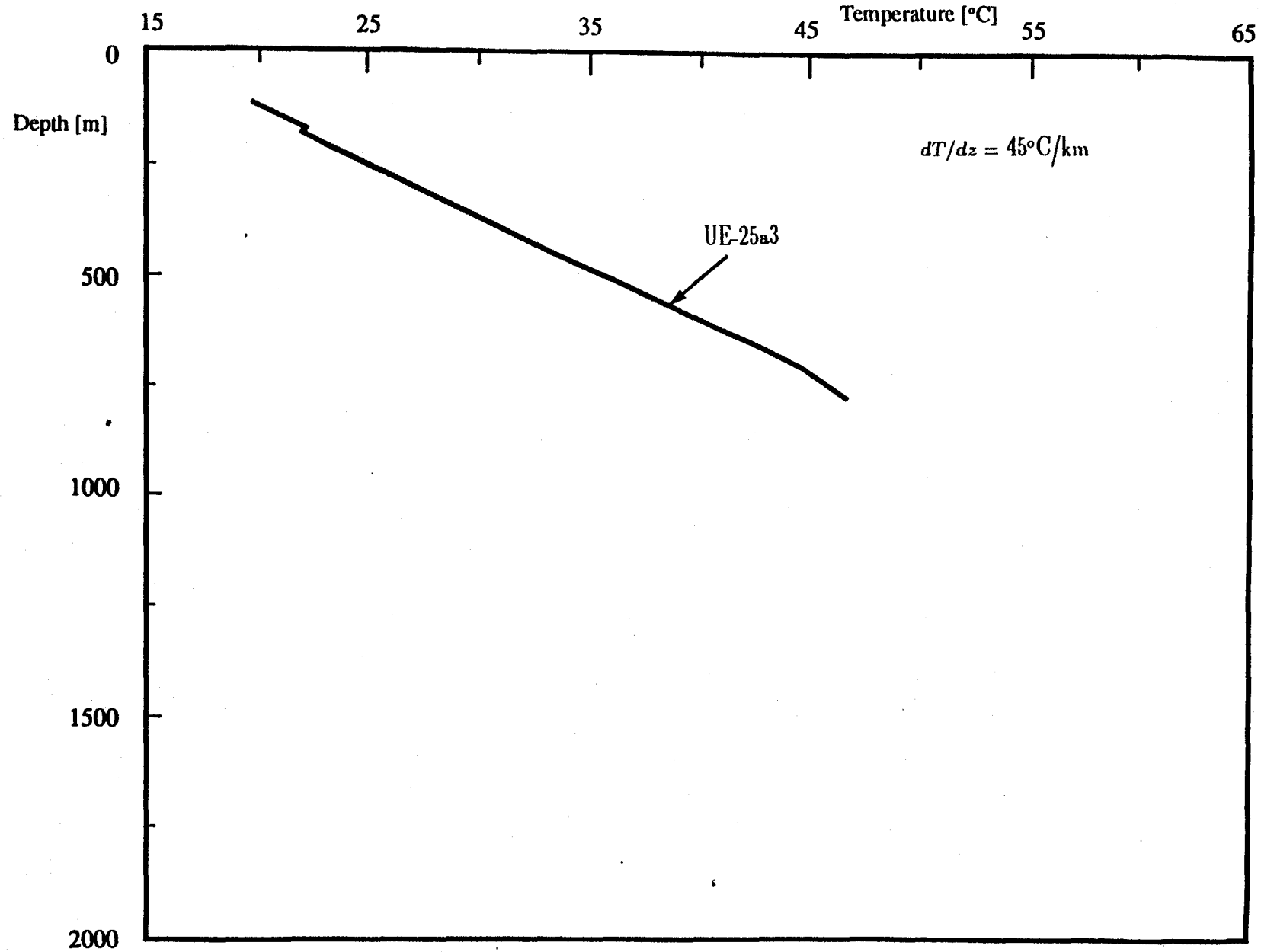

Downhole temperature profiles. Borehole UE-25a3. North-western margin of the Skull Mountain hydraulic "source" region. From Sass and Lachenbruch, 1982.

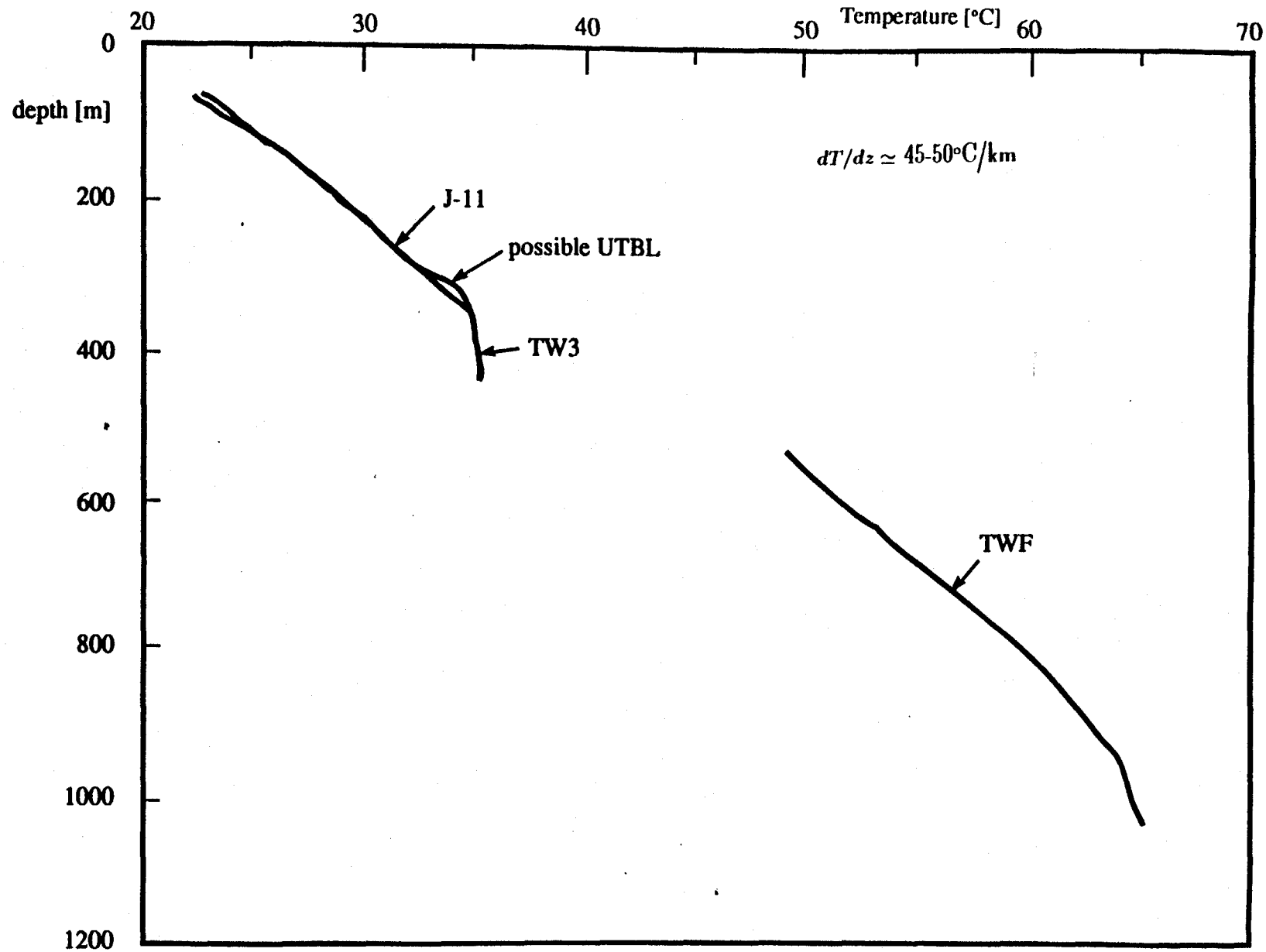

Downhole temperature profiles. Boreholes J-11, TWF, and TW3. Skull Mountain hydraulic "source" region. From Sass and Lachenbruch, 1982.

Figure 1-5d

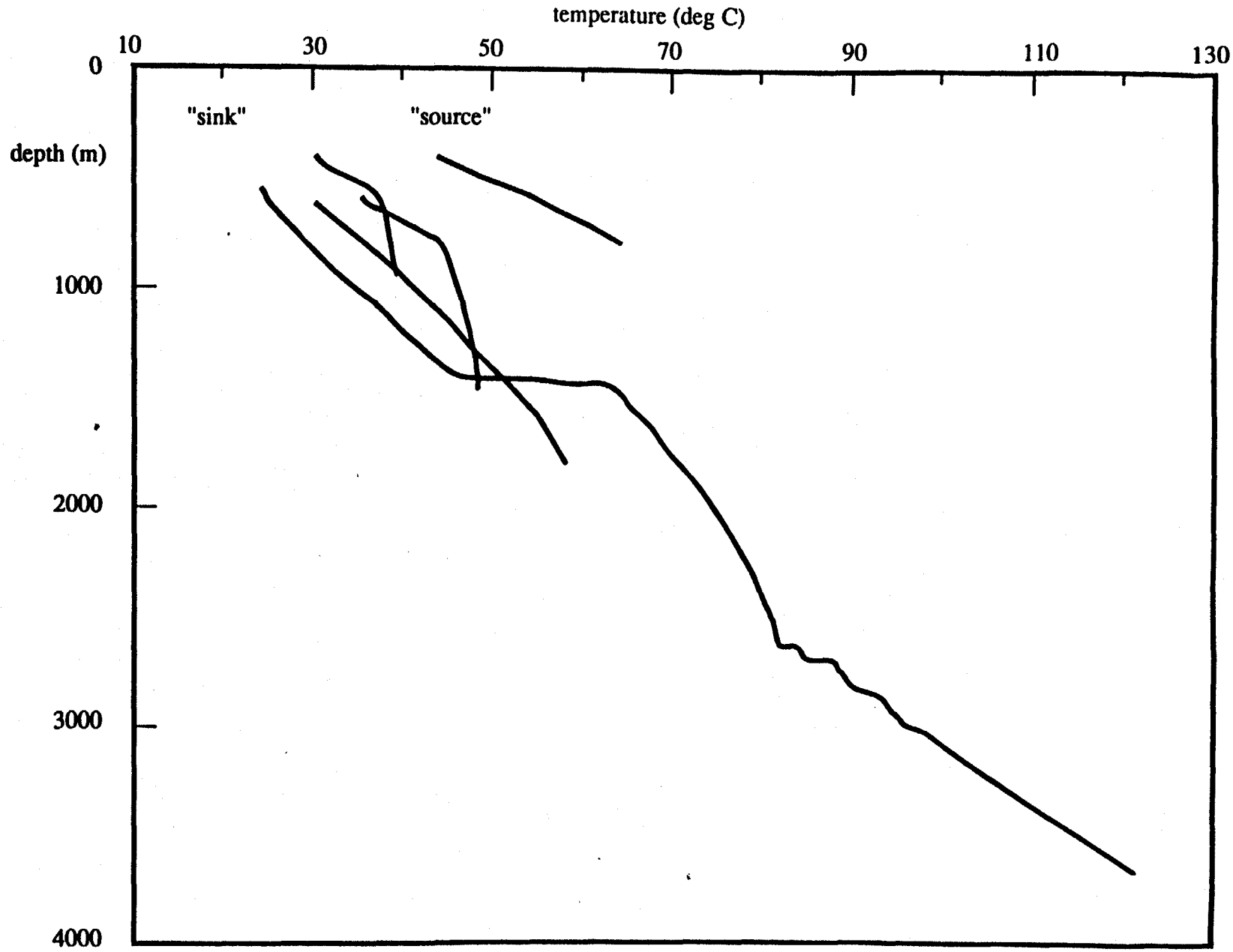

Downhole temperature profiles. Pahute Mesa hydraulic "sink" and "source" regions. Modified from Sass and Lachenbruch, 1982.

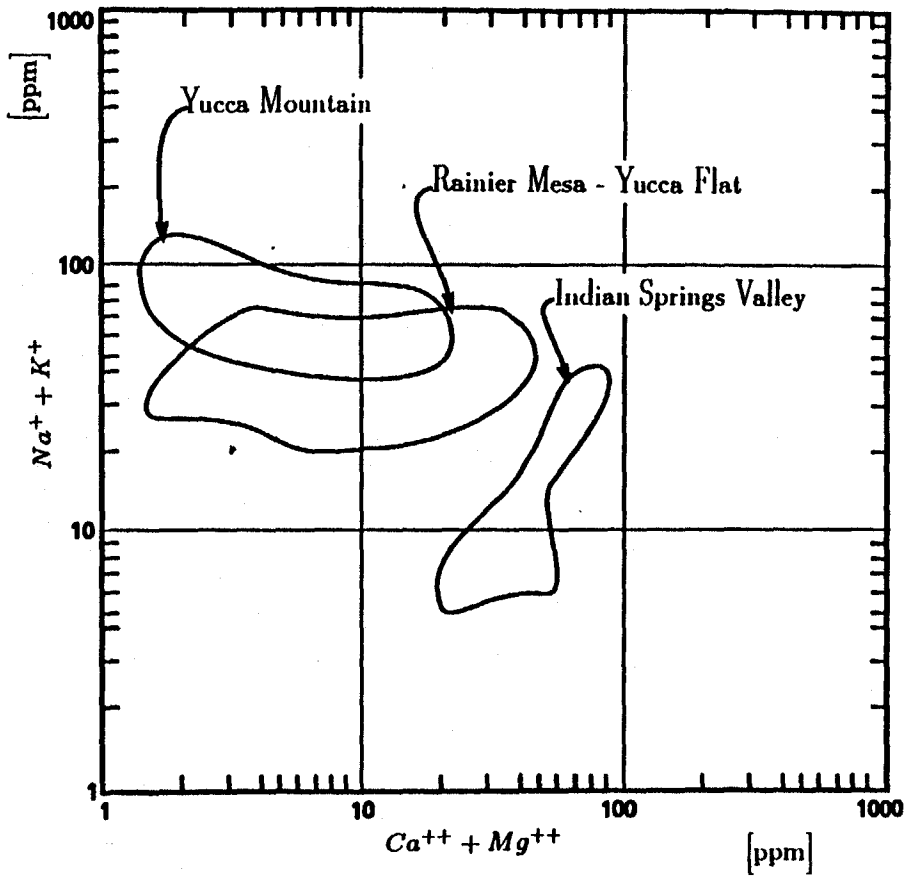

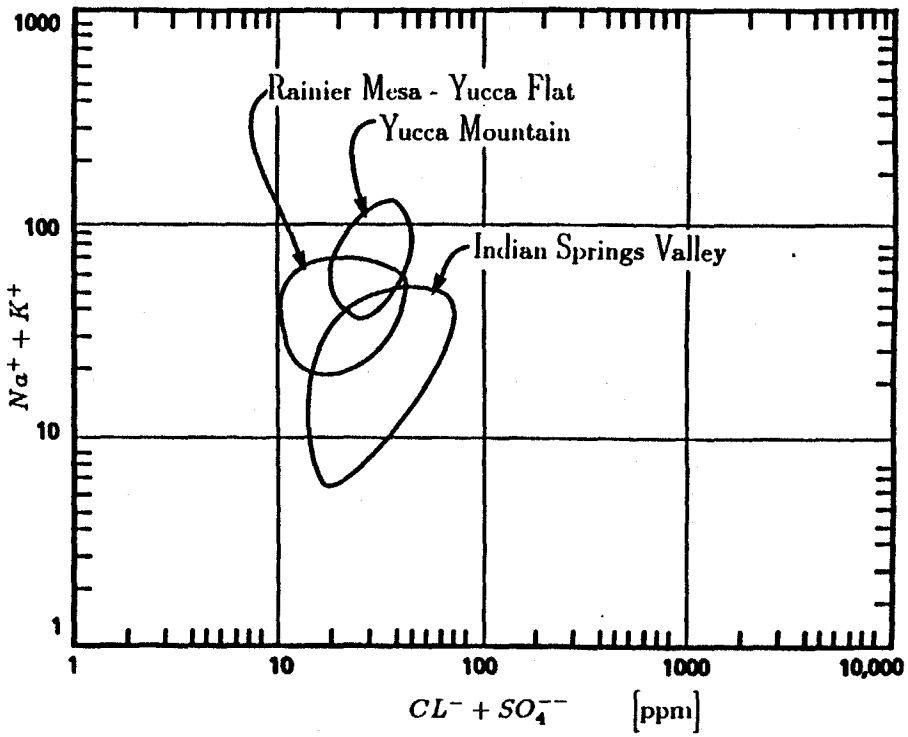

Groundwater chemistry. Hydraulic "sink" and dilated regions. The Nevada Test Site hydrosphere.

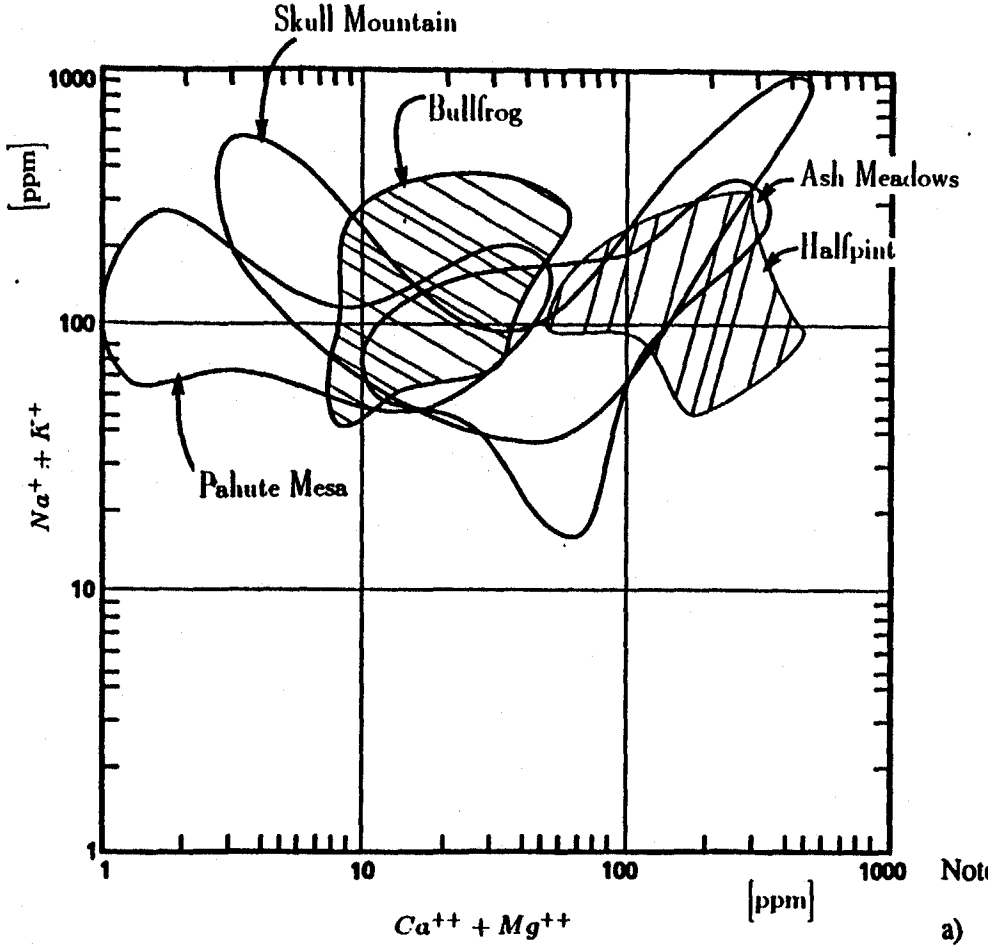

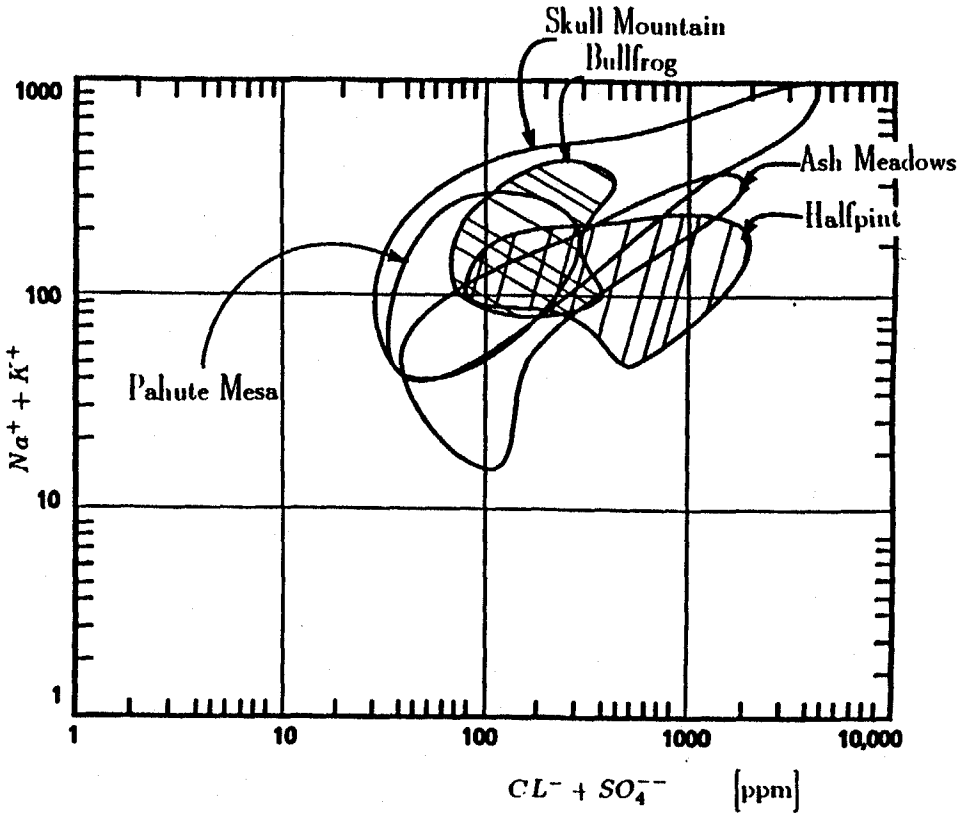

Note:

a) fluids result from intermixing of at least two end-members;

b) one end-member is represented by poorly evolved meteoric recharge; and

c) the other member is represented by deep and chemically evolved fluids.

Groundwater chemistry. Hydraulic "source" regions. The Nevada Test Site hydrosphere.

- If the Nevada Test Site hydrosphere is a self-organized system indeed then, it may be expected that the hydraulic "source" regions contain fluids which, in terms of various isotopic signatures, are distinct from the hydraulic "sink" fluids.

- Specifically, relative to the hydraulic "sink" fluids, fluids residing in the contemporary hydraulic "source" regions should exhibit:

  a) higher concentrations of the dissolved uranium and lower values of the $^{234}U/^{238}U$ activity ratio;

  b) higher values of the $^{87}Sr/^{86}Sr$ ratio;

  c) higher values of the $\delta^{13}C$ ratio and lower carbon -14 concentrations;

  d) higher magnitudes of the "oxygen isotopic shift"; and

  e) negative values of the "hydrogen isotopic shift".

  Note:

  a) each of the above expectations has a rational base;

  b) the derivation of these expectations is a lengthy process and will not be presented here; and

  c) other isotopic expressions are conceivable.

Expected relative isotopic expressions of the contemporary hydraulic "source" regions. The Nevada Test Site hydrosphere.

- At the Nevada Test Site, the U-content vs. $^{234}U/^{238}U$ field from samples of the hydraulic "source" fluids is distinct from the corresponding field from samples of the hydraulic "sink" fluids.

Conclusion: **The Nevada Test Site hydrosphere is a self-organized dynamic system and consists of a number of the Benard-Rayleigh dissipative structures.**

Self-organization. The Nevada Test Site hydrosphere - dissolved uranium data.

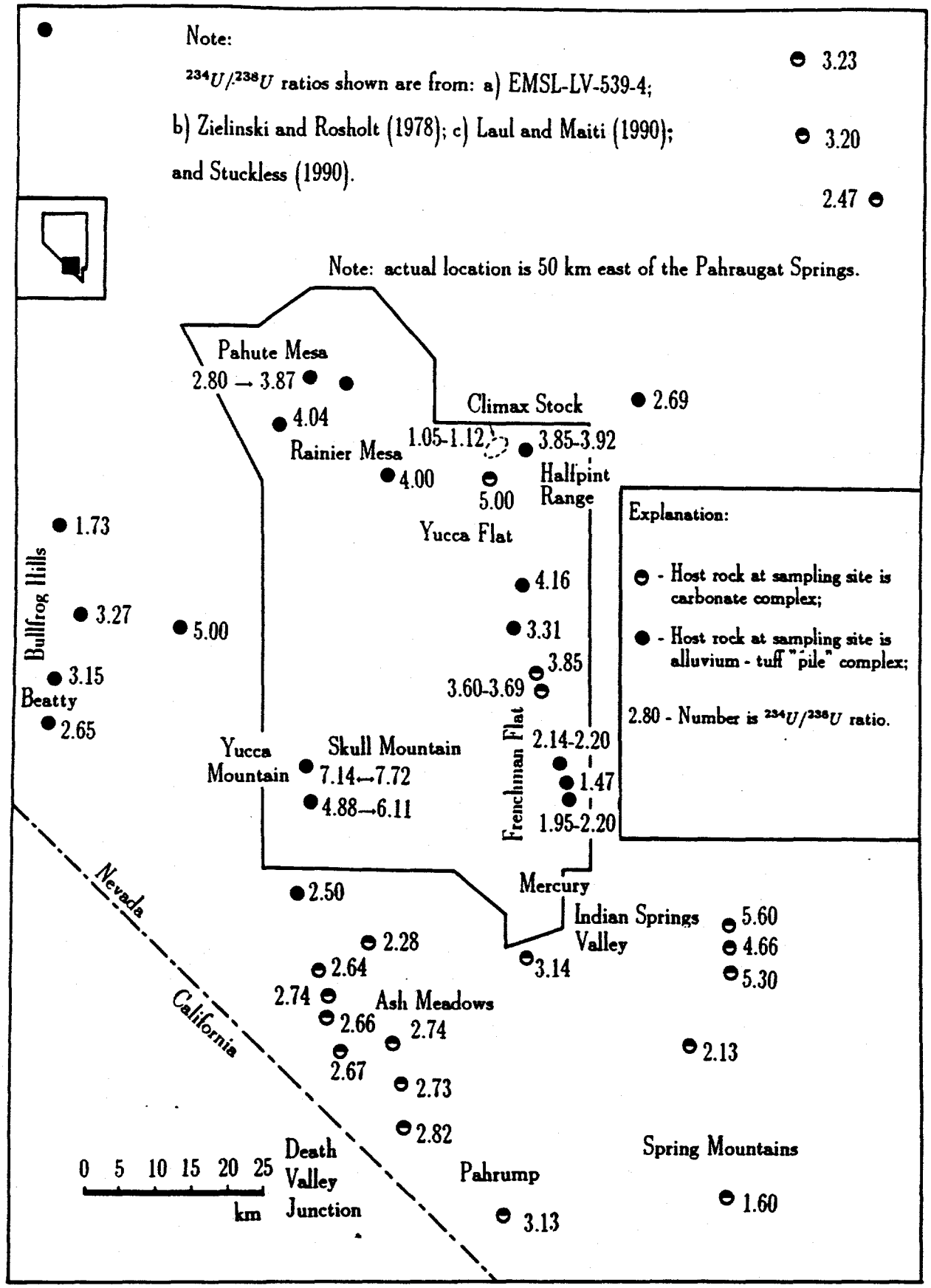

$^{234}U/^{238}U$ ratio. The Nevada Test Site hydrosphere.

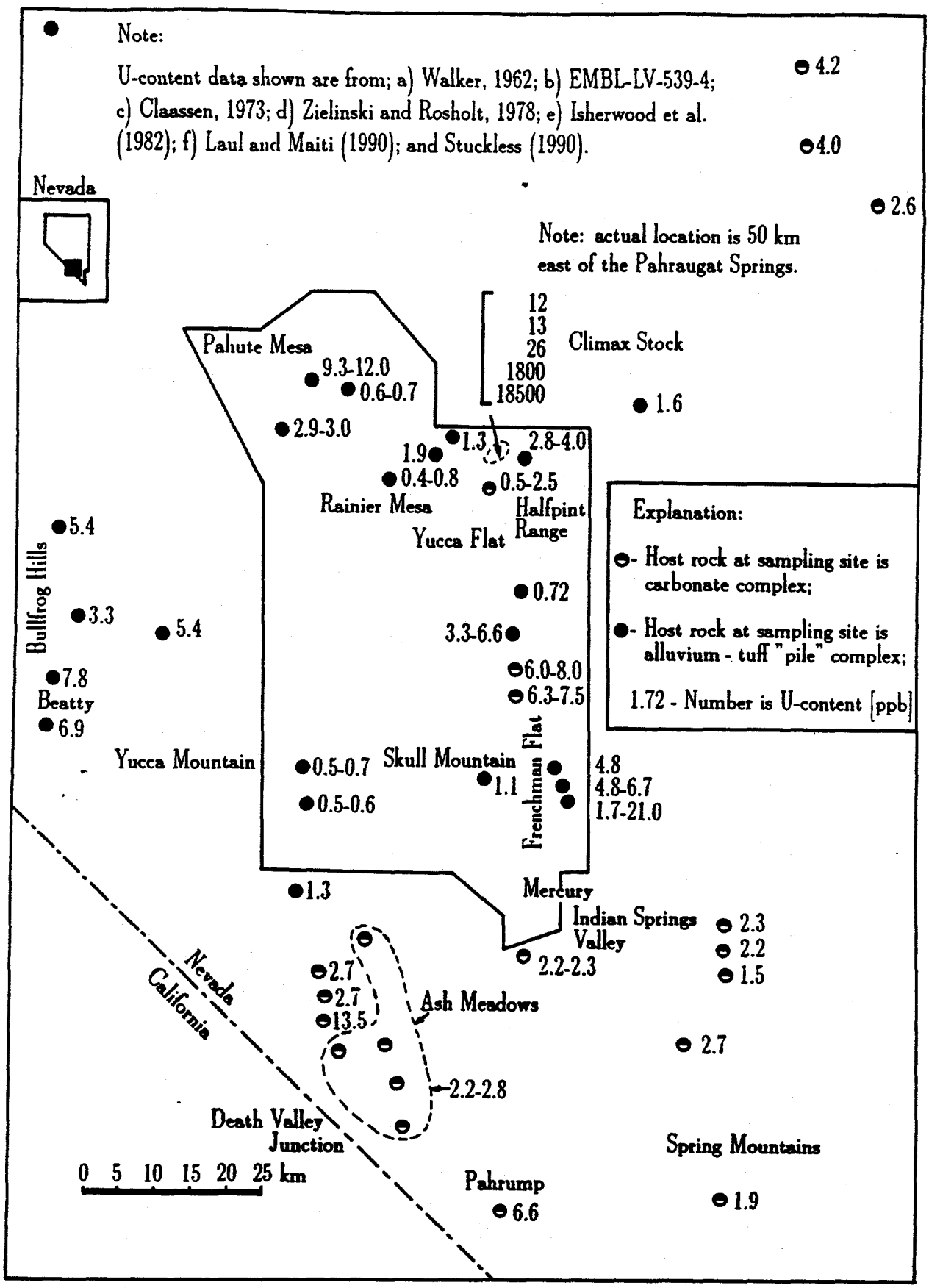

U content. The Nevada Test Site hydrosphere.

Figure 1-12

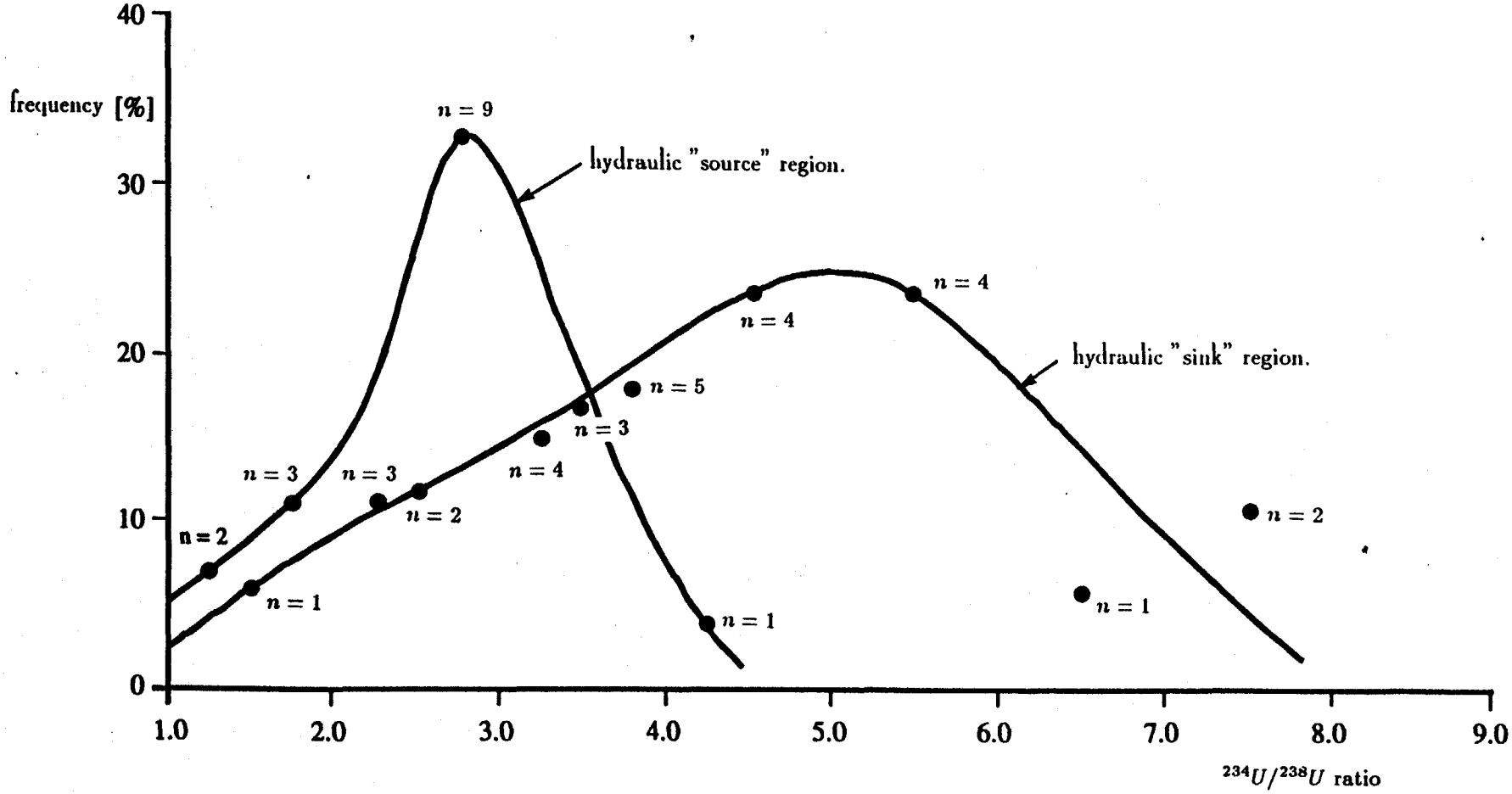

Note:

a) n = 27 for hydraulic "source" regions; n = 17 for hydraulic "sink" regions.

Isotopic character of the dissolved uranium. Water samples from the hydraulic "source" and "sink" regions. The Nevada Test Site hydrosphere.

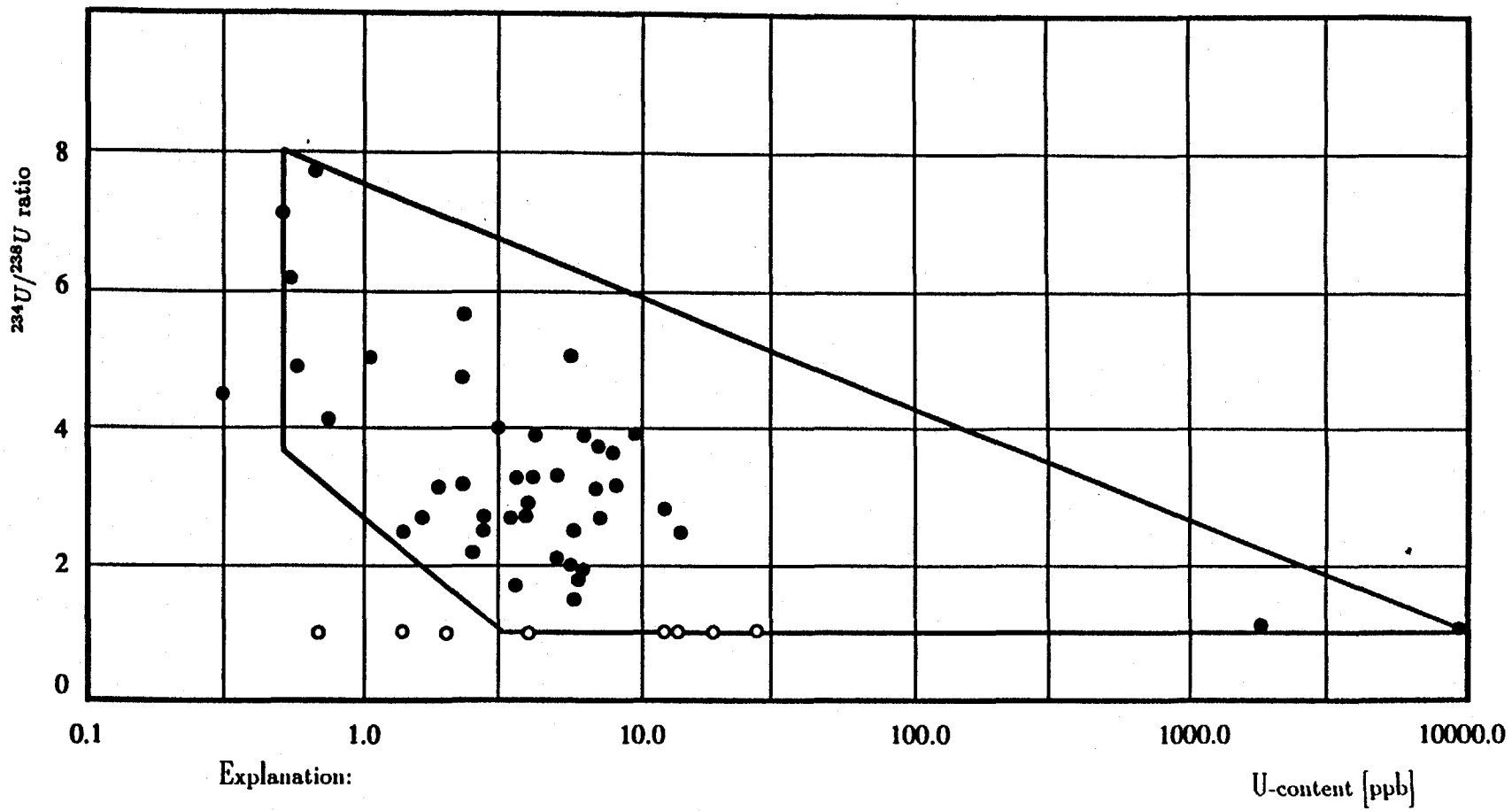

$^{234}U/^{238}U$ ratio vs U-content field. Nevada Test Site subsurface fluids.

Figure 1-14

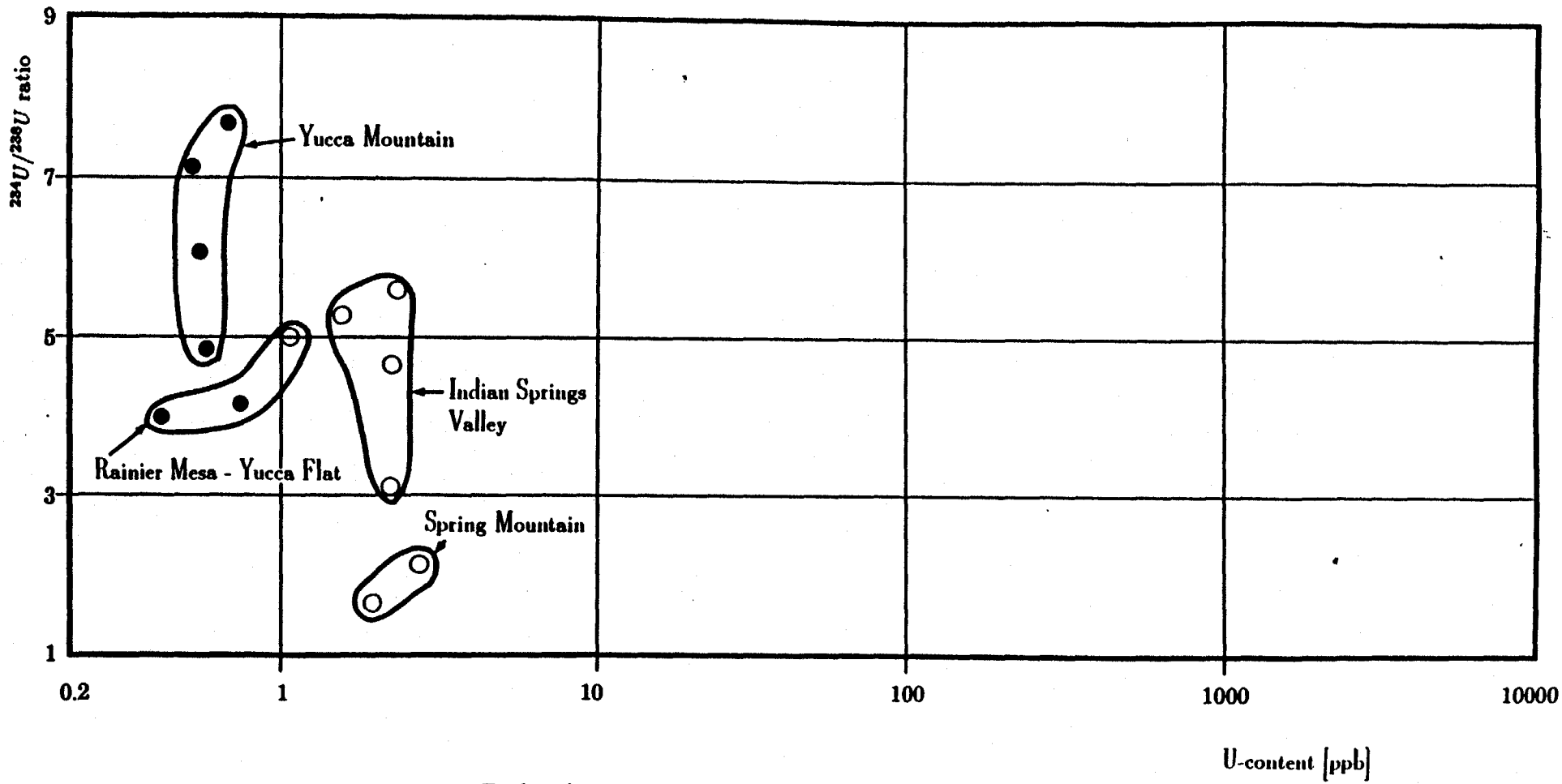

Explanation:

- ● - sample represents fluids from the tuff pile; and
- ○ - sample represents fluids from the Paleozoic carbonates.

$^{234}U/^{238}U$ vs U-content field. Hydraulic "sink" and dilated regions. The Nevada Test Site hydrosphere.

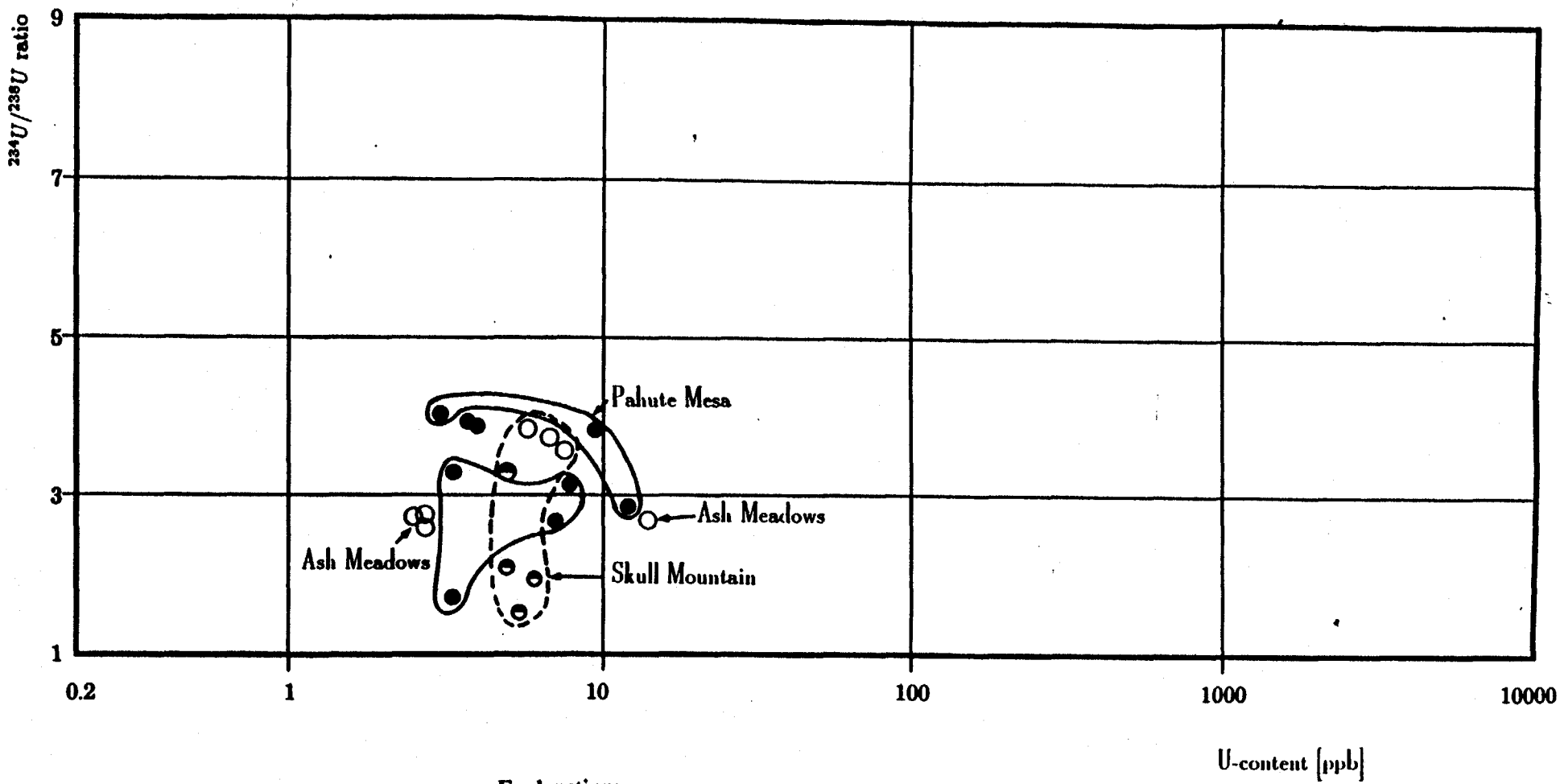

Explanation:

- ● - sample represents fluids from the tuff pile;
- ○ - sample represents fluids from the Paleozoic carbonates; and
- ⊖ - sample represents fluids from alluvium.

Note:

a) the Climax Stock perched fluids were excluded from this plot.

$^{234}U/^{238}U$ vs U-content field. Hydraulic "source" regions. The Nevada Test Site hydrosphere.

- At the Nevada Test Site, the $^{87}Sr/^{86}Sr$ ratios from samples of the hydraulic "source" fluids are distinct from the corresponding ratios from samples of the hydraulic "sink" fluids.

Conclusion: **The Nevada Test Site hydrosphere is a self-organized dynamic system and consists of a number of the Benard-Rayleigh dissipative structures.**

Self-organization. The Nevada Test Site hydrosphere - dissolved strontium data.

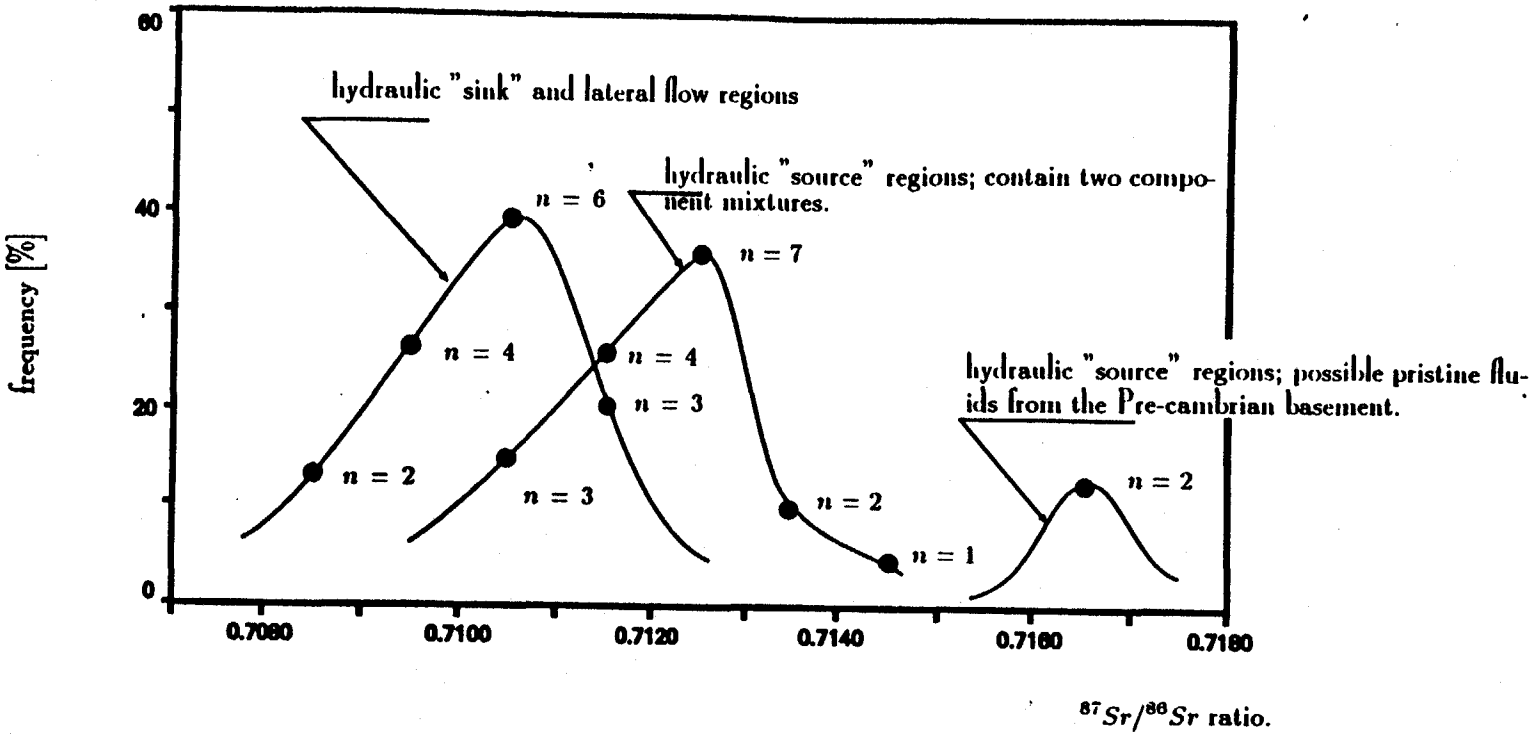

Note:

a) total number of samples: n = 15; and

b) isotopic data are from Stuckless (1990).

Comparision of the $^{87}Sr/^{86}Sr$ ratios. The Nevada Test Site "source" and "sink" regions.

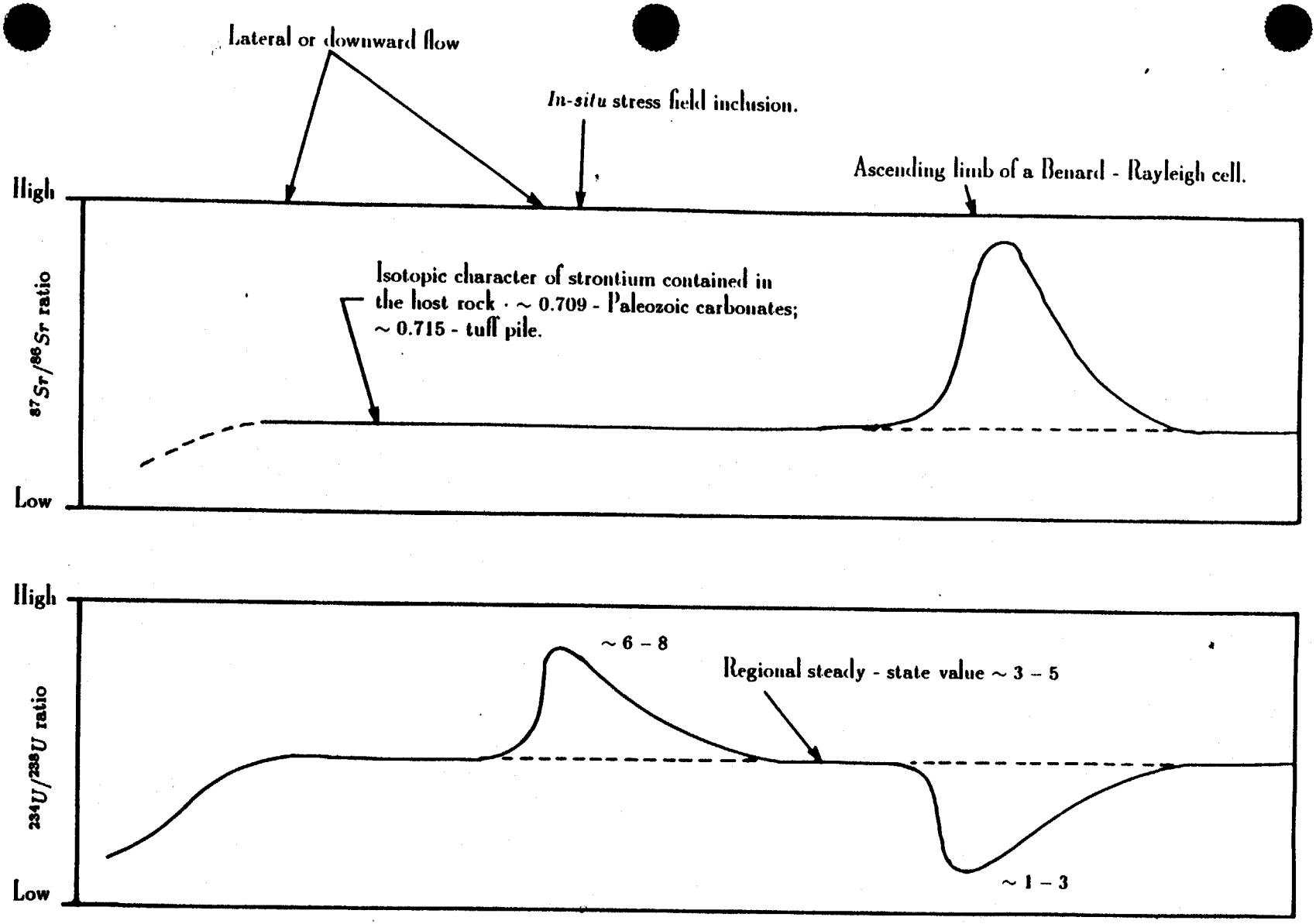

Note:

Fluids residing in the hydraulic "source" regions exhibit paired isotopic signature; relative to fluids from the hydraulic "sink" regions, the hydraulic "source" fluids simultaneously exhibit: i) lower values of the $^{234}U/^{238}U$ activity ratio; and ii) higher values of the $^{87}Sr/^{86}Sr$ ratio.

Conceptual understanding of spatial distribution of the strontium and uranium isotopic ratios. The contemporary Nevada Test Site hydrosphere.

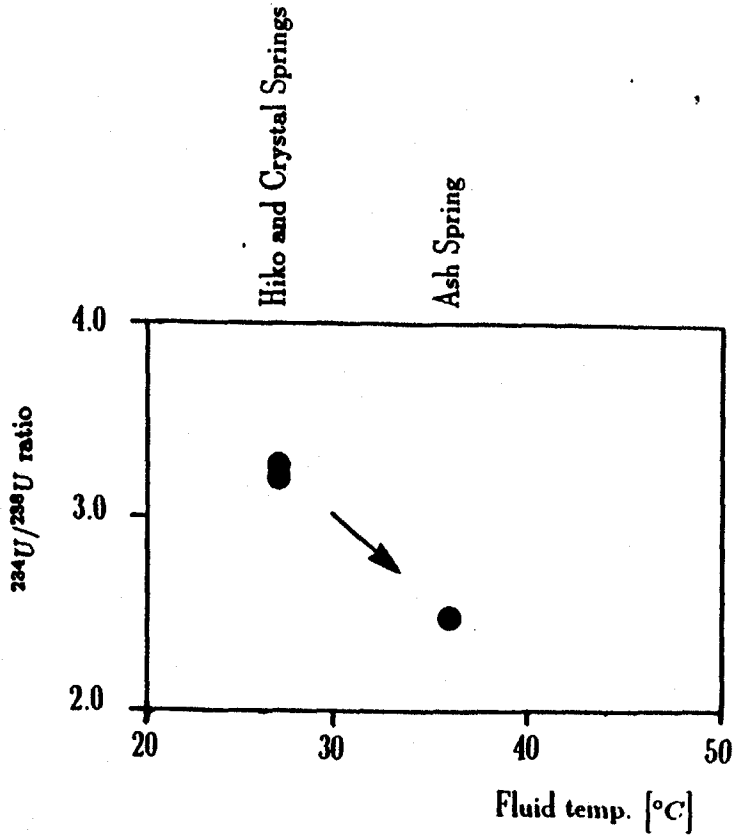

a) isotopic character of dissolved uranium.

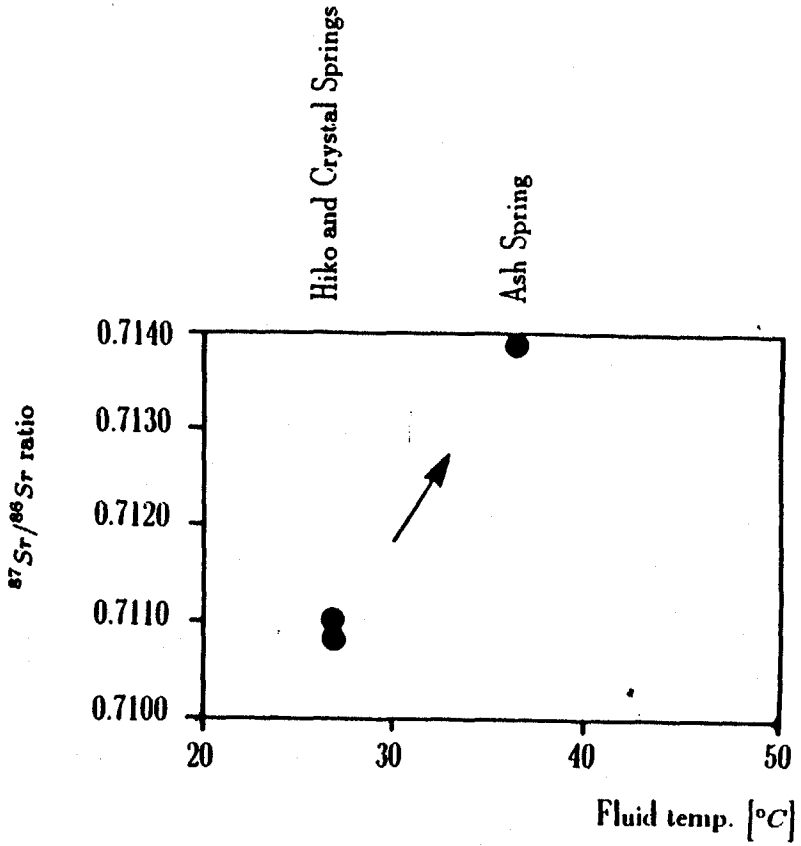

b) isotopic character of dissolved strontium.

Note:

a) isotopic and fluid temperature data are from Stuckless (1990).

Temperature vs. isotopic characters of dissolved uranium and strontium. Pahranagat Valley, Nevada.

- At the Nevada Test Site, the calcite saturation index - log(Q/K), calculated from water compositions using the EQ3 chemical equilibrium computer program, for the hydraulic "source" fluids is greater than the corresponding index for the hydraulic "sink" fluids.
- Both the carbon-14 and carbon-13 contents from samples of the hydraulic "source" fluids are distinct from those from samples of the hydraulic "sink" fluids.

Conclusions:

a) the Nevada Test Site hydrosphere is a self-organized dynamic system and consists of a number of the Bernard-Rayleigh dissipative structures;

b) degassing of CO_2 from the upwelling "source" fluids may be an important factor of the overall thermodynamic scheme;

c) for the hydraulic "sink" fluids, carbon from the atmosphere - biosphere source is a dominant factor; and

d) for the hydraulic "source" fluids, carbon from the subterranean source (dissolution of the Paleozoic carbonates and degassing of deep-seated igneous bodies) is a dominant factor.

Self-organization. The Nevada Test Site hydrosphere - dissolved carbon data.

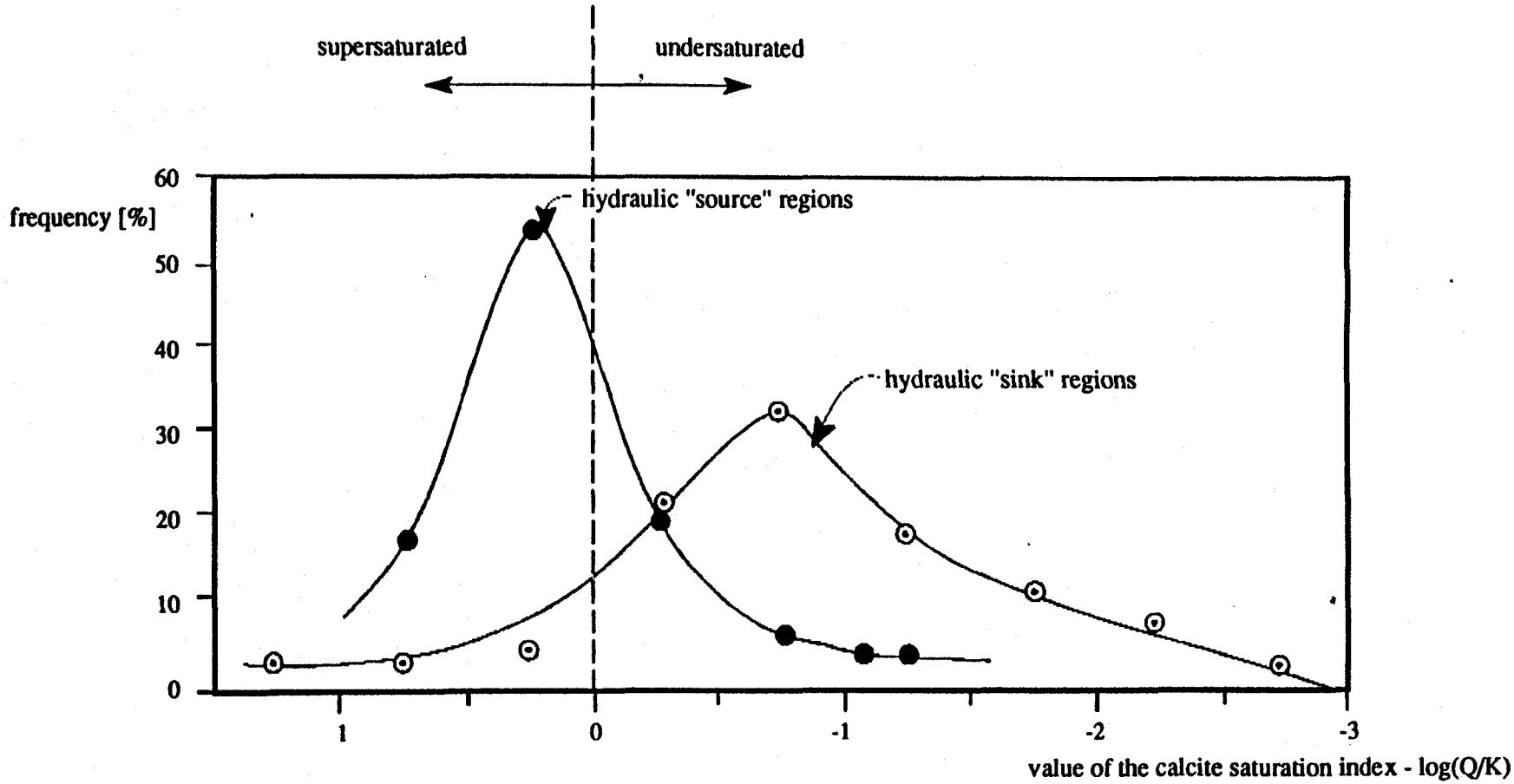

Note:

a) log (Q/K) data are from Kerrisk (1987);

b) N=52 for hydraulic "source" regions; N=64 for hydraulic "sink" regions; and

c) Q - the ion activity product, K - the equilibrium constant for the solubility reaction.

Calcite saturation index. Water samples from the Nevada Test Site hydraulic "sink" and "source" regions.

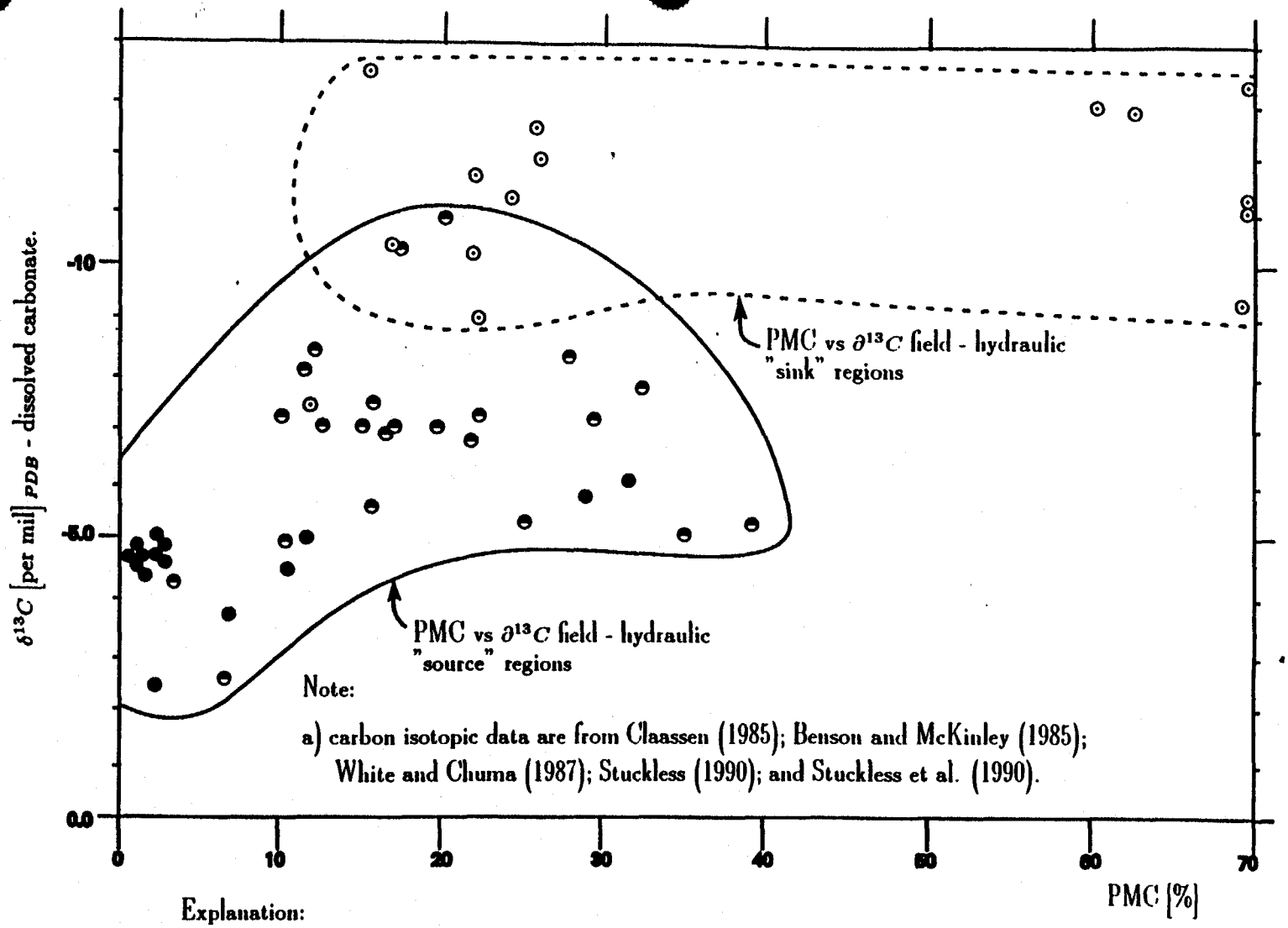

$\delta^{13}C$ vs. PMC field. Water samples from the Nevada Test Site hydrosphere.

Figure 1-23

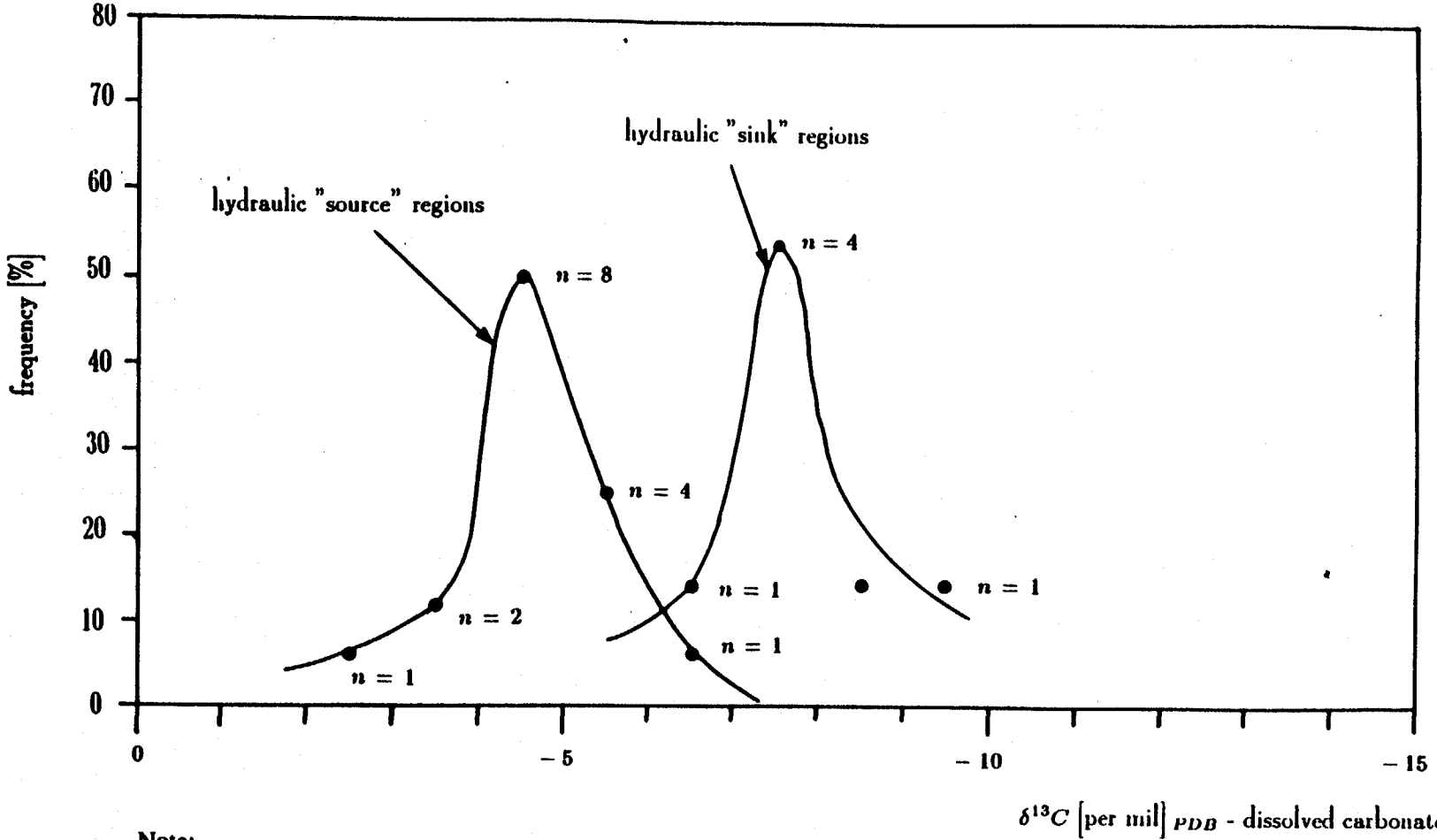

Note:

a) N = 16 for hydraulic "source" regions; N = 7 for hydraulic "sink" regions.

Isotopic character of the dissolved carbon. Water samples from the Paleozoic carbonate based hydraulic "sink" and "source" regions.

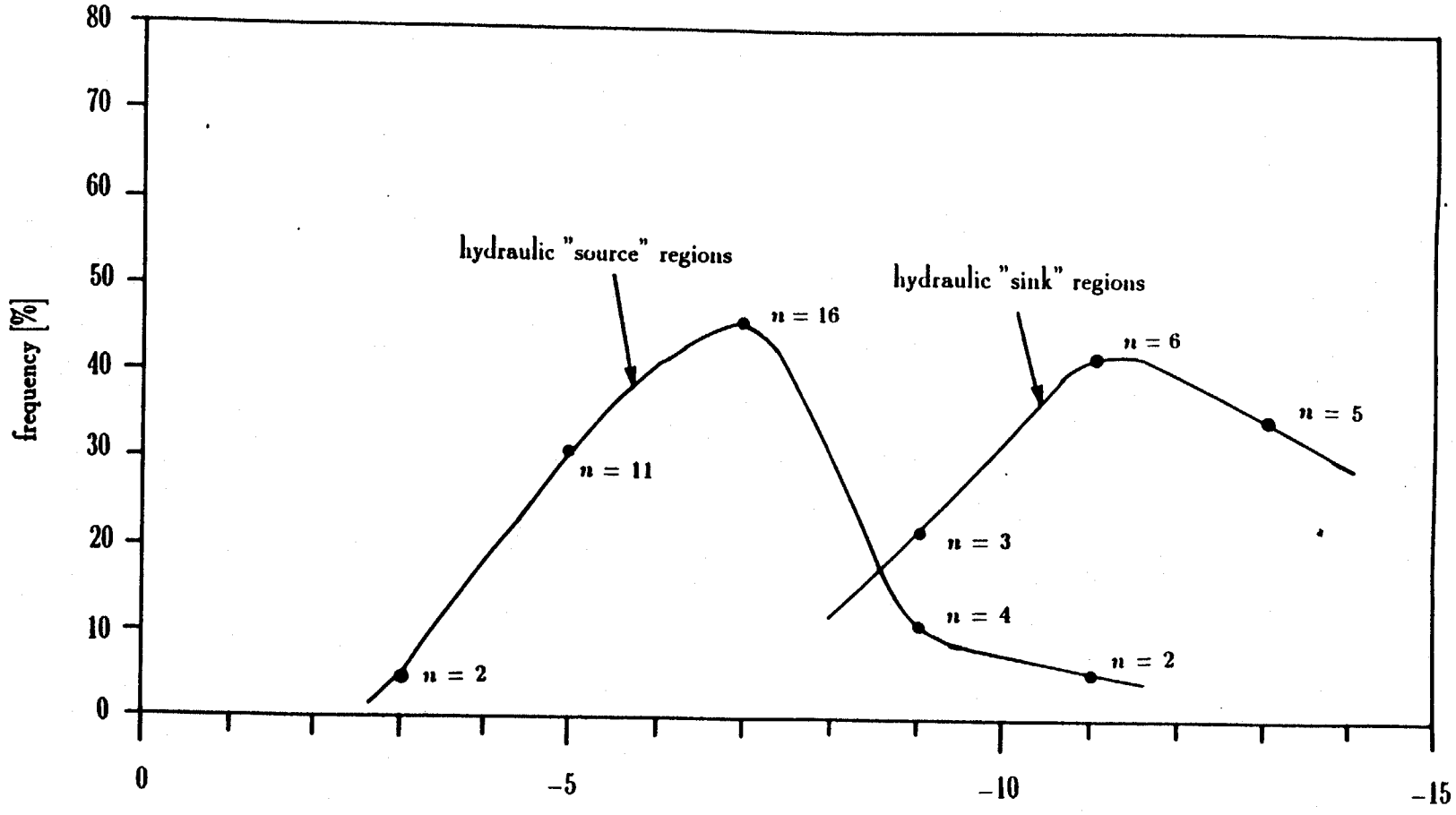

Note:

a) N = 35 for hydraulic "source" regions; N = 14 for hydraulic "sink" region.

Isotopic character of the dissolved carbon. Water samples from the alluvium - tuff pile hydraulic "source" and "sink" regions.

- o At the Nevada Test Site, the "oxygen isotopic shift" from samples of the hydraulic "source" fluids is greater than that from samples of the hydraulic "sink" fluids.

- o Both the deuterium content and the oxygen -18 content, from samples of the Nevada Test Site subsurface fluids, reflect altitudes of the local land surface.

- o Relative to the hydraulic "sink" fluids, the hydraulic "source" fluids exhibit both the negative "hydrogen isotopic shift" and the positive "oxygen isotopic shift".

Conclusion:

a) The Nevada Test Site hydrosphere is a self-organized dynamic system and consists of a number of the Benard-Rayleigh dissipative structures.

b) Partially, the Nevada Test Site subsurface fluids are derived from the local atmospheric precipitation, (i.e., recharge is widespread and not restricted to the high altitude regions.)

c) The Nevada Test Site subsurface fluids are, at least, two-component mixtures (oxygen shifted and deuterium depleated geothermal fluids intermixed with the recharging local atmospheric precipitation.)

Self-organization. The Nevada Test Site hydrosphere - deuterium and oxygen data.

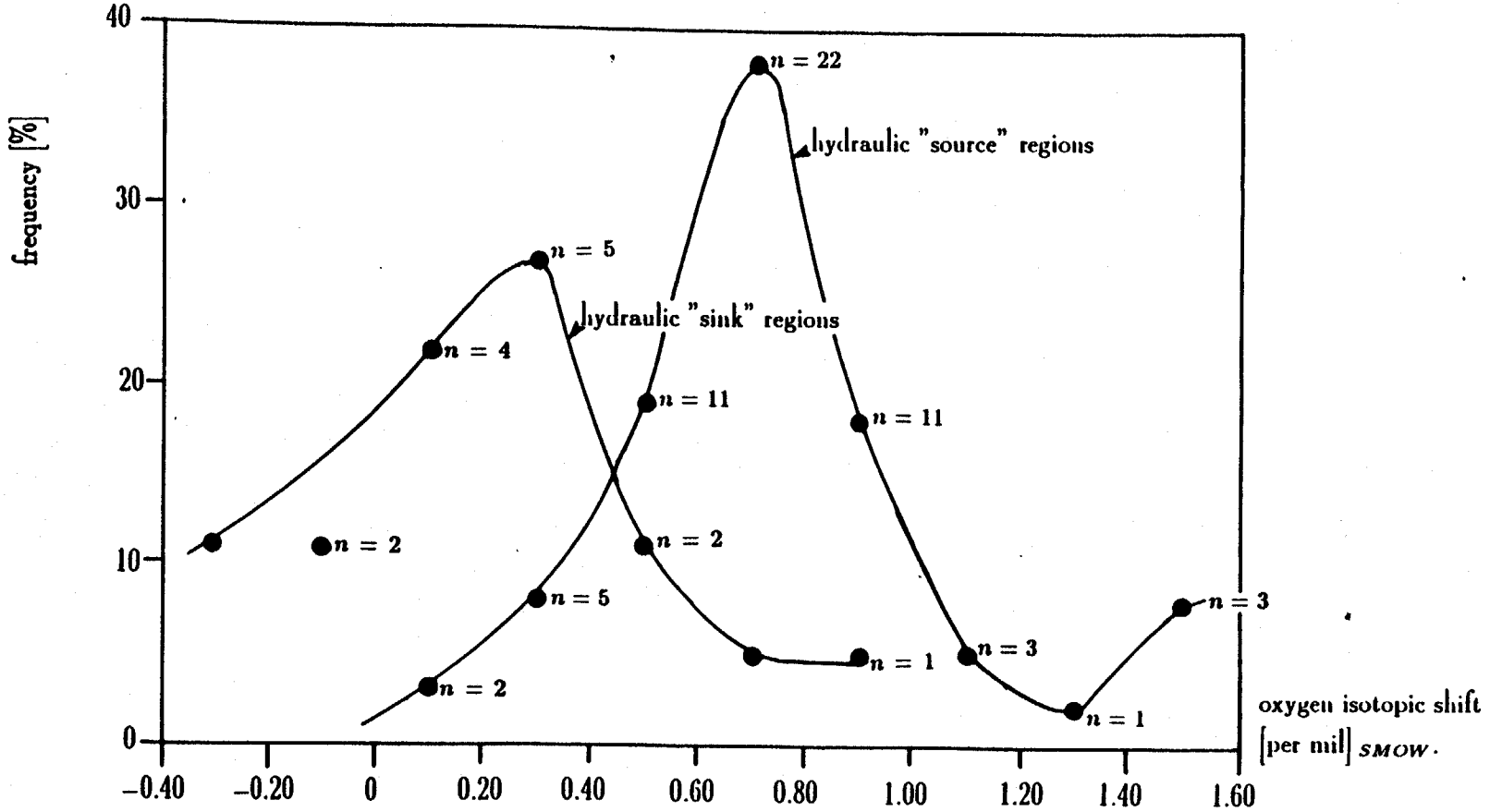

Note:

a) samples are bulk samples pumped out of large segments of exploratory wells - sampling "smoothing" may be involved, and the observed oxygen isotopic shift may be smaller than the actually present one:

b) oxygen isotopic shift $\Delta\delta^{18}O = (\delta D_{ob} - 10)/8 - \delta^{18}O_{ob}$; and

c) oxygen isotopic data are from Isherwood et al. (1982), Benson and McKinley (1985), Claassen (1985), White and Chuma (1987), Stuckless (1990), and Stuckless et al. (1990).

Comparison of magnitudes of the oxygen isotopic shift. The Nevada Test Site "sink" and "source" regions.

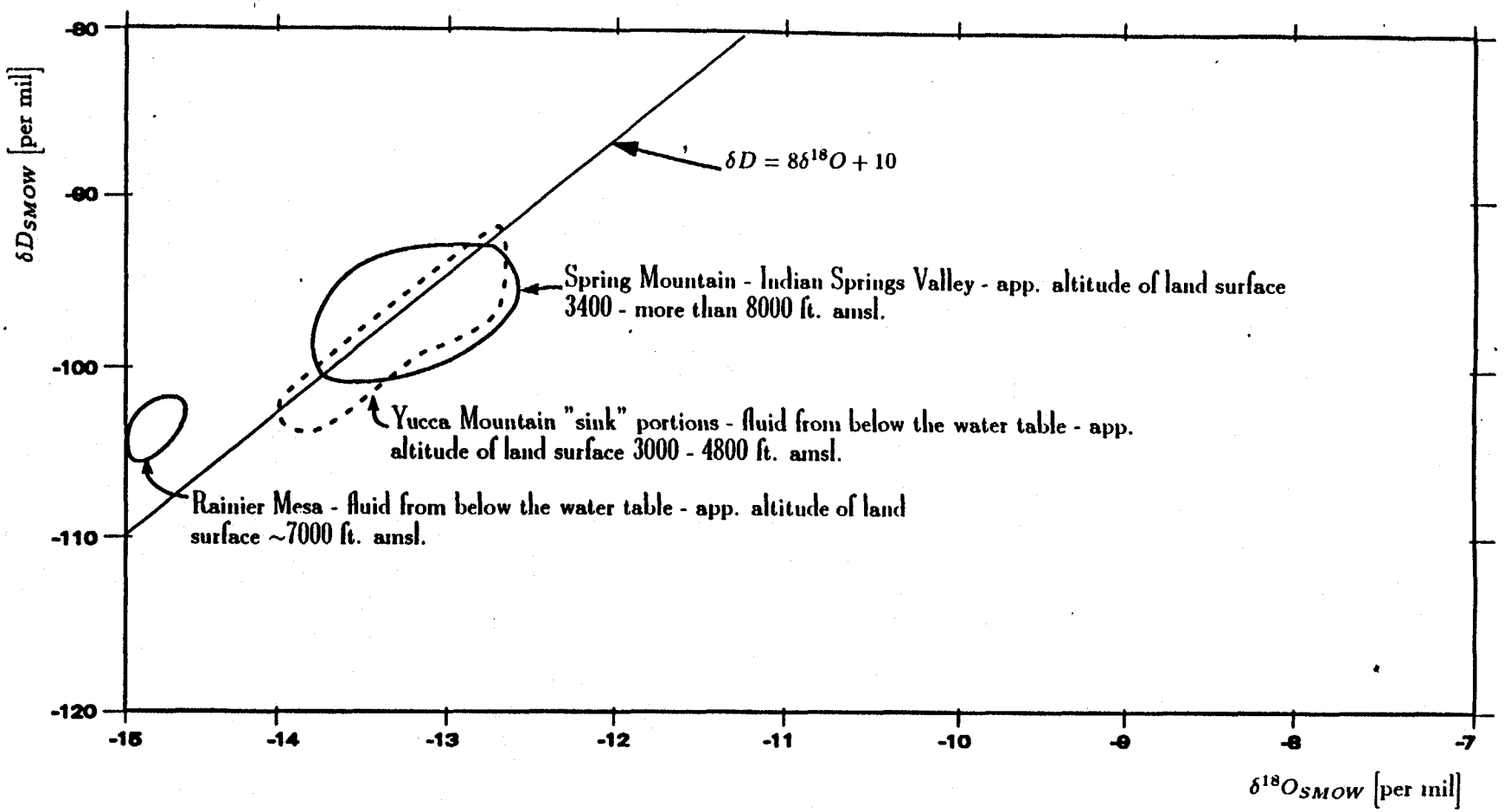

Note:

a) Spring Mountain fluids are contemporary fluids; and

b) Yucca Mountain and Rainier Mesa fluids from below the water table are older fluids - ^{14}C ages are comparable to those of fluids from the "source" regions.

Relationship between the observed isotopic compositions, the meteoric water line, and altitude of the local land surface. Fluids from the hydraulic "sink" regions. The Nevada Test Site hydrosphere.

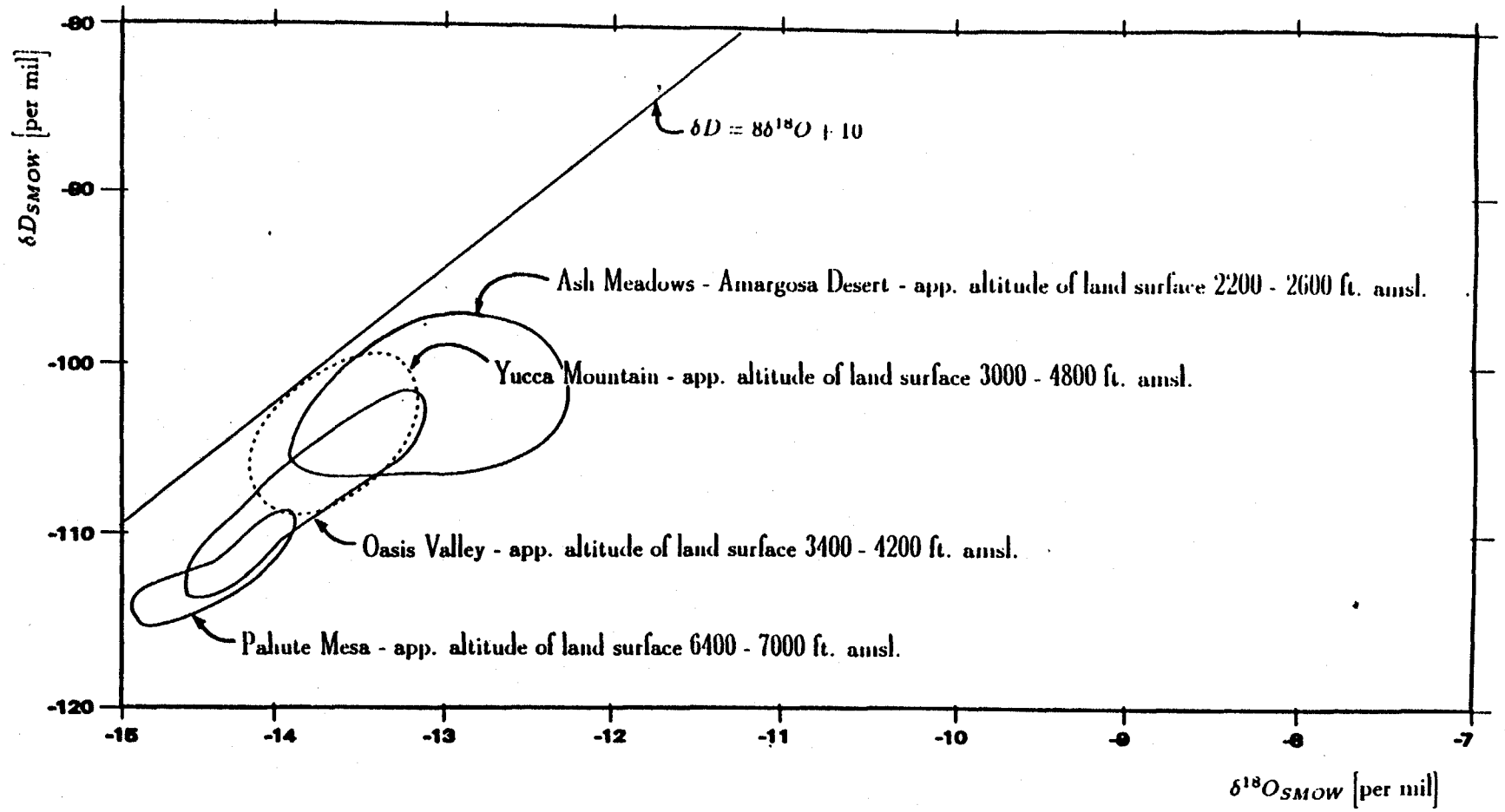

Relationship between the observed isotopic compositions, the meteoric water line, and altitudes of the local land surface. Fluids from the hydraulic "source" regions. The Nevada Test Site hydrosphere.

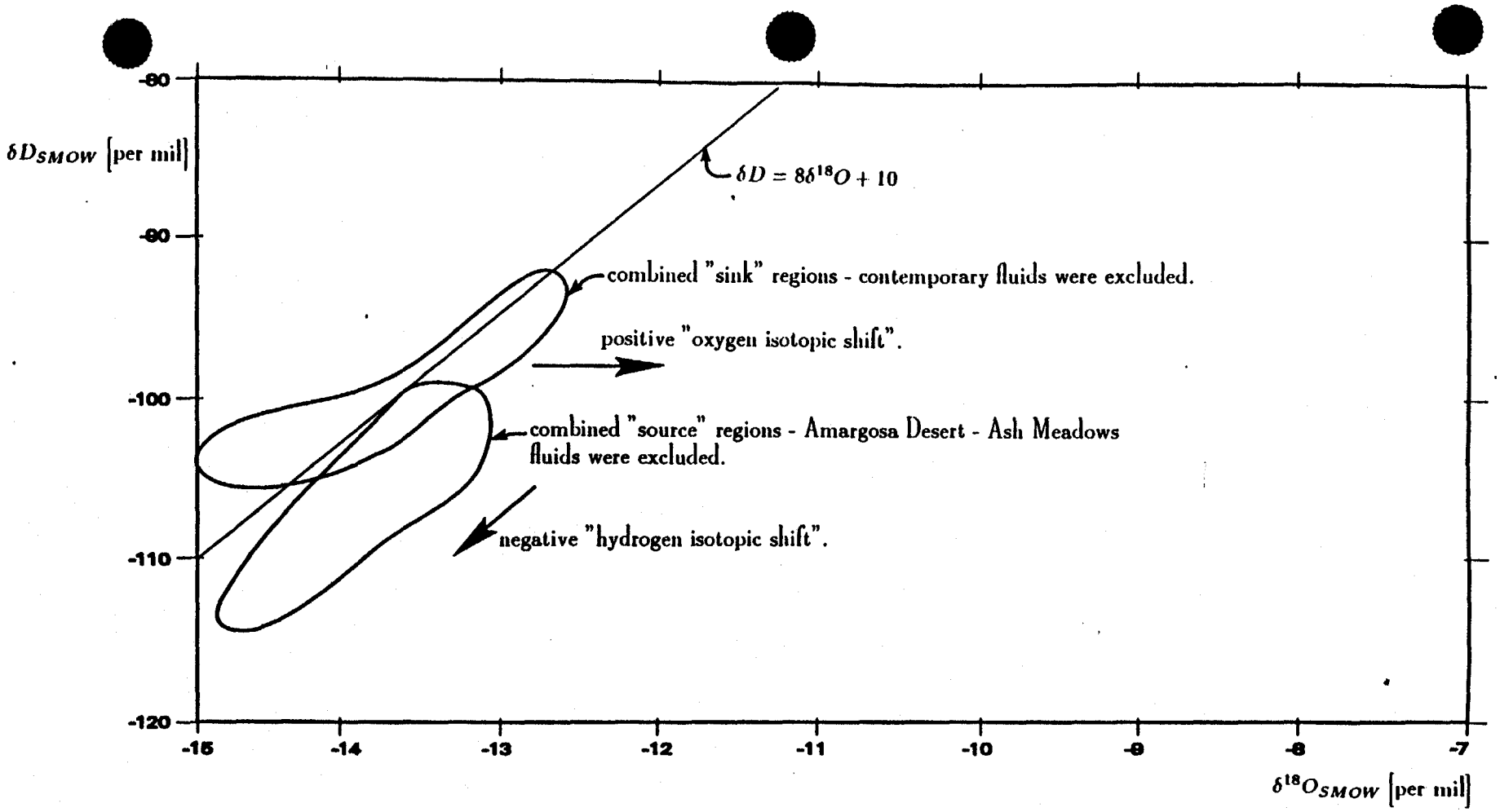

Note:

a) comparison is based on data from regions with comparable altitudes of the land surface; and

b) comparison is based on data from fluid samples with comparable PMC.

Comparison of isotopic compositions. "Sink" and "source" regions - The Nevada Test Site hydrosphere.

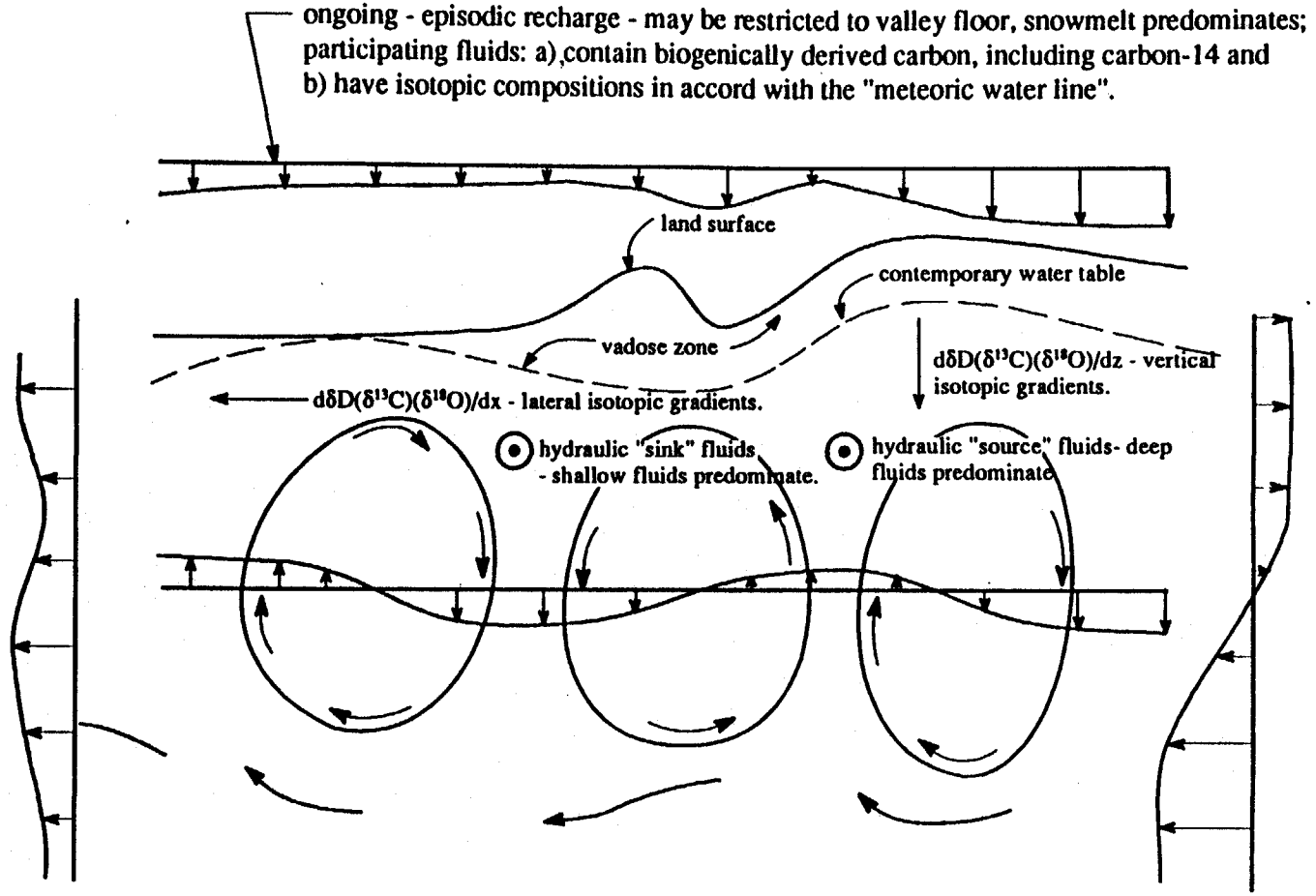

Note:

a) lateral and vertical isotopic gradients are produced by spatially variable intermixing of deep and shallow fluids.

Conceptual understanding of isotopic hydrochemistry. The Nevada Test Site hydrosphere.

Overall Conclusions

i) The Nevada Test Site hydrosphere exhibits very pronounced spatial heterogeneity involving simultaneously a number of hydrologic parameters (dh/dz, dT/dz, fluid chemical and isotopic compositions).

ii) It may reasonably be expected that, the traditional patterns of hydrologic thoughts [i.e., a) absence of thermally driven fluid motion; b) fluid motion restricted to shallow lithospheric parts; c) "no upward flow boundary conditions" - at some litho-structural interface; and d) hydraulic conductivity structure related to the local litho-stratigraphic framework, etc.] do not apply in this case.

iii) Along a horizontal flow path, hydraulic circumstances alternate between those of the hydraulic "source" regions and those of the hydraulic "sink" regions.

Conclusions - presentation #1.

Issue - Is it reasonable to presume that, for the Nevada Test Site hydrosphere, the anticipated changes in position of the local water table may be measured in terms of hundreds of meters ?

Statement of the issue - presentation #2

Figure 2-1

- Approximate altitude of the local land surface is ~ 4700 ft, Ekren and Sargent, 1965.

- Approximate altitude of the regional water table is:

  a) ~ 2420 ft, Domenico, 1972; and
  b) closest wells encountered water table at ~ 2784 ft (Eleane Frm. - east) and ~ 3755 ft (upstream), Winograd and Thordarson, 1975.

- Absence of any cover (including "pedogenic carbonates") suggests that age of the deposit may be as young as Holocene.

- Presence of gypsum indicates that, the deposit parent fluids are:

  a) deep-seated; and
  b) were involved in geothermal circulations.

Basic data and main observations - the Whamonie $CaSO_4$ and $CaCO_3$ mounds.

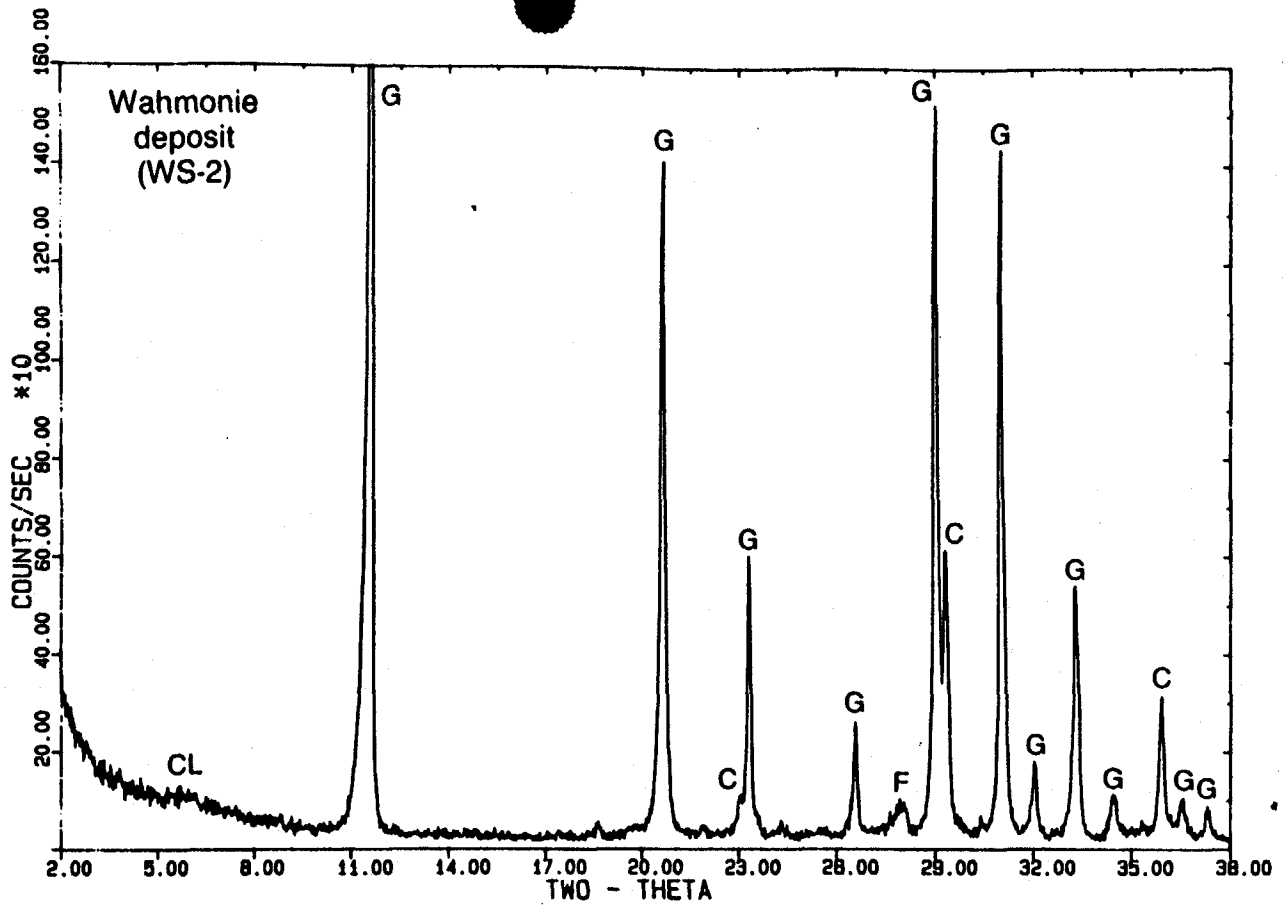

x-ray defractogram

The Paleospring Mound at Wahmonie. Although the only active warm springs close to Yucca Mountain are in Oasis Valley, there is a paleospring mound on the Nevada Test Site above Wahmonie, 28 km east of Yucca Mountain (fig. 1B). This spring mound consists of almost pure gypsum with minor calcite (fig. 14) and appears to represent deposits from an old hot-water discharge centered in the Wahmonie ore district, which was onced mined for gold, silver, and copper (Bell and Larson 1982.). As at Tonopah, this hydrothermal system combines precious metals with sulfur-bearing mineralogy. Silica sinter, however, does not occur at Wahmonie. In its abundance of gypsum and lack of silica, the paleospring mound at Wahmonie is quite different from the fault-related calcite-silica deposits near Yucca Mountain.

From Vaniman et al., (1988).

Wahmonie Spring mounds - introductory information.

Figure 2-3a

At the Nevada Test Site, a deposit of gypsum, a few meters thick, was found near Whamonie. The outcrop of this deposit is located about 6 km northwest of Skull Mountain (Vaniman et al., 1988). The deposit occurs at the ground surface, in a topographic setting that precludes playa deposition, and in an area where the vadose zone is more than 500 m thick. It consists of almost pure gypsum with minor calcite, **and leaves little doubt that it represents a warm-water paleo-spring discharge** (Vaniman et al., 1988). Not much is known about the age of activity of this spring; field appearance of the outcrop, however, is one of a young deposit. The Whamonie paleo-spring mound occurs in a hydraulic setting where a) groundwaters are enriched in sulfate anion (Section 4.5.2); b) the intensity of flux of terrestrial heat is locally increased, (Section 4.3.2); c) the localized low-seismic velocity anomaly is present (Section 3.4.1); and d) hydrothermal convection system is locally developed (Sass et al., 1980). In this situation, it is reasonable to speculate that factors which are responsible for the Whamonie gypsum mound, may also be involved in the contemporary hydrology of Skull Mountain. In order to purdue such a hypothesis any further, however, it is necessary to establish the age of activity of the Whamonie mound. This age is a single most important data need that is required for a complete understanding of contemporary hydrology of the Skull Mountain area. A very modest field effort, consisting of mapping and trenching, is required to resolve this important issue.

From Szymanski, 1989.

Concurrent with drilling at Calico Hills, geophysical studies conducted at Wahmonie indicated that the granite, which occurs at the surface, would be only marginally large enough for a repository at the depth needed. These studies, plus surface mapping, also suggested that the granite within reasonable depths was probably altered by hydrothermal solutions (Smith et al., 1981; Hoover et al., 1982). In addition to the altered granite, local surface deposits from recent warm springs indicate upward seepage of groundwater, possibly from great depths. For these reasons, Wahmonie was eliminated from consideration in the spring of 1979.

From DOE, 1984 - based on USGS, 1980 letter.

Wahmonie Spring mounds - introductory information.

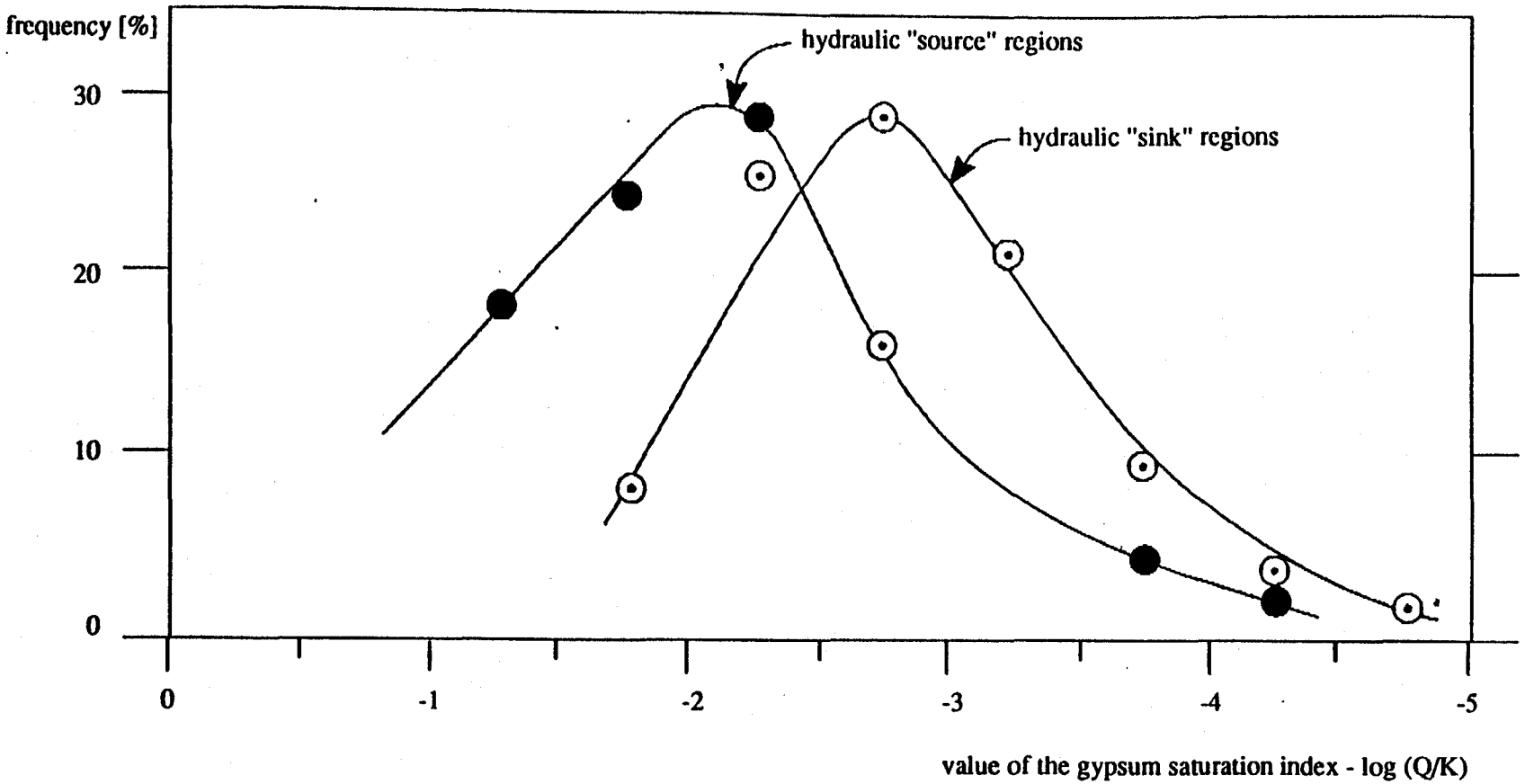

Note:

a) log (Q/K) data are from Kerrisk;

b) N = 48 for hydraulic "source" regions, N = 61 for hydraulic "sink" regions; and

c) Q - the ion activity product, K - the equilibrium constant for the solubility reaction.

Gypsum saturation index. Water samples from the Nevada Test Site hydraulic "sink" and "source" regions.

- It is reasonable to conclude that, the parent fluids for the Whamonie gypsum mound have carried values of the gypsum saturation index log (Q/K) > 0.

- At the Nevada Test Site, none of the fluids sampled and analyzed have yielded positive values of the gypsum saturation index.

Conclusion: the parent fluids for the Wahmonie gypsum mound were upwelded from a depth measured in terms of kilometers.

Depth of fluid circulation, as indicated by the Whamonie Spring mounds.

Figure 2-5

- An interpretation of the depth of fluid circulation is an important aspect of considerations regarding potential magnitudes of the tectonically induced rises of the water table.

- Three independent lines of evidence indicate that, at the Nevada Test Site, the depth of groundwater circulation is large, namely:

  i) presence of the fresh Whamonie mounds;

  ii) the hydraulic "source" fluids residing in the Paleozoic carbonate complex carry abnormally high values of the $^{87}Sr/^{86}Sr$ ratio, from 0.7118 to as much as 0.7149 . [a) in the pristine state, fluids equilibrated with the marine limestones of Early Paleozoic age should carry values of the $^{87}Sr/^{86}Sr$ ranging from 0.7082 to less than 0.7100, Faure (1986); b) the elevated values of the $^{87}Sr/^{86}Sr$ ratio indicate that, at the Nevada Test Site, there is an upward fluid flux from the Pre-cambrian basement; and c) stratigraphic thickness of the Paleozoic carbonate complex exceeds ~ 2 km]; and

  iii) some of the hydraulic "source" fluids residing in the Mesozoic non-carbonate rocks carry abnormally high values of the $\delta^{13}C$ ratio, e.g. a) sampling site #1 in Thirsty Canyon, $\delta^{13}C$ = -2.52 per mil $_{PDB}$, White and Chuma (1978); b) the Yucca Mountain borehole USW H-3, $\delta^{13}C$= -4.9 per mil $_{PDB}$, Benson and McKinley (1985); and c) the Climax Stock perched waters, $\delta^{13}C$ = -3.54 and -4.57 per mil $_{PDB}$, Isherwood et al. (1982). [a) the high values of the $\delta^{13}C$ ratio may be taken to indicate that fluids contain carbon derived through dissolution of the underlying Paleozoic carbonates; b) for sites with abnormally high values of the $\delta^{13}C$ ratio, the Paleozoic carbonates are known to occur at a depth ranging from ~ 1.5 to 4.0 km]; and

- At the Nevada Test Site, the depth of groundwater circulation may reasonably be presumed to be in excess of ~ 5 km.

Interpretation of the depth of groundwater circulation for the Nevada Test Site.

Figure 2-6

Overall Conclusions

The Whamonie mounds provide direct and clear testimony that:

i) at the Nevada Test Site, the tectonically induced (seismic and/or geothermal) rises of the local water table may be as large as a few hundred of meters;

ii) at the Nevada Test Site, presence of the Benard-Rayleigh instabilities must be anticipated - confirms the results of dT/dz and Ra - Rc analyses; and

iii) downplaying potential magnitudes of the tectonic rises of the local water table [based on: a) beliefs, Dudley et al. (1989); b) reported global observations of hydrologic effects of earthquakes; and c) erroneous numerial simulations] **is totally without merit.**

Conclusions - presentation #2

Figure 2-7

Issue - Intraformation time and history of fluids emerging from Cane Spring orifice.

Interpretation Options

I - solely perched infiltrating recharge (conventional wisdom).

II - two end-member mixture, i.e. a) deep-seated fluids overflowing from an active hydraulic mound; and b) infiltrating recharge (J.S.S. proposition).

Statement of the issue - presentation #3.

Figure 3-1

- The Cane Spring travertines are regarded as a modern analog for the Yucca Mountain calcite-opaline silica deposits, based on:

  - morphology, texture, and composition; and
  - $^{234}U/^{238}U$ activity ratio and U-content.

- Based on direct field observations it is clear that, the parent fluids for the Cane Spring travertines are spring fluids emerging from the local bedrock. They are not contemporary rainfall infiltrating through soil horizon; source of the dissolved SiO_2 and Ca^{++} is not a windblown dust.

- The Skull Mountain perched fluids may reasonably be interpreted to be the combined results of: a) local retardation of infiltrating recharge; and b) local retardation of fluids ejected from below the water table.

The Cane Spring travertines - a modern analog for the Yucca Mountain calcite-opaline silica deposits.

Figure 3-2

Cane Spring Fault

CSF 1: The sample point is located approximately 0.5 mi southwest of Cane Spring on a normal fault within the Tertiary volcanics. At this point, the normal fault is subparallel to the Cane Spring Fault and strikes N50°E and dips 83° to the northwest. The faulting has produced a small outcrop of a grey-white pumice agglomerate (Twtb) which underlies a reddish-brown rhyodacite flow (Twf). Both of these volcanic units are part of Tertiary Wahmonie Formation. The laminar tuffaceous travertine occurs as thick, flow-like layers of very white carbonate, coating the exposed face (fault scarp) of the pumice agglomerate outcrop. The travertine is hard and relatively brittle on the outer surface, appearing similar to solution/precipitation lamination, but is very powdery underneath. There appears to be a rind of altered material between this caliche and the underlying pumice. The travertine is definitely related to the fault producing this scarp, but the relationship between the age of this carbonate and the last movement on the normal fault is unclear. No slickensides are present on the travertine, which suggests that it postdates the last movement. The fault is terminated in the southwest by overlying (unfaulted) Tertiary alluvium and colluvium (Tac) and in the northeast by the Cane Spring Fault. Allowing for the possibility of minor movement along this small fault block in response to left-lateral motion on the Cane Spring Fault, the travertine could be as young as Quaternary in age, although the bulk of the normal faulting in this area undoubtly occurred in late Tertiary times.

CSF 2: The sample point is located on the Cane Spring Fault approximately 0.5 mi southwest of Cane Spring. The fault strikes N60°E and locally dips 80° to the northwest. It separates Quaternary alluvium and colluvium (Qac) on the downthrown (NW) block from Tertiary alluvium and colluvium (Tac). The Qac consists of loose, partly caliche-cemented sand and gravel, whereas the Tac is a well indurated sandy gravel consisting of rhyodacite, dacite, and rhyolotic tuff clasts, some up to 2 ft in diameter cemeted in place. Near the base of the scarp, which is well exposed in an arroyo, platy tuffaceous travertine is present only within 0.5 ft of the fault filling fractures between blocks of Tac parallel to the scarp face. The travertine is white and relatively hard although somewhat thin (<1/8 in.). There are no slickensides present, indicating formation certainly postdates the last movement on the Cane Spring Fault, although the exact relationship remains unclear.

Description of samples analyzed and dated by Knauss, 1981. From Knauss, 1981.

Sample No.	Fraction	Activity (dpm/g)				Concentration (ppm)		Activity ratio			$CaCO_3$ (%)
		^{232}Th	^{230}Th	^{238}U	^{234}U	Th	U	$\frac{^{230}Th}{^{234}U}$	$\frac{^{230}Th}{^{232}Th}$	$\frac{^{234}U}{^{238}U}$	
CSF 1	Leach	.021 ±.003	.79 ±.02	1.99 ±.05	2.87 ±.06	.09 ±.01	2.67 ±.06	.27 ±.01	37.7 ±5.7	1.44 ±.04	78.0
	Residue	.11 ±.01	2.18 ±.07	5.87 ±.15	8.94 ±.19	.45 ±.06	7.87 ±.20	.24 ±.01	19.8 ±2.7	1.52 ±.04	-
CSF 2	Leach	.24 ±.01	.25 ±.01	4.61 ±.14	5.68 ±.17	.97 ±.03	6.18 ±.19	.043 ±.002	1.04 ±.04	1.23 ±.03	68.31
	Residue	1.80 ±.05	1.29 ±.04	9.60 ±.38	10.8 ±.4	7.41 ±.20	12.9 ±.5	.119 ±.006	.72 ±.03	1.13 ±.04	-

Sample No.	Uncorrected (x 10^3 yr)	Isochron plot (x 10^3 yr)
CSF 1	34	41
CSF 2	4.8	2

U/Th data and U/Th dates. Cane Spring travertines. From Knauss, 1981.

The Vadose Zone

General

The vadose zone constitutes the upper portion of a groundwater system. It is located between the land surface and the uppermost continuous potentiometric surface, which is the water table. In the Death Valley groundwater system, thickness of the vadose zone ranges from a few meters, at and near the discharge areas, to as much as 600 m, in the central and recharge areas. In the vadose zone, water content, expressed as a percentage of interstitial space, is highly variable. It ranges from 60 to 75 percent, ± 15 percent. In local areas, however, the degree of saturation is higher and fractures contain "free" waters. Such waters may be removed from the host rock by pumping and gravitational drainage.

Spatial distribution of water content in the vadose zone may be viewed as resulting from mixing of two patterns of distribution. The first pattern is a systematic change in moisture content as a function of depth and time (Ross, 1984). Near the ground surface, moisture content and suction potential fluctuate with precipitation events and with season. At depth, however, the fluctuations damp out, and there is a constant downward flux of water under the unit head gradient. Both, the suction potential and the effective hydraulic conductivity, are constant. Near the water table, moisture content is high and suction potential has a small negative value.

The second pattern is a random occurrence of bodies of "free" waters. Such bodies owe their existance either to local retentions or to local additions of fluids. Their origin may be related to many factors, some of which are a) local heterogeneity in the hydraulic conductivity structure, that may be caused either by lithologic composition or by an *in situ* stress field; b) locally increased infiltration, that may be the result of either atmospheric precipitation or man action; and c) injection of fluids from below the water table, that may be caused by either thermal or *in situ* stress rises of the water table.

For the purposes of these conceptual considerations, it is useful to recognize three forms of occurrence of the bodies of "free" water in the vadose zone. These are a) perched waters b) semi-perched waters; and c) hydraulic mounds. The perched waters are separated from the underlying continuous body of groundwater by a sequence of "undersaturated" rocks. The semi-perched waters have higher hydraulic head than the underlying body of groundwater. In contrast to the perched waters, however, the semi-perched waters are not separated from the underlying groundwater by an "undersaturated" sequence. Such water, similarly as the perched waters, owe their existence to local hydraulic conductivity contrasts, that restrict downward movement of fluids and thus prevent equilibrium of hydraulic pressures across them. Within a hydraulic mound, however, the values of hydraulic potentials are higher than those in the upstream areas; locally, equipotential surfaces are bent upward. Such a bending is caused by local upwelling of fluids, that may be related either to "forced" or to "mixed" convection. Unlike both the perched and semi-perched bodies of water, hydraulic mounds owe their existence to local "upward-fluid-flux" boundary conditions, rather than to the local hydraulic conductivity contrasts.

Conceptual importance of the Cane Spring perched body.

Figure 3-5a

Once encountered, bodies of "free" water pose an interesting and very important conceptual dilemma. Conceivably, there are two conceptual possibilities that need to be considered. The first possibility is, that a body of "free" water represents meteoric water directly from atmospheric precipitation that has been caught during downward infiltration through the vadose zone, by rocks whose hydraulic transmissivity is very low. Most, if not all, of the researchers concerned with Death Valley groundwater system regarded this possibility as an adequate explanation of all "free" water occurring in the vadose zone of that system. The second possibility is, that at least, some bodies of "free" waters are the result of tectonic injection from below the water table. These bodies, therefore, represent tectonically induced hydraulic mounds, either active or relict.

It is rather obvious, that selection of a correct conceptual possibility regarding the origin of bodies of "free" water in the vadose zone, entails very profound implications as far as conceptual understanding of the Yucca Mountain groundwater system is concerned. Consequently, such a selection shall be made with due caution and based on adequate data base. Such a data base should include the following categories of information: a) chemical and isotopic composition of fluids involved; b) local tectonic and hydrologic setting; c) contemporary and paleo-temperatures; d) volume of fluid; and e) values of hydraulic potentials, including their time- and space-dependence.

In the Death Valley groundwater system, bodies of "free" water are known to be present at several locations. Such bodies were encountered in many exploratory boreholes (Walker, 1962; Winograd and Thordarson, 1975; and Czarnecki, 1987). They were also encountered in underground workings in Rainier Mesa and Climax Stock (Thordarson, 1965; and Isherwood et al., 1982). At the Nevada Test Site, bodies of perched water feed several springs, that yield small quantities of water. Examples of such springs are Cane Spring, Topopah Spring, and Pavits Spring (Thordarson and Robison, 1971; and Schoff and Moore, 1968).

For purposes of subsequent considerations, four examples of bodies of "free" water were selected for closer examinations. These four examples are from the following locations: a) Greenwater Range; b) Skull Mountain; c) Rainier Mesa; and d) Climax Stock. The locations are shown on plate 4.5.2.1-1.

From Szymanski (1989).

Conceptual importance of the Cane Spring perched body.

Figure 3-5b

The Skull Mountain Hydrologic Anomaly

Plates 4.5.2.3-1 through 4.5.2.3-3 present the hydrologic setting of Skull Mountain area. This area is located in the southern sector of the Nevada Test Site, between Frenchman and Jackass Flats. Hydrology of this area is known based on subsurface explorations with boreholes, and was described by Winograd and Thordarson, 1975. Around Skull Mountain, altitudes of the "regional" water table range from 2,420 to 2,380 feet above mean sea level (Plates 4.5.2.3-2 and 4.5.2.3-3). A sharp increase in position of the water table occurs west of the Mercury Highway (Plate 4.5.2.3-3). This increase was encountered in two wells. The first well, Well #73-68, was drilled to a depth of 1,504 feet. Winograd and Thordarson, 1975, reported that "drillers first reported water at a depth of approximately 660 feet. Several days after completion of drilling, the water level stood 518 feet below land surface," which corresponds to an altitude of about 2,982 feet above mean sea level. This altitude is more than 500 feet higher than the regional water table downstream in the neighboring Frenchman Flat (Plate 4.5.2.3-3). Winograd and Thordarson, 1975, reported that "Well #77-68 penetrated 1,093 feet of the valley fill aquifer and 150 feet of the welded tuff aquifer. The water level in Well #77-68 stands at a depth of 796 $\pm$ 5 feet, or at an altitude of about 2,784 feet above the mean sea level; this altitude is approximately 370 feet higher than the water level in either valley-fill or the welded-tuff aquifers east of the Mercury Highway" (Plate 4.5.2.3-3). The water level in Well #77-68 is also 364 feet higher than water levels upstream, north and northeast from Skull Mountain, (Plate 4.5.2.3-2). Winograd and Thordarson, 1975, concluded that " because of the moderate to high transmissivity of the valley-fill and the welded-tuff aquifers, the anomalously high water level in Well #77-68 cannot be ascribed to perching or semi-perching of water within strata of low gross transmissivity or to the existence of steep hydraulic gradients within the aquifers."

Farther west of the Mercury Highway, west and south of Wells #77-69 and #77-68, perched waters were encountered in three wells: #73-66, #75-66a, and #75-66 (Plate 4.5.2.3-3). In addition, two small springs are found in the area: Cane Spring and Pavits Spring. The springs occur at altitudes of 4,060 and 3,940 feet above mean sea level, respectively. The perched waters, feeding the springs and encountered in the three wells, are situated as much as 1,200 to 1,600 feet higher than the "regional" water table downstream in Frenchman and upstream in Yucca Flats.

Based on groundwater chemistry data compiled by Winograd and Thordarson, 1975, (plate 3), it appears that around Skull Mountain there is a noticeable increase in the sulfate content of groundwater. North, east, and west from Skull Mountain, the sulfate content is low, say less than 2 milliequivalents per liter. Immediately around Skull Mountain, however, the sulfate content is several times greater. The sulfate rich water were encountered in three wells: #68-69, #73-66, and #74-61. Plate 4.5.2.3-4 presents the results of chemical analyses of water samples obtained from Well #68-69, and from three depth intervals in test Well #73-66.

Well #68-69 is located in central Mercury Valley, a few kilometers southeast from Skull Mountain. A sample of water bailed from this well yielded highly anomalous results (Plate 4.5.2.3-4). The total dissolved solids content was found to be equal to 5,420 milligrams per liter. Sodium constituted about 75 percent of the total cations, and sulfate about 95 percent of the anions.

The results of chemical anaylses of water samples swabbed during the drill-stem tests in Well #73-66 (depth intervals 77 to 693 feet and 1,565 to 1,695 feet), and pumped from the Paleozoic carbonates (depth 3,140 to 3,400 feet) are shown on Plate 4.5.2.3-4. The location of Well #73-60 is shown on

Conceptual importance of the Cane Spring perched body.

Plate 4.5.2.3-3. The sulfate content increases depthward from 34 to 181 mg/L. The samples of perched water, from depth interval 1,565 to 1,695 feet, was high in total dissolved solids (981 mg/L), high in sodium (424 mg/L), but very low in calcium (4 mg/L).

Well #74-61 is located in central Jackass Flat, approximately 8 km west of Skull Mountain. Winograd and Thordarson, 1975, reported that the sulfate content of water from this well is high, about 9 mg/L. In contrast, the sulfate content of water from two nearby wells, Wells #74-57 and #73-58, is less than 0.5 mg/L. These differences suggest that "dissolution of pyrite" in upstream areas, hydrothermally altered Calico Hills for example, should not be held responsible for the locally increased content of sulfate anions (Winograd and Thordarson, 1975).

Geothermal conditions around Skull Mountain were considered in Section 4.3.2. It can be recalled that a) the area contains the low seismic velocity anomaly (Plate 3.4.1-3); b) *in situ* temperatures of groundwater are higher than those in the surrounding regions; and c) around Well UE-25a3, the hydrothermal convection system is present. The in situ temperature of perched water, encountered in Well #73-66 at a depth of 1,565 to 1,695 feet, is equal to 33.5°C (Plate 4.5.2.3-4). This temperature is about 12°C higher than the corresponding temperature of semi-perched waters at Rainier Mesa (Plate 4.3.2-3 and 4.3.2-4). In the Paleozoic carbonates, the *in situ* temperature of groundwater in Well #73-66, at a depth interval 3,140 to 3,400 feet, was found to be 64.5°C (Plate 4.5.2.3-4). This temperature is 10 to 30°C higher than the corresponding temperatures at Yucca Mountain and around Yucca Flat (Plates 4.3.2-2 and 4.3.2-7).

The possible depthward increase in the value of hydraulic potentials within the body of perched water, as noted during drilling Well #73-68; the progressive increase in altitudes of the water table in Wells #77-68 and #73-68; and an anomalously high water level in the valley-fill aquifer as encountered in Well #77-68, relative to the upstream areas; all suggest that groundwaters involved in the Skull Mountain hydrologic anomaly may not be "ordinary" meteoric water infiltrating through the vadose zone. Such a suspicion is somewhat strengthened by both the groundwater chemistry and geothermal data. It is possible, that the anomalous waters may be related to the underlying aquifer and are, in fact, expressing a deep rooted hydraulic mound. Spatial correspondence between the location of the inferred hydraulic mound and the low-seismic velocity anomaly on Plate 3.4.1-3 suggests that the proposed explanation has merit and should be explored further. In any event, it is rather obvious that the current data base is not sufficient to either substantiate or refute that or any other explanation.

1989 Recommendation

An investigation of the known bodies of perched and semi-perched water, that occur within the vadose zone of the Death Valley groundwater system, should be performed. A main purpose of this task is to evaluate the possibility that some of these bodies represent tectonically induced hydraulic mounds, either remnant or active. There are three outstanding candidates for this study: a) the apparent hydraulic mound underneath Greenwater Range; b) the hydrologic anomaly in the vicinity of Skull Mountain; and c) the apparent hydraulic mound between Climax Stock and Emigrant Valley. The investigation should be sufficiently broad in scope to permit a definition of lateral and vertical gradients of a) hydraulic potentials; b) *in situ* temperature; and c) isotopic and chemical composition of groundwater.

From Szymanski (1989).

Conceptual importance of the Cane Spring perched body.

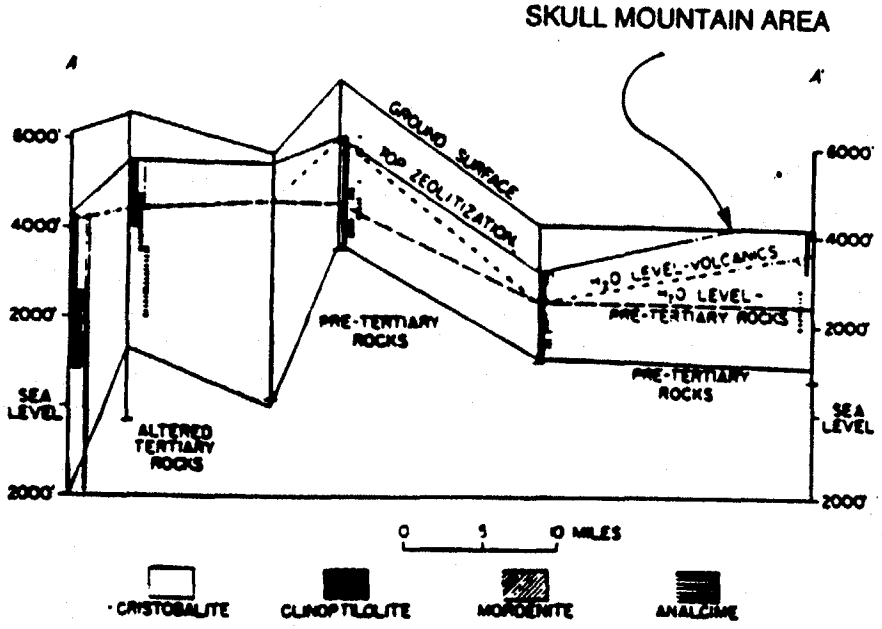

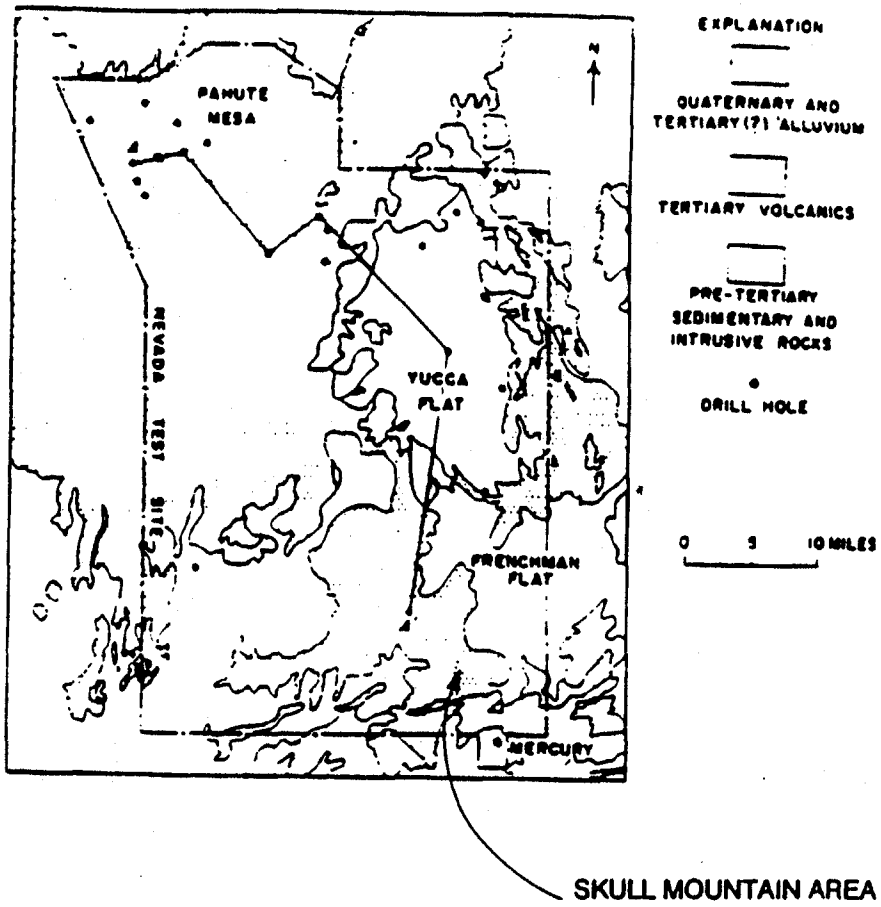

General hydrology of Yucca Flat and Frenchman Flat. Nevada Test Site. From Hoover, 1968.

Figure 3-5e

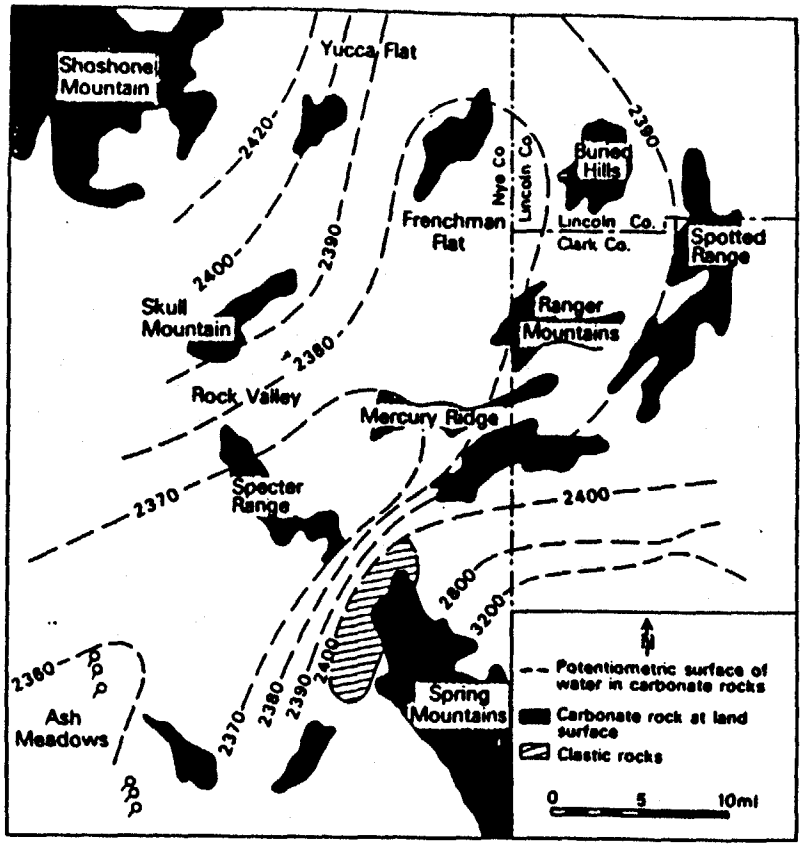

Potentiometric setting of the Skull Mountain area. Nevada Test Site. From Domenico, 1972.

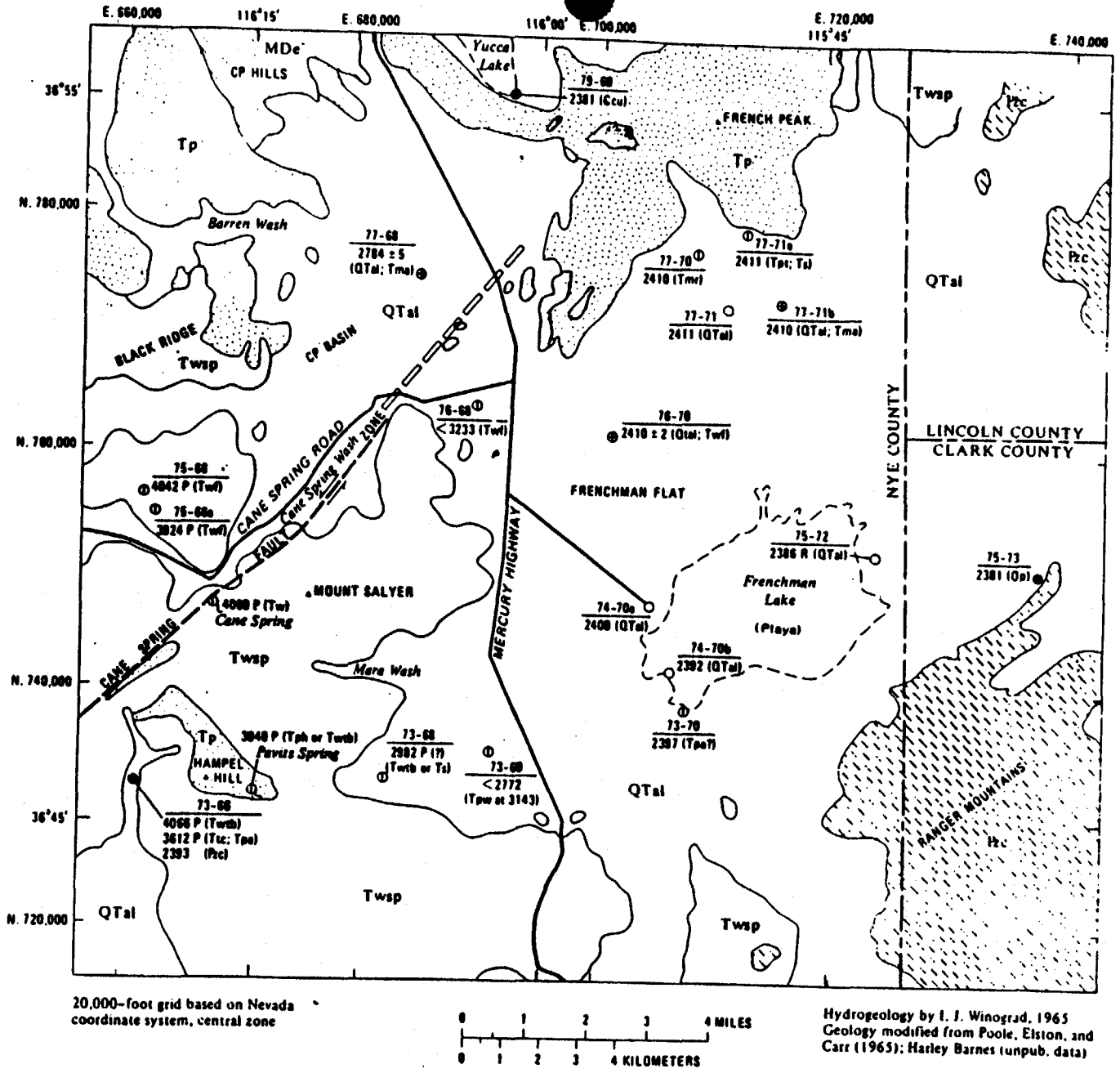

Local hydrologic conditions near Skull Mountain. Nevada Test Site. From Winograd and Thordarson, 1975.

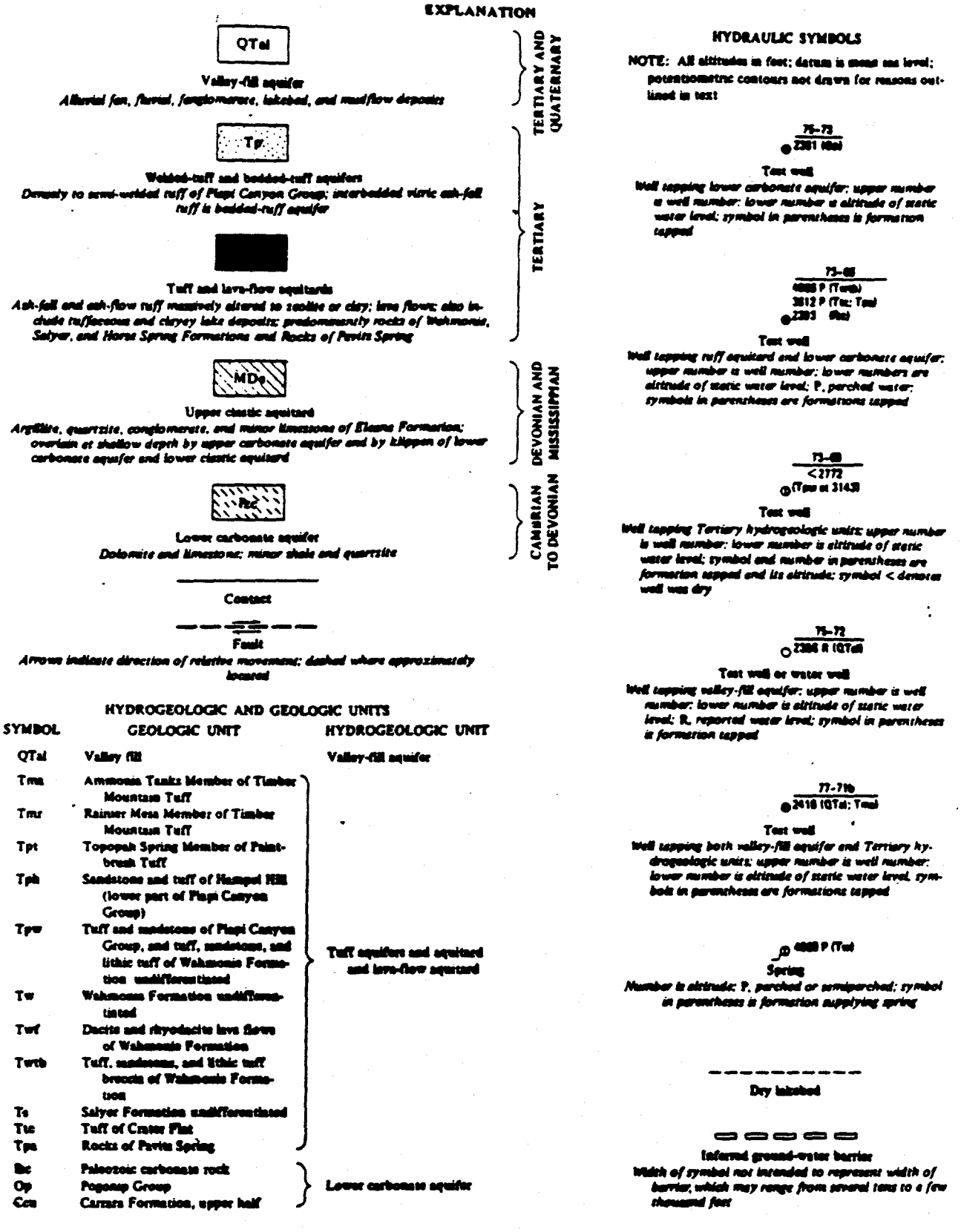

Explanation of symbols used on Figure 3-5g. From Winograd and Thordarson, 1975.

Chemical analysis of water from test well 68–69. Mercury Valley, Nye County

	Milligrams per liter[1]	Milliequivalents per liter
Silica (SiO_2)	23	---
Calcium (Ca)	281	14.02
Magnesium (Mg)	90	7.40
Sodium (Na)	1,290	56.12
Bicarbonate (HCO_3)	98	1.61
Carbonate (CO_3)	Tr	---
Sulfate (SO_4)	3,600	74.99
Chloride (Cl)	[2]35	.99
Dissolved solids (sum)	5,420	---
Hardness as $CaCO_3$ (total)	1,070	---
pH	6.1	---

[1]Analysis by Smith-Emery Co. of Los Angeles, Calif., 1951. Sodium, sulfate, dissolved solids, and hardness have been rounded to Survey standards.
[2]Erroneously reported as 96 by Schoff and Moore (1964, p. 27).

Chemical analyses of water from three depth intervals in test well 73–66, Rock Valley, Nye County

[Analyses by U.S. Geol. Survey, Denver, Colo]

Depth interval (ft)	77–693	1,565–1,695	3,140–3,400
Major constituents, in milligrams per liter			
Silica (SiO_2)	32	14	31
Calcium (Ca)	13	4.0	68
Magnesium (Mg)	1.0	.0	30
Sodium (Na)	98	424	63
Potassium (K)	6.4	4.4	9.6
Bicarbonate (HCO_3)	199	719	273
Carbonate (CO_3)	0	68	0
Sulfate (SO_4)	34	110	181
Chloride (Cl)	32	35	11
Physical characteristics and computed values			
Dissolved solids, in milligrams per liter calculated	327	981	634
Hardness as milligrams per liter $CaCO_3$:			
Total	37	10	293
Noncarbonate	0	0	65
Specific conductance (μmhos per cm at 25°C)	492	1,640	751
pH	7.3	8.8	7.3
Temperature (°C)	22.0	33.9	64.5

Results of chemical analyses of water samples from Well #68-69 and Well #73-66. From Winograd and Thordarson, 1975.

- ^{3}H content is less than 6pCi/L (detection limit) - fluid is older than ~ 30 years.
- Value of the $\delta^{14}C$ ratio is -71.9 $\pm$ 9 per mil or PMC = 92.8% - the calculated uncorrected age is ~ 600 years B.P.
- Chemical and isotopic composition of the Cane Spring discharge fluctuate about the median "sink" - "source" values.
- Sharp increases in TDS (end of 1983 and beginning of 1985) reflected through sharply increased values of the $\delta^{18}O$ and $\delta^{13}C$ ratios.
- Possible monotonic decrease in $\delta^{18}O$, SiO_2, and temperature.
- Relatively large value of the "oxygen isotopic shift".

Note:

a) all of the above observations indicate that the Cane Spring fluids result from transient intermixing of two end-members; and

b) the discending "sink" fluids and the ascending "source" fluids are these end-members.

Characteristics of the Cane Spring fluids.

Site Name	Date (MDY)	del D	del 18O	del 13C	Tritium pCi/l
Cane spring	03/06/81	-	-	-	<60.0
	03/10/81	-	-11.6	-	-
	04/02/81	-	-	-	<6.0
	05/06/81	-	-11.6	-	-
	10/27/81	-89.0	-11.2	-	-
	12/03/81	-	-10.9	-	-
	02/08/82	-87.0	-9.9	-	-
	03/26/82	-	-	-	<6.0
	05/26/82	-88.0	-11.6	-	-
	06/17/82	-	-10.9	-	-
	08/16/82	-	-11.7	-	-
	12/02/82	-	-11.2	-	-
	02/14/83	-	-9.5	-	-
	04/10/83	-	-12.2	-	-
	06/08/83	-	-10.2	-	-
	08/17/83	-	-10.1	-	-
	10/05/83	-	-7.1	-10.1	-
	01/04/84	-92.0	-11.1	-	-
	02/10/84	-90.0	-10.9	-	-
	04/10/84	-90.0	-10.3	-	-
	06/06/84	-90.0	-12.0	-	<6.0
	08/03/84	-95.0	-10.9	-	-
	10/10/84	-88.0	-11.0	-	-
	11/02/84	-89.0	-11.0	-	-
	11/15/84	-88.0	-11.2	-	<6.0
	01/10/85	-90.0	-11.0	-	<6.0
	02/12/85	-91.0	-11.0	-	-
	03/12/85	-91.0	-11.5	-	-
	04/11/85	-89.0	-10.4	-	-
	05/08/85	-89.0	-10.6	-10.1	-
	06/13/85	-88.0	-11.2	-8.8	-
	07/08/85	-91.0	-11.1	-9.3	-
	08/07/85	-89.0	-11.0	-8.9	-
	09/11/85	-90.0	-10.6	-9.2	-
	10/10/85	-90.0	-11.0	-10.0	-
	11/15/85	-91.0	-11.1	-	-
	11/15/85	-89.0	-11.1	-10.7	-
	12/16/85	-90.0	-10.8	-12.0	-
	12/16/85	-89.0	-10.8	-10.7	-
	01/15/86	-88.0	-11.1	-	-

Site Name	Date (MDY)	del D	del 18O	del 13C	Tritium pCi/l
Cane spring (cont)	01/15/86	-89.0	-10.6	-11.0	-
	02/12/86	-90.0	-11.1	-	-
	02/12/86	-89.0	-10.8	-	-
	03/10/86	-88.0	-11.1	-	-
	04/23/86	-90.0	-11.4	-	-
	04/23/86	-90.0	-11.0	-	-
	05/20/86	-91.0	-11.0	-	-
	05/20/86	-94.0	-10.9	-	-
	06/10/86	-87.0	-10.7	-	-
	06/10/86	-85.0	-10.7	-	-
	07/22/86	-89.0	-11.0	-	-
	07/22/86	-89.0	-11.0	-	-
	08/19/86	-90.0	-10.8	-	-
	08/19/86	-92.0	-11.0	-	-
	09/17/86	-91.0	-11.0	-	-
	09/17/86	-90.0	-11.0	-	-
	10/17/86	-90.0	-11.4	-	-
	10/17/86	-90.0	-11.2	-	-
	11/19/86	-91.0	-11.4	-	-
	11/19/86	-92.0	-11.2	-	-
	12/10/86	-95.0	-11.2	-	-
	12/10/86	-88.0	-11.0	-	-

Fluid isotopic data. Cane Spring. From Lyles et al., (1990)

Figure 3-7

Appendix C

Site Name	Date (MDY)	Temp C	EC fld	EC lab	pH fld	pH lab	Ca	Mg	Na	K	Cl	SO4	HCO3 lab	SiO2	NO3
Cane spring															
	07/11/80	15.5	340.0	-	-	-	-	-	-	-	-	-	-	-	-
	01/13/81	12.1	300.0	440.0	6.03	7.78	35.0	9.5	41.9	5.99	20.3	28.0	186.0	66.0	15.90
	03/06/81	11.0	365.0	433.0	7.10	7.04	35.0	9.5	40.8	5.22	20.1	29.2	187.0	65.0	13.60
	04/02/81	10.0	360.0	-	-	-	-	-	-	-	-	-	-	-	-
	05/04/81	13.5	340.0	450.0	7.05	7.34	34.9	10.0	42.9	6.64	19.9	28.0	213.0	66.0	13.30
	06/08/81	14.5	334.0	453.0	6.95	7.55	36.7	10.3	41.7	6.36	19.4	28.1	209.0	64.0	11.50
	07/31/81	20.0	400.0	-	-	-	-	-	-	-	-	-	-	-	-
	09/01/81	16.0	300.0	-	-	-	-	-	-	-	-	-	-	-	-
	10/26/81	12.5	-	434.0	-	7.64	32.3	9.3	39.4	5.41	21.2	28.9	190.0	66.0	-
	02/08/82	6.0	440.0	-	-	-	-	-	-	-	-	-	-	-	-
	03/25/82	10.5	360.0	433.0	-	7.63	35.0	9.8	40.4	6.12	21.6	32.8	191.0	61.0	11.90
	04/28/82	14.0	350.0	-	-	-	-	-	-	-	-	-	-	-	-
	05/26/82	14.9	319.0	420.0	-	7.72	34.1	9.7	40.5	6.27	19.6	28.5	188.0	62.0	-
	06/17/82	14.0	360.0	439.0	-	7.83	34.9	9.6	39.0	7.01	20.3	30.4	188.0	64.0	13.90
	08/16/82	-	-	403.0	-	7.62	32.5	9.0	37.4	6.25	18.7	27.0	173.0	62.0	14.60
	10/04/82	15.0	320.0	442.0	-	7.78	35.9	10.5	42.0	6.38	20.4	28.9	190.0	65.0	9.96
	12/02/82	11.0	270.0	445.0	-	7.60	35.2	10.4	43.3	6.16	21.1	28.9	196.0	65.0	14.50
	02/15/83	12.0	460.0	440.0	-	7.76	34.6	10.1	44.4	5.77	20.7	29.7	192.0	65.0	13.40
	04/15/83	12.0	305.0	478.0	7.82	7.82	40.6	10.9	43.7	6.14	26.1	46.9	186.0	62.0	12.90
	06/07/83	15.0	320.0	443.0	-	7.68	37.3	10.5	42.7	6.76	21.7	33.5	184.0	64.0	17.00
	08/16/83	18.0	320.0	417.0	-	7.70	32.5	9.6	39.7	6.66	19.2	29.0	172.0	64.0	19.40
	10/06/83	15.0	420.0	539.0	-	7.59	45.2	12.0	47.0	7.25	30.5	54.5	199.0	63.0	14.80
	01/04/84	12.0	330.0	467.0	-	7.53	38.2	11.1	44.5	6.26	23.5	36.3	194.0	64.0	16.30
	02/10/84	8.7	540.0	470.0	-	7.59	39.6	11.4	46.6	6.30	23.7	38.9	199.0	64.0	16.50
	04/05/84	11.3	529.0	453.0	-	7.71	37.3	10.8	43.7	6.08	22.0	34.5	188.0	61.0	15.20
	06/06/84	14.0	310.0	416.0	-	7.86	34.9	9.7	39.5	6.20	19.5	27.2	171.0	60.0	20.20
	08/07/84	18.0	-	423.0	-	7.74	33.1	9.2	40.1	6.71	19.7	30.1	179.0	63.0	17.50
	10/11/84	10.5	496.0	450.0	-	7.67	36.8	10.6	44.0	6.69	22.1	31.2	196.0	65.0	17.40
	11/02/84	-	-	455.0	-	7.87	36.7	10.7	42.7	6.45	22.1	31.2	196.0	67.0	17.50
	11/16/84	-	476.0	452.0	-	7.71	36.0	10.8	43.3	6.58	23.6	30.9	194.0	65.0	17.30
	01/11/85	8.8	663.0	627.0	-	7.57	54.2	15.1	55.0	7.19	45.0	87.0	184.0	65.0	16.50
	02/13/85	-	-	520.0	-	7.54	43.1	12.3	46.8	6.44	31.9	61.1	181.0	62.0	17.00
	03/13/85	10.2	539.0	512.0	-	7.60	42.2	11.8	43.8	6.21	30.3	53.7	183.0	61.0	15.90
	04/12/85	14.2	515.0	488.0	-	7.72	38.6	10.6	44.8	6.27	27.5	48.9	182.0	59.0	15.40
	01/16/86	10.4	454.0	416.0	-	7.54	31.3	9.6	38.3	7.88	19.6	28.0	181.0	65.0	12.10

Note:

a) concentration of $CL^- + SO_4^-$ ions ranges from 46.7 to 132 ppm;
b) concentration of $Ca^{++} + Mg^{++}$ ions ranges from 40.9 to 69.3 ppm;
c) concentration of HCO_3^- ions ranges from 171 to 213 ppm; and
d) concentration of $K^+ + Na^+$ ions ranges from 43.6 to 62.2.

Fluid chemistry data. Cane Spring. From Lyles et al. (1990)

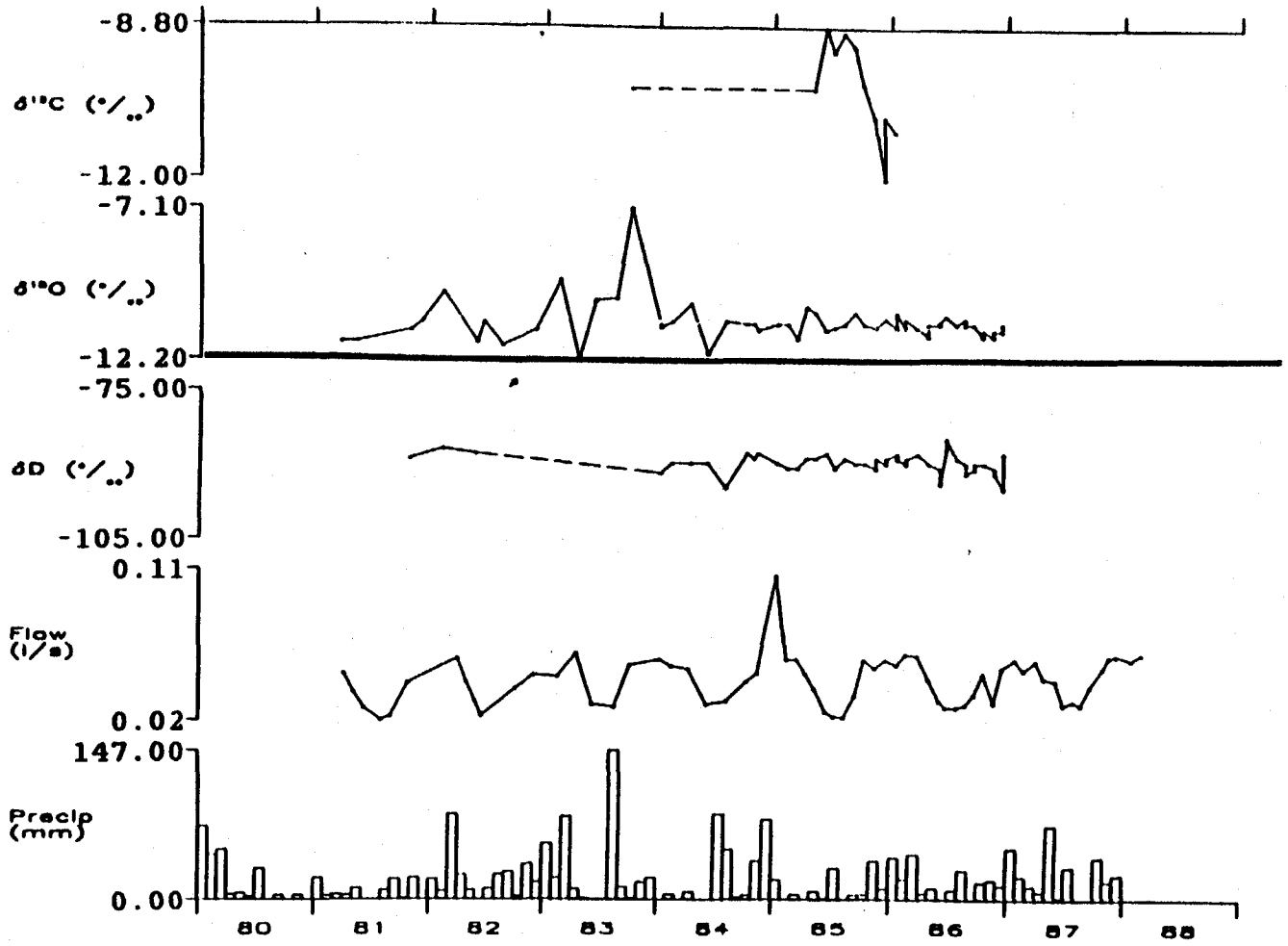

Cane Spring. Fluid isotopic composition, time-series. From Lyles et al., 1990.

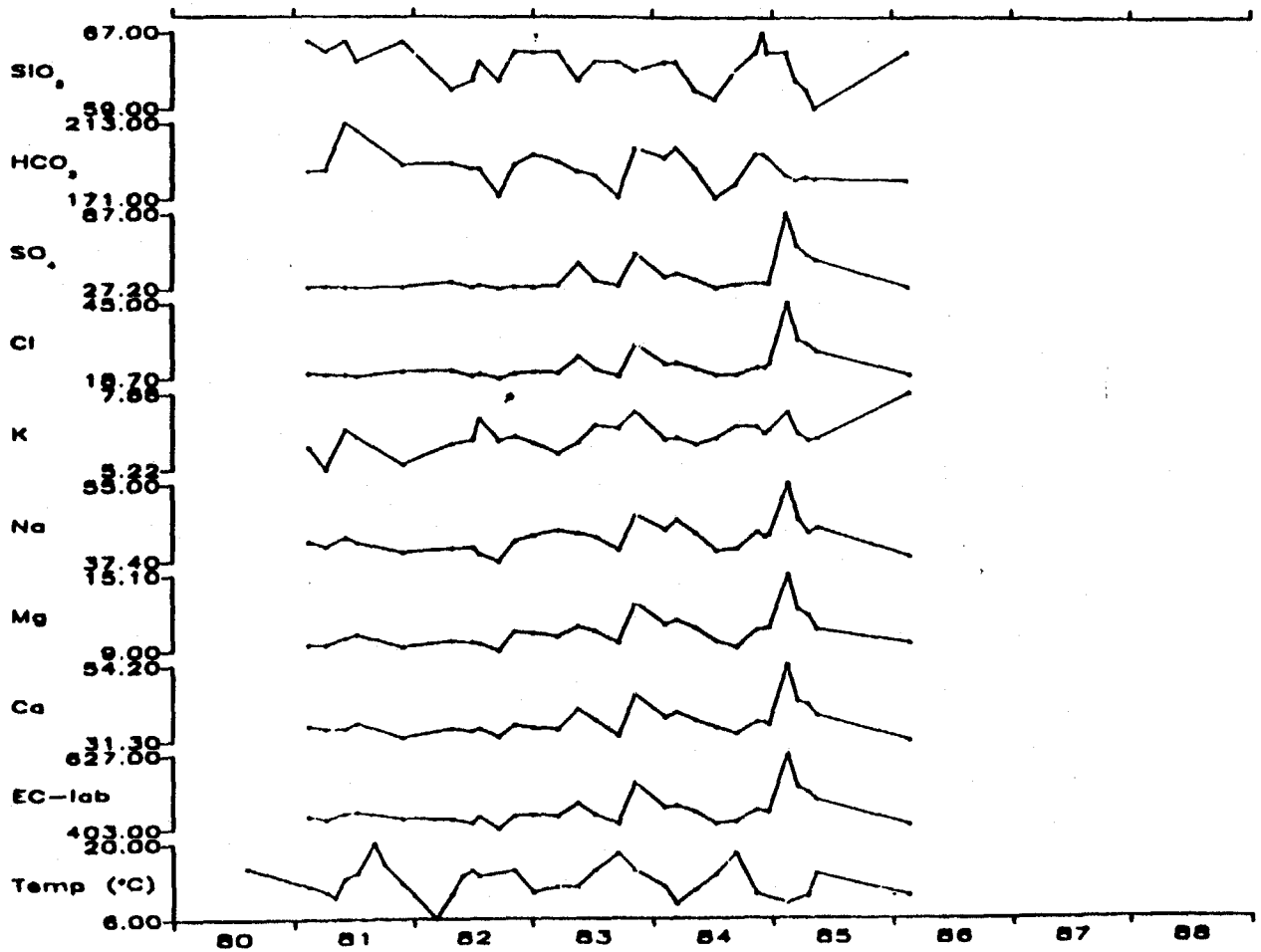

Cane Spring. Fluid chemical composition, time-series. From Lyles et al., 1990.

Variable	Min.	Max.	Mean	SDEV	Coef. Var.**	n***
Temp. (°C)	6.0	20.0	12.9	3.0	23.3	31
EC-lab*	403.0	627.0	457.7	45.9	10.0	29
pH-lab	7.04	7.87	7.65	0.17	2.2	29
Ca (mg/*l*)	31.3	54.2	37.1	4.64	12.5	29
Mg (mg/*l*)	9.0	15.1	10.5	1.27	12.1	29
Na (mg/*l*)	37.4	55.0	42.8	3.48	8.1	29
K (mg/*l*)	5.22	7.88	6.40	0.53	8.3	29
Cl (mg/*l*)	18.7	45.0	23.2	5.52	23.8	29
SO_4 (mg/*l*)	27.2	87.0	36.3	13.47	37.1	29
HCO_3 (mg/*l*)	171.0	213.0	188.7	9.71	5.1	29
SiO_2 (mg/*l*)	59.0	67.0	63.6	1.99	3.1	29
NO_3 (mg/*l*)	9.96	20.2	15.24	2.43	15.9	27

* µmhos/cm @ 25°C
** SDEV/mean x 100
*** Number of observations

a) summary statistics, from 01, 1981 to 01, 1986 - ion chemistry, fluids from the Cane Spring.

Physical Parameter		log - Saturation Index	
pH-lab	7.65	Anhydrite	-2.89
Temperature	12.9°C	Calcite	-0.13
log Pco_2	-2.45	Dolomite	-0.67
		Gypsum	-2.20

b) saturation indexes - WATEQDR for mean Cane Spring chemistry.

Water chemistry data - the Cane Spring perched body. From Lyles et al., 1990.

Variable	Min.	Max.	Mean	SDEV	Coef. Var.**	n***
Temp. (°C)	5.0	28.5	14.7	8.0	54.4	9
EC-lab*	96.0	119,0	110.8	8.1	7.3	6
pH-lab	6.89	7.55	7.09	0.25	3.5	6
Ca (mg/*l*)	6.0	7.2	6.7	0.4	6.0	6
Mg (mg/*l*)	1.3	1.6	1.4	0.1	7.1	6
Na (mg/*l*)	9.4	12.8	11.4	1.2	10.5	6
K (mg/*l*)	4.50	6.99	6.01	0.87	14.5	6
Cl (mg/*l*)	1.6	4.7	2.9	1.2	41.4	6
SO_4 (mg/*l*)	6.6	10.8	8.1	1.6	19.8	6
HCO_3 (mg/*l*)	34.6	58.0	52.0	9.0	17.3	6
SiO_2 (mg/*l*)	25.0	60.0	48.7	13.3	27.3	6
NO_3 (mg/*l*)	0.31	5.10	1.89	2.23	118.0	4

* µmhos/cm @ 25°C
** SDEV/mean x 100
*** Number of observations

a) summary statistics, from 03, 1981 to June, 1982 - ion chemistry, fluids from the Topopah Spring.

Physical Parameter		log – Saturation Index	
pH-lab	7.09	Anhydrite	-3.48
Temperature	14.7°C	Calcite	-1.87
log Pco_2	-2.42	Dolomite	-4.25
		Gypsum	-3.41

b) saturation indexes - WATEQDR for mean Topopah Spring chemistry.

Water chemistry data - Topopah Spring perched body. From Lyles et al., 1990.

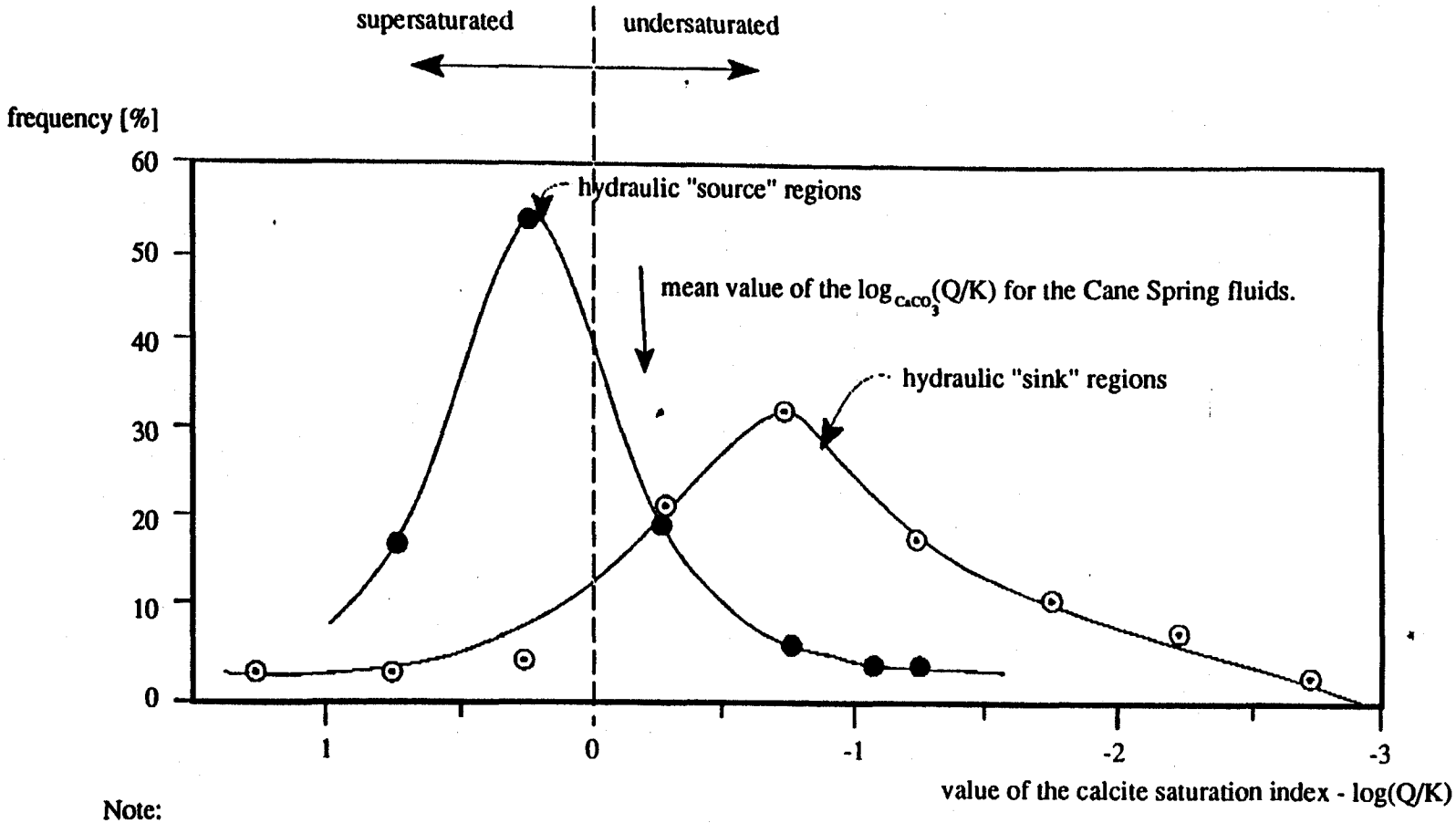

Note:

a) log (Q/K) data are from Kerrisk (1987);

b) N = 52 for hydraulic "source" regions; N = 64 for hydraulic "sink" regions; and

c) Q - the ion activity product, K - the equilibrium constant for the solubility reaction.

Calcite saturation index. Water samples from the Nevada Test Site hydraulic "sink" and "source" regions relative to the Cane Spring fluids.

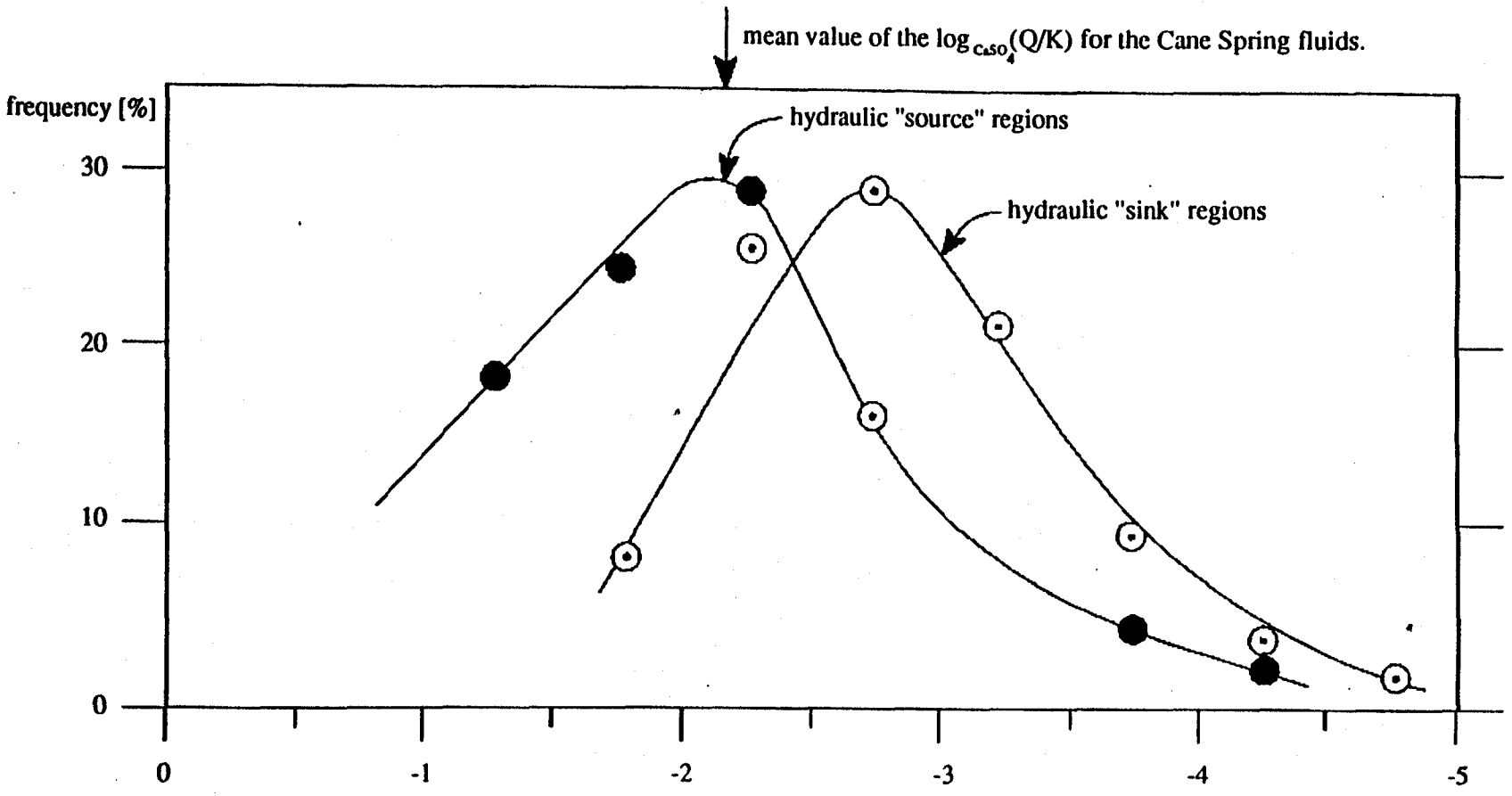

Note:

a) log (Q/K) data are from Kerrisk (1987);

b) N = 48 for hydraulic "source" regions; N = 61 for hydraulic "sink" regions; and

c) Q - the ion activity product, K - the equilibrium constant for the solubility reaction.

Gypsum saturation index. Water samples from the Nevada Test Site hydraulic "sink" and "source" regions relative to the Cane Spring fluids.

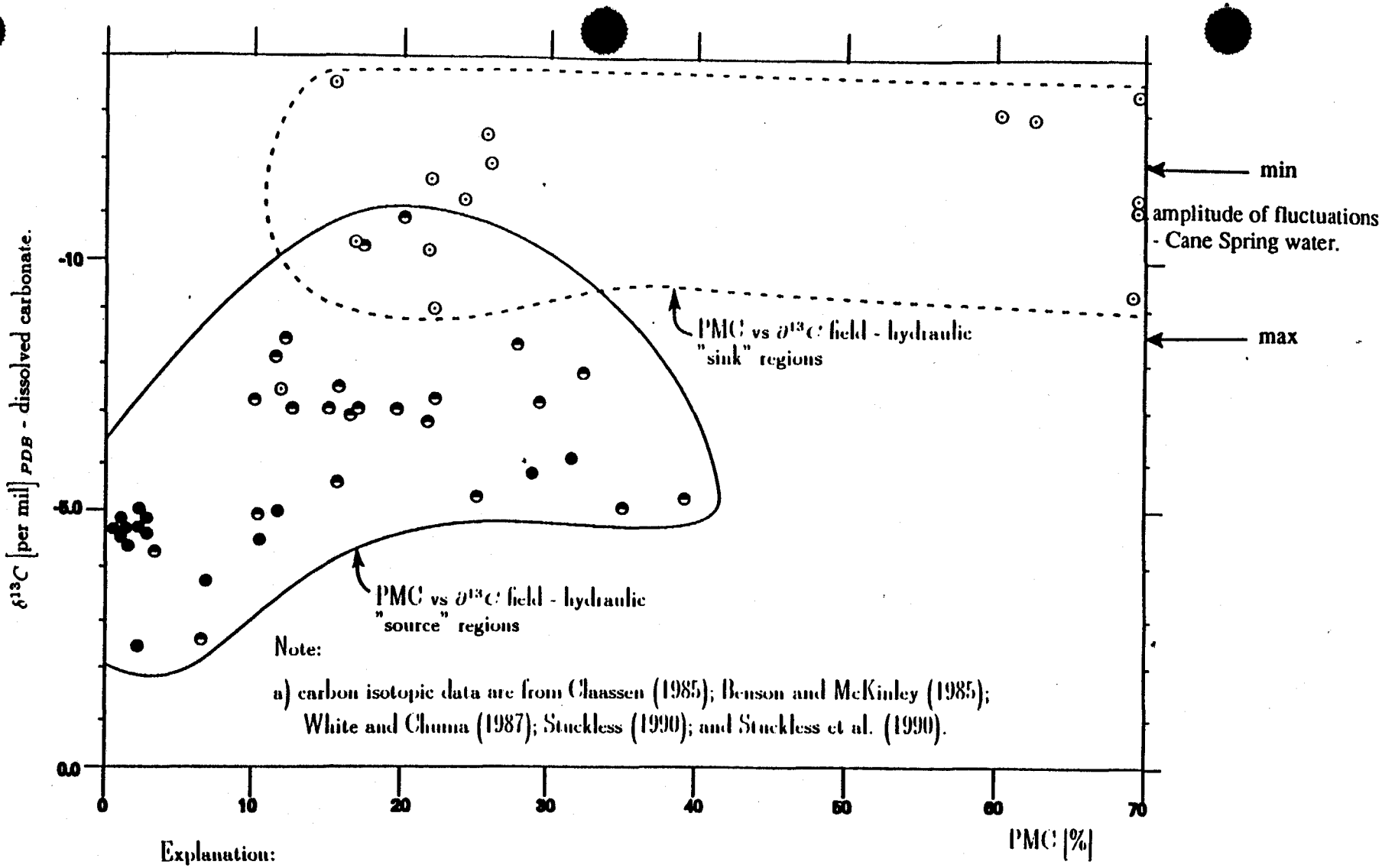

Explanation:

- ○ - sample represents the tuff "pile" based hydraulic sink region;
- ⊖ - sample represents the tuff "pile" based hydraulic source region; and
- ● - sample represents the Paleozoic carbonates based hydraulic source region.

$\delta^{13}C$ vs. PMC field. Water samples from the Nevada Test Site hydrosphere relative to the Cane Spring fluids.

Figure 3-15

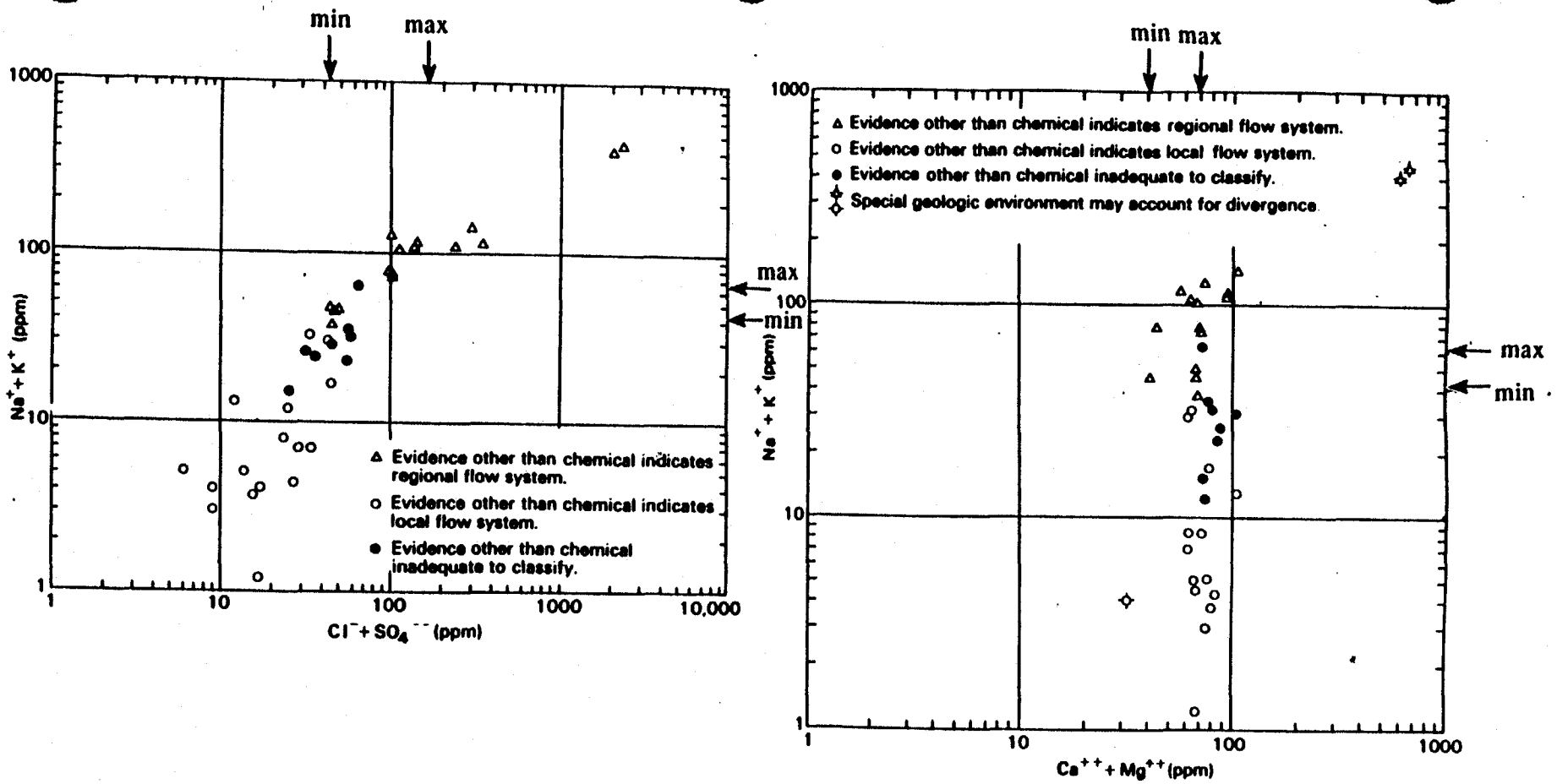

Explanation:

← max

amplitude of fluctuations - Cane Spring water.

← min

Comparison of groundwater chemistry. The Nevada Test Site subsurface fluids and the Cane Spring perched fluids. Modified from Domenico, 1972.

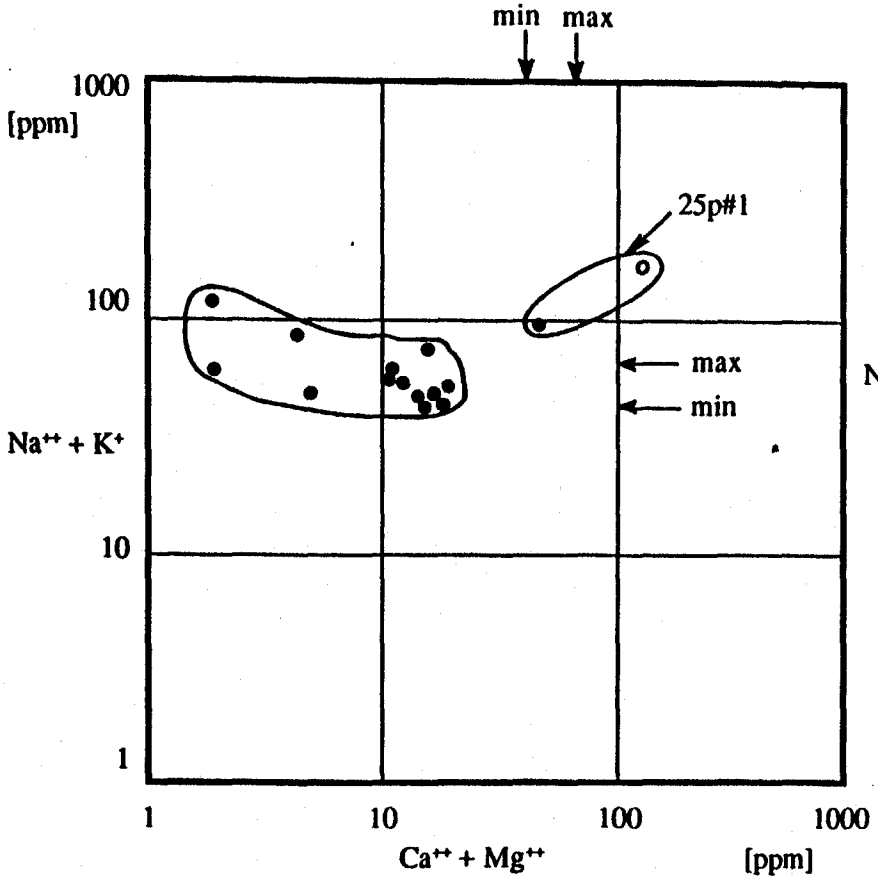

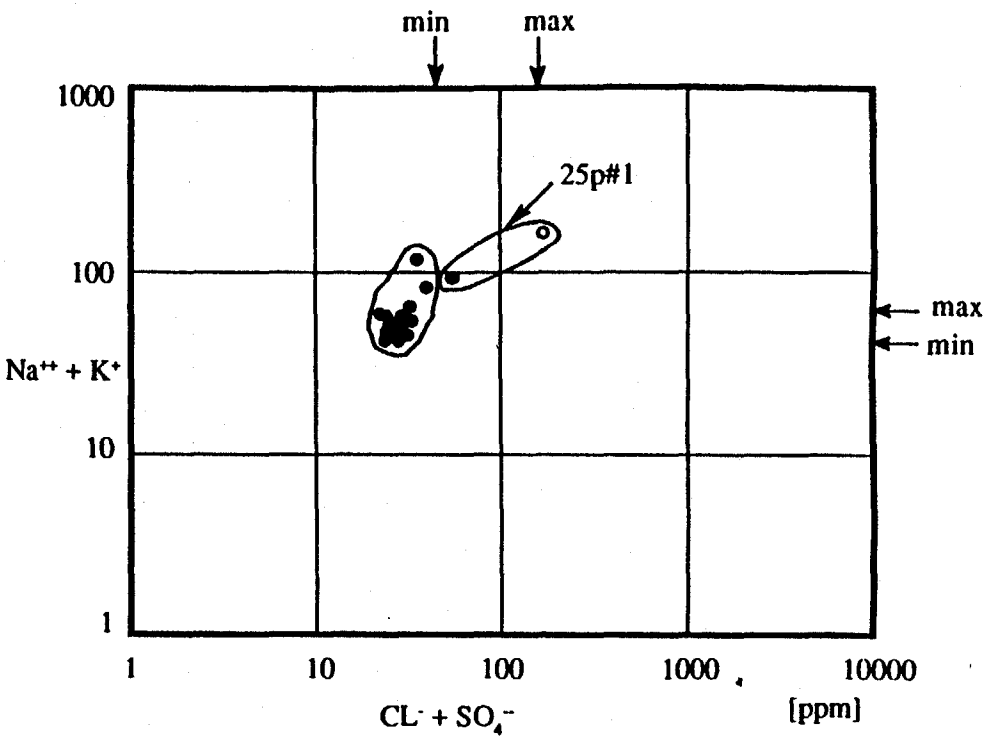

Explanation:

- ● - sample represents fluids from within the Yucca Mountain *in-situ* stress field inclusion;
- o - sample represents deeper fluids from the underlying hydraulic "source".

← max
← min
amplitude of fluctuations - Cane Spring water.

Groundwater chemistry. Summary. Yucca Mountain dilated region relative to the Cane Spring fluids.

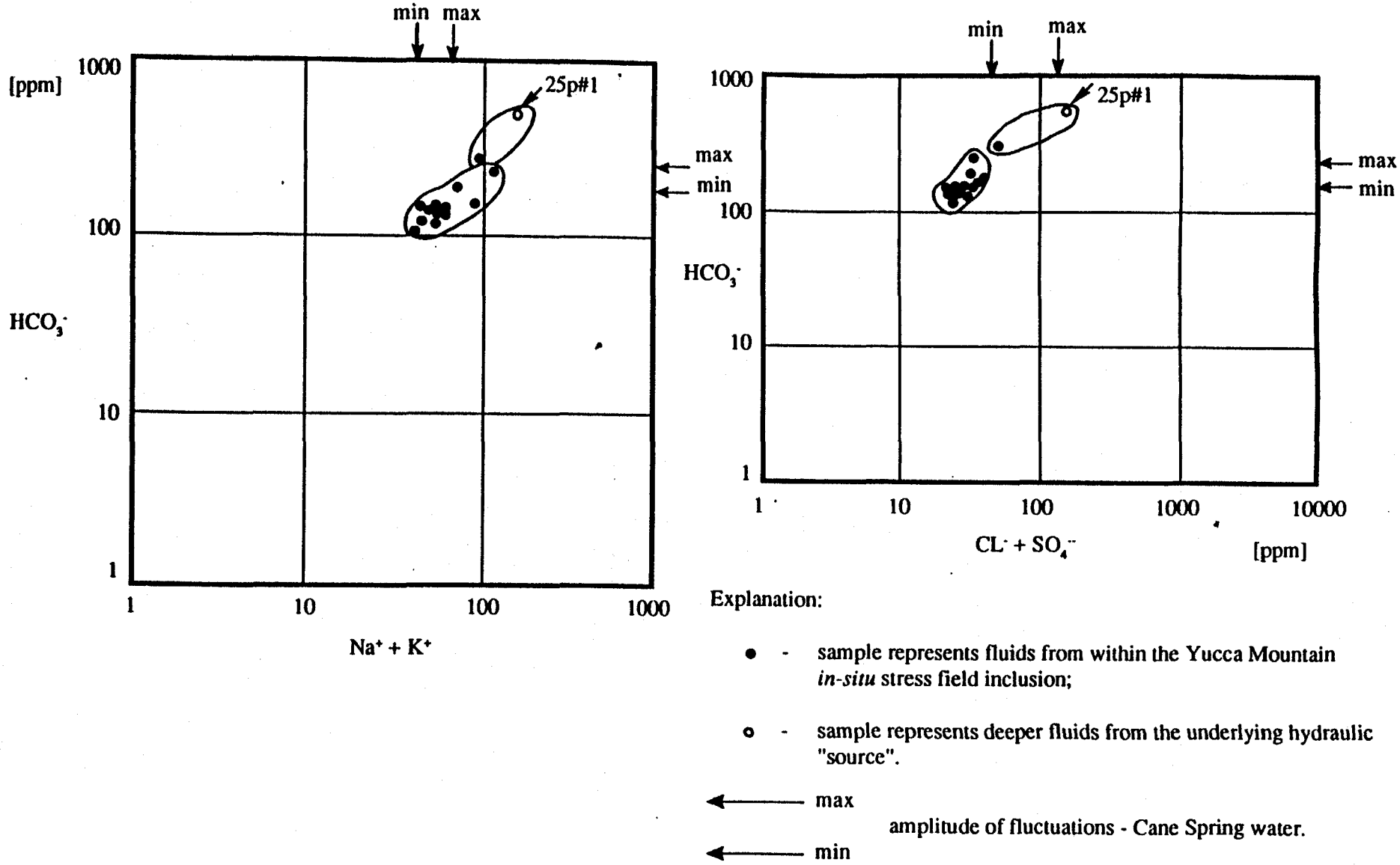

Explanation:

- ● - sample represents fluids from within the Yucca Mountain *in-situ* stress field inclusion;
- o - sample represents deeper fluids from the underlying hydraulic "source".

← max

amplitude of fluctuations - Cane Spring water.

← min

Groundwater chemistry. Summary. Yucca Mountain dilated region relative to the Cane Spring fluids.

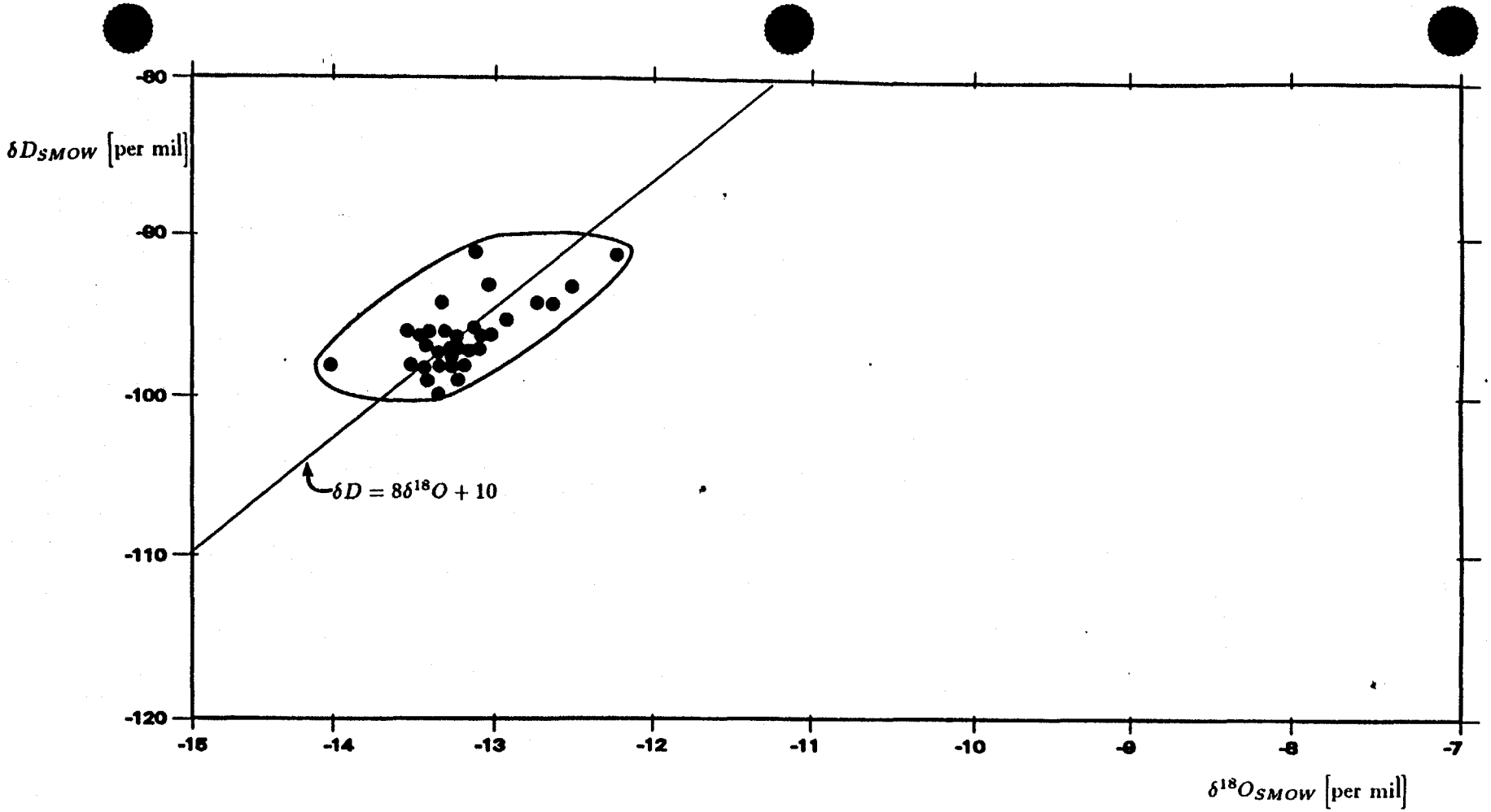

Note:

a) the U12n.03 seep is into tunnel, samples were obtained ~ 400m below the ground surface;

b) fluid is known to be directly from atmospheric precipitation;

c) fluid does not exhibit any oxygen shift, indicating that evaporative enrichment is nil;and

d) isotopic data are from Russell (1987).

Reference - evaporative enrichment in the Rainier Mesa recharge.

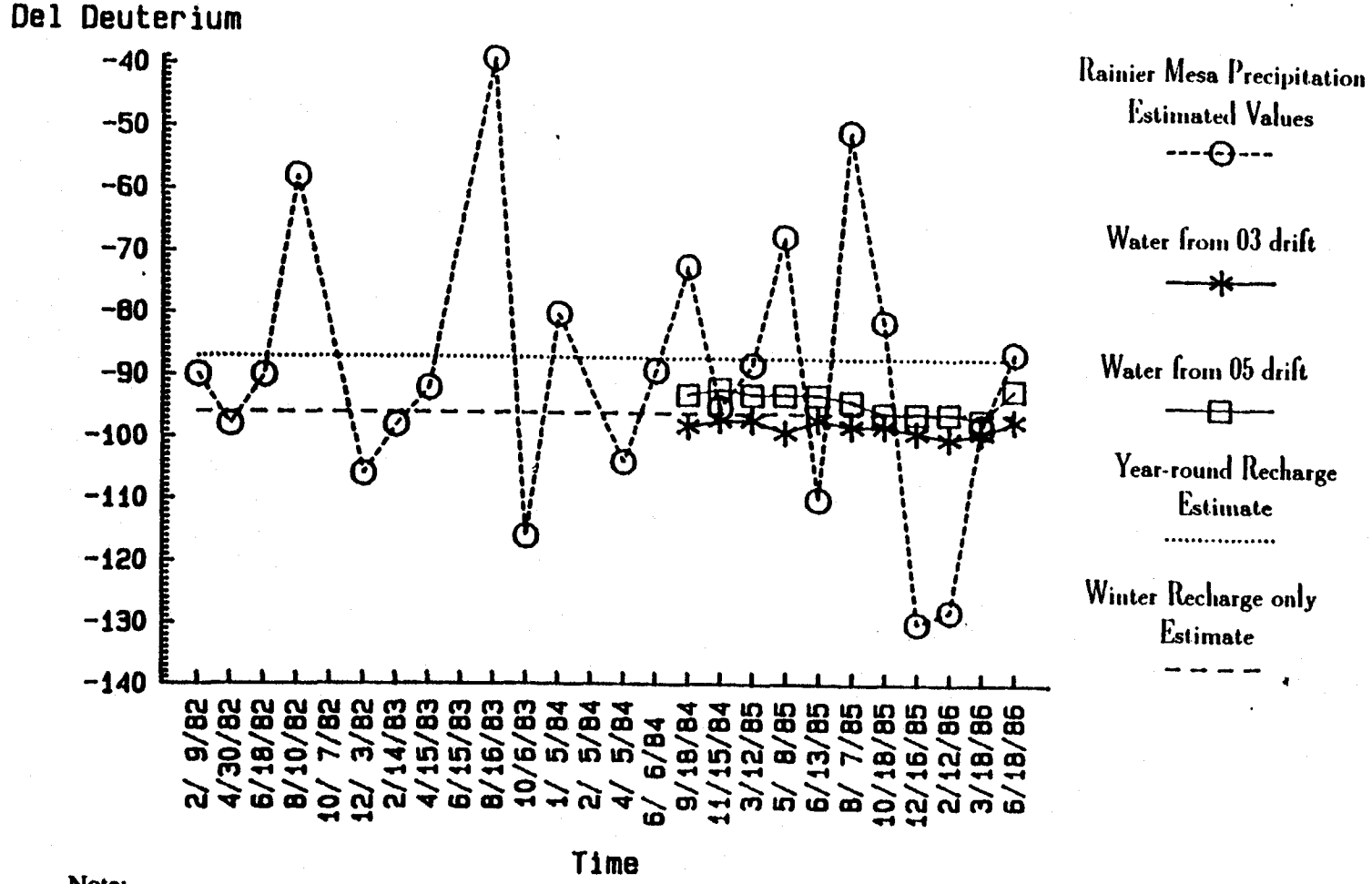

Note:

a) for the infiltrating recharge, δD fluctuations are very small;

b) mean value for the year-round recharge is δD ~ - 87 per mil $_{SMOW}$; and

c) mean value for the winter-recharge is δD ~ - 96 per mil $_{SMOW}$.

Reference - temporal variability in value of the δD ratio, from samples of the infiltrating recharge. Rainier Mesa. From Russell, 1987.

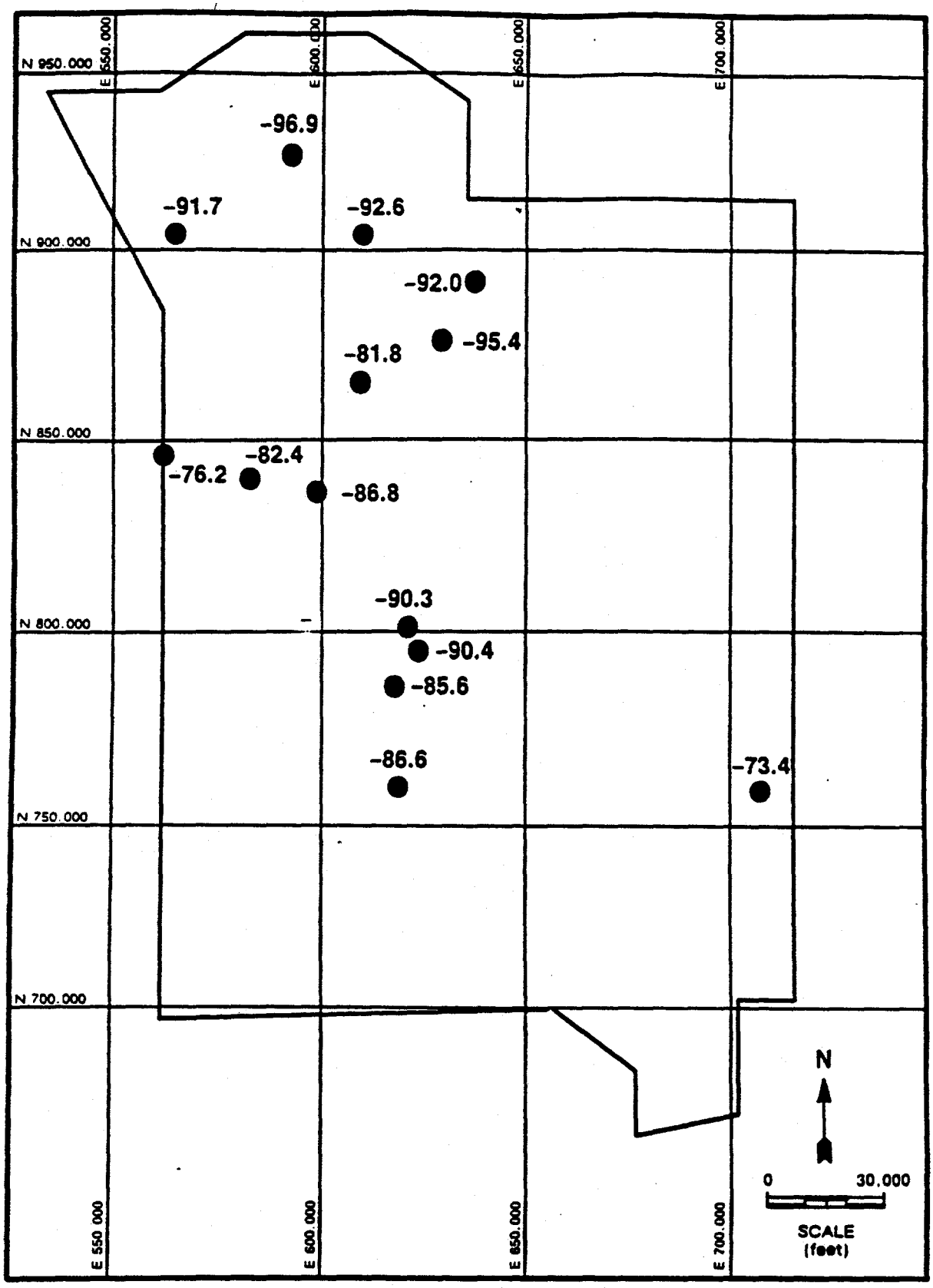

δD_{SMOW} weighted average - contemporary meteoric precipitation over the Nevada Test Site area. From Ingraham et al., 1990.

Figure 3-21

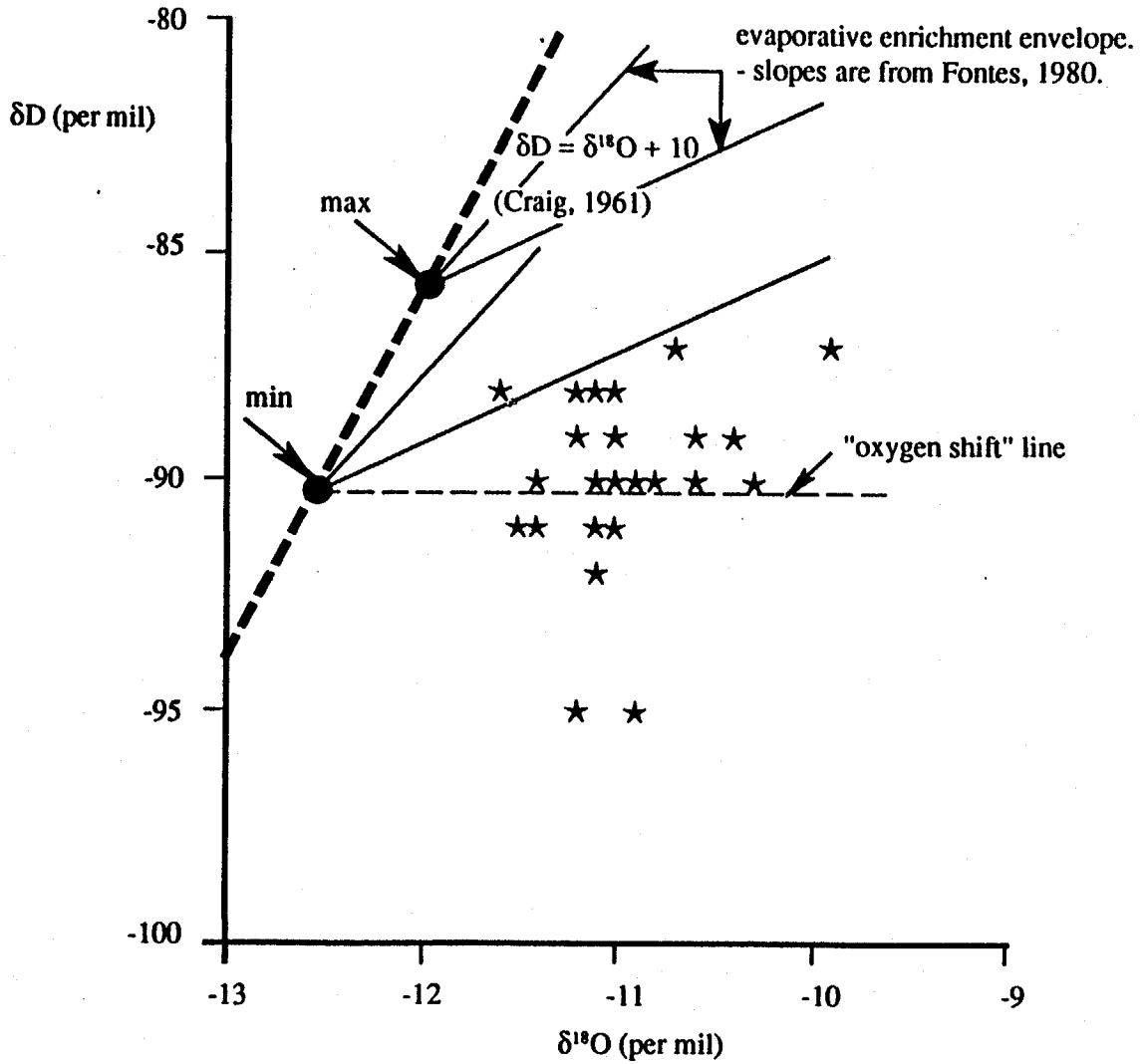

Origin of the observed "oxygen isotopic shift" (fluid ←→rock exchange reactions or evaporative enrichment). Cane Spring discharge.
Modified from Lyles et al., 1990.

Figure 3-22

Overall conclusions

- Apart from the traditional patterns of hydrologic thoughts, there is no rational reason, what-so-ever, to regard the Cane Spring fluids as solely representing the perched infiltrating recharge (interpretation Option I).

- a) The overall setting of the Cane Spring (thermal, hydraulic, and hydrochemical); b) the chemical and isotopic composition of the discharging fluids; c) the observed fluctuation of the chemical and isotopic compositions; and d) the observed "oxygen isotopic shift" are all consistant with the interpretation Option II.

- The Cane Spring travertines are modern analog for the Yucca Mountain calcite-opaline silica deposits.

Conclusions - presentation #3.

Figure 3-23

Issue - Intraformation time and history of the parent fluids for the Yucca Mountain calcretes, surficial fault - fracture infilings, and subsurface veins (depth 0 - 700 m).

Interpretation options.

I - **the *per descensum* deposits**, i.e. a) the parent fluids are fresh meteoric fluids; b) dissolved solids are leached out of the local soil horizon and provided by windblown dust; and c) carbon originates from the atmosphere - biosphere source.

II - **the *per ascensum* deposits**, i.e. a) the parent fluids are evolved fluids from the hydraulic "source" regions; b) dissolved solids are leached out of the parent fluid host rock; and c) carbon originates from both the biosphere source and the subterranean source (dissolution of the Paleozoic carbonates and deep-seated igneous bodies).

Presentation content.

Part I - Critique of the *per descensum* interpretations of the origin of the Yucca Mountain calcretes and surficial veins, as proposed by Quade and Cerling (1990).

Part II - Direct field evidence for the *per ascensum* origin of the Yucca Mountain calcretes and surficial veins.

Part III - Isotopic and geochemical evidence for the *per ascensum* origin of the Yucca Mountain calcretes and surficial veins.

Statement of the issue - presentation #4.

Figure 4-1

Part I - Critique of the *per descensum* interpretations of the origin of the Yucca Mountain calcretes and surficial veins, as proposed by Quade and Cerling (1990).

Part I - title page.

Figure 4-1-1

- Quade and Cerling (1990) favor the *per descensum* origin for the Yucca Mountain calcretes and surficial veins - interpretation option I.

- Two lines of evidence were put forth in support of this conclusion, namely:

  i) the $\delta^{13}C$ vs $\delta^{18}O$ field, from samples of the Yucca Mountain calcretes and surficial veins, is claimed to be uniquelly compatible with the $d\delta^{13}C/dz$ and $d\delta^{18}O/dz$ gradients, as observed in the results of isotopic analyses of the cobble encrustations; and

  ii) the isotopic character of carbon dissolved in the parent fluids for the Yucca Mountain calcretes and surficial veins, as interpreted based on the results of isotopic analyses of samples of these calcretes and veins, is claimed to be similar to that dissolved in soil water.

- In my considered opinion, "the *per descensum* interpretations of the origin of the Yucca Mountain surficial deposits, as proposed by Quade and Cerling (1990), lack a proper foundation. As a matter of fact, the very oxygen -18 and carbon -13 data, that were used in developing the *per descensum* interpretations, may be used to successfully discredit these interpretations".

The *per descensum* interpretations advocated by Quade and Cerling (1990) - general information.

Figure 4-1.2

- Comparative analyses of the $d\delta^{13}C/dz$ and $d\delta^{18}O/dz$ gradients.
  - i) the observed values of the isotopic gradients, from the Quade et al, (1988) cobble encrustations;and
  - ii) the expected values of the isotopic gradients, for the groundwater produced cobble encrustations and distal calcretes.
- Comparative analyses of the $\delta^{13}C$ vs $\delta^{18}O$ fields.
  - i) the carbonate gangue veins from the Carlin - Cortez disseminated gold deposits;
  - ii) the Amargosa Basin *per ascensum* deposits;
  - iii) the reference cobble encrustations; and
  - iv) the Yucca Mountain calcite-opaline silica deposits.

Content - the comparative analyses of the isotopic gradients and the $\delta^{18}O$ vs $\delta^{13}C$ fields.

Figure 4-1.3

Sample No.	Elevation (m)	$\delta^{13}C_{PDB}$	$\delta^{18}O_{PDB}$
SM-1a	840	-2.0	-9.0
SM-1b	840	-1.9	-7.8
SM-1c	840	-1.2	-7.8
SM-2b	1550	-3.1	-8.8
SM-2b	1550	-4.0	-11.2
SM-2c	1550	-5.2	-12.3
SM-3a	1950	-5.4	-11.2
SM-3b	1950	-5.0	-11.6
SM-3c	1950	-5.8	-10.4
SM-3(B)a	1900	-4.3	-11.0
SM-3(B)b	1900	-3.6	-9.4
SM-3(B)c	1900	-4.8	-9.2
SM-4a	2270	-8.1	-13.1
SM-4b	2270	-6.0	-8.2
SM-4c	2270	-5.8	-9.2
SM-4d	2270	-7.3	-11.4
SM-5a	2490	-8.62	-12.2
SM-5b	2490	-8.4	-12.2
SM-5b-rerun	2490	-8.4	-12.5
SM-5c	2490	-8.8	-11.5
SM-6a	2740	-9.11	-12.2
SM-6b-1	2740	-8.08	-11.8
SM-6b-2	2740	-8.7	-12.6
SM-6c	2740	-8.0	-11.7
TC-1a	300	3.4	-2.8
TC-1b	300	4.1	-2.6
TC-1c	300	2.5	-5.6
GM-1a	1830	-8.3	-11.0
GM-1a -1m	1830	-6.9	-11.6
GM-1c	1830	-6.5	-10.4
GM-1d	1830	-7.2	-11.0
GM-2a-90cm	1575	-6.3	-9.4
GM-2b	1575	-5.8	-8.8
GM-2c	1575	-5.5	-9.7
GM-3a	1160	-2.0	-6.7
GM-3b	1160	-0.9	-7.1
GM-3c	1160	-1.8	-7.0
GM-4a	900	-2.4	-6.8
GM-4b	900	-1.3	-7.5
PaM-1a	300	-1.7	-0.4
PaM-1b	300	-0.4	-3.5
PaM-1c	300	0.9	-6.2
PiVM-1a	1675	-6.1	-11.1
PiVM-1d	1675	-6.1	-11.9
PiVM-2a	2130	-8.1	-11.2
PiVM-2b	2130	-7.5	-10.0
PiVM-2c	2130	-7.7	-11.2

Carbon and oxygen isotopic data. Cobble encrustations - region around the Nevada Test Site. From Quade et al., 1988.

Figure 4-1.4

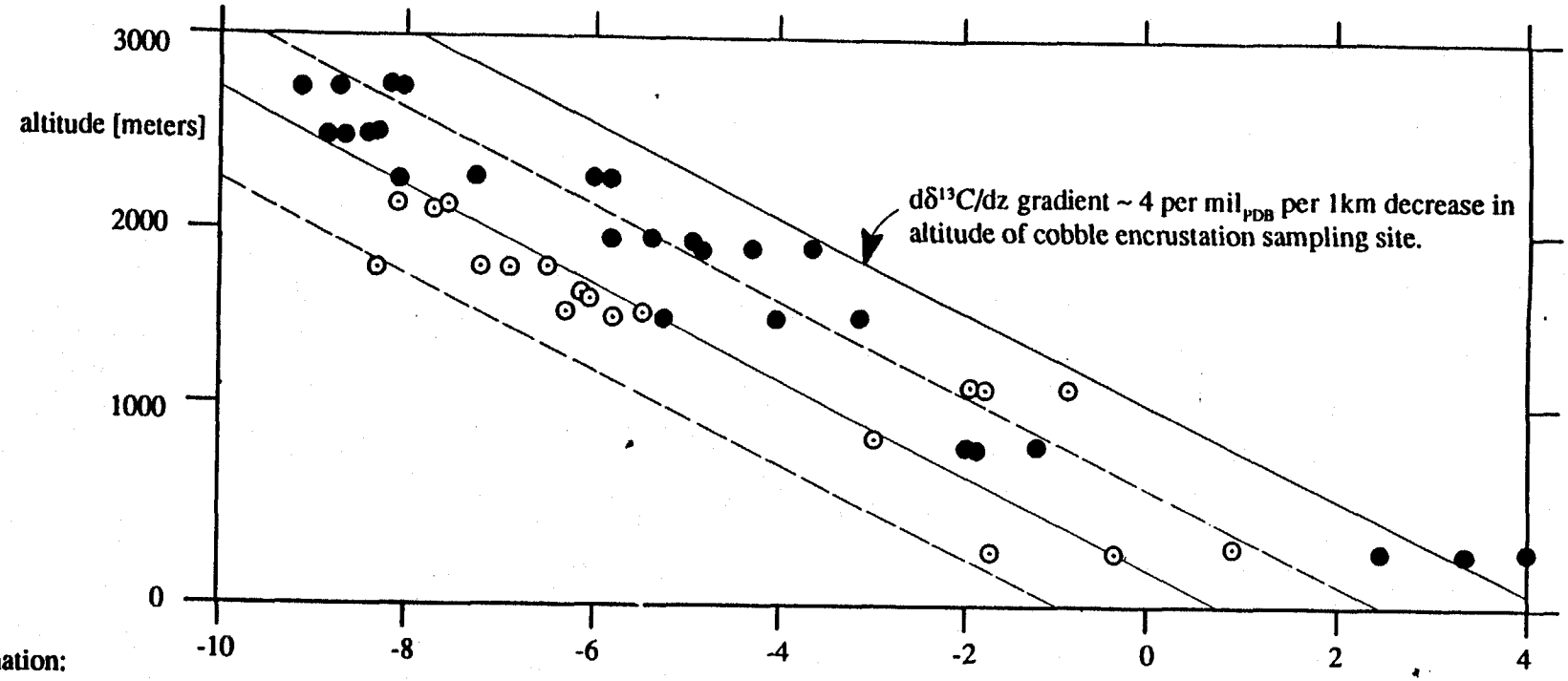

Explanation:

● - calcareous bedrock; and

⊙ - non-calcareous bedrock.

Note:

a) carbon contained in the cobble encrustations developed over the calcareous bedrock is about 2 per mil PDB "heavier";
b) this observation may be taken to indicate that, partially, parent fluids for the cobble encrustations acquire their carbon-13 content from the underlying bedrock;
c) the $d\delta^{13}C/dz$ gradient has been computed assuming that, for a fixed altitude and character of the underlying bedrock, the parent fluids have carried values of the $\delta^{13}C$ ratio varying by $\Delta\delta^{13}C \sim 3$ per mil $_{PDB}$; and
d) the above assumption is reasonable, for either the *per descensum* pedogenic fluids or the *per ascensum* pedogenic fluids, and is justified by the results of actual measurements.

Isotopic character of carbon contained in the cobble encrustations as a function of altitude of land surface.

Figure 4-1.5

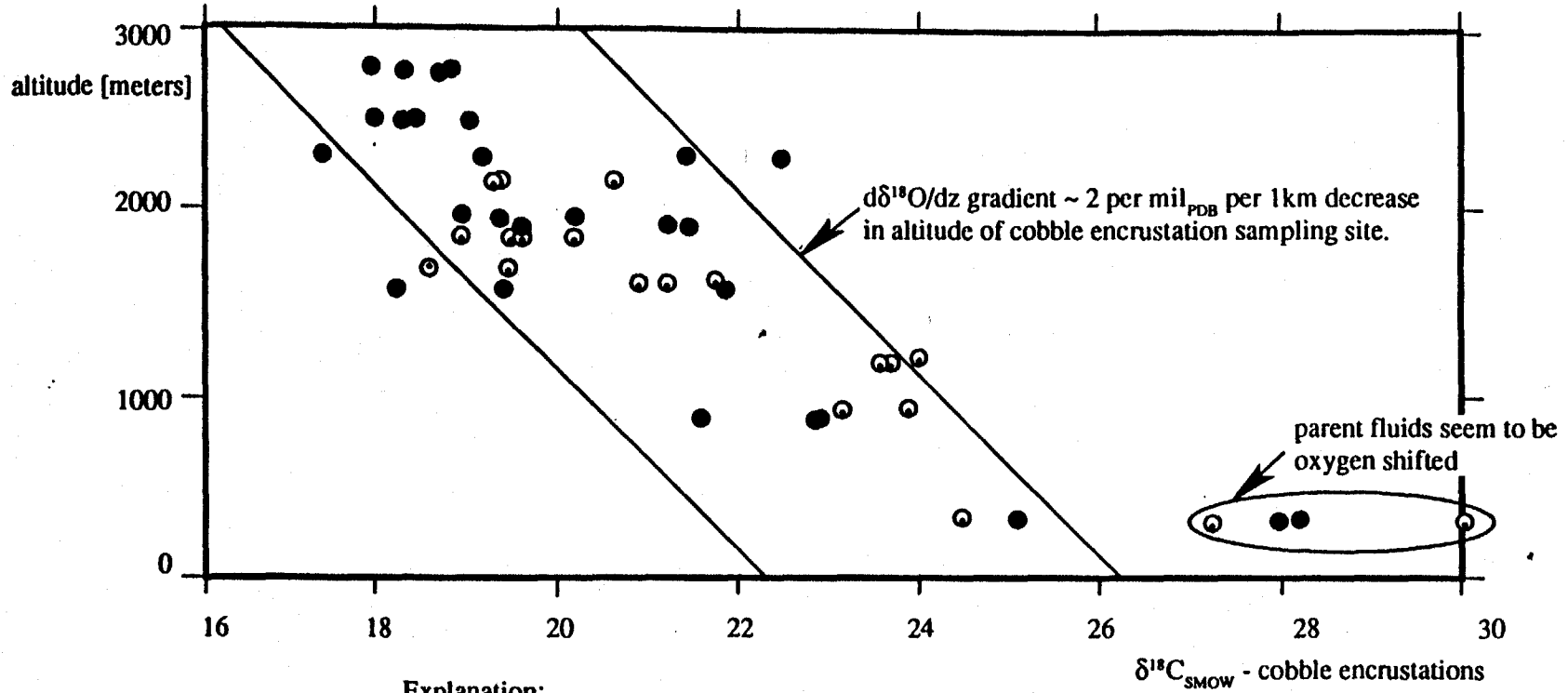

Explanation:

- ● - calcareous bedrock; and
- ⊙ - non-calcareous bedrock.

Note:

a) $\delta^{18}O_{SMOW} = 1.03086 \cdot \delta^{18}O_{PDB} + 30.86$, Frtiz and Fontes (1980);
b) the $d\delta^{18}O/dz$ gradient has been computed assuming that, for a fixed altitude, the parent fluids have carried values of the $\delta^{18}O$ ratio varying by $\Delta\delta^{18}O \sim 4$ per mil_{SMOW}; and
c) the above assumption is reasonable, for either the *per descensum* pedogenic fluids or the *per ascensum* pedogenic fluids, and is justified by the results of actual measurements.

Isotopic character of oxygen contained in the cobble encrustations as a function of altitude of land surface.

Figure 4-1.6

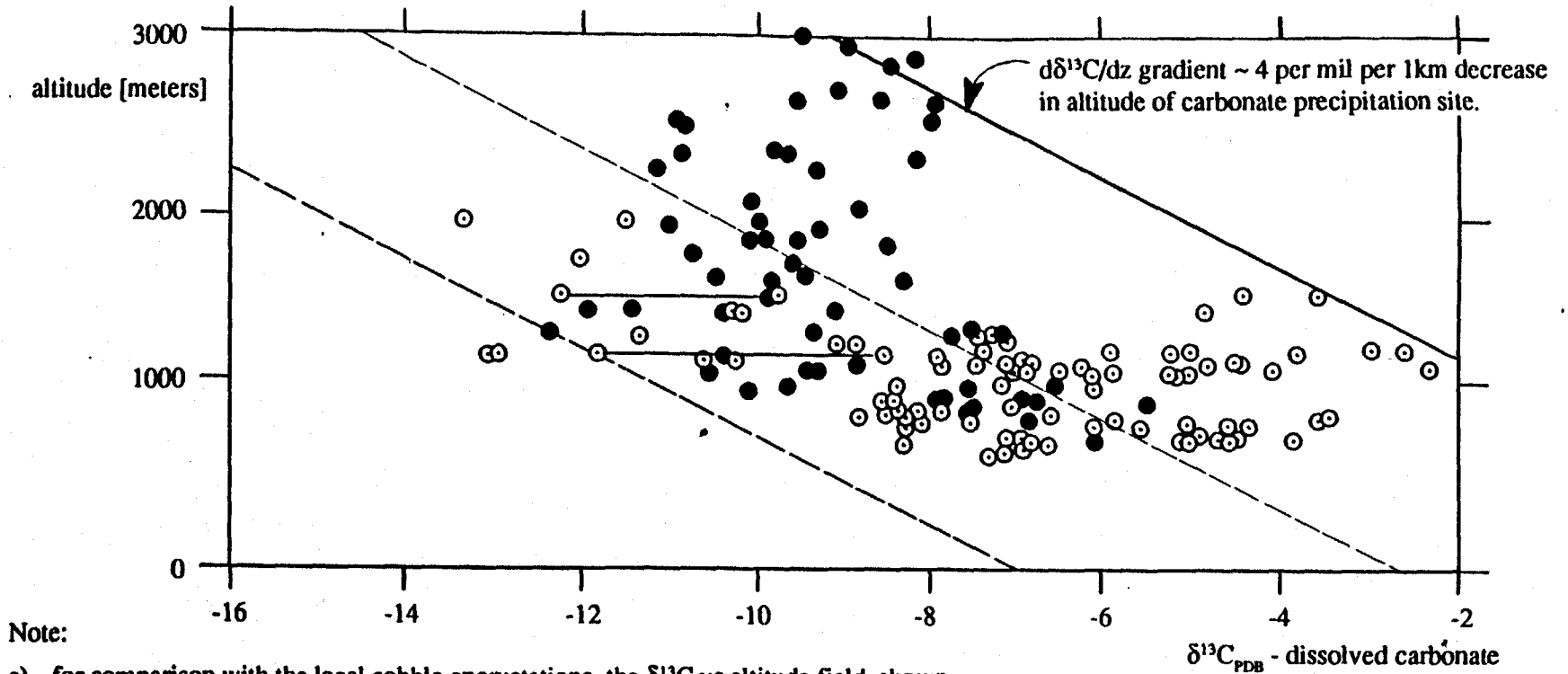

Note:

a) for comparison with the local cobble encrustations, the $\delta^{13}C$ vs altitude field, shown between solid and dashed lines, should be shifted by the equilibrium fractionation factor $10^3 \ln\alpha_{CaCO_3 - HCO_3^-} \sim 2$ per mil_{PDB};

b) relative to the observed $\delta^{13}C$ vs altitude field from the local cobble encrustations, the expected $\delta^{13}C$ vs altitude field, for the *per ascensum* cobble encrustations and distal calcretes, is about a factor of two wider;

c) the increased width of the expected $\delta^{13}C$ vs altitude field may be accounted for by recognizing that fluids which carry isotopically "light" carbon (situated between two dashed lines) are the calcium-poor fluids residing in the tuff "pile" based hydraulic "sink" regions - such fluids are not involved in precipitation of the local cobble encrustations; and

d) the expected value for the $\delta^{13}C$ vs altitude gradient, from samples of the *per ascensum* cobble encrustations and distal calcretes, is $d\delta^{13}C/dz \sim 4$ per mil_{PDB} per 1km decrease in altitude of carbonate precipitation site.

Explanation:

- ● - groundwater data (well and spring), from Hershey, 1989; and
- ○ - the Nevada Test Site groundwater data (well and springs), from Isherwood et al., 1982; Claassen, 1985; Kerrisk, 1987; White and Chuma, 1978; Spencer, 1990; Stuckless, 1990; and Lyles et al., 1990.

tielines represent the Whiterock Spring fluids and the Cane Spring fluids.

Isotopic character of carbon dissolved in the Nevada Test Site subsurface fluids, as a function of altitude of land surface, and the expected $\delta^{13}C$ vs altitude gradient and field for the *per ascensum* cobble encrustations and distal calcretes.

Figure 4-1.7

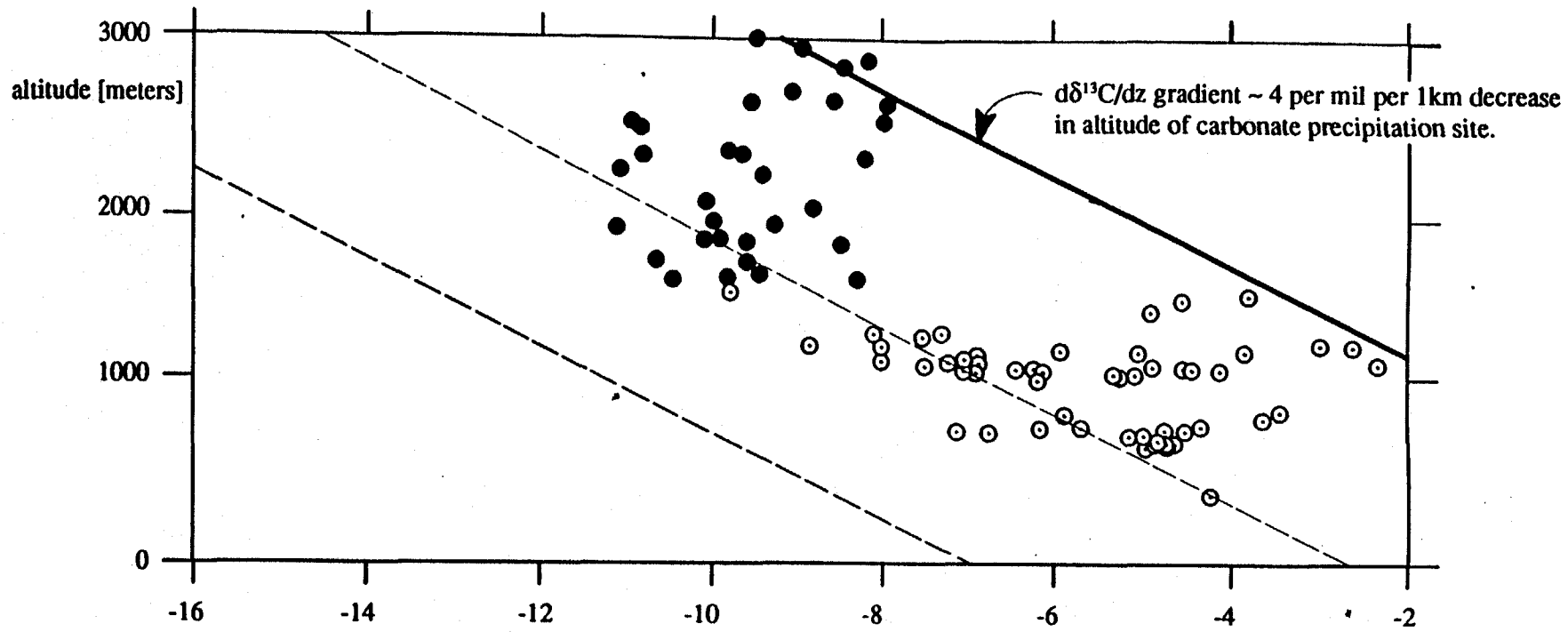

Explanation

- ● - groundwater data (well and spring) from the Spring Mountain area above altitude of 1600m, here, the host rock consists presumably exclusively of the Paleozoic carbonates, from Hershey, 1989; and
- O - groundwater data from the Nevada Test Site hydraulic "source" regions - here, the resident fluids are supersaturated with respect to calcite and, potentially, may discharge at the topographic surface.

Note:

a) selective usage of the carbon isotopic data is an attempt to exclude the calcium-poor fluids residing in the tuff "pile" based hydraulic "sink" regions; and
b) both the expected $\delta^{13}C$ vs altitude gradient and the expected $\delta^{13}C$ vs altitude field, for the *per ascensum* cobble encrustations and distal calcretes, are similar to the corresponding gradient and field, as observed by Quade et al. (1988) for the local cobble encrustations.

Isotopic character of carbon dissolved in the Nevada Test Site calcium-rich subsurface fluids ("source" plus carbonate rock based fluids) as a function of altitude of land surface and the expected values of the $\delta^{18}O$ gradient and for the per ascensum cobble encrustations and distal calcretes.

Figure 4-1.8

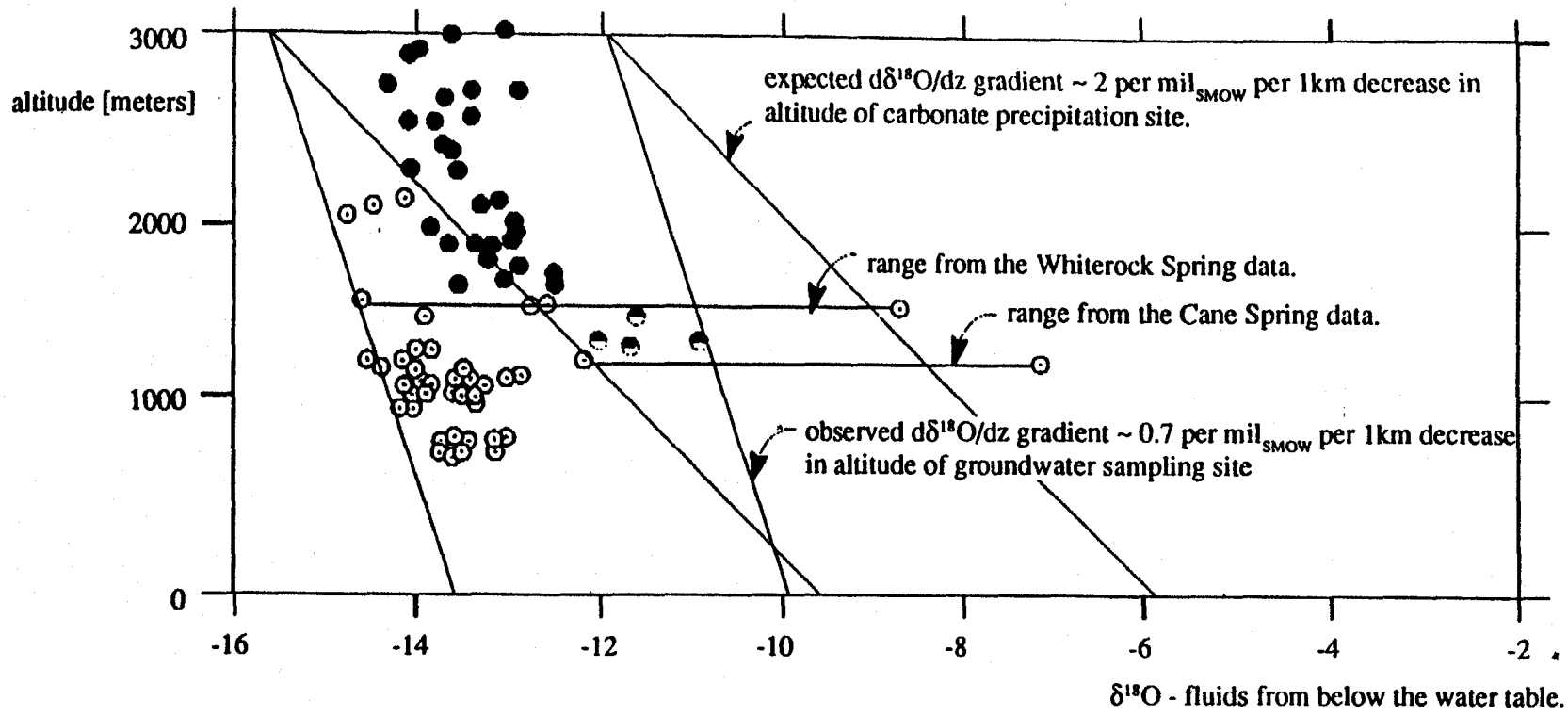

Explanation:

- ● - groundwater data (spring and well) from the Spring Mountain area above altitude of 1600m, from Hershey, 1989;
- ◒ - groundwater data (possibly "oxygen shifted") from the Spring Mountain area, from Hershey, 1989; and
- ○ - groundwater data from the Nevada Test Site hydraulic "source" regions, from Isherwood et al., 1982, Claassen, 1965, Kerrisk, 1987, White and Chuma, 1987, Benson and McKinley, 1985, Stuckless et al., 1990, and Lyles et al., 1990.

Isotopic character of oxygen contained in the Nevada Test Site calcium-rich subsurface fluids ("source" plus carbonate rock based fluids), as a function of altitude of land surface, and the expected $\delta^{18}O$ vs altitude gradient and field for the *per ascensum* cobble encrustations and distal calcretes.

Figure 4-1.9

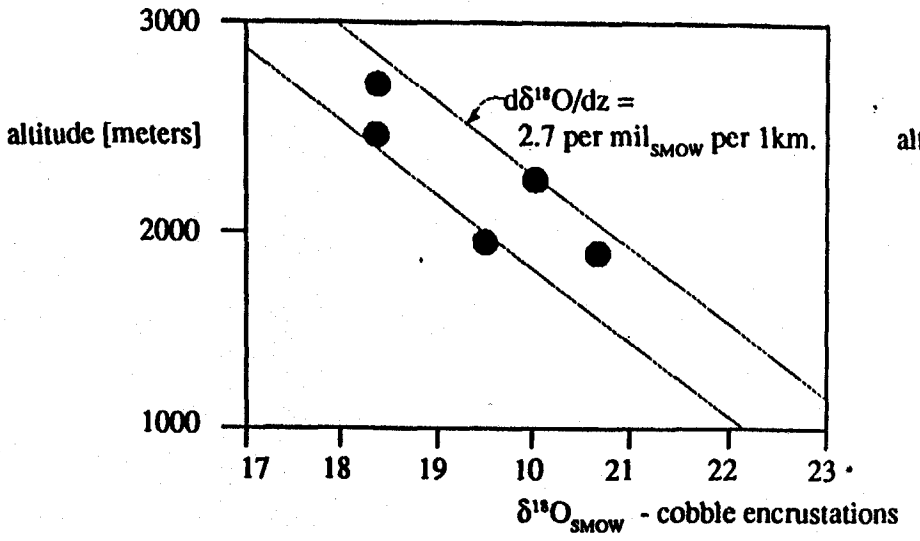

a) mean value of the isotopic composition vs altitude gradient - cobble encrustations from the Spring Mountain area, above altitude of 1800m.

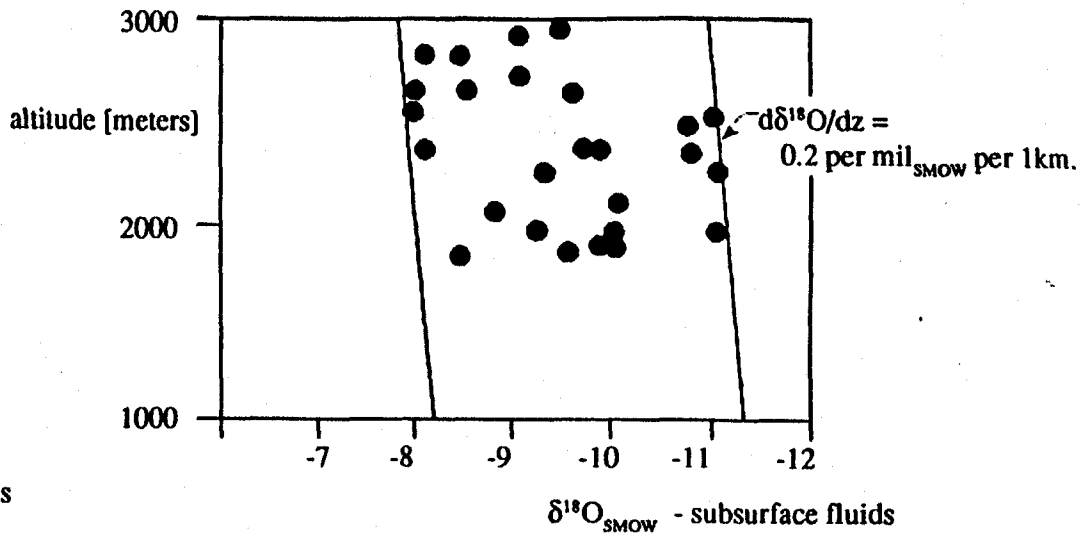

b) the isotopic composition vs altitude gradient - subsurface fluids from the Spring Mountain area, above altitude of 1800m.

Note:

a) isotopic data, as shown, are from Hershey (1989) and are computed from Quade et al. (1988);

b) the observed isotopic composition vs altitude gradient, from samples of the *sensu lato per descensum* cobble encrustations from the Spring Mountain area, is the combined results of two altitude dependent factors, namely; i) the oxygen -18 evaporative enrichment; and ii) the oxygen -18 content of the local subsurface fluids; and

c) the interpreted value for the oxygen -18 evaporative enrichment vs altitude gradient, from samples of the groundwater cobble encrustations, is $d\delta^{18}O/dz = +2.5$ per mil_{SMOW} per 1km decrease in altitude of carbonate precipitation site.

Isotopic character of oxygen contained in the Nevada Test Site calcium-rich fluids ("source" plus carbonate rock based fluids), as a function of altitude of land surface, and the expected $\delta^{18}O$ vs altitude gradient and field for the *per ascensum* cobble encrustations and distal calcretes.

Figure 4-1.10

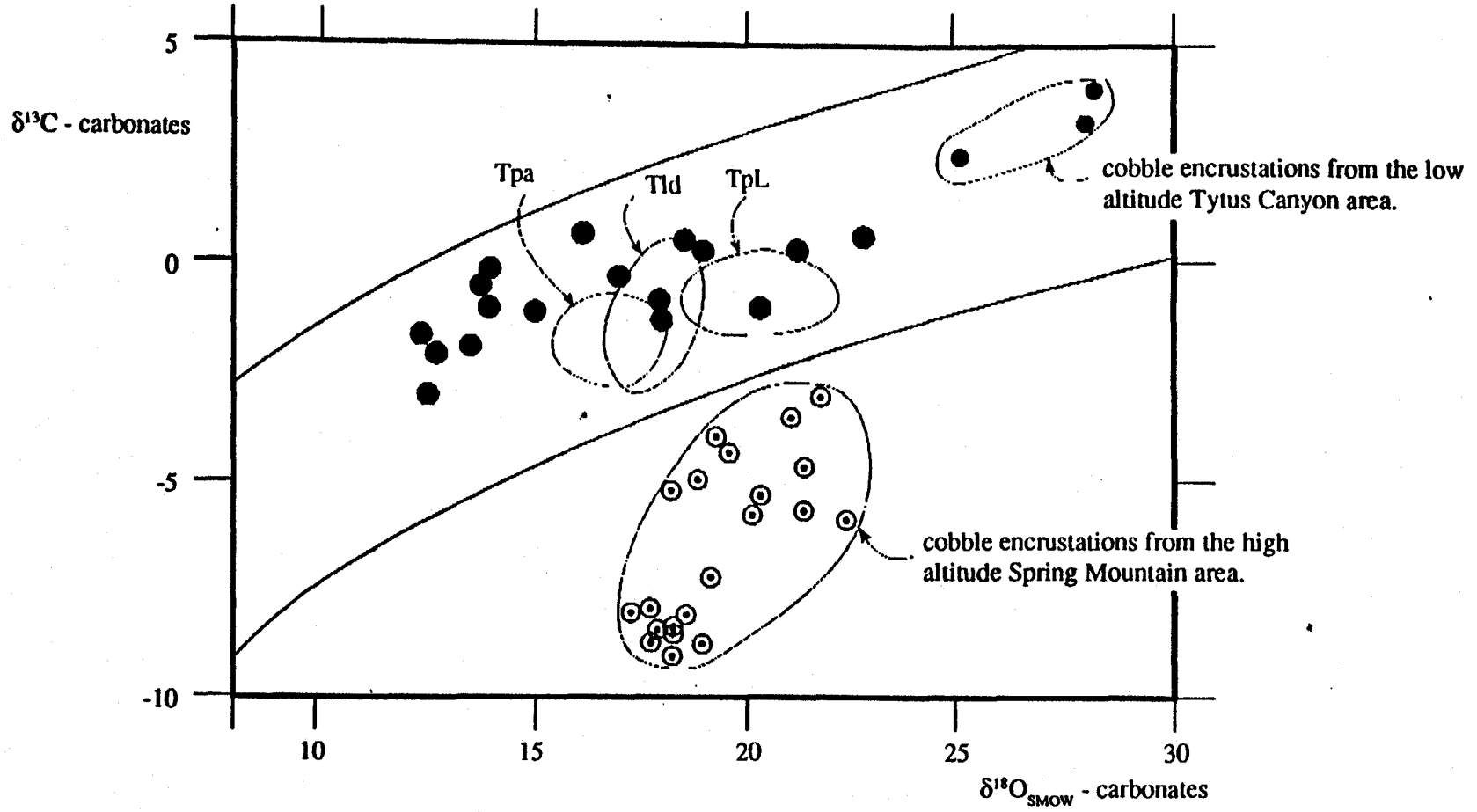

Explanation:

- ● - sample represents the carbonate gangue minerals from the Carlin and Cortez gold deposits; Tpa, Tld, and TpL denote lithofacies from the Amargosa Basin deposits;
- ● - sample represents the cobble encrustations, collected at altitudes less than 1550m and from the carbonate bedrock sites; and
- ⊙ - sample represents the cobble encrustations, collected at altitudes more than 1550m and from the Spring Mountain carbonate bedrock sites.

Isotopic comparative analyses - the Carlin and Cortez carbonate gangue minerals, the Amargosa Basin deposits, and the reference cobble encrustations.

Figure 4-1.11

Note:

a) the isotopic data, as shown, are from: Rye (1985); Hay et al. (1986); and Quade et al. (1988);

b) the observed trend toward the increasing carbon -13 and oxygen -18 contents, for all of the considered lithofacies but excluding the cobble encrustations from the high altitude Spring Mountain area, may be accounted for by assuming that: i) all of the lithofacies were precipitated from fluids that, in the pristine state, have carried similar carbon - oxygen isotopic signatures; ii) the precipitation temperatures and the degree of evaporation are, respectively, the highest and the lowest for the vein - proximal lithofacies; iii) values of CO_2 partial pressure are the highest for the vein - proximal lithofacies; and iv) the progressive carbon -13 diffusional enrichment, the precipitation temperature controlled fractionation factors, and the progressive oxygen -18 evaporative enrichment, are responsible for the observed isotopic gradients.

c) the observed two-fold clustering of the isotopic data, from the reference cobble encrustations, may be taken to indicate that two genetically different populations are involved;

d) the cobble encrustations encountered in the low altitude Tytus Canyon area represent the *sensu stricto per ascensum* population - it was suggested, in the January 18 letter, that the cobble encrustations representing this population were precipitated from the highly evolved *per ascensum* fluids, discharged from nearby no longer active springs; and

e) the cobble encrustations encountered in the high altitude Spring Mountain area represent the *sensu lato per descensum* population - it was suggested, in the January 18 letter, that the cobble encrustations representing this population were precipitated from seasonal run-off fluids, evaporating through the topographic surface. [Longwell et al. (1965), while discussing "gravel firmly cemented with calcium carbonate" from the Kyle and Lee Canyon areas, have used unmistakably clear language "the carbonate cement no doubt was dissolved either from the fragments or from the parent bedrock in the range." For both the Kyle Canyon cobble encrustations and the Lee Canyon cobble encrustations there is no rational reason to: i) call for the dubious *sensu stricto per descensum* concepts; and ii) insist for the solely atmosperic - biospheric source of carbon. Furthermore, to account for the observation made by Quade et al. (1988) that, relative to the non-carbonate bedrock sites the cobble encrustations from the carbonate bedrock sites contain isotopically "heavier" carbon, there is again no rational reason to propose that differing ecosystems are residing over the respective sites.]

Isotopic comparative analyses - the Carlin and Cortez carbonate gangue minerals, the Amargosa Basin deposits, and the reference cobble encrustations. (continued)

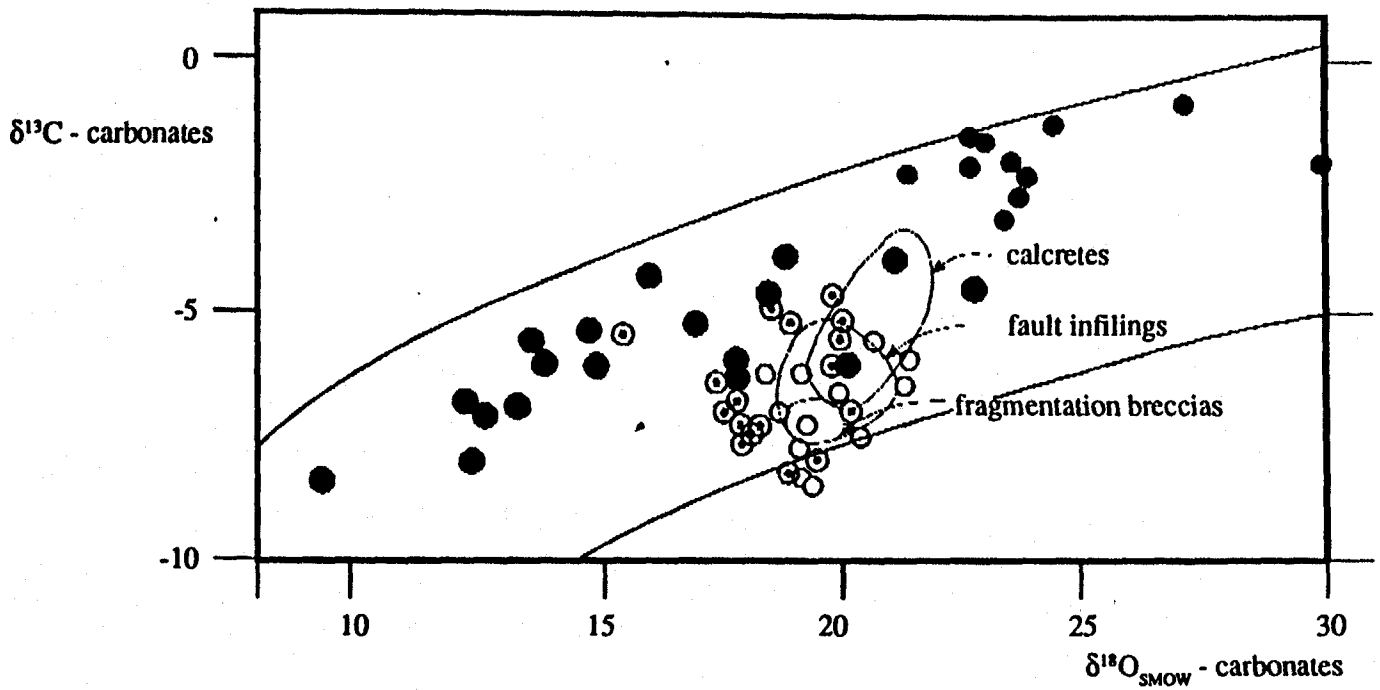

Explanation:

- ● - sample represents the carbonate gangue minerals from the Carlin and Cortez gold deposits - value shown has been adjusted by -5 per mil_{PDB} to account for the non-carbonate bedrock;
- ● - sample represents the cobble encrustations, collected at altitudes less than 1500m and from the non-carbonates bedrock sites;
- ○ - sample represents the cobble encrustations, collected at altitudes more than 1500m and from the non-carbonate bedrock sites; and
- ⊙ - sample represents the calcite-silica veins from the Yucca Mountain vadose zone (depth ranging from 34 to 611 m).

Isotopic comparative analyses - the normalized Carlin and Cortez carbonate gangue minerals, the Yucca Mountain surficial and subsurface calcite-opaline silica deposits and the reference cobble encrustations.

Figure 4-1.12

Note:

a) the isotopic data, as shown are from: Rye (1985), Szabo and Kyser (1985), Quade et al. (1988), and Whelan and Stuckless (1990);

b) the isotopic compositions of the Carlin and Cortez carbonate gangue veins, as shown, have been normalized to account for the respective differences in lithology of the host rock - the assumed normalization factor is -5 per mil_{PDB}; and

c) the observed trend toward the increasing carbon -13 and oxygen -18 contents, for all of the considered lithofacies, may be accounted for by assuming that: i) all of the lithofacies were precipitated from fluids that, in the pristine state, have carried similar carbon - oxygen isotopic signatures; ii) the precipitation temperatures and the degree of evaporation are, respectively, the highest and the lowest for the breccia cement - vein lithofacies;. iii) values of the CO_2 partial pressure are the highest for the vein-breccia cement lithofacies; and iv) the progressive diffusional carbon -13 enrichment, the precipitation temperature controlled fractionation factors, and the progressive evaporative oxygen -18 enrichment, are responsible for the observed isotopic gradients.

Isotopic comparative analyses - the normalized Carlin and Cortez carbonate gangue minerals, the Yucca Mountain surficial and subsurface calcite-opaline silica deposits and the reference cobble encrustations. (continued)

- Values of the isotopic compositions vs altitude gradients, observed based on samples of the local cobble encrustations, are:

  i) $d\delta^{13}C/dz \sim +4$ per mil_{PDB} per 1km decrease in altitude of the deposit sampling site; and
  ii) $d\delta^{18}O/dz \sim +2$ per mil_{SMOW} per 1km decrease in altitude of the deposit sampling site.

- For the *per ascensum* cobble encrustations and distal calcretes, the expected value of the carbon -13 content vs altitude gradient is $d\delta^{13}C/dz \sim +4$ per mil_{PDB} per 1km decrease in altitude of the deposit precipitation site - this expectation is based on the carbon-13 content vs altitude gradient, as observed from samples of the calcium-rich subsurface fluids.

- For the *per ascensum* cobble encrustations and distal calcretes, the expected value of the oxygen -18 content vs altitude gradient is $d\delta^{18}O/dz \sim +2$ per mil_{SMOW} per 1km decrease in altitude of the deposit precipitation site - this expectation is based on:

  i) the oxygen-18 content vs altitude gradient, as observed from samples of the calcium-rich subsurface fluids;
  ii) the observed mean ambient temperature vs altitude gradient; and
  iii) the interpreted oxygen -18 evaporative enrichment vs altitude gradient.

- In addition to yielding the comparable values of the isotopic gradients, the calcium-rich subsurface fluids also carry values of the $\delta^{18}O$ and $\delta^{13}C$ ratio that are comparable to those interpreted for the parent fluids of both the Yucca Mountain calcretes and veins and the local reference cobble encrustations.

Summary - comparative analyses of the isotopic compositions vs altitude gradients.

Figure 4-1.13

- Evidently, the observation made by Quade and Cerling (1990), that the $\delta^{13}C$ and $\delta^{18}O$ ratios from samples of the local cobble encrustations change progressively with changing altitude of the sampling site, if considered together with the similar observation, made based on the expected ratios for the *per ascensum* cobble encrustations and distal calcretes, has a two-fold meaning:

  i) either the *per ascensum* process yields cobble encrustations and distal calcretes that, in terms of the isotopic compositions vs altitude gradients, are similar to those produced via the *per descensum* process; or

  ii) the assumption of the *per descensum* origin for the local cobble encrustations, as proposed by Quade et al. (1988); Quade et al. (1989); and Quade and Cerling (1990), is **FALSE**.

- The above conclusion, if considered together with the conclusion from Figure 4-1.20, indicates that the *per descensum* interpretations of the origin of the Yucca Mountain calcretes and veins, as proposed by Quade and Cerling (1990), are devoid of any scientific bases.

Overall conclusions - comparative analyses of the isotopic compositions vs altitude gradients.

Evaluations of carbon isotopic compatibility.

i) the interpreted carbon isotopic composition of parent fluids for the Yucca Mountain calcretes and surficial veins; and

ii) the observed and interpreted carbon isotopic composition of the *per descensum* pedogenic fluids for the Yucca Mountain area.

Content - evaluations of carbon isotopic compatibility, the parent fluids for the Yucca Mountain calcite-opaline silica deposits and the Yucca Mountain *per descensum* pedogenic fluids.

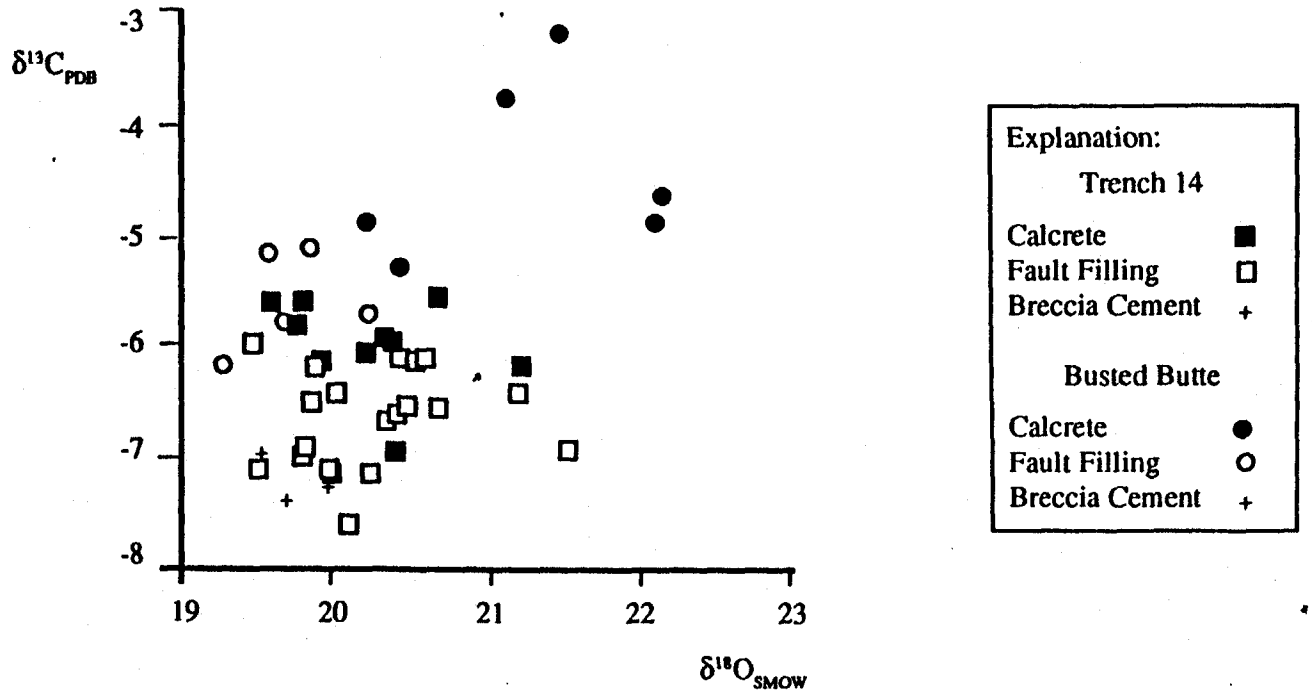

Note:

a) the observed range for the $\delta^{13}C$ ratio, from samples of the Yucca Mountain calcretes and surficial veins, is from -3.0 to -7.5 per mil_{PDB}, isotopic data are from Whelan and Stuckless, 1990;

b) for precipitation temperature T = 15°Celcius, the equilibrium fractionation factor $10^3 ln\alpha_{CaCO_3 - HCO_3^-} = 1.75$ per mil_{PDB}; and

c) the interpreted range for the $\delta^{13}C$ ratio, for the parent fluids of the Yucca Mountain calcretes and surficial veins, is from -4.75 to -9.25 per mil_{PDB}.

The interpreted range of values for the $\delta^{13}C$ ratio - the parent fluids for the Yucca Mountain calcretes and surficial veins.

Figure 4-1.16

- A mean value of the $\delta^{13}C$ ratio for CO_2 gas respired from the vadose zone, as observed at Yucca Mountain and Amargosa Narrows, is $\delta^{13}C$ = **-18.36 and -20.0 per mil$_{PDB}$**, respectively, Yang et al., 1986; Thorstenson et al., 1989, and White and Chuma, 1987 - the Yucca Mountain value is based on samples that carry PMC > 100 percent and were collected at a depth ranging from 0 to 12.8m.

- A mean value of the $\delta^{13}C$ ratio for soil gas, as observed at various locations throughout the Nevada Test Site, is $\delta^{13}C$ = **-20.5 per mil$_{PDB}$**, Boughton, 1986.

- The equilibrium isotopic fractionation factor $10^3 \ln\alpha_{HCO_3^- - CO_2(g)} = 9.483 \bullet 10^3 \bullet T^{-1} - 23.89$, Turi (1986) - for 15°Celsius, the fractionation factor is ~ 9 per mil$_{PDB}$.

- Dissolution of CO_2 gas respired from the vadose zone, with the observed range from -18.36 to -20.5 per mil$_{PDB}$, may be expected to yield the *per descensum* pedogenic fluids with the $\delta^{13}C$ ratios ranging from **-9.36 to -11.5 per mil$_{PDB}$**.

Isotopic character of carbon dissolved in the *per descensum* pedogenic fluids, interpreted based on the observed $\delta^{13}C$ ratios from samples of the Nevada Test Site vadose zone gases.

Figure 4.1.17

- A mean value for the $\delta^{13}C$ ratio from samples of shallow alluvium - based fluids, as observed around Amargosa Narrows, is $\delta^{13}C$ = **-11.3 per mil$_{PDB}$** (range of the observed values is **from -9.59 to -13.05 per mil$_{PDB}$**), White and Chuma (1987).

- A value of the $\delta^{13}C$ ratio from samples of shallow tuff "pile" - based fluids, as observed in the Yucca Mountain borehole UE-29 a#2 (depth to the water table is 29m, and PMC ranges from 60 to 62.3 percent), is $\delta^{13}C$ = **-13.0 per mil$_{PDB}$**, Benson and McKinley, 1985.

- A value of the $\delta^{13}C$ ratio for the Nevada Test Site soil water, as interpreted based on laboratory soil-leaching experiments, is $\delta^{13}C$ = **-12.0 per mil$_{PDB}$** (the observed range for leached water is from **-9.6 to - 16.4 per mil$_{PDB}$**), Spencer (1990).

Isotopic character of carbon dissolved in the *per descensum* pedogenic fluids, based on direct measurements and on soil-leaching experiments.

Figure 4-1.18

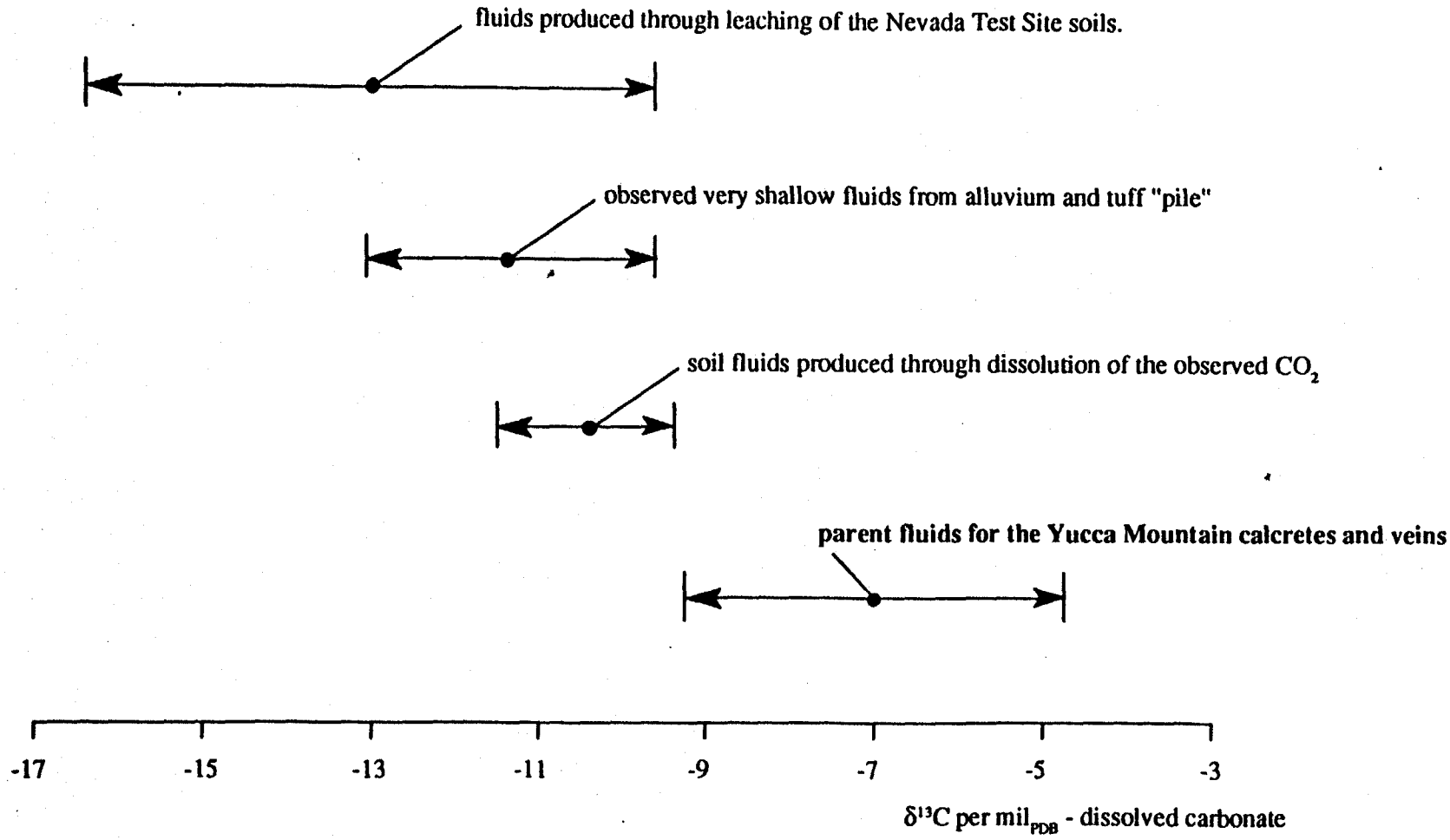

Summary - comparison of carbon isotopic compositions, the *per descensum* pedogenic fluids and the parent fluids for the Yucca Mountain calcretes and surficial veins.

The $\delta^{13}C$ range from -4.75 to -9.45 per mil_{PDB}, interpreted for the parent fluids of the Yucca Mountain calcretes and surficial veins, is too "heavy" to permit genetic association with the local *per descensum* pedogenic fluids alone.

Conclusion - evaluations of the carbon isotopic compatibility.

Overall Conclusions

- Summing up the conclusions from Figures 4-1.14 and 4-1.20, the *per descensum* interpretations of the origin of the Yucca Mountain calcite-opaline silica deposits, as proosed by Quade and Cerling (1990), lack scientific basis.

Conclusion - Part I.

Figure 4-1.21

Part II - Direct field evidence for the *per ascensum* origin of the Yucca Mountain calcretes and surficial veins.

Part II - title page.

Figure 4-2.1

With reference to the third main objection, I would like to make two statements. On the one hand, it seems to me that by suggesting "he arrived at his conclusion *a priori*," you are unfair and inadvertently, I am sure, misleading a reader. As far as the *a priori* conclusions are concerned, the January 18 letter contains the unmistakenly clear language. Figure 44 from this letter expresses my utmostly sincere viewpoint that: **"To an experienced field geologist, the *per ascensum* origin at the Yucca Mountain calcite-silica deposits, based on common sense considerations of abundant field evidence alone, is obvious. The gamut of isotopic data only confirms the *a priori* known, and reasonably secure, conclusion."** I am certain you are aware that both the carbon–13 and the oxygen–18 considerations, whether pertaining to a parent fluid or a therefrom precipitated mineral compound, fall into a category of "plausibility arguments." Such considerations seldom, if ever, yield uniquely constrained interpretations. For example, by intermixing a little of the biogenically derived CO_2 [for a start, produced by an adjustable mixture of plants with both the C–3 metabolic pathways and the C–4 (CAM) metabolic pathways] with a little of the atmospheric CO_2 and employing various "desert ecosystem" and "soil diffusional" carbon–13 enrichment corrections, one may duplicate the carbon isotopic compositions of all of the CO_2 genetic species, that are known to exist in the terrestrial environment. Similarily, it is possible to explain, or duplicate, the oxygen–18 content of parent fluids, as interpreted for a particular accumulation of calcium carbonate, in a number of widely differing ways. This is so because an interpreter is commonly free to employ various combinations of assumptions that pertain to: i) the oxygen–18 content for the pristine parent fluids; ii) the conditions of subsequent isotopic alterations of these fluids; and iii) the conditions of precipitated compound–parent fluid isotopic fractionations. Considering the substantial uncertainties that may be associated with these assumptions and their combinations, it is neither surprising nor inappropriate for experienced field geologists, while attempting to resolve the origin dilemma for the Yucca Mountain opals and calcites, to rely primarily on the direct and quite informative field observations. This prudent preference, however, does not entitle you to declare that Szymanski has "arrived at this conclusion *a priori*." Please be advised that, favoring common sense considerations and well established principles, Szymanski has concluded *a priori*, but only to reject *a priori* the isotopic illusions and obscurations.

On the other hand, however, two statements contained in the March 6 letter [specifically: i) "no field observations are presented, only a testimonial;" and ii) "what are these common sense considerations?"] seem to be encouraging me to take a sufficient time and to share with you the direct field observations that justify my viewpoints regarding the obviously *per ascensum* origin of the Yucca Mountain calcite–silica deposits. Perhaps, to get familiar with the direct and abundant field evidence, it would be most appropriate for you to visit the Yucca Mountain area and examine it first hand. Whenever your schedule permits, I stand ready to escort you and further discuss this important topic. In the meantime, however, let me share with you seven fairly simple, yet reliable, lines of the direct field evidence.

First, around Yucca Mountain, the observable rates of the *sense stricto per descensum* accumulations, for both calcium carbonate and opaline silica, are vanishingly small, or nearly so. Such a state of affairs is indicated by the directly observable absence of: i) a discernible calcite–opaline silica accumulation at the surface of the Lathrop Wells cinder core; and ii) a discernible calcite–opaline silica cement bounding grains that comprise of thin stringers of basaltic ash occurring, for example, in the interior of the Trench #14 vein. The most conservative age estimate, for both the cinder core and the basaltic ash stringers, is ~ 10^4 years B.P. The vanishingly small rates for the hypothetical *per descensum* accumulations, as deduced here for the Yucca Mountain area, are in accord with viewpoints expressed by a number of the *per descensum* advocates. Machette (1985), for example, has stated that: "Carbonate accumulations rates in the Roswell–Carlsbad area of southeastern New Mexico, over the past 500,000 years, exceed 0.5g/cm^2/1000 years and are the highest in the Southwest. At the other extreme, calcic soils in the Beaver, Utah, area have accumulated carbonate at rates of about 0.14g/cm^2/1000 years; this rate is 25 to 75 percent of equivalent–age soils in New Mexico."

The *per ascensum* vs *per descensum* dialogue with Quade and Cerling.

Second, the Yucca Mountain fault infilings, up to a few inches wide, typically exhibit M–textures in a sense that they consist of pure mineral phases, conspicuously lacking internal impunities such as detrital clays, silts, sands, pebbles, and small boulders. One is hard pressed to imagine either open or progressively opening bedrock fissure which, while being filled up with the vanishingly small rates by the *per descensum* deposits, remains isolated from either the overlying soil cover or the detritus that is being transported at the topographic surface by wind action and runoff, including occassional flash floods. To account for the observed M–textures, it is necessary to assume the presence of a non–delinquent "cleaning agent" that removes the ever supplied wind– and water–borne detritus. In sharp contract to the descending fluids, the upwardly flowing *per ascensum* fluids would satisfactorily fulfill this necessary role.

Third, the Yucca Mountain calcite deposits occur in the form of vertical veins emplaced through bodies of fairly loose eolian sand. Such veins may be observed in the interior of sand ramps developed on both the west and east sides of Busted Butte. You may agree that even a stout, but reasonably inquisitive, proponent of the *per descensum* origin for these veins is immediately stuck on two unanswerable questions, namely: i) how to form a vertical fissure a few inches wide in a fairly loose sand, and ii) how to keep such a fissure open during a time span that is required for the slowly accumulating *per descensum* infiling? When dealing with both of these questions, however, the *per ascensum* advocate is blessed with the decisive advantage. In the context of his preferences, the questions become pale in comparison. He will point out that a mineralized fluid contained in the ejected slug, from the underlying bedrock fault, seeps through walls of the propagating vertical fissure. The associated drop in the CO_2 partial pressure creates an opportunity for the dissolved calcium carbonate to come out of the ejected solution. Walls of the propagating fissure become stronger and, under the supporting influence of the fluid pressure, may remain open and accommodate the *per ascensum* calcium carbonate infiling.

Fourth, the Yucca Mountain calcretes occur in the form of four textural varieties. These are: i) the GS–textured calcretes – the allogenic clasts are in direct contact and the authigenic cement occurs in undilated pore space; ii) the F–textured calcretes – the allogenic clasts "float" in the authigenic cement; iii) the M–textured calcretes – the authigenic cement constitutes more than 90 percent of a specimen total volume; and iv) the laminated M– and GS–textured calcretes – laminae of fine cemented, but grain supported, sand separate individual laminae of the detritus–free authigenic cement. To account for the observed textural diversity, the *per descensum* advocates must rely on a dubious concept that the enlargement of pore space may be caused by the authigenic cement crystallization pressures. If such advocate is reasonably inquisitive, however, soon he will become confronted with two unanswerable questions, namely: i) why the calcretes of clearly comparable ages exhibit the observed textural diversity? – presumably the authigenic cement crystallization pressures exert their dilatory influence indiscriminately; and ii) why the M–textured calcretes are laminated with the GS–calcretes? – presumably the authigenic cement crystallization pressures act in all direction but not selectively normal to the topographic surface. When dealing with both of these questions, the *per ascensum* advocate is again blessed with the decisive advantage. Such advocate will immediately point out that: i) the authigenic cement formation rates, for a number of reasons, vary in a spatio–temporal sense; ii) the authigenic cement precipitates both directly at the topographic surface and below the topographic surface – the ejected *per ascensum* fluids may flow either on the topographic surface or through pre–existing alluvial, colluvial, or eolian deposits; and iii) the authigenic cement formation occurs in association with ubiquitous introduction of the allogenic clasts, be it by wind action, runoff, or flash floods. Clearly, the spatio–temporally varying rates for both the authigenic cement precipitation and the allogenic clasts introduction are recorded through the textural diversity, as observed for the Yucca Mountain calcretes. A fast, and the topographic surface direct, precipitation yields both the M–textured calcretes and the laminated M– and GS–textured calcretes. A slower, but still the topographic surface direct, precipitation lends to formation of the F–textured calcretes. Here, the authigenic cement precipitation rates are comparable to the allogenic

The *per ascensum* vs *per descensum* dialogue with Quade and Cerling.

Figure 4-2.2b

clast introduction rates. Finally, the GS–textured calcretes are produced when the ejected *per ascensum* fluids flow through the pre–existing accumulations of various detritus.

Fifth, typically the Yucca Mountain surficial infilings of the fault related fissures exhibit nearly vertically banded textures. As it may be observed in Trenches #8 and #14, for example, these infilings consist of veins which, in turn, are composed of bands of calcium carbonate alternating with bands of opal–CT. You may agree that the observed mineral phase alternations may be taken as indicating that, either the parent fluids chemistry or the mineral phases precipitation conditions were alternating between those favoring precipitation of opals–CT and those favoring precipitation of micritic calcites. Alternatively, it may also be assumed that the opal–CT bands represent the epigenetic replacement of the earlier micritic calcites. In any event, one may reasonably conclude that either i) the parent fluids for the Yucca Mountain fault infilings or ii) the conditions of precipitaiton of these infilings were fluctuating either episodically or continuously. Whether episodic or continuous, the fluctuation involving both of the above factors are not the expected characteristics of the *per descensum* pedogenic processes. Here again, therefore, the *per descensum* proponents are confronted with the unanswerable question. For the *per ascensum* advocate, however, finding the answer to this question presents little challenge. Immediately he will point out that both the fluctuating chemical composition of the parent fluids and the fluctuating conditions of the mineral phases precipitation are typical feastures of most geothermal systems. During certain periods of activity of such systems, for example, the parent fluids carry high values of CO_2 partial pressure. The calcite precipitation is favored because of the rapid CO_2 escape from the parent solution. During some other periods of activity, however, the parent fluids may carry low values of the CO_2 partial pressure and in this case, progressive cooling of the parent fluids dominates the mineral phases formation process. The opal precipitation may be favored because of the SiO_2 prograde solubility with temperature.

Sixth, at Yucca Mountain, the calcite–silica deposits are known to occur throughout the entire thickness of the local vadose zone; they also occur below the local water table. As it may be observed in rock cores extracted from the Yucca Mountain bedrock, the subsurface veins are both texturally and compositionally similar to the local surficial fault infilings. Both of the calcite–silica deposits yield comparable uranium–thorium ages and, as was pointed out in the January 18 letter, carry comparable concentrations of oxygen–18 and carbon–13. There is no rational reason, therfore, to even suspect that the subsurface veins may have been produced via depositional processes that are distinct from those involved in the precipitation of the surficial fault infilings and veins. To account for the clearly evident affinity, the *per descensum* proponents are forced to carry the "pedogenic" actions well below the soil horizons, and even below the water table. For the *per ascensum* advocate, however, to describe this proposition as ridiculous is to elevate its status by undue flattery.

Seventh, some of the Yucca Mountain calcretes and opals occur in the form of the hydro–clastic breccia dike cements and of the hydraulic fracturing residua. Both of these forms may be directly observed on the eastern flank of the so–called Harper Valley, situated just west of Busted Butte. After examining the attached Figures 4-2.3 and 4-2.4, you may agree that the referenced features indeed represent the *per ascensum* injections veins and dikes. To sum up my response to the third main objection, it seems appropriate to cite words once employed by Dr. T. R. Harper to describe his impressions after a rather extensive geological reconnaissance of the Yucca Mountain area. "It shouts at you, it screams at you – this was produced by a forceful injection of fluids."

The *per ascensum* vs *per descensum* dialogue with Quade and Cerling.

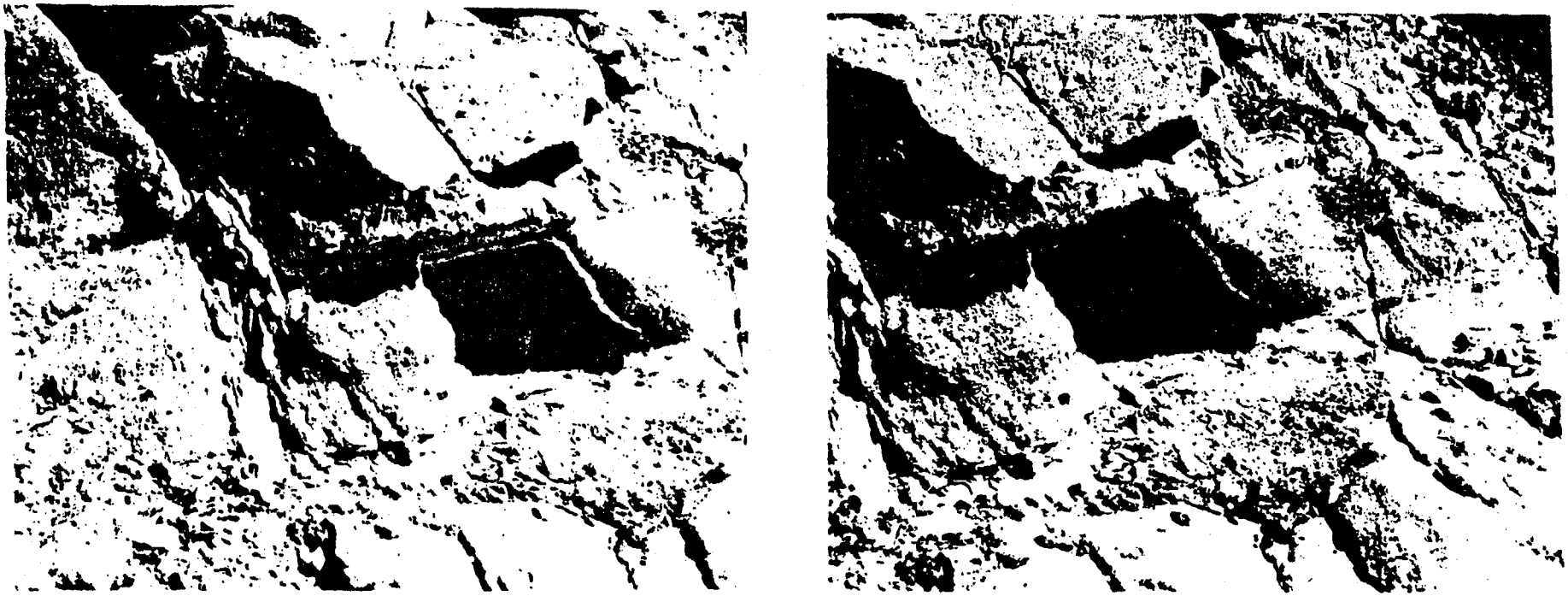

Note:

a) the host rock for the hydraulic fracture calcite residuum is the bedded tuff from the "caprock zone" of the Topopah Spring Member;

b) presence of both the locally very intense oxidation and the jasperoidal opals indicates that the observed bedded tuff alteration is caused by hydrothermal solutions; and

c) two different views of the same calcite residuum are shown.

Hydraulic fracture calcite residuum - eastern flank of the Harper Valley, southern part of the Yucca Mountain area.

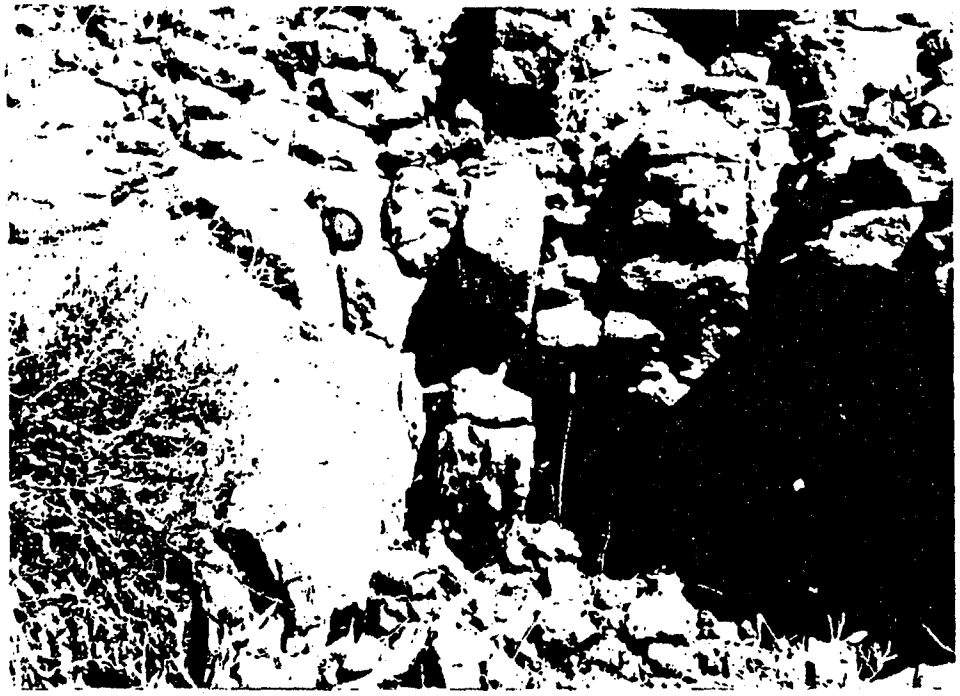

a) opaline silica cement.

b) mixed calcite-opaline silica cement.

Note:

a) the host rock for the injection breccia dikes is the "columnar zone" of the Tiva Canyon Member; and

b) the breccia dikes contain clasts lithologically similar to the underlying Topopah Spring Member.

Hydro-clastic injection breccia dikes - eastern flank of the Harper Valley, southern part of the Yucca Mountain area.

Overall Conclusions

- The directly observable field evidence indicates that the Yucca Mountain calcite-opaline silica were precipitated in fluids discharging from the local bedrock.

- The assumption of the *per descensum* origin, for these deposits, leads to a multiple conflict with the direct field observations.

Conclusions - Part II.

Figure 4-2.5

Part III - Isotopic and geochemical evidence for the *per ascensum* origin of the Yucca Mountain calcretes and surficial veins.

Part III - title page.

Figure 4-3.1

- As far as the origin of the Yucca Mountain calcretes and veins is concerned, the already available isotopic and geochemical data clearly indicate that the *per ascensum* origin of these deposits is secure beyond a reasonable doubt.

- Seven independent lines of evidence may be put forth in support of this conclusion, these are:

  i) the interpreted U-content vs $^{234}U/^{238}U$ activity ratio field, for the parent fluids of the Nevada Test Site calcretes and subsurface veins, overlaps with the corresponding field from the local geothermal fluids;

  ii) the observed values of the $^{87}Sr/^{86}Sr$ ratio, from samples of the Yucca Mountain calcretes and surficial veins, are identical to those from samples of the local geothermal fluids;

  iii) the observed values of the $\delta^{13}C$ ratio, from samples of the Yucca Mountain calcretes and surficial veins, are identical to those from samples of: a) worldwide groundwater calcretes; b) some of the worldwide travertines; c) carbonate gangue minerals from hydrothermal ore deposits; d) the Yucca Mountain subsurface veins, occurring down to a depth of at least 700m; and e) the *per ascensum* deposits, expected to be produced from the local geothermal fluids;

  iv) the observed values of the $\delta^{18}O$ ratio, from samples of the Yucca Mountain calcretes and surficial veins, are identical or comparable to those from samples of: a) some of the worldwide travertines; b) some of carbonate gangue veins from the Carlin and Cortez disseminated gold deposits of Nevada; c) the *per ascensum* deposits from the Ash Meadows Basin; d) the Yucca Mountain subsurface veins, occurring down to a depth of at least 700m; and e) the *per ascensum* deposits, expected to be produced from the local geothermal fluids;

  v) considerations of the observed $\delta^{18}O$ ratios, from samples of the Yucca Mountain calcretes and surficial veins, lead to a conclusion that the precipitation temperatures may have been in a range from 15 to as much as 53°Celsius;

  vi) considerations of the observed $d\delta^{18}O/dz$ (depth) gradient, from samples of the Yucca Mountain calcretes and subsurface veins, lead to a conclusion that during formation of these deposits values of the geothermal gradient (dT/dz) were a factor 1.5 - 2.5 higher than the observed contemporary geothermal gradient; and

  vii) considerations of the observed chemical, REE, and isotopic compositions of samples of the Yucca Mountain interstitial fluids, centrifuged from the vadose zone cores, lead to a conclusion that these fluids are relict geothermal fluids.

The *per ascensum* origin of the Yucca Mountain calcretes and surficial veins - summary of isotopic and geochemical evidence.

Figure 4-3.2

- The interpreted U-series characteristics of the parent fluids for the Nevada Test Site calcite-silica deposits are: a) value of the $^{234}U/^{238}U$ activity ratio ranging from 1.0 to ~ 3.5; and b) value of the U-concentration varying over a range of 1-2 orders of magnitude.

- The interpreted U-content vs. $^{234}U/^{238}U$ field, for the parent fluids of the Nevada Test Site calcite-silica deposits, overlaps with the corresponding field from samples of the local geothermal fluids.

Conclusion:

a) The Nevada Test Site calcite-silica deposits, including: a) calcretes; b) surficial fault-infilings; and c) subsurface veins, were formed via the *per ascensum* process; and

b) In the past, the Nevada Test Site hydrosphere have experienced the "source" ⟷ "sink" transformations.

Isotopic affinity between the parent fluids for the calcite-silica deposits and the local geothermal fluids - the U-content vs. $^{234}U/^{238}U$ field.

Figure 4-3.3

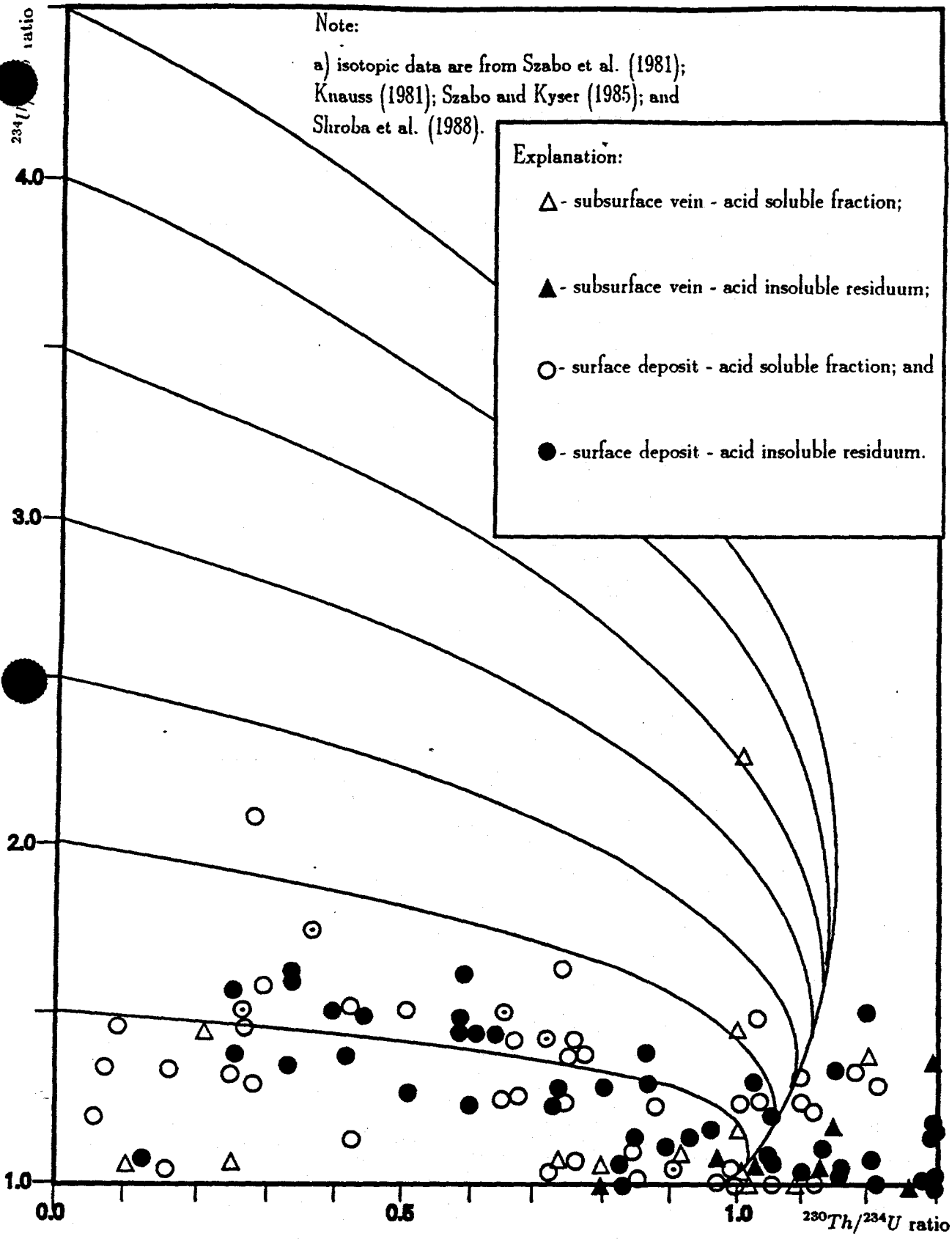

$^{234}U/^{238}U$ and $^{230}Th/^{234}U$ activity ratios. The Nevada Test Site calcite-silica deposits.

Figure 4-3.4

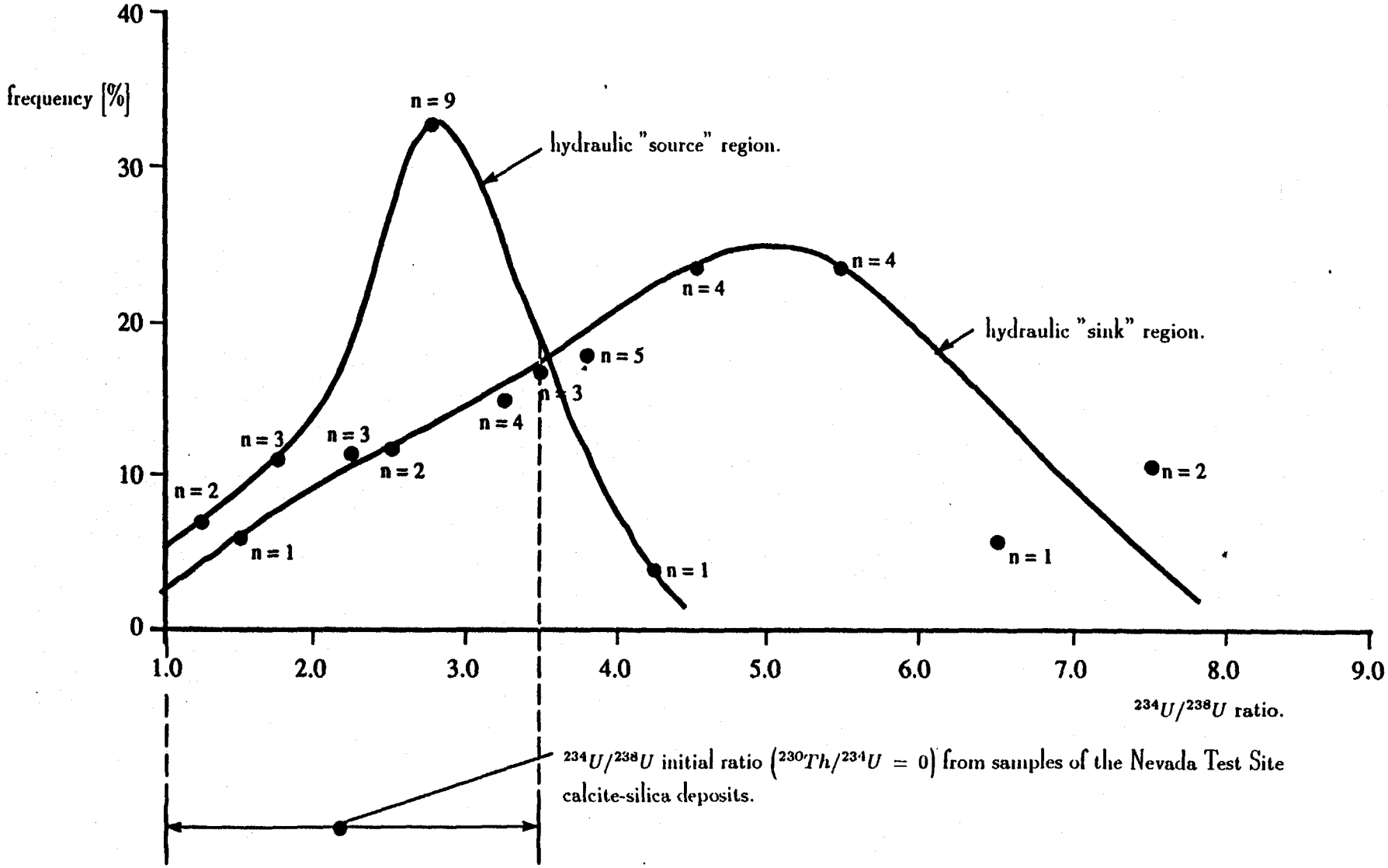

Comparison of the $^{234}U/^{238}U$ activity ratios. The Nevada Test Site calcite-silica deposits and the local geothermal fluids.

Figure 4-3.5

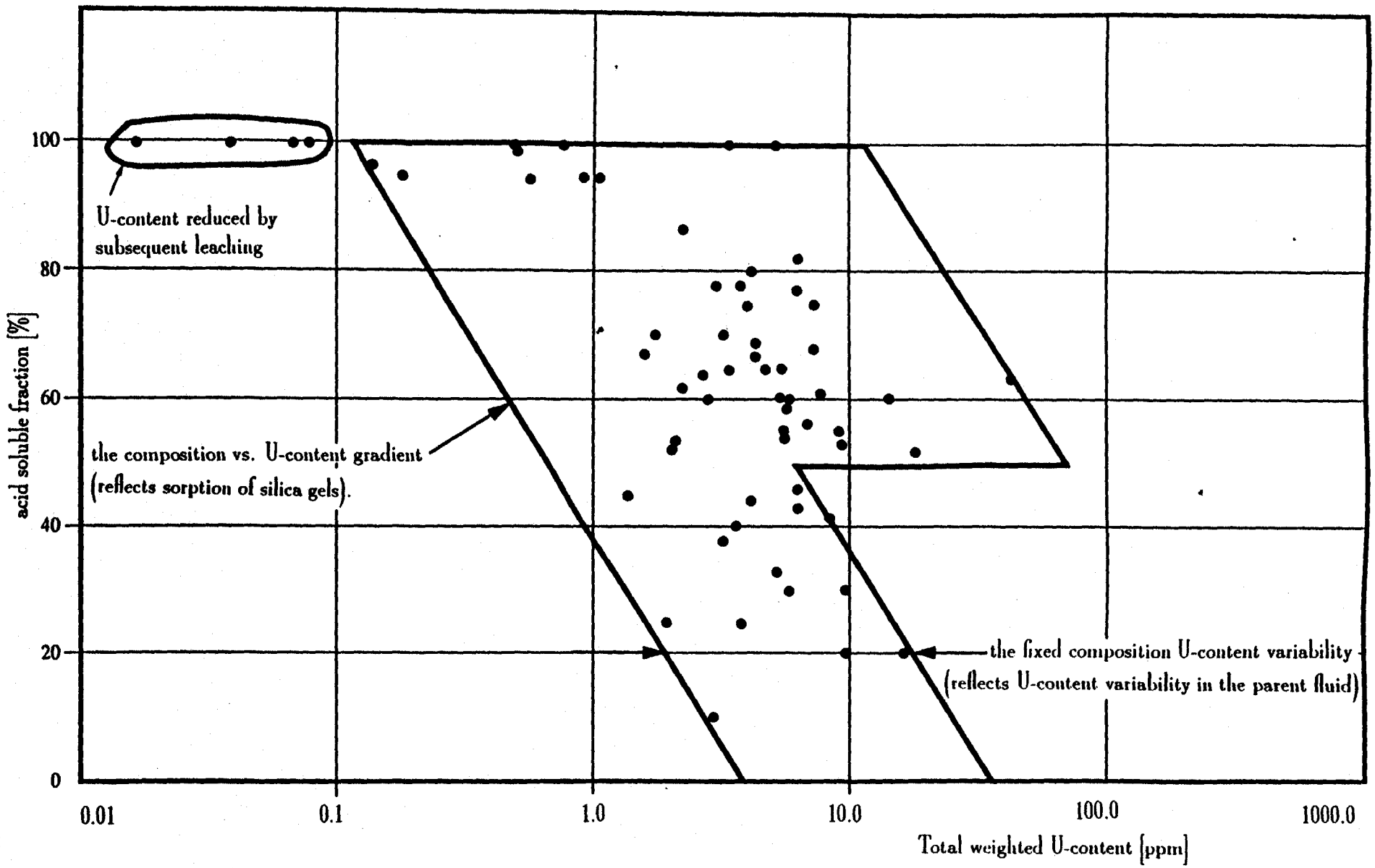

Total U-content vs. percentage of acid-soluble fraction. Calcite-silica deposits from the Nevada Test Site.

Figure 4-3.6

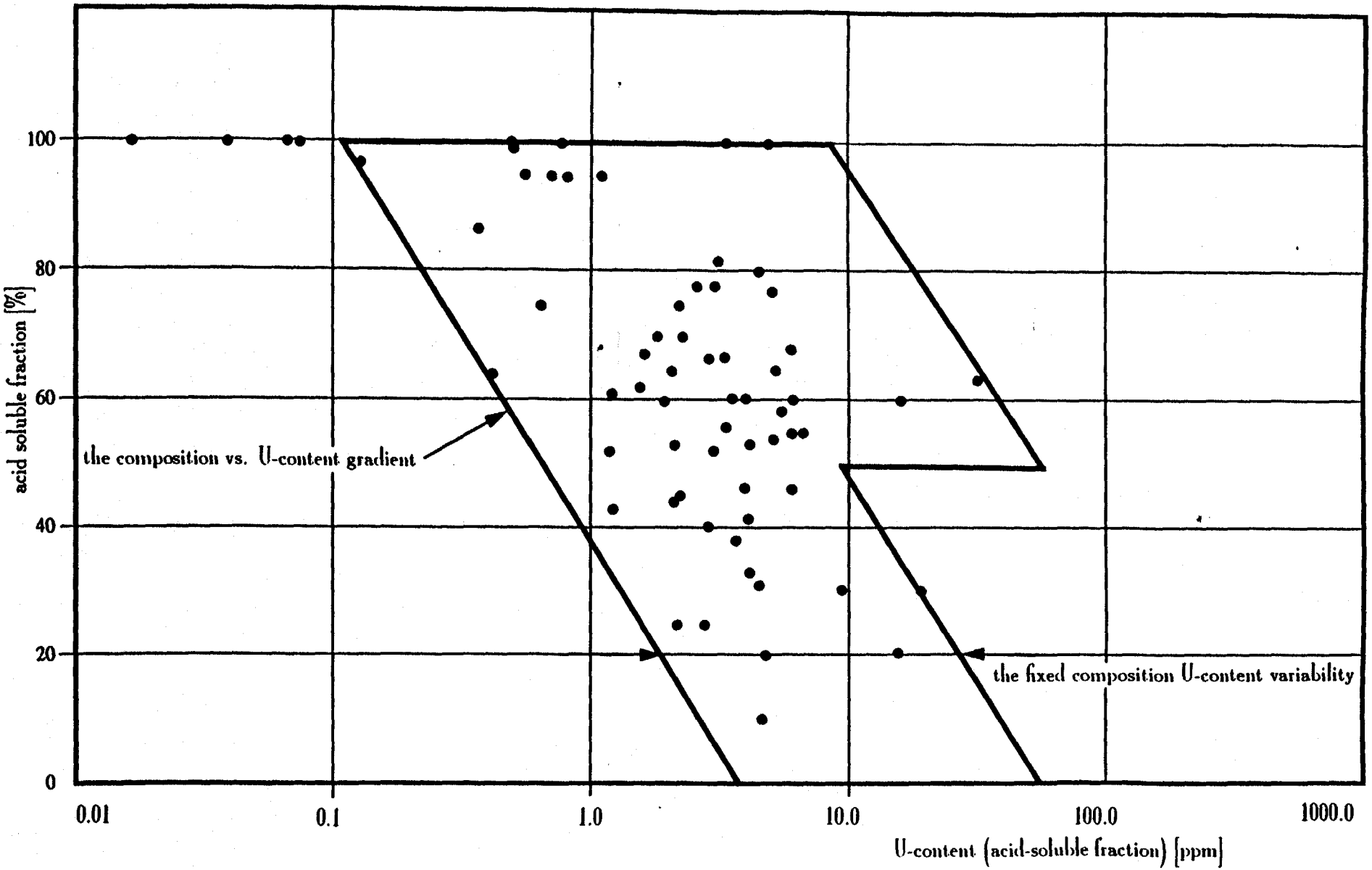

U-content vs. percentage of acid-soluble fraction. Calcite-silica deposits from the Nevada Test Site.

Figure 4-3.7

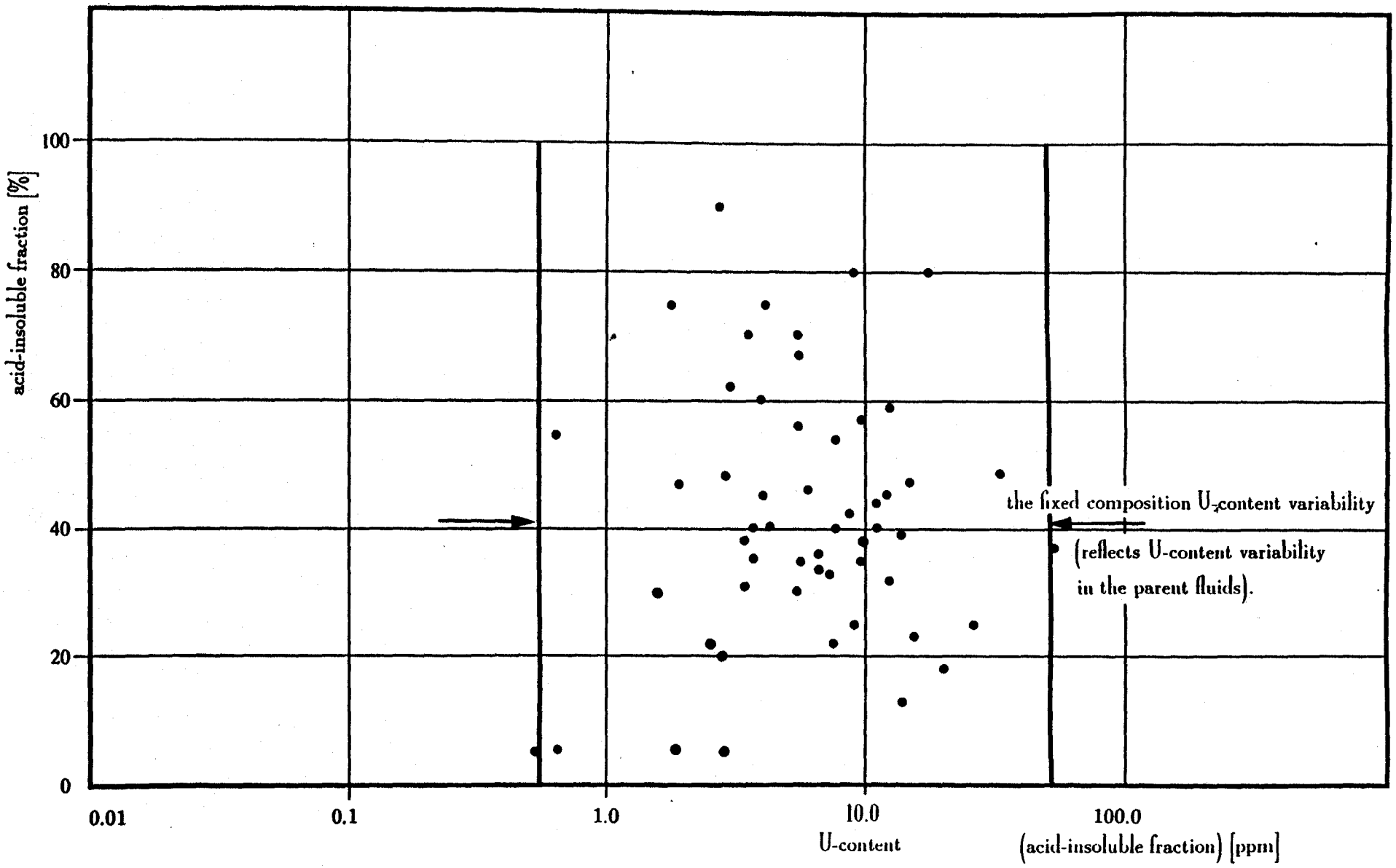

U-content vs. percentage of acid-insoluble fraction. Calcite-silica deposits from the Nevada Test Site.

Figure 4-3.8

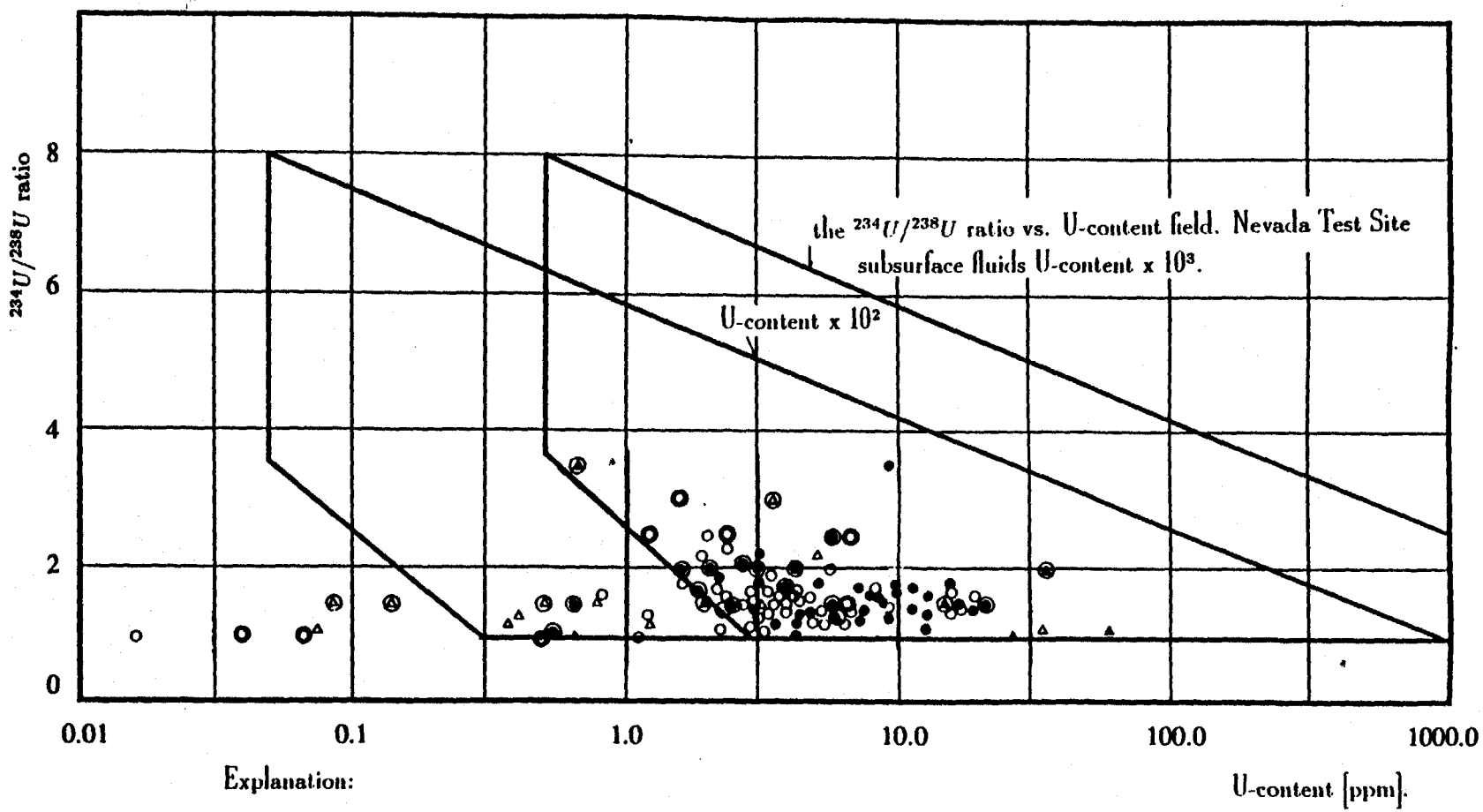

Explanation:

△ - subsurface vein - acid soluble fraction;

▲ - subsurface vein - acid insoluble residuum;

○ - surficial deposit - acid soluble fraction;

● - surficial deposit - acid insoluble residuum;

◎ - $^{234}U/^{238}U$ ratio plotted is a minimum value.

The Nevada Test Site calcite-silica deposits and the Nevada Test Site subsurface fluids.

Figure 4-3.9

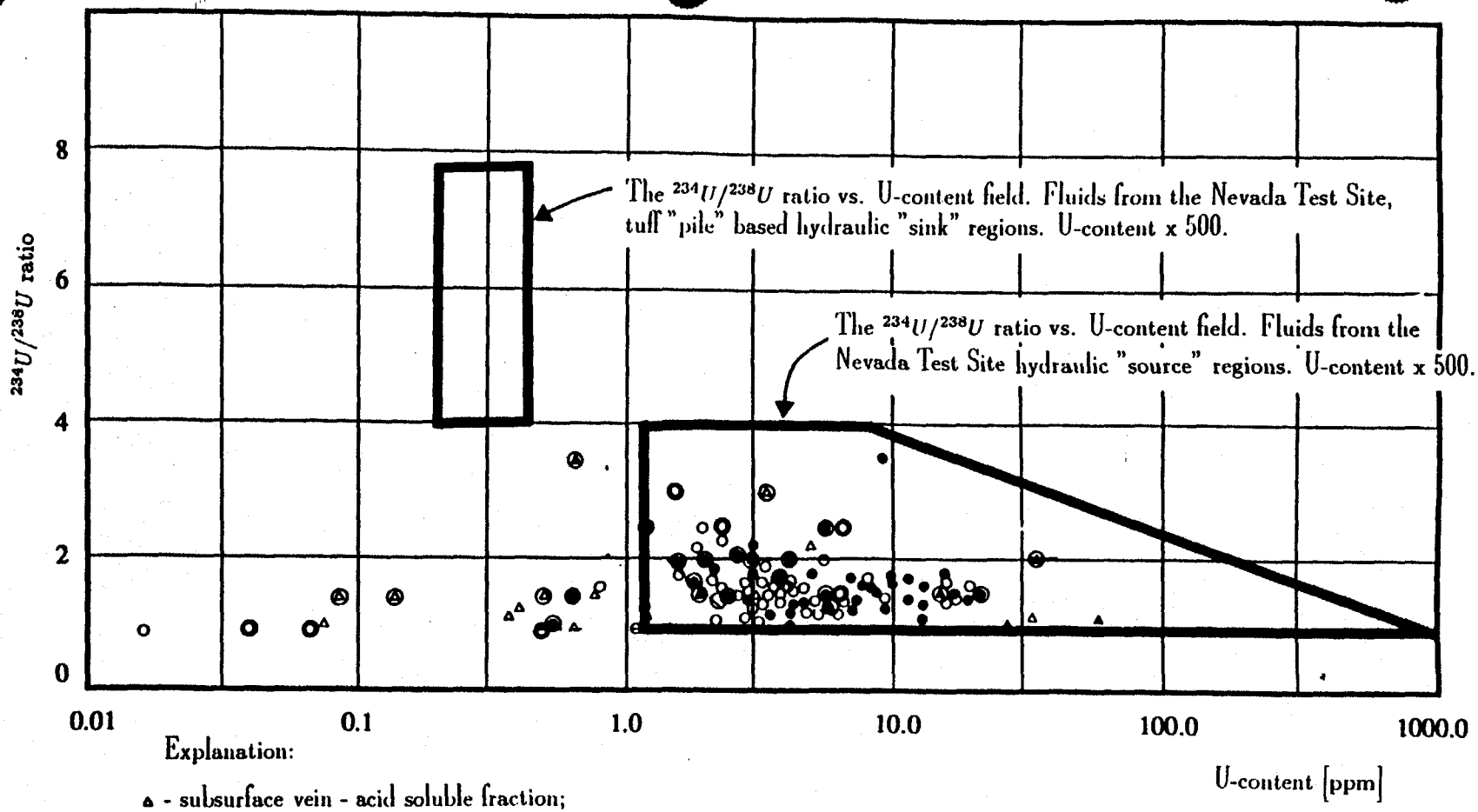

The Nevada Test Site calcite-silica deposits and the Nevada Test Site subsurface fluids.

Figure 4-3.10

- The $^{87}Sr/^{86}Sr$ ratios, from samples of the Yucca Mountain surficial calcite-silica deposits, are similar to those from samples of the Northern and Southern Latium travertines.

- The $^{87}Sr/^{86}Sr$ ratios, from samples of the Yucca Mountain surficial calcite-silica deposits, are similar to those from samples of the local geothermal fluids.

Conclusion:

a) The Yucca Mountain surficial calcite-silica deposits were formed via the per ascensum process; and

b) In the past, the Yucca Mountain hydrosphere have experienced the "source" ⟷ "sink" transformations.

Isotopic affinity between the parent fluids for the calcite-silica deposits and the local geothermal fluids - $^{87}Sr/^{86}Sr$ ratio.

Figure 4-3.11

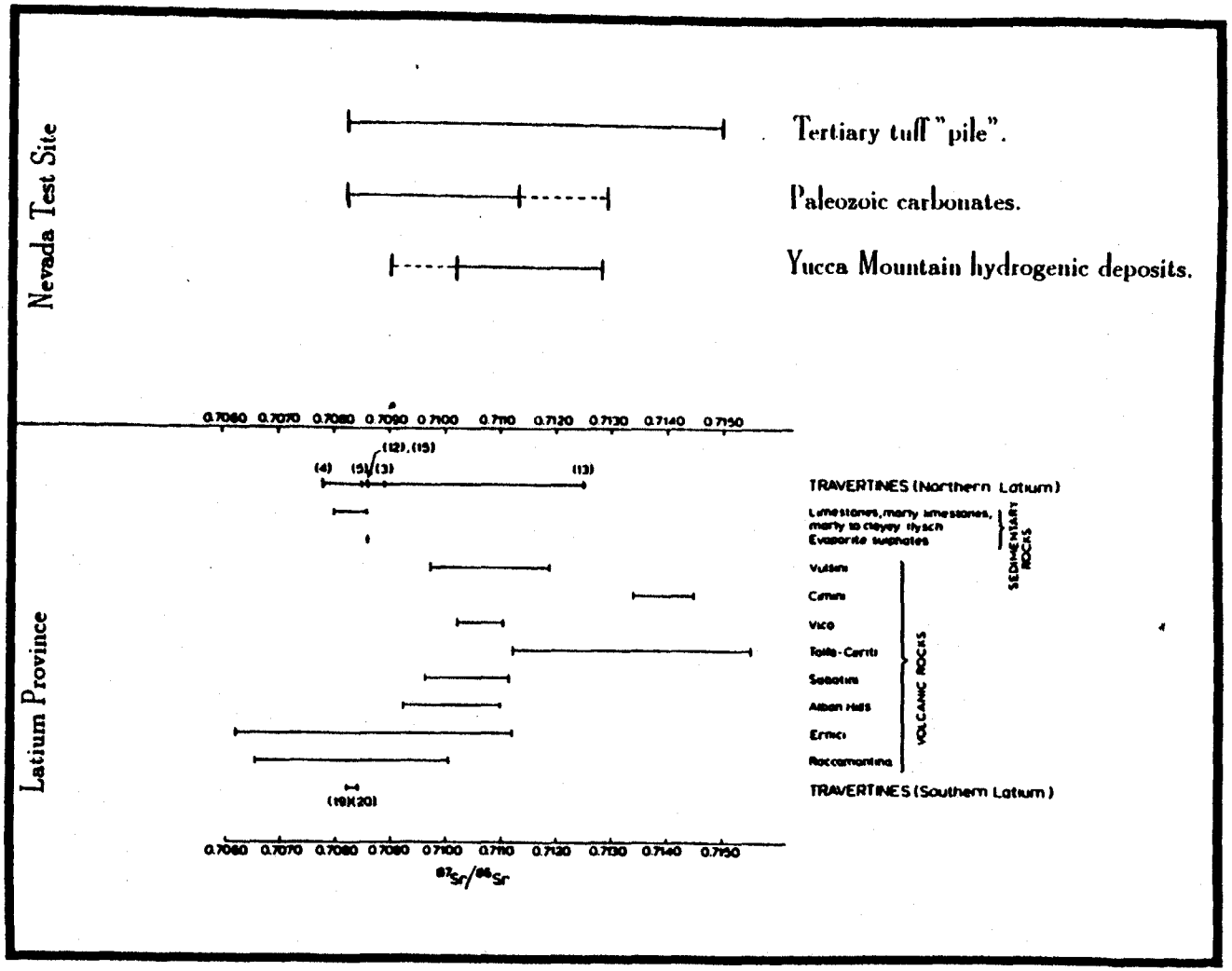

Comparison of the $^{87}Sr/^{86}Sr$ ratios from the Nevada Test Site calcite-silica deposits with those from the Italian Latium Province travertines. Modified from Turi, 1986.

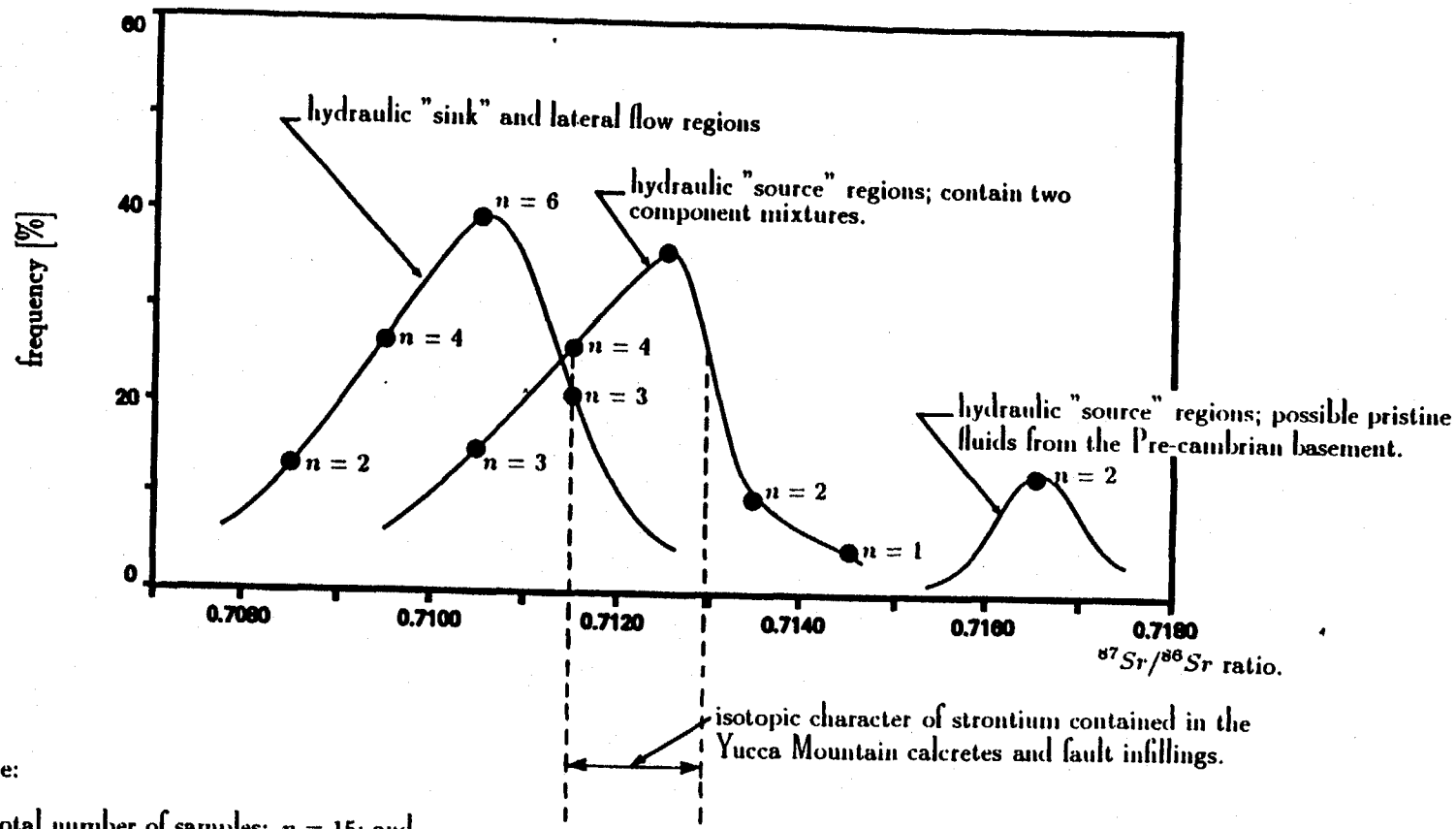

Note:

a) total number of samples: $n = 15$; and

b) isotopic data are from Marshall et al. (1990); Stuckless (1990); Peterman (1990); and Stuckless et al. (1990).

Comparison of the $^{87}Sr/^{86}Sr$ ratios. The Yucca Mountain calcite-silica deposits and the Nevada Test Site subsurface fluids.

Figure 4-3.13

- The values of the $\delta^{13}C$ ratio from samples of the Yucca Mountain surficial calcite-silica deposits are compatible with those: a) from the worldwide groundwater calcretes; b) from some of the worldwide travertines; c) from carbonate gangue veins from gold-bearing hydrothermal ore deposits; d) from the Yucca Mountain subsurface veins (occurring down to a depth of at least ~ 600 m); and e) from the local geothermal fluids.

Conclusion:

a) **The Yucca Mountain calcite-silica deposits, including: a) calcretes; b) surficial fault in-filings; and c) subsurface veins, were formed via the *per ascensum* process; and**

b) **In the past, the Yucca Mountain hydrosphere have experienced the "source" ⟷ "sink" transformations.**

Isotopic affinity between the parent fluids for the calcite-silica deposits and the local geothermal fluids - carbon.

Figure 4-3.14

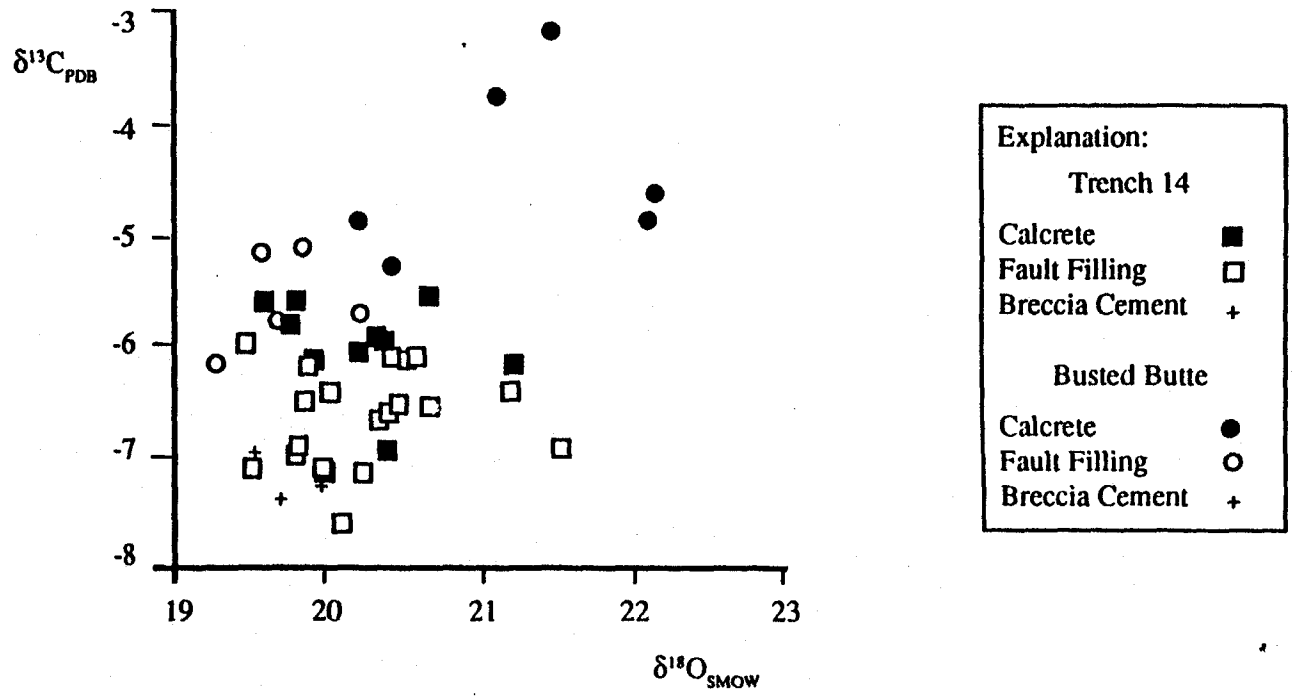

Note:

a) the carbon-oxygen part of the isotopic fingerprint, for the Yucca Mountain surficial calcite-silica deposits, is a range of values for the $\delta^{18}O$ and $\delta^{13}C$ ratios;

b) the observed range for the $\delta^{13}C$ ratio is from -3.0 to -7.5 per mil_{PDB} ; and

c) the observed range for the $\delta^{18}O$ ratio is from 19.2 to 22.0 per mil_{SMOW} .

Carbon-oxygen isotopic fingerprint. The Yucca Mountain surficial calcite-silica deposits. From Whelan and Stuckless, 1990.

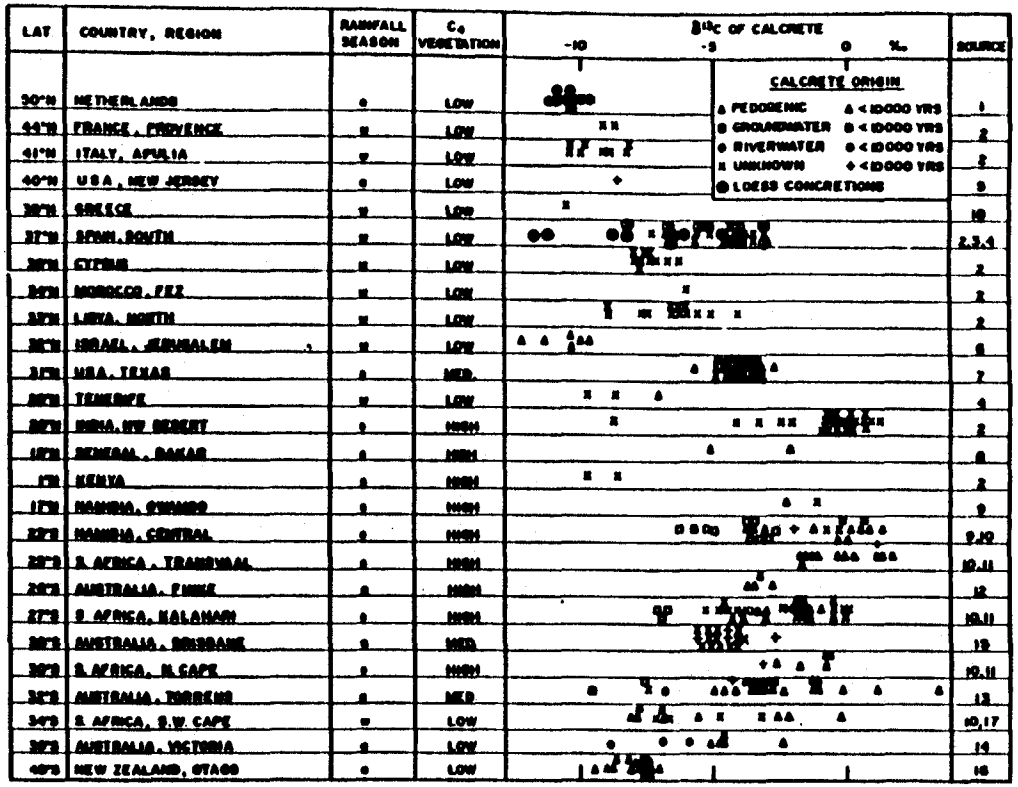

Results of isotopic comparison: the observed Yucca Mountain range, from -3.0 to -7.5 per mil$_{PDB}$, is similar to that observed for some of the worldwide groundwater calcretes.

Carbon isotopic file - isotopic character of carbon contained in groundwater calcretes, worldwide data. From Talma and Netterberg (1983).

Figure 4-3.16

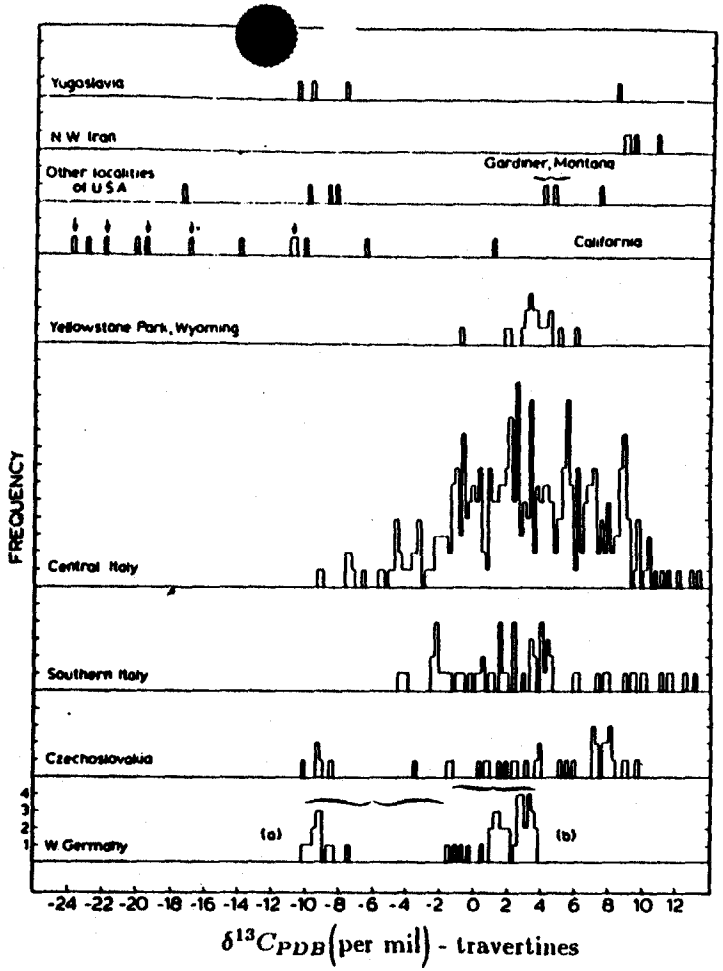

Note:

a) In some regions, carbon contained in travertine deposits is largely derived from dissolution of marine limestones and, therefore, mean values for the $\delta^{13}C$ ratio tend to be positive, say +3.0 per mil $_{PDB}$; and

b) In other regions, however, carbon contained in travertine deposits is isotopically "lighter" than that derived exclusively from marine limestones. A number of factors may be involved, including: i) participation of biogenically produced CO_2 ($\delta^{13}C$ values ranging from −35 to −10 per mil $_{PDB}$); and ii) participation of CO_2 from deep, igneous sources ($\delta^{13}C \sim -7$ per mil $_{PDB}$).

Results of isotopic comparison: the observed Yucca Mountain range, from −3.0 to −7.5 per mil $_{PDB}$, is "lighter" than that from travertines produced as the result of marine limestone dissolution alone.

Carbon isotopic file - isotopic character of carbon contained in travertines, worldwide data. From Turi, 1986.

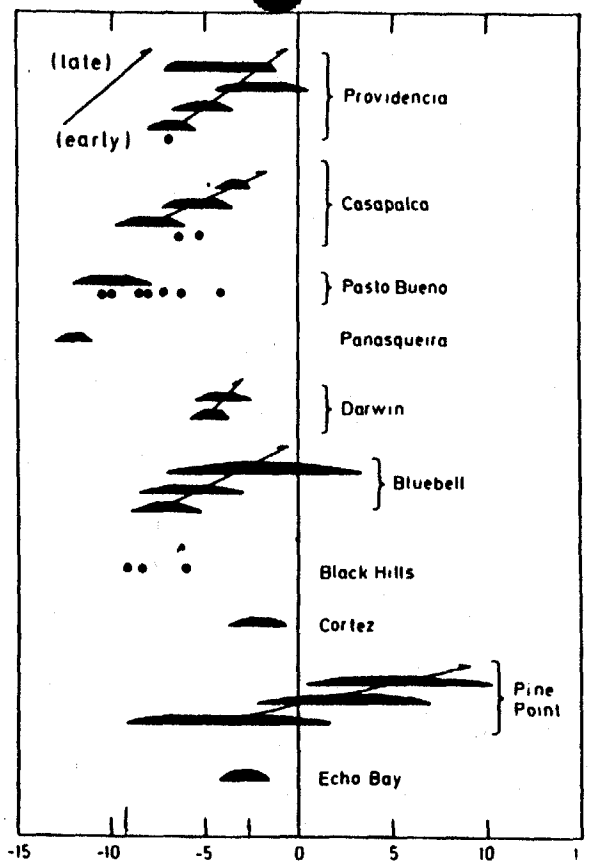

Note: $\delta^{13}C(\text{per mil})_{PDB}$ - carbonate gangue from hydrothermal ore deposits

a) The isotopic character of carbon contained in CO_2 derived from deep-seated, igneous sources is described by a mean value of the $\delta^{13}C$ ratio of about -7 per mil_{PDB}; and

b) Depending upon the reaction temperature ($10^3 \ln\alpha_{HCO^-_3 - CO_{2(g)}} = 9.483 \cdot 10^3 \cdot T^{-1} - 23.89$), dissolution of the igneous CO_2 may yield geothermal fluids with values of the $\delta^{13}C$ ratio ranging from +1 (temp. ~ 20°Celsius) to -14 per mil_{PDB} (temp ~ 300°Celsius).

Results of isotopic comparison: the observed Yucca Mountain range, from -3.0 to -7.5 per mil_{PDB}, is similar to that contained in carbonate gangue minerals from hydrothermal ore deposits.

Carbon isotopic file - isotopic character of carbon contained in carbonate gangue minerals from a number of hydrothermal ore deposits. From Hoefs, 1987.

Figure 4-3.18

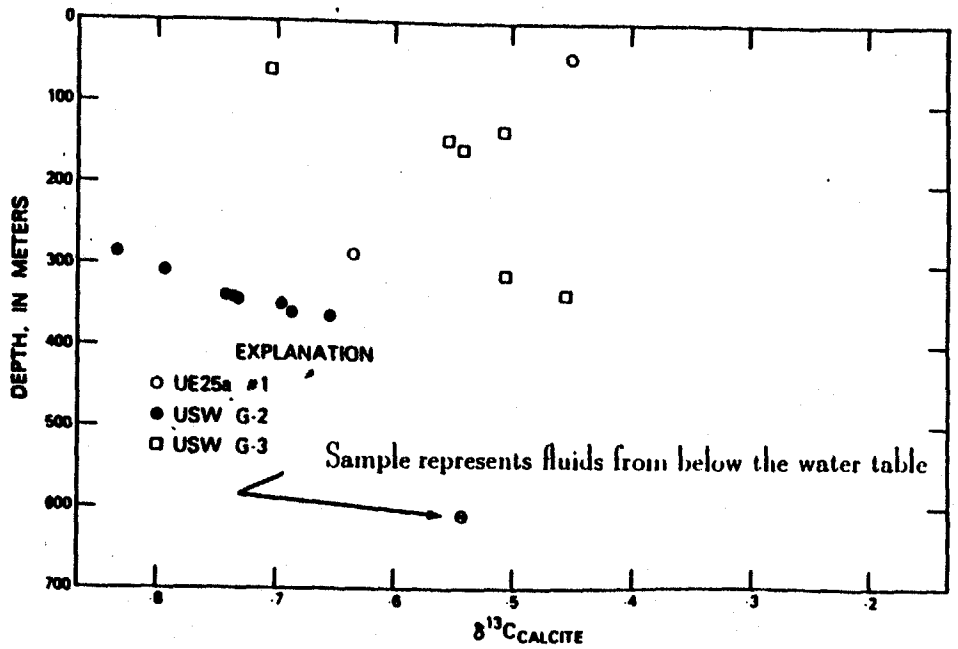

Results of isotopic comparison: the observed Yucca Mountain range (surficial deposits), from −3.0 to −7.5 per mil $_{PDB}$, is similar as that from samples of calcite silica veins from both the vadose zone and below the water table.

Carbon isotopic file - isotopic character of carbon contained in the Yucca Mountain subsurface veins. From Szabo and Kyser, 1990.

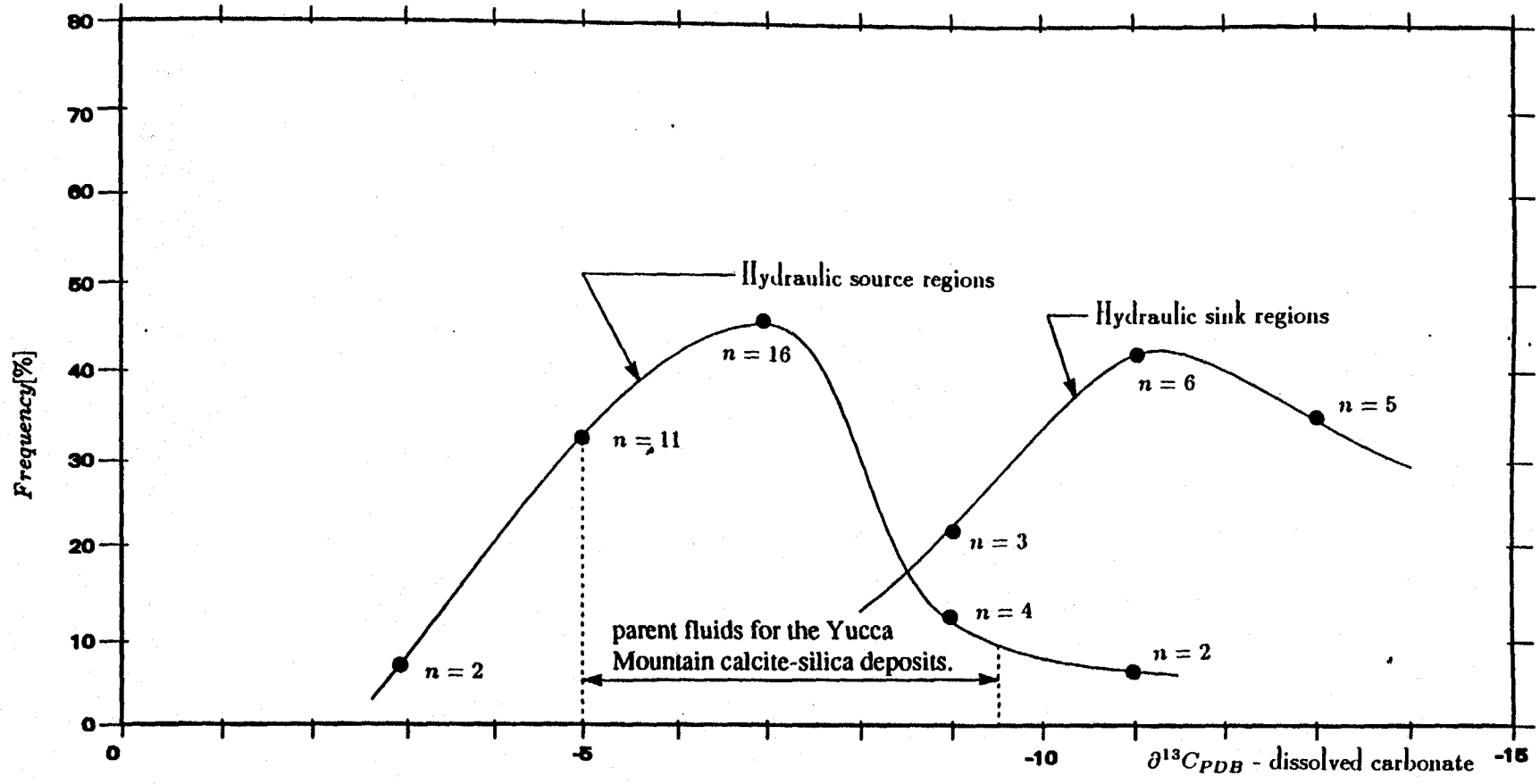

Note: Isotopic data from Claassen, (1985), Benson and McKinley (1985), and White and Chuma (1987).

Results of isotopic comparison: the observed Yucca Mountain range, from -3.0 to -7.5 per mil_{PDB}, is similar to that expected for deposits produced by local geothermal fluids.

Comparison of the $\delta^{13}C$ ratio. The Yucca Mountain calcite-silica deposit and the Nevada Test Site subsurface fluids.

Figure 4-3.20

- Values of the $\delta^{18}O$ ratio from samples of the Yucca Mountain surficial calcite-silica deposits are compatible with those: a) from some of the Carlin and Cortez (Nevada) carbonate gangue veins; b) from some of the worldwide travertines; c) from local *per ascensum* deposits; d) from the Yucca Mountain subsurface veins (occurring down to a depth of at least ~ 600 m); e) from the Yucca Mountain subsurface fluids; and f) from the Nevada Test Site geothermal fluids.

Conclusion:

a) **The Yucca Mountain calcite-silica deposits, including: a) calcretes; b) surficial fault in-filings; and c) subsurface veins, were formed via the *per ascensum* process; and**

b) **In the past, the Yucca Mountain hydrosphere have experienced the "sink" ⟷ "source" transformations.**

Isotopic affinity between the parent fluids for the calcite-silica deposits and the geothermal fluids - oxygen.

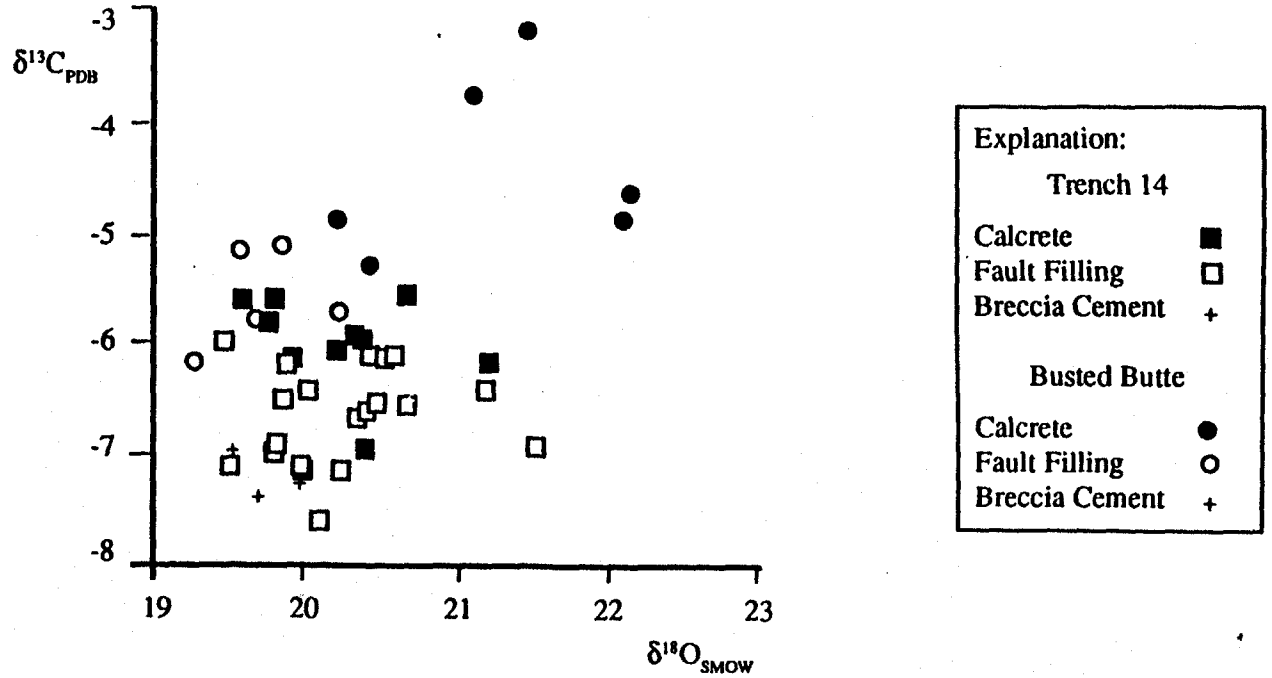

Note:

a) the carbon-oxygen part of the isotopic fingerprint, for the Yucca Mountain surficial calcite-silica deposits, is a range of values for the $\delta^{18}O$ and $\delta^{13}C$ ratios;

b) the observed range for the $\delta^{13}C$ ratio is from -3.0 to -7.5 per mil_{PDB} ; and

c) the observed range for the $\delta^{18}O$ ratio is from 19.2 to 22.0 per mil_{SMOW} .

Carbon-oxygen isotopic fingerprint. The Yucca Mountain surficial calcite-silica deposits. From Whelan and Stuckless, 1990.

Figure 4-3.22

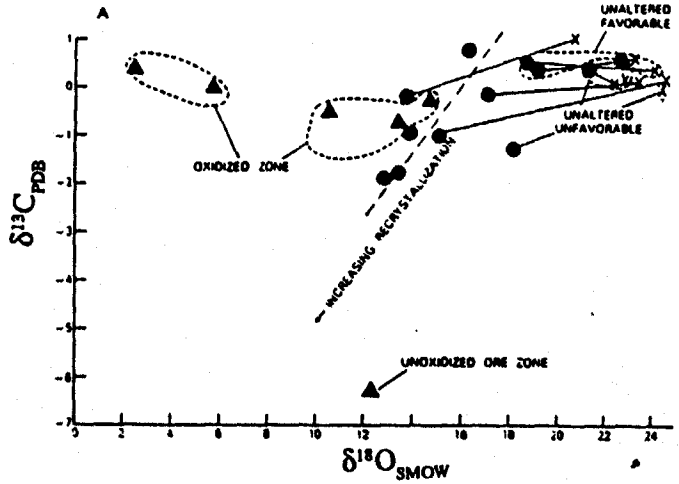

a) the Carlin disseminated gold deposit of Nevada.

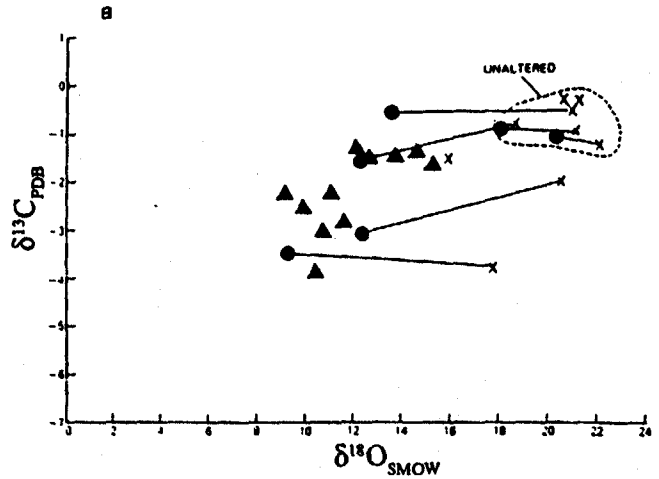

b) the Cortez disseminated gold deposit of Nevada.

Explanation:

▲ - sample represents altered host rock and calcite veins in oxidized and unoxidized zones;

● - sample represents calcite veins;

x - sample represents dolomite; and

tielines connect coexisting calcite and dolomite

Note:

a) calcite veins from the oxidized zone at Carlin, and all the veins at Cortez, have oxygen - isotopic compositions similar to that of the calcite component in the altered host rock;

b) other veins were derived from low-temperature groundwater.

Results of isotopic comparison: the observed Yucca Mountain range, from 19.2 to 22.0 per mil_{SMOW}, is similar to some of the Carlin and Cortez carbonate gangue veins.

Oxygen isotopic file - isotopic character of oxygen contained in carbonate gangue veins from the Carlin and Cortez gold deposits. From Rye, 1985.

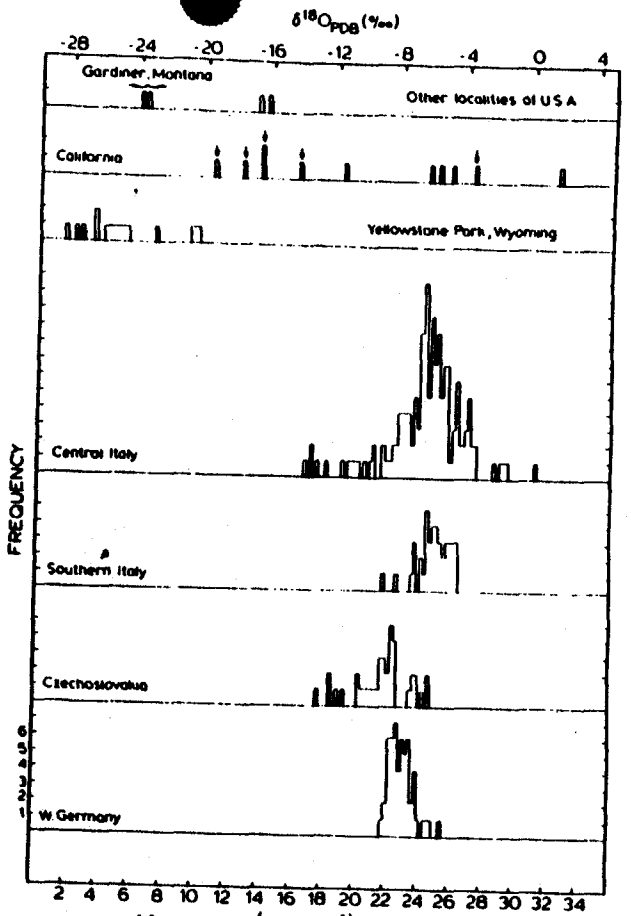

Note:

a) A value of the $\delta^{18}O$ ratio, from a sample of a particular travertine deposit, reflects three main factors, namely: i) oxygen -18 content for the parent fluid; ii) precipitation temperature; and iii) conditions of precipitation and the resulting value of the isotopic fractionation factor; and

b) Various combinations of the controlling factors are possible and, consequently, the worldwide travertine deposits exhibit a very wide range of the $\delta^{18}O$ ratio, from +2 to about +32 per mil $_{SMOW}$.

Results of isotopic comparison: the observed Yucca Mountain range, from 19.2 to 22.0 per mil $_{SMOW}$, is within the corresponding range from the worldwide travertine deposits.

Oxygen isotopic file - isotopic character of oxygen contained in travertines, worldwide data. From Turi, 1986.

Figure 4-3.24

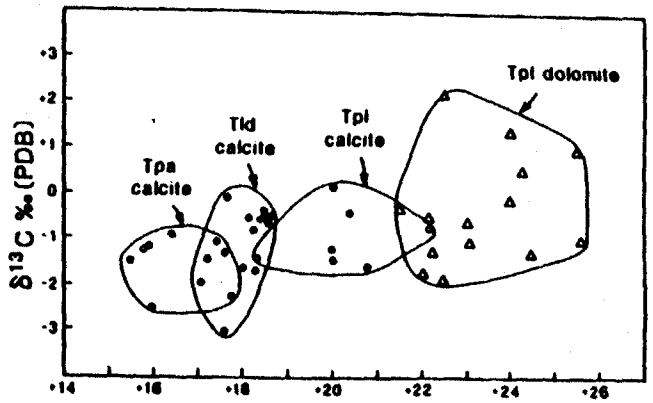

Note:

a) Both the $\delta^{13}C$ vs. lithology gradient and the $\delta^{18}O$ vs. lithology gradient may reasonably be attributed to an increasing residence time, at the topographic surface, of the deposits parent fluids;

b) The increasing residence time for the parent fluid, at the topographic surface, is accompanied by: i) decreasing precipitation temperature; ii) increasing kinetic fractionation effects; and iii) increasing oxygen -18 and carbon -13 evaporative enrichment - each of these factors may account for the observed gradients;

c) Tpa denotes soft - chalky limestone; Tld denotes dense nodular and fenestral limestone; Tpl denotes carbonate rocks and minerals disseminated in claystones;

d) At the Ash Meadows topographic surface, the ambient temperatures are likely to be 5 to 10° Celsius higher than the corresponding temperatures at Yucca Mountain - the resulting differences in the equilibrium fractionation factor range from 1 to 2 per mil $_{SMOW}$, the Yucca Mountain values being larger; and

e) Differences in values of the $\delta^{13}C$ ratio, between the Ash Meadows deposits and the Yucca Mountain surficial deposits, are directly attributable to the corresponding differences in the parent fluids host rocks.

Results of isotopic comparison: the observed Yucca Mountain range, from 19.2 to 22 per mil$_{SMOW}$, if adjusted for the differing equilibrium fractionation factors is compatible with the oxygen -18 content of the Ash Meadows *per ascensum* carbonates.

Oxygen isotopic file - isotopic character of oxygen contained in the *per ascensum* deposits from the Ash Meadows Basin, Nevada. From Hay et al., (1986).

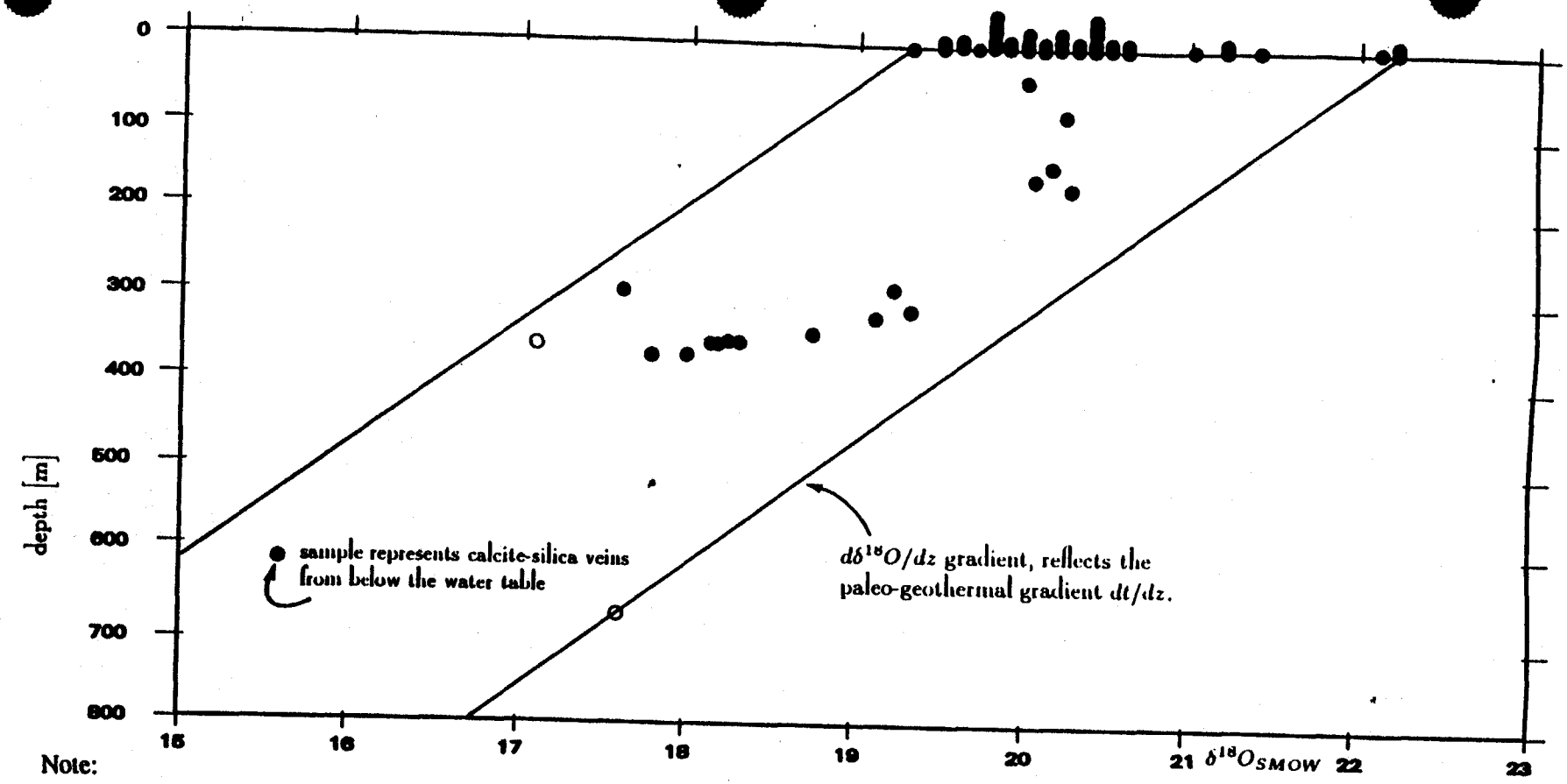

Note:

a) The entire observed Yucca Mountain range of the $\delta^{18}O$ ratios for carbonate deposits, from 15.4 to 22.0 per mil_{SMOW}, is very similar to that observed for the Ash Meadows Basin deposits, Figure 4-3.25; and

b) The above similarities indicate that, the differences in oxygen -18 contents from samples of the respective surficial deposits are caused by the respective differences in either the precipitation temperatures or the isotopic fractionation factor, but not by major differences in the oxygen -18 contents of the respective parent fluids.

Results of isotopic comparison: the observed Yucca Mountain range, from 19.2 to 22 per mil_{SMOW}, if adjusted for the differing percipitation temperatures, is compatible with the observed oxygen -18 content of the Yucca Mountain subsurface veins.

Oxygen isotopic file - isotopic character of oxygen contained in the Yucca Mountain calcite-silica subsurface veins. Data from Szabo and Kyser (1990) and Whelan and Stuckless (1990).

Figure 4-3.26

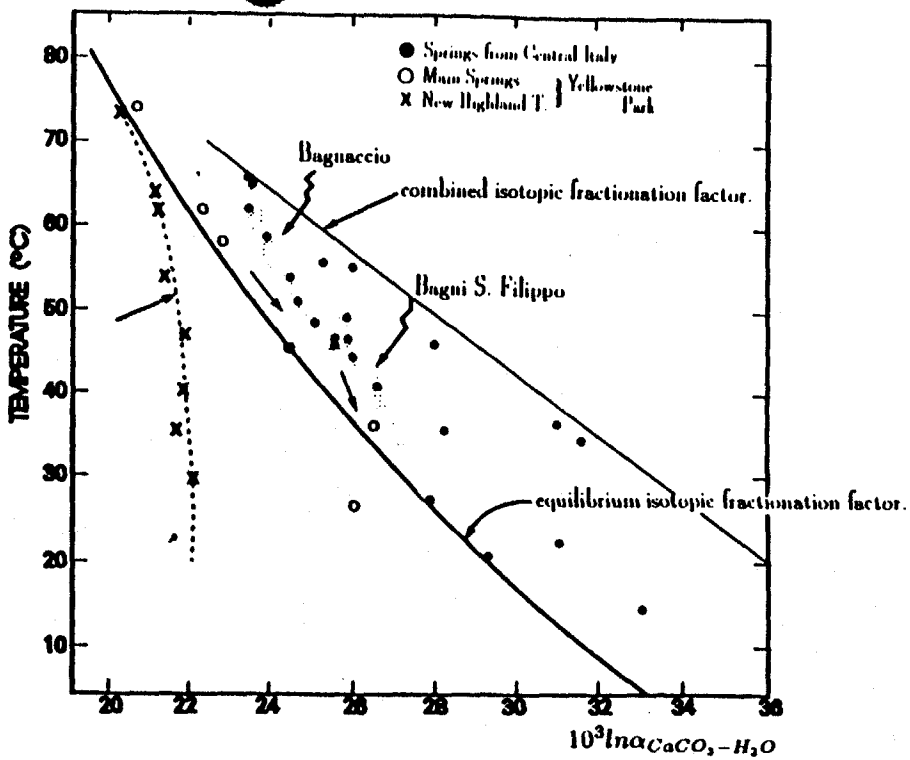

Note:

a) During natural depositions of travertines, the conditions of equilibrium isotopic fractionation are seldom attained, mainly as a consequence of the kinetic or non-equilibrium processes;

b) Depending upon conditions of precipitation, the combined or actual isotopic fractionation factor ($10^3 ln\alpha_{CaCO_3-H_2O}$) may be both larger and smaller than the equilibrium fractionation factor; and

c) At a precipitation temperature of T ~20° Celsius, the combined isotopic fractionation factor may be assumed to range from 22 to 36 per mil *SMOW*.

Oxygen isotopic fractionation data from travertine depositing springs of Central Italy and Yellowstone Park. From Turi, 1986.

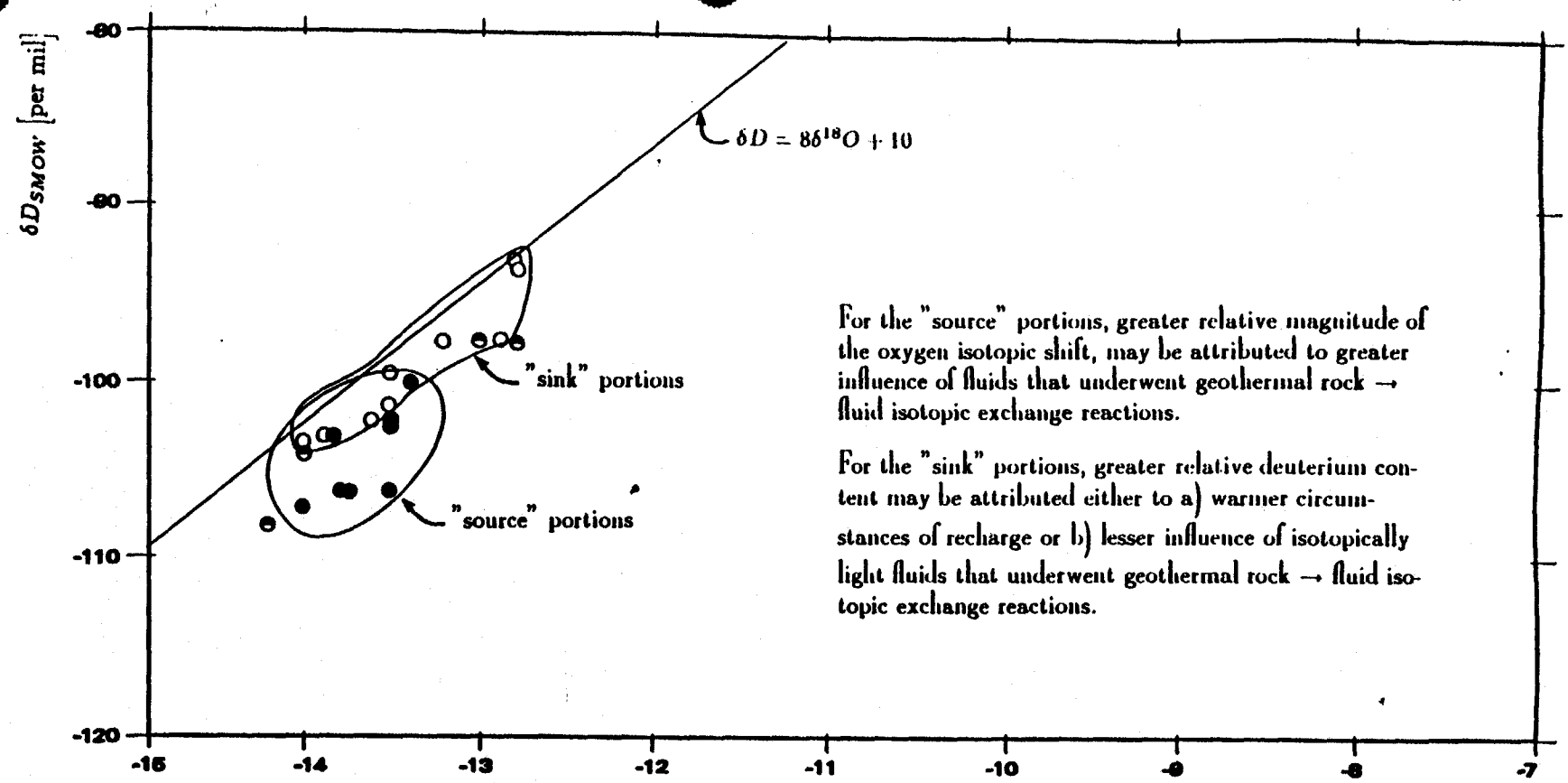

Note:

a) The observed range of values for the $\delta^{18}O$ ratio, from samples of the contemporary Yucca Mountain subsurface fluids, is from −14.2 to −12.7 per mil $_{SMOW}$; samples are bulk water samples pumped out of large segments of exploratory wells - sampling "smoothing" may be involved, and the observed range may be smaller than the actually present one; and

b) If the parent fluids, for the Yucca Mountain surficial deposits, have carried the same oxygen −18 contents then, the combined isotopic fractionation factor was in a range from 31.9 to 35.2 per mil $_{SMOW}$, which is permissible by the empirical fractionation data from Figure 4-3.27.

Results of isotopic comparison: the observed Yucca Mountain range, from 19.2 to 22 per mil $_{SMOW}$, is compatible with that expected for deposits produced by the contemporary Yucca Mountain subsurface fluids.

Oxygen isotopic file - isotopic character of oxygen contained in the contemporary Yucca Mountain subsurface fluids. Data from Benson and McKinley, 1985.

Figure 4-3.28

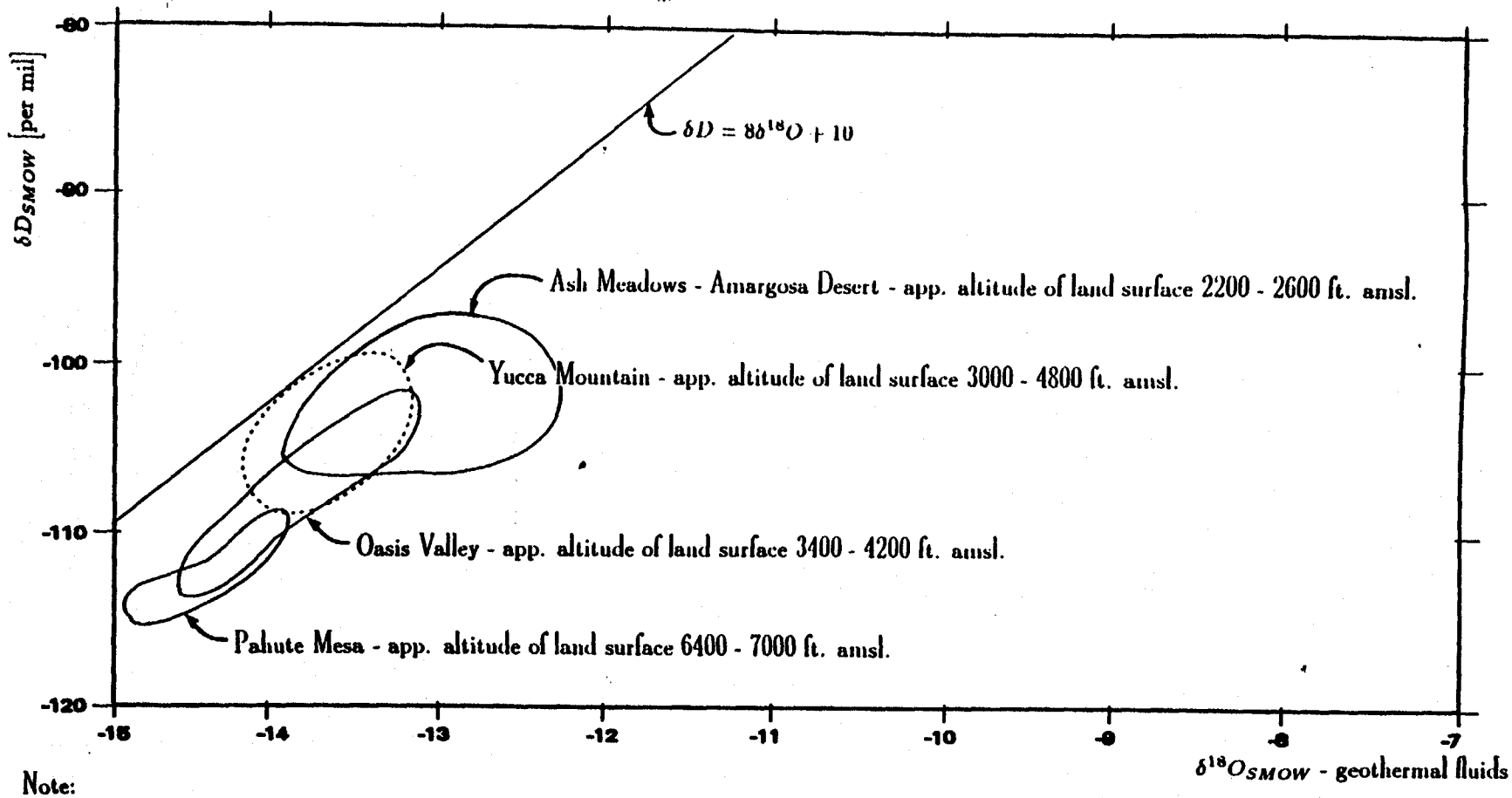

Note:

a) The observed range of values for the $\delta^{18}O$ ratio, from samples of the contemporary Nevada Test Site geothermal fluids, is from −14.8 to −12.3 $_{SMOW}$; samples are bulk samples pumped out of large segments of exploratory wells - sampling "smoothing" may be involved, and the observed "oxygen isotopic shift" may be smaller than the actually present one; and

b) If the parent fluids, for the Yucca Mountain surficial deposits, have carried the same oxygen - 18 contents then, the combined isotopic fractionation factor was in a range from 31.5 to 36.8 per mil $_{SMOW}$, which again is permissible by the empirical fractionation data from Figure 4-3.27.

Results of isotopic comparison: the observed Yucca Mountain range, from 19.2 to 22.0 per mil $_{SMOW}$, is compatible with that expected for deposits produced by the contemporary Nevada Test Site geothermal fluids.

Oxygen isotopic file - isotopic character of oxygen contained in the contemporary Nevada Test Site geothermal fluids. Data from Claassen, 1985; Benson and McKinley, 1985; and White and Chuma, 1987.

- Consideration of: a) the oxygen -18 content of the precipitants; b) the assumed oxygen -18 contents of the parent fluids; and c) the reasonable isotopic fractionation effects lead to a conclusion that, the precipitation temperatures for the Yucca Mountain surficial calcite-silica deposits may have been in a range from 15 to as much as 53°Celsius.

- The available data do not allow for further narrowing of the interpreted precipitation temperature range. Thus, the considerations of precipitation temperatures alone neither support nor contradict each of the two postulated modes of formation of the Yucca Mountain surficial calcite-silica deposits.

Conclusion: Based on considerations of the precipitation temperatures alone, both the *per ascensum* origin and the *per descensum* origin, for the Yucca Mountain surficial calcite-silica deposits, are permissible.

Precipitation (crystallization) temperatures, based on the oxygen -18 content of the Yucca Mountain surficial calcite-silica deposits.

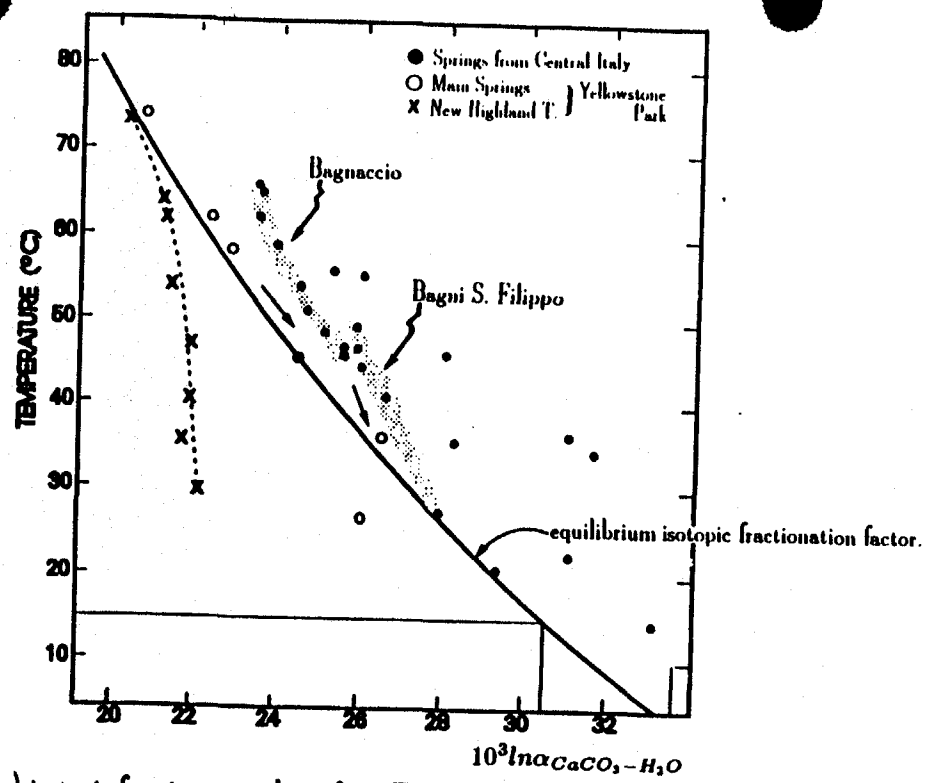

a) isotopic fractionation data, from Turi (1986).

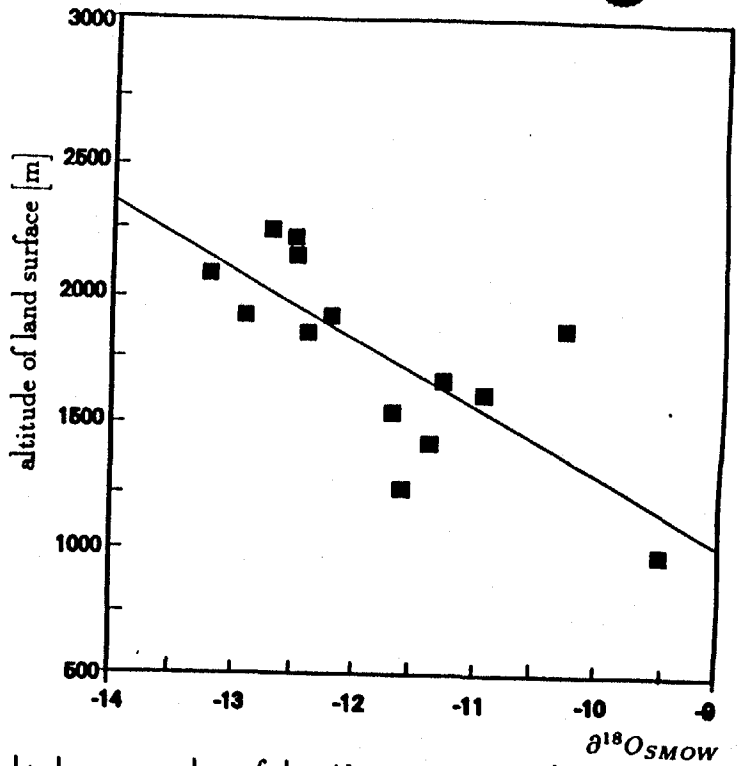

b) weighted average values of the $\delta^{18}O$ ratio - atmospheric precipitation at the Nevada Test Site, from Ingraham et al., (1990).

Note:

a) In performing this reconstruction, it has been assumed that: i) the parent fluids, for the Yucca Mountain surficial fluids, were isotopically identical to the contemporary atmospheric precipitation (at altitudes ranging from 1250 to 1400m, $\delta^{18}O$ values range from -11.7 to -11.3 per mil $_{SMOW}$); and ii) the non-equilibrium isotopic fractionation effects were absent, such that the combined isotopic fractionation factor $10^3 ln\alpha_{CaCO_3-H_2O} = 2.78 \cdot 10^6/T^2 - 2.82$;

b) The *minimum* and *maximum* values for the combined fractionation factor ($10^3 ln\alpha_{CaCO_3-H_2O} = 2.78 \cdot 10^6/T^2 - 2.82$) are 30.5 and 33.7, respectively;

c) The corresponding range for the precipitation temperatures is from 0 to ~ 14° Celsius; and

d) The measured contemporary *in-situ* temperatures, at and near the topographic surface, range from 15 to 21° Celsius, Sass et al., (1987) - the paleo and contemporary temperatures discrepancy indicates that one or both of the assumptions, employed to determine the paleo temperature, are false.

Reconstruction A - the precipitation temperatures for the Yucca Mountain surficial deposits, based on oxygen -18 contents from samples of these deposits.

Figure 4-3.31

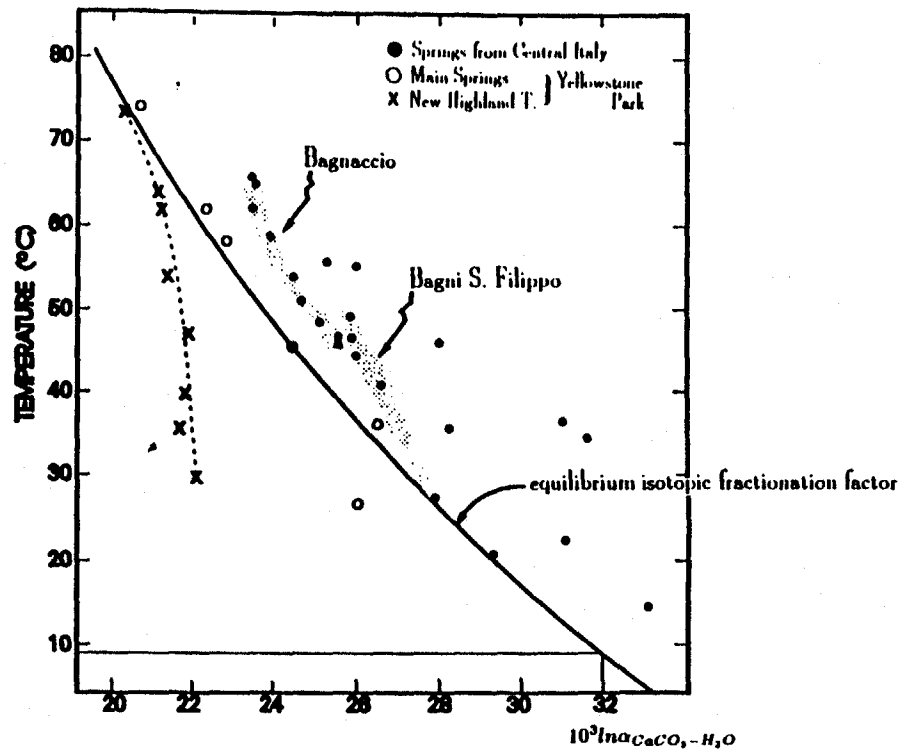

Note:

a) In performing this reconstruction, it has been assumed that: i) during a time span represented by the surficial deposits, the isotopic compositions of the parent fluids were the same as those observed below the water table at the present time ($\delta^{18}O$ values ranging from −14.2 to −12.7 per mil $_{SMOW}$, Figure 4-3.28. ii) the non-equilibrium isotopic fractionation effects were absent, such that the combined isotopic fractionation factor $10^3 ln\alpha_{CaCO_3-H_2O} = 2.78 \cdot 10^6 / T^2 - 2.82$;

b) The minimum and maximum values for the combined fractionation factor ($10^3 ln\alpha_{CaCO_3-H_2O} = 2.78 \cdot 10^6 / T^2 - 2.82$) are 31.9 and 36.2 per mil $_{SMOW}$, respectively; and

c) The corresponding range for the precipitation temperatures is from 8 to below 0° Celsius - this abnormally low range indicates that one or both of the employed assumptions are false.

Reconstruction B - the precipitation temperatures for the Yucca Mountain surficial deposits, based on oxygen -18 contents from samples of these deposits.

Figure 4-3.32

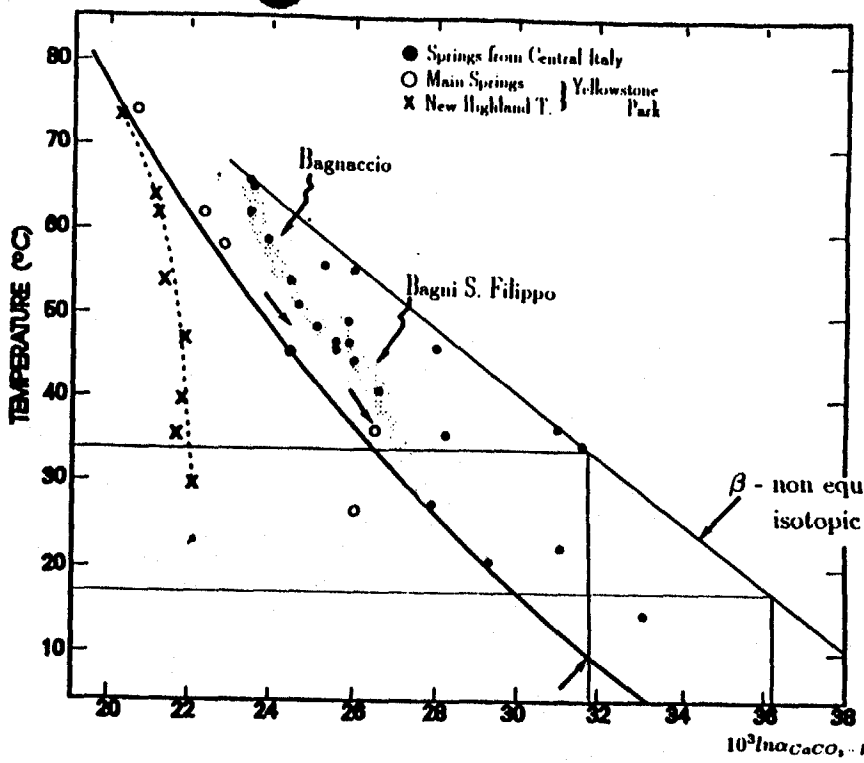

β - non equilibrium component for the combined isotopic fractionation factors.

Note:

a) In performing this reconstruction, it has been assumed that: i) during a time span represented by the surficial deposits, the isotopic compositions of the parent fluids were the same as those observed below the water table at the present time ($\delta^{18}O$ values ranging from −14.2 to −12.7 per mil $_{SMOW}$, Fig4-3.28); ii) the combined isotopic fractionation factor was larger that the equilibrium fractionation factor, such that $10^3 ln\alpha_{CaCO_3-H_2O} = 2.78 \cdot 10^6/T^2 - 2.82 + \beta$; and iii) the non-equilibrium isotopic fractionation is caused by a rapid escape of CO_2 from the parent solution; isotopically lighter CO_2 is eliminated preferentially, and $CaCO_3$ acquires it's oxygen from both H_2O and CO_2;

b) The minimum and maximum values for the combined isotopic fractionation factor ($10^3 ln\alpha_{CaCO_3-H_2O} = 2.78 \cdot 10^6/T^2 - 2.82 + \beta$) are 31.9 and 36.2, respectively; and

c) The corresponding range for the precipitation temperatures is from 18 to 34° Celsius.

Reconstruction C - the precipitation temperatures for the Yucca Mountain surficial deposits, based on oxygen -18 contents from samples of these deposits.

Figure 4-3.33

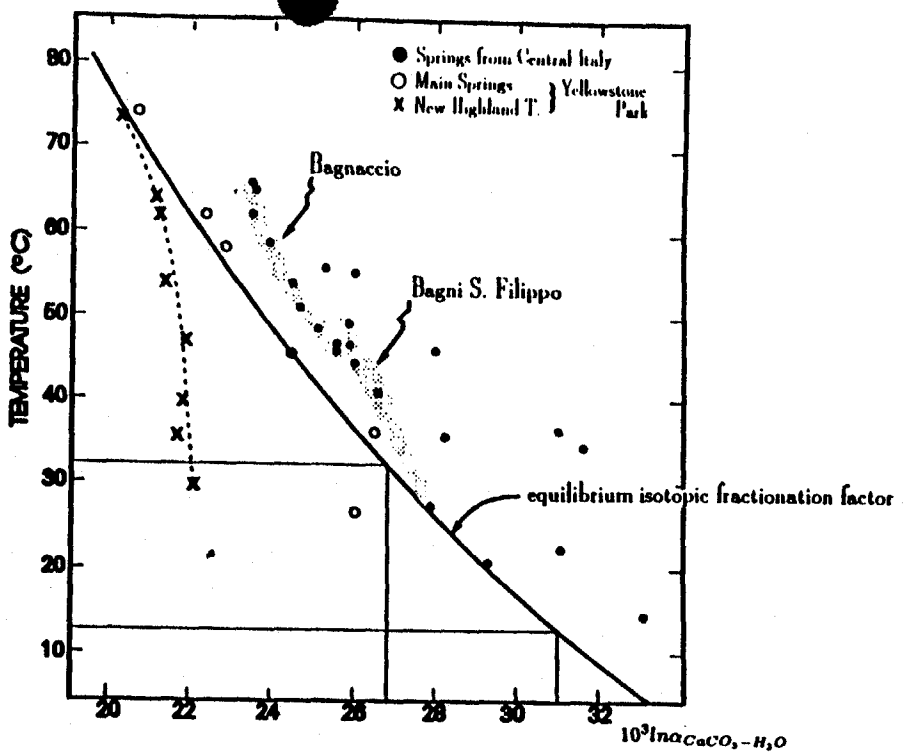

Note:

a) In performing this reconstruction, it has been assumed that: i) the parent fluids, for the Yucca Mountain surficial deposits, were isotopically heavier than the contemporary Yucca Mountain subsurface fluids, $\Delta\delta^{18}O \sim 5$ per mil $_{SMOW}$ (-9.2 to -7.7 per mil $_{SMOW}$); and ii) the non-equilibrium isotopic fractionation effects were absent, such that the combined isotopic fractionation factor $10^3 ln\alpha_{CaCO_3-H_2O} = 2.78 \cdot 10^6/T^2 - 2.82$;

b) The minimum and maximum values for the combined fractionation factor ($10^3 ln\alpha_{CaCO_3-H_2O} = 2.78 \cdot 10^6/T^2 - 2.82$) are 26.9 and 31.2 per mil, respectively; and

c) The corresponding range for the precipitation temperatures is from 13 to $\sim 32°$ Celsius.

Reconstruction D - the precipitation temperatures for the Yucca Mountain surficial deposits, based on oxygen -18 contents from samples of these deposits.

Figure 4-3.34

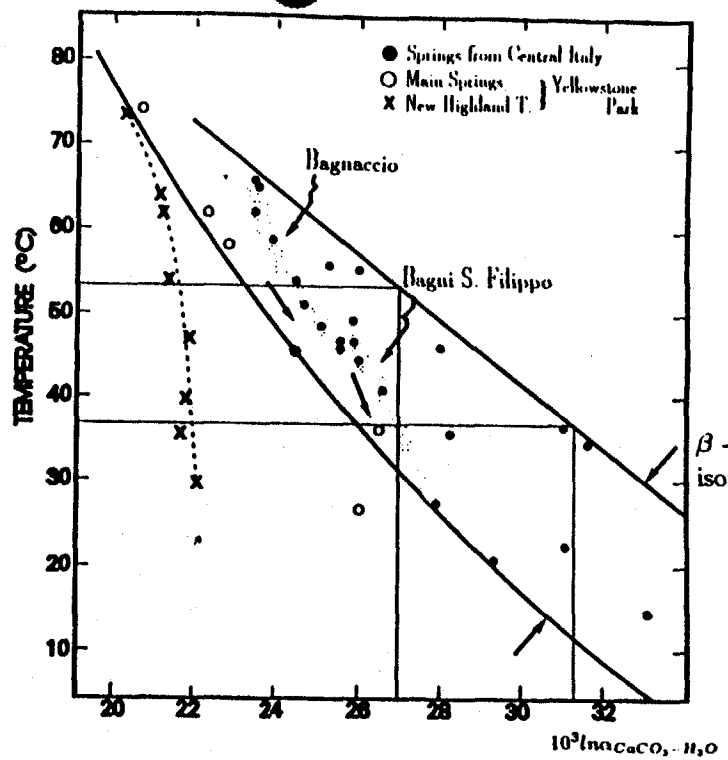

β - non-equilibrium component for the combined isotopic fractionation factor

Note:

a) In performing this reconstruction, it has been assumed that: i) the parent fluids, for the Yucca Mountain surficial deposits, were isotopically heavier than the contemporary Yucca Mountain subsurface fluids, $\Delta\delta^{18}O \sim 5$ per mil $_{SMOW}$ (−9.2 to −7.7 per mil $_{SMOW}$,); the combined isotopic fractionation factor was larger than the equilibrium fractionation factor, such that $10^3 ln\alpha_{CaCO_3-H_2O} = 2.78 \cdot 10^6/T^2 - 2.82 + \beta$; and iii) the non-equilibrium isotopic fractionation is caused by a rapid escape of CO_2 from the parent solution; isotopically lighter CO_2 is eliminated preferentially, and $CaCO_3$ acquires it's oxygen from both H_2O and CO_2;

b) The minimum and maximum values for the combined isotopic fractionation factor ($10^3 ln\alpha_{CaCO_3-H_2O} = 2.78 \cdot 10^6/T^2 - 2.82 + \beta$) are 26.9 and 31.2 per mil, respectively; and

c) The corresponding range for the precipitation temperatures is from 38 to 53° Celsius.

Reconstruction E - the precipitation temperatures for the Yucca Mountain surficial deposits, based on oxygen -18 contents from samples of these deposits.

Figure 4-3.35

- Without having reliable information regarding both the isotopic compositions for the parent fluids and the isotopic fractionation conditions, it is not possible to specify a reliable, but at the same time, narrow range for the precipitation temperatures for the Yucca Mountain surficial deposits. Based on information presently at hand all that may be said, with some degree of certainty, is that temperatures could have been anywhere within a range from 15 to as much as 53°Celsius, consistently with the *per ascensum* origin for the deposits.

- The currently available data do not allow for ruling out the possibility that the precipitation temperatures, for all of the considered samples, were within the 15 - 20°Celsius ambient temperature range. As a consequence, based on the results of considerations of the precipitation temperature alone, the *per descensum* origin for the Yucca Mountain surficial deposits can not be rejected.

- A more reliable and definitive picture of the geothermal circumstances of precipitation, for the Yucca Mountain calcite-silica deposits, may be derived from considerations of the paleo-geothermal gradients. This is so because such considerations may be performed on relativistic basis and, therefore, do not require knowledge of the absolute isotopic composition for the deposits parent fluids.

Summary - the precipitation temperature reconstructions. The Yucca Mountain calcite-silica deposits.

- Considerations of: a) the $d\delta^{18}O/dz$ from samples of the calcite-silica deposits; b) the reasonable spatio-temporal variability of the oxygen -18 content for the parent fluids; and c) the reasonable isotopic fractionation effects lead to a conclusion that, during formation of the Yucca Mountain calcite-silica deposits, the geothermal gradient (dT/dz) was a factor 1.5-2.5 higher than the contemporary geothermal gradient.

Conclusion: a) The paleo- and contemporary geothermal gradient discrepancy indicates that precipitation of the calcite-silica deposits was accompanied by a significant warming up of the vadose zone, and occurred as the per ascensum process; and

b) In the past, the Yucca Mountain hydrosphere have experienced the "sink" ⟷ "source" transformations.

Paleo-geothermal gradient, based on the $d\delta^{18}O/dz$ gradient.

- A reliable interpretations of the Yucca Mountain paleo-geothermal, based on the observed $d\delta^{18}O/dz$ gradient from samples of the local calcite-silica deposits, constitutes an important aspect of resolving the dilemma that surrounds the origin of these deposits.

- A reliable demonstration that, in the Yucca Mountain vadose zone, the geothermal gradients undergo temporal fluctuations, with amplitudes say $\Delta dT/dz \sim 10 - 15$°Celsius per 1km of depth, would constitute a fairly definitive demonstration that: i) episodically, the Yucca Mountain vadose zone was being inundated with warm fluids from below the water table; and ii) all of the Yucca Mountain calcite-silica deposits were formed via the *per ascensum* process.

- A reliable interpretation of the paleo-geothermal gradient is difficult to perform. This is so because such an interpretation requires two assumptions. These assumptions are: i) the oxygen -18 contents of the parent fluids, for spatially and temporally different samples, were either the same of the $\delta^{18}O$ variability is both known and fixed in the spatio-temporal sense; and ii) the non-equilibrium isotopic fractionation effects are either absent or, relative to the equilibrium fractionation curve, maintain a know relationship.

- It is not possible to exactly specify the oxygen -18 content of the parent fluids for the Yucca Mountain calcite-silica deposits. This is so because: i) the contemporary Yucca Mountain subsurface fluids exhibit the $\delta^{18}O$ spatial variability of ~1.5 per mil_{SMOW} - this variability is known based on bulk fluid samples pumped out of large borehole segments, sampling "smoothing" may be involved, and the actual $\delta^{18}O$ spatial variability may be larger, say $\Delta\delta^{18} \sim 3$ per mil_{SMOW}; and ii) for the time-spans represented by the Yucca Mountain calcite-silica deposits, the locally known value for the $\delta^{18}O$ temporal variability ranges from 2.7 to about 4 per mil_{SMOW}.

Interpretations of the paleo-geothermal gradients, based on the observed $d\delta^{18}O/dz$ gradient - general remarks.

- We do not know much about the non-equilibrium fractionation effects, as such effects pertain to the Yucca Mountain calcite-silica deposits. In view of substantial errors that potentially may be involved, it is prudent to consider three fractionation scenarios.

- The first scenario is that, the non-equilibrium isotopic fractionation effects are either absent or depth invariant. In this case, the paleo-geothermal gradient estimates are fairly reliable. The observed constant depth $\delta^{18}O$ variability, from samples of the deposits, may reasonably be regarded as reflecting the spatio-temporal $\delta^{18}O$ variability in the parent fluids for these deposits.

- The second scenario is that, for some or all of the considered samples, the combined isotopic fractionation factor exceeds the equilibrium fractionation factor and the difference is depth variant. In this case, down to some depth, the observed constant depth $\delta^{18}O$ variability, from samples of the deposits, reflects; i) the spatio-temporal $\delta^{18}O$ variability in the parent fluids, together with; ii) the spatio-temporal variability of the combined isotopic fractionation factor. It is difficult to separate these two variabilities and, consequently, the paleo-geothermal gradient estimates may not be reliable. Because it is likely that the non-equilibrium fractionation effects diminish depthward, the paleo-geothermal gradient estimates, for deeper portions of the vadose zone, may be regarded as more reliable than those for shallower portions.

- The third scenario is that, for some or all of the considered samples, the combined isotopic fractionation factor is smaller than the equilibrium fractionation factor and the difference is depth variant. Here again, it is difficult to properly interpret the observed constant depth $\delta^{18}O$ variability, from samples of the deposits. As a consequence, the reliability of the paleo-geothermal gradient estimates may be low, particularly for shallow parts of the vadose zone.

Interpretations of the paelo-geothermal gradient, based on the observed $d\delta^{18}O/dz$ gradient - general remarks.

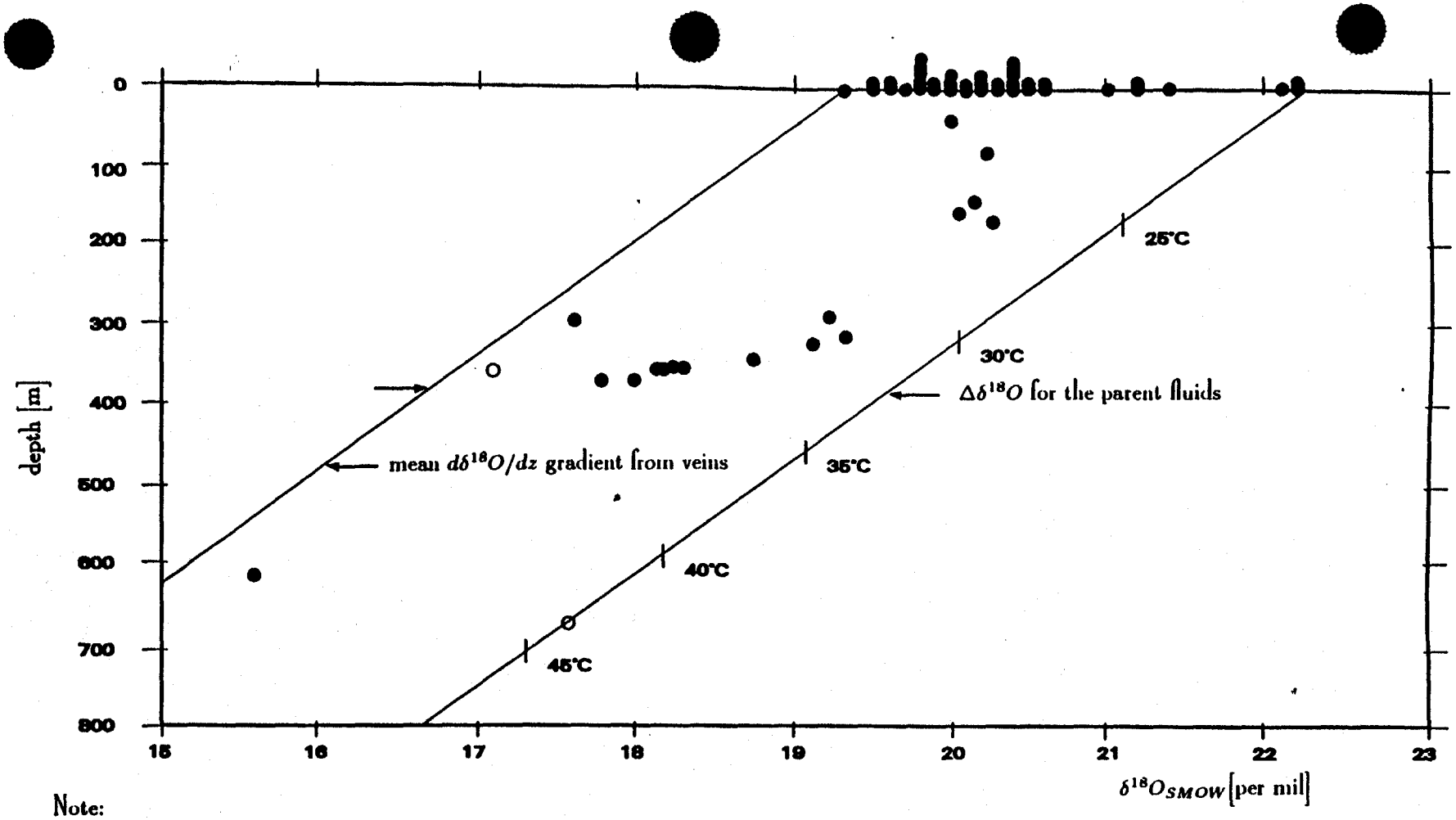

Note:

a) In performing this reconstruction, it has been assumed that: i) at the topographic surface, the precipitation temperature for calcretes and veins was T ~20° Celsius; ii) the constant depth variability of the oxygen -18 content, from samples of the calcite-silica deposits, reflects the spatio-temporal variability of the oxygen -18 content in the parent fluids, $\Delta\delta^{18}O \sim 3$ per mil; and iii) the non- equilibrium isotopic fractionation effects are absent and, therefore, $10^3 ln\alpha_{CaCO_3-H_2O} = 2.78 \cdot 10^6/T^2 - 2.82$ - where T is precipitation temperature in ° Kelvin; and

b) Value of the paleo-geothermal gradient is dT/dz ~ 35° Celsius per 1km increase in depth - the corresponding contemporary geothermal gradient ranges from 20 to 24° Celsius per 1km increase in depth.

Reconstruction A - the Yucca Mountain paleo-geothermal, based on the oxygen -18 content of samples of the local calcite-silica deposits.

Figure 4-3.40

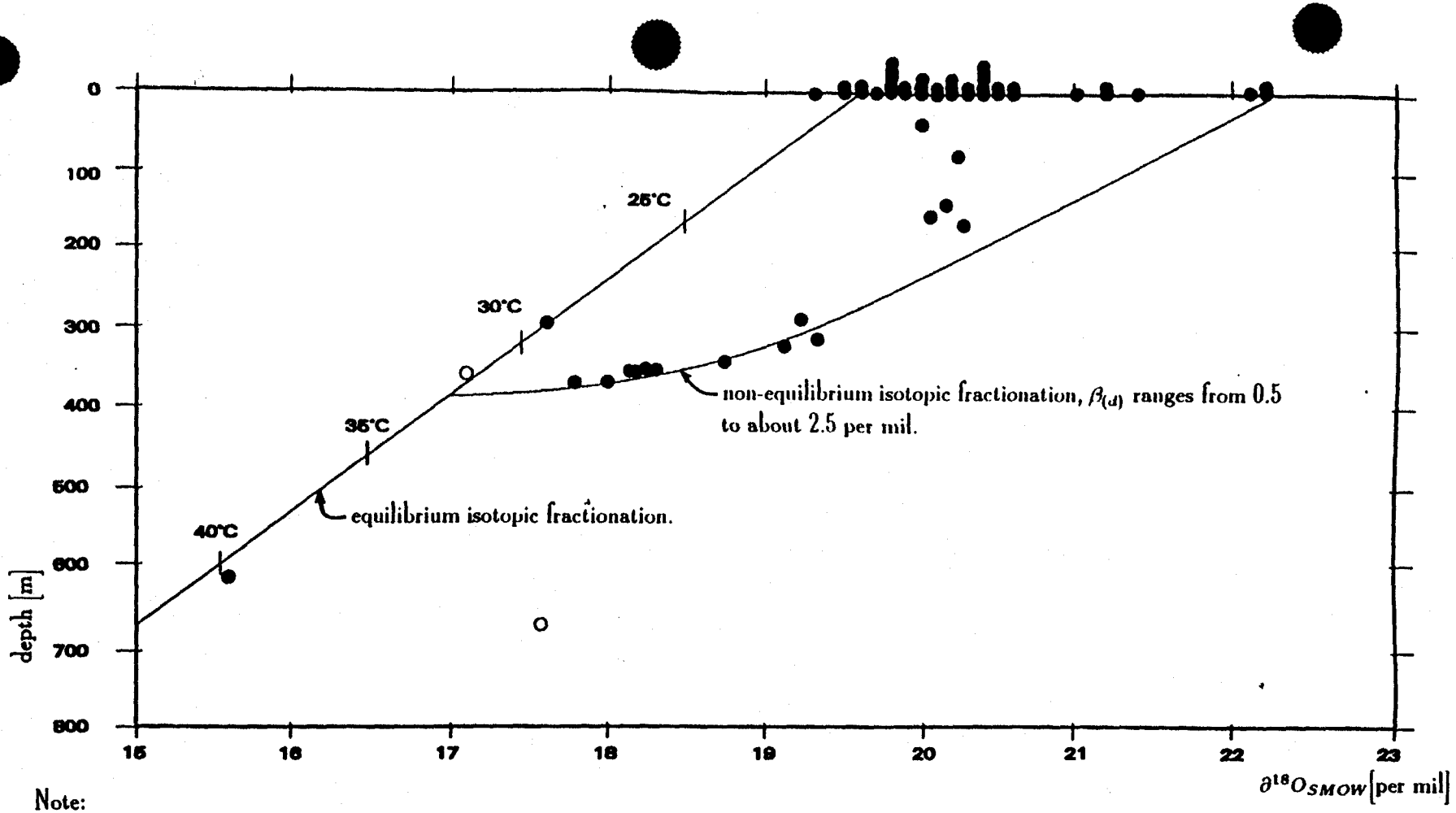

Note:

a) In performing this reconstruction, it has been assumed that: i) at the topographic surface, the precipitation temperature for calcretes and veins was T ~20° Celsius; ii) the oxygen -18 content of the parent fluids, for spatio-temporarly different samples, was the same; iii) the constant depth variability of the oxygen -18 content, from samples of the calcite-silica deposits, is attributable to the non-equilibrium isotopic fractionation effects, such that combined $10^3 ln\alpha_{CaCO_3-H_2O} = 2.78 \cdot 10^6/T^2 - 2.82 + \beta_{(a)}$; and iv) the non-equilibrium fractionation is caused by a rapid, and depth variant escape of CO_2 from the parent solution - the CO_2 degassing rate decreases depthward, and $CaCO_3$ acquires its oxygen from both H_2O and CO_2; and

b) Value of the paleo-geothermal gradient is dT/dz ~33° Celsius per 1km increase in depth - the corresponding contemporary geothermal gradient ranges from 20 to 24° Celsius per 1km increase in depth.

Reconstruction B - the Yucca Mountain paleo-geothermal, based on the oxygen -18 content of samples of the local calcite-silica deposits.

Figure 4-3.41

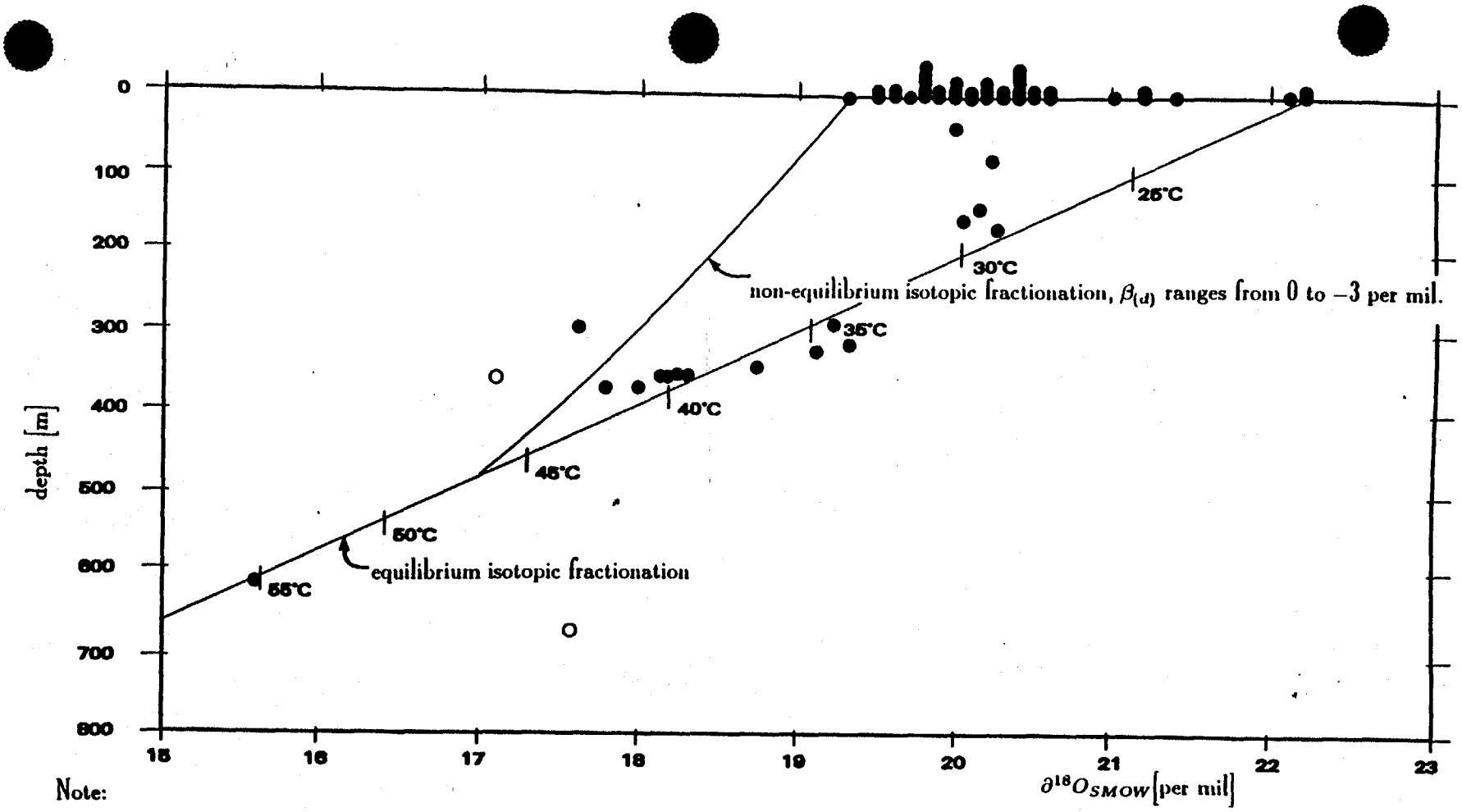

Note:

a) In performing this reconstruction, it has been assumed that: i) at the topographic surface, the precipitation temperature for calcretes and veins was T ~20° Celsius; ii) the oxygen −18 content of the parent fluids, for spatio-temporally different samples, was the same; iii) the constant depth variability of the oxygen −18 content, from samples of the calcite-silica deposits, is attributable to the non-equilibrium isotopic fractionation effects, such that combined $10^3 ln\alpha_{CaCO_3-H_2O} = 2.78 \cdot 10^6/T^2 - 2.82 - \beta_{(d)}$; and iv) the non-equilibrium fractionation is caused by a rapid upward movement of the parent fluids - the $CaCO_3$ nucleation occures prior to its deposition and, consequently, the deposited $CaCO_3$ records, temperatures that are higher than those prevailing at the actual deposition sites; and

b) Value of the paleo-geothermal gradient is dT/dz ~58° Celsius per 1km increase in depth - the corresponding contemporary geothermal gradient ranges from 20 to 24° Celsius per 1km increase in depth.

Reconstruction C - the Yucca Mountain paleo-geothermal, based on the oxygen -18 content of samples of the local calcite-silica deposits.

Figure 4-3.42

- Figure 4-3.44 presents a summary of reconstructions of the Yucca Mountain paleo-geothermal gradient. The contemporary geothermal gradient, as measured in Well USW G-3 by Sass et al., (1987), is used as a reference.

- In all cases considered, the reconstructed paleo-geothermal gradient is significantly greater than the geothermal gradient, as measured in the corresponding wells. Values of the contemporary geothermal gradient are: i) Well UE-25a, dT/dz ~ 22°Celsius per 1km of depth; ii) Well USW G-2, dT/dz ~ 24°Celsius per 1km of depth; iii) Well USW G-3, dT/dz ~ 22°Celsius per 1km of depth; and iv) Well USW G-4, dT/dz ~ 20°Celsius per 1km of depth.

- The reconstructed values of the paleo-geothermal gradient are: i) reconstruction by Szabo and Kyser (1990) - dT/dz ranging from 17, near the topographic surface, to 50°Celsius per 1km of depth, in deeper parts of the vadose zone; ii) reconstruction A - dT/dz ~ 35°Celsius per 1km of depth; iii) reconstruction B - dT/dz ~ 33°Celsius per 1km of depth; and iv) reconstruction C - dT/dz ~ 58°Celsius per 1km of depth.

- The interpreted temporal fluctuations of values of the geothermal gradient indicate that, the Yucca Mountain vadose zone was being episodically invaded by warm fluids from below the water table. Evidently, the resulting warming up of the vadose zone was accompanied, and recorded, by the episodic precipitation of the calcite-silica veins.

- As far as the origin of the calcite-silica deposits is concerned, the available oxygen -18 and carbon -13 data are convincing and clear. Both the surficial deposits and the subsurface veins were produced via the *per ascensum* process.

Summary - the paelo-geothermal gradient reconstruction.

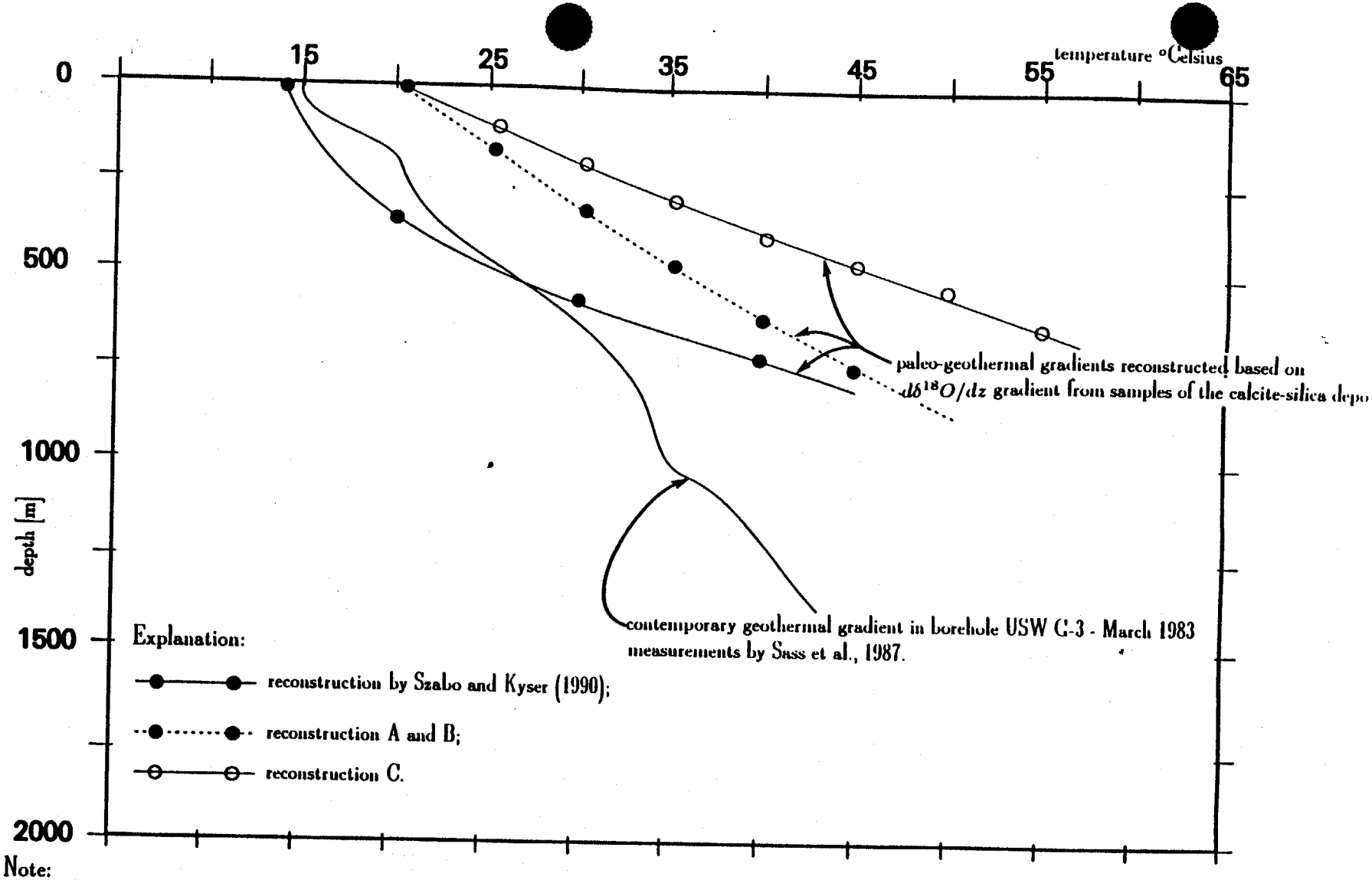

Note:

a) Each of the considered cases yields the paleo- geothermal gradient that is substantially higher than the contemporary geothermal gradient; and

b) The geothermal gradients discrepancy indicates that precipitation of the calcite-silica deposits was accompanied by a significant warming up of the vadose zone and, therefore, occurred as the *per ascensum* process.

Comparison between the contemporary geothermal gradient and the paleo-geothermal gradients, as reconstructed based on the dδ^{18}O/dz gradient from samples of the calcite-silica deposits and using various assumptions.

Figure 4-3.44

- At Yucca Mountain, the vadose zone interstitial fluids exhibit strong REE and bulk chemical affinity with the local deep-seated geothermal fluids. The latter fluids are upwelling along the Tertiary/Paleozoic fault contact and were encountered in borehole UE-25p#1, depth ~1200 m.

- The δD and $\delta^{18}O$ isotopic composition of the intersitial fluids may be explained by assuming that these fluids are the result of intermixing of fresh meteoric fluids with the older geothermal fluids. The observed "hydrogen-oxygen isotopic shift" is directly attributable to the *in situ* evaporative deuterium and oxygen -18 enrichment.

Conclusion: **The Yucca Mountain interstitial fluids are, in part, the relict geothermal fluids.**

Chemical and isotopic affinity between the vadose zone interstitial fluids and the local geothermal fluids. Yucca Mountain.

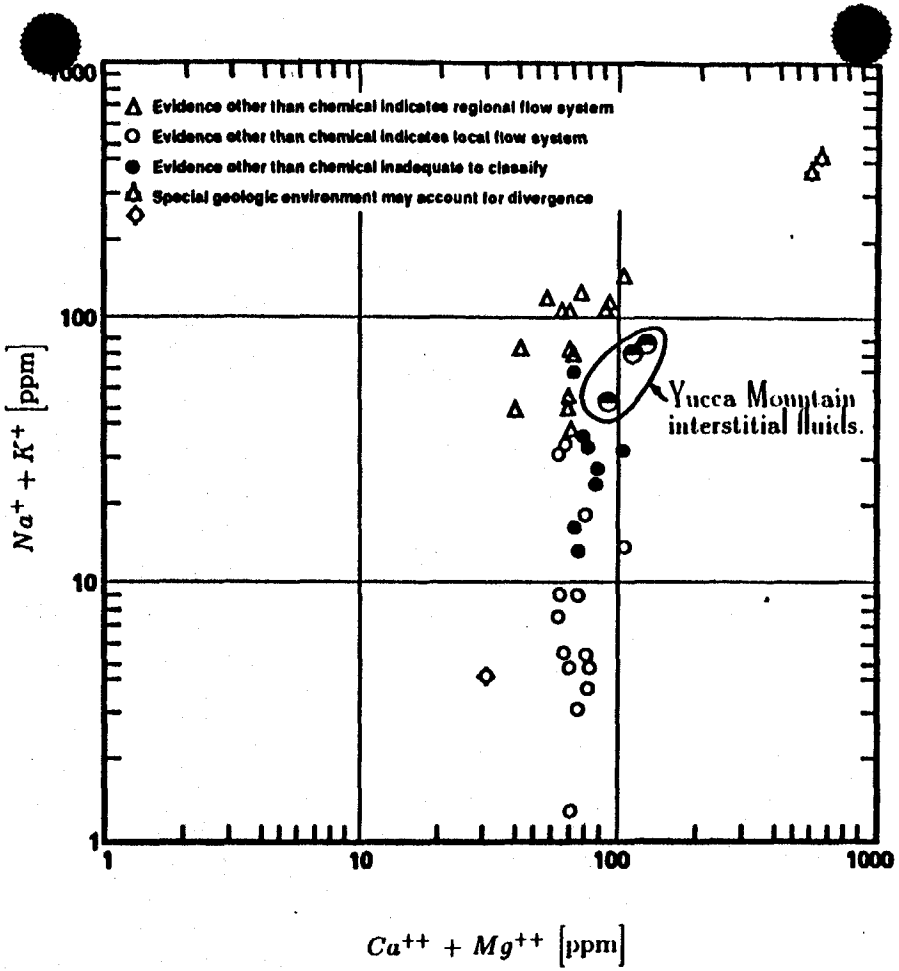

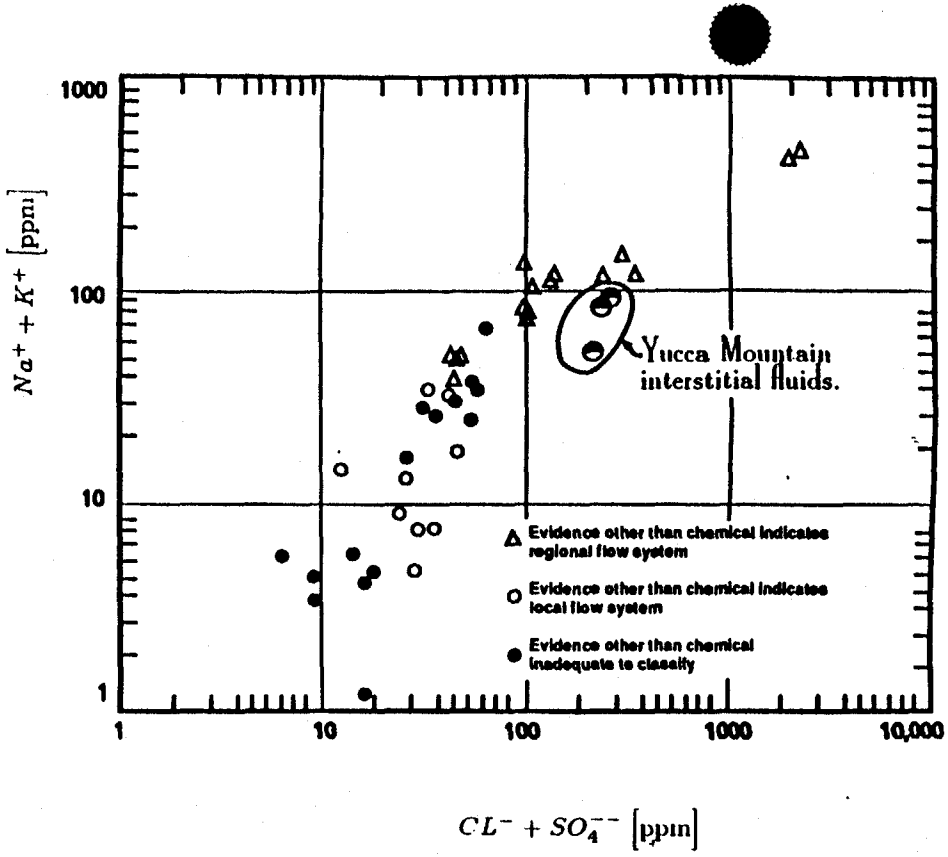

Note:

a) fluid chemistry data for the Yucca Mountain interstitial fluids are from Yang et al. (1989).

A comparison of geochemical compositions of fluids - the Yucca Mountain interstitial fluids and fluids from the carbonate - based flow system of Nevada. Modified from Domenico, 1972.

Figure 4-3.46

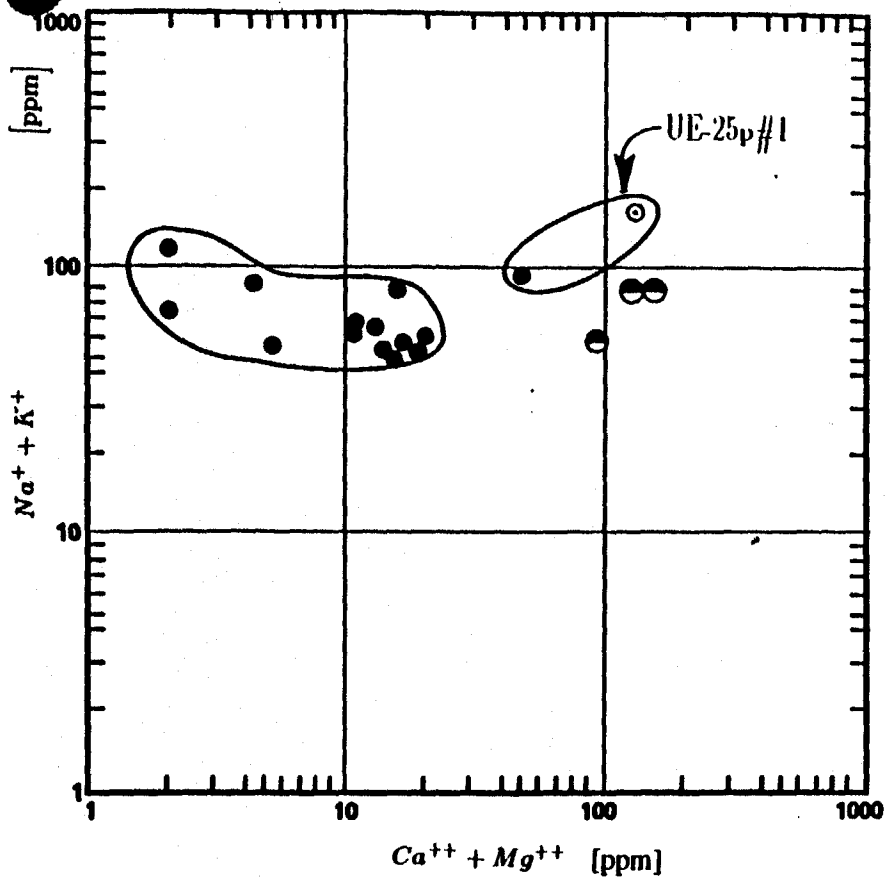

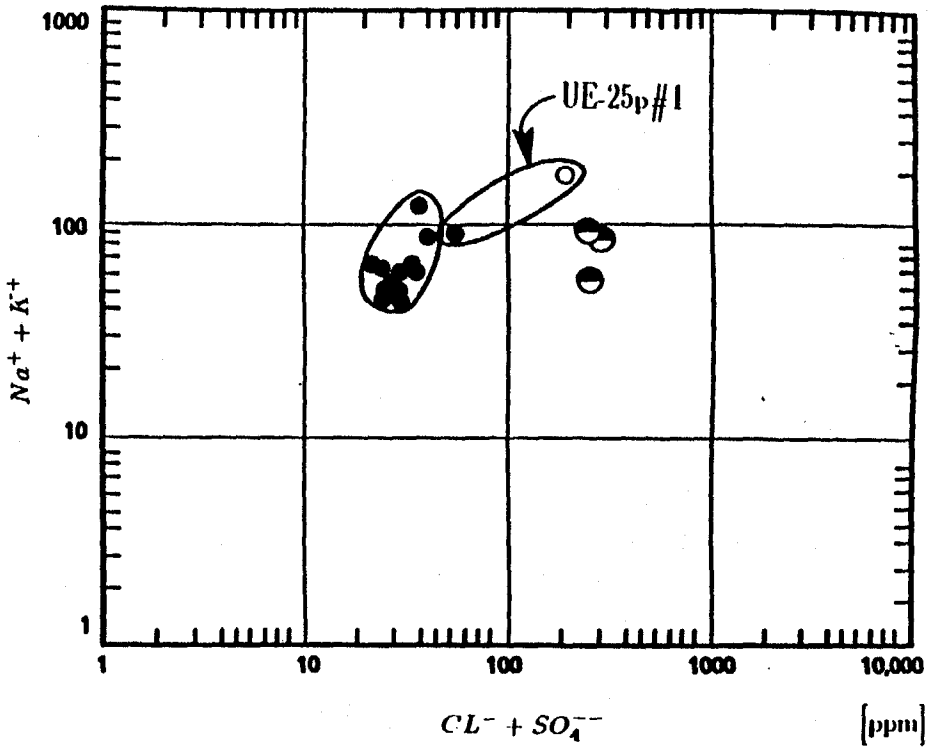

Note:

a) fluid chemistry data are from Benson and McKinley (1985) and Yang et al. (1989).

Explanation:

- ● - sample represents fluids from within the Yucca Mountain *in-situ* stress field inclusion;
- ○ - sample represents deeper fluids from the underlying hydraulic "source";
- ◒ - sample represents interstitial fluids from the local vadose zone.

A comparison of chemical compositions of subsurface fluids. Fracture water from below the water table against interstitial water from the vadose zone, Yucca Mountain

Figure 4-3.47

TABLE 3 Trace element data for J-12 and J-13 Well waters

Sample #	J-12	error	J-13	error	SLRS-1*	cert. val
pH (field)	7.3		--			
pH (lab)	7.69					
F(ppm)	2.00					
Cl(ppm)	7.5					
NO3(ppm)	8.2					
SO4(ppm)	22.2					
HCO3(ppm)	117					
Li	50	10	40	10	1.5	
B	130	10				
Na(ppm)	41.8	1.3				10.4
Mg(ppm)	2.45	0.15	2.4	0.2		5.89
Al	1.2	0.6	0.6			23.6
Si(ppm)	25.6	1.1	30	5		
Cl(ppm)	7.5	0.5				
K	5.6	0.7				1.3
Ca(ppm)	15	0.2	14	5	25	25.1
Sc	<1		<3		0.34	
Ti	0.08		0.1		0.7	
V	4	1	6	1	0.73	0.68
Cr	0.37	0.12	0.33	0.03	0.26	0.36
Mn	0.15	0.06	<0.3		1.19	1.77
Fe	3	1	3	1	27.5	31.6
Co	<0.01		<0.01		0.023	0.043
Ni	0.03	0.01	0.05	0.01	0.7	1.07
Cu	0.2	0.08	0.6	0.2	2.8	3.56
Zn	2.7	0.5	2.4	0.5	0.85	1.3
As	9	3	8	3	0.53	0.55
Rb	0.2	1.1	6.5	1	0.83	
Sr	35	1	33	2	133	136
Y	0.0025	0.0008	0.0025	0.0008	0.28	
Mo	5	0.5	5.3	0.1	0.82	0.79
Pd	<0.01		<0.01			
Cd	<0.05		<0.05		0.011	0.018
Sb	0.15	0.01	0.21	0.01	0.57	0.93
I	2		2		2.22	
Te	<0.01		<0.03		<0.01	
Cs	0.56	0.02	0.66	0.16	0.0032	
Ba	1.75	0.35	178.6		21.5	22.2
La	0.0004		0.0003		0.04	
Ce	<0.005		0.0006		0.066	
Pr	<0.001		<0.001		0.01	
Nd	<0.001		<0.001		0.037	
Sm	<0.001		<0.001		0.03	
Eu	<0.001		<0.001		0.0014	
Gd	<0.001		<0.001		0.005	
Tb	<0.001		<0.001		0.0007	
Dy	<0.001		<0.001		0.0035	
Ho	<0.001		<0.001		0.0006	
Er	<0.001		<0.001		0.003	
Tm	<0.001		<0.001		0.0003	
Yb	<0.001		<0.001		0.0028	
Lu	<0.001		<0.001		0.0004	
Hf	0.001		<0.002			
Ta	<0.001		<0.001			
W	1.0	0.3	2.0	0.4	0.13	
Re	0.056	0.01	0.0020.83		0.003	
Pt						
Au					0.0006	
Tl	0.01	0.004	0.008			
Pb	0.2	0.08	0.3	0.1	0.082	0.108
Bi	<0.001		<0.003		0.001	
Th	0.0001	0.00003	0.0004	0.0002	0.003	
U	0.56	0.13	0.4	0.14	0.25	0.28

* Riverine Water Reference Material for Trace Metals (National Research Council Canada)

Note:

a) concentrations are in ppb unless noted;

b) water samples are from below the water table;

c) host rock is rhyolitic tuff;

d) $logP_{CO_2}$ ranges from −2.10 to −2.11 atm. and PMC = 29.2 - 32.2 percent; and

e) SLRS-1, Riverine Reference Standard.

The results of trace element analyses. Water samples from J-12 and J-13 Wells. From Smith (1991).

TABLE 4. Trace element data for Pore Water Samples from UZ#4

Sample #	Pore wat 6110926	error	USGS (reported)	Pore wat 6110923	error	USGS (reported)
pH			6.5			6.5
SO4(ppm)						190
U	80			65	10	
B						
Na(ppm)			48			53
Mg(ppm)	27	5	21	25	1	23
Al				<5		
Si(ppm)			74			78
Cl(ppm)			160			210
K			5			14
Ca(ppm)	120	10	120	110	10	130
Sc	<3	1		0.4		
Ti				<3		
Cr	<9	<3		0.4	0.1	
Mn	133	25	150	14	3	90
Fe	35	5	150	<20		<3
Co				<1		
Ni	40	10		<80	16	
Cu	40	10		10	1	
Zn	150	15		71	5	
Rb	23	2		12	2	
Sr	1020	110		1180	110	
Y	0.3	0.1		0.21	0.05	
Mo	1880	180		1400	30	
Cd				1.4	0.3	
Sb	1			0.7	0.2	
I	50			40		
Cs	0.5	0.1		0.44	0.05	
Be	27	3		18	1	
La	<0.1			0.007	0.007	
Ce	<0.1			0.046	0.02	
Pr	<0.04			<0.008		
Nd	<2			<0.05		
Sm	<0.3			<0.006		
Eu	<0.06			<0.006		
Gd	<0.2			<0.003		
Tb	<0.03			0.013	0.005	
Dy	0.09	0.03		0.032	0.008	
Ho	<0.1			0.022	0.008	
Er	0.14	0.04		0.12	0.02	
Tm	0.05	0.02		0.04	0.01	
Yb	0.5	0.2		0.5	0.10	
Lu	0.14	0.05		0.16	0.05	
Hf	0.01			0.3	0.1	
Ta	0.5			<0.2		
W	600	200		330	50	
Re	0.2	0.08		0.2	0.1	
Pt	0.2	0.1		0.2	0.05	
Au	0.12	0.05		0.2	0.1	
Tl	0.2			0.2		
Pb	0.25	0.1		1.7	0.3	
Bi	<0.03			<0.1		
Th	0.0024	0.0006		<0.01		
U	0.45	0.06		0.13	0.03	

Note:

a) concentrations are in ppb unless noted;

b) samples represent the interstitial fluids from the Yucca Mountain vadose zone;

c) host rock is unwelded rhyolitic tuff; and

d) samples of fluid were extracted by centrifugation.

The results of trace element analyses. Interstitial fluids from the Yucca Mountain vadose zone (borehole UZ-4). From Smith (1991).

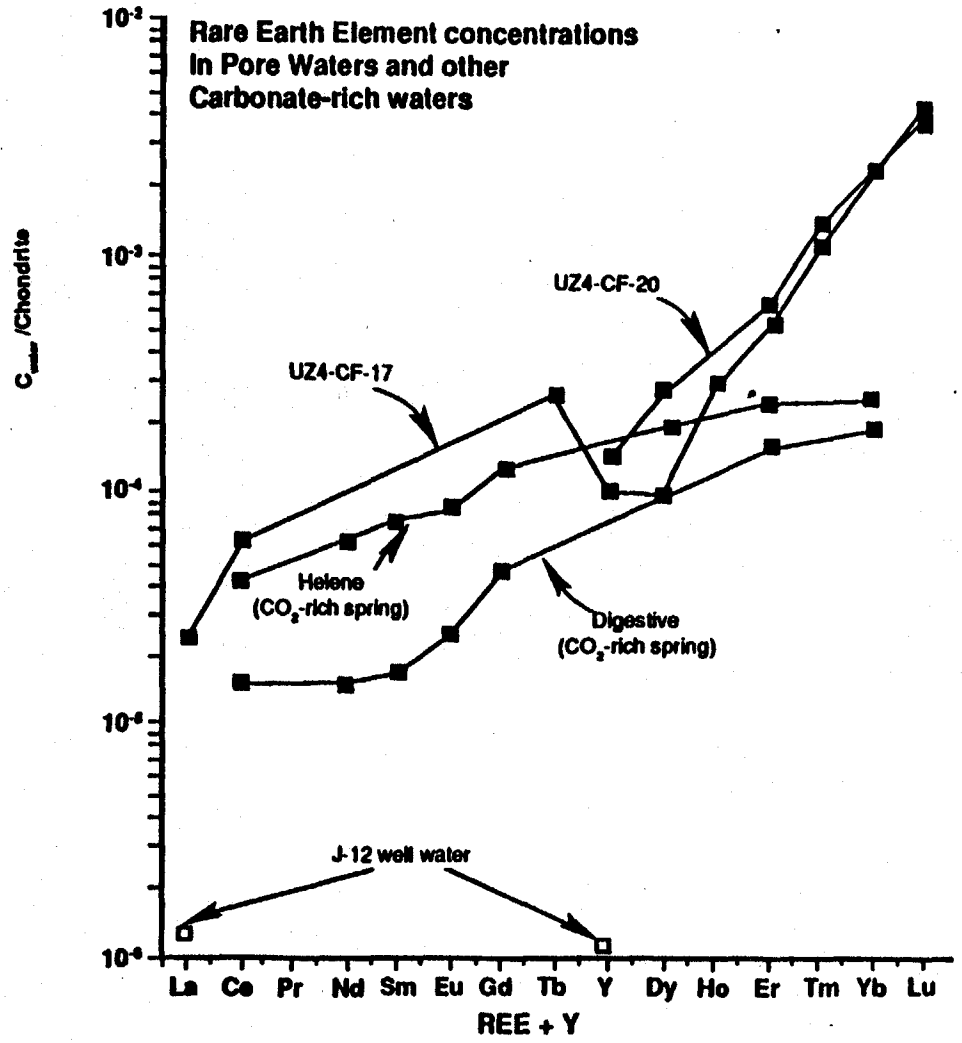

Note:

a) the expected REE abundance pattern for interstitial fluids from the rhyolitic tuffs is one of the high abundances of the light rare earth elements (i.e., La → Sm);

b) the observed REE abundance pattern is one of the high relative abundances of the heavy rare earth elements (Tb → Lu);

c) the interstitial fluids carry high concentrations of the alkaline earth elements (i.e., Mg, Ca, Sr, and Ba) - this suggests dissolution of the Paleozoic carbonates, which occur 1km below; and

d) the complexation of HREE by carbonate rich waters explains the abnormally high HREE concentrations.

Comparison of trace element abundances. The local subsurface fluids (Well J-12), the intersitial fluids from the Yucca Mountain vadose zone (UZ4-CF-17 and UZ4-CF-20), and the CO_2 - rich fluids from Vals-les-Baines (Helene and Digestive). From Smith, 1991.

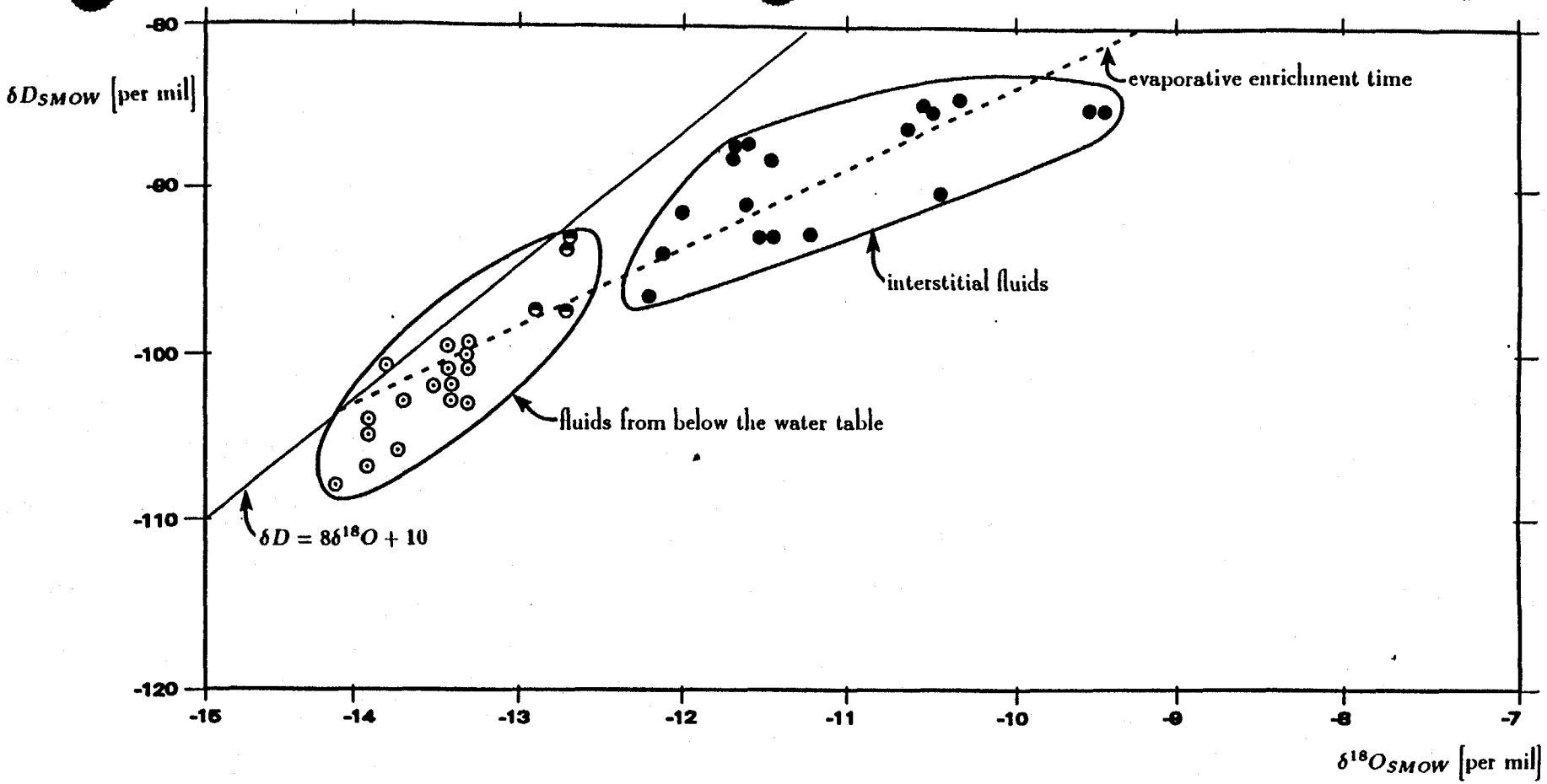

Explanation:

● - sample represents interstitial fluids from the vadose zone (^{14}C age ~ 10^3 – 4.9 x 10^3 years B.P.);

◒ - sample represents fluids from below the water table (^{14}C age ~ 3.8 x 10^3 - 9.9 x 10^3 years B.P.);

○ - sample represents fluids from below the water table (^{14}C age ~ 12 x 10^3 - 18.5 years B.P.).

Note:

a) isotopic data are from Benson and McKinley (1985) and Yang et al. (1989).

A comparison of isotopic chemical compositions, interstitial fluids and fluids from below the water table. Yucca Mountain.

Figure 4-3.51

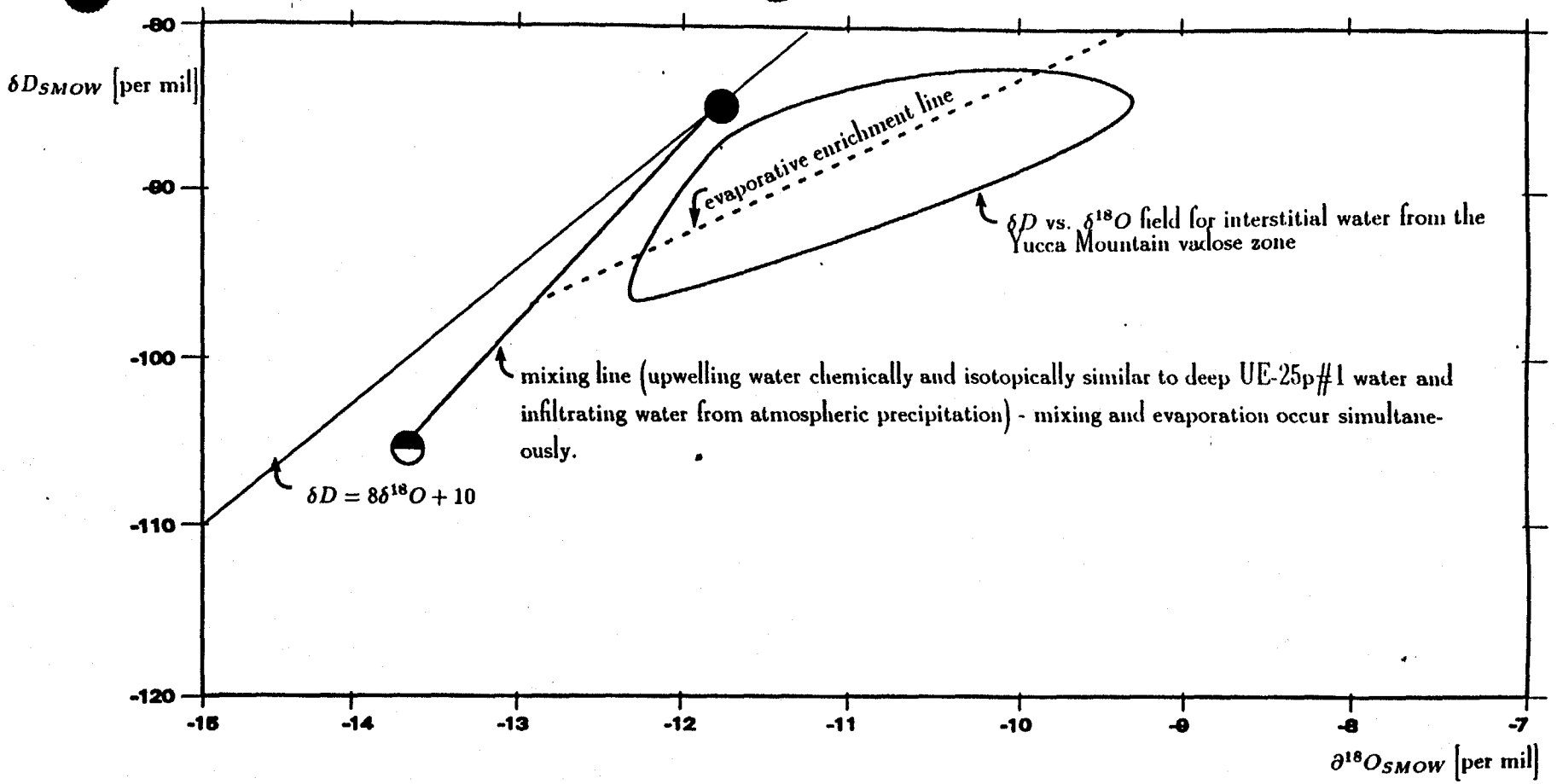

Explanation:

- isotopic composition of deep water from Well UE-25p#1 (Benson and McKinley, 1985);

- mean isotopic composition of the Yucca Mountain recharge (isotopic smoothing - based on studies at Rainier Mesa, altitude correction $d\delta D/dz \sim 1.3$ per mil per 10^2m, Dansgaard, 1964.)

Interpretation of meaning of chemical and isotopic compositions of interstitial water from the Yucca Mountain vadose zone.

Figure 4-3.52

Overall conclusions

The results of isotopic considerations, of the Yucca Mountain calcite-silica deposits and of the Nevada Test Site subsurface fluids, allow for two firm conclusions to be drawn.

Conclusion I - The isotopic characters of uranium, strontium, carbon, and oxygen contained in the Yucca Mountain calcretes, surficial fault-infillings, and subsurface veins are, for all practical purposes, identical. It is virtually certain, therefore, that all these deposits were precipitated from the common parent fluids.

Conclusion II - The isotopic characters of uranium, strontium, carbon, and oxygen contained in the Yucca Mountain calcite-silica deposits are identical to those of uranium, strontium, carbon, and oxygen dissolved and contained in the Nevada Test Site geothermal fluids. It is virtually certain, therefore, that the parent fluids for these deposits were the upwelled geothermal fluids.

Conclusions - Part III.

Issue - Origin of the Yucca Mountain "mosaic" breccias.

Interpretation options

I - all of the Yucca Mountain "mosaic" breccias are the so-called "pedogenic fragmentation breccias" [i.e., i) the calcite-silica matrix cement is developed via the *per descensum* pedogenic process; ii) the F-texture is produced through "forces of crystallization"; and iii) the breccia clasts are produced without fluid involvement].

II - all of the Yucca Mountain "mosaic" breccias are the so-called "hydrothermal eruption breccias", either fragmentation or explosive [i.e., i) the calcite-silica matrix cement is developed via the *per ascensum* process; ii) the F-texture indicates very rapid rates of the matrix cement formation; and iii) the bedrock clasts are produced with fluid pressure involvement]; and

III - the Yucca Mountain "mosaic" breccias are combined products of both of the above processes [i.e. i) some are the pedogenic fragementation breccias; and ii) some are the hydrothermal eruption breccias].

Statement of the issue - presentation #5.

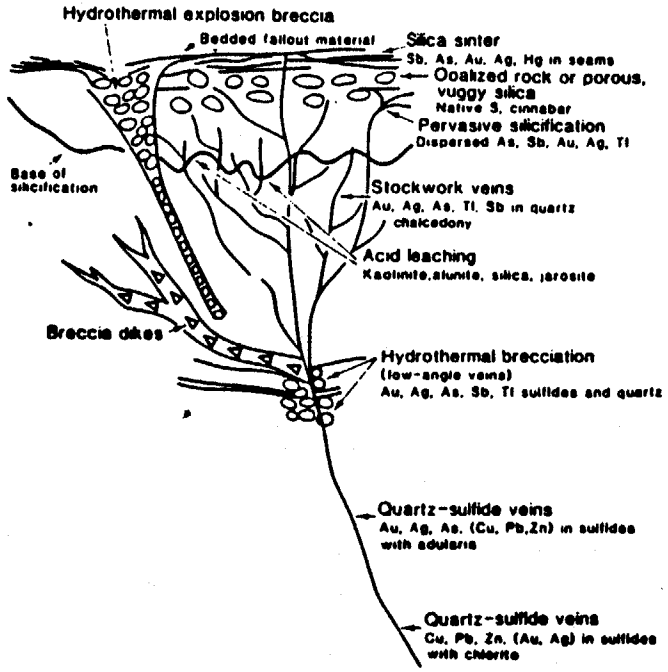

Note:

a) the vertical geothermal zoning, as depicted, is found in association with the hot-spring precious metal bearing deposits;

b) fluids that are involved in formation of both the extensive silicification and the hydrothermal brecciation does not have to carry significant concentrations of the path finders and the precious metals; and

c) the vertical geothermal zoning, as shown, does not need to be present in the Yucca Mountain area.

A possible mechanism for extensive silicification and brecciation, as observed in the Yucca Mountain area. From Berger (1985).

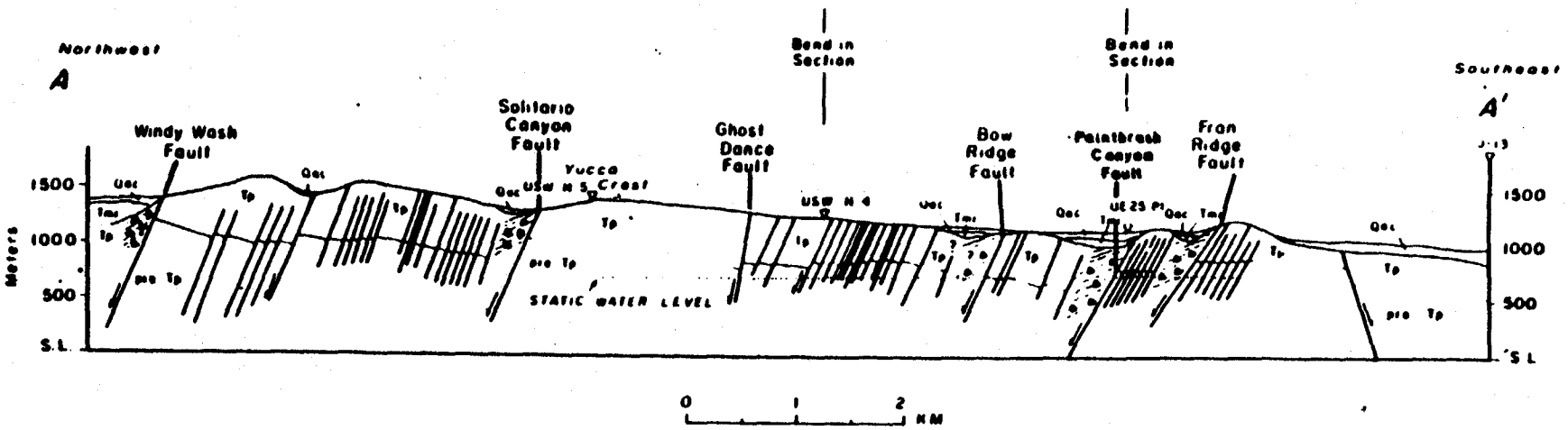

In making such a traverse, an observer would encounter five sizeable and youthful faults (Plates 3.3.2.3-4 and 3.3.2.3-5). These faults are a) the Fran Ridge Fault; b) the Paintbrush Fault; c) the Bow Ridge Fault; d) the Solitario Canyon Fault; and f) the Windy Wash Fault. The observer would also notice the presence of two types of thought provoking materials. These materials occur along traces of each of the local faults and consist of a) "mosaic" breccias; and b) veins and aprons composed of opaline silica, calcite, with minor sepiolite. The combined thickness of these materials relative to the total length of the traverse, is considerable (Plate 3.3.2.3-5)

from Szymanski (1989).

Geologic section across Yucca Mountain showing location and thickness of mosaic breccias. From Scott and Bonk, 1985.

The "mosaic" breccias consist of angular fragments of the country rock embedded in a matrix composed mainly of opaline silica and calcite. Remarkable characteristics of these breccias are: a) "matrix" support texture (individual clasts are not in direct contact with each other); b) very large volumetric strain, ranging from several percent to tens of percent; and c) very isotropic character of the volumetric strain (the amount of dilation is similar in all three mutually perpendicular directions). All of these characteristics indicate that the "mosaic" breccias are either "fragmentation" breccias or "explosive" breccias. The term "explosive" breccia is employed here to denote a breccia for which formation of the clasts and the matrix is the result of a common process and, in the case of clasts, requires large and fast build-ups of fluid pressure (e.g., hydrothermal eruptions, wallrock fragmentation of an active geothermal system by vibratory ground motion, and fragmentation of host rock caused by very rapid increases of the mean effective stress followed by the geothermal circulation of fluids.) In contrast, the term "fragmentation" breccia is used here to denote a breccia for which formation of the clasts and the matrix is the result of two independent processes occurring at the same time and place (e.g., mass wasting and filling-up of a bedrock opening within which minerals are precipitating from upwelling deep-seated fluids; and rapid cementation of a mass wasting fill of a topographic depression, whether structural or erosional, by mineral rich fluids discharging from nearby faults and fissures). Hanson et al., 1987, on the basis of field inspection, diagnosed the Yucca Mountain breccias as **"hydrothermal eruption breccias"**.

Characteristics of the "mosaic" breccias. From Szymanski (1989).

Another important characteristic of the "mosaic" breccias is their age. Although, little is known about this topic there are, however, some bases for constraining the problem. First, the "mosaic" breccias contain fragments of mineral products from the vapor phase mineralization and from devitrification of the country rock (Hanson et al., 1987). This suggests that the formation of "mosaic" breccias occurred after deposition of the country rock. This inference is supported by two other observations: a) "mosaic" breccias do not appear to be "stratum (ash sheet) bound"; and b) occurrences of these breccias are not restricted solely to pyroclastic materials, they also occur in carbonates of Paleozoic age. Second, the "mosaic" breccias commonly form wallrocks of the calcite-silica veins. Some of these veins extend from the bedrock into alluvium of Late Quaternary age.

Taken together, the above two cross-cutting relationships constrain the age formation of the "mosaic" breccias as between Late Miocene to Late Quaternary time. Recognizing the considerable thickness of these breccias and their age, relative to the time of solidification of the country rock, an additional inference may be drawn. This inference is that the "mosaic" breccias are polygenetic, and that they represent a considerable time span.

Characteristics of the "mosaic" breccias. From Szymanski (1989).

		Ag	As	Au	Cu	Hg	Mo	Pb	Sb	TL	Zn	Bi	Cd
Mean values - Yucca Mnt. [ppm]		0.026	3.07	0.001	6.88	<0.10	0.10	0.25	0.25	0.50	1.00	0.25	0.10
silicified "mosaic" breccia from Trench #14	north wall	0.034	7.93	0.004	7.15	0.122	0.507	7.75	<0.247	<0.494	23.0	0.504	<0.099
	north wall	0.423	110.0	0.005	27.9	0.700	65.3	154.0	24.6	<0.497	33.2	<0.249	2.12
	south wall	0.031	7.31	0.002	4.52	0.147	0.422	5.31	<0.245	<0.49	19.0	<0.245	<0.090

Our surface geochemical sampling of faults and fracture zones does, however, show weakly anomalous bismuth, zinc, lead, and molybdenum. Statistical analysis indicates correlations among these elements. The anomalous samples could represent a very distal geochemical halo around a concentration of base metals in the deep subsurface.

From Castor and Tingley, 1990.

Note:

a) the average base metal concentrations for the Yucca Mountain area are from Castor et al., (1989);

b) the base metal concentrations from samples of the Trench #14 "mosaic" brcccia are from Larson et al. (1988); and

c) the noticeably higher concentrations of the base metals, relative to the corresponding mean concentrations for the Yucca Mountain area, indicate that hydrothermal fluids were involved in formation of the Trench #14 "mosaic" breccias.

Base metal concentration for the Yucca Mountain area.

(expressed in parts per million)

	Ag	As	Au	Cu	Hg	Mo	Pb	Sb	Tl	Zn	Bi	Ga	Se	Te
1)	0.423	110	0.005	27.9	0.799	65.3	154	24.6	<0.49	33.2	<0.249	1.90	<0.995	<0.497
1a)	0.129	10.0	0.002	6.49	0.202	1.11	15.0	0.763	<0.487	44.6	<0.243	1.15	<0.973	<0.487
1b)	-	-	-	-	0.036	-	-	-	-	-	-	-	-	-
2)	0.048	15.6	0.004	11.1	0.373	1.23	16.4	10.1	<0.488	90.8	<0.244	<0.488	<0.977	<0.488
2a)	-	-	-	-	0.085	-	-	-	-	-	-	-	-	-
3)	<0.015	5.89	0.001	2.71	0.349	1.80	10.7	2.90	<0.498	147	<0.249	<0.498	<0.996	<0.498
3a)	-	-	-	-	0.012	-	-	-	-	-	-	-	-	-
4)	0.048	11.2	0.001	4.11	0.553	2.29	14.8	6.36	<0.492	75.5	<0.246	<0.492	<0.984	<0.492
4a)	-	-	-	-	0.048	-	-	-	-	-	-	-	-	-
5)	0.049	11.2	0.002	2.95	2.02	1.58	46.6	2.89	<0.492	892	<0.246	<0.492	<0.983	<0.492
5a)	-	-	-	-	0.012	-	-	-	-	-	-	-	-	-
6)	0.141	14.1	0.001	14.4	3.08	2.54	78.6	8.69	<0.487	344	<0.244	<0.487	<0.975	<0.487
6a)	-	-	-	-	0.024	-	-	-	-	-	-	-	-	-
7)	0.054	1.77	0.001	2.35	0.160	0.759	3.27	<0.247	<0.494	50.0	<0.247	0.845	<0.987	<0.494
7a)	0.054	1.83	<0.0005	3.11	0.185	0.686	3.49	<0.245	<0.49	46.3	<0.245	0.799	<0.979	<0.49
7b)	0.049	1.57	0.001	1.68	0.170	0.637	2.93	<0.25	<0.5	49.4	<0.25	0.576	<0.999	<0.5
7c)	-	-	-	-	<0.050	-	-	-	-	-	-	-	-	-
8)	0.04	3.09	<0.0005	1.28	0.214	0.688	4.02	<0.245	<0.49	41.1	<0.245	0.606	<0.979	<0.49
8a)	0.055	3.05	<0.0005	1.31	0.184	0.712	4.02	<0.248	0.523	44.0	<0.248	0.684	<0.992	<0.49
8b)	0.053	3.51	0.001	1.57	0.177	0.883	4.31	<0.245	<0.491	44.7	<0.245	0.650	<0.982	<0.49
8c)	-	-	-	-	<0.050	-	-	-	-	-	-	-	-	-
9)	0.048	4.34	<0.0005	1.23	0.154	0.703	3.68	<0.247	<0.494	43.1	<0.247	0.535	<0.989	<0.494
9a)	0.051	3.84	<0.0005	1.17	0.178	0.698	3.60	<0.244	<0.488	38.8	<0.244	0.524	<0.976	<0.488
9b)	0.047	4.09	<0.0005	1.16	0.171	0.680	3.49	<0.246	<0.491	41.1	<0.246	0.559	<0.982	<0.491
9c)	-	-	-	-	<0.050	-	-	-	-	-	-	-	-	-

1) [x]3SW195B: north wall, fractured Tiva Canyon Member with weak silicification, ± drusy quartz in lithophysae, analysis from Weiss et al. (1989). **

1a) Split of hand-sample remaining from 3SW-195B. **

1b) [z] Later split of hand-sample remaining from 3SW-195B.

2) [x]3SW329: south wall, siliceous buff to white carbonate vein filling. *

2a) [z]Split of hand-sample remaining from 3SW329.

3) [x]3SW331: south wall, dark purplish, silicified breccia of Tiva Canyon Member between calcareous veins. *

3a) [z]Split of hand-sample remaining from 3SW331.

4) [x]3SW333: south wall, siliceous margin of 1-2 cm thick white calcareous vein. Margin is composed of buff to light brown silica vein material containing small, dark colored, silica-replaced fragments of Tiva Canyon Member. *

4a) [z]Split of hand-sample remaining from 3SW333.

5) [x]3SW335: north wall, silicified breccia of Tiva Canyon Member with bleached groundmass surrounding drusy quartz-lined lithophysal cavities, _ 2 meters east of thick, white, calcareous vein. *

5a) [z]Split of hand-sample remaining from 3SW335.

6) [x]3LT029: south wall, silicified breccia of Tiva Canyon Member, purplish rock fragments in buff siliceous matrix. *

6a) [z]Split of hand-sample remaining from 3LT029.

7) 3SW433; dense, lithophysal Tiva Canyon Member, east side of Exile Hill. **

7a) Duplicate split of 3SW433. **

7b) Triplicate split of 3SW433. **

7c) [z]Split of hand-sample remaining from 3SW433.

8) 3SW435; dense, lithophysal Tiva Canyon Member, east side of Exile Hill. **

8a) Duplicate split of 3SW435. **

8b) Triplicate splite of 3SW435. **

8c) [z]Split of hand-sample remaining from 3SW435.

9) 3SW437; dense, lithophysal Tiva Canyon Member, east side of Exile Hill. **

9a) Duplicate split of 3SW437. **

9b) Triplicate split of 3SW437. **

9c) [z]Split of hand-sample remaining from 3SW437.

Except as noted, analyses by Geochemical Services Inc., using inductively-coupled plasma emission spectrography; * = 10 gram digestion; ** = 15 gram digestion. Values as reported by G.S.I.; number of significant figures does not indicate precision or accuracy of analyses.

[x] denotes analyses from Weiss et al. (1989b).

[z] denotes mercury analyses by the Nevada Mining and Analytical Laboratory, Nevada Bureau of Mines and Geology, using atomic absorption methods.

Precious metals and indicator-element abundences - rock-chip samples from Trench #14 and vicinity.
From Weiss et al. (1990).

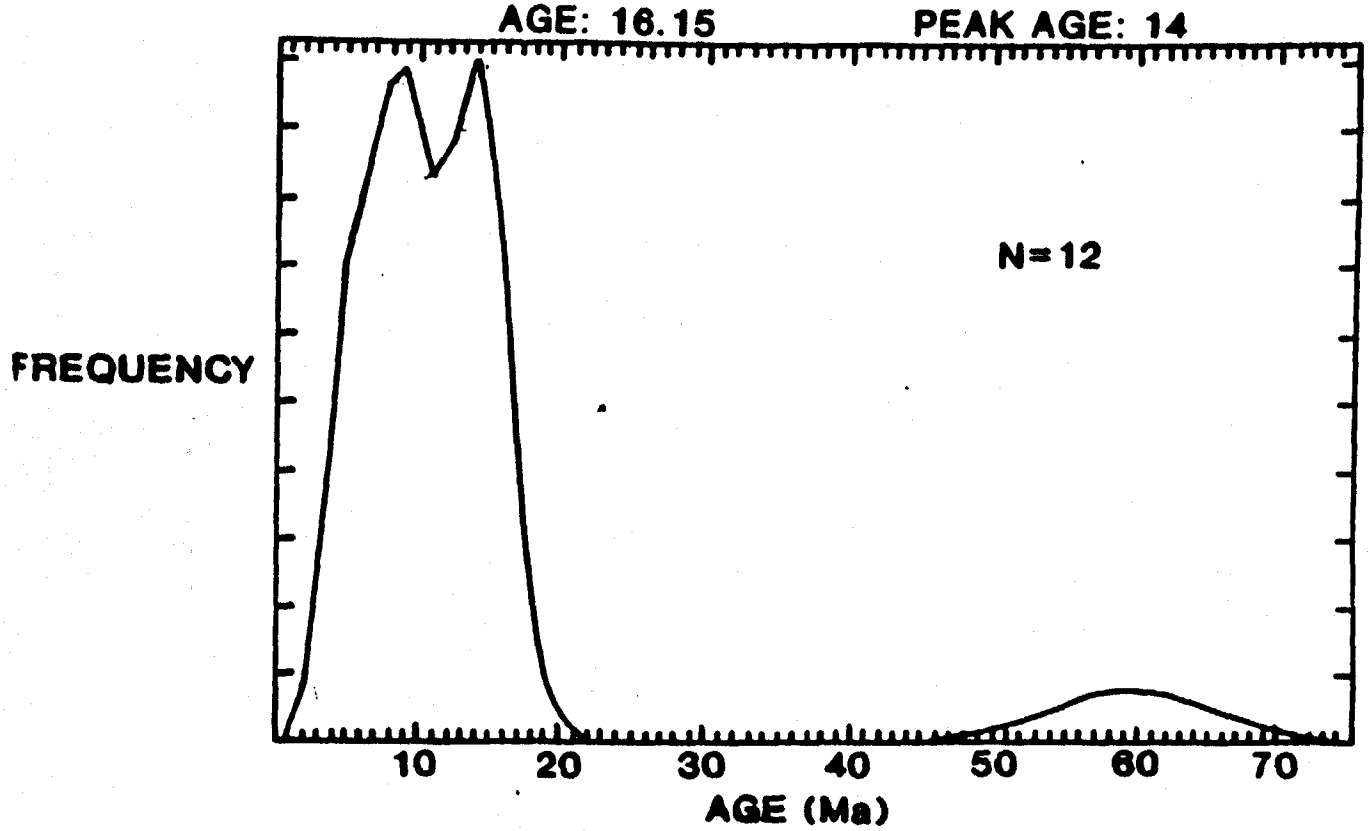

Note:

a) presence of zircons with the fission track ages substantially different than the age of emplacement of the country rock indicates that, the zircons hosting "mosaic" breccias were formed after emplacement and solidification of the tuff "pile"; and

b) presence of zircons with the fairly young fission track ages (say less than 7 x 10^6 years B.P.) indicates that either i) the "mosaic" breccias are of the Plio-Quaternary age or ii) the "mosaic" breccias are polygenetic and partially were formed during the Plio-Quaternary time.

Fission - track ages - samples of the "mosaic" breccias from Busted Butte. From Naeser (1990).

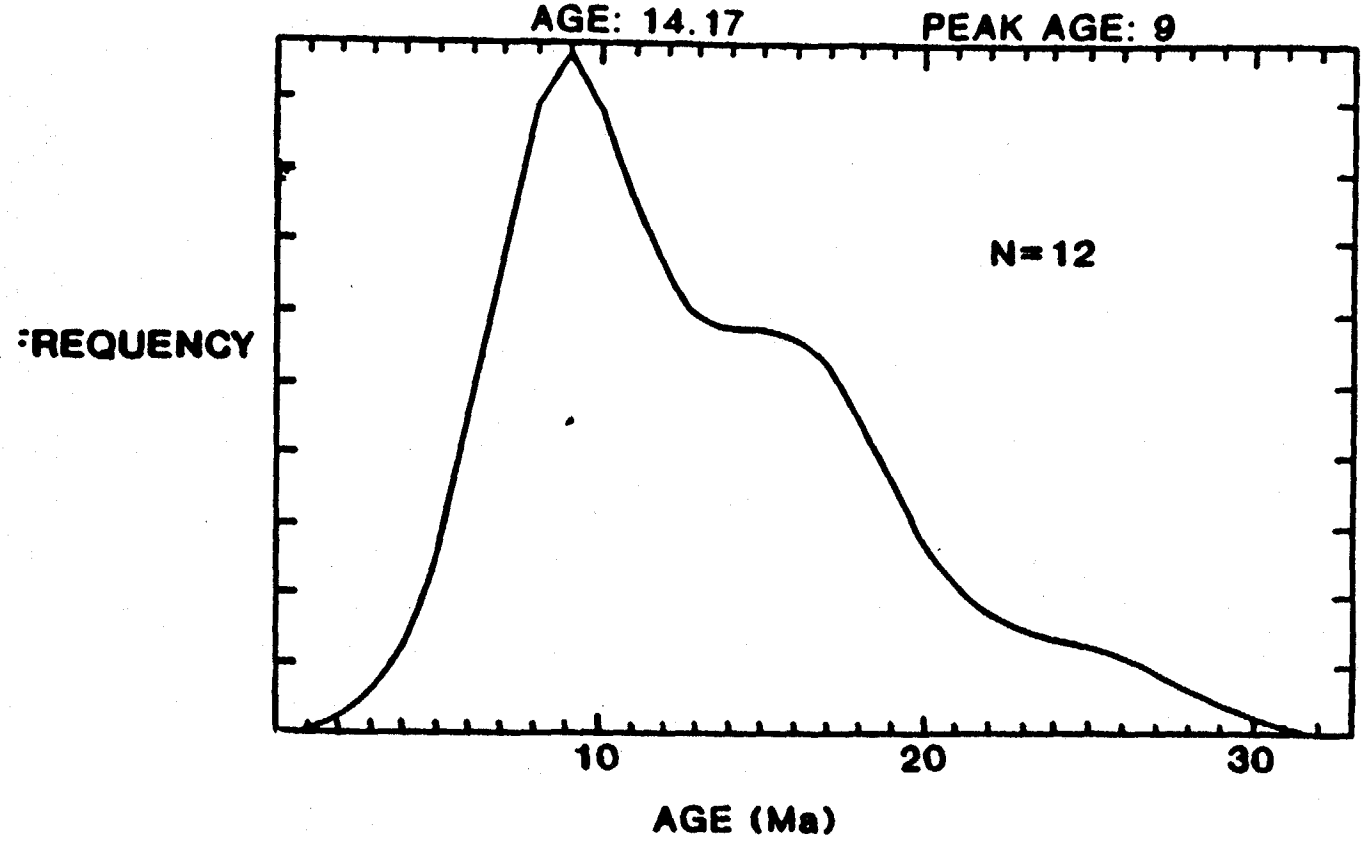

Note:

a) presence of zircons with the fission track ages substantially different than the age of emplacement of the country rock indicates that, the zircons hosting "mosaic" breccias were formed after emplacement and solidification of the tuff "pile"; and

b) presence of zircons with the fairly young fission track ages (say less than 7 x 10^6 years B.P.) indicates that either i) the "mosaic" breccias are of the Plio-Quaternary age or ii) the "mosaic" breccias are polygenetic and partially were formed during the Plio-Quaternary time.

Fission - track ages - samples of the "mosaic" breccia from Trench #14. From Naeser (1990).

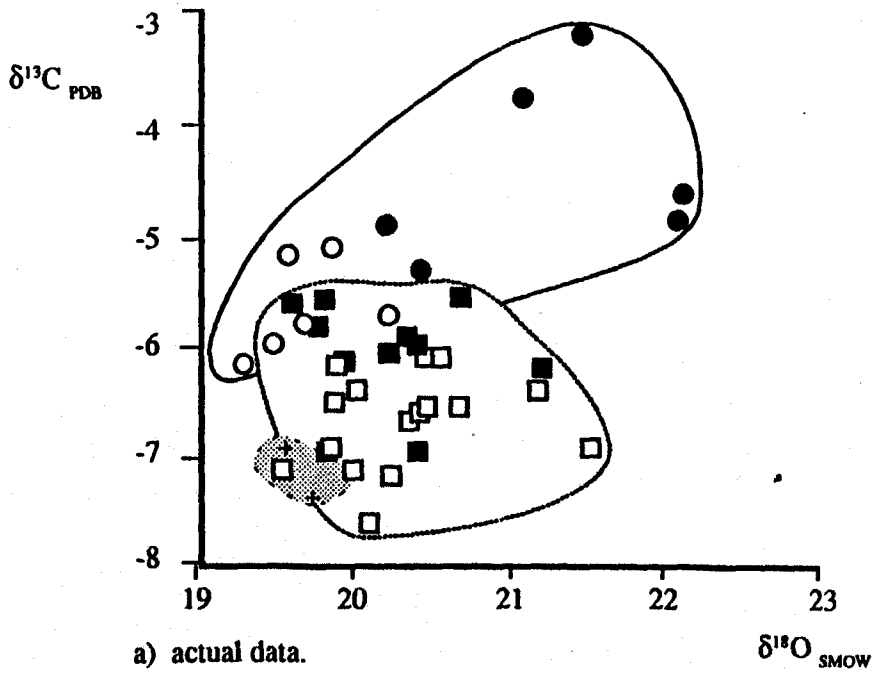

a) actual data.

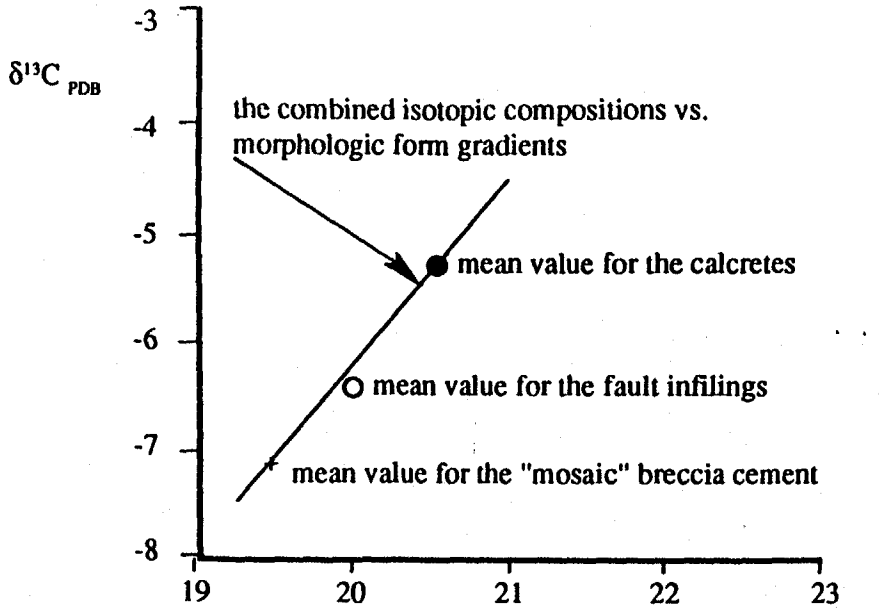

b) mean values.

Explanation:

■ and ● - sample represents the Yucca Mountain calcretes;

□ and ○ - sample represents the Yucca Mountain fault infiling; and

\+ - sample represents the Yucca Mountain "mosaic" breccia.

The isotopic compositions vs. morphological form gradients, the Yucca Mountain calcite-silica deposits.

Figure 5-9a

Note:

a) the isotopic data are from Whelan and Stuckless (1990);

b) the Yucca Mountain calcite-opaline silica deposits occur as three morphological varieties, namely: i) the "mosaic" breccia cement; ii) the fault infilings, and iii) the calcretes;

c) the $\delta^{18}O$ vs $\delta^{13}C$ fields from the distinguished morphological forms are sufficiently similar to assume that all of these forms were precipitated in the parent fluids which, in the pristine state, have carried similar values of the $\delta^{13}C$ vs $\delta^{18}O$ ratio;

d) it may reasonably be assumed that: i) the degree of departure from the pristine state, resulting from either the oxygen -18 evaporative enrichment or the carbon -13 diffusional enrichment, was the lowest for the parent fluids of the "mosaic" breccia cement, somewhat higher for the parent fluids of the fault infilings, and still higher for the parent fluids of the calcretes; and ii) the mineral precipitation temperatures were the highest for the "mosaic" breccia cement, somewhat lower for the fault infilings, and still lower for the calcretes;

e) the observed isotopic compositions vs. morphological form gradients may reasonably be taken as indicating: i) for the oxygen -18 gradient, the combined influence of the mineral precipitation temperature and the oxygen-18 evaporative enrichment, and ii) for the carbon -13 gradient, the carbon -13 diffusional enrichment; and

f) the observed isotopic compositions vs. morphological form gradients are consistant with the *per ascensum* origin of the Yucca Mountain calcite-silica deposits - similarily as is the case for the Amargosa Basin deposits, the Yucca Mountain distal calcretes are isotopically "heavier" than their proximal counterparts.

The isotopic compositions vs. morphological form gradients, the Yucca Mountain calcite-silica deposits. (continued)

Overall Conclusions

The already available geochemical and isotopic data indicate that:

i) apart from the wishful thinking, there is no rational bases to regard some or all of the Yucca Mountain "mosaic" breccias as the "pedogenic fragmentation breccias";

ii) there is no rational bases to regard the majority of the Yucca Mountain "mosaic" breccias as syn-depositional with emplacement of the local tuff "pile";

iii) the Yucca Mountain "mosaic" breccias may reasonably be regarded as the epigenetic "hydrothermal eruption breccias", either explosive or fragmentation; and

iv) most likely, the Yucca Mountain "mosaic" breccias are polygenetic, their development appears to be an ongoing process (some of the "mosaic" breccias may be of the Plio-Quaternary age).

Note:

a) presence of zircons with the fairly young fission track ages **demands** an answer regarding circumstances of the zircons introduction into the separated fault openings;

b) a particularly alarming possibility is that, the thermally reset zircons are **indigenous** to the Yucca Mountain area and are related to fairly young silicic injections; and

c) the direct field observations indicate, that, at Yucca Mountain, the silicic injections are present. [such injections are younger than oxidation of the welded tuffs from either the Tive Canyon Member of the Topopah Spring Member; however, no upper age limit is apparent.]

Conclusions - presentation #5.

Figure 5-10

Issue - Origin of carbon that: a) is contained in carbon dioxide respired from the Yucca Mountain vadose zone; and b) is dissolved in the Nevada Test Site hydrosphere.

Interpretation options

I - all carbon is derived solely from the atmosphere-biosphere source (conventional wisdom); and

II - a) the vadose zone CO_2 is a two end-member mixture [a) CO_2 from the atmosphere-biosphere source; and b) CO_2 from degassing of the upwelling hydraulic "source" fluids]; and

b) carbon dissolved in the hydrosphere originates from three distinct sources, each with spatially varying importance [a) CO_2 from the atmosphere-biosphere source; b) carbon acquired through dissolution of the Paleozoic carbonates; and c) CO_2 produced through degassing of deep-seated igneous bodies] (J.S.S. proposition).

Statement of the issue - presentation #6.

Figure 6-1

Part I - Origin of carbon dioxide respired from the Yucca Mountain vadose zone.

Part I - title page

Figure 6-2

- Quade and Cerling (1990) have performed their carbon isotopic analyses of the cobble encrustations, and of the Yucca Mountain calcretes and surficial veins, assuming that all carbon contained in vadose zone gases and dissolved in subsurface fluids originates solely from the atmosphere-biosphere source.

- This is a reasonable assumption but only for terrains that are devoid of: a) carbonate and other carbon bearing rocks; and b) Plio-Quaternary volcanism. At the Nevada Test Site, however, there is direct and clear evidence that both of these complicating circumstances are present.

- In the absence of evidence to the contrary and recognizing that the Nevada Test Site upwelling hydraulic "source" fluids carry values of the calcite saturation index log (Q/K) > 0, it is only prudent to expect that, in the Yucca Mountain vadose zone, the resident CO_2 may be a three end-members mixture. The potential end-members are: i) the atmospheric CO_2 - mean value of the $\delta^{13}C$ ratio is -7.0 per mil $_{PDB}$, Keeling (1961); ii) the biogenically derived CO_2 - mean value of the $\delta^{13}C$ ratio is -24 per mil $_{PDB}$, for ~ 85 percent biomass with the C-3 metabolic pathway; and iii) the subterranean CO_2 - for volcanic and geothermal areas, value of the $\delta^{13}C$ ratio ranges from 0 to -9 per mil $_{PDB}$, Deines (1980).

General remarks - interpretation of the origin of CO_2 respired from the Yucca Mountain vadose zone.

- Interpretations of the results of studies of spatio-temporal distribution of the carbon indexes ($\delta^{13}C$, PMC, and log P_{CO_2}), from samples of the Yucca Mountain vadose zone CO_2, must be made recognizing that, at the vadose zone base, there are very substantial lateral temperature gradients, dT/dx 10°Celsius per 1km.

- The lateral temperature gradients, with the observed magnitudes, virtually assure that, in the Yucca Mountain vadose zone, convective circulations of gaseous phases are taking place.

- Fluctuations involving both the barometric pressure and the atmospheric temperature virtually assure that the convective circulations occur as the non-periodic flow, Lorentz (1963);

- It may be expected, therefore, that $\sigma\phi_{xyz(t)} \neq 0$ [for a given sampling site, $\sigma\phi_{xyz(t)}$ denotes amplitude of fluctuations involving either the $\delta^{13}C$ ratio, the PMC index, or the log P_{CO_2} index].

Introduction - interpretation of the results of studies of spatio-temporal distribution of the carbon indexes in the Yucca Mountain vadose zone.

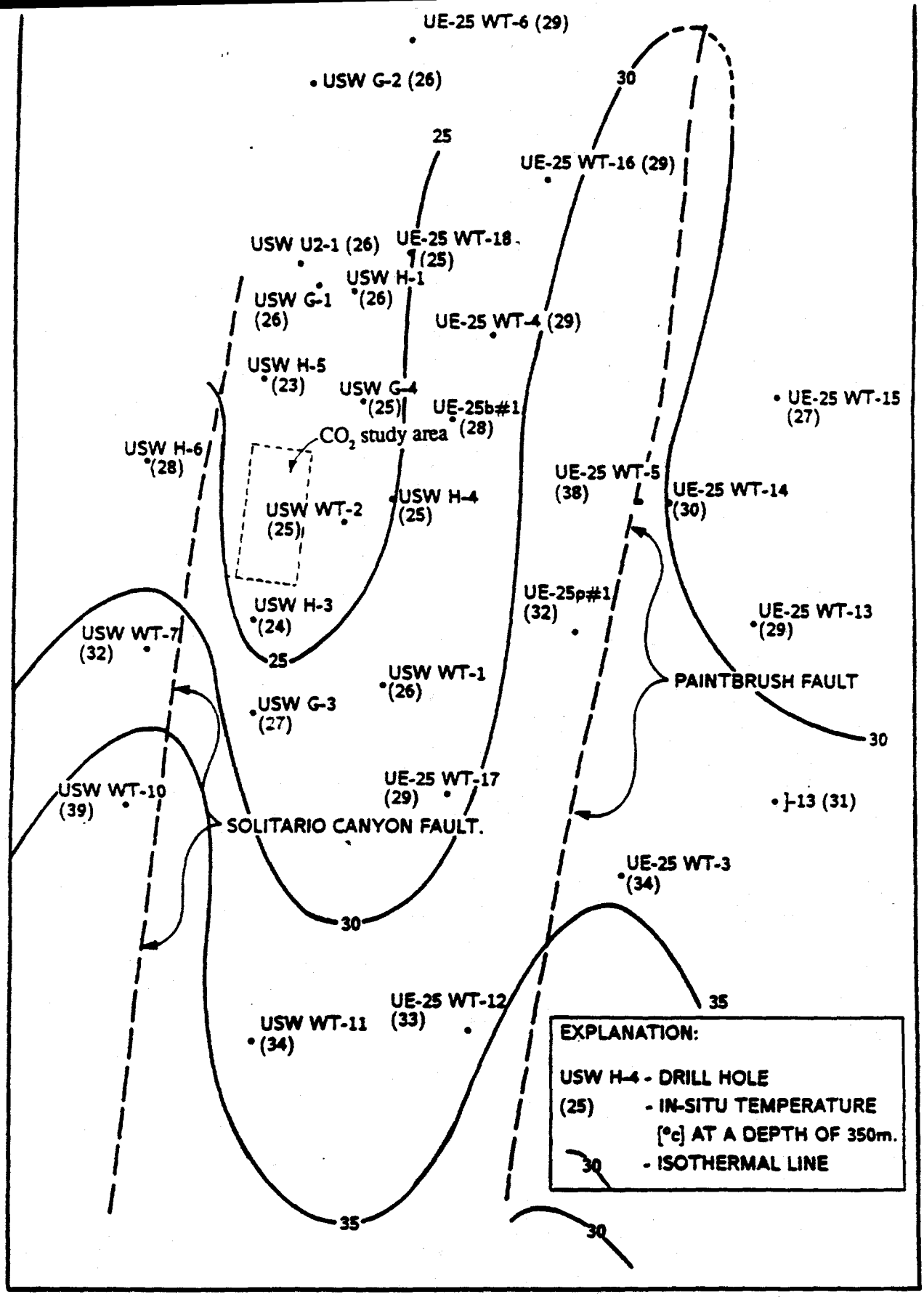

Location of the CO_2 study area. Relative to *in-situ* temperatures at a depth of 350 m. Yucca Mountain - vadose zone. From Szymanski, 1989.

Figure 6-5

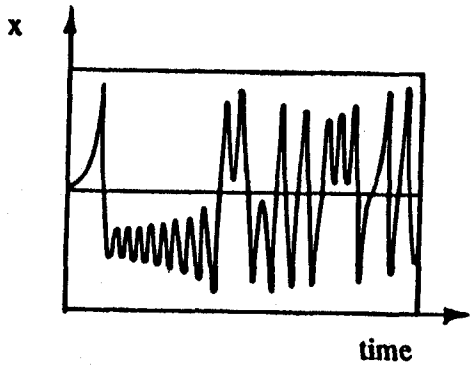

a) time-series

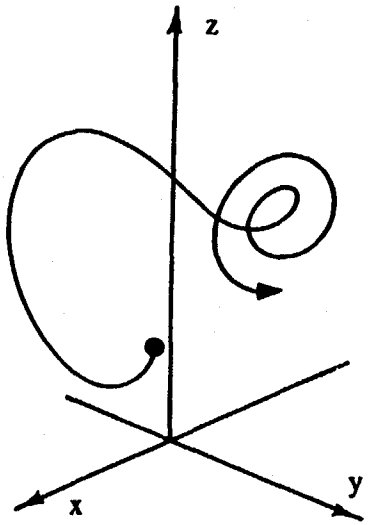

b) phase-space representation

Note:

a) $dx/dt = -\sigma x + \sigma y$, $dy/dt = Rx - y - xz$, and $dz/dt = -bz + xy$ - Lorentz's equations from Kelis-Borok (1990);

b) fluctuations x, y, z characterize the intensity of convection stream, horizontal and vertical temperature gradients, respectively;

c) σ, b, and R are numerical parameters; and

d) dx/dt controls values of the $\delta^{13}C$ ratio, the PMC index, and the partial pressure log P_{CO_2}.

Non-periodic convective flow. Modified from Gleick (1987) and Kelis-Borok (1990).

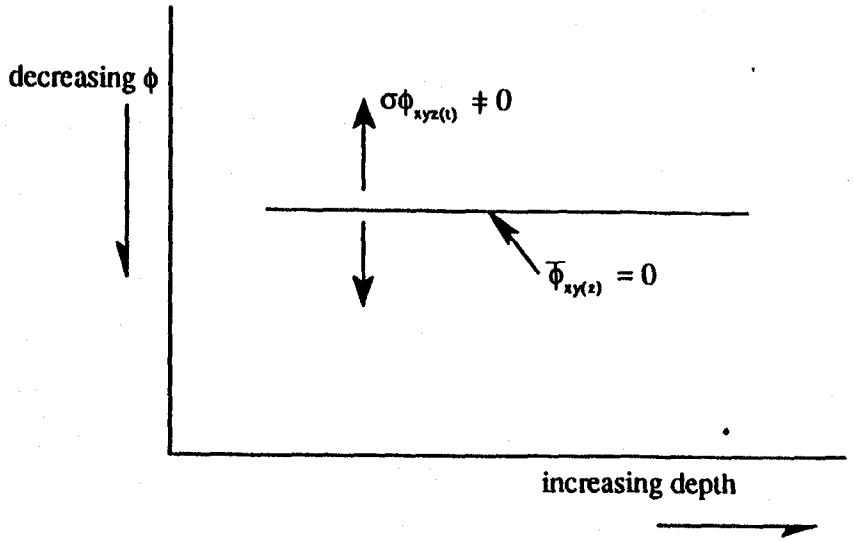

a) CO_2 originates solely from the atmosphere-biosphere source.

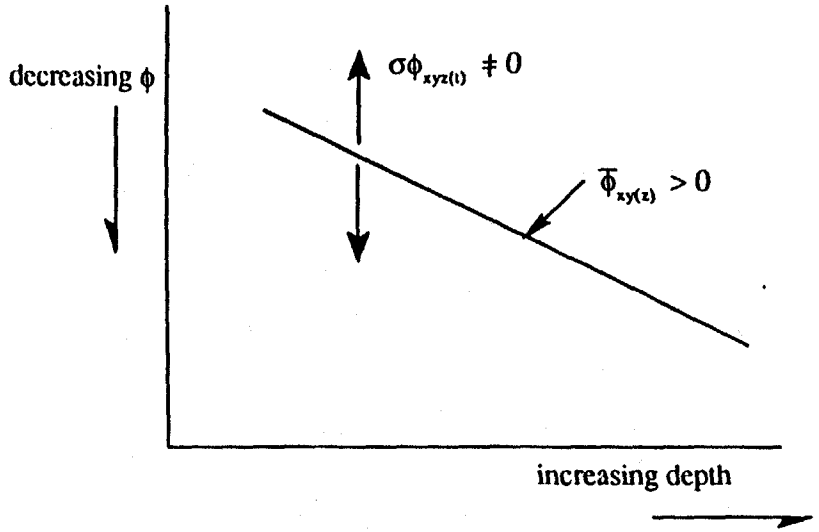

b) CO_2 originates from both the atmospher-biosphere source and the subterranean source.

Explanation:

ϕ - denotes value of either the $|\delta^{13}C|$ ratio or the PMC index, $\overline{\phi}$ denotes mean value;

$\overline{\phi}_{xy(z)}$ - denotes $\overline{\phi}$ vs depth gradient, for a given vertical reference profile; and

$\sigma\phi_{xyz(t)}$ - denotes amplitude of ϕ fluctuations, for a given reference point.

Note:

a) the subterranean source yields CO_2 that, relative to the atmosphere-biosphere derived CO_2, contains smaller concentrations of carbon-14 and carbon-12.

Interpretation key - origin of CO_2 respired from the Yucca Mountain vadose zone.

Figure 6-7

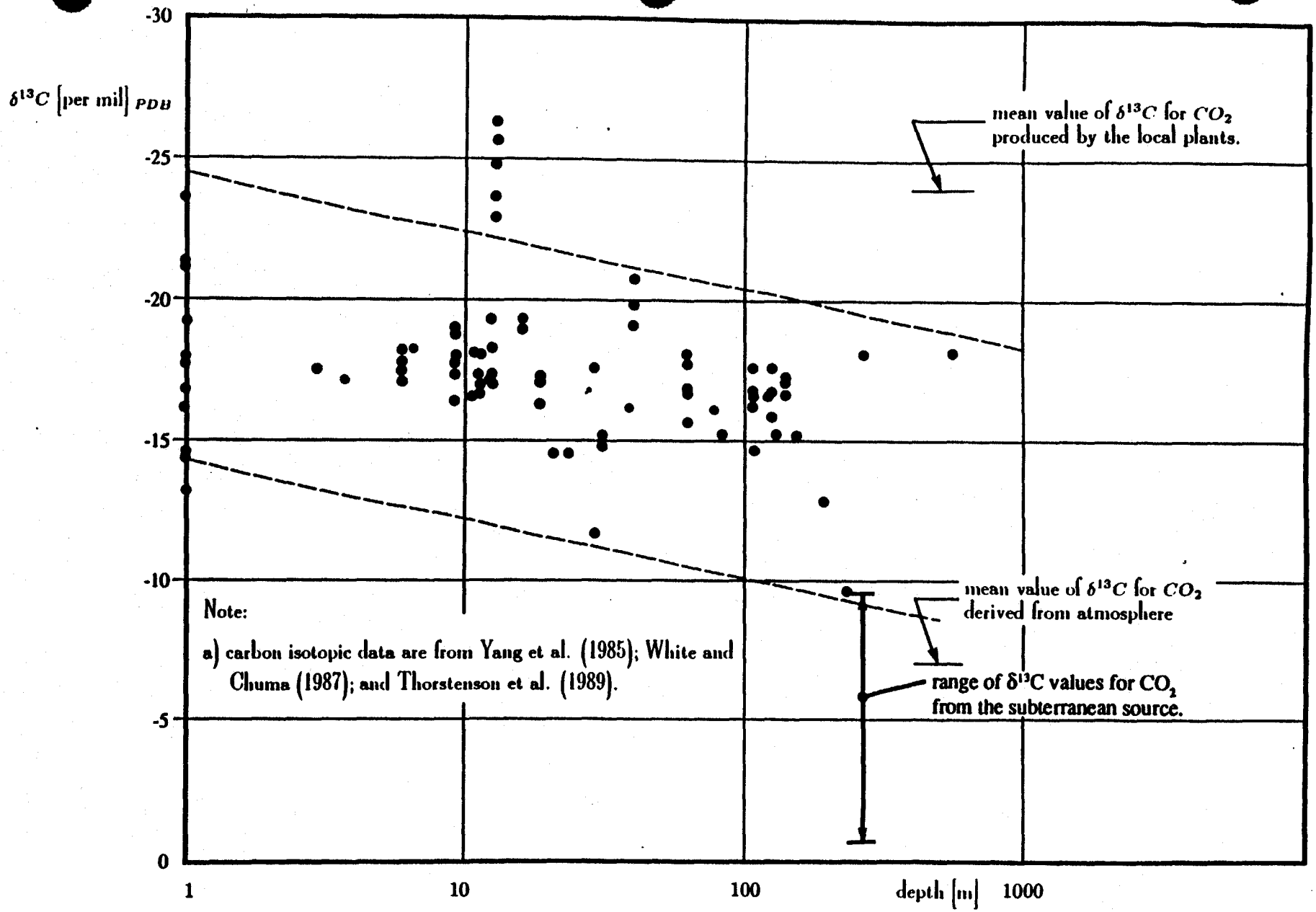

Isotopic character of carbon contained in carbon dioxide from the vadose zone as a function of depth.

Figure 6 8

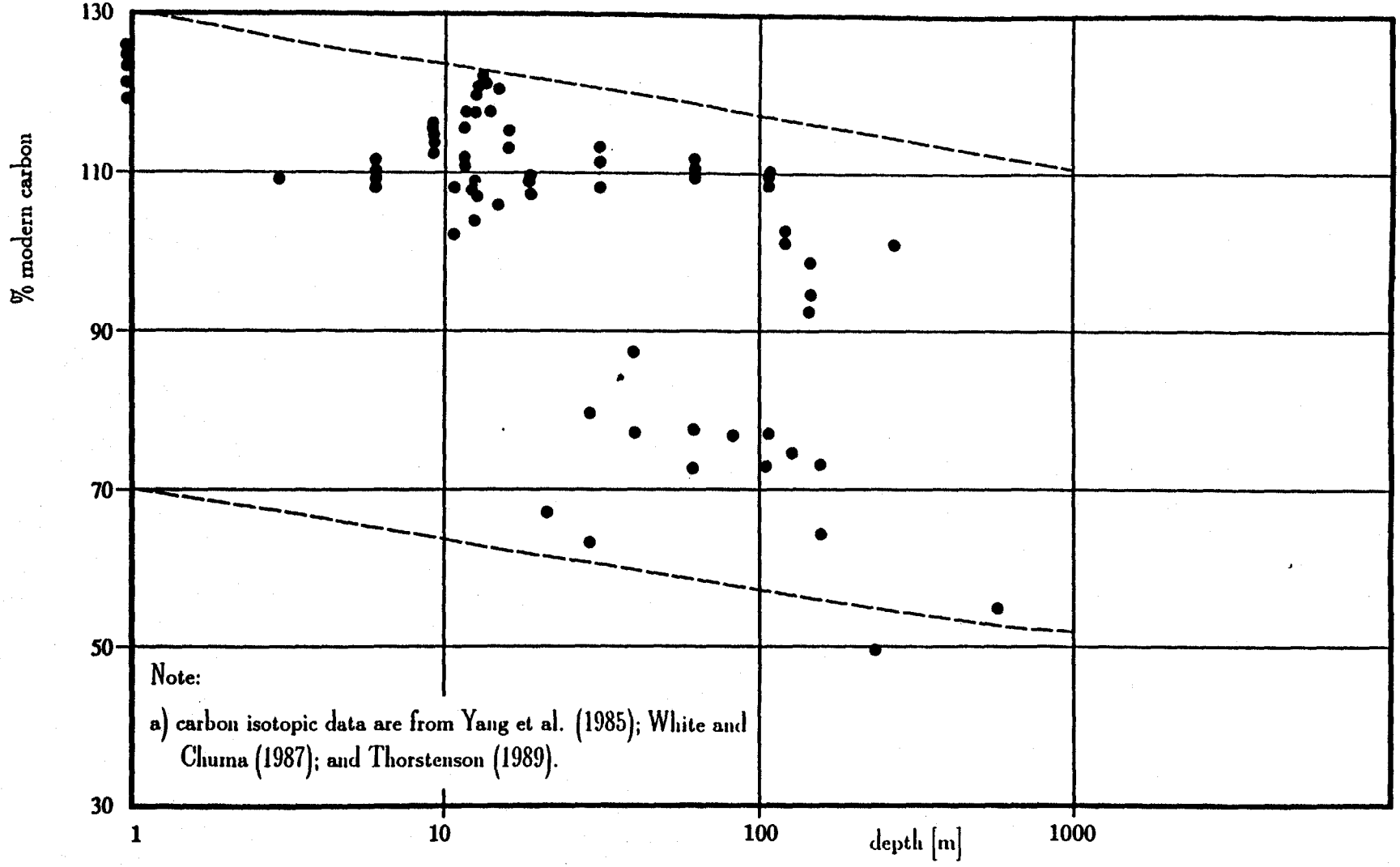

^{14}C content in carbon dioxide from the vadose zone as a function of depth.

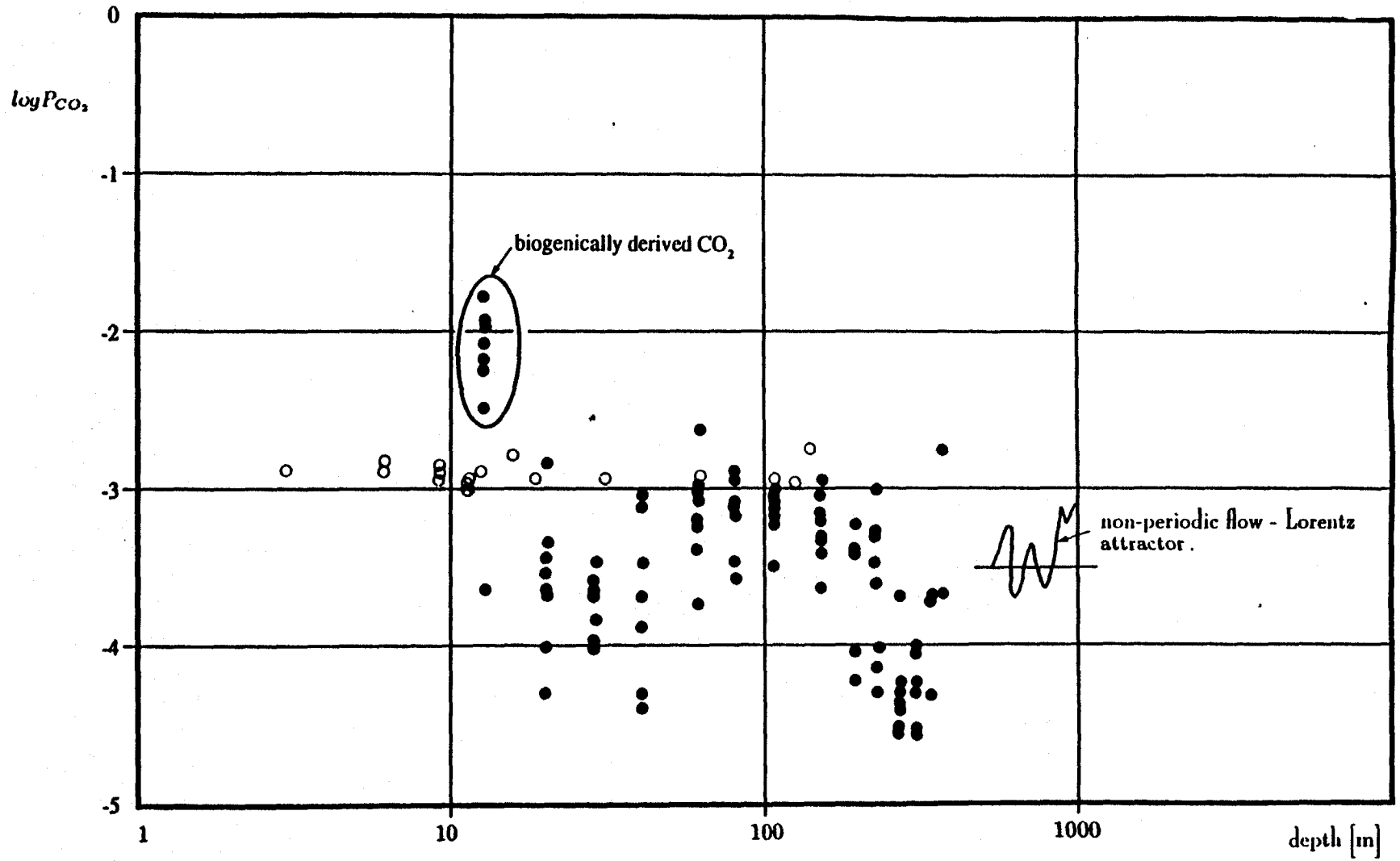

Explanation:

- USW UZ-1 - time history, period from November 1983 to June 1985, see Yang et al. (1989) for details; and
- UZ6S and N-borehole data represent one-time measurements.

$logP_{CO_2}$ as a function of depth and time. Carbon dioxide from the Yucca Mountain vadose zone

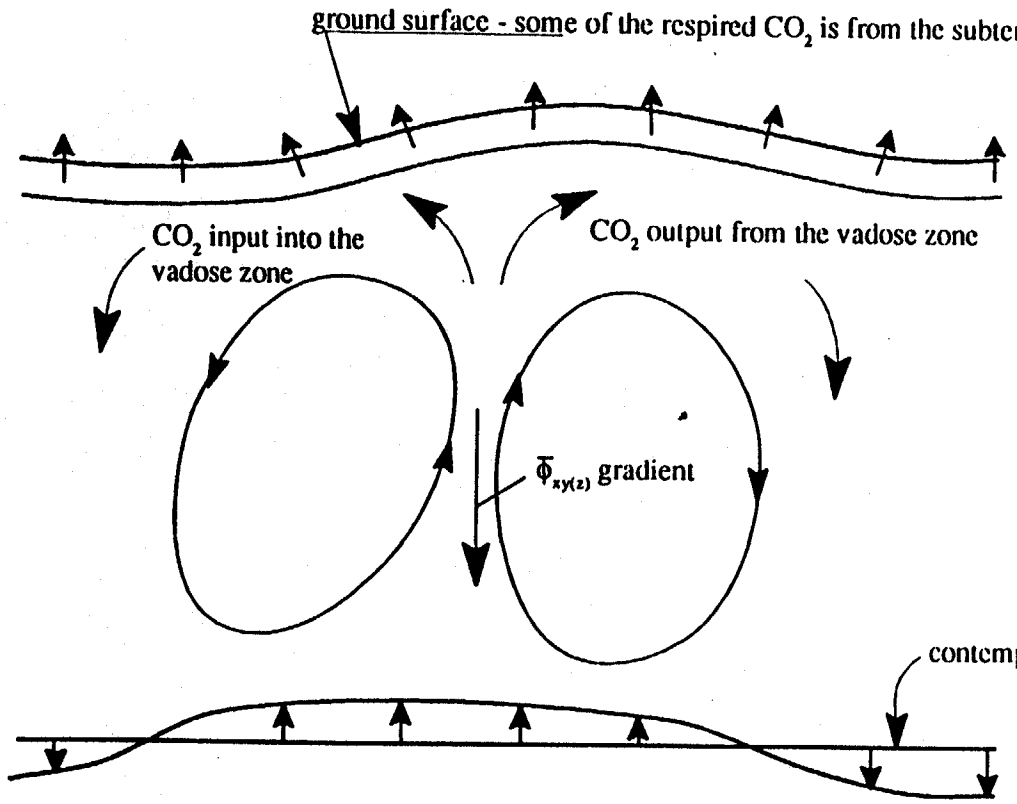

The atmosphere-biosphere CO_2 source - value of the $\delta^{13}C$ ratio ranges from say -15 to -24 per mil $_{PDB}$, and PMC > 100 percent.

Non-periodic flow of gaseous phases - lacks spatio-temporal consistency.

The subterranean CO_2 "source", in line with the CO_2 "sink" [for the subterranean CO_2 source - value of the $\delta^{13}C$ ratio may range from -1 to -9 per mil $_{PDB}$; and PMC $\rightarrow$ 0 percent].

for the "source" region, dT/dx $\rightarrow$ 10°C per 1km.

for the "sink" region, dT/dx $\rightarrow$ 0°C per 1km.

Conceptual understanding, spatio-temporal distribution of the carbon indexes - the Yucca Mountain vadose zone.

Part II - Origin of carbon dissolved in the Nevada Test Site subsurface fluids, from below the water table.

Part II - title page

Figure 6-12

- The spatial analyses of the chemical and carbon isotopic data, from samples of the Nevada Test Site subsurface fluids, lead to the following observations:

  i) at the Nevada Test Site, there is a positive log P_{CO_2} gradient from hydrosphere → vadose zone → atmosphere, but not vice versa;

  ii) fluids residing in the Nevada Test Site hydraulic "source" regions are supersaturated with respect to calcite, while their "sink" counterparts are undersaturated;

  iii) relative to the hydraulic "sink" fluids, fluids residing in the hydraulic "source" regions carry considerably lower concentrations of carbon-14;

  iv) relative to the hydraulic "sink" fluids, fluids residing in the hydraulic "source" regions carry noticeably higher values of the $\delta^{13}C$ ratio;

  v) relative to the tuff "pile" based fluids, fluids residing in the Paleozoic carbonates carry noticeably higher values of the $\delta^{13}C$ ratio; and

  vi) the Paleozoic carbonates based fluids carry values of the $\delta^{13}C$ ratio that are conspicuously lower than values expected for fluids equilibrated with the marine limestones.

Observations resulting from the carbon analyses of samples of the Nevada Test Site subsurface fluids.

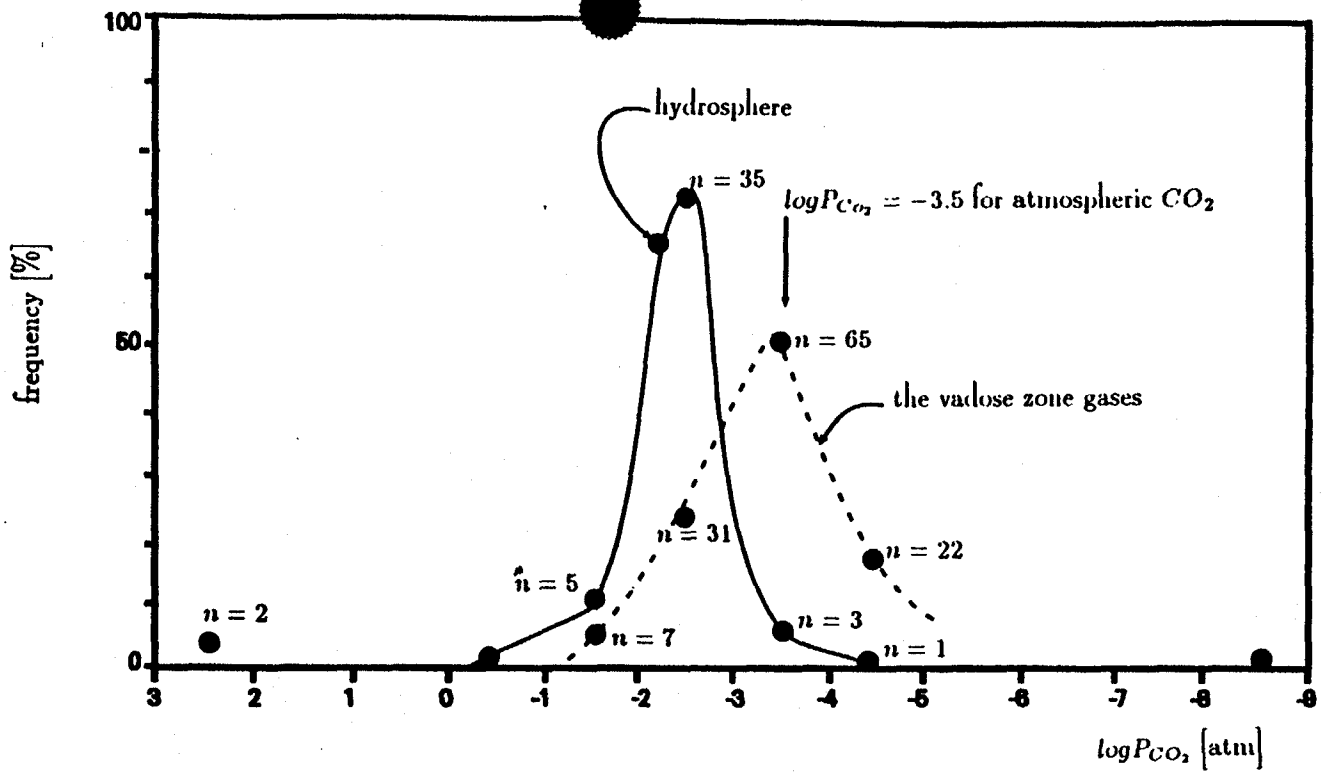

Note:

a) N = 47 samples for the hydrosphere, N = 125 for the vadose zone; and

b) $logP_{CO_2}$ data from the vadose zone and from the hydrosphere are from White and Chuma (1978), Yang et al. (1985), Thordarson et al. (1989), and Kerrisk (1987).

Histogram. Partial pressure of $C0_2$. The Nevada Test Site hydrosphere.

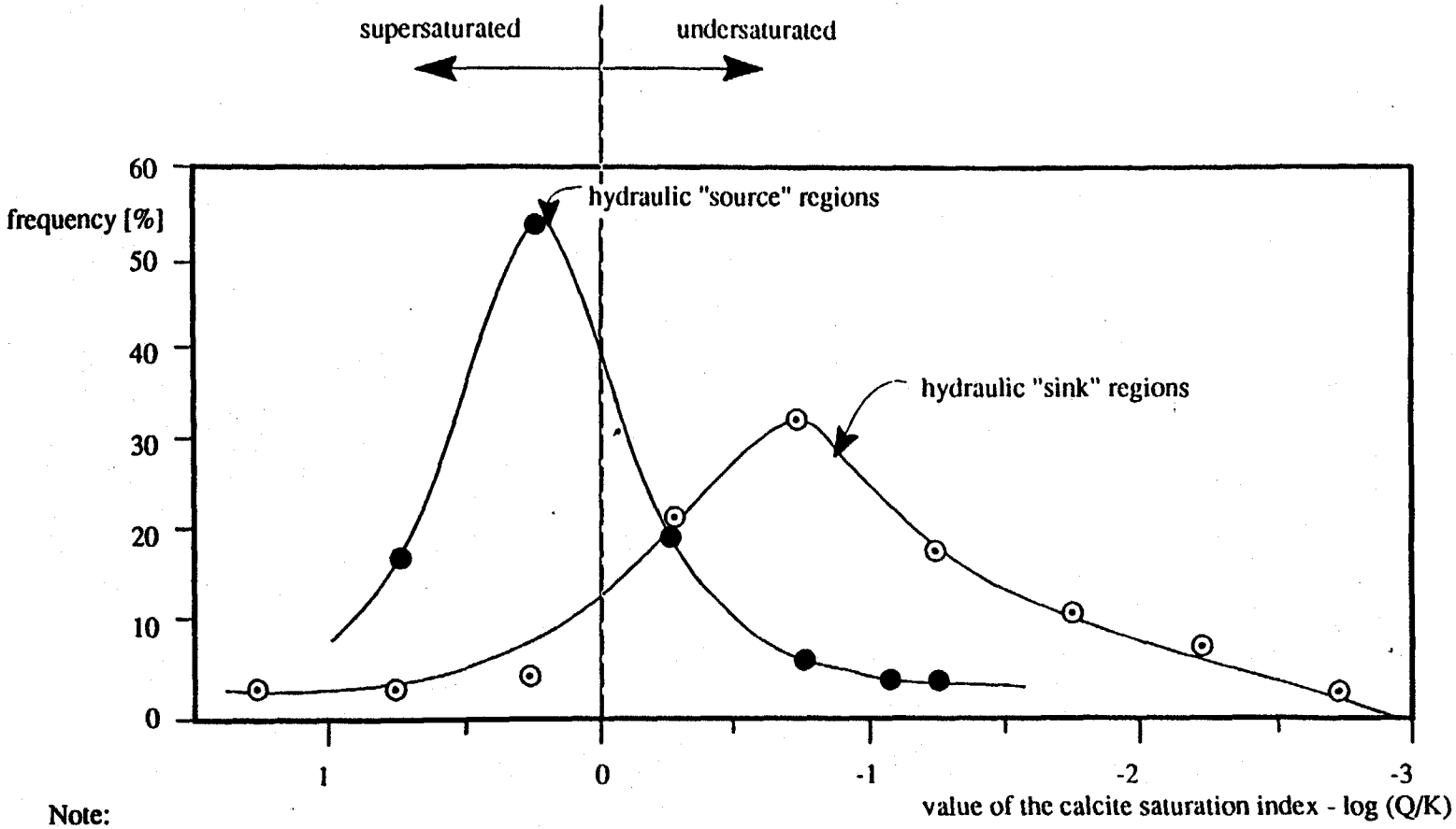

Note:

a) log (Q/K) data are from Kerrisk (1987);

b) N = 52 for hydraulic "source" regions; N = 64 for hydraulic "sink" regions; and

c) Q - the ion activity product, K - the equilibrium constant for the solubility reaction.

Calcite saturation index. Water samples from the Nevada Test Site hydraulic "sink" and "source" regions.

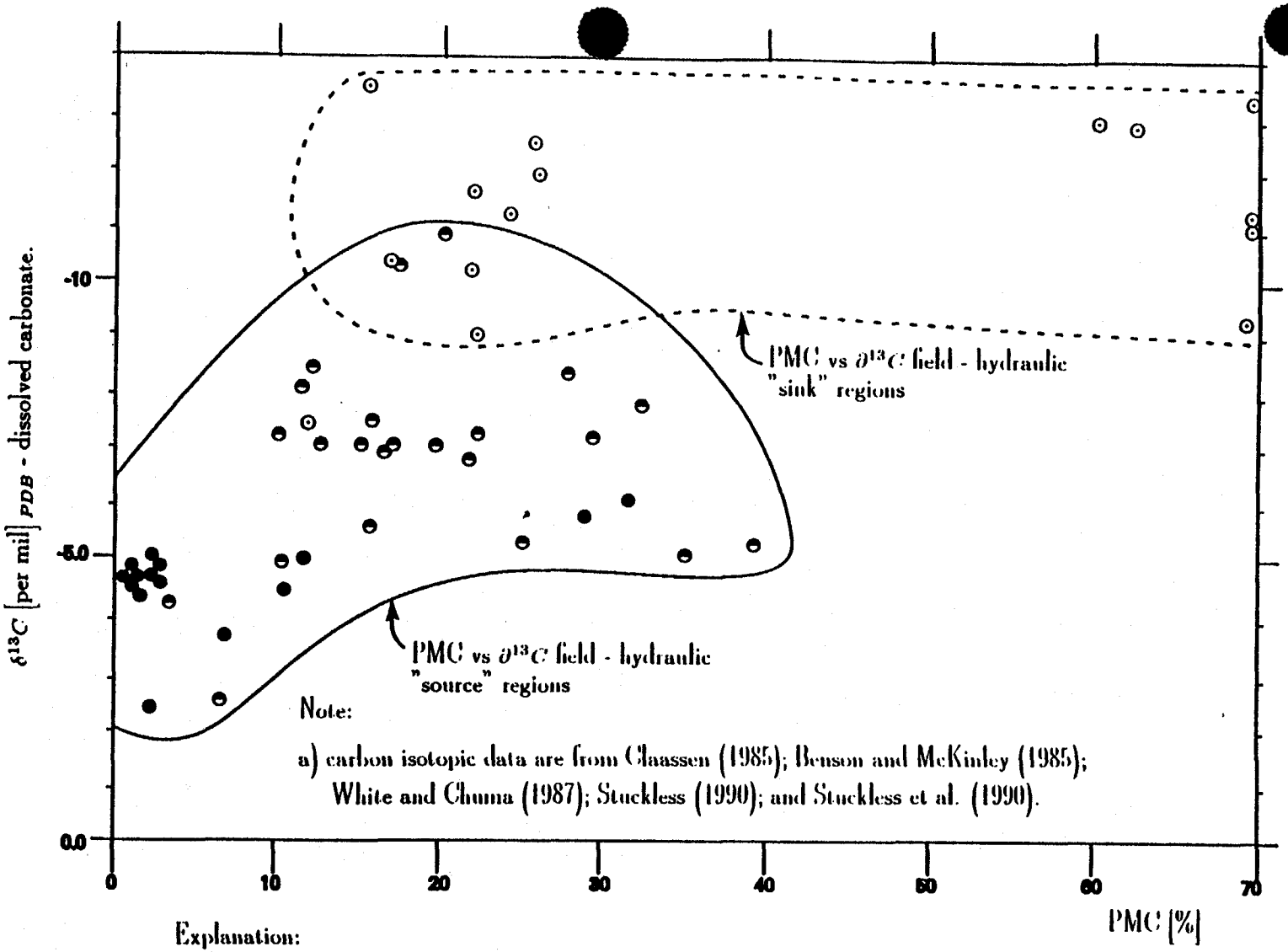

Explanation:

- ○ sample represents the tuff "pile" based hydraulic sink region;
- ⊖ sample represents the tuff "pile" based hydraulic source region; and
- ● sample represents the Paleozoic carbonates based hydraulic source region.

$\delta^{13}C$ vs PMC field. Water samples from the Nevada Test Site hydrosphere.

Figure 6-16

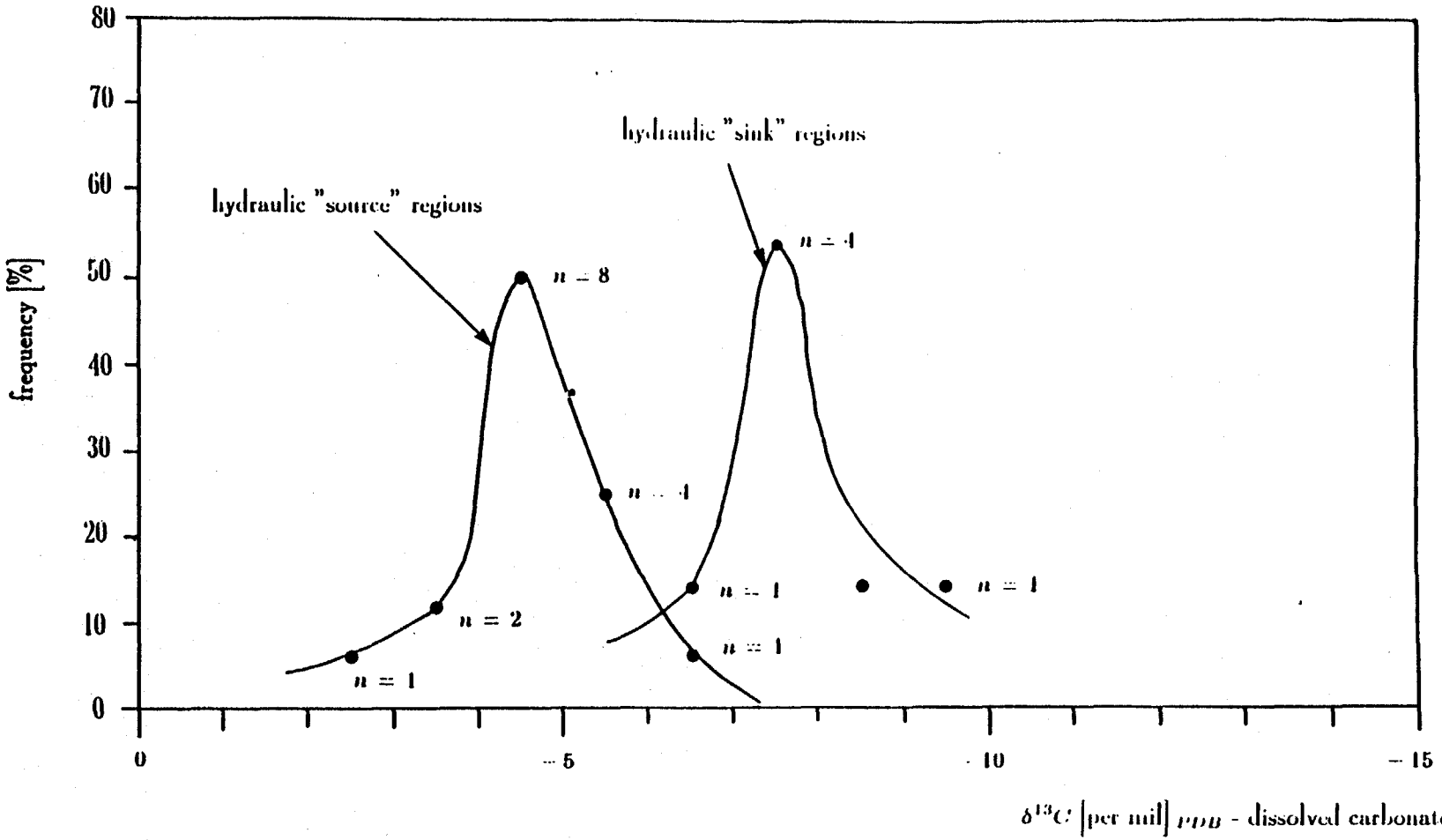

Note:

a) N = 16 for hydraulic "source" regions; N 7 for hydraulic "sink" regions.

Isotopic character of carbon. Water samples from the Paleozoic carbonate based hydraulic "sink" and "source" regions.

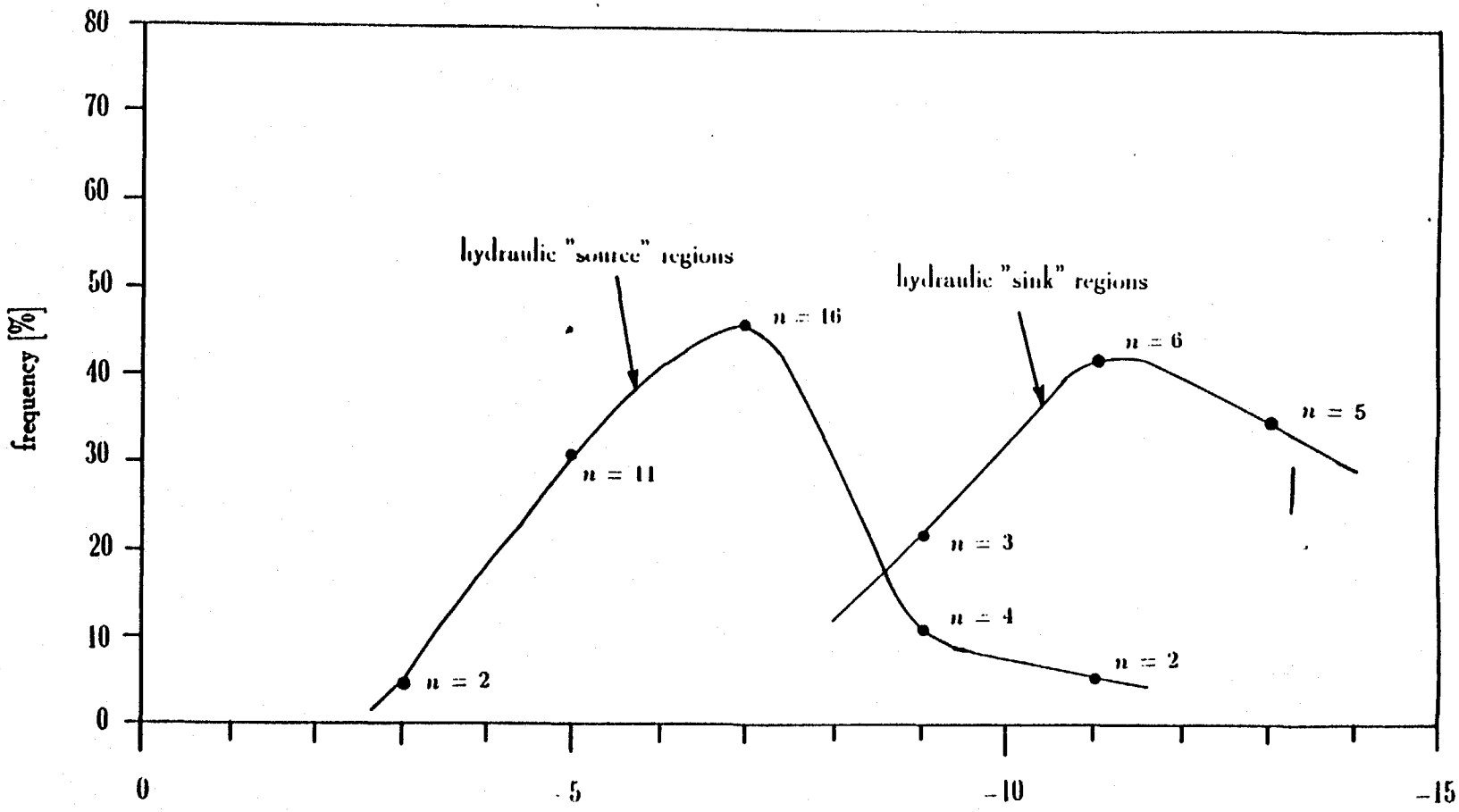

Note:

a) N = 35 for hydraulic "source" regions; N = 14 for hydraulic "sink" region.

Isotopic character of carbon. Water samples from the alluvium-tuff pile hydraulic "source" and "sink" regions.

Figure 6-18

- To account for the observations made, from the results of spatial analyses of the carbon isotopic data, the following four interpretations may be put forth:

  i) Observation that the upwelling "source" fluids carry positive values of the calcite saturation index, if coupled together with the observed direction of the log P_{CO_2} gradient, may reasonably be taken to indicate that, at the Nevada Test Site, local degassing of CO_2 from the hydrosphere is taking place;

  ii) Observation that the hydraulic "source" fluids carry both the lower concentrations of carbon-14 and the lower values of the $\delta^{13}C$ ratio may reasonably be taken to indicate that, at the Nevada Test Site, the atmosphere-biosphere CO_2 source is not a dominant factor in controlling the isotopic character of carbon dissolved in the upwelling geothermal fluids. The atmosphere-biosphere CO_2 source, however, appears to be the main factor controlling the isotopic character of carbon dissolved in the discending "sink" fluids;

  iii) Observation that, relative to the tuff "pile" based fluids, fluids residing in the Paleozoic carbonates carry higher values of the $\delta^{13}C$ ratio may reasonably be taken to indicate that some of the carbon, dissolved in the Nevada Test Site hydrosphere, is acquired through dissolution of the local marine limestones; and

  iv) Observation that, relative to the expected values of the $\delta^{13}C$ ratio for fluids equilibriated with marine limestones, the Paleozoic carbonates based fluids carry abnormally low values of the $\delta^{13}C$ ratio does not appear to have an unequivocal interpretation. To account for this observation, however, two interpretations may be proposed. On the one hand, it may be assumed that the Paleozoic carbonate based fluids carry fairly significant concentrations of old and isotopically "light" carbon from the atmosphere-biosphere CO_2 source. On the other hand, however, it is equally plausible that, at the Nevada Test Site, there is an additional source of carbon dioxide. It may reasonably be suspected that, this additional source of carbon dioxide is either a) partially molten sub-lithospheric mantle, or b) therefrom derived igneous bodies residing in the crust. It is important to note that, the local presence of, at least, three such bodies may be interpreted based on: a) the results of studies of the P-wave residuals from teleseismic events, as performed by Monfort and Evans (1982); and b) the results of seismic reflection survey made in Amargosa Desert, as reported by Brocker et al. (1989). Furthermore, the partially-incipiently molten state of the local sub-lithospheric mantle is indicated by both the direct field observations regarding rather conspicuous presence of the Plio-Quaternary volcanism [yielding Hy- to Ne-normative alkali basalts and hawaiites] and the results of seismic tomography studies of the sub-lithospheric mantle, Monfort and Evans (1982); Szymanski (1989); and EOS (1990).

Interpretations of observations resulting from the spatial analyses of the carbon isotopic data.

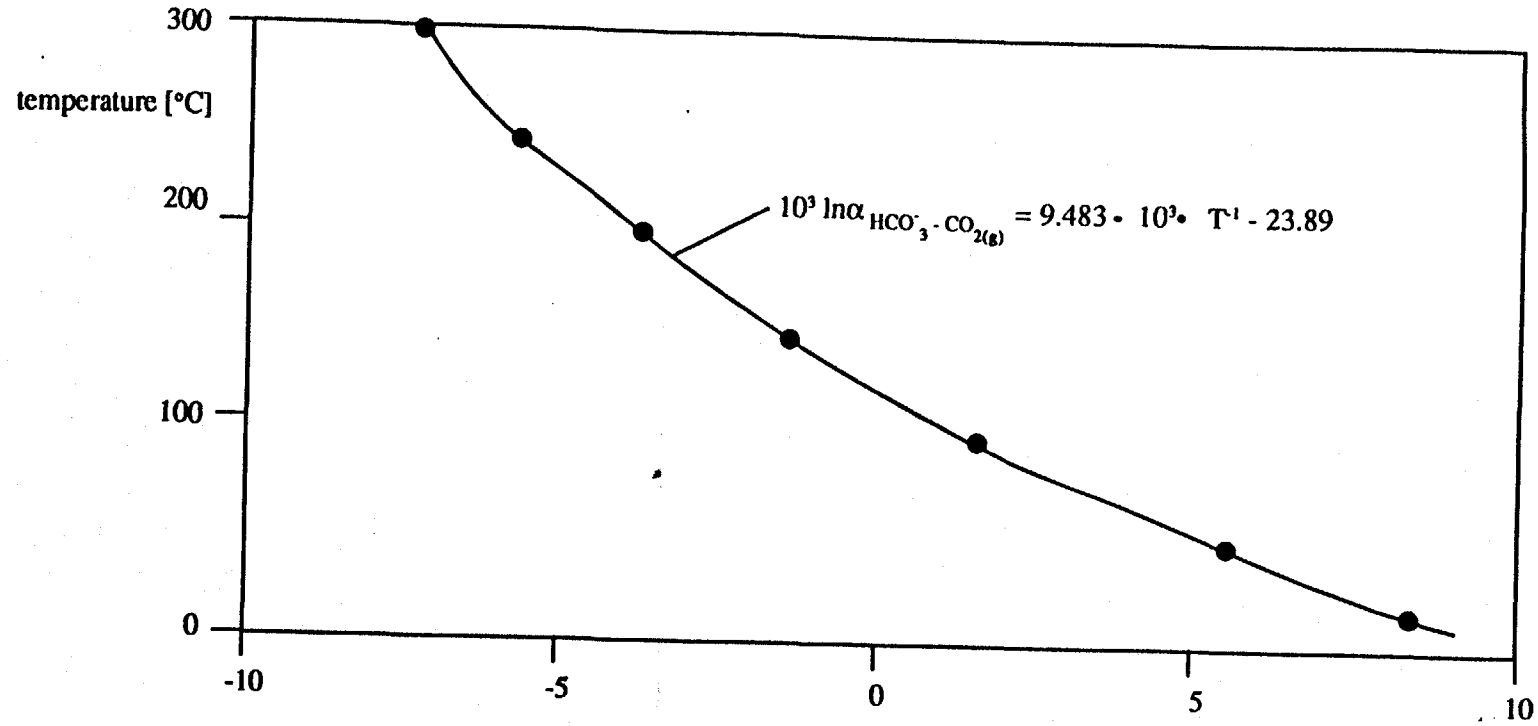

Note:

a) the fractionation equation is from Turi (1986);

b) mean value of the $\delta^{13}C$ ratio, for the sub-lithospheric mantle indigenous CO_2, may be taken as ~-6 per mil $_{PDB}$, Hoefs (1987);

c) depending upon reaction temperature, dissolution of the sub-lithospheric mantle indigenous CO_2 may be expected to produce fluids with values of the $\delta^{13}C$ ratio ranging from + 1.45 (T = 20°Celsius) to -10 per mil $_{PDB}$ (T = 200°Celsius); and

d) the expected range of the $\delta^{13}C$ ratio, for fluids produced through dissolution of the sub-lithospheric mantle indigenous CO_2, is similar to that observed for the Nevada Test Site geothermal fluids.

Plausibility assessment - hypothesis that the abnormally low values of the $\delta^{13}C$ ratio, for the Paleozoic carbonates based "source" fluids, may be reflecting influx of the sub-lithospheric mantle indigenous CO_2 .

Figure 6-20

- A fairly firm support for the hypothesis that, at the Nevada Test Site, some of the circulating carbon is derived from the local deep-seated (igneous) sources of carbon may be inferred from the results of carbon isotopic studies of samples of the carbonate gangue minerals associated with the hydrothermal ore deposits. Specifically, the results of such studies indicate that:

  i) the parent fluids for the hydrothermal ore deposits, typically, carry values of the $\delta^{13}C$ ratio ranging from -2 to more than -10 per mil $_{PDB}$, Hoefs (1987);

  ii) the hydrothermal ore forming fluids carry the dissolved carbon that is: a) isotopically "lighter" than carbon acquired during dissolution of marine limestones; and b) isotopically "heavier" than carbon produced by the biogenic sources;

  iii) during early stages of the ore forming periods, which presumably correspond with peaks of igneous activity and periods with the most intense influx of the deep-seated CO_2, the hydrothermal fluids carry relatively low values of the $\delta^{13}C$ ratio. [This very consistant observation may be taken to indicate that: a) dissolution of the deep-seated CO_2 is occurring at fairly high temperatures and b) the deep-seated carbon source predominates]; and

  iv) during vanishing stages of the ore forming periods, which presumably correspond with termination of igneous activity and periods with the accordingly reduced influx of the deep-seated CO_2, the hydrothermal fluids carry higher values of the $\delta^{13}C$ ratio [This observation may be taken to indicate that: dissolution of the deep-seated CO_2 is occurring at lower temperatures; and b) the marine limestone reservoir of carbon becomes important].

Further plausibility assessment - hypothesis that the abnormally low values of the $\delta^{13}C$ ratio, for the Paleozoic carbonates based "source" fluids, may be reflecting influx of the sub-lithospheric mantle indigenous CO_2.

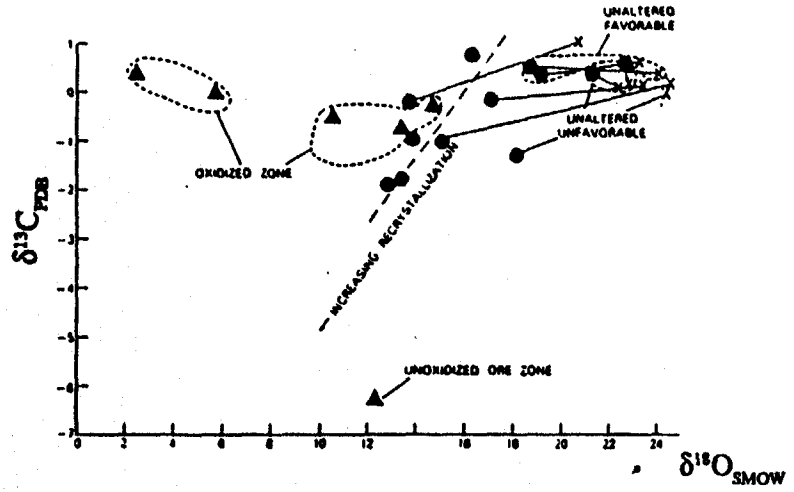

a) the Carlin disseminated gold deposit of Nevada

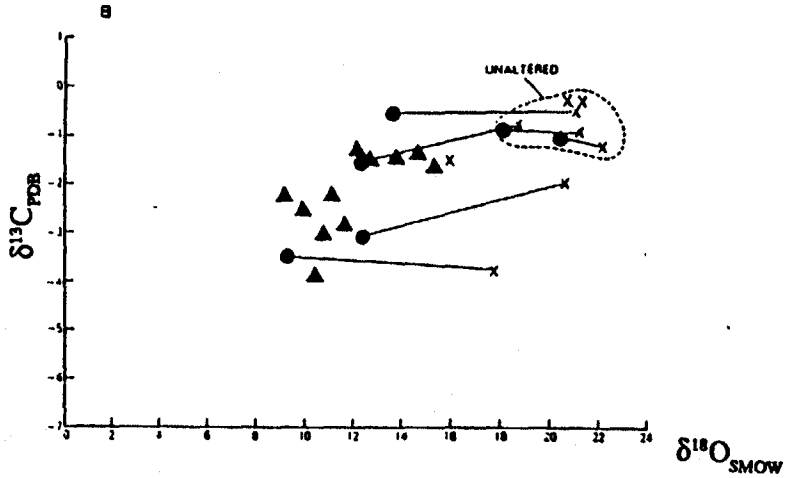

b) the Cortez disseminated gold deposit of Nevada

Note:

a) for both deposits host rock is the Paleozoic limestone;

b) samples of the carbonate gangue minerals, from the Carlin and Cortez deposits, yield values of the $\delta^{13}C$ ratio ranging from +1 to -2 per mil $_{PDB}$ and from 0 to -4 per mil $_{PDB}$, respectively;

c) White (1985) have reported that both of the gold accumulations were formed at a temperature ranging from 150 to 200°Celsius - the corresponding value of the equilibrium fractionation factor is $10^3 \ln\alpha_{HCO^-_3 - CO_{2(g)}} = \sim -3.0$ per mil $_{PDB}$, Hoefs (1987);

d) the parent fluids for the Carlin and Cortez deposits have carried values of the $\delta^{13}C$ ratio ranging from -2 to -5 per mil $_{PDB}$ and from -3 to -7 per mil $_{PDB}$, respectively; and

e) observation that the marine limestone based, and hydrothermal ore forming, fluids have carried the abnormally low values of the $\delta^{13}C$ ratio may be taken to indicate the deep-seated (igneous) origin of the dissolved carbon.

The isotopic character of carbon contained in the carbonate gangue minerals associated with the Carlin and Cortez disseminated gold deposits of Nevada.

Figure 6-22

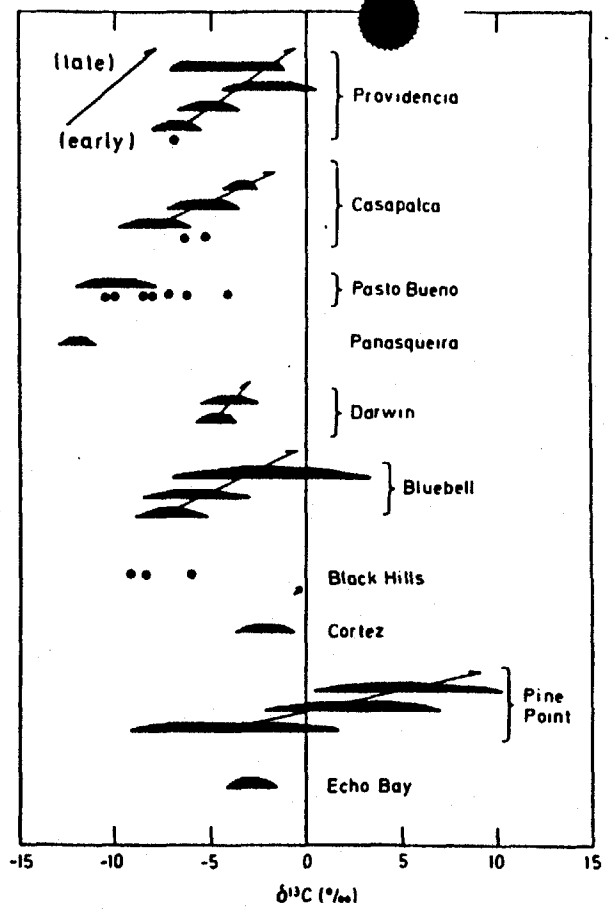

Explanation:

- carbonate gangue minerals; and
- fluid inclusion

Note:

a) relict fluids entrapped in fluid inclusions from samples of the carbonate gangue minerals, associated with various hydrothermal ore deposits, yield values of the $\delta^{13}C$ ratio ranging from -4 to about -10 per mil $_{PDB}$;

b) for individual ore deposits, the different generations of the carbonate gangue minerals are arranged from early to late, as shown by arrows;

c) the observed trend toward the isotopically "heavier" carbon (with decreasing age of the carbonate gangue minerals) may be taken to indicate that, as the volcanic activity and the resulting geothermal circulations decay, the contribution of CO_2 from the deep-seated igneous sources also decays; and

d) observation that the hydrothermal ore forming fluids carry values of the $\delta^{13}C$ ratio ranging from -2 to about -10 per mil $_{PDB}$ may be taken to indicate the deep-seated (igneous) origin of the dissolved carbon, Hoefs (1987).

The isotopic character of carbon contained in samples of the carbonate gangue minerals associated with various hydrothermal ore deposits. From Hoefs (1987).

Overall conclusions - **the result of isotopic considerations of carbon contained in the Yucca Mountain vadose zone and dissolved in fluids comprising the Nevada Test Site hydrosphere, allow for two important conclusions to be drawn.**

Conclusion I - The carbon dioxide respired from the Yucca Mountain vadose zone is provided by two independent CO_2 sources. These are: i) the atmosphere-biosphere; and ii) the subterranean fluids.

Conclusion II - At the Nevada Test Site, the circulating carbon appears to be provided by three independent sources of carbon. These are: i) the atmosphere-biosphere; ii) the Paleozoic carbonates; and iii) the deep-seated igneous bodies.

Note:

a) both the igneous origin of some of the Yucca Mountain carbon dioxide and the presence of fairly young silicic injections (suggested by the fission track ages of zircons) are, at this time, speculative propositions; and

b) as far as the proposed utilization of the Yucca Mountain area is concerned, however, both of these speculative propositions are of CRITICAL importance and, therefore, will be addressed by J.S.S. during this forthcoming field season.

Conclusions - presentation #6.

Figure 6-24

REFERENCES

Benson, L.V., and H. Kleiforth, 1989. **Stable Isotopes in Precipitation and Groundwater in the Yucca Mountain Region, Nevada — Paleoclimatic Interpretations,** In Peterson, D.H., ed., Aspects of Climate Variability in the Pacific and Western Americas, Geophysical monograph 55, p. 41–19.

Benson, L.V., and P. W. McKinley, 1985. **Chemical Composition of Groundwater in the Yucca Mountain Area, Nevada, 1971–8.** USGS Open-File Report 85–484, 10p.

Berger, B.R., 1985. **Geologic–Geochemical Features of Hot–Spring Precious–Metal Deposits.** USGS Bulletin 1646.

Blankenagel, R.K., and J. E. Weir, Jr., 1973. **Geohydrology of the Eastern Part of Pahute Mesa, Nevada Test Site, Nye County, Nevada.** USGS Professional Paper 712–B, the USGS, Washington, DC.

Boughton, C. 1986. **Integrated Geochemical and Hydraulic Analysis of the Nevada Test Site Groundwater Systems,** Masters Thesis, 135p., University of Nevada, Reno.

Brocher, T.M., P.E. Hart, and S.F. Carle, 1989. **Feasibility Study of the Seismic Reflection Method in Amargosa Desert, Nye County, Nevada.** USGS Open–File Report 89–133, Menlo Park, CA.

Castor, S.B., S.C. Feldman, and J.V. Tingley, 1989. **Mineral Evolution of the Yucca Mountain Addition, Nye County, Nevada.** Report to Science Applications International Corporation.

Castor, S.B., and J.V. Tingley, 1990. **Mineral Potential Report for the U.S. Department of Energy Administrative Land Withdrawal Application for the Yucca Mountain Addition.**

Claassen, H.C., 1973. **Water Quality and Physical Characteristics of Nevada Test Site Water–Supply Wells.** USGS Open–file Report USGS–474–158.

Claassen, H.C., 1985. **Sources and Mechanisms of Recharge for Groundwater in the West–Central Amargosa Desert, Nevada – A Geochemical Interpretation.** USGS Professional Paper 712, p. F1–F31.

Dansgaard, W., 1964. **Stable Isotopes in Precipitation.** Tellus, 16.

Deines, P., 1980. **The Isotopic Composition of Reduced Organic Carbon.** In Handbook of Environmental Isotope Geochemistry, v.1, P. Fritz and J. Ch. Fontes (editors). Elsevier.

DOE (U.S. Department of Energy), 1984. **Draft Environmental Assessment, Yucca Mountain Site, Nevada Research and Development Area, Nevada.** DOE/RW–0012, Washington, DC.

Domenico, P.A., 1972. **Concepts and Models in Groundwater Hydrology.** Earth and Planetary Sciences, McGraw–Hill International Series.

Dudley, W.W., G.E. Barr, D.A. Chesnut, and C.J. Fridrich, 1989. **Review of a Conceptual Model and Evidence for Tectonic Control of the Ground–Water System in the Vicinity of Yucca Mountain, Nevada.** US DOE, Las Vegas, NV.

Ekren, E.B., and K.A. Sargent, 1965. **Geologic Map of the Skull Mountain Quadrangle, Nye County, Nevada.** Geologic Quadrangle Map GQ–387, USGS.

EOS, 1990. **First Tomographic Study of Western U.S. Completed Transactions, American Geophysical Union,** Vol.71, No. 38.

Faure, G., 1986. **Principles of Isotope Geology.** John Wiley and Sons, Inc., New York.

Fontes, J. Ch., 1980. **Environmental Isotopes in Groundwater Hydrology.** In Handbook of Environmental Isotope Geochemistry, v.1, P. Fritz and J. Ch. Fontes (editors). Elsevier.

Friedman, I., 1970. **Some Investigations of the Deposition of Travertine from Hot Springs.** The Isotopic Chemistry of a Travertine – Depositing Spring. Geochim, Cosmochim. Acta, 34.

Fritz, P. and J. Ch. Fontes, 1980. **Introduction.** In Handbook of Environmental Isotope Geochemistry, v.1, P. Fritz and J. Ch. Fontes (editors). Elsevier.

Garside, L.J., and J.H. Schilling, 1972. **Geothermal Exploration and Development in Nevada.** Geothermal Overviews of the Western United States: Geothermal Resource Council Conf., El Centro, 1972.

Gleick, J. 1987. **Chaos – Making a New Science.** Penguin Books.

Hanson, G.N., V.R. Baker, P.M. Bethke, P.J. Hudleston, and G.R. Roguemore, 1987. **Report of the Peer Review Panel on the Proposed Program of Studies of the Calcite and Opaline–silica Deposits in the Yucca Mountain Area, Nevada.**

Hay, R.L., R. E. Pexton, T.T. Teague, and T.K. Kyser, 1986. **Spring–Related Carbonate Rocks, Mg Clays, and Associated Minerals in Pliocene Deposits of the Amargosa Desert, Nevada and California.** Geological Society of America Bulletin, 97.

Hershey, R.L., 1989. **Hydrogeology and Hydrogeochemistry of the Spring Mountain, Clark County, Nevada.** M.S. Thesis, University of Nevada, Las Vegas, NV.

Hoefs, J., 1987. **Stable Isotope Geochemistry.** Springer–Verlag.

Hoover, D.L., 1968. **Genesis of Zeolites, Nevada Test Site.** Geological Society of America Memoir 110, E.B. Eckel, (ed).

Ingraham, N.L., R.L. Jacobson, J.W., Hess, and B.F. Lyles, 1990. **Stable Isotopic Study of Precipitation and Spring Discharge on the Nevada Test Site.** Water Resources Center. Desert Research Institute. University of Nevada System. Publication #45078.

Isherwood, D., J. Harrar, and E. Raber, 1982. **Characterization of Climax Granite Ground Water.** UCRL–53–309, Lawrence Livermore National Laboratory, Livermore, CA.

Keeling, C.D., 1961. **The Concentration and Isotopic Abundance of Atmospheric Carbon Dioxide in Rural Areas.** Geochim, Cosmochim. Acta, 13.

Keilis–Borok, V.I., 1990. **The Lithosphere of the Earth as a Nonlinear System with Implications for Earthquake Prediction.** Reviews of Geophysics, 2

Kerrisk, J.G., 1987. **Groundwater Chemistry at Yucca Mountain, Nevada, and Vicinity.** LA–10929–MS, Los Alamos National Laboratory, Los Alamos, NM.

Knauss, K.G., 1981. **Dating Fault Associated Quaternary Material from the Nevada Test Site Using Uranium–Series Methods.** UCRL–53231, Lawrence Livermore National Laboratory, Livermore, CA.

Larson, L.T., D.C. Noble, S.I. Weiss, M.R. Jackson, and A.K. Chamberlain, 1988. Task 3 Report for January, 1987–June, 1988: **Volcanic Geology and Evaluation of Potential Mineral and Hydrocarbon Resources of the Yucca Mountain Area.**

Laul, J.C., and T.C. Maiti, 1988. **Natural Radionuclides in Groundwater from J–13 Well at the Nevada Test Site.** Draft DOE report.

Laul, J.C., and T.C. Maiti, 1990. **Natural Radionuclides in Groundwater from J–13 Well at the Nevada Test Site.** High Level Radioactive Waste Management Proceedings, American Nuclear Society, Las Vegas, NV.

Longwell, C.R., E.H. Pampeyan, B. Bowyer, and R.J. Roberts, 1965. **Geology and Mineral Deposits of Clark County, Nevada.** Mackay School of Mines – University of Nevada, Reno, NV.

Lorenz, E.N., 1963. **Deterministic Non–Periodic Flow.** Journal of the Atmospheric Sciences, vol.20.

Lyles, B.F., J. Edkins, R.L., Jacobson, and J.W. Hess, 1990. **Time–Series Analysis of Ion and Isotope Geochemistry of Selected Springs of the Nevada Test Site, Nye County, Nevada.** Water Resources Center. Desert Research Institute. University of Nevada System. Publication #45068.

Major, J., 1977. **California Climate in Relation to Vegetation.** In M.G. Barbour and J. Major (editors). Terestrial Vegetation of California. John Wiley, New York.

Marshall, B.D., Z.E. Peterman, K. Futa, J.S. Stuckless, S.A. Mahan, J.S. Downey, and E.D. Gutentag, 1990. **Origin of Carbonate Deposits in the Vicinity of Yucca Mountain, Nevada: Preliminary Results of Strontium–Isotope Analyses.** High-Level Radioactive Waste Management Proceedings. American Nuclear Society, Las Vegas, NV.

Monfort, M.E., and J.R. Evans, 1982. **Three–Dimensional Modeling of the Nevada Test Site and Vicinity From Teleseismic P–Wave Residuals.** USGS–OFR–82–409, the USGS, Menlo Park, CA.

Quade, J., T.E. Cerling, and J.R. Bowman, 1988. **Systematic Variations in $\delta^{13}C$ and $\delta^{18}O$ of Soil Carbonate Along Elevation Transects in the Southern Great Basin, USA.** Update Report: The Paleohydrology and Paleoenvironments in the Vicinity of the Proposed Yucca Mountain Nuclear Waste Repository. W.G. Spaulding, ed.

Quade, J., T.E. Cerling, and J.R. Bowman, 1989. **Systematic Variations in the Carbon and Oxygen Isotopic Composition of Pedogenic Carbonate Along Elevation Transects in the Southern Great Basin, United States.** Geological Society of America Bulletin, v.101.

Quade, J., and T.E. Cerling, 1990. **Stable Isotopic Evidence for a Pedogenic Origin of Carbonates in Trench 14 Near Yucca Mountain, Nevada.** Science, Vol.

Rye, R.O., 1985. **A Model for the Formation of Carbonate–Hosted Disseminated Gold Deposits Based on Geologic, Fluid–Inclusion, Geochemical, and Stable–Isotope Studies of the Carlin and Cortex deposits, Nevada.** USGS Bulletin 1646.

Russell, C.E., 1987. Hydrogeologic Investigations of Flow in Fractured Tuffs, Rainier Mesa, Nevada Test Site, M.S. Thesis, University of Nevada–Reno, Reno, NV.

Sass, J.H., H. Lachenbruch, 1982. **Preliminary Interpretation of Thermal Data from the Nevada Test Site.** USGS–OFR–82–973, Open–File Report, the USGS, Denver, CO.

Saas, J.H., A.H. Lachenbruch, W.W. Dudley, S.S. Priest, and R.J. Munroe, 1987. **Temperature, Thermal Conductivity, and Heat Flow near Yucca Mountain, Nevada: Some Tectonic and Hydrologic Implications.** UGSG Open–File Report, the USGS, Denver, CO.

Shroba, R.R., D.R. Muhs, and J.N. Rosholt, 1988. **Physical Properties and Radiometric Age Estimates of Surficial and Fracture–Fill Deposits Along a Portion of the Carpetbag Fault System, Nevada Test Site, Nye County, Nevada.** DOE/NV/10583–1.

Smith, 1991. Personal Communication to Dr. D.L. Livingston.

Spencer, E.B., 1990. **A Radiocarbon Study of Groundwater in the Western Nevada Test Site and Vicinity.** M.S. Thesis, University of Nevada–Reno, Reno, NV.

Stewart, I., 1989. **Does God Play Dice? – The Mathematics of Chaos.** Basil Blackwell Ltd., Oxford, UK.

Stuckless, J.S., 1990. Presentation to the National Academy of Sciences Panel on Coupled Hydrologic/Tectonic/Hydrothermal Systems at Yucca Mountain.

Stuckless, J.S., 1990. **An Evaluation of Evidence Pertaining to the Origin of Vein Deposits.** Draft USGS Report.

Stuckless, J.S., J.F. Whelan, and W.C. Steinkampf, 1990. **Isotopic Discontinuities in Ground Water Beneath Yucca Mountain, Nevada.** Draft USGS Report.

Szymanski, J.S., 1989. **Conceptual Considerations of the Yucca Mountain Groundwater System with Special Emphasis on the Adequacy of this System to Accommodate a High–Level Nuclear Waste Repository.** DOE Internal Report.

Szabo, B.J., W.J. Carr, and W.C. Gottschall, 1981. **Uranium–Thorium Dating of Quaternary Carbonate Accumulations in the Nevada Test Site Region, Southern Nevada.** USGS–OFR–81–119, Open–File Report, the USGS, Denver, CO.

Szabo, B.J., and T.K. Kyser, 1985. **Uranium, Thorium Isotopic Analyses and Uranium–Series Ages of Calcite and Opal, and Stable Isotopic Compositions of Calcite from Drill Cores UE–25a1, USW G–2, and USW G–3/GU3, Yucca Mountain Nevada.** USGS–OFR–85–224, Open–file Report, the USGS, Denver, CO.

Szabo, B.J., and T.K. Kyser, 1990. **Ages and Stable–Isotopic Compositions of Secondary Calcite and Opal in Drill Cores from Tertiary Volcanic Rocks of the Yucca Mountain Area, Nevada.** Geological Society of America Bulletin, v.102.

Talma, A.S., and F. Netterberg, 1983. **Stable Isotope Abundances in Calcretes. In Residual Deposits: Surface Related Weathering Processes and Materials.** Wilson, R.C.L. (ed). The Geological Society of London.

Thorstenson, D.C., E.P. Weeks, H. Hess, and J.C. Woodward, 1989. **Physical and Chemical Characteristics of Topographically Affected Airflow in an Open Borehole at Yucca Mountain, Nevada.** Focus '89 Nuclear Waste in the Unsaturated Zone Proceedings.

Turi, B., 1986. **Stable Isotope Geochemistry of Travertines In Handbook of Environmental Isotope Geochemistry.** v.2, P. Fritz and J. Ch. Fontes (editors). Elsevier.

U.S. Environmental Protection Agency, 1976. **Environmental Monitoring Report for the Nevada Test Site and Other Test Areas Used for Underground Nuclear Detonations.** EMSL–LV–539–4.

Vaniman, D.T., D.L. Bish, and S. Chipera, 1988. **A Preliminary Comparison of Mineral Deposits in Faults near Yucca Mountain, Nevada, with Possible Analogs.** LA–11289–MS, Los Alamos National Laboratory, Los Alamos, NM.

Walker, G.E., 1962. **Ground Water in the Climax Stock, Nevada Test Site, Nye County, Nevada.** USGS Report TEI–813, the USGS, Denver, CO.

Weiss, S.I., D.C. Noble, and L.T. Larson, 1990. Task #3 Report in Evaluation of the Geologic Relations and Seismotectonic Stability of the Yucca Mountain Area. Progress Report 30, September 1990. Center for Neotectonic Studies, Mackay School of Mines, University of Nevada, Reno, NV.

Whelan, J.F., and J.S. Stuckless, 1990. **Reconnaissance $\delta^{13}C$ and $\delta^{18}O$ Data from Trench 14, Busted Butte, and Drill Hole G–4. Yucca Mountain, Nevada Test Site.** Draft USGS Report.

White, A.F., 1979. **Geochemistry of Ground Water Associated with Tuffaceous Rocks, Oasis Valley, Nevada.** USGS Professional Paper 712–E, the USGS, Washington, DC.

White, A.C., H.C. Claassen, L.V. Benson, 1980. **The Effect of Dissolution of Volcanic Glass on the Water Chemistry in a Tuffaceous Aquifer, Rainier Mesa, Nevada.** USGS–WSO1536–Q, Water Supply Paper, the USGS, Washington, DC.

White, A.F., and H.J. Chuma, 1987. **Carbon and Isotopic Mass Balance Models of Oasis Valley–Fortymile Canyon Groundwater Basin, Southern Nevada.** Water Resources Research, v.23, No.4.

Winograd, I.J., and W. Thordarson, 1975. **Hydrogeologic and Hydrochemical Framework, South–Central Great Basin, Nevada–California, with Special Reference to the Nevada Test Site.** USGS Professional Paper 712–C, pp. C1–C126, Washington, DC.

Yang, I.C., H.H. Herbert, E.P. Weeks, and D.C. Thorstenson, 1985. **Analysis of Gaseous–Phase Stable and Radioactive Isotopes in the Unsaturated Zone, Yucca Mountain, Nevada.** Proceedings of the NWWA Conference on Characterization and Monitoring of the Vadose Zone, Nevember 19–21, 1985, Denver, CO.

Yang, I.C., 1989. **Conceptual Model of Unsaturated Zone Ground Water Flows at Yucca Mountain in Nevada, Based on Geochemical Isotopic Data.** Draft USGS Report Submitted for Release as Proceedings for the April 1990 International High–Level Radioactive Waste Management Conference.

Zielinski, R.A., and J.N. Rosholt, 1978. **Uranium in Waters and Aquifer Rocks at the Nevada Test Site, Nye County, Nevada.** USGS Jour. Res., 6, 489.